24th World Mining Congress

MINING IN A WORLD OF INNOVATION

October 18-21, 2016 • Rio de Janeiro /RJ • Brazil

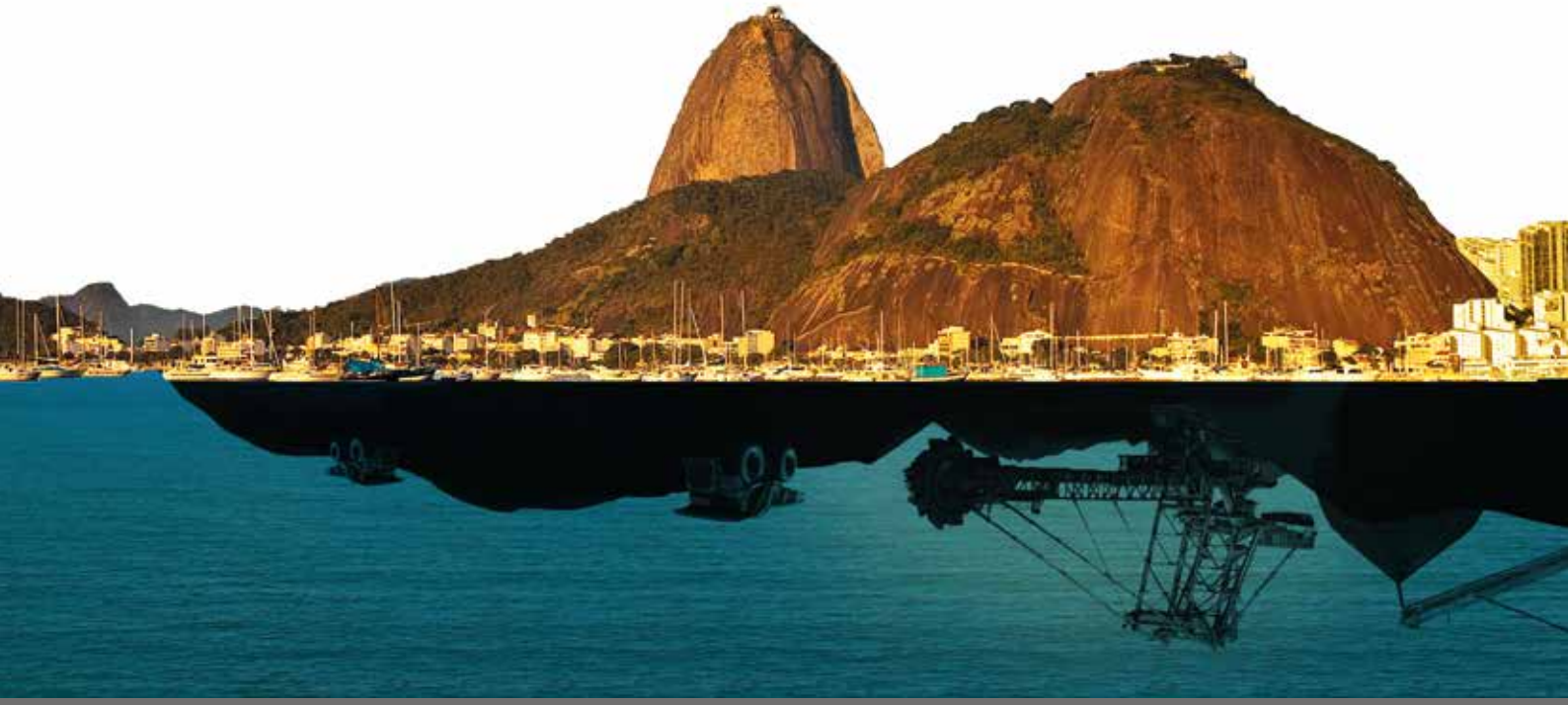

24th World Mining Congress **PROCEEDINGS**

MINERAL PROCESSING

Promotion:

IBRAM
INSTITUTO BRASILEIRO DE MINERAÇÃO
Brazilian Mining Association
Cámara Minera de Brasil

Diamond Sponsorship:

VALE

Votorantim Metais

Gold Sponsorship:

SINFERBASE
Sindicato Nacional da Indústria da Extração do Ferro e Metais Básicos

Silver Sponsorship:

CBMM

Bronze Sponsorship:

AngloAmerican

HYDRO

KINROSS

Special Sponsorship:

ANGLOGOLDASHANTI

Steel Sponsorship:

GERDAU

Special Support:

ANEPAC

GBR
Global Business Reports

MINISTÉRIO DE MINAS E ENERGIA

MINISTÉRIO DA CIÊNCIA, TECNOLOGIA, INOVAÇÕES E COMUNICAÇÕES

BRASIL
GOVERNO FEDERAL

Communication Agency:

Profissionais do Texto
COMUNICAÇÃO CORPORATIVA

Operations Management:

HYRNASTHA
INOVAR

Executive Producer and Marketing:

panda

Commercial Partner – India:

IndusExposium

Commercial Partner – Canada/USA:

AMP

Promotion:

IBRAM
INSTITUTO BRASILEIRO DE MINERAÇÃO
Brazilian Mining Association
Cámara Minera de Brasil

24th World Mining Congress **PROCEEDINGS**

MINERAL PROCESSING

October 18-21, 2016
Rio de Janeiro /RJ • Brazil

IBRAM
INSTITUTO BRASILEIRO DE MINERAÇÃO
Brazilian Mining Association
Câmara Minera de Brasil

IBRAM sede
SHIS QL 12, Conjunto 0 (zero), Casa 04,
Lago Sul – Brasília/DF – CEP: 71.630-205
Phone: +55 (61) 3364-7272 / (61) 3364-7200
ibram@ibram.org.br

IBRAM Minas Gerais
Rua Alagoas, 1270, 10 º andar
Funcionários – Belo Horizonte/MG
CEP: 30130-168
Phone: + 55 (31) 3223-6751
ibram-mg@ibram.org.br

IBRAM Amazônia
Travessa Rui Barbosa, 1536 – B. Nazaré
Belém/PA – CEP: 66035-220
Phone: + 55 (91) 3230-4066
ibramamazonia@ibram.org.br

www.ibram.org.br

https://www.facebook.com/InstitutoBrasileirodeMineracao/

Catalog Card

24th World Mining Congress (24: 2016: Rio de Janeiro, RJ)

24th World Mining Congress PROCEEDINGS – MINERAL PROCESSING / Brazilian Mining Association/Instituto Brasileiro de Mineração (Org). 1ed. - Rio de Janeiro: IBRAM, 2016. e-book

Event held between 18th to 21st October 2016.

Available at: www.wmc2016.org.br and www.ibram.org.br

336 p.

ISBN: 978-85-61993-11-5 e-book

1- Mining. 2- Innovation. 3- Mineral Processing. I- Title. II- 24th World Mining Congress. III- Instituto Brasileiro de Mineração.

CDU: 622/5: 502/504

VALE INSTITUTE OF TECHNOLOGY

VALE

Access **www.itv.org** and be part of our team of researchers,
academics, masters' degree and post-graduation students.

Vale Institute of Technology

Created in 2009 with the purpose of stimulating innovation, competitiveness and sustainability in Vale's operations, Vale Institute of Technology (ITV) is a non-profit organization that develops research activities, with emphasis on H2 and H3 horizons as well as training of resources human at post-graduate level. ITV has two locations: one in Belém in the State of Pará, focused on matters related to Sustainable Development, and the other in Ouro Preto, MG, dedicated to Mining and Mineral processing topics.

At the ITV unit in Belém, Vale has been offering a *Master's Degree Program in the Sustainable Use of Natural Resources in Tropical Regions* since 2012. This is a unprecedented initiative in Brazil as it is the first course offered in conjunction with a company from the mineral sector to obtain certification from the Coordination for the Improvement of Higher Education Personnel (Coordenação de Aperfeiçoamento de Pessoal de Nível Superior - Capes), of the Ministry of Education.

In Minas Gerais, ITV launched a pioneering partnership with Universidade Federal de Ouro Preto (UFOP) to structure the *Master's Degree Course in Instrumentation, Control and Mining Process Systems, and Master's Degree Course in Mineral Engineering*. This course has been approved by Capes in 2015 and classes began in 2016. Another innovative partnership that has been being developed is with the ISPT-Instituto Superior Profissional de Tete, Mozambique, consisting in the offer of courses for the Master's Degree Program in Mining at ISPT. These courses are supported financially and operationally by Vale and Capes.

ITV also provides Specialization courses in Mining for Vale's employees and other courses for professional qualification, as well as research activities comprising levels from scientific research to post-doctoral degree.

Luiz Mello

In partnership with Capes, Vale offers academic postdoctoral scholarships for Brazilians and foreigners to researchers who are selected to work at Vale Institute of Technology units, further bringing together the academic community and Vale, expanding the potential generation of innovation and wealth for Vale and Brazil.

Performance Segments

ITV activities are focused across three key segments: Research, Education and Entrepreneurship, following the cycle through which scientific production evolves, creating practical application and generation of concrete benefits for the company. For further information visit: www.itv.org or send an e-mail: info.itv@itv.org.

It is a pleasure for us to participate in the 24th edition of the World Mining Congress - WMC 2016, being held for the first time in Brazil, and we can introduce you to some of the technological, research and innovation solutions in the Mining Sector. It is our commitment to share knowledge, innovation and technology towards the sustainable development of the operations and processes in global mining.

I hope that everyone enjoys the most of the World Mining Congress!

Luiz Mello
CEO of Vale Institute of Technology
Technology and Innovation Executive Manager of Vale

José Fernando Coura

On behalf of the Brazilian Mining Association - IBRAM and its associates, I would like to offer a warm welcome to all the participants of the 24th edition of the World Mining Congress - WMC 2016. This is the first time that the WMC, recognized as one of the most important world mining events, is being held in Brazil. The central theme of this congress is "Mining in a World of Innovation", one of the most current and important issues in the management of mining-sector businesses.

The 24th WMC began to take shape in 2012 when representatives from businesses and entities of the mining sector, as well as the Brazilian government, joined forces to support the country's bid, before the International Organizing Committee, to host the congress (IOC). This was well-deserved, given Brazil is one of the international exponents of mining.

The presentation of the Brazilian bid was made by IBRAM's presidency in conjunction with our Director of Mineral Issues, Marcelo Ribeiro Tunes. It fell to him to deliver the speech underlining the qualities that make IBRAM suitable to organize such an event, of the city of Rio de Janeiro (RJ) to attract and host event participants, and the Brazilian mining industry; factors which proved decisive in convincing the IOC members to choose Brazil as the host of the event in 2016.

With this significant vote of confidence, we are certain that the 2016 WMC will be the stage of an intense diffusion of knowledge, of discussions on the best way forward, and deep analyses of the current and future landscape of the mining industry. Without a doubt, it will also serve as a way to strengthen relationships and enable dialogue between the most diverse actors of the sector's extensive production chain on an international level.

We know that the last few years have been challenging for the mining industry and "innovation" is the key word for new business and the future of the sector itself. The economic environment has altered the rhythm of supply and demand, impacting ore prices and making it more difficult for mining companies to outline their next steps both locally and globally. Nevertheless, this moment offers an opportunity for mining to lay the way for a return to greater productivity in the future.

This is the proposal of the 24th edition of the WMC, amongst others. We also intend to technically and scientifically promote and support cooperation to develop more stages in the sustainable development of operations and processes in the mining sector.

With an optimistic vision of the prospects of the mineral sector, I hope that IBRAM, via this grand event, can awaken the public interest to debate the future of mining and identify innovative actions to further strengthen the mining industry around the world.

We wish everybody an excellent World Mining Congress!

José Fernando Coura
CEO of the Brazilian Mining Institute

Murilo Ferreira

Brazil has a historic vocation for mineral extraction activities, and since the mid-18th century they have practically dominated the dynamics of its economy. Rich in world-class minerals, the country has emerged as one of the leading global players in the mining industry, and it is now the second largest iron ore producer and one of the most significant agents in international trading and exports of this commodity.

The mining industry has become one of the most important pillars of Brazil's development. Despite the decline in iron ore prices and demand in the international markets, especially due to the slowdown in Chinese consumption, and despite the end of the super-cycle, the mining sector has continued to play a key role in maintaining Brazil's balance of trade surplus.

In addition to its positive impacts in the macroeconomic sphere in Brazil, mining has also become a driver of social development, particularly as it has a multiplier effect on other economic activities, contributing to the expansion of various production chains and consequently to the generation of jobs and income. It is noteworthy that in the municipalities where mining companies operate, Human Development Index ratings have been higher than the average figures for their respective states, and much higher than in non-mining municipalities.

In a country like Brazil, whose economic growth, as already mentioned, is strongly dependent upon the expansion of mining activities, the creation of the Brazilian Mining Association, which will turn 40 in December, was essential and absolutely necessary. This is a date to be celebrated, above all because IBRAM has played its role to support and strengthen mining activities with dynamism, efficiency and innovative practices. The sector's companies and organizations can count on a body that assertively and competently represents, coordinates and integrates them, defending their interests and generating conditions conducive to the sustainable development and competitiveness of their businesses.

The holding in Brazil of the 24th edition of the World Mining Congress, organized by an entity of IBRAM's quality, is a milestone and an excellent opportunity for the sector to share ideas, discuss, reflect and find stimuli and feasible ways forward at a time when we need to face the end of the mining super-cycle. The theme of the Congress could not be more appropriate, and I am sure that by its end, promising directions will have been mapped to strengthen the mining industry across the world.

Murilo Ferreira
Chief Executive Officer, Vale S.A.

Professor Jair Carlos Koppe

Mining has been extremely important to the World's economic growth and prosperity for centuries. The mining industry is currently facing an economic and social crises that can impact strongly the mineral production and productivity. In this scenario several challenges must be addressed, among them complex mineral deposits of low grades, water, social and environmental issues as well as declining commodity prices. Considering that the world is changing dramatically in all aspects this is the moment for innovation in mining. The WMC 2016 is under the umbrella of Mining in a World of Innovation in the proper moment. This is a nice opportunity to change our ways in mining technology considering the new evolving technologies such as automation, sensors, cloud computing, data analytics that can increase the mining production and efficiency in the entire value chain. Let's take this moment to spread our experience among academy, industries, practitioners and professionals of the mining sector focusing in the future of a world in constantly innovation.

We would like to thanks all the contributions done by the authors invited speakers and participation of delegates that will make WMC 2016 a very successful meeting. Special thanks to the members of the Scientific Committees that helped in the paper analysis ensuring the quality of the conference.

Welcome to the WMC 2016.

Professor Jair Carlos Koppe
Congress Chairperson

Józef Dubiński

Hermínio Oliveira

The 24th World Mining Congress is one of the most important mining events worldwide and is going to be held in Rio de Janeiro, Brazil, from October 18 to 21, 2016. The premiere of the World Mining Congress took place 58 years ago, in September 1958, in Warsaw, Poland. Currently, the WMC organization gathers 45 mining nations from all over the world.

Each World Mining Congress, which takes place in a different host-nation, is always a great mining occasion for the international community that represents science and industry figures involved in the exploration of mineral assets. We can assert that this congress points to the most significant directions for global mining development and determines priorities for the activities of all institutions related to mineral activity. The same approach is going to be adopted during the 24th World Mining Congress, which is going to concentrate on the theme of "Mining in a World of Innovation". Nowadays, and increasing number of countries hold great knowledge potential on mining. The challenges aforementioned demand mutual cooperation, exchange of technical knowledge and professional experience, as well as assistance to those in need. Personally, I believe that our generation of the world mining society – the heirs of our illustrious ancestors – will follow their accomplishments and guide the organization of the World Mining Congress into a new direction, to assure many more years of effective services to global mining and to the people who have taken part in this challenging activity, yet still necessary for all humankind.

Józef Dubiński
Professor and Doctor of Engineering
Corresponding Member PAS
Chairman of the World Mining Congress International Organizing Committee

HONORARY CHAIRPERSONS

JOSÉ FERNANDO COURA
President-Director of the Brazilian Mining Association (IBRAM)

MURILO FERREIRA
Chief Executive Officer of VALE

SPECIAL HONOUREE

GEOLOGIST MARCELO RIBEIRO TUNES
Director of Mining Affairs at the Brazilian Mining Association (IBRAM)
Former General-Director of the National Department of Mineral Production (DNPM)

CONGRESS CHAIRPERSON

PROFESSOR JAIR CARLOS KOPPE
Federal University of Rio Grande do Sul (UFRGS)

CONGRESS CO-CHAIRS

PROFESSOR EDUARDO BONATES
Federal University of Campina Grande (UFCG)

PROFESSOR ENRIQUE MUNARETTI
Federal University of Rio Grande do Sul (UFRGS)

PROFESSOR GEORGE VALADÃO
Federal University of Minas Gerais (UFMG)

PROFESSOR ISSAMU ENDO
Federal University of Ouro Preto (UFOP)

PROFESSOR LUIS ENRIQUE SÁNCHEZ
University of São Paulo (USP)

CONGRESS TECHNICAL COORDINATION

RINALDO CÉSAR MANCIN
Director of Environmental Affairs at the Brazilian Mining Association (IBRAM)

WORLD MINING CONGRESS CHAIR

M.SC. ENG. JACEK SKIBA
Secretary General of the World Mining Congress

PROF. JÓZEF DUBIŃSKI
World Mining Congress Chairperson and Managing Director of the Central Mining Institute, Katowice, Poland

NATIONAL SCIENTIFIC ADVISORY COMMITTEE

AARÃO DE ANDRADE LIMA – UFCG

ANDRÉ CARLOS SILVA – UFG

ANDRÉ CEZAR ZINGANO – UFRGS

ANTÔNIO EDUARDO CLARK PERES – UFMG

ANTÔNIO PEDRO F. SOUZA – UFCG

CARLOS HOFFMANN SAMPAIO – UFRGS

CARLOS OTÁVIO PETTER – UFRGS

CLÁUDIO LÚCIO L. PINTO – UFMG

DINIZ TAMANTINI RIBEIRO – VALE

EDMO DA CUNHA RODOVALHO – UNIFAL

ENRIQUE MUNARETTI – UFRGS

EUNÍRIO ZANETTI – ITV/VALE

GÉRMAN VINUEZA – ITV/VALE

GEORGIO DI TOMI – USP

IVO ANDRÉ HOMRICH SCHNEIDER – UFRGS

JOÃO FELIPE C. L. COSTA – UFRGS

JOSÉ BAPTISTA OLIVEIRA – UFBA

JOSÉ MARGARIDA DA SILVA – UFOP

JULIO CESAR DE SOUZA – UFPE

LAURINDO DE SALLES LEAL FILHO – ITV/VALE

LINEU AZUAGA AYRES DA SILVA – USP

LUIZ ENRIQUE SÁNCHEZ – USP

MICHEL MELO OLIVEIRA – CEFET/ARAXÁ

MÔNICA CARVALHO – UFPB

PAULO SALVADORETTI – UFRGS

RICARDO CABRAL DE AZEVEDO – USP

ROBERTO CERRINI VILLAS–BÔAS – CETEM
(in memorian)

RODRIGO DE LEMOS PERONI – UFRGS

VLÁDIA CRISTINA SOUZA – UFRGS

WILSON TRIGUEIRO DE SOUZA – UFOP

INTERNATIONAL SCIENTIFIC ADVISORY COMMITTEE

ABANI R. SAMAL, PH.D
University of Utah, US

DR. ANDRE XAVIER
Canadian International Resources and Development Institute (CIRDI), Canada

MR. G.P. KUNDARGI
Chairman-cum-Managing Director, MOIL Limited, India

DR. BISWAJIT SAMANTA
Indian Institute of Technology, India

MR. M. BILGIN KAYNAR
Deputy Chairman Turkish National Committee, Turkey

PROF. DR. CARSTEN DREBENSTEDT
Institut für Bergbau und Spezialtiefbau, Germany

PH.D. DEBORAH J. SHIELDS
Colorado State University, US

PROF. DR. DOMINGO JAVIER CARVAJAL GÓMEZ
Universidad de Huelva, Spain

PROF. ERNEST BAAFI
The University of Wollongong, Australia

PROF. DR. ENG. JAN PALARSKI
Silesian University of Technology, Poland

PROF. DR. ENG. STANISŁAW PRUSEK
Central Mining Institute, Katowice, Poland

DR. FARSHAD RASHIDI-NEJAD
University of New South Wales, Australia

PROF. FERRI HASSANI
Mc Gill University, Canada

PROF. DR. FIDELIS TAWIAH SUORINENI
University of New South Wales, Australia

PROF. GIDEON CHITOMBO
The University of Queensland, Australia

DR. HUA GUO
Queensland Centre for Advanced Technologies
(QCAT), Australia

PROF. HOOMAN ASKARI–NASAB
University of Alberta, Canada

MR.SC. IVAN COTMAN
KAMEN d.d. (Ltd.), Croatiia

PROF. ING. VLADIMÍR SLIVKA
Technical University of Ostrava, Czech Republic

24th World Mining Congress
MINING IN A WORLD OF INNOVATION
October 18-21, 2016 • Rio de Janeiro /RJ • Brazil

Summary

A REVIEW OF LARGE COPPER CONCENTRATOR DESIGNS – TYPES OF FLOWSHEETS, EQUIPMENT SELECTION AND INDUSTRY TRENDS

*David G. Meadows
Global Manager of Metallurgy
Bechtel Mining & Metals
Phoenix, Arizona
USA

*(*Corresponding author: dmeadows@bechtel.com)*

24th World Mining Congress
MINING IN A WORLD OF INNOVATION
October 18-21, 2016 • Rio de Janeiro /RJ • Brazil

LARGE COPPER CONCENTRATOR DESIGN – TYPES OF FLOWSHEET, EQUIPMENT SELECTION AND INDUSTRY TRENDS

ABSTRACT

With the continuing processing of higher ore throughput rates at lower ore feed grades, concentrator process plant sizes have continued to grow from the once large 30,000 tpd plant to now over 120,000 tpd single line plants. Simplification has come about by the continuing advancement of larger equipment sizes such as cone crushers, grinding mills and flotation cells. In more recent years greater emphasis has been placed on energy efficiency and the use of high pressure grinding rolls particularly for processing hard competent ores has been more noticeable. This paper reviews the current design aspects across some of the concentrators recently built by Bechtel and others and reviews the overall plant designs and operational considerations.

KEYWORDS

Concentrator, High Pressure Grinding Rolls (HPGR), Mineralogy, Testwork, Flowsheet

INTRODUCTION AND BACKGROUND

As the minerals industry moves forward in this downturned market it is also faced with the challenge of more complexly mineralogical occurring deposits of giant copper porphyries. The deposits are often vast in size and the measured resource size over 5,000,000 tonnes of contained copper is not uncommon. Often new orebody discoveries are at greater depth and associated with harder competent ore types, with much finer disseminated value copper minerals. At the same time, the overall grades of the deposits are lower than the past. In the 1980's several copper concentrators were built with a throughput rate of approximately 30,000 tpd. These plants were characterized by single line grinding circuits and streamlined downstream processing due to the increase in equipment sizes. With the now lower feed grades plant capacities have continued to increase and the latest projects with 240,000 tpd plants have been constructed and have been set into operation.

PROCESS MINERALOGY DICATES PROCESS ROUTE

In order to determine the process route options an understanding of the mineralization is essential. The application of process mineralogy is a key step in the development process. Process mineralogy is an inter-discipline of the fields of mineralogy and mineral processing.

Due to the continued development of more complex ores, the role and importance of process mineralogy will continue to gain more attention. One of the most important goals of the mineral processor is to establish a process route to enable recovery of as much of the target mineral(s) as possible from the ore being treated and to perform this with the best overall economics. The test work planning will explore all the unit processes of the flowsheet step by step as well as some potential interactions such as recycle streams and recycle water etc.

For the majority of copper ores, the final concentrate grades and recoveries are influenced by the copper mineralogical occurrence, together with other factors such as grain size, liberation and association.

The economically most important minerals of copper are summarized with the respective percentage of contained metal in the right hand column of Table 1. In broad terms of processing, the process routes will follow either an oxide route or a sulphide route. Occasionally circuits also include a

combined step for treatment of sulphides/mixed ores. The focus of this paper relates to the sulphide route in concentrator design.

Table 1 - Economic Copper Minerals

Mineral	Classification	Composition	% Copper Contained
Malachite	Oxide	$Cu_2(CO_3)OH)_2$	58
Chalcopyrite	Sulphide	$CuFeS_2$	35
Chrysocolla	Oxide	$(Cu,Al)_2H_2Si_2O_5(OH)_4 \cdot n(H_20)$	34
Chalcocite	Sulphide	Cu_2S	80
Bornite	Sulphide	Cu_5FeS_4	63

Hydrometallurgical process routes for copper oxide ores (such as malachite and chrysocolla) have followed a traditional stage crushing, agglomeration, heap leaching, solvent extraction and electrowinning (SX-EW) route with the final electrolytic high quality metal being produced at the project site. Although there have been some advances in the hydrometallurgical side including bacterial leaching and pressure leach circuits, the traditional copper concentrator route has been the 'workhorse' circuit for the vast majority of greenfield and brownfield sulphide deposits. In the past two decades a significant number of concentrators have been built, covering geographical spans from Armenia to Zambia. The overall block flow diagram for a copper concentrator is shown in Figure 1. There are a number of variations on this depending on associated mineralization, for example copper-molybdenum ores will have an additional molybdenum flotation circuit.

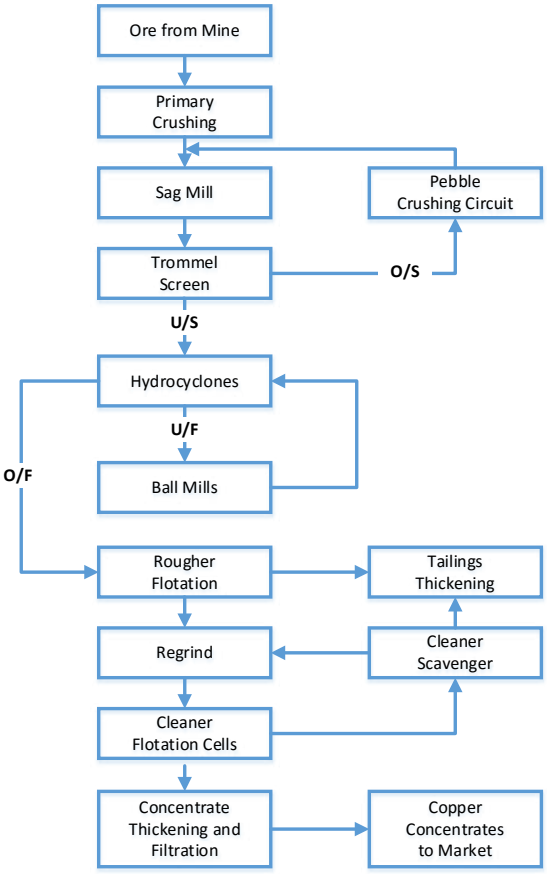

Figure 1 – Concentrator Block Flow Diagram – SABC Comminution Circuit

TESTWORK AND FLOWSHEET DEVELOPMENT

The development of a suitable process route to treat an orebody would appear to be relatively simple but requires a great deal of thought and consideration. Prior to going ahead with the test program it is essential that a close interaction is established between the mine geologist, the mining engineers and the metallurgical group. These aspects are broadly categorized by the geometallurgy theme and set the stage for the future success of the work.

Once a deposit has been drilled and a variety of test samples are available a metallurgical test program can be initiated. The metallurgical test program must be carefully planned and be well structured in nature. In broad terms the test program will cover:

- Samples selected and lithology aspects (including variability testing)
- Mineralogy
- Comminution Circuit Design including HPGR testing
- Flotation Circuit Design
- Solid Liquid Separation steps including thickening of concentrates and tailings, together with concentrates filtration
- Tailings deposition aspects
- Environmental aspects such as dust generation, effect on water quality of recycle and final discharge
- Concentrate sample analysis for marketing and downstream process considerations.

With the continued pressures on project development costs, adequate test work is even more imperative nowadays as new mined ore bodies have more complex mineralogy, and have larger ore variation across the deposit. Test work programs are not only essential to the effective process design and accurate equipment sizing but also contribute to timely start-ups for greenfield projects. Further, these changing ore bodies do not always fit within the framework of currently available test work databases and installations.

The effects of inadequate sample selection and test work are evident in some of the SAG mill sizing errors made in recent years; many non-optimum flowsheet designs as noted in start-up analysis by T. McNulty and others. Underperforming plants can often be traced back to the sample selection and quality of test work planning at the beginning of project.

TYPES OF FLOWSHEET

The process design basis must allow for a flexible circuit design and at the same time take into account the key findings of the metallurgical test work. Flowsheet simplification and flexibility requires careful planning as well as close referencing to what has been done in the past, what has worked well and what lessons are learnt. Engagement of the appropriate skill sets and mix of design, operation and maintenance teams are all part of the important blend to a successful flowsheet.

The choice of flowsheet is based on a variety of factors which will be derived from the test work results, energy efficiency considerations as well as various economic considerations, coupled together with project site location and skill sets etc. Benchmarking and adaption of proven technology are of paramount importance in the process development phase.

As shown above the typical format of a copper concentrator flow diagram is reflected in Figure 1. In some of the recent projects a number of variations of this have been built. These can be summarized as:

Concentrator Comminution Circuit

- Three stage crushing and ball milling (traditional circuits of 1940's to 1970's) Morenci, Bougainville Copper, Cananea etc. This still has its merits in some parts of the world.
- Stage Crushing and HPGR (Cerro Verde shown in Figure 2) for improved energy circuit usage.
- Precrushing ahead of the SAG mill to reduce the feed size to the SAG mill and to accommodate harder difficult to SAG mill ores (e.g. Copper Mountain).
- Advancing the crushed pebbles directly to the ball mills thereby taking the load off the SAG mill and allow the ball mills to effectively reduce the pebble size (Centinela and Los Bronces).

Concentrator Downstream Circuit

- Standardization of rougher and cleaner/cleaner scavenger flotation cell sizes. Porphyry copper concentrators float various sulphide minerals using xanthates or specialty collectors at an alkaline pH range of 8 to 12.
- Inclusion of separate roughing and scavenging regrind circuits using IsaMill™
- Jameson cells directly after the regrind circuit with the Jameson cell concentrate going directly to final concentrate.
- Elimination of tailings thickeners in some cases.

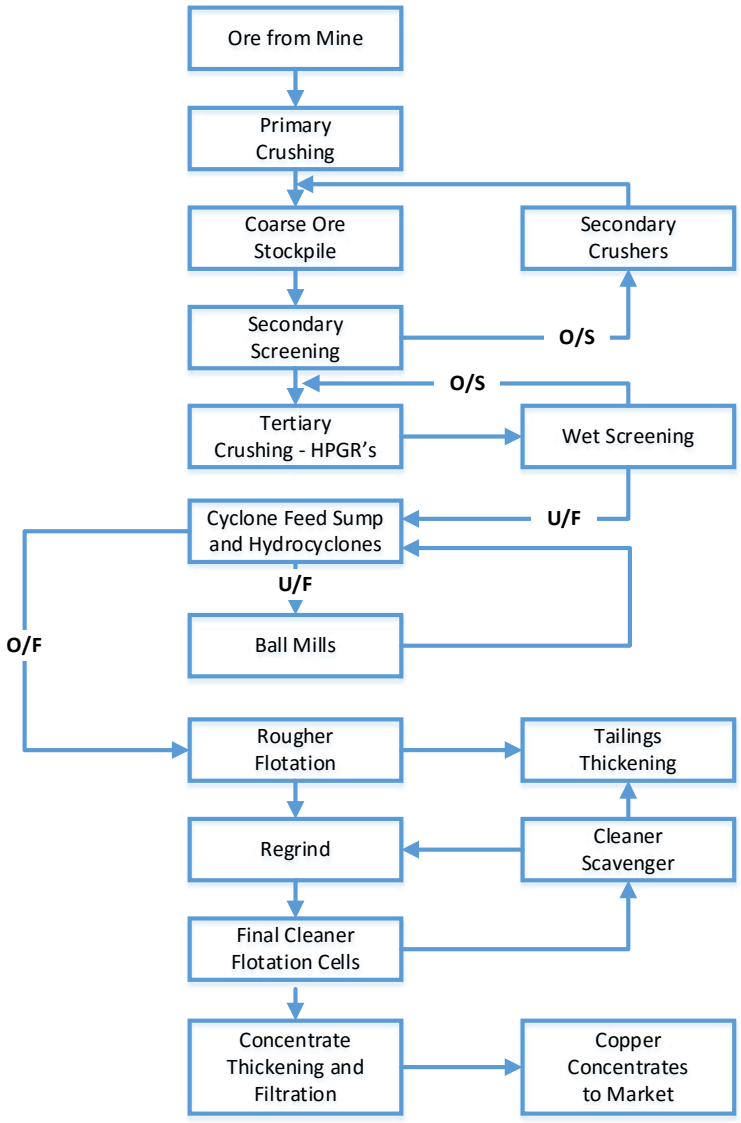

Figure 2 - Concentrator Block Flow Diagram with HPGR comminution circuit

PROCESS AND PLANT DESIGN

The integral parts of the concentrator design are key to the plant being able to process its nameplate capacity and achieved the desired metal recovery, combined with the lowest lifecycle cost. There are a variety of key aspects that influence the plant design and layout. House F.F article on 'An engineer's guide to process-plant layout 'comments that 'it is reasonable to state that the siting and development of the plant is of an art rather than an exact science'. This statement still holds true and a significant contribution for this comes from the plant layout specialist and team of designers.

Nowadays new mineral deposits are often discovered in extremely remote locations and in the case of the Andes in Latin America often at very high altitudes and extremely rugged terrain. To the maximum extent possible ways to take advantage of the terrain should be a key focus (for example use of gravity flow). This can allow a more functional design and also result in energy savings due to less pumping requirements etc. Emphasis should also be placed on the relative distances between the areas being set out. This focus allows the overall plant footprint to be compressed so as to minimize earthwork

requirements and take advantage of certain topographical features. This must consider the functionality of each of the process areas as well as maintenance and access considerations – such as drive through areas.

Other features such as support wall construction should also be taken into consideration. In the past five or so years there has been a growing trend of more open air plant concepts with as a minimum the complete flotation plant open and only (if any partial) lighter designed structures and covering around the grinding area. This has proven to be very successful in many of the recent Bechtel projects such as Las Bambas and OGP1 flotation and downstream area. Other key recent design aspects have included the use of tower cranes in the downstream flotation area. Also travelling gantry type cranes have been more noticeable designs. Some other areas of interest have included minimum standby pumping systems and minimum grinding area laydown areas. Figure 3 is a typical 3D rendition of a large open air concentrator.

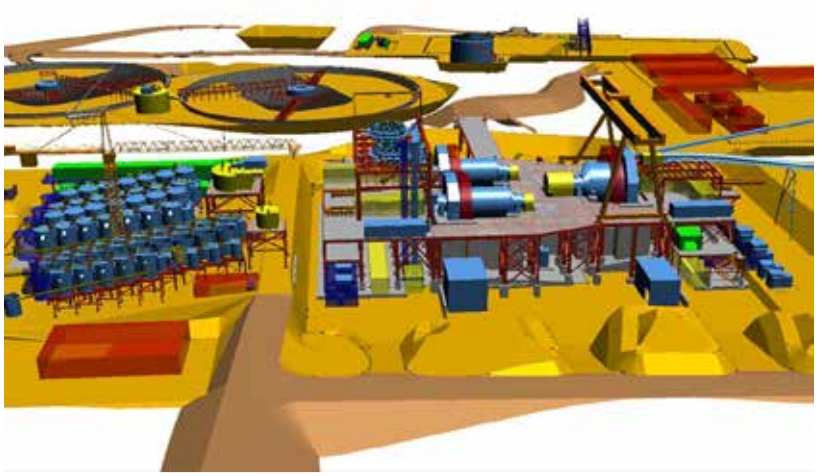

Figure 3 – Overall Concentrator Layout

EQUIPMENT SELECTION AND TRENDS

The following is a summary by areas of some of the recent industry trends and developments in the equipment selection for copper concentrators by unit process:

Primary Crushing

For the larger capacity concentrators, the primary crusher is still dominated with the gyratory crushers that process over 9,000 tph of ore. The Gyratory Crushers are now up to a size of 60 by 110E with up to 1,200 kW installed on the Superior crushers and 160 by 3000 Fuller units. The most noticeable design developments include the FLSmidth top service model and the Metso new arched spider design. These have allowed safer, improved maintenance with reduced downtime.

Precrush/Stage Crushing

The inclusion of a pre-crushing step ahead of the SAG mill has been more noticeable on a series of projects treating very hard competent ores. Two of the most recent installations in North America have included Raptor XL2500 cone crushers. These include Copper Mountain's copper concentrator and Osisko gold project in Canada. Also recently First Quantum's Sentinel Project in Zambia installed two MP2500 cone crusher by Metso as part of its pre-crush circuit ahead of the SAG mills. For stage crushing plants the noticeable advancement has been in the use of larger cone crushers such as the MP1250 crusher by Metso and the Raptor XL1100 unit by FLSmidth.

SAG-Ball Milling

With the exception of Cerro Verde, the SAG-Ball mill grinding circuits have dominated all the large concentrator designs in the past two decades. Progressive increases in sizes of both the SAG and Ball mill have allowed the overall grinding circuit to be simplified and the footprint to be reduced. SAG mills of 12.2 metre in diameter and drive ratings of 28 MW are very common with over fifteen worldwide installations. Ball mill sizes have also increased to 8.5 metre diameter with 22 MW gearless drive motors. Bechtel's introduction of a trommel screen/vibrating screen combination have permitted high throughput single line plants such as Escondida Phase IV, OGP1 etc.

High Pressure Grinding Rolls (HPGR)

Cerro Verde set the stage in the copper industry with the development of its first (Cerro Verde I) concentrator featuring HPGR's. With a processing rate of 108,000 tpd this concentrator included four 2.4/1.7 Krupp Polysius units each equipped with 5 MW motors in its tertiary crushing stage. After the plant ramped up to capacity and with improved development of the HPGR roll surface the roll life of 6,000 hours has been greatly exceeded with current achievements over 8,000 hours. More recently Metso developed its first large scale HPGR machine with its 3 metre diameter HRC3000 unit (see Figure 4). The single unit is installed at Freeport's Metcalf Concentrator in the USA and processes over 6,000 tph including recycle. Roll life hours are predicted to be over 10,000 hours. Also the reduced edge recycle rate has been recognized.

Figure 4 - HRC3000 at Metcalf Concentrator

Flotation

Flotation cells have continued to increase in size with the demands to process higher throughput rates. In the past three years the most noticeable cell installations have been the e500 m3 Outotec Flotation cell at Kevista in Finland. The cell is installed at the head of the rougher flotation circuit and has operated extremely well with good metallurgical performance and low power requirements. More recently FLSmidth completed its 600 m3 flotation cell installation at Robinson Mine in Nevada, USA. This installation is at the end of the rougher scavenger row. The testing is still ongoing including evaluating different rotors such as the next STEPTM which combines its best modeling and expertise in rotor design.

Another very interesting development has been the introduction of the Woodgrove Technologies Inc. Staged Flotation Reactor (SFR) units (see Figure 5). Woodgrove Technologies Inc. has continued to develop the machines and now a number of rougher applications are in progress. The SFR offers huge potential to reduce flotation area footprint and also significantly decrease operating costs through reduced

energy usage and air usage. Jameson cells have appeared in one or two flowsheets but more in specialized applications and few in number.

Figure 5 – Staged Flotation Reactors

Regrind

Due to the more complex mineralogy focus on regrind and regrind size has increased. Metso's VTM Vertimills more or less became the newer workhorse machine for regrinding circuits. More recently a number of projects required finer regrind sizes and IsaMill™ M3000 units (1500 kW) were introduced into the regrind circuit to offer lower energy input for a given liberation size. Last years introduction of the Outotec's HIG Mill has gained a lot of attention and a number of successful installations including Kevista HIG have enabled this to be a feasible option in emerging projects.

Concentrate Thickening and Filtration

Concentrate thickener sizes have increased marginally over time. Due to its modest diameter the majority of concentrate thickeners are elevated steel designs. Outotec's Larox Pressure filters are no doubt the industry benchmark for copper concentrate filtration. The PF144 m2 units (with 6m2 plates) have been used in several installations for copper concentrates such as Escondida's Laguna Seca and Antamina. Also of note is Centinela's 166m2 unit that has been installed including a chloride wash step. These filters produce a low moisture content product within the transportable moisture limits. FLSmidth's APF and Metso's horizontal presses provide good alternatives with the larger units processing concentrate rates of over 100 tph per filter.

Tailings thickening and Filtration

Tailings thickener size has now increased to the largest units in operation in copper processing being 125 metre diameter and other 135 metres in ground thickeners units being up in other process industries. Associated torque ratings have been increased for the high rate units. There has been a greater emphasis placed on attainment of higher thickener underflow densities and hence there has been a progression from conventional shallow sloped units to steeper slope high density units to some applications with paste technology such as those in service at Centinela in Chile and one of the most noticeable being the NICICO's Sarcheshmec Copper Mine in Iran.

In a number of recent large concentrator studies in Chile options towards filtered tailings have been evaluated using pressure filtration methodologies. Since the horizontal press sizes have now increased to 4 m by 2 m units, the processing capability of such units is over 15,000 tpd per unit. So realistically for a

100,000 tpd concentrator six to eight units may be capable of processing the entire tailings and then the material can be dry stacked into a more compressed tailings dam footprint.

Water Recovery

In copper concentrators the fresh water consumption rate is in the vicinity of 0.35m3/t to 0.50m3/t. As the concentrator sizes have grown so have the process water requirements and in certain areas of the world such as Chile available water resources are of concern. Most of the focus has been on tailings thickening and achievement of maximum underflow densities as well as tailings filtration considerations. Some operations such as Sierra Gorda and Centinela use sea water as the medium.

INDUSTRY PROJECTS – RECENT DEVELOPMENTS

As described above plant throughput sizes have continued to grow over time. Table 2 provides a snapshot to some of the large new concentrators that have just come on line in the last five years. As would be expected a significant portion of these plants are in Peru and Chile and the other projects in emerging copper producing countries such as Mongolia and Kazakhstan. Escondida and Cerro Verde are amongst the top three largest copper mining operations in the world.

Table 2 – Summary of New Large Copper Concentrators and Highlights

Concentrator	Plant Capacity tpd	Year into Operation	Comments
Centinela	95,000	2012	First large concentrator with sea water medium. Use of 300m3 rougher flotation cells
Antapaccay	70,000	2012	First standardized concentrator design approach – Xstrata
Oyu Tolgoi	100,000	2011	Recent major copper concentrator project in Mongolia
Toromocho	115,000	2014	Largest 12.2 m (40ft) SAG and 8.53 m (28 ft) Ball mills in world at time
OGP1 (Escondida)	152,000	2015	Largest copper mine – combined with Laguna Seca/Los Colorados. Largest rougher circuit flotation volume at 14,700 m^3
Las Bambas	140,000	2015	Large logistically challenged site at 4200 masl. Expandable to 200,000 tpd
Bozshakol	80,000	2016	Largest ever copper project in CIS region
Cerro Verde II	240,000	2015	Largest HPGR circuit in copper processing

CONCLUSION

With the declining ore grades seen within the copper industry concentrator throughput rates have continued to grow and some of the recent projects have demonstrated that the new range of concentrators could be in the 240,000 tpd to 300,000 tpd range. With these higher throughputs the unit process equipment has continued to be pushed and multiple line comminution circuits are inevitable at these rates particularly related to HPGR type circuits.

There should be a continued attempt to explore larger equipment sizes but importantly investigation into innovative ways to process copper ores and achieve a higher energy efficient means of comminution.

With the larger throughput concentrators water usage and recycle must also have a greater level of attention since the water requirements are huge at these processing rates and certain parts of the world have a scarcity of water sources available.

ACKNOWLEDGEMENTS

The author would like to thank a number of individuals in Bechtel Mining & Metals including Paige Wilson and Bill Imrie, together with the valuable contributions from Ken Winship from the Copper Centre of Excellence Plant Design Group.

REFERENCES

Blois, M.D.S & Talocchino L. (1993, November) 'Plant siting and layout – A metallurgist perspective' SA Institute of Mining and Metallurgy, School of Metallurgical Process Design in the 90's

Chapman, T.G. (n.d) 'Concentration of copper in North America' United States Department of the Interior Bureau of Mines, Bulletin 392.

House, F.F. (1969, July 28) 'An engineer's guide to process-plant layout' Chemical Engineering 120

Malghan, S.G. (1986) 'Typical flotation circuit configurations' Chapter 4 concentration and dewatering section

Malhotra, D., Taylor, R.T., Spiller, E. and LeVier, M. (2009) Recent advances in mineral processing plant design' Society for Mining, Metallurgy and Exploration, USA

Schodde, R (2010, March) 'The key drivers behind resource growth: An analysis of the copper industry over the last 100 years' MinEx Consulting, Phoenix, Arizona, USA

Vanderbeek, J.L., Linde, T.B., Brack, W.S. & Marsden, J.O. (2006) 'HPGR implementation at Cerro Verde'. Proc. International Autogenous and Semi-Autogenous Grinding Technology. Vol IV.

Malhotra, D., Taylor, R.T., Spiller, E. and LeVier, M. Recent advances in mineral processing plant design' Society for Mining, Metallurgy and Exploration, USA. 2009

ANALYSIS OF BENEFICIATION OF VARIOUS COAL TYPES DEPENDABLY ON ANALYTIC MOISTURE OF RESEARCHED MATERIAL

*T. Niedoba[1], A. Surowiak[1] and P. Pięta[1]

[1]AGH University of Science and Technology,
Faculty of Mining and Geoengineering,
Department of Environmental Engineering and Mineral Processing,
al. Mickiewicza 30, 30-059 Kraków, Poland,
(Corresponding author: tniedoba@agh.edu.pl)*

24th World Mining Congress
MINING IN A WORLD OF INNOVATION
October 18-21, 2016 • Rio de Janeiro /RJ • Brazil

ANALYSIS OF BENEFICIATION OF VARIOUS COAL TYPES DEPENDABLY ON ANALYTIC MOISTURE OF RESEARCHED MATERIAL

ABSTRACT

On the basis of the previously published investigations with application of observational tunnels method to multidimensional analysis of various coal types it was stated that the features which are sufficient to properly recognize type of coal were analytic moisture, sulfur contents and volatile parts contents. Furthermore, it was also stated that analytic moisture is a crucial parameter to proper identification of coal type. This is the reason that the coal beneficiation analysis will be presented in this paper with particular consideration of analytic moisture as the main feature. The analysis was done for three types of coal: 31, 34.2 and 35. For each of these coals the separation for particle size fractions was performed. Then, for each fraction values of five various coal features were determined. Additionally, the material was also divided into particle density fractions and analyzes were performed for each such fraction. The authors performed statistical analysis of data, including step regression analysis to determine which coal features influence significantly on the values of analytic moisture which is treated as the main feature allowing the recognition of coal type. Then, for each type of coal the distribution function describing this feature of coal was found by means of least squared method. Finally, the similarities between mean values of analytic moisture for all analyzed types of coal were verified by performing statistical Cochran-Cox test. The results were statistically analyzed and conclusions were made.

KEYWORDS

Hard coal, statistical analysis, multidimensional analysis, approximation, type of coal, statistical test

INTRODUCTION

The basic starting point of this paper is acceptance of the assumption that the grained material is being characterized by multidimensional random variable $W=(w_1, w_2, \ldots, w_n)$ where $w_i=(i=1, \ldots, n)$ are the properties of the researched material [Tumidajski, 1997]. In works [Jamróz and Niedoba, 2014; 2015; Niedoba, 2013, 2015; Niedoba et al., 2015] the identification of the coal type was conducted by means of observational tunnels method. On the basis of the obtained results it was stated that three coal properties, including analytic moisture, sulfur contents and volatile parts contents are sufficient to identify correctly a coal type. The crucial feature to that purpose is analytic moisture. In this work, the analysis of random variable representing analytic moisture for various coal types will be conducted on the basis of statistical methods (variance analysis, regression analysis, determination of random variable's distribution function). To this purpose, the grained material was divided into particle fractions because of its size and density. It was assumed that for each type coal, material representing the same fraction (the same size d and density ρ) creates one measured object for which ash contents, sulfur contents, volatile parts contents as well values of analytic moisture and combustion heat were determined. In this way the mapping $(d, \rho) \rightarrow (w_1, w_2, w_3, w_4, w_5)$ was done, where w_1 is ash contents, w_2 – sulfur contents, w_3 – volatile parts contents, w_4 – analytic moisture, w_5 – combustion heat. The results of measurements for the individual types of coal were presented with details in [Niedoba, 2013].

METHODOLOGY AND RESULTS

Three types of coal, types 31 (energetic coal), 34.2 (semi-coking coal) and 35 (coking coal) in the Polish classification were used in the investigation. They originated from three various Polish coal mines and all of them were initially screened on a set of sieves of the following sizes: -1.00, -3.15, -6.30, -8.00, -10.00, -12,50, -14.00, -16.00 and -20.00 mm. Then, the size fractions were additionally separated into density fractions by separation in dense media using zinc chloride aqueous solution of

various densities (1.3, 1.4, 1.5, 1.6, 1.7, 1.8 and 1.9 g/cm^3). The fractions were used as a basis for further consideration and additional coal features were determined by means of chemical analysis. For each density-size fraction such parameters as combustion heat, ash contents, sulfur contents, volatile parts contents and analytical moisture were determined, making up, together with the mass of these fractions, seven various features for each coal.

Regression analysis

First, the material was divided into fractions because of particle size and it was determined by means of classical regression and step regression which factors influence significantly on analytic moisture value for coals of type 35 and 31. It was decided not to do this part for coal, type 34.2 because of the lack of some data. The obtained results were presented in Table 1.

Table 1 - Regressive functions for analytic moisture, coals of types 31 and 35.

Particle size d [mm]	Function for coal type 35	R	Function for coal type 31	R
0.50-1.00	w_4=0.318w_2+0.894	0.789	w_4=-2.076w_2+6.077	0.893
1.00-3.15	w_4=0.102w_3-0.681w_2+1.116	0.946	w_4=-0.025w_1-1.481w_2+0.096w_3-0.531	0.959
3.15-6.30	w_4=-0.070w_1-0.898w_2-0.018w_3-1.272ρ+8.928	0.993	w_4=0.165w_3-2.100ρ-4.987	0.900
6.30-8.00	w_4=-0.097w_1-0.506w_3+19.490	0.922	w_4=-1.156w_2+0.192w_3+2.163ρ-5.057	0.872
8.00-10.00	w_4= -2.920ρ+7.596	0.893	w_4=-0.079w_3+2.797	0.800
10.00-12.50	w_4=0.107w_3+0.114	0.989	w_4=0.067w_1+1.191	0.843
12.50-14.00	w_4=-0.060w_1-0.111w_3+7.800	0.860	w_4= 0.041w_3+0.548ρ-0.242	0.720
14.00-16.00	w_4=-0.002w_1+3.606	0.876	w_4=0.060w_1-0.050w_2-4.310ρ+6.887	0.939
16.00-20.00	w_4=-0.047w_3+2.275	0.801	w_4=0.646w_2-0.089w_3-0.089ρ+7.233	0.987

The juxtaposition of the factors having significant influence on analytic moisture in individual fractions is presented in Table 2.

Table 2 - Factors having significant influence on analytic moisture

Size d [mm]	Coal type 35	Coal type 31
0.50-1.00	w_2	w_2
1.00-3.15	w_2, w_3	w_1, w_2, w_3
3.15-6.30	w_1, w_2, w_3, ρ	w_3, ρ
6.30-8.00	w_1, w_3	w_2, w_3, ρ
8.00-10.00	ρ	w_3
10.00-12.50	w_3	w_1
12.50-14.00	w_1, w_3	w_3, ρ
14.00-16.00	w_1	w_1, w_2, ρ
16.00-20.00	w_3	w_2, w_3, ρ

By analyzing Table 2 it can be stated that for fractions of lower size ([0.50, 1.00], [1.00, 3.15]) the biggest influence on the value of analytic moisture is generated by the feature w_2 which is sulfur contents. For medium fractions ([3.15], [6.30, 8.00], [8.00, 10.00]) the biggest influence is generated by the feature w_3 which is volatile parts contents. And for the coarse fractions ([10.00, 12.50], [12.50, 14.00], [14.00, 16.00], [16.00, 20.00]) the biggest influence is generated by the feature w_1, which is ash contents.

Distribution function for analytic moisture

The significant part of comparing random variables determined in various populations is investigation of their distribution functions. Let's do the research of random variable referring to analytic moisture of investigated particle. The fitting of probability distribution function was done for three types of coal. After some experiments, it was stated that the most fitted distribution function for coals, types 31 and 34.2 was Weibull distribution function (called also as RRB), while for coal, type 35 the best was logistic distribution function [Dobosz, 2001; Tumidajski, 1997]. These distribution functions are given by the following functions:

- For coal, type 35

$$F(w) = \frac{1}{1+335541exp(-11.38w)} \quad (1)$$

- For coal, type 34.2

$$F(w) = 1 - exp\left(-\frac{w^{4.20}}{0.91}\right) \quad (2)$$

- For coal, type 31

$$F(w) = 1 - exp\left(-\frac{w^{6.74}}{716.03}\right) \quad (3)$$

where w is analytic moisture and $F(w)$ - a distribution function of it.

The obtained results are presented in Tables 3-5, as well on Figs 1-3.

Table 3 - Distribution function for analytic moisture, coal type 35

Analytic moisture w [%]	Yield [%]	Empirical distribution function $F_0(w)$	Theoretical distribution function $F(w)$
0.80-1.00	6.87	6.87	7.70
1.00-1.10	41.14	48.01	44.82
1.10-1.20	10.54	58.55	58.93
1.20-1.30	19.44	77.99	81.74
1.30-1.40	12.05	90.04	93.32
1.40-1.50	7.20	97.24	97.76
1.50-1.60	1.52	98.76	99.26
1.60-1.70	1.24	100.00	99.76

Table 4 - Distribution function for analytic moisture, coal type 31

Analytic moisture w [%]	Yield [%]	Empirical distribution function $F_0(w)$	Theoretical distribution function $F(w)$
1.00-2.00	0.33	0.33	0.23
2.00-2.50	2.66	2.99	3.45
2.50-3.00	5.07	8.06	12.73
3.00-3.50	27.95	36.01	34.28
3.50-4.00	28.73	64.74	66.75
4.00-4.50	29.82	94.56	92.27
4.50-5.50	5.41	99.97	99.56

Table 5 - Distribution function for analytic moisture, coal type 34.2

Analytic moisture w [%]	Yield [%]	Empirical distribution function $F_0(w)$	Theoretical distribution function $F(w)$
0.50-0.70	11.21	11.21	12.02
0.70-0.90	26.47	37.68	34.86
0.90-1.10	24.41	62.09	66.52
1.10-1.30	29.97	92.06	90.49
1.30-1.50	7.38	99.44	98.88
1.50-1.70	0.56	100.00	99.96

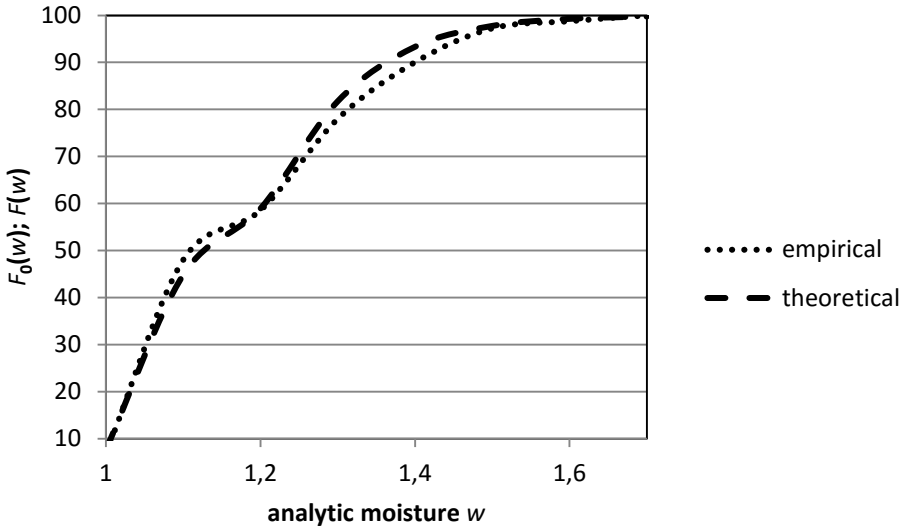

Figure 1 - Distribution functions of analytic moisture, coal type 35

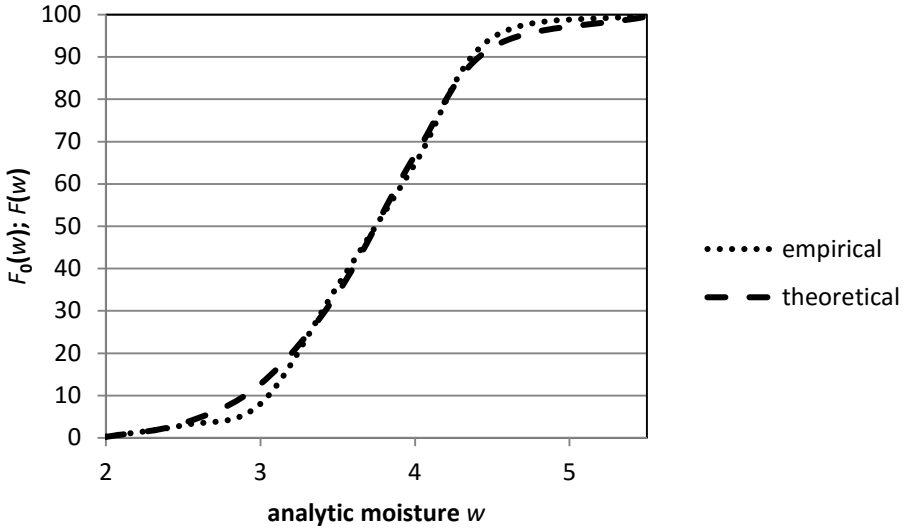

Figure 2 - Distribution functions of analytic moisture, coal type 31

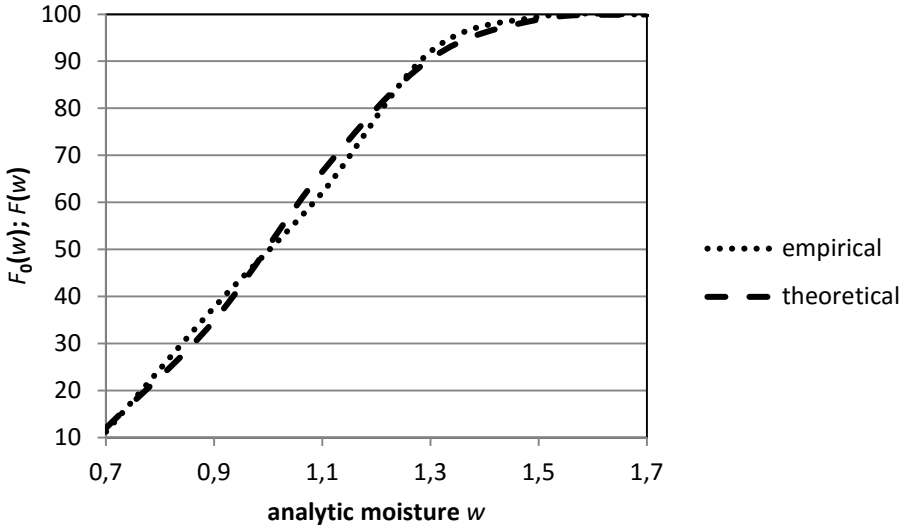

Figure 3 - Distribution functions of analytic moisture, coal type 34.2

As the measure of the fitting of the curves the value of mean standard error was accepted (MSE), given by the equation

$$MSE = \sqrt{\frac{\sum_{i=1}^{n}\left(F(w)-F_0(w)\right)^2}{n-2}} \quad (4)$$

where n is number of fractions

The results of calculated mean standard errors were presented in Table 6.

Table 6 - Values of mean standard errors for approximated functions

	Coal, type 35	Coal, type 31	Coal, type 34.2
MSE	3.11	2.62	2.78

Analyzing the obtained results is visible that for coals, types 31 and 34.2 the values of mean standard errors are very similar and for both types of coals, the best fitted distribution function is Weibull distribution function. For coal, type 35, the best fitted distribution function is logistic distribution function. If it is accepted that for this coal the approximation supposes to be done also by means of Weibull distribution functions then its form is

$$F(w) = 1 - exp\left(-\frac{w^{6.84}}{3.66}\right) \quad (5)$$

However, the value of the MSE is then much higher and is equal to 4.35.

Verification of statistical test

Because the distribution functions for analytic moisture for coals, types 31 and 34.2 are from the same family of distribution functions (Weibull) and for coal, type 35 this kind of approximation is also acceptable it was decided to check whether analytic moisture is crucial to identify the type of coal by means of verification of hypothesis about equality of mean values. Because the condition of equality between variances is not fulfilled (such tests as Bartlett's, Cochran's and Hartley's showed that the hypothesis of equality between variances must be rejected) [Krysicki et al., 2012; Pięta, 2015] the hypothesis about equality of mean values was verified for coal types in pairs. Let's mark mean value of analytic moisture as m_1 for coal, type 35, m_2 for coal, type 31 and m_3 for coal, type 34.2. The results of measurements of analytic moisture for individual size fractions were presented in Table 7.

Table 7 - Values of analytic moisture according to particle size fraction and coal type.

Particle size d [mm]	Analytic moisture, coal type 31 [%]	Analytic moisture, coal type 35 [%]	Analytic moisture, coal type 34.2 [%]
0.50-1.00	2.44	1.02	0.68

1.00-3.15	2.92	1.08	0.68
3.15-6.30	2.95	1.22	0.90
6.30-8.00	3.00	1.34	0.99
8.00-10.00	3.00	1.36	1.07
10.00-12.50	3.02	1.36	1.09
12.50-14.00	3.04	1.38	1.10
14.00-16.00	3.30	1.38	1.19
16.00-20.00	3.63	1.41	1.20

In purpose of verifying hypotheses about equality of mean values the Cochran-Cox test was used [Krysicki et al., 2012] determined by the formula

$$C = \frac{m_i - m_k}{\sqrt{\frac{{s_i}^2}{n_i - 1} + \frac{{s_k}^2}{n_k - 1}}} \quad (6)$$

where ${s_i}^2$ (${s_k}^2$) is value of variance for i^{th} (k^{th}) coal type; n_i (n_k) – quantity of sample for i^{th} (k^{th}) coal type.

The critical value on the significance level α is given by the equation

$$c(1-\alpha, n_i, n_k) = \frac{\left(\frac{{s_i}^2}{n_i - 1} t_\alpha (n_i - 1) + \frac{{s_k}^2}{n_k - 1} t_\alpha (n_k - 1)\right)}{\frac{{s_i}^2}{n_i - 1} + \frac{{s_k}^2}{n_k - 1}} \quad (7)$$

where t_α is quintile of t-Student distribution function for n_i-1 (n_k-1) levels of freedom.

The values of Cochran-Cox test were presented in Table 8.

Table 8 - Values of Cochran-Cox test - particle size fractions taken into consideration

Hypothesis H_0	Value of the test C	Critical value c (0.975; 8; 8)
H_0: m_1=m_2	14.23	
H_0: m_1=m_3	22.53	2.31
H_0: m_2=m_3	4.09	

Because the critical area for alternative hypothesis H_1: $m_i \neq m_k$ is in form $(-\infty, C) \vee (C, +\infty)$, so for all three hypotheses the value of the test is within critical area. That means that on significance level α=0.05 the hypotheses about equality of mean values of analytic moisture should be rejected. Furthermore, it is worthy to underline that for some particle size fractions analytic moisture depends significantly on particle density. That is why the similar analysis was conducted also for material divided into density fractions. The results of measured analytic moisture dependably on density were presented for each type of coal in Tables 9-11. The unequal amount of results in individual particle density fractions is the effect of lack of some measurements results.

Table 9 - Results of analytic moisture dependably on particle density for coal, type 35

Density ρ [g/cm^3]	Analytic moisture w [%]
<1.30	1.43 1.34 1.45 1.30 1.36 1.32 1.30 1.07 1.02
1.30-1.40	1.15 1.20 1.21 1.21 1.11 1.10 1.19 1.09
1.40-1.50	1.25 1.26 1.28 1.32 1.20 1.10 1.14 0.97 1.03
1.50-1.60	1.44 1.25 1.32 1.39 1.38 1.14 1.29 0.93 1.04
1.60-1.70	1.43 1.39 1.47 1.31 1.40 1.09 1.50 1.05 1.10
1.70-1.80	1.54 1.42 1.61 1.47 1.51 1.32 1.46 1.08 1.18
1.80-1.90	1.65 1.53 1.51 1.64 1.57 1.65 1.16 1.47 1.13

Table 10 - Results of analytic moisture dependably on particle density for coal, type 31

Density ρ [g/cm^3]	Analytic moisture *w* [%]
<1.30	4.03 3.59 3.23 4.06 3.75 3.27 3.18 4.15 4.39
1.30-1.40	3.74 2.94 3.36 2.68 3.62 3.64 3.94 2.55 5.41
1.40-1.50	3.36 3.23 3.87 2.68 3.24 3.64 3.60 2.55 3.54
1.50-1.60	4.20 3.30 3.40 2.31 2.95 2.96 3.21 2.80 3.20
1.60-1.70	3.32 2.89 2.40 1.95 2.65 2.76 2.55 2.65 3.45
1.70-1.80	2.45 2.65 2.19 1.41 1.71 2.80 2.31 2.35 2.89
1.80-1.90	2.01 2.66 2.23 1.32 2.49 2.11 2.19 2.29 2.51

Table 11 - Results of analytic moisture dependably on particle density for coal, type 34.2

Density ρ [g/cm^3]	Analytic moisture *w* [%]
<1.30	1.20 1.23 1.04 1.02 1.48 1.15 1.11 0.85 0.64
1.30-1.40	1.35 0.73 1.87 0.93 1.18 1.10 0.93 0.88 0.64
1.40-1.50	1.11 1.02 1.34 1.11 1.30 1.09 0.83 0.64 0.82
1.50-1.60	1.24 0.95 1.11 1.22 1.10 0.92 0.80 0.62
1.60-1.70	0.81 1.11 1.06 1.01 0.92 0.42 0.52
1.70-1.80	0.72 0.37 1.26 0.93 0.95 1.31 0.56 0.81
1.80-1.90	1.06 1.01 0.92 0.63

On the basis of presented results the verification of hypothesis about equality of mean values of analytic moisture was conducted for various coal types in individual particle density fractions. Again, Cochran-Cox test was used to this purpose. The results were presented in Table 12.

Table 12 - Values of Cochran-Cox test - particle density fractions taken into consideration

Density [g/cm^3]			<1.30		1.30-1.40		1.40-1.50		1.50-1.60		1.60-1.70		1.70-1.80		1.80-1.90	
H_0	Test value C	Critical value *c*	*C*	*c*	*C*	*c*	*C*	*c*	*C*	*c*	*C*	*c*	*C*	*c*	*C*	*c*
$m_1=m_2$	9.23	2.31	7.94	2.31	13.56	2.31	10.78	2.31	9.13	2.31	5.49	2.31	4.90	2.31		
$m_1=m_3$	2.34	2.31	0.23	2.31	1.58	2.31	2.48	2.34	3.87	2.40	4.16	2.35	4.99	2.91		
$m_2=m_3$	16.07	2.31	7.90	2.31	13.56	2.31	1.18	2.32	11.13	2.35	7.45	2.33	7.92	2.61		

Analyzing the obtained results it is worthy to notice that almost in every fraction the hypothesis about equality of mean values of analytic moisture should be rejected. Only in particle density fractions (1.30-1.40) and (1.40-1.50) this hypothesis can be accepted for coals, types 35 and 34.2. And for pairs of coal types 35 and 31, as well as 34.2 and 31 all hypotheses for all particle density fractions are supposed to be rejected.

CONCLUSIONS

The conducted statistical analysis showed that analytic moisture is the obligatory feature to identify type of coal and its ability to beneficiation. However, because of the fact that comparing the coals, types 35 and 34.2 the hypothesis H_0 about equality of mean values of analytic moisture should not be rejected in two cases and in other cases the value of Cochran-Cox test *C* was only slightly higher than the critical value *c* it seems to be necessary to use also other coal features to recognize and identify properly the type of coal. These features can be volatile parts contents or sulfur contents. The obtained results are in complete accordance with the results presented in works [Jamróz and Niedoba, 2014; 2015; Niedoba, 2013; Niedoba et al., 2015].

ACKNOWLEDGEMENT

The paper is an effect of statutory work no. 11.11.100.276.

REFERENCES

Dobosz M. (2001). *Statistical analysis of research*. Akademicka Oficyna Wydawnicza, Warszawa. [in Polish]

Jamróz D., Niedoba T. (2014). *Application of Observational Tunnels Method to select Set of Features Sufficient to Identify a Type of Coal*. Physicochemical Problems of Mineral Processing vol. 50(1), pp. 185-202.

Jamróz D., Niedoba T. (2015). *Comparison of Selected Methods of Multi-parameter Data Visualization Used for Classification of Coals*. Physicochemical Problems of Mineral Processing, vol. 51(2), pp. 769-784.

Krysicki J., Bartos D., Dyczka W., Królikowska K., Wasilewski M. (2012). *Probability and mathematical statistics, part II*. PWN, Warszawa. [in Polish]

Niedoba T. (2013). *Multidimensional characteristics of random variables in description of grained materials and their separation processes*. Wydawnictwo IGSMiE PAN, Series: Studia, Rozprawy, Monografie, vol. 192, Krakow. [in Polish]

Niedoba T. (2015). *Application of Relevance Maps in Multidimensional Classification of Coals Types*. Archives of Mining Sciences, vol. 60(1), pp. 93-106.

Niedoba T., Surowiak A., Jamróz D. (2015). *Methods of determining crucial properties to identify the type of coal*. Proceedings of XVI Balkan Mineral Processing Congress, ed. Ćalić N. et al., Belgrade, vol. 1, pp. 69-74.

Pięta P. (2015). *One-dimensional and two-dimensional analyses of hard coal separation in a jig*. Journal of Polish Mineral Engineering Society, vol. 1(35), pp. 133-135.

Tumidajski T. (1997). *Stochastic analysis of grained materials features and their separation processes*. Wydawnictwo AGH, Kraków. [in Polish]

TABLE OF CONTENTS

ANALYSIS OF THE MILLING CIRCUIT PERFORMANCE OF VALE FERTILIZANTES FROM ARAXÁ, MG, BRAZIL

*ROCHA, B.G.[1] and JUNIOR, H.D.[2]

Universidade Federal dos Vales do Jequitinhonha and Mucuri. Campus Janaúba – MG – Brazil.

Department of Mining and Petroleum Engineering. Universidade de São Paulo. São Paulo – SP – Brazil.
*(*Corresponding author: barbara.rocha@ufvjm.edu.br)*

24th World Mining Congress
MINING IN A WORLD OF INNOVATION
October 18-21, 2016 • Rio de Janeiro /RJ • Brazil

ANALYSIS OF THE MILLING CIRCUIT PERFORMANCE OF VALE FERTILIZANTES FROM ARAXÁ, MG, BRAZIL

ABSTRACT

Computational simulation and mathematical representation of real system operation has aided professionals in designing new installations and in optimizing the performance of industrial circuits already implemented. Mathematical modeling concepts were used in this work, with the JKSimMet® simulator, for the equipment of the industrial circuit to mill and to classify the phosphate ore from Vale Fertilizantes in Araxá, MG, Brazil. The aim was to obtain improvements in the performance rates of the milling circuit and in the production of finer concentrate, abiding by the specification of the FCA – Fine Concentrate Apatite. From the samplings conducted in the milling circuit, mass balance exercises and individual model adjustments were conducted. The adjustments were made in rod mill, ball mill and cyclone models. Later, the individual models were integrated so as to constitute robust platforms for simulating primary and secondary milling in the circuit of Vale Fertilizantes in Araxá, MG. The simulations indicated significant improvements, with capacity increments and a finer product, in addition to allowing the investigation of potential gains from the increase in classification efficiency.

KEYWORDS

Phosphate; Fertilizers; Simulation; Comminution; Grinding.

INTRODUCTION

In modern society, there is a growing demand for high quality products that meet the strict content and grain size distribution specifications. The demand for mineral goods and the exhaustion of better potential mines, lead to the exploration of mines previously considered non-economic. Hence, it is important to develop new processing routes, equipment and ways of forecasting the influence that such modifications might have on the performance of the circuit focused.

A way of assessing modifications in processes is the mathematical representation of real system operation. By using integrated simulation systems, mathematical modeling allows the efficient and fast study of alternatives for solving more complex alterations, which involve several sectors of a processing mill.

Aiming to help professionals in the mineral industry area, computational simulation has been used for adopting procedures that enhance the performance of processing circuits thus reducing the operational cost. It allows analyzing the viability of incrementing the feeding flow of a milling line without hindering there ach of the grain size distribution required, for example.

It is worth mentioning that this analysis is performed avoiding complex, expensive and usually inconclusive tests, at industrial scale (NASCHENVENG, 2003). The aim of this study was to apply mathematical modeling to the equipment and processes of the industrial circuit of phosphate ore milling and classification of Vale Fertilizantes S.A., located in Araxá, MG, Brazil, and a platform of adjusted models to provide the computational simulation of the adjusted operations.

MATERIALS AND METHODS

In order to calibrate models and form a base for simulations, a full sampling was carried out at the 311 Processing Plant of Vale Fertilizantes S.A., in Araxá, MG, Brazil. The sampled circuit is presented in Figure 1.

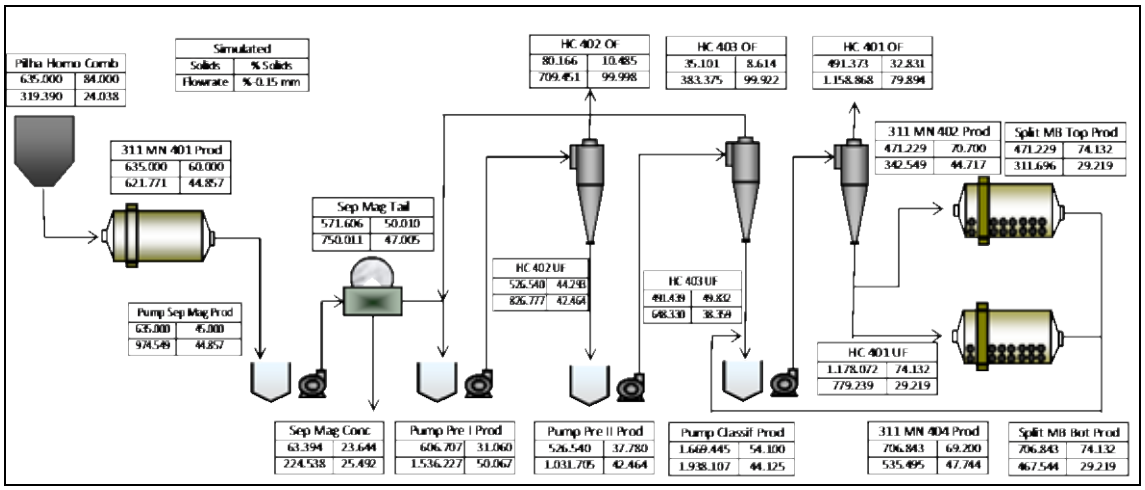

Figure 1. Process flow of the sampled circuit.

The new milling circuit feeding consists in retaking the homogenization pile, formed by crushed ore. After processed in the rod mill, the ore is submitted to magnetic separation in low-intensity barrels, to separate magnetite from the flow directed to the pre-classification stage. Two cyclone nests form the pre-classification stage, generating natural sludge and a deslimed product, the latter being directed to a milling stage in two ball mills, which operate in parallel in aclosed and directly configured circuit with a cyclone nest.

Sampling procedures

The sampling was conducted at 15-minute intervals of 1 hour and 10 minutes. Two distinct samples were collected, one for grain size analysis and the other for determining the percentage of solids at the eighteen points defined in the circuit.

The samples were collected into 20-L plastic buckets, being approximately 6 kg of pulp obtained at each sampled point. The containers were duly sealed and taken to the Sample Treatment Laboratory of the same plant, in the city of Araxá. The determination of the minimum mass of material obtained at each sampling point was based on the method proposed by Barbery (1972).

The material underwent wet mechanical sieving for 30 minutes. Along the processing, the output water was collected for determining the passing fraction at 0.038 mm. The sieving set was composed of *decks* with the following meshes: 0.600; 0.425; 0.300; 0.212; 0.150; 0.106; 0.075; 0.053 and 0.038

mm. The material retained at 0.600 mm was wet-sieved again in circular sieves with 200 mm in diameter. The samples were then oven dried, weighed in electronic scales, packed in plastic bags and sent to the Laboratory of Simulation and Ore Treatment Process Control of EPUSP, São Paulo, Brazil.

Simulations

Four simulations were conducted so as to explore (a) the possibility of increasing the feeding flow of the circuit, thus keeping the milling product specification constant and (b) the possibility of obtaing a finer secondary product. These simulations were carried out in the JKSimMet® simulator, after the model adjustment procedures of primary and secondary milling operations. The simulations were the following:

- Simulation 1: Incremental increase by10% of the circuit new feeding flow;
- Simulation 2: Dilution of the pulp at the classification stage of the milling closed circuit to 50%;
- Simulation 3: Sequential increases in the percentage of solids of the ball mills operation; dilution of the pulp at the feeding of the classification stage and increasing the diameter of the apex of the classification cyclones (from 110 mm to 127 mm).

RESULTS AND DISCUSSIONS

The results from each simulation were compared to the Base Case, the latter referring to the operation conditions of the industrial circuit along the sampling, as obtained from the calibration of the models employed.

Simulation 1

In Simulation 1, the new feeding flow of the milling circuit was increased by 10%. Table 1 presents the summary of the results as compared to the Base Case.

Table 1. Milling circuit performance – Simulation 1.

Equipment	Flow	Solid Flow (t/h)		% Solids		Pulp Flow (m^3/h)		P_{80} (mm)	
		Base Case	Simulation 1	Base Case	Simulation 1	Base Case	Simulation 1	Base Case	Simulation 1
Rod Mill	Feed	635	699	60,0	60,0	622	684	32,1	32,1
	Product	635	699	60,0	60,0	622	684	0,933	1,07
Pre-classification I	Feed	607	644	31,1	31,1	1536	1631	0,781	0,848
	Underflow	527	552	44,3	45,9	827	823	0,896	0,980
	Overflow	80	92	10,5	10,5	710	808	0	0
Pre-classification II	Feed	527	552	37,8	37,8	1032	1082	0,896	0,980
	Underflow	491	532	49,8	53,4	648	632	0,951	1,01
	Overflow	35,1	20,2	8,6	4,3	383	451	0	0
Classification	Feed	1669	1867	54,1	54,1	1938	2167	0,447	0,469
	Underflow	1178	1334	74,1	76,8	779	820	0,598	0,619
	Overflow	491	532	32,8	31,1	1159	1347	0,151	0,153
Primary Ball Mill	Feed	471	534	70,7	70,7	343	388	0,598	0,619
	Product	471	534	70,7	70,7	343	388	0,367	0,387
Secondary Ball Mill	Feed	707	801	69,2	69,2	536	607	0,598	0,619
	Product	707	801	69,2	69,2	536	607	0,326	0,347

Note: Base case versus Simulation 1.

According to the data listed in Table 1, the increase in the circuit flow by 10% did not cause significant alterations in the percentages of solids, pulp out flows or water flows. The P_{80} of the rod mill product increased by about 15%.

The overflow outflow of the pre-classification rose considerably, indicating an increase in the participation of the natural sludge. In the classification, the increase in pulp outflow caused an increase in the cyclones pressure, with thread operation (Table 2).

The reduction ratio of the rod mil, considered high in the Base Case, was reduced in Simulation 1 (Table 2), also being deemed high for the open circuit, even when considering the classification effect caused by the rods in the mil load transfer dynamics. Both the feeding and the products of the ball mils presented higher P_{80} in Simulation 1.

Alterations on the P_{80} of the circuit final product was considered minimal in Simulation 1, increasing from 0.151 mm (Base Case) to 0.153 mm (Simulation 1).

Simulation 2

In Simulation 2, the percentage of solids of the feeding flow of the secondary closed circuit classification cyclone was reduced from 54% (Base case) to 50% (Simulation 2). Table 2 presents the summary of the results as compared to the Base Case.

Table 2. Milling circuit performance – Simulation 2.

Equipment	Flow	Solid Flow (t/h)		% Solids		Pulp Flow (m^3/h)		P_{80} (mm)	
		Base Case	Simulation 2	Base Case	Simulation 2	Base Case	Simulation 2	Base Case	Simulation 2
Rod Mill	Feed	635	635	60,0	60,0	622	622	32,1	32,1
	Product	635	635	60,0	60,0	622	622	0,933	0,93
Pre-classification I	Feed	607	591	31,1	31,1	1536	1497	0,781	0,754
	Underflow	527	508	44,3	44,1	827	804	0,896	0,871
	Overflow	80	83	10,5	11,1	710	693	0	0
Pre-classification II	Feed	527	508	37,8	37,8	1032	996	0,896	0,871
	Underflow	491	489	49,8	51,4	648	616	0,951	0,90
	Overflow	35,1	19,5	8,6	4,9	383	380	0	0
Classification	Feed	1669	1994	54,1	50,0	1938	2617	0,447	0,414
	Underflow	1178	1505	74,1	79,0	779	870	0,598	0,519
	Overflow	491	489	32,8	23,5	1159	1747	0,151	0,136
Primary Ball Mill	Feed	471	602	70,7	70,7	343	438	0,598	0,519
	Product	471	602	70,7	70,7	343	438	0,367	0,364
Secondary Ball Mill	Feed	707	903	69,2	69,2	536	684	0,598	0,519
	Product	707	903	69,2	69,2	536	684	0,326	0,332

Note: Case base versus Simulation 2.

For Simulation 2, Table 2 indicates an increase in the circulating load and cyclone pressure, with the consequent reduction in the P_{80} of the circuit product, from 0.151 mm to 0.136 mm.

The finest cut of the classification cyclones impacted the percentage of solids of the underflow, from 74% in the Base Case, to 79% and increased the feeding from 1669 t/h to 1994 t/h of solids. The combination of these two changes resulted in the rope discharge operation in the underflow of the hydrocyclones manifold (Table 2).

Simulation 3

Simulation 3 considered: a) an increasing in the percentage of solids of the ball mil feed; b) dilution of the flow feeding the hydrocyclone classifier and c) increasing the hydrocyclone apex (from 110 mm to 1127 mm) in order to obtain a finer cut.

The comparison of the milling circuit performance between the Base Case and Simulation 3 is presented in Table 3.

Table 3. Milling circuit performance – Simulation 3.

Equipment	Flow	Solid Flow (t/h)		% Solids		Pulp Flow (m^3/h)		P_{80} (mm)	
		Base Case	Simulation 3	Base Case	Simulation 3	Base Case	Simulation 3	Base Case	Simulation 3
Rod Mill	Feed	635	635	60,0	60,0	622	622	32,1	32,1
	Product	635	635	60,0	60,0	622	622	0,933	0,93
Pre-classification I	Feed	607	591	31,1	31,1	1536	1497	0,781	0,754
	Underflow	527	508	44,3	44,1	827	804	0,896	0,871
	Overflow	80	83	10,5	11,1	710	693	0	0
Pre-classification II	Feed	527	508	37,8	37,8	1032	996	0,896	0,871
	Underflow	491	489	49,8	51,4	648	616	0,951	0,90
	Overflow	35,1	19,5	8,6	4,9	383	380	0	0
Classification	Feed	1669	2319	54,1	50,0	1938	3044	0,447	0,382
	Underflow	1178	1830	74,1	75,6	779	1164	0,598	0,454
	Overflow	491	489	32,8	22,1	1159	1880	0,151	0,125
Primary Ball Mill	Feed	471	732	70,7	75,0	343	473	0,598	0,454
	Product	471	732	70,7	75,0	343	473	0,367	0,338
Secondary Ball Mill	Feed	707	1098	69,2	75,0	536	709	0,598	0,454
	Product	707	1098	69,2	75,0	536	709	0,326	0,307

Note: Case base versus Simulation 3.

Changes in the solids percent of the feeding flows to the hydrocyclones operating in closed circuit with the ball mills increased the circuit circulating load ratio. Therefore, the hydrocyclones pressure also increased from 36 kPa (Base Case) to 87 kPa (Simulation 3).

As regards to the Base Case, the P_{80} of the hydrocyclone overflow reduced to 0.125 mm in Simulation 3, also increase the percentage of solids of the underflow. These changes also reflected in the hydrocyclone feed rate that from 1669 t/h (Base Case) to 2319 t/h (Simulation 3). Considering the pre-classification stages I and II, no relevant alterations were observed.

The results from Simulation 3 indicated a product with finer grain size, according to the FCA (Fine Concentrated Apatítico) product specifications.

CONCLUSIONS

The simulations performed described the use of modeling for diagnosing the industrial circuit operation selected, as well as investigating alternatives for performance improvement.

In Simulation 1, a new feeding flow was raised by 10%, resulting in an increase of the product P_{80} (the cyclones *overflow*).

Simulation 2 indicated that, altering the percentage of solids fed to the hydrocyclone classifiers, significant changes were observed in the P_{80} of the hydrocyclones overflow products. The P_{80} values changed from 0.151 mm (Base Case) to 0.136 mm (Simulation 2). It also increased the circulating load causing rope discharge operation in the hydrocyclones underflow products.

Regarding to Simulation 3, the changes proposed resulted in: significant changes in the P_{80} of the hydrocyclone overflow product that was reduced to 0.125 mm; the circuit circulating load increased and as a consequence the circuit throughput also increased; it was also observed an increase in the hydrocyclones pressure. The results from Simulation 3 yielded a product with finer grain size, according to the FCA product specifications

ACKNOWLEDGEMENTS

The authors thank Vale Fertilizantes for the support in the execution of the study, as well as for authorizing its publication.

REFERENCES

BARBERY,G. Derivation of a formula to estimate the mass of a sample for size analysis. Trans AusIMM, 81 (784), March, C49-C51, 1972.

NASCHENVENG, A.C. Modelagem e simulação do circuito de moagem da Ultrafértil. São Paulo, 2003. 101 p. Dissertação (Mestrado) – Escola Politécnica, Universidade de São Paulo.

BAUXITE FINES RECOVERY VIA DESLIMING AND CONCENTRATION

N. G. Bigogno[1], R. S. Junior.[2], C. F. Andrade[3], C. M. V. Deursen[4], E. M. Dias [5] and F. T. M. Araújo[6]

1. Process Engineer
2. Bauxite and Alumina Technology Development Manager
3. Operational Unit Manager Votorantim Metais
4. Process Consultant Votorantim Metais
4. Mining Process Engineer Votorantim Metais
5. Metallurgical Engineer.
*(*Corresponding author: nilson.bigogno@vmetais.com.br)*

24th World Mining Congress
MINING IN A WORLD OF INNOVATION
October 18-21, 2016 • Rio de Janeiro /RJ • Brazil

BAUXITE FINES RECOVERY VIA DESLIMING AND CONCENTRATION

ABSTRACT

Votorantim Metais is one of the majors producers of primary aluminium of Brazil and operates an industrial complex in the municipality of Aluminium. This industrial complex comprises an alumina refinery, a smelter and aluminium transformation units and processes bauxite from different mines. One of these mines is situated in Miraí city, in Minas Gerais state (Brazil'S southeast region). This site comprises mining and bauxite washing operations. The washing plant is set to recover the coarse fraction of the bauxite by scrubbing and screening. The fraction finer than 1.0 mm is rejected as a pulp to a dam. Several studies concluded that part of this material might be recovered by removing the clay and concentrating the lighter fraction, richer in alumina, by removing the heavy fraction, richer in iron minerals and quartz. The equipment considered for these operations are hydrocyclones and spiral concentrators. This processing route was developed by applied research done in laboratory scale, proven in a pilot application and confirmed in a single industrial processing line. Recovering this fraction of the bauxite will increase the mass recovery of Miraí plant up to 20%.

KEYWORDS

Bauxite; ore dressing; concentration; fines recovery.

INTRODUCTION

The Votorantim Group started as a textile factory and was commissioned in 1918 in the municipality of Votorantim, São Paulo state. Since then, Votorantim has been diversifying its activities. Industrial operations now include cement, mining and metallurgy (aluminum, zinc and nickel), steel, pulp, orange juice, and electricity generation.

The aluminium business includes four bauxite mines, a refinery, a smelter and plastic transformation units and a mega project, Alumina Rondon. To produce aluminium, the bauxite is mined and transported by railway to the refinery where up to 1 million tons of alumina can be produced, resulting in nearly 500 thousand tons of metal per year.

From the 230 million tons of bauxite produced every year worldwide, roughly 60 million tons are form beneficiating operations. Bauxite beneficiation is typically done via size separation. The beneficiation of bauxite is done in order to increase the low temperature available alumina grade (THA or total hydrate alumina, the alumina that is recoverable at 150° C Bayer process), to reduce the reactive silica grade (RS) or both. This type of beneficiation process uses the difference in relative concentration of both materials in different size ranges. Commonly, THA is in coarser fractions and RS, in finer fractions of the run of mine.

This is also the process that is applied in beneficiating the bauxite from Miraí. There, the run of mine bauxite is fed into crushers, disaggregated in a washing drum or scrubber and separated by size in two sets of screens; being the undersize of the first the feed of the second one. Both oversizes are jointly staked as product, and the undersize of the secondary screen is disposed as a pulp in a reject dam.

The mass recovery of each bauxite is a consequence from natural condition of the deposit and the process applied. Since typical operations "wash" bauxite, the material characteristic taken into account is the particle size. If it is coarse enough, it is product and if it is fine, the material is rejected. This approach is justifiable if there is a clear distinction in THA and RS grades along the particle size

distribution (PSD). Indeed, if the THA grade is high enough and the RS is low enough up to a certain size, this size should the cut size for the process.

This rationale may be applied in the bauxite found in the municipality of Miraí and implies in a cut size of roughly 850 µm (eventually a little smaller). But, at this cut size, the mass recovery of the operation is just over 40 %. In order to increase this mass recovery, finer particles should be recovered. However, even though the RS grades are low for particles as fine as 40 µm, the THA grades are in the low 30%, lower than the product at 43% THA. With the purpose of reaching the same THA values, a concentrating operation must be implemented.

PREVIOUS WORK REVIEW

Other bauxite mines beneficiate the fine bauxite fraction via classification with hydrocyclones separating the minus 40 µm. This cut is justifiable due to the size of kaolinite particles, mass recovery below 40 µm and size range where hydrocyclones are applicable. Kaolinite reacts with NaOH, being this mineral the RS bearer for the low temperature Bayer process. Kaolinte has 46.6% of SiO2 and has Al2Si2O5(OH)4 as chemical formula. This means that if the bauxite has 3.0% of RS, it actually has 6.4% of kaolinite. It is relevant to state that not all kaolinite particles are free from gibbsite particles (or available alumina bearing particles) and this lack of liberation limits the amount of separable RS.

Several operations in northern Brazil process their fine bauxite only via hydrocyclones achieving acceptable THA and RS grades and mass recovery. This is also the case of Alumina Rondon, a Votorantim Metais project. The process flow of Alumina Rondon is in image 1. This circuit is in a rougher-cleaner-cleaner configuration, where the underflow of the first cyclone battery is the feed to the second, the underflow of the second feeds the third being its underflow the fine product to be dewatered.

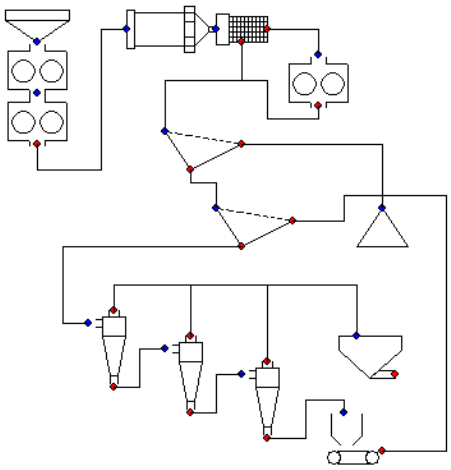

Figure 1 – Alumina Rondon simplified flow chart

Other processing routes may include froth flotation and magnetic or density concentration. [source] These operations deal with alternative differentiation characteristics of the material, respectively natural or selectively induced hydrophobicity, magnetic or a combination of factors such as size, specific gravity, shape, rugosity, porosity etc. The combination of these factors describes the behavior of the particle when suggested to a force within a fluid and is referred as the hydraulic diameter of the particle. Such material peculiarities were considered when developing the laboratory approach with the minus 850 µm bauxite from Miraí, as well as similar operations that deal with bauxite from the same region.

In other Votorantim operation, in the municipality of Itamarati de Minas, a processing route, similar to the concept proposed to Miraí fines, was successfully applied to increase the mass recovery of the plant. This concentrating route received the undersize of the product screen, removed the RS rich clay (or the minus 40 µm) in a hydrocyclone battery and concentrated the bauxite in spiral separators

separating quartz and iron bearing particles. After concentration, the THA rich fraction, or the lighter fraction, was dewatered and composed the bauxite product of the plant. The fine bauxite recovery circuit is exposed in image 2.

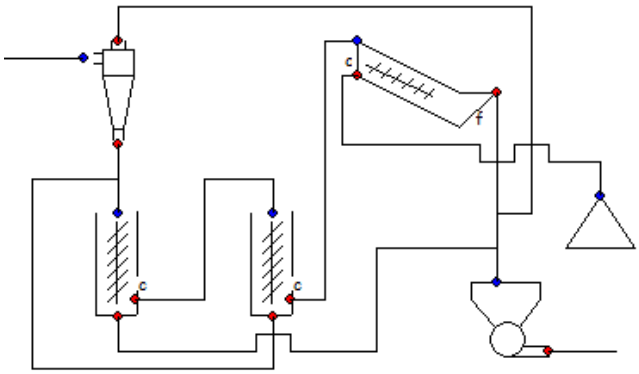

Figure 2 – Itamarati bauxite fines recovery flow chart

The bauxite processed in Miraí was subject in several previous works [source] where the ultimate goal was to increase the mass recovery without any negative consequences in the THA and RS grades. Other processing routes proposed for these bauxite fines included several unit operations as described earlier. In the authors' opinion, these options were not further developed and built due to their complexity and capital costs. These were taken into account in this new approach.

PROCESS FLOW DIAGRAM DEFINITION

The first activity developed to understand the material properties in order to design the flow chart was to obtain the bauxite fines composition per size fraction. This was done by wet screening a typical tailings sample in a series of screens and then analyzing each size fraction by XRF and for THA and RS. The results, as listed in table 1, confirmed the expectation that the coarser particles have higher THA and lower RS grades.

Table 1 – Composition of bauxite fines per size fraction and above accumulated

Mesh	PSD		Grades per fraction					Grades above accumulated				
	Simple Retained	Accumulated Retained	$Al_2O_3^T$	$Fe_2O_3^T$	SiO_2^T	THA	RS	$Al_2O_3^T$	$Fe_2O_3^T$	SiO_2^T	THA	RS
(µm)	(%)	(%)	(%)	(%)	(%)	(%)	(%)	(%)	(%)	(%)	(%)	(%)
850	0.7	0.7	53.5	11.1	5.2	48.6	1.8	53.5	11.1	5.2	48.6	1.8
600	1.1	1.8	49.9	10.6	11.3	45.3	1.6	51.2	10.8	9.0	46.5	1.7
425	1.9	3.6	45.3	11.9	17.5	40.5	1.5	48.2	11.4	13.4	43.4	1.6
300	3.8	7.5	38.6	13.4	27.0	33.5	1.4	43.3	12.4	20.4	38.3	1.5
212	4.6	12.1	33.9	17.2	30.4	27.6	1.3	39.7	14.2	24.2	34.2	1.4
150	6.5	18.5	30.6	22.1	28.2	23.4	1.1	36.5	17.0	25.6	30.4	1.3
106	5.1	23.7	27.7	25.4	26.5	21.3	0.9	34.6	18.8	25.8	28.4	1.2
75	7.6	31.3	27.3	28.4	19.9	20.9	1.2	32.8	21.1	24.3	26.6	1.2
53	5.1	36.4	27.1	30.4	17.1	21.3	0.9	32.0	22.4	23.3	25.8	1.2
38	4.9	41.3	29.1	30.8	13.0	23.4	1.1	31.7	23.4	22.1	25.6	1.2
20	6.2	47.5	33.1	30.2	8.8	25.5	2.3	31.9	24.3	20.4	25.5	1.3

Bottom	52.5	100	38.6	25.0	10.9	23.6	9.3	35.4	24.7	15.4	24.5	5.5

At first, it is possible to observe that the mass is evenly distributed along the different sizes except for minus 20 µm fraction, which has 52.5% of the initial mass. Another observation is that only particles coarser than 425 µm have THA and RS grades within the product range. In addition, the mass of particles coarser than 425 µm is 3.6% of the bauxite fines fraction, or, in typical values, less than 2% of the run of mine mass.

The iron bearing particles occur through all the PSD, with grades higher than 20% under 212 µm. As might be also noted, the RS is low throughout all the PSD, with a steep increase below 20 µm. As the XRF measures the amount of silicon atoms in the sample, the difference between RS and SiO2T is a fair approach of the quartz quantity in the sample. With this it is possible to assert that the quartz particles are concentrated between 425 and 106 µm.

This sample was also tested via qualitatively XRD and the main minerals and their densities are listed in table 2.

Table 2 – Minerals in bauxite fines and their densities

Mineral	Density g/cm³
Gibbsite	2.3 – 2.4
Quartz	2.6 – 2.7
Hematite	4.9 – 5.3
Kaolinite	2.6

The densities stated above are the true densities of perfect grains of the mineral, and might be used as a reference to interpret the hydraulic diameter of the particle, since that density and particle size have major influence in the hydraulic diameter. There is no objective determination of the hydraulic diameter by reason of the difficulties of measuring each property of the particle and combining them to create a single value for direct comparison. However, it is possible to infer the relative behavior of particles in terms of the hydraulic diameter by doing specific laboratory experiments and a pilot plant test.

Carrying out a dense liquid separation test assisted in developing the process flow. This test consists in placing the material in a fluid with a controlled density and letting it float or settle. In this case, particles put in a solution of bromoform - CHBr3. The bromoform was diluted with ethanol so that the solution density was 2.5 g/cm³. In this solution, it was possible to separate the particles in three groups: the buoyant, the slow settling and the fast settling fractions. This test was done with discrete particle sizes and the fractions smaller than 38 µm were not tested. With size reduction, other forces start to have a relevant influence in the particle mobility in a fluid, and, for this case, particles smaller than 38 µm could not be efficiently separated. In table 3 follow the composition of each fraction.

Table 3 – Buoyant, fast and slow settling fractions in bromoform solution

	Fraction	Mass recovery from bauxite fines	THA	RS
	+300 µm			
1	buoyant	4	55.0	1.3
2	slow settling	2.6	18.8	1.9
3	fast settling	0.8	14.2	0.7
	-300 +106 µm			
4	buoyant	4.9	54.9	1.4

5	slow settling	6.2	15.2	0.7
6	fast settling	5.1	7.6	0.4
	-106 +38 μm			
7	buoyant + slow settling	10.2	34.3	1.2
8	fast settling	7.5	5.3	0.4

A possible product from a separation process that relies on density differences is the combination of the results listed in lines 1, 4 and 7. This material, by doing a weighted average from obtained grades, has 43.9% THA and 1.3% RS. Lines 1 and 4 are results from size ranges where the separation process was efficient enough to allow distinction between buoyant and slow settling. The result in line 7 is from finer material and its separation was less effective, resulting in poorer product.

The laboratory tests did not included dewatering tests since this phenomenon has lower complexity and might be accessed through existing models or by operating references. References [source] show that the moisture of clay free bauxite fines is between 15 to 20% regardless of the dewatering equipment used, e.g. belt filter, dewatering screen etc.

From the results obtained in the tailings technological characterization, a pilot essay was designed. This pilot test included a hydrocyclone for clay classification and spiral concentrator for iron and quartz separation. When a spiral concentrator is fed a dilute pulp mixture of minerals of different specific gravities and sizes, the low hydraulic diameter particles are more readily suspended by the water and attain relatively high tangential velocities so that they climb toward the outer rim of the spiral trough. At the same time, the higher hydraulic diameter, non-suspended grains migrate along the spiral surface at the lowest portion of the spiral cross section. In this case, small hydraulic concentrate is selectively directed into the spiral trough near the outside of the spiral surface through the use of adjustable product splitters. The splitters allow three products to be obtained: small, mixed and high hydraulic diameter particles.

The objective of this test was to obtain a richer in THA material in the small diameter fraction. Other products of this test included the clay fraction in the hydrocyclones overflow, the iron richer fraction in the higher diameter of the spiral and a mixed material, richer in quartz. This processing route was inspired by the dense liquid tests.

The processing route comprehended:
Desliming at 40 μm in hydrocyclones;
Underflow concentration in a rougher spiral;
Low hydraulic diameter of the rougher spiral concentration in a cleaner step;
Intermediate material from the rougher spiral concentration in a scavenger step;

The samples from the pilot test were obtained by simultaneously collecting the products from each stage. With that, it was possible to access the following mass partition estimation.

As may be seen in table 4, for a typical sample and in the cyclone, rougher-cleaner spiral configuration the product obtained had THA and RS within product ranges, resp. 41.3% and 3.16%.

Table 4 – Grades obtained in the pilot test for a typical sample

	Mass recovery	THA	RS	Fe2O3T
1 Feed	100.0	26.3	8.34	17.7
2 Overflow	53.1	18.9	13.4	21.1
3 Underflow	46.9	34.7	2.59	13.9
4 Rougher feed	46.9	34.7	2.59	13.9

5	High	6.10	11.6	1.32	33.6
6	Intermediate	9.30	25.3	2.43	17.9
7	Low	31.5	41.9	2.88	8.83
8	Cleaner feed	31.5	41.9	2.88	8.83
9	High	3.10	23.0	0.70	16.1
10	Intermediate	10.4	45.5	1.61	10.5
11	Low	18.0	43.1	3.99	6.61
12	Scavenger feed	9.30	25.3	2.43	17.9
13	High	1.02	13.1	0.30	30.7
14	Intermediate	2.00	20.0	0.68	14.5
15	Low	6.3	29.0	3.33	16.90
10+11+15	Product	34.7	41.3	3.16	9.64

More interestingly than evaluating the grades, is to check if the obtained densities are as expected, i.e. within gibbsite range for product, quartz range for intermediate and closer to hematite for the reject. Table 5 shows these densities values and the expectation is confirmed.

Table 5 – Product specific gravities

	Specific gravity		
	Rougher	Cleaner	Scavenger
High	3.21	2.60	3.22
Intermediate	2.61	2.39	2.52
Low	2.40	2.34	2.44

The less dense material is the low hydraulic diameter product of the cleaner step. On the other hand, the denser are the high diameter product from the rougher and scavenger steps.
The pilot plant results established that the proposed processing route is effective in separating the gibbsite bearer particles from other sufficiently to have a product with acceptable grades. The next step is to build a single processing line in the beneficiation plant in order to demonstrate the processing rout at full scale. This will also enable the operators to learn from the equipment and how to deal with feed variability prior having the necessary number of equipment to process the whole reject.

The proposed industrial plant flow chart is in image 3 and includes a hydrocyclone, a rougher-cleaner arrangement for spiral concentrator and dewatering screens.

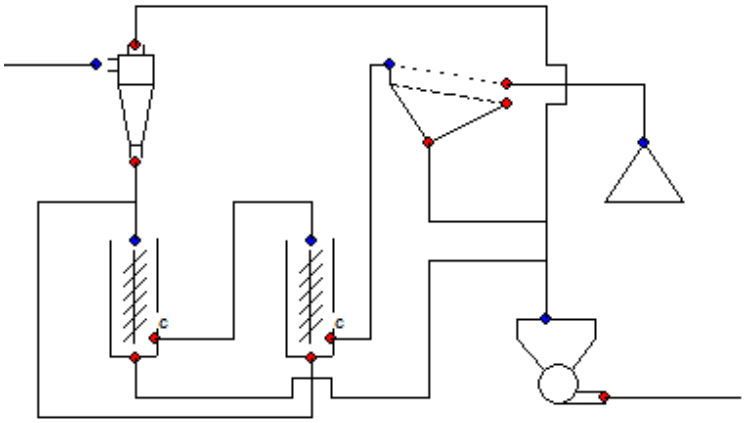

Figure 3 – Proposed flow diagram for Miraí fines recovery circuit

CONCLUSION

The laboratory tests and the pilot run demonstrated that it is possible to obtain a fine bauxite product similar to the one obtained in the coarse fraction. The coarse fraction characteristics follow in table 6.

Table 6 – Mirai bauxite characteristics

Characteristic	Unit	Value
THA	(%)	44.0
RS	(%)	3.0
Total Alumina	(%)	48.0
Total Silica	(%)	11.0
Alumina bearer	(%)	gibbsite
Total Organic Carbon	(%)	0.2
Iron	(%)	12.5
Settling Rate (HX)	(m/h)	30
WI	(kWh/st)	11
Moisture	(%)	12
PSD	P95 (mm) P05 (mm)	50 1.0

REFERENCES

CHAVE, A.P.; BERGERMAN, M.G.; ABREU, C, A,V.; BIGOGNO, N**.** *Concentration of bauxite fines via gravity concentration.* Itamarati de Minas, 2009

VOTORANTIM (Brasil). *Memorial CBA 50 Ano*s**.** São Paulo: Grupo Votorantim, 2013.

BERGERMAN, M.G. *Produção mais limpa no tratamento de minérios: caso da Companhia Brasileira de Alumínio, Mina de Itamarati de Minas, MG*. São Paulo: Escola Politécnica da Universidade de São Paulo, 2003.

KURUSU, R.S. *Flotação de finos de bauxita*. São Paulo: Escola Politécnica da Universidade de São Paulo, 2005.

JUNIOR, H.D.; JATOBÁ, T.L.A.; GOMES, W.L.; SENEFONTE, R. *Caracterização tecnológica do rejeito de bauxita da Unidade Miraí.* São Paulo: HDA S/S Ltda, 2014

BENEFICIATION OF INDUSTRIAL MINERALS USING A TRIBO-ELECTRIC BELT SEPARATOR

F.J. Hrach[1] and K.P. Flynn[1], *P. J.Miranda[1]

[1]ST Equipment & Technology LLC
101 Hampton Avenue
Needham MA 02494 USA
*(*Corresponding author: pmiranda@titanamerica.com)*

24th World Mining Congress
MINING IN A WORLD OF INNOVATION
October 18-21, 2016 • Rio de Janeiro /RJ • Brazil

BENEFICIATION OF INDUSTRIAL MINERALS USING A TRIBO-ELECTRIC BELT SEPARATOR

ABSTRACT

Triboelectric charging has been around for thousands of years. In ancient Greece, the triboelectric effect was initially by observation of small fibers of clothing adhering to amber jewelry. By rubbing the fibers, the situation became worse. Even during this age, people wondered about the effect. Next, in the 18th century, one of our nations cofounders, Benjamin Franklin, performed several experiments utilizing the phenomenon. Triboelectric charging is based on materials becoming electrostatically charged based on contact or friction from other particles. Examples of triboelectric charging include rubbing fur with glass or a comb through hair. During this process, electrons from materials will jump from one material to another and therefore become charged due to differences in surface electron affinity (or work function).

Recently, ST Equipment & Technology, LLC (STET) has developed a processing system based on tribo-electrostatic separation. This dry technology provides the mineral processing industry a means to beneficiate fine materials. In contrast to other electrostatic separation processes that are typically limited to particles greater than 75µm in size, the triboelectric belt separator is ideally suited for separation of very fine (<1µm) to moderately coarse (500µm) particles with very high throughput. The high efficiency multi-stage separation through internal charging/recharging and recycle results in far superior separations that can be achieved with a conventional single-stage free-fall tribo-electrostatic separator. The triboelectric belt separator technology has been used to separate a wide range of materials including mixtures of glassy aluminosilicates/carbon, calcite/quartz, talc/magnesite, and barite/quartz. Separation results are presented and economic comparison of using the tribo-electrostatic belt separation versus conventional flotation for barite/quartz separation is evaluated.

KEYWORDS

Industrial minerals, dry separation, calcium carbonate, talc, barite, quartz, tribo-electrostatic charging, belt separator, fly ash

INTRODUCTION

The triboelectric effect, better known as triboelectric charging, is caused when certain different materials become frictionally charged by contacting each other. During this process, electrons from one material will be transferred to another material. When the materials are then separated, excess electrons will be left on one material while the other material will be electron deficient, therefore, both materials will behave in a charged state based on losing or gaining electrons. The sign and magnitude of the charge difference depends partly on the difference in electron affinity (or work function) between the particle types. For example, rubbing your hair with a balloon will build up negative charge on the balloon, leaving your hair positively charged. Even though the triboelectric effect is well known, it can be unpredictable, however, scientific advancements have been completed for separation of certain materials utilizing the triboelectric effect. Separation can then be achieved using an externally applied electric field.

The lack of access to fresh water is becoming a major factor affecting the feasibility of mining projects around the world. According to Hubert Fleming, former global director for Hatch Water, "Of all the mining projects in the world that have either been stopped or slowed down over the past year, it has been, in almost 100% of the cases, a result of water, either directly or indirectly" Blin (2013). Dry mineral processing methods offer a solution to this looming problem. Wet separation methods such as froth flotation require the addition of chemical reagents that must be handled safely and disposed of in an environmentally responsible manner. Inevitably, it is not possible to operate with 100% water recycle, requiring disposal of at least of portion of the process water, likely containing trace amounts of chemical reagents.

Dry methods such as electrostatic separation will eliminate the need for fresh water and offer the potential to reduce costs. Electric separation methods that utilize contact, or tribo-electric, charging are particularity interesting because of their potential to separate a wide variety of mixtures containing conductive, insulating, and semi-conductive particles.

ST Equipment and Technology (STET), a subsidiary of Titan America, has developed a full scale triboelectric mineral separator. The technology can successfully separate fly ash and minerals at approximately 40 tons per hour. For fly ash, separation of the carbon component (Ecotherm) and the aluminosilicate based component (Proash) has been proven at a lab scale demonstration, pilot plant demonstration, and full scale implementation of the technology with in the United States and worldwide. Ecotherm products produced using the technology can be placed back into the coal fired power plant or transported offsite for further caloric use, such as kiln furnace fuel. Secondly, the Proash product is an excellent replacement for portlandite cement based on its Pozzolanic properties. By successfully using the triboelectrostatic separators, utility plants using coal fired technology are able to successfully use a waste product and transform it to a product of use in the cement industry along with recovering the unused carbon from the fly ash.

Besides being utilized in the fly ash industry, this technology has been used to successfully separate minerals from each other. For example, calcite purification along with quartz rejection has been successfully tested using this type of technology. Secondly, removing magnesite from talc was also successful. Lastly, increasing barite purification to the required clients level as also been completed. Each of these accomplishments are discussed below.

TRIBO-ELECTROSTATIC BELT SEPARATION

In the tribo-electrostatic belt separator (Figures 1 and 2), material is fed into the thin gap 0.9 – 1.5 cm between two parallel planar electrodes. The particles are triboelectrically charged by particle to particle interaction. For example, in the case of coal combustion fly ash, a mixture of carbon particles and silicate based mineral particles, the positively charged carbon and the negatively charged minerals are attracted to opposite electrodes. The particles are then swept up by a continuous moving open-mesh belt and conveyed in opposite directions. The belt moves the particles adjacent to each electrode toward opposite ends of the separator. The electric field need only move the particles a tiny fraction of a centimeter to move a particle from a left-moving to a right-moving stream. The counter current flow of the separating particles and continual triboelectric charging by carbon-mineral collisions provides for a multistage separation and results in excellent purity and recovery in a single-pass unit. The high belt speed also enables very high throughputs, up to 40 tons per hour on a single separator. By controlling various process parameters, such as belt speed, feed point, electrode gap and feed rate, the device produces low carbon fly ash at carbon contents of 2 % ± 0.5% from feed fly ashes ranging in carbon from 4% to over 30%.

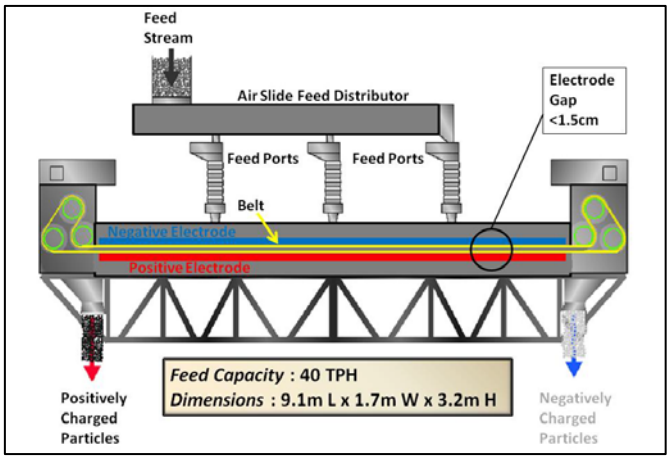

Figure 1- Schematic of triboelectric belt separator

The separator design is relatively simple. The belt and associated rollers are the only moving parts. The electrodes are stationary and composed of an appropriately durable material. The belt is made of plastic based material. The separator electrode length is approximately 6 meters (20 ft.) and the width 1.25 meters (4 ft.) for full size commercial units. The power consumption is less than 2 kilowatt-hour per ton of material processed with most of the power consumed by two motors driving the belt.

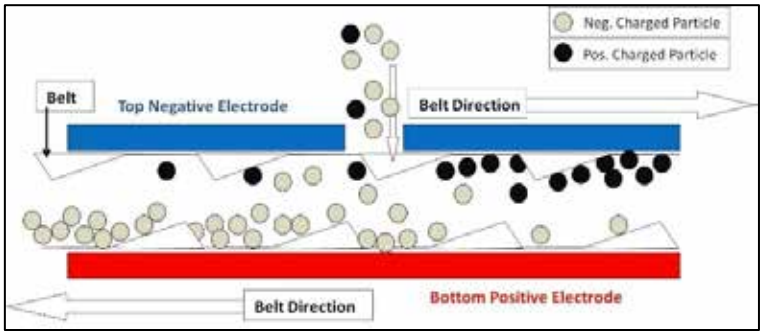

Figure 2- Detail of separation zone

The process is entirely dry, requires no additional materials, and produces no waste water or air emissions. In the case of carbon from fly ash separations, the recovered materials consist of fly ash reduced in carbon content to levels suitable for use as a pozzolanic admixture in concrete and a high carbon fraction which can be burned at the electricity generating plant. Utilization of both product streams provides a 100% solution to fly ash disposal problems.

The tribo-electrostatic belt separator is relatively compact. A machine designed to process 40 tons per hour is approximately 9.1 meters (30 ft.) long, 1.7 meters (5.5 ft.) wide and 3.2 meters (10.5 ft.) high. The required balance of plant consists of systems to convey dry material to and from the separator. The compactness of the system allows for flexibility in installation designs.

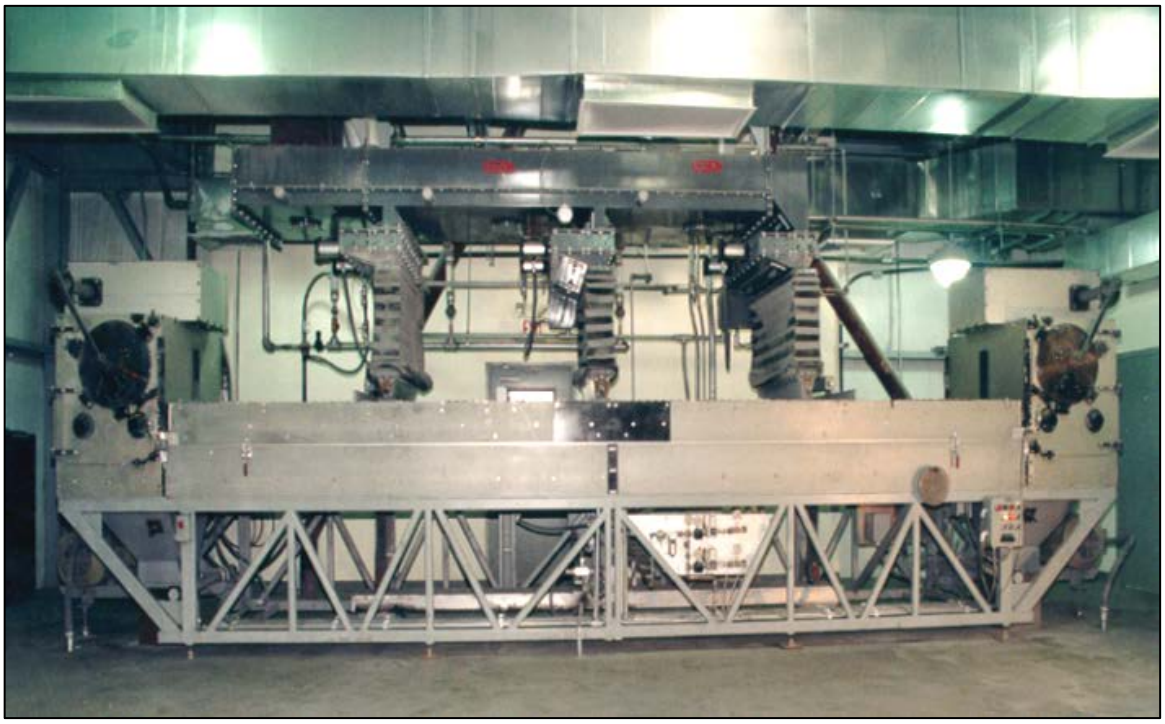

Figure 3- Commercial tribo-electrostatic belt separator

APPLICATIONS OF TRIBO-ELECTROSTATIC BELT SEPARATION

Coal Combustion Fly Ash

The tribo-electrostatic belt separation technology was first applied industrially to the processing of coal combustion fly ash in 1995. The technology is effective in separating carbon particles from the incomplete combustion of coal, from the glassy aluminosilicate mineral particles in the fly ash. The technology has been instrumental in enabling recycle of the mineral-rich fly ash as a cement replacement in concrete production due to its pozzolanic properties. Since 1995, over 20,000,000 tonnes of fly ash has been processed by the 19 tribo-electrostatic belt separators installed in the USA, Canada, UK, Poland, and South Korea. The industrial history of fly ash separation is listed in Table 1.

Table 1 - Industrial Application of Tribo-electrostatic belt separation for fly ash

Utility / power station	Location	Start of commercial operations	Facility details
Duke Energy – Roxboro Station	North Carolina USA	1997	2 Separators
Talen Energy- Brandon Shores	Maryland USA	1999	2 Separators
Scottish Power- Longannet Station	Scotland UK	2002	1 Separator
Jacksonville Electric-St. Johns River Power Park	Florida USA	2003	2 Separators
South Mississippi Electric Power -R.D. Morrow	Mississippi USA	2005	1 Separator
New Brunswick Power-Belledune	New Brunswick Canada	2005	1 Separator
RWE npower-Didcot Station	England UK	2005	1 Separator
Talen Energy-Brunner Island Station	Pennsylvania USA	2006	2 Separators
Tampa Electric-Big Bend Station	Florida USA	2008	3 Separators two-pass scavenging
RWE npower-Aberthaw Station	Wales UK	2008	1 Separator
EDF Energy-West Burton Station	England UK	2008	1 Separator
ZGP (Lafarge Cement /Ciech Janikosoda JV)	Poland	2010	1 Separator
Korea Southeast Power- Yeongheung	South Korea	2014	1 Separator
PGNiG Termika-Sierkirki	Poland	Scheduled 2016	1 Separator

Mineral Applications-Calcium Carbonate

When applying the technology to industrial minerals, success was achieved in the removal of quartz and other acid insoluble contaminants from finely ground calcium carbonate. Acid insoluble (AI) testing is a standard method of measuring the amount of undesirable contaminants in calcium carbonate. Silicates, such as quartz, mica, and talc, tend to tribo-charge strongly negative relative to carbonates.

Because of this technology, successful separations have been achieved on over 11 sources of calcium carbonate tested at both the pilot-scale and demonstration plant. Improvement in product brightness is also achieved for many sources of calcium carbonate as the tribo-electrostatic belt separation technology is also effective in removing trace amounts of dark contaminates such as graphite and metal sulfides. Monthly average results for a pilot-scale continuously operating separator processing calcium carbonate is shown in Table 2. This demonstration plant used a continuously operating pilot-scale separator with average feed rate 10 tonne per hour.

Table 2- Demonstration plant separation results for calcium carbonate

Month	Avg. Feed grade (%AI)	Avg. Product grade (%AI)	Product Mass Yield (wt.%)	Calcium carbonate recovery (%)	AI rejection to by product (%)
Feb	3.3%	0.6%	86%	89%	84%
March	3.7%	0.6%	89%	92%	87%
April	4.1%	0.6%	89%	92%	88%
May	4.0%	0.7%	89%	92%	84%
June	4.7%	0.6%	89%	93%	89%

Mineral Applications-Talc

The tribo-electrostatic belt separation technology is also effective in removal of magnesite, quartz, and other dark colored contaminants from finely milled talc. Batch pilot-scale single-pass separation test results for a representative talc ore is shown in Figure 4. Talc content is estimated by loss-on-ignition (LOI) measurements assuming a simple mixture of talc and magnesite. The talc feed was first milled to 95% passing 325 mesh (45 microns) then processed in a pilot-scale tribo-electrostatic belt separator in batch mode. Feed moisture level (as measured by relatively humidity) was adjusted by drying and/or by the addition of water to the feed batch prior to tribo-electrostatic separation testing. For this talc ore, a talc concentrate with 88% grade was produced with 80% recovery with this technology in a single pass.

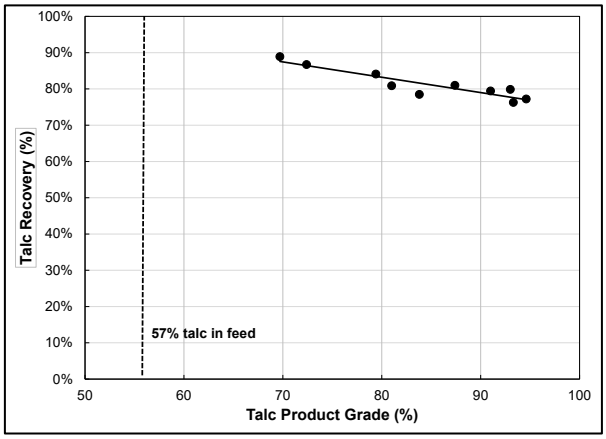

Figure 4- Pilot-scale separation results for a representative talc sample

Mineral Applications-Barite

The tribo-electrostatic belt separation technology is also effective in removing quartz and other low specific gravity (SG) components from barite used as a weighting agent in drilling applications. The American Petroleum Institute (API) specification requires that the barite be milled to a particle size with less than 3% retained on a 200 mesh (0.075 mm) sieve. Low grade barite from several sources milled to this specification has been successfully tested to produce a barite product that meets the API specification

13A-7 of 4.2 SG minimum in a single-pass (rougher separation only) for barites with a feed specific gravity of 3.78 or higher.

Batch pilot-scale single-pass separation test results for upgrading a representative low-grade barite ore sample is shown in Figure 5. The results are also presented showing the increase in barite product SG in Figure 6. For this low grade barite feed, with an average 3.75 SG, the tribo-electrostatic belt separator was able to produce API 13A-20 grade (4.1 SG barite) in a single pass, and produce API 13A-7 grade (4.2 SG barite) in a second pass (rougher and cleaning separation only, without scavenging). Scavenging of the tailings would significantly improve the overall barite recovery.

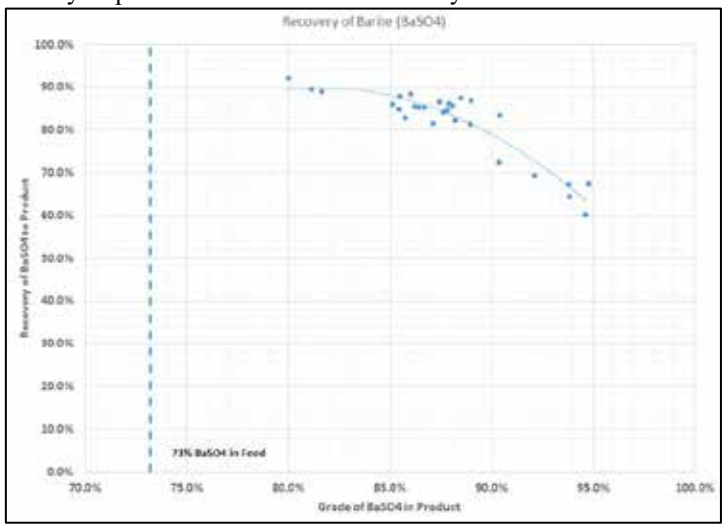

Figure 5- Separation Results for representative low-grade barite

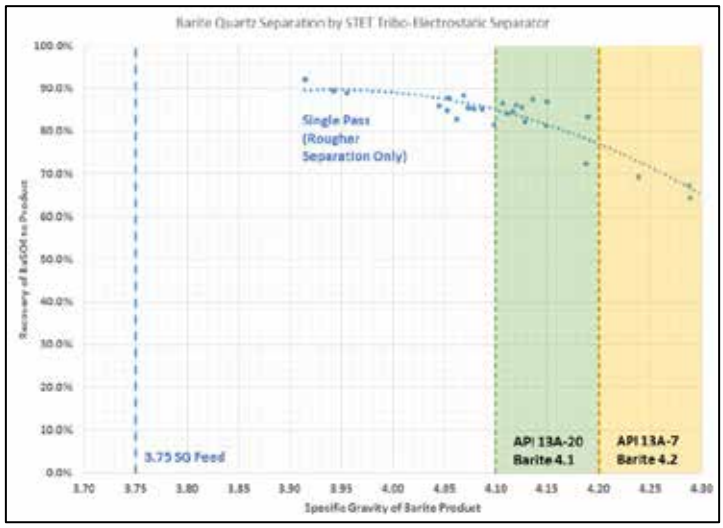

Figure 6- Specific gravity improvement for low-grade barite with cleaning

In addition to these examples, the tribo-electrostatic belt separation technology has been demonstrated to effectively beneficiate potash (sylvite/halite/kieserite), mineral sands (ilmenite/rutile/zircon/quartz), phosphate (apatite/dolomite/quartz), and graphite/quartz. Since the separator can process materials with particle sizes from about 0.5 mm to less than 0.001 mm, and is effective for both insulating and conductive materials, the technology greatly extends the range of applicable materials over conventional electrostatic separators. Since the tribo-electrostatic process is entirely dry, its use will eliminate the need for final product drying and liquid waste handling from flotation processes.

COST OF TRIBO-ELECTROSTATIC BELT SEPARATION

Comparison to Conventional Flotation for Barite

A comparative cost study was commissioned by STET and conducted by Soutex Inc., a Quebec Canada based engineering company with extensive experience in both wet flotation and electrostatic separation process evaluation and design. The study compared the capital and operating costs of tribo-electrostatic belt separation process to conventional froth flotation for the beneficiation of a low-grade barite ore. Both technologies upgrade the barite by removal of low density solids, mainly quartz, to produce an API drilling grade barite with greater than 4.2 SG. Flotation results were based on pilot plant studies conducted by the Indian National Metallurgical Laboratory, NML (2004). Tribo-electrostatic belt separation results were based on pilot plant studies using similar feed ores. The comparative economic study included flowsheet development, material and energy balances, major equipment sizing and quotation for both flotation and tribo-electrostatic belt separation processes. The basis for both flowsheets is the same, processing 200,000 t/y of barite feed with SG 3.78 to produce 148,000 t/y of drilling grade barite product with SG 4.21 g/ml. The flotation process estimate did not include any costs for process water, or water treatment.

Flowsheets were generated by Soutex for the barite flotation process (Figure 7), and tribo-electrostatic belt separation process (Figure 8).

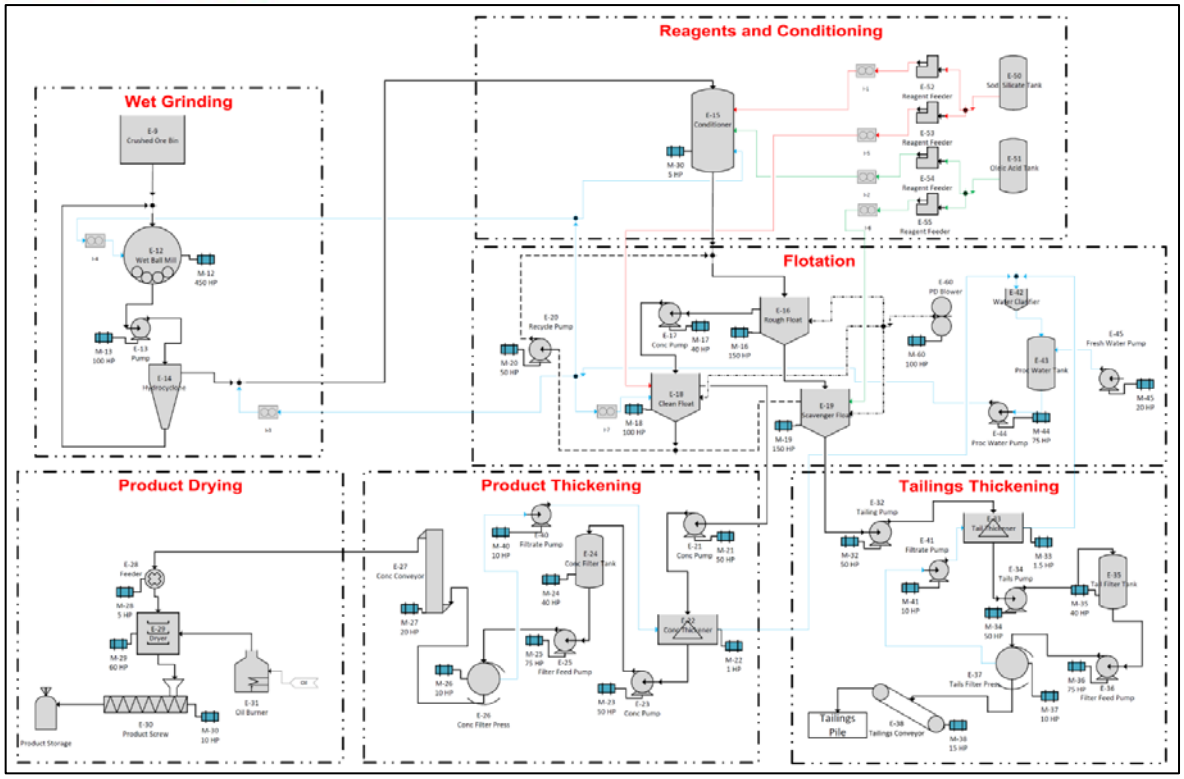

Figure 7- Barite flotation process flowsheet

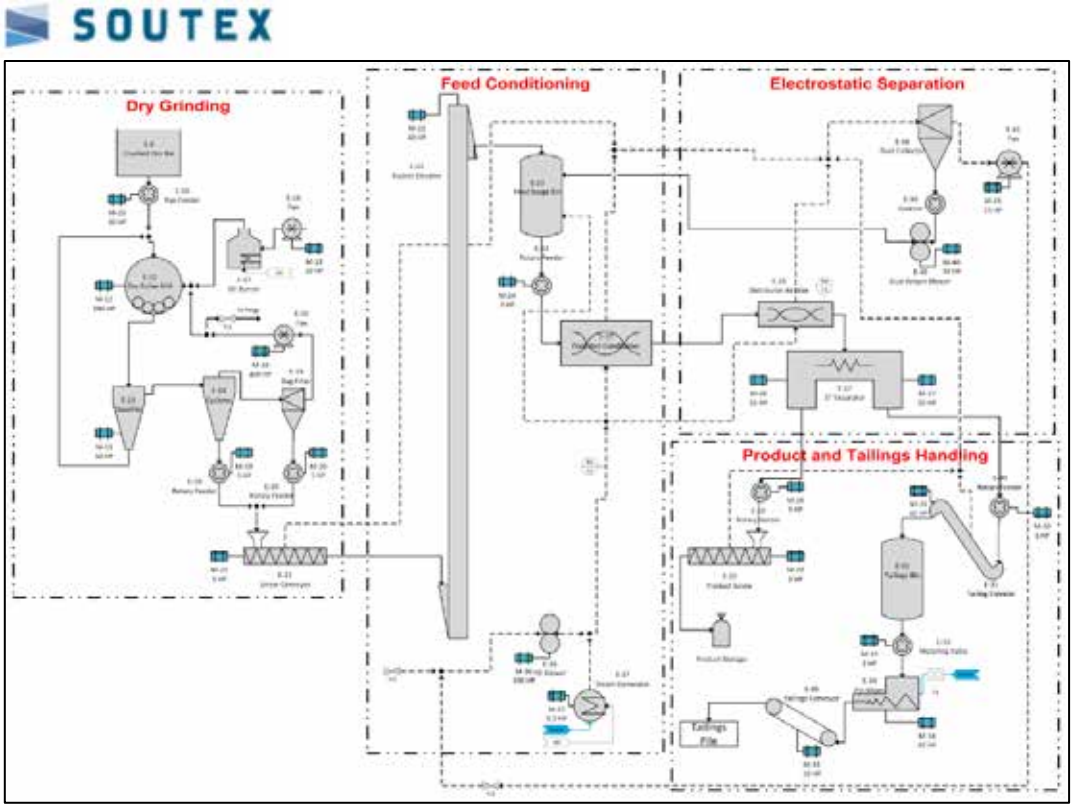

Figure 8 - Barite tribo-electrostatic belt separation process flowsheet

Theses flowsheets do not include a raw ore crushing system, which is common to both technologies. Feed grinding for the flotation case is accomplished using a wet pulp ball mill with cyclone classifier. Feed grinding for the tribo-electrostatic belt separation case is accomplished using a dry, vertical roller mill with integral dynamic classifier.

The tribo-electrostatic belt separation flowsheet is simpler than flotation. Triboelectostatic belt separation is achieved in a single stage without the addition of any chemical reagents, compared to three-stage flotation with oleic acid used as a collector for barite and sodium silicate as a depressant for the silica gangue. A flocculant is also added as a reagent for thickening in the barite flotation case. No dewatering and drying equipment is required for tribo-electrostatic belt separation, compared to thickeners, filter presses, and rotary dryers required for the barite flotation process.

Capital and Operating Costs

A detailed capital and operating cost estimate was performed by Soutex for both technologies using equipment quotations and the factored cost method. The operating costs were estimated to include operating labor, maintenance, energy (electrical and fuel), and consumables (e.g., chemical reagent costs for flotation). The input costs were based on typical values for a hypothetical plant located near Battle Mountain, Nevada USA. The total cost of ownership over ten years was calculated from the capital and operating cost by assuming an 8% discount rate. The results of cost comparison are present as relative percentages in Table 3.

Table 3 - Cost Comparison for Barite Processing

	Wet Beneficiation	Dry Beneficiation
Technology	Froth flotation	Tribo-electrostatic belt separation
Purchased Major Equipment	100%	94.5%
Total CAPEX	100%	63.2%
Annual OPEX	100%	75.8%
Unitary OPEX ($/ton conc.)	100%	75.8%
Total Cost of Ownership	100%	70.0%

The total purchase cost of capital equipment for the tribo-electrostatic belt separation process is slightly less than for flotation. However, when the total capital expenditure is calculated to include equipment installation, piping and electrical costs, and process building costs, the difference is large. The total capital cost for the tribo-electrostatic belt separation process is 63.2% of the cost of the flotation process. The significantly lower cost for the dry process results from the simpler flowsheet. The operating costs for the tribo-electrostatic belt separation process is 75.5% of the flotation process due to mainly lower operating staff requirements and lower energy consumption.

The total cost of ownership of the tribo-electrostatic belt separation process is significantly less than for flotation. The study author, Soutex Inc., concluded that the tribo-electrostatic belt separation process offers obvious advantages in CAPEX, OPEX, and operational simplicity.

CONCLUSION

The tribo-electrostatic belt separator provides the mineral processing industry a means to beneficiate fine materials with an entirely dry technology. The environmentally friendly process can eliminate wet processing and required drying of the final material. The process requires little, if any, pre-treatment of the material other than grinding and operates at high capacity – up to 40 tonnes per hour by a compact machine. Energy consumption is low, less than 2 kWh/tonne of material processed. Since the only potential emission of the process is dust, permitting is relatively easy.

A cost study comparing the tribo-electrostatic belt separation process to conventional froth flotation for barite was completed by Soutex Inc. The study shows that the total capital cost for the dry tribo-electrostatic belt separation process is 63.2% of the flotation process. The total operating cost for tribo-electrostatic belt separation is 75.8% of operating cost for flotation. The study's author concludes that the dry, tribo-electrostatic belt separation process offers obvious advantages in CAPEX, OPEX, and operational simplicity

CHARACTERIZATION OF GOLD MINERALS USING SEM, XRF AND LIBS TECHNIQUES

Gurinder K. Ahluwalia[1] and Jacquelyn Maccoon[2]

1. College of The North Atlantic, 1600 Nichols Adam Highway, Labrador city, NL, Canada
2. Hitachi high tech, Montreal Canada

24th World Mining Congress
MINING IN A WORLD OF INNOVATION
October 18-21, 2016 • Rio de Janeiro /RJ • Brazil

CHARACTERIZATION OF GOLD MINERALS USING SEM, XRF AND LIBS TECHNIQUES

ABSTRACT

The ability to more accurately determine the concentration of metallurgical and mineralogical properties of ore and precious metals prior to chemical treatment is vital to optimizing extraction process efficiency for the mining industry. In the present work we have characterized rock and mineral samples for estimation of gold content. The samples were obtained from a gold mining industry in the north eastern province of Newfoundland and Labrador in Canada. Three non-destructive techniques viz. Scanning Electron Microscopy (SEM), Laser Induced Breakdown spectroscopy (LIBS) and X-ray fluorescence (XRF) were for characterization. These techniques will be discussed in detail. SEM is an important tool whereby images of a sample are produced by scanning it with a focused beam of electrons. The electrons interact with atoms in the sample, producing various signals that can be detected and that contain information about the sample s surface topography and composition. The electron beam is generally scanned in a raster scan pattern, and the beam s position is combined with the detected signal to produce an image. Resolution better than 1 nanometer can be obtained using SEM. X-ray Fluorescence involves emission of characteristic "secondary" (or fluorescent) X-rays from a material that has been excited by bombarding with high-energy X-rays. The phenomenon is widely used for elemental and chemical analysis at the micro and nanometer scale. LIBS is a spark spectrochemical sensor technology in which a laser beam is directed at a sample to create a high temperature micro plasma and a detector used to collect the spectrum of light emission and record its intensity at specific wavelengths. We have made qualitative and quantitative investigations of the samples using the three techniques for the estimation of gold for the mining industry.

KEYWORDS

SEM, LIBS, XRF, Gold minerals, Mining

INTRODUCTION

In the present work we used three experimental techniques for quantitative and qualitative analysis of the powder and rock samples obtained from anaconda gold mining industry. The basic principles underlying the three are given below. Experimental results obtained using these techniques will be discussed in the following section.

1. Scanning Electron Microscopy (SEM)

Analysis of powder samples for determination of mineral content was done using a Hitachi SU3500 scanning electron microscope. A scanning electron microscope (SEM) produces images of a sample by scanning it with a focused beam of high energy electrons. The electron beam is scanned in a raster scan pattern, and the beam's position is combined with the detected signal to produce an image. SEM can achieve resolution better than 1 nanometer. The most common SEM mode is detection of secondary electrons emitted by atoms excited by the electron beam. The number of secondary electrons that can be detected depends, among other things, on the angle at which beam meets surface of specimen i.e. on specimen topography. By scanning the sample and collecting the secondary electrons that are emitted using a special detector, an image displaying the topography of the surface is created. The signals produced by an SEM include secondary electrons (SE), reflected or back-scattered electrons (BSE), photons of characteristic X-rays and light (cathodoluminescence) (CL), absorbed current (specimen current) and transmitted electrons. Secondary electron detectors are standard equipment in all SEMs. In the standard detection mode, secondary electron imaging or SEI, the secondary electrons are emitted from very close to the specimen surface. Consequently, SEM can produce very high-resolution images of a sample surface, revealing details less than 1 nm in size. Back-scattered electrons (BSE) are beam electrons that are reflected from the sample. The very narrow electron beam enables a large depth of field yielding a characteristic three-dimensional appearance useful for understanding the surface structure of a sample. A wide range of magnifications is possible, from about 10 times (about equivalent to that of a powerful hand-lens) to more than 500,000 times.

2. X-ray Fluorescence (XRF)

X-ray fluorescence (XRF) is the emission of characteristic "secondary" (or fluorescent) X-rays from a material that has been excited by bombarding with high-energy X-rays or gamma rays. The phenomenon is widely used for elemental and chemical analysis, particularly in the investigation of metals, rocks, glass, ceramics and building materials. Analytical measurements for elemental content can be classified in three ways:

1. Qualitative Analysis: Determination of identity of the elements comprising a sample with no information regarding the amount or concentration.
2. Semi-quantitative analysis: Quantitative analysis with additional information regarding the relative amounts of constituent elements. For XRF measurements the identity of all elements above the detection limit is established quickly with great accuracy. Use of sophisticated algorithms like Bayesian method employed by Bruker systems renders identification of all peaks with excellent certainty. In addition to this, the corrected and deconvoluted counts provide an excellent measure of the relative amounts of each element with respect to that element. For example, one can accurately assess the relative amounts of Fe across all samples but one cannot make any judgments on the relative amounts of Cr to Fe based on the corrected counts. For this one must have a suitable calibration data set.
3. Quantitative analysis: Identification of all elements present above the detection limit and their true concentrations based on calibration against a suitable data set with known standards. For XRF in particular these calibration standards must closely match the matrix, or general composition of the samples to be analyzed.

3. Laser Induced Breakdown spectroscopy (LIBS)

LIBS is a spark spectrochemical sensor technology in which a laser beam is directed at a sample to create a high temperature micro plasma and a detector used to collect the spectrum of light emission and record its intensity at specific wavelengths. In practice, detection limits are a function of the a) plasma excitation

temperature, b) light collection window, and c) line strength of the viewed transition. The optimization of LIBS event timing is important for efficient capture of high resolution line spectra. The optimum "gate" time for turning on the spectrometer, and avoiding the masking broadband bremsstrahlung emission, is typically one or two microseconds after the plasma initiation. Short femtosecond or picoseconds laser excitation pulse widths produce plasma with 10x faster bremsstrahlung continuum emission decay times. As a result of the shorter broadband background emission duration, ultra-short pulse LIBS allows for more efficient capture of fine line emission spectra often without the need for gated detectors. The detection limits for elements analyzed via LIBS technique are typically found in the parts per million (ppm) ranges. Detection limit values are influenced by matrix effects, instrumentation, environment and measurement parameters.

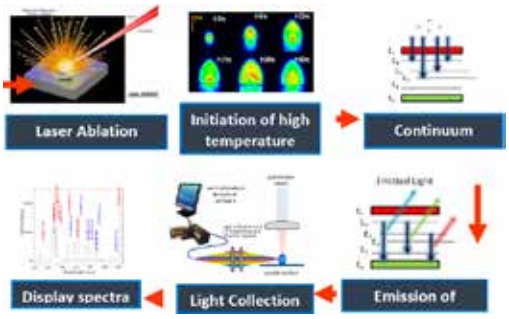

Figure 1- Schematic representation of the basis of LIBS technique

4. Comparison of techniques

Table 1 shows a comparison of different techniques for characterization of minerals.

Table 1- Comparison of different techniques for characterization of minerals

	SIMS	AES	SEM/EDS	XRF	GD-MS	LIBS
Depth profiling resolution	1 – 20 nm	10 -100 A	0.5 – 3 μm	> 1 μm	100 to 300 nm	30 to 100 nm
Lateral resolution	> 10 μm	0.01 - 2 μm	0.2 to 2 μm	10's μmto 1 mm	>1000 μm	10 μm
Measurement time for 2 micron film	hours	hours	minutes	minutes	10's minutes to hr	seconds
Detection limit	ppb	1000 to 10000 ppm	1000 to 10000 ppm	100 to 1000 ppm	Sub-ppm	ppm
Sample preparation	Minor sectioning to put into the sample holder	Little prep (sample must be conductive)	Coating with Ir or Au	Minor palletizing or little prep	Minor surfacing cleaning; mainly conductive sample	Little sample prep
Measurement environment	High vacuum	High vacuum	High vacuum	In air	High vacuum	In air/ in chamber with buffer gas
Elemental coverage	Most elements in the periodic table	Most elements in the periodic table (except H & He)	Difficult for elements lighter than Carbon	Difficult for elements lighter than Sodium	Most elements in the periodic table	Most elements in the periodic table
Instrument cost	500K to 1 Mil USD	350 to 500K USD	500 to 750K USD	80 to 150K USD	400 to 800 K USD	130 to 230K USD

EXPERIMENTAL RESULS AND DISCUSSION

1. SEM

SEM micrographs were taken on 16 powdered samples. Pictures and the quantitative spectra of two of them are shown in figures 2-7 indicating a clear presence of gold along with some other elements listed in Tables 2-4.

Sample 1

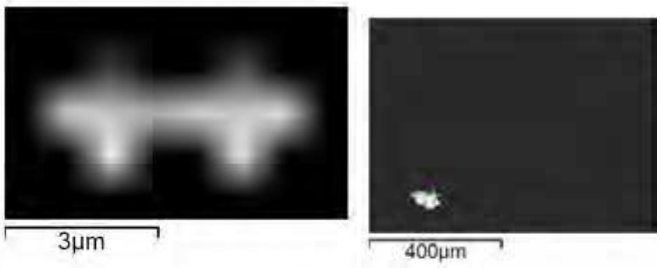

Figure 2- SEM micrograph of one of the samples at different scales

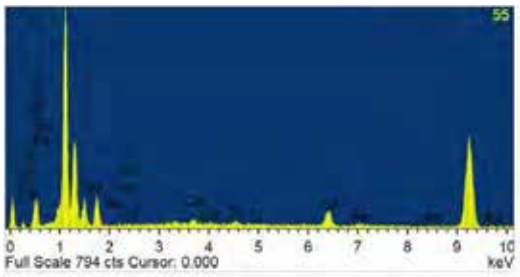

Figure 3- Quantitative results for sample 1 at position 1

Table 2- Quantitative results for sample 1 at position 1

Quant Results:

Name	Value	Error	Units
O	50.60	2.97	Wt%
Au	35.95	2.93	Wt%
Fe	10.06	0.91	Wt%
Ca	1.83	0.50	Wt%
Ti	1.48	0.53	Wt%
S	0.07	0.59	Wt%

Morphology Results:

Name	Value	Units
Area	6.97	sq. µm
Aspect Ratio	2.01	
Beam X	227.00	pixels
Beam Y	627.50	pixels
Breadth	2.52	µm
Direction	170.69	degrees
ECD	2.98	µm
Length	5.08	µm
Perimeter	12.78	µm
Shape	1.86	

Sample 1 position 2

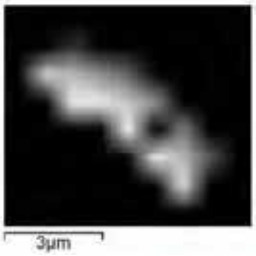

Figure 4 - SEM micrograph of the sample at position 2

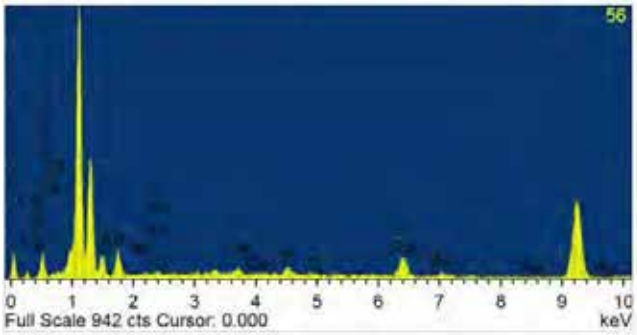

Figure 5 - Quantitative results for sample 1 at position 2

Table 3- Quantitative results for sample 1 at position 2

Quant Results:

Name	Value	Error	Units
O	47.34	3.34	Wt%
Au	32.35	3.41	Wt%
Fe	14.05	1.23	Wt%
Ti	3.78	0.84	Wt%
Ca	2.49	0.56	Wt%
S	0.00	0.00	Wt%

Morphology Results:

Name	Value	Units
Area	12.55	sq. µm
Aspect Ratio	2.36	
Beam X	236.00	pixels
Beam Y	627.50	pixels
Breadth	2.85	µm
Direction	150.94	degrees
ECD	4.00	µm
Length	6.73	µm
Perimeter	16.33	µm
Shape	1.89	

Sample 2

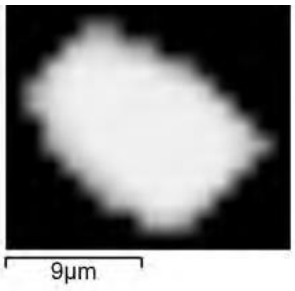

Figure 6- SEM micrograph of the second sample

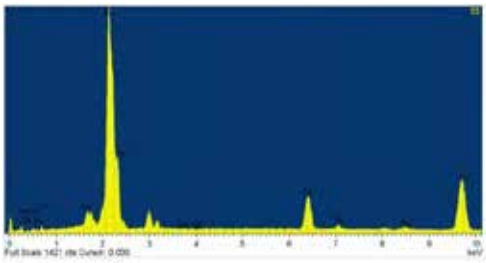

Figure 7 – Quantitative results for sample 2

Table 4 - Quantitative results for sample 2

Quant Results:				Matching Classes:	
Name	Value	Error	Units	Name	Rank
Au	78.86	1.70	Wt%	Au	1
Fe	16.27	0.86	Wt%	Marked	Marked
O	4.85	1.67	Wt%	Analysis Date: 8/20/2014 5:54:04 PM	
Ca	0.01	0.29	Wt%		

2. XRF

XRF data was taken on three samples and the results are summarized in table 5.

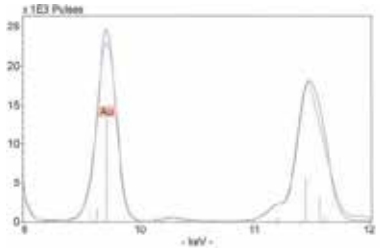

Figure 8 – Characteristic spectra of pure gold

Figure 8 shows the characteristic (gold) Au L-lines pattern. The red trace is the raw data and the blue trace is the Bayesian curve fit provided by the Bruker Artax software package. This curve fit is based on a Fundamental Parameters spectral correction and deconvolution algorithm and is an excellent confirmation tool. Figure 9 shows the spectra for one of the samples #23 with clear indication of the presence of gold. A separate set of measurements with an integration period of 180s were taken to enhance the detection of Au.

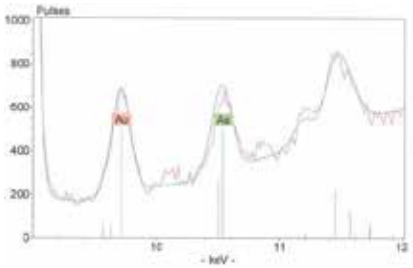

Figure 9 – XRF spectra of sample #23

A significant amount of arsenic was also detected in the samples.

Table 5- Results of XRF taken on three rock samples.

Corrected Counts	As	Au	Cr	Ga	W
15-P1	352	339	1300	1431	751
15-P2	697	229	645	1283	985
140922-P1	524	1084	188	1765	3516
140922-P2	927	716	99	1431	2141
140922-P3	481	-1	699	765	1261
140923-large-P1-gold colour	3689	3687	2029	80	311
140923-large-P2	1018	-1	320	717	387
140923-small-P1	655	0	1077	1	6940

3. LIBS:

All Samples were analyzed using ASI's J200 LIBS 266 EC. Samples analyzed in 3 areas containing different mineral types using 1 mm^2 raster areas. Gold colored mineral areas were compared with known Au sample. Analysis resulted in detection of elements associated with calcite ($CaCO_3$) and iron pyrite (FeS_2). Other detected major elements included Mg, K, Cu, Al, Si.

Figure 10- Sample #23 used for analysis using LIBS and XRF.

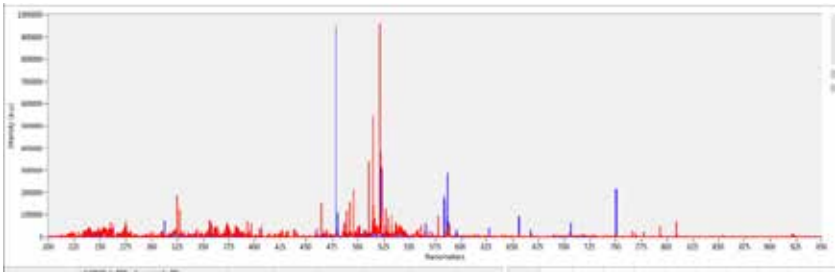

Figure 11 – LIBS spectra for sample #23

Conclusion

Composition and quantitative analysis was done for rock and powder samples obtained from gold mining industry. The techniques of SEM was found to be ideal for both analysis. XRF confirmed the presence of gold in the samples whereas LIBS provided marginally accurate results.

Acknowledgements: The author Gurinder K. Ahluwalia thankfully acknowledges the help provided by Scott McGeorge at Transition technologies for taking the XRF and LIBS data and Hitachi technologies for SEM analysis.

COAL MINE METHANE (CMM) FOR SAFE MINING & GREENHOUSE GAS REDUCTION

*Balaswamy Akala

Former CMD, Central Coalfields Ltd. & Central Mine Planning & Design Institute,
Secretary General, Indian Coal Forum,
Member, Intnl. Organizing Committee (IOC) of the World Mining Congress (WMC),
Member, Executive Committee of the Indian National Committee (INC) of WMC.
Tel: +91 44 n24415068, Cell: + 91 9899279391and + 91 9884062700

*(*Corresponding author: akala_b@yahoo.com)*

24th World Mining Congress
MINING IN A WORLD OF INNOVATION
October 18-21, 2016 • Rio de Janeiro /RJ • Brazil

COAL MINE METHANE (CMM) FOR SAFE MINING & GREENHOUSE GAS REDUCTION

ABSTRACT

Geologists knew that coal is a gas source rock, but, as this gas is in an adsorbed state, its potential was little known because of no gas show. Methane in coal seams, if allowed to remain, can form explosive mixture with mine air. Coalmining community always viewed methane as a menace and danger. But, once this gas is extracted either before mining, during mining or after mining; it is a form of energy. Depending upon how and from where it is extracted, it is called Coal Bed Methane (CBM), Coal Mine Methane (CMM), Abandoned Mine Methane (AMM) or Ventilation Mine Methane (VAM). CMM is the process of extracting methane either during or after coal mining operations.

Historically, coal mining and methane coexisted and many countries witnessed deadly explosions due to methane ignition. Though underground mechanization and mining techniques improved, the only way of keeping mines safe was by ventilation to reduce the concentration of methane in the mine air. However, following such disasters, US Bureau of Mines aggressively pursued research in 1970s to find ways to remove methane from coal seams before mining them and things became different in USA. Encouraged by the experiments conducted on the wells drilled in coal seams, using technology from the oil and gas industry, methane was extracted in advance of coal mining and mining started becoming safer and more productive. As a result, coal seams became CBM reservoir targets in early 1980s.

The paper delves with the necessity to pursue CMM process by discussing the background, benefits, viable methane recovery methods and the technology with a view to encourage and make the stake holders participate actively in U S Environmental Protection Agency's (EPA's) Coalbed Methane Outreach Program (CMOP). Methane must become the friend of miner in order to make this initiative a success. Reducing emissions, making it near zero, from active underground mines recovering and utilizing drained gas should be the ultimate goal of CMM process. EPA's CMM global initiative will have to yield such results to make the coal mining safer and convert it as a source of energy, besides reducing greenhouse gas and global warming.

KEYWORDS

CBM, CMM, AMM, VAM, EPA, CMOP, CIL, MTY, GRI, JWR, CONSOL

INTRODUCTION

Methane is an odorless, colorless and flammable gas, formed during coalification and in the coal seams, so formed; it stays in an adsorbed state. Because of its danger in underground mines, the coal mining community calls it “fire damp”. While mining coal in underground mines, it floats and gets concentrated as a layer on the roof portion of the workings. Being highly combustible, methane can form explosive mixture with the mine air. Mixture of 5 to 14% methane in mine air is highly explosive and is the cause of many mine disasters in the past

But, once methane is captured and recovered either before mining, during mining or after mining, it is a form of energy. It is called CBM, if extracted from coal seams before mining, CMM if extracted during mining and AMM if extracted after mining. Methane that is vented to the atmosphere from the mine ventilation system is normally called VAM. Removing fugitive methane gas from underground coal mines and using it in profitable and practical ways can improve worker safety, enhance mine productivity, increase revenues, and reduce greenhouse gas emissions.

PAST CONCEPTION

Coalmining community viewed methane as a menace and danger**.** The knowledge of methane occurring with coal beds is as old as the mining itself. However, it was treated more as a hazard than a resource. Being highly explosive, coalmines faced many deadly explosions in the past due to this gas and such explosions were a common occurrence due to inadequate ventilation in mines.

Geologists have long known coal as a source rock for many conventional reservoirs. However, until the early 1980s coal seams generally were not considered to be a reservoir target, even though producers often drilled through coal seams when going to deeper horizons. The potential of this resource was overlooked because often there was little or no gas show (because of its adsorbed state) and people did not believe that a thin, shallow horizon could contain economic quantities of gas. Moreover, coal seams initially produce water, not gas.

The first thing that any mining supervisor does in an underground coalmine, before doing other jobs, is to test for this gas in the coalfaces and in the general mine atmosphere so as to rule out its presence. He is well trained for gas testing and is, normally, the first examination that he needs to pass to become a mine supervisor. Gas in the coalface and in mine workings is a matter of danger. Immediate safety measures need be taken to remove the presence of gas and to keep the gas percentage levels within the permitted limits as per mines’ regulations. There are many instances where coal mining is stopped because of the danger created by methane. So, besides the danger, presence of methane in coalmines results adverse economic implications. There are cases, where the mining operations are temporarily stopped or even abandoned, for safety as well as economic reasons, when the gas emissions are excessive. This is how methane was conceived in the past.

COALMINING AND METHANE - HISTORY

Coal Mining

Large-scale coal mining started during the Industrial Revolution and coal provided the main source of primary energy for industry and transportation in the West from the 18th century to the 1950s. Coal remains an important energy source, due to its low cost and abundance when compared to other fuels, particularly for electricity generation. It is likely to remain so at least for the next 30 years or so. However,

coal is also mined today on a large scale by open pit methods wherever the coal strata strike the surface and is relatively shallow.

Britain developed the main techniques of underground coal mining from the late 18th century onward, with further impetus and technology improvement in 19th and early 20th century. Poland, Germany, France, Russia, USA, Australia, South Africa joined in pursuing underground coal mining methods and brought lot many improvements. So much so, the efficiency, production and productivity levels have surpassed expectations. Besides technological improvements, safety in mines also improved. In later years China too joined in the race and opened many underground mines. India kept its normal pace in underground technology and concentrated more on opencast mining methods.

Since 1970 environmental issues became increasingly important, including the health of miners, destruction of the landscape from strip mines and mountaintop removal, air pollution and coal combustion's contribution to climate change due to global warming. During the same period, oil and gas gradually started becoming alternative fuel to coal. The worldwide trend to replace coal as a source of energy, particularly for electricity, by oil, natural gas and new energy sources such as solar, wind, nuclear etc is gaining substantial momentum.

India has a long history of commercial coal mining covering nearly 220 years starting from 1774 by East India Company in the Raniganj Coalfield. The annual coal production, which was 6.12 mts in the year 1900 rose to 18 mts by the end of 1st World War (1920). After witnessing a slump in the early thirties, it rose to 30 mts by 1946. After Independence in 1947, the country embarked upon the 5-year development plans. At the beginning of the 1st Plan, annual production went upto 33 mts.

On account of safety, social and scientific reasons, the Central Government took a decision to nationalize the private coalmines. After the nationalization of coalmining in 1973, the mining activity in India proceeded in a systematic and scientific manner. Coal India Ltd. (CIL), the public sector holding company, is pursuing major part of the coal sector in the country. The country’s coal production in 2015 has reached to a level of 650.00 MTY. However, major proportion of coal is being produced from opencast mines at shallow depths. Acknowledging the need to extract more coal from deep seams, the country has taken many steps to encourage underground mining. In the year 1993, coal mining was opened to private operators engaged in steel/cement production and power generation, for their captive use. With the passing of Coal Mines (Special Provisions) Act 2015, wherein commercial coal mining is opened in the country, underground coal mining also will play a major contributory role and help increase the coal production in the future years to come.

Methane

Most of the explosions in the past were caused by methane (firedamp) ignitions followed by coal dust explosions. Coal Mining has always been dangerous, because of explosions, roof cave-ins, and the diffi-culty of mines rescue. To cite a few, the worst single disaster in British coal mining history was at Senghenydd in the South Wales coalfield. On the morning of 14 October 1813, an explosion and subsequent fire killed 436 men and boys. Only 72 bodies were recovered. It followed a series of many extensive Mining accidents in the Victorian era such as the Oaks explosion of 1866 and the Hartley Colliery Disaster of 1862.

China has suffered a string of deadly mining disasters, despite a nationwide safety crackdown. In 2004, there were more than 6400 deaths in floods, explosions and fires. In Northern China's Shaanxi province, an explosion in October 2003 killed 148 and a blast in November 2003 killed 166 miners. In Feb. 2005, a gas explosion in China’s Northeast Mine killed 203. This is the deadliest such disaster reported since Communist Rule began in 1949.

Poland, though has a remarkably good mine safety record, too witnessed gas explosions in the past. 8 (eight) miners died in 2006 and 15 trapped in a deep underground coal mine in South Poland.

In USA too, many disaters occurred due to gas explosions.The Monongah Mine disaster of Monongah West Virginia 6 December 1907 was the worst of many mining disasters in American history. The explosion was caused by the ignition of methane gas (also called "firedamp"), which in turn ignited the coal dust. The lives of 362 men were lost in the underground explosion.

In India, 7 (seven) gas (firedamp) explosions occurred in the last 55 years, killing 394 workmen in all. The deadliest was in Chinnakuri colliery of Raniganj coalfield, West Bengal, in the year 1958, killing 175 workmen. In 1965, at Dhori Colliery, East Bokaro Coalfield, Jharkhand, 265 men died in a coal dust explosion, said to be initiated by firedamp. Even after the year 2000, there were as many as 8 major gas explosions, across the coal producing countries, claiming many lives in coal mines. They were:

Year	Country	Number of fatalities
2005	China	214
2006	USA	12
2006	Kazakhstan	43
2006	India	50
2007	Russia	108
2007	Ukraine	80
2010	USA	29
2010	Turkey	30

CHANGE IN OUTLOOK

Following series of gas disasters in coal mines across the world and in USA, US Bureau of Mines aggressively pursued research to find ways to remove methane from coal seams before mining them. In 1971, the Bureau began installing five-spot well patterns at eleven locations across the United States, and conducted experiments on these wells using technology from the oil and gas industry. Production rates from these initial wells were less than 10 Mcfd. After stimulating the wells with hydraulic fracture treatments, one well in the Warrior Basin produced 50 Mcfd. This initial success led to the drilling of additional wells in the Warrior Basin during the mid and late 1970s.

Concurrent with the Warrior Basin projects, Amoco Production Company began developing technology for producing gas from coal seams in the western United States. Amoco's first major success came in the San Juan Basin with the Cahn #1 well. After this well was de-watered for twelve months, its production rate reached 1 MMcfd. This success initiated the Coalbed gas development of the Cedar Hill Field in this western basin.

In 1983, the Gas Research Institute (GRI) initiated research that catalyzed the development of Co-albed gas as a new source of natural gas. At the end of 1983, there were some 165 CBM wells in the United States with an estimated total annual production of 67 Bcf. By the end of 1993, annual production had increased to 705 Bcf from 6500 wells. To date, the Warrior Basin and the San Juan Basin have been the most active Coalbed gas areas in the United States. As producers in the United States began to better unders-tand Coalbed gas production mechanisms, adapt well completion technology, and hear of Coalbed gas suc-cesses, they came to view Coalbed gas not as a mining hazard, but as an important component in the U.S. domestic natural gas supply.

CBM can be ideal fuel for co-generation power to bring in higher efficiency and is a preferred fuel for new thermal power plant on important counts such as lower capital investment, higher operational efficiency and environmental friendliness. CBM is a potential energy resource in many of the major coal mining countries of the world. Extraction of methane beforehand and during mining, as an additional energy source, is not only economically and environmentally profitable, but also makes the underground mining safer by reducing the degree of gassiness in mines.

Since the beginning of the Coalbed gas industry, operators have relied greatly on technology from the mining and petroleum industries to evaluate and develop Coalbed gas properties. Much of this conventional oil and gas technology applies to Coalbed gas operations, but often it must be modified. In some cases, Coalbed gas operations require entirely different techniques. The unique characteristics of coal reservoirs often are responsible for the need to use a different engineering approach.

The success of CBM production in the United States has sparked intense interest worldwide, particu-larly among several coal-rich nations in Eastern Europe and Asia. Leaders in these countries view Coalbed methane as a key strategic resource for gaining energy independence. In an effort to develop this resource, these countries are actively seeking Coalbed methane technology from the United States.

Development of CBM in India has started in 90s. So, methane, the 'firedamp' has become 'sweet gas', be-cause of its lack of hydrogen sulfide and 'Coalbed Methane (CBM)' because of its utility as enegry.

CAPTURING METHANE

Having realized the danger that methane poses in the coalmines and understood the reservoir characteristics where this useful gas is stored in coal seams and shales, the only way left to mitigate its danger and to reap the benefits is to capture it from source. In the process of pursuing this objective, efforts were initiated to degasify the coal seams, in advance, from the underground workings. The purpose was to simply reduce the gas emission, and so the associated danger, to the mine workings in the coal seams being worked. Therefore, the gas so captured by drilling holes (in seam) from the underground workings, was simply vented out to the atmosphere. In due course, the process, which started as a degasification, got diversified and strengthened by improvised methods and resorting to use the gas that was extracted.

Coalmines already employ a range of technologies for recovering methane. These methods have been developed primarily for safety reasons, as a supplement to ventilation systems. The major degasification techniques used at U.S. coalmines are vertical wells (from surface), long-hole and short-hole horizontal boreholes (in seam), and gob wells (from surface). Vertical wells and in-mine horizontal boreholes, which recover methane in advance of mining, produce nearly pure methane. In contrast, gob wells, which recover post-mining methane, may recover methane that has been mixed with mine air.

The quality of the gas determines how it may be used. Methane recovered from degasification can be used for pipeline injection, power generation, on-site use in a thermal coal drying facility, or sale to nearby commercial or industrial facilities. At present, most recovered coalmine methane is sold through natural gas pipelines.

Even where degasification systems are used, mines still emit significant quantities of methane via ventilation systems. Currently, technologies are in development that would catalytically oxidize the low con-centrations of methane in ventilation air, producing usable thermal heat as a by-product. Mines that are already recovering methane represent opportunities for utilities to work with the mine operators to develop a use strategy for the gas that is already being recovered. Utilities may also be able to participate in projects at coalmines that are not currently recovering any methane in conjunction with mining, by implementing pro-jects that include both gas recovery and utilization

CBM DEVELOPMENT PROCESS

Here, the discussion on CBM is restricted, as a prelude, only to understand and pursue CMM in the coal mines. The CBM or CMM development process will mainly depend upon the total gas content in the given coal seam. Coal, being a source rock and a reservoir rock for methane, is the result of depositional environment and burial history of plant matter that affects the composition of gas as well as gas content, diffusivity, permeability and the gas storage capacity of coal. Coalbed Methane (CBM) is the phrase used, when methane is extracted from the virgin coal basins where coal mining will not take place for long time to come. For this purpose, this is also called Virgin Coalbed Methane (VCBM). Extraction of CBM is classified as production from an unconventional reservoir, mainly due to the absence of a conventional trapping me-chanism. In a coal bed reservoir, methane gas is adsorbed to molecular structure of the coals and is therefore trapped in this state by natural pressure equilibrium. Whereas, in conventional sandstone and limestone re-servoirs, gas occurs in a free or dissolved phase, but in CBM reservoirs, gas exists more or less in a condensed, liquid- like state. Coal has high micro-porosity with large internal surface areas and, therefore, adsorbs and retains large amounts of gas.

Coal reservoirs often require pumping water before gas is produced to reduce reservoir pressure and release the gas. Commercial CBM production typically requires a physical process called desorption, which reduces the natural pressures on the reservoir and allows methane gas and water to flow out (detach) from the coals. Desorption can be induced through drilling and, in many cases, a process called dewatering. Most CBM plays require the drilling, completion and production of several adjacent wells to adequately reduce the pressure in the coals.

Dewatering simply involves the production of water from the coal seams. During the dewatering phase, which can last from 6 to 36 months, methane gas production typically accelerates and water production declines. CBM properties typically have long economic lives, ranging from 10 to 25 years. The three principal factors that determine the ultimate recovery of methane gas from coal beds are:

1. The permeability or flow characteristics of the coals, which are related to depth and fracturing.
2. The thickness of the coals.
3. The gas content of the coals.

Generally, most CBM is produced from bituminous coals, which are medium rank coals that are between lignite (low rank, low heat content) and anthracite (high rank, high heat content). Because of these and other coal reservoir characteristics, successfully developing a coalbed gas property, as a CBM Project, requires careful evaluation of the geologic and reservoir properties.

STATUS OF CBM DEVELOPMENT

CBM is a form of natural gas extracted from coal beds. In recent decades it has become an important source of energy in United States, Canada, and other countries. Australia has rich deposits where it is known as coal seam gas. Also called coalbed gas, the term refers to methane adsorbed into the solid matrix of the coal. It is called 'sweet gas' because of its lack of hydrogen sulfide.

It was the United States of America where the CBM development process started first, as far back as, in 70s. As years passed, it became so prominent that CBM constituted a substantial 10% of natural gas production in the country. So much so, there were as many as 24,000 CBM wells in Powder River basin alone. The production which peaked to 1.966 tcf in 2008 came down to 1.71 tcf in 2011 and further to 1.404 tcf in 2014. Most of the CBM plays are in the Rocky Mountain States of Colorado, Wyoming and New Mexico, besides Alabama.

In Australia commercial recovery of CBM began in 1996. As of 2013, production from Bowen, Surat and Sydney basins of Queensland and New South Wales made up about ten percent of Australia's gas production. Demonstrated reserves were estimated to be 33 trillion cubic feet as of January 2012.

In Canada too, Western Canadian Sedimentary Basin (WCSB) is a vast sedimentary basin underlying 1,400,000 square kilometres (540,000 sq mi) of Western Canada including southwestern

Manitoba, southern Saskatchewan, Alberta, northeastern British Columbia and the southwest corner of the Northwest Territories. It contains about 90 percent of Canada's usable coal resources, and so the CBM, with a massive wedge of sedimentary rock extending from the Rocky Mountains in the west to the Canadian Shield in the east.

As of 2013, Alberta, which is estimated to have about 170 trillion cubic feet (4.8 trillion cubic metres) of economically recoverable coalbed methane, is the only province with commercial coalbed methane wells. British Columbia is estimated to have approximately 90 trillion cubic feet (2.5 trillion cubic metres) of coalbed gas.

Kazakhstan, could witness large scale CBM development process in the years to cone. The country is said to have an estimated reserves of 900 billion m3 of gas in its main coalfields.

China is one of the world's leading coal producers and consumers and boasts a total of 30-35 trillion cubic meters of CBM resources. However, the country had the highest rate of coalmine accident fatalities in the world. Methane, which is blamed for 70 percent to 80 percent of the coalmine accidents nationwide, is the No. 1 killer factor that endangers coalmine security. Therefore, Methane captures and harnessing has won greater attention from the Chinese government. Coalmine gas harnessing is paramount in China's endeavor to improve safety in coalmines across the country. Though it is considered as an arduous, complicated and long-standing task to harness gas and prevent gas accidents in coalmines, the country has determined to pursue CBM/CMM development process, The country's partnership and cooperation with the American companies is expected ti yield fruits in the efforts to probe for effective ways to harness and make a good of use of gas, Most advanced construction technology in the CBM environment, namely the unbalanced multi-lateral horizontal well drilling technique, has been introduced to sink three new test wells in Laochang of Yunnan and Shouyang of north China's Shanxi Province.

In India, the CBM potential is estimated to more than 162 TCF (4.6 TCM). 33 blocks have been allotted till now, out of which 4 blocks are producing about 8 mscmd of gas and 3 are ready to produce.

CMM AND COAL MINING

CMM is the phrase used, in the context, where methane is extracted to degasify the coal seam in advance, with a view to minimize gas emissions in to the proposed working mine, which otherwise would have made its way in to the mine workings and made it unsafe for mining operations. It is also used in the context when methane is extracted from the working mines or from the abandoned mines. In recent years, several of the gassiest mines have begun making beneficial use of recovered gas, primarily sales into the pipeline system. Most coalmine methane recovery in the U.S. is at active underground mines, with the remainder from inactive or abandoned underground mines. Because the distribution of gassiness among underground mines is so skewed, a small number of the very gassy mines have offered the greatest need to degasify as well as the greatest economic opportunities to use the gas.

Methane is released during mining and post-mining activities. Methane emissions are typically divided into the following categories:

1. Underground Mining: In underground mining, methane is released into the mine workings during mining. Mining regulations require methane to be diluted in the ventilation air, and then vented to the atmosphere. Mines can also remove methane before and during mining by using degasification systems. The gas can be vented, flared (not currently done in many countries), or recovered for its energy content. Emissions are reduced if recovered gas is flared or used. Up to 50 to 60 percent of methane can typically be recovered with degasification.

2. Surface Mining: During surface mining, methane is released directly to the atmosphere as the overlying rock strata are removed. No emissions mitigation options are being used at this time. In

theory, some pre-mining degasification and recovery could occur at gassy surface mines. However, the low gas content of surface mines relative to that of underground mines makes it unlikely that significant recovery would be technically feasible, let alone cost-effective.

3. Post-Mining Activities: Some methane still remains in the coal after mining and is released during subsequent processing and transportation of coal. No proven mitigation options exist at this time.

4. Abandoned Mines. Methane emissions from closed or abandoned mines are not quantified and not included in inventory estimates, but may be significant. In some cases, degasification techniques can, and have been used to, remove methane from abandoned underground mines. There is uncertainty as to whether and at what rate the methane present in these mines would have been emitted

A Success Story of CMM Operation in the US is the combined operation of mining coal from deep underground coalmines by Jim Walter Resources, Inc (JWR) and extraction of methane in advance by Black Warrior Methane Corp. in the state of Alabama, USA. It comprises of mining high quality coal from Alabama's Blue Creek seam from 3 deep (around 1800 ft) underground mines and related methane gas operations. The growth and success of Jim Walter Resources' coal mining operations have continued to fuel the success of the company's coal seam degasification business. Black Warrior Methane Corpn. was formed in 1981 to recover and market methane gas principally from the Blue Creek Coal seam on lands owned or leased by the company. The original motivation for the business was to reduce, in advance of mining, the level of methane concentrations in and around the mining operations and to augment productivity by decreasing the amount of gas to be ventilated from the mines. Today, it represents one of the most extensive and comprehensive commercial programs for coal seam degasification in the United States, producing more than 30 mcfd of gas from its 400-plus wells.

Another example of successful CMM plays, from 1980s, is the combined coal and gas extraction by CONSOL Energy Inc. Their coal mines are highly technical operating environments that require specialized training. The technological advances and CMM operations, which include coal bed methane extraction, have helped make the mining process safer and more productive. Simultaneous operation of coal mines and the gas wells in their leaseholds help improve mine safety and higher coal productivity.

CONSOL’s Coal Division operates 12 coal mining complexes in four states in the United States, including Pennsylvania, West Virginia, Virginia and Utah and produces more than 65 million tons of coal. CONSOL’s Gas Division includes yearly production of nearly 128 billion cubic feet of coalbed methane.

These leading companies use three methods for extracting methane from coal seams:

1. Vertical wells drilled from the surface;
2. Underground horizontal drilling used primarily for improving longwall operations; and
3. Gob wells which pump gas from the area left after longwall mining has taken place.

CMM Potential in India

In India, Jharia Coalfield has been a storehouse of Medium Coking Coals (Vitrinite reflectance 0.9 to 1.3%) and has been mined extensively during the past, mostly through vertical shafts. Most of the workings are goaved and few are also standing on pillars. Coal mining areas of CIL and other coal blocks hold at least 30% of the estimated 75 billion tonnes of coal resources in India. These coal mines are spread in eight states, which are estimated to have 50 tcf (1.4 tcm) of CBM reserves. Many of its acreage are gaseous and unsafe mines, where safe mining of coal is possible only after the extraction of CBM and, therefore, come under potential CMM plays for the capture and utilization of methane from the existing as well as the abandoned coal mines.

The idea is to capture methane from the identified mines or group of mines, collect the gas so captured and utilize it for power generation. The capture/degasification system can be of three types, namely (1) before/ahead of (ii) during (iii) after mining. All three methods are required to be applied in the mines identified for the project, because these mines are in different stages of mining. Four methods, which are proven, can be adopted for extraction of methane. They are

1. Vertical Wells for ahead of mining, wherein vertical wells are drilled through coal seam(s) and completed by hydro fracturing or open hole cavitations for extraction and draining gas prior to mining.

2. Cross Measure Boreholes for pre-draining the overlying strata, wherein long holes are drilled at an angle to the strata from the existing mine entries to pre drain the overlying strata.

3. Horizontal Wells for during mining, wherein long holes are drilled into the coal seams from development entries of the mine to drain gas from the un-mined areas of coal seams. Higher recovery is expected in Roof & Pillar sections by drilling longer holes far in advance of mining. In this case as well as in the case of cross measure boreholes, gas transmission line and vertical borehole will be used to transport methane to surface.

4. Gob Wells for abandoned mines, wherein predrilled gob well (just above the roof of the lower most coal seam being worked) is drilled to drain gas from the worked out panels.

There is huge potential to capture and collect methane gas from selected group of underground coalmines in Jharia and Raniganj coalfields of India and utilize the gas, so collected, by mixing it together with waste coal/washery rejects for power generation. The activities can be planned for near term methane recovery, designed for cost effective operation and expected to be financially supporting. Methane from Coalbed (CBM) and coalmine (CMM) is an emerging energy resource and if not extracted before and in conjunction with mining of coal, would vent away causing loss of valuable environment friendly energy and also will bring damage to environment. This is an innovative programme, the first of its kind in India, by which methane being a green house gas and a hazard for coal mining would not be allowed to mix with the atmosphere. As a result, this project will help reduce global methane emission to a small, but useful extent..

MINES SAFETY

Mining is the oldest means by which the mankind has progressed to the stage that we see today. In spite of the fact that it was, and is, hazardous; mining continues to be the basic requirement for sustaining the progress. The basic human instinct to safeguard life has contributed to make and keep mining as safe as possible.

The two factors that were bothering mining community, right from the beginning, were the uncertainty in the rock behavior (that caused innumerable accidents both in numbers and deaths) and the gas (that was causing a sense of fear and havoc in coal mining due to ignitions and explosions) all over the world. Both the factors drew the attention of the research agencies and, as a result of concerted and continued efforts; these are, to a very large extent kept under control. The consoling factor is that, now we know how to deal with these hazards.

Coming to methane and mines safety, there are only two ways of handling it in coal mining. The first is the age old and tested method to keep it away from the mine workings by adequately ventilating the coal faces and the general mine atmosphere so that the methane percentage in the mine air is never allowed to become explosive. The second method is to drain the gas from coal seam in advance, so that its emission to mine workings is reduced to the minimum and does not bother the coalmining operations in as much proportion as it would have had it not been drained in advance.

However, the fact of the matter is that a combination of both would be required for ensuring guaranteed safety in mines on account of methane emission in to the mine workings. This is how; the firedamp (methane the menace) can be made as a mate and a friend.

GLOBAL CMM INITIATIVE

Efforts are on, globally, to capture methane from source in the coal seams so that it does not become a gas of danger but to be of use as energy. In the process, the methane, the GHG, emission is also reduced to help protect environment. The effective program that is being pursued is the EPA's Coalbed Methane Outreach Program (CMOP), which is a voluntary program with a goal of reducing methane emissions from coal mining activities. CMOP's mission is to promote the profitable recovery and utilization of coal mine methane (CMM). Coal mine methane is a potent greenhouse gas that contributes to climate change if emitted to the atmosphere. CMM can also create an explosive hazard inside mines. But if CMM is recovered safely and used for energy, it is a valuable, clean-burning fuel source.

Since 1994, CMOP has worked cooperatively with the coal mining industry in the U.S. and internationally to reduce CMM emissions. By helping to identify and implement methods to recover and use CMM instead of emitting it to the atmosphere, CMOP has played a key role in the United States' efforts to reduce greenhouse gas emissions and address global climate change. The goal is:

- To reduce greenhouse gas emissions
- To achieve the profitable recovery and use of CMM
- To promote use of a clean energy source

The extent of Methane Emissions from Coal Mines is very large. In underground mines, it can create an explosive hazard to coal miners, so it is removed through ventilation systems. In some instances, it is necessary to supplement the ventilation with a degasification system consisting of a network of boreholes and gas pipelines. In abandoned mines and surface mines, methane might also escape to the atmosphere through natural fissures or other diffuse sources. Coal mine methane is emitted from five sources:

- Degasification systems at underground coal mines (also commonly referred to as drainage systems). These systems may employ vertical and/or horizontal wells to recover methane in advance of mining (known as "pre-mine drainage") or after mining (called "gob" or "goaf" wells).
- Ventilation air from underground mines, which contains dilute concentrations of methane.
- Abandoned or closed mines, from which methane may seep out through vent holes or through fissures or cracks in the ground.
- Surface mines, from which methane in the coal seams is directly exposed to the atmosphere.
- Fugitive emissions from post-mining operations, in which coal continues to emit methane as it is stored in piles and transported.

International Emissions of CMM

Coal mine methane emissions are globally distributed among the world's key coal-producing countries. Methane is a well-mixed gas in the atmosphere and emissions reductions anywhere in the world are important to reducing the total global burden of CMM emissions. The global CMM emissions total 120 MMTCE. The pie diagram appended below shows the county wise percentage of CMM emissions. While China emits around 40% of methane from coal related activity, US come second in line. Therefore these countries need to take concerted steps to reduce the emissions. That does not mean that other countries may relax. As the ultimate goal is to make the emissions near zero, all other countries also need to take steps in the direction of reducing methane emissions.

For many years, CMOP has been actively engaged to help promote recovery and utilization of coal mine methane in many key coal-producing countries, including China, India, Poland, the Russian Federation, and Ukraine.

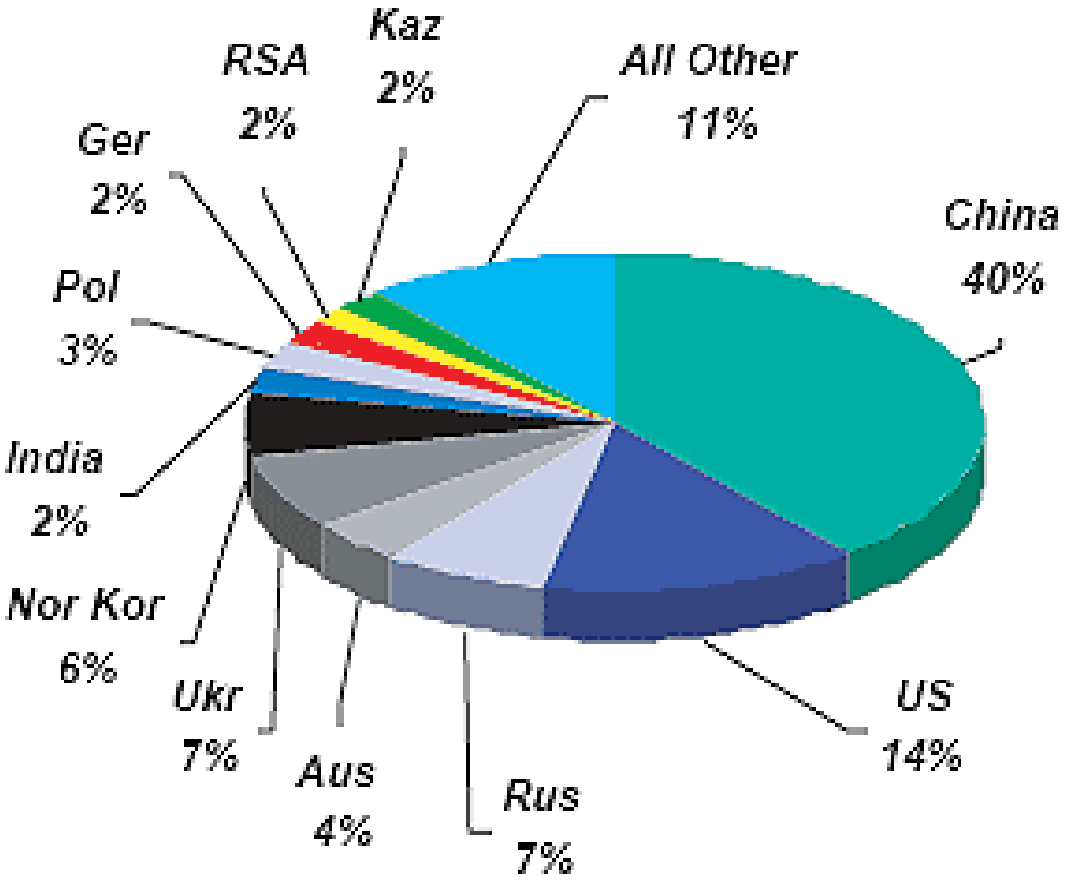

Benefits of Capturing and Using Coal Mine Methane

There are numerous benefits to capturing and using coal mine methane, including:

- Reducing greenhouse gas emissions
- Conserving a local source of valuable, clean-burning energy
- Enhancing mine safety by reducing in-mine concentrations of methane
- Providing revenue to the mine

Recovery and Use of Coal Mine Methane

Technology is readily available to recover methane – the major component of natural gas – from coal mines. Specific CMM end-uses depend on the gas quality, especially the concentration of methane and the presence of other contaminants.

Worldwide, CMM is most often used for power generation, district heating, boiler fuel, or town gas, or it is sold to natural gas pipeline systems. CMM can also be used in many other ways:

- Coal drying
- Heat source for mine ventilation air

- Supplemental fuel for mine boilers
- Vehicle fuel as compressed or liquefied natural gas (LNG)
- Manufacturing feedstock
- Fuel source for fuel cells

Viable methane recovery and use projects are significant, even in the absence of a price signal for methane emissions. As the breakeven price for methane reductions rises, the mitigation potential grows.

Accomplishments

EPA's CMOP has assisted the coal mining industry in successfully increasing its methane recovery by 50 percent between 1994, when the program was launched, and 2009. These emissions reductions are due to active underground mines recovering and utilizing drained gas. In 2009, the U.S. coal mining industry recovered and used about 81 percent of all drained coal mine methane (CMM).

Between 1994 and 2009, U.S. CMM emissions reductions have effectively removed the equivalent of more than 263 million metric tons of carbon dioxide from the atmosphere. These avoided emissions are equivalent to 654 billion cubic feet of methane – 588 from active underground mines and the remaining 66 from abandoned underground mines.

CMOP has been successful in encouraging and facilitating the development of environmentally friendly and economically sound CMM recovery and utilization projects. Accomplishments since the program's launch in 1994 include the following:

- CMOP has developed detailed profiles of 50 active underground coal mines that represent opportunities for recovering and using coal mine methane.
- CMOP has prepared assessments for project opportunities at abandoned underground coal mines and surface coal mines.
- There are currently about 14 coal mine methane recovery and utilization projects at active underground coal mines, and about 38 projects recovering methane from abandoned underground coal mines.

CONCLUSION

The map below shows such countries where the EPA’s CMOP has worked around the world for over a decade to bring awareness, pass on the knowledge and practice the right practices to capture methane in advance, during and after coal mining for promoting the coal mine methane (CMM) development and use.

EPA has supported 17 grants for projects promoting coal mine methane recovery and utilization under the Global Methane Initiative. To date, these projects are located in China, India, Mongolia, Nigeria, and Poland. The Global Methane Initiative, CMOP also supports Coal mine/Coalbed methane (CMM/CBM) Clearinghouses or other in-country collaborative efforts in numerous countries, including the following China, India, Kazakhstan, Poland, Russian Federation and Ukraine. CMOP also works in close collaboration with the United Nations Economic Commission for Europe (UN-ECE) and with the International Energy Agency (IEA) on coal mine methane issues. The IEA recently published a report that documents successful methane recovery and use policies around the world.

.

Methane must become the friend of miner in order to make this initiative a success. Had the mining engineer started capturing methane and removed it from the coal seams before mining, the coal mining history would have been different. It is better late than never and the future mining should be free from methane emissions from the mine workings. CMM global initiative will have to yield such results to make the coal mining safe, besides reducing global warming.

REFERENCES

EIA's and CMOP's Publications

COMPUTATIONAL FLUID DYNAMICS SIMULATION OF COOLING SYSTEM FOR COPPER SMELTER GASES BY TENIENTE CONVERTER WITH EVAPORATIVE COOLER

*S. Pérez [a], Y. Aguilera [a], J. Hurtado [a], J. Vargas [a]

[a] *Universidad de Santiago de Chile, Avenida Libertador Bernardo O'Higgins nº 3363, Santiago, Chile*

*(*Corresponding author: sebastian.perez@usach.cl)*

24th World Mining Congress
MINING IN A WORLD OF INNOVATION
October 18-21, 2016 • Rio de Janeiro /RJ • Brazil

ABSTRACT COMPUTATIONAL FLUID DYNAMICS SIMULATION OF COOLING SYSTEM FOR COPPER SMELTER GASES BY TENIENTE CONVERTER WITH EVAPORATIVE COOLER

ABSTRACT

In smelting copper sulphide gases from the Teniente type copper convertor are highly corrosive and toxic, which must be treated to avoid environment impacting.

In the present study, a simulation methodology for system of capturing and cooling gases is proposed by means of Computational Fluid Dynamics (CFD), which considerate the collection hood and evaporative cooler for gases from Teniente copper convertor.

Using the proposed methodology is possible to obtain a simulation model of the behavior of gases produce in Teniente Copper Convertor with an error between 3% and 13%. This indicates that in practical terms the trends for metallurgical gases along its route by the hood and cooling chamber are reliable to predict the dynamic thermal behavior of the gas fluid within the network management gases studied.

KEYWORDS

collection hood – Computational Fluid Dynamics simulation – Evaporative Cooler – Gases from Copper Sulfides smelting

INTRODUCTION

Generally, the percentage of mine copper (Assays), is about 1% value, very distant from 99.99% purity copper should have to be marketed, and therefore it is necessary to process the ore into several stages to achieve the required purity for marketing [18]. In the case of copper sulfide minerals, once the rock is removed from the mine, it is transported to the concentrator plant, where it is subjected to crushing and grinding processes to then be concentrated by the flotation process. The concentrate from the concentrator plant contains about 30 to 35% copper, which is filtered and sent to the smelter to continue the process.

In the smelter, the concentrate is subjected to fusion and conversion, which in this case is done in a Teniente type converter [18]. This equipment operates at high temperatures to smelt the concentrate. At this stage of the process an important release of gases is produced at high temperature.

Some of the main chemical reactions generated in the fusion of copper sulphide which allow to observe the composition of the smelter gases are described in equations 1 to 7:

$$2CuFeS_{2(s)} + O_{2(g)} = Cu_2S + 2FeS + SO_{2(g)} \quad \text{Equation (1)}$$

$$FeS_{2(s)} + O_{2(g)} = FeS + SO_{s(g)} \quad \text{Equation (2)}$$

$$Cu_5FeS_{4(s)} + O_{2(g)} = 5Cu_2S + FeS + SO_{2(g)} \quad \text{Equation (3)}$$

$$2CuS_{(s)} + O_{2(g)} = Cu_2S + SO_{2(g)} \quad \text{Equation (4)}$$

$$FeS_{(l)} + \frac{3}{2}O_{2(g)} = FeO + SO_{2(g)} \quad \text{Equation (5)}$$

$$3FeO + \frac{1}{2}O_{2(g)} = Fe_3O_4 \quad \text{Equation (6)}$$

$$2FeO + SiO_2 = Fe_2SiO_4 \quad \text{Equation (7)}$$

The generated gas due to fusion and conversion of copper concentrates mainly contain SO_2. Also, in the industrial process it contains variable parts of acid fog, H_2O, arsenic, selenium, among others, it is captured and sent to the gas managing system where gas conditioning is performed and which supplies the gas cleaning plants (GCP) to free them of dust, acid fog and other impurities, leaving a high SO_2 content gas, which is converted into SO_3 and which is reacted with water to produce H_2SO_4 [9].

The process line conditioning gases before reaching the gas cleaning plant consists of several teams which perform critical functions such as capturing, cooling and primary cleaning of particulate matter suspended in the gases. Each of these functions must satisfy specific conditions required for the proper operation of the gas handling system and of the following processes in the gas treatment line, mainly the gas cleaning plant.

In this study, a new methodology is developed through computer simutaltion of fluid mechanics of transfer phenomena associated with the fluid dynamics of the gas collection hood in the evaporative cooler. This makes it possible to better understand the phenomena that govern the process and their interactions.

METHODOLOGY

The work focuses on modeling and computer simulation from the point of view of thermo fluid dynamics, which includes heat transfer phenomena for two of the main components of gas management network in the CT line in Caletones smelter. These correspond to the first section of the network and are composed of the gas collection hood [5] and the evaporative cooler [8].

The studied gas management network begins with the collection of the gases released from the Teniente converters to the gas hood placed over the converter [10] which has the task of capturing and cooling the gases entering the hood due to pressure differences [17] caused by induced draft fans located downstream of the network. In the gas hood, the first cooling stage takes place [16] mainly due to gas dilution with air at room temperature (average temperature 25 ° C) and mixed with the process gas produced from the melting converter, where temperature drop is estimated from 1200 ° C to approximately 600 ° C [15].

After being captured and diluted, the gas this passes through the evaporative cooling chamber, where there are lances that inject air and cold water to the gas flow. This system uses evaporated water combined with a humidified medium to cool the gas temperature as it passes through the chamber [19]. The gas temperature drops to about 350 ° C due to phase change from liquid to steam.

Reaching a temperature close to 350 ° C is an important operating parameter because it is the temperature required for the operation in the following process, consisting in the gas cleaning by the electro-static precipitator.

The present study was performed by modeling and computer simulation of the gas passing through these devices [11, 14] using ANSYS CFX software.

Modeling is conducted based on certain assumptions such as:

- Equipment discretization is performed considering the structural drawings of the smelting.
- Modeling was done considering species, depending on the generation of metallurgical gases.
- The gases behave as ideal gas.

- Steady state flow.

- Environmental conditions considered are 81,060 Pascal pressure at 25 ° C temperature (temperature around the smelting sections).

1.1. **Simulation Methodology**

The steps for carrying out the simulation are summarized as follows:

1.- Generation of three-dimensional geometry of the capturing hood and evaporative cooler.

2.- Geometry meshing.

3.- Definition of boundary conditions

4.- Simulation

5.- Validation of results

2.2 Theory of Physical Models

Computational fluid dynamics is a tool that is based on solving the transport equations in each control volume for a volumetric discretization of the domain [14].
The number of transport equations to be solved depends on the number of models necessary to describe the fluid dynamics of the problem of interest [7].

To model the behavior of the gas mixture in the converter output a model species or multi-component is chose [4], since it is used for molecular gas interactions and all calculated variables are weighted by the mass fractions of each component.

The species transport model does not allow chemical reactions, this assumption is acceptable, since the percentage of SO_2 converted into SO_3 corresponds to figures below 3%.

The turbulence model used for this work is called "Shear Stress Model" (SST) which effectively combines the robustness and accuracy of the *k-omega* model near the wall with model *k-epsilon,* which is an appropriate model in fields away from wall [13].

Spray System Modeling

One of the main mechanisms of heat transfer in the evaporative cooling chamber for the gases from the Teniente converter is by changing the water's liquid-gas phase through a SONIC type spray nozzles mechanism which inject water by air pressure into the hot gases entering the cooling chamber.

This research models the heat absorbed by the lances through a thermal sink represented by the volume of the cone of dispersion produced by spray nozzles, and enter a source of mass at the base of the cone, considering the effect of the entering mass.

The geometrical parameters necessary to describe the volume of the cone generated by the lances are the length and angle of injection, the length of the cone produced under average operating conditions of the SONIC lances is about 50 [cm] and the angle of injection is obtained geometrically from that observed in the operation see Figure 1a.

The evaporative cooler studied has nine water injection lances whose location was modeled on the design plans. Figure 1b shows the distribution of the lances.

Continuity source is applied to the red side and the total volume is the thermal sink, as shown in figure 1c.

The amount of heat absorbed by each lance is calculated using equation (8).

$$Q = \dot{m} \cdot h_1 - \dot{m} \cdot h_2 \qquad \text{Equation (8)}$$

With $\dot{m}$ being the mass water flow and h, the specific enthalpy of phase change, condition 2 represents the condition of the water outlet (nozzle) and 1 represents the condition of saturated steam reached when

mixed with the temperatures of the metallurgical gases. The compositions of the gases in the continuity source are specified in the following points.

The fine rain generated by the lances is produced by mixing water with compressed air to about 6.2 [bar] (90 PSIG), the air entering the lance is approximately 198 [Nm / h] and the water used on average reaches 160 [l / min].

The heat absorbed by each lance corresponds approximately to 1MW, then, the heat absorbed by the nine is 9 MWt.

2.3 Boundary Conditions

Boundary conditions are understood as the input data to perform the resolution of the proposed mathematical model, some of which were data directly measured on the gas cooling system and other previously calculated in previous work [15].

Figure 2a, shows the 3D geometric model of the gas cooling system incorporated in CFX 14.5 [4].

The boundary conditions imposed on the model are detailed below.

Inlet

The "inlet" condition is the starting point of metallurgical gases, geometrically located in the midplane of the Teniente converter, it is assumed, for purposes of the simulation, that the copper fill level reaches said free surface.

As input, the mass flow is considered, with a value of m = 33.63 kg / s at 1250 ° C. Additionally, there is the composition of the mass fraction metallurgical gases, which are reported in Table 1.

Environment

Boundary condition "Environment" means the air parcel as environment surrounding the Teniente converter and the suction bell, represented by a "box" called "Ambiente" illustrated in figure 2c. The main objective of simulating this condition is to obtain the infiltration of environment air through the radial clearance there is between the converter and the cooling hood. This boundary condition is simulated by a *opening* type boundary condition, where "artificial walls" are created at the borders, leaving the fluid without restrictions for entering or exiting the box.

Table 2 shows the composition of the environment air considered for this simulation. Composition considered at atmosphere pressure at 20°C.

It is important to mention at this point that the data entered into the boundary condition "inlet" and "environment" were measured in the smelting works.

Cooling System Walls

Boundary condition of the system walls is all internal sides of the plates that are in contact with the fluid, that is, the hood and the evaporative cooling chamber. Table 3 exposes a summary of the used border conditions.

Figure 2c shows the distribution of all the zones named in Table 3.

The temperatures obtained in Table 3 are the result of thermal images [6, 12] and the energy balance performed on the walls, as shown in equation (9).

$$(T_1 - T_2) \cdot \Delta x \cdot k = A \cdot h_{ev} \cdot (T_2 - T_{amb}) + \sigma \cdot \varepsilon \cdot A \cdot (T_2^4 - T_{amb}^4) \quad \text{Equation (9)}$$

Where condition 1 is the wall in contact with the gases inside the cooler, and condition 2 is the wall in contact with the environment.

Lances

In the modeling is not performed directly to the phase change of water droplets, but rather, the effect on the metallurgical gases, that is, it causes a decrease in the exit temperature and a source of continuity.

The mass fraction of fluid in the SONIC injection system corresponds to environment air 0.0263 and a H_2O with 0.9737.

Outlet

The outlet condition is entered by pressure applied over the area as shown in Figure 2c. This pressure corresponds to an average pressure value of -36 [Pa] in a normal workday.

2.4 Mesh Network

To define the mesh, a mesh sensitivity analysis has been performed, which was performed by simulating identical configuration and different mesh, using a finer one each time until we observe variation in results.

Figure 2b shows the mesh used for computational fluid dynamics simulation, with approximately 4 million elements and 1 million nodes.

One of the important parameters to be considered refers to the mesh quality [2, 3], this work is taken as a criterion orthogonal quality and skewness. The resulting values are shown in Table 4.

For reference, the quality criteria for an orthogonal grid were of least 0.2 for good quality mesh and 1 for excellent quality. For skewness quality the value was of 0.5 or more for good quality and 0 for excellent.

2.4 **Solution Convergence**

The simulation was carried out considering a stationary model, where the convergence criteria for the equations of continuity, momentum and energy correspond to the waste stabilization with values below $1.0x10^{-3}$ which reach over 10 thousand time steps as shown in figure 3.

RESULTS

The following figures show the results of simulations for the cooling system of metallurgical gases from the Teniente converter.

Figure 4a shows the velocity vectors of the gas in the converter entering the cooling system, and the velocity vectors of the environment air that dilute and cool the exiting gases is observed in the Teniente converter. It is also possible to observe the behavior of the internal flow identifying recirculation zones of the flow and the maximum speed, which reaches 31 m/s.

Figure 4b, shows the power lines that are generated in the converter cooling system of the Teniente Converter. Vorticity of the flow is seen as it passes through the cooling system generating areas of preferential flow.

Figure 5, shows the contours of temperature where the effect of the evaporative cooler injection lances can be seen represented by an area of low temperature at the outlet of the collection hood. Temperatures range between 20 ° C for injection fluids as environmental air and water injected by the lances and 1244 ° C for gases from the merger-conversion copper process.

Figure 6. shows the contours of temperature at the exit of the evaporative cooling chamber. The temperature distribution seen is not symmetrical despite the shape of the analyzed geometry.

3.1 **Simulation of the CT Cooling System Validation**

For the corresponding validation of the simulation, data from temperature sensors measurements recorded on February 12, 13 and 14 of 2013, at an interval of 1 minute measurement were used.

Note that in the case of validations, average registration data submitted by each pair of sensors are used. The sensor record identified as 53-TT-303, which represents the average temperature between the sensor 53-TT-303B and 53-TT-303A. Similarly there is a registration called sensor 53-TT-299 which records the average between the sensor 53-299A and 53-TT-TT-299B. This variable is represented by the red line (see figure 7a) which unites the measuring point of both sensors.

Figure 7b shows the associated temperature contour associated to the plan of the measurement points.

Analyzing the data tendency shown in figure 8a, it can be seen that the highest percentage of registered data is grouped around 630 ° C. Using the "Function calculator" simulation tool [4] for generating a control line on the simulation plane in the same location on the 53-TT-303 sensor, an average value is obtained of 826.3K, that is 553 ° C. Comparing this result with the value of the larger trend of figure 8a with a marginal error close to 13%.

By generating a control line located in the simulation corresponding to the 53-TT-209 sensor is possible to know the simulated temperature for the line corresponding to 647K control, that is, 374 ° C.

The trend value obtained by plotting the measurements delivered by the sensor in figure 8b, is about 385 ° C, then, if this is considered as "true value" and compared with the simulation, there is an error close to 3% in the simulation.

DISCUSSION

Considering the results of the simulations with an acceptable percentage of error we obtain that maximum temperatures resulting from the cooler are around 410 ° C, the resulting temperature is interesting to analyze, since the gases are driven to an electrostatic precipitator, the which operates with gases at temperatures between 320 - 400 ° C [1] so the exiting temperature obtained in the simulation results indicate the existence of episodes where the electrostatic precipitator does not operate at its highest efficiency point. As the gas cleaning process is not completely efficient in the electrostatic precipitator, it is expected to see certain deviations in the following processes.

It is possible to observe that the cooling system of the Teniente Converters dissipates 17 MW, where about 35% of the heat is dissipated by dilution in the area of the capturing hood and 41% is dissipated by injecting water and air through injection lances.

The large amount of dissipated energy suggests the possibility of implementing cogeneration systems energy from waste heat.

CONCLUSIONS

Using computational fluid mechanics it is possible to generate a representative modeling and simulation process of capturing and cooling of gases from Teniente copper converter type.

By comparing the results obtained by simulation with the data recorded by the sensors, these differences obtained are within a range of 3% and 13%. This mainly implies that the trends obtained by simulation and which metallurgical gases follow along their route through the hood and evaporative cooling chamber are reliable to predict the dynamic thermal behavior of the gas fluid, and so observations can be made to improve equipment and processes.

Through simulation it is possible to know the internal flow characteristics of the feedback system and cooling of gases, such as vorticity areas, areas with preferential flow circulation, speeds and temperatures inside the equipment.

ACKNOWLEDGEMENTS

This work has been conducted thanks to Universidad de Santiago de Chile, Faculty of Engineering; Proyecto DICYT 051615PC Usach; Codelco Chile, El Teniente Caletones Division; DIMIN Usach.

REFERENCES

Bibliographical References

[1] Air Pollution Training Institute (APTI)., 1998. Electrostatic Precipitator Operation', in *Electrostatic Precipitator Plan Review, pp. 1-21*.

[2] Ansys Inc. 2009. *Modeling and Meshing Guide*, U.S.A. pp. 15-25

[3] ANSYS Inc. 2011. *ANSYS FLUENT Theory Guide*, U.S.A. pp. 668-670

[4] ANSYS Inc. 2010. 'ANSYS CFX Tutorials ', Canonsburg, U.S.A. pp. 239-260

[5] Arellano A.E., 1998. *Estudio de flujo de gases en campanas extractoras de convertidores de cobre*, Universidad de Santaigo de Chile, Santiago.

[6] Astarita T., Carlomagno G.M., 2013. 'Infrared Thermography for Thermo-Fluid-Dynamics', in *Experimental Fluid Mechanics*, Springer, London, England, pp. 23-125.

[7] Bird R., Stewart W., Lightfoot E., 1992. *Fenómenos de Transporte*, in I Jonh Weley & Sons (ed.), Reverte S.A. Barcelona, España, pp. 95-137

[8] Campos Yañez, L.A., 2005. *Estudio de enfriamiento de gases metalurgicos en camara evaporativa. Fundición de cobre Puerto Ilo-Peru, Universidad de Santiago de Chile, Santiago, Chile, pp. 50-182*.

[9] Comisión Chilena del Cobre, 2004. Inventario Nacional de Fuentes de Emisión de Dioxinas y Furanos, Chile, pp. 207-230.

[10] Díaz Humeres, MA 2007. *Estudio de sistema de extracción de gases en convertidores de cobre*, Universidad de Santiago de Chile, Santiago, Chile.

[11] Ducoste, J 2008. An Overview of Computational Fluid Dynamics, *MBR Training Seminar*, Belgium.

[12] FLIR Systems AB 2011, 'Guía de termografía para mantenimiento predictivo', Madrid, España.

[13] Ghahremanian, S y Moshfegh, B 2011, 'Numerical and experimental verification of initial, transitional and turbulent regions of free turbulent round jet', *20th AIAA Computational Fluid Dynamics Conference*, American Institute of Aeronautics and Astronautics, Honolulu, Hawaii.

[14] Patankar SV., 1980, *Numerical Heat Transfer and Fluid Flow*, CRC press Taylor & Francis, U.S.A.

[15] Rodríguez A., C 2008, *Modelo de Operación para Manejo de Gases de la Fundición Caletones*, Pontificia Universidad Catolica de Valparaiso, Valparaiso, Chile.

[16] Safe P, Matson S y Deakin, J., 2002, *Effective Design Of Converter Hoods*, TMS Annual Meeting and Exhibition, Texas, U.S.A. pp. 1-11

[17] Safe P., Stephens R.L., 2000, 'Peirce-Smith Converter Hood Design Analysis Using Computational Fluid Dynamics Modeling', *EPD Congress 2000*, The Minerals, Metals & Materials Society, Texas, U.S.A. pp. 51-61

[18] Sanchez, M y Imris, I 2006, La secuencia en la piroextracción del cobre, *Pirometalurgia del cobre y comportamiento de sistemas fundidos*, Universidad de Concepción , Concepción , Chile. pp. 19-39

[19] Sheng, C. y Agwu Nnanna A.G., 2012, Empirical correlation of cooling efficiency and transport phenomena of direct evaporative cooler, Applied Thermal Engineering, U.S.A. pp. 48-55 doi:10.1016/j.applthermaleng.2012.01.052

FIGURES

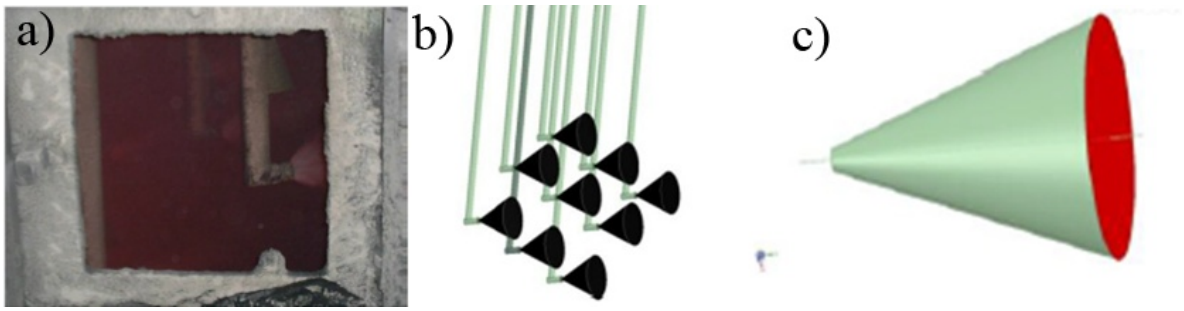

Figure 1. a) Injection mechanism, SONIC. b) Volume distribution, lances SONIC. c) Cone lances SONIC.

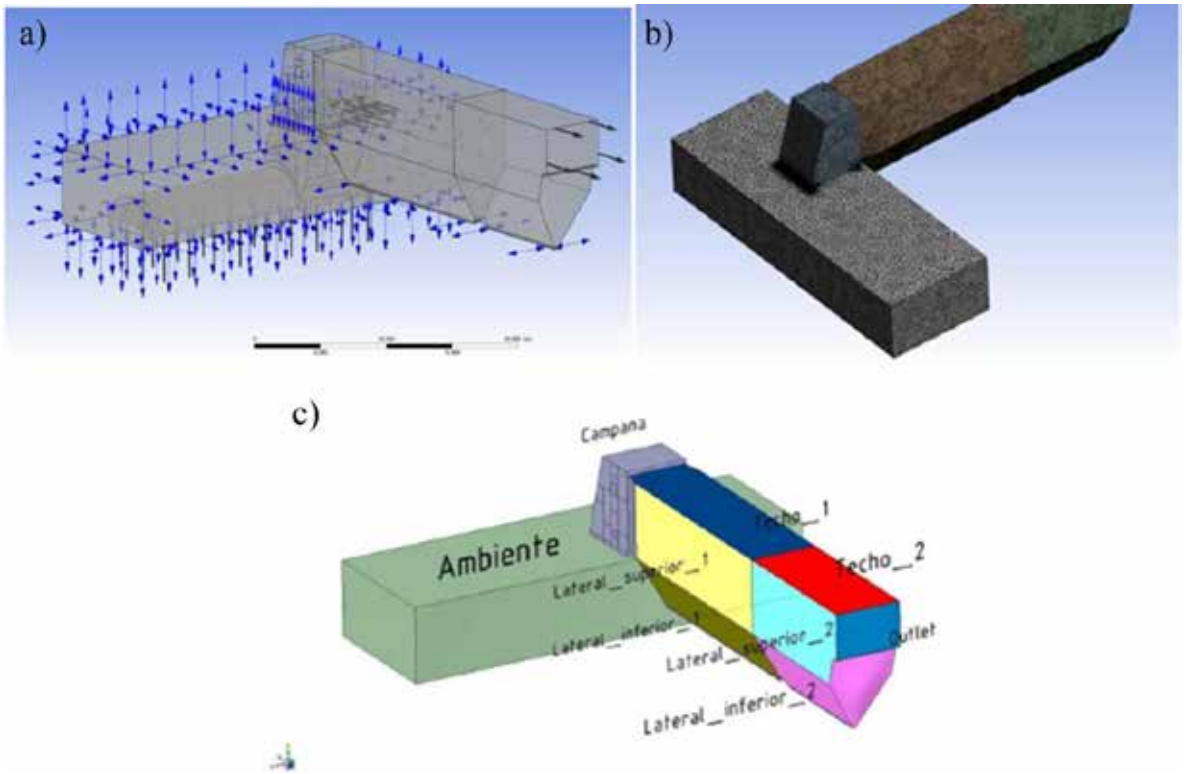

Figure 2. a) Geometric 3D model of gas cooling system incorporated into CFX 14.5 b) Mesh for CFD simulation. c) Distribution of walls, Teniente converter cooling system.

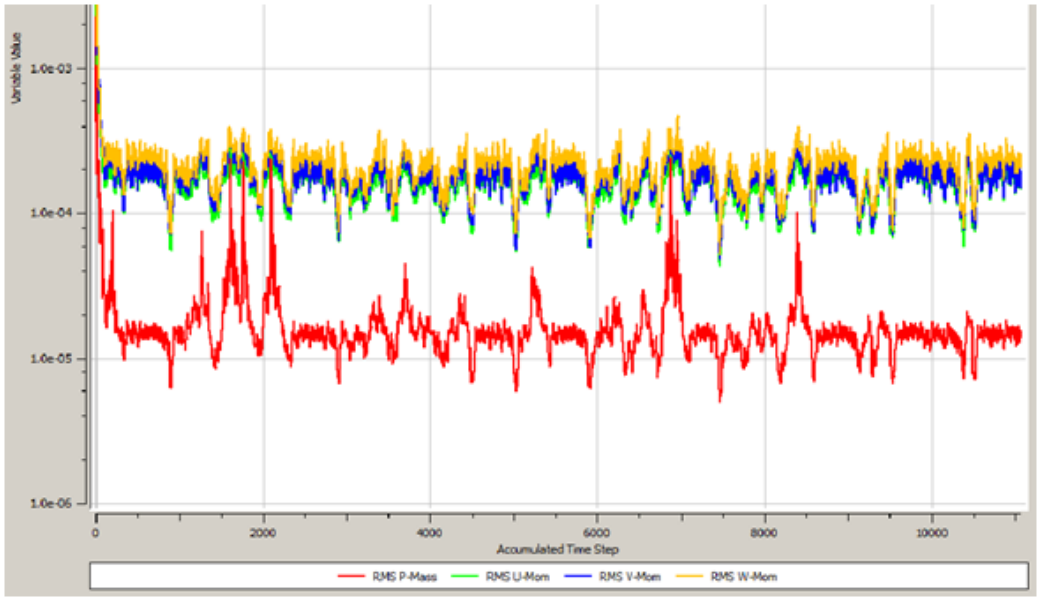

Figure 3. Graph of Waste.

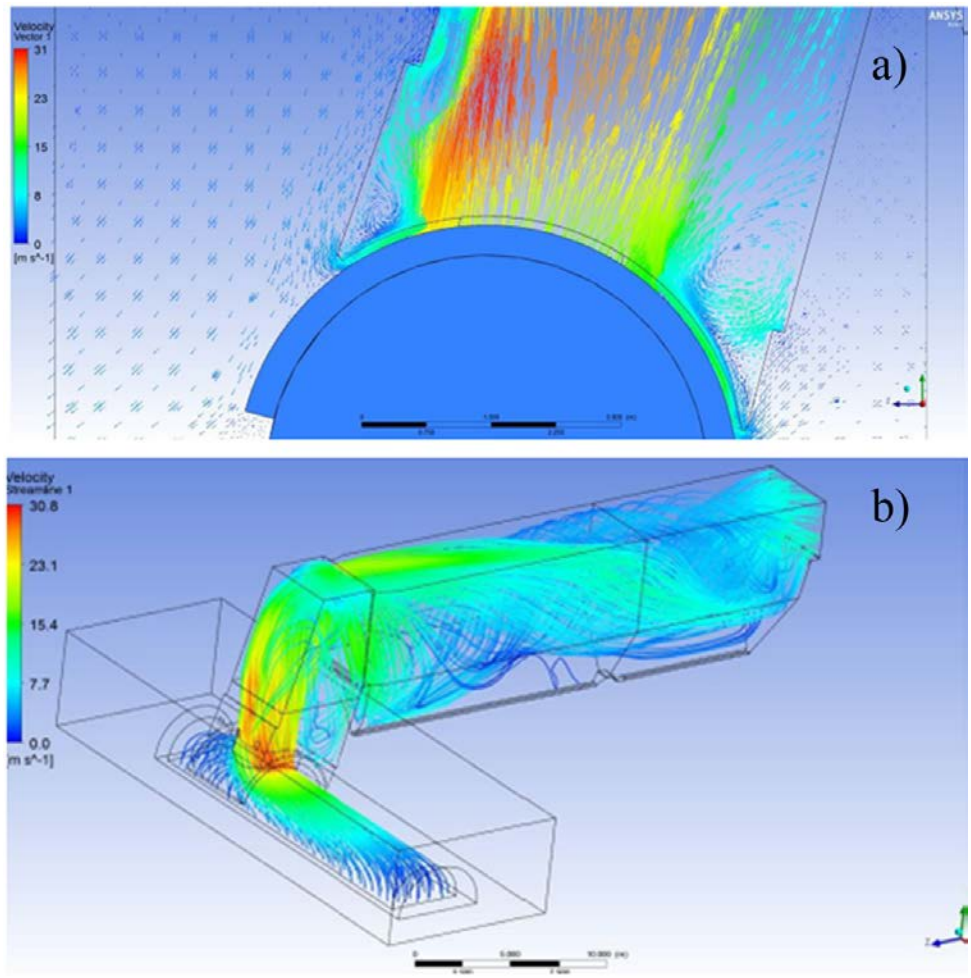

Figure 4. a) Gas velocity profile at the exit of the Teniente Converter. b) Current lines of gas velocity, Teniente converter cooling system.

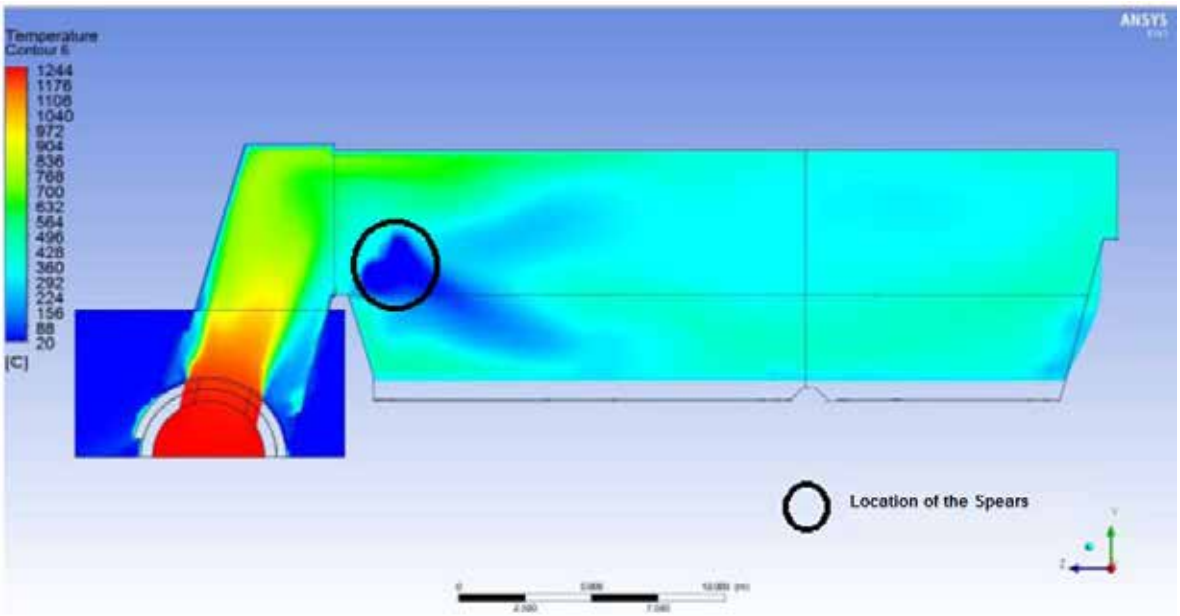

Figure 5. Temperature contour, medium plan of the gas cooling system of the Teniente converter.

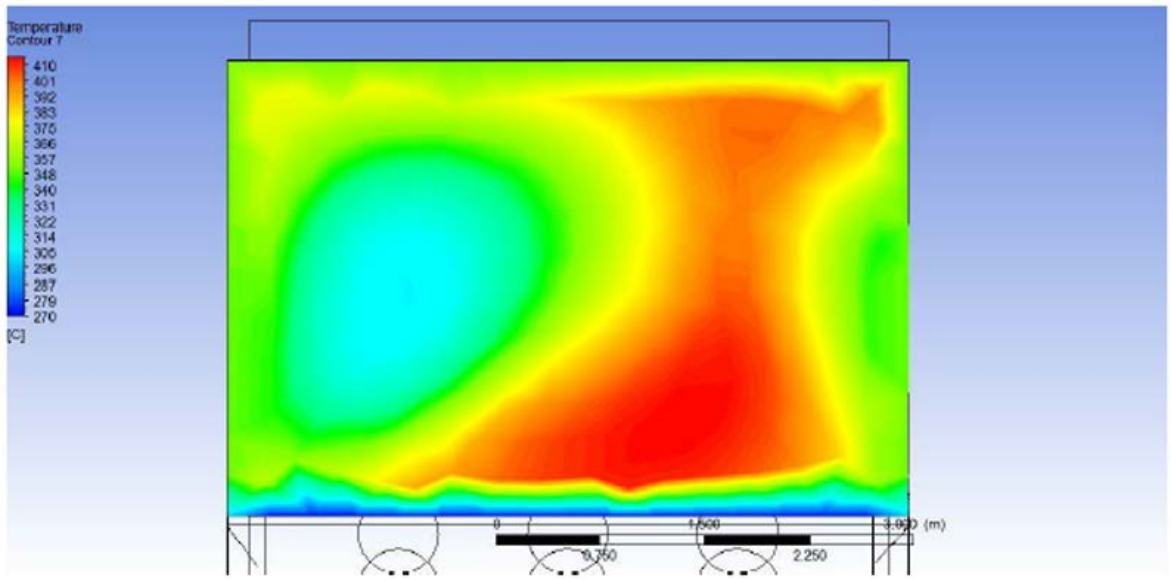

Figure 6. Temperature contour, outlet of the Teniente converter cooling chamber.

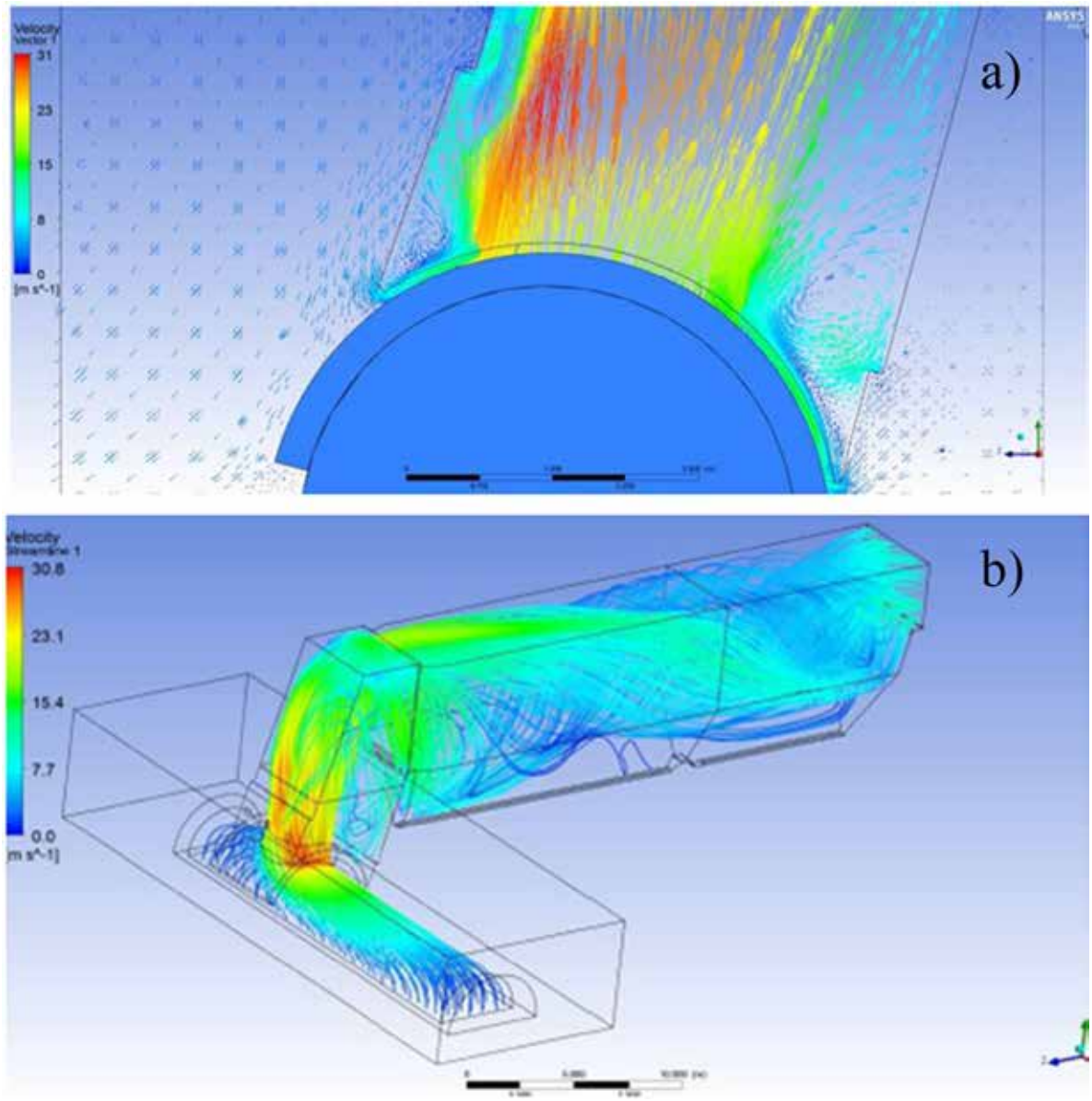

Figure 7. a) Location of the evaporative cooler temperature sensors. b) Contour of the temperature on the control surface.

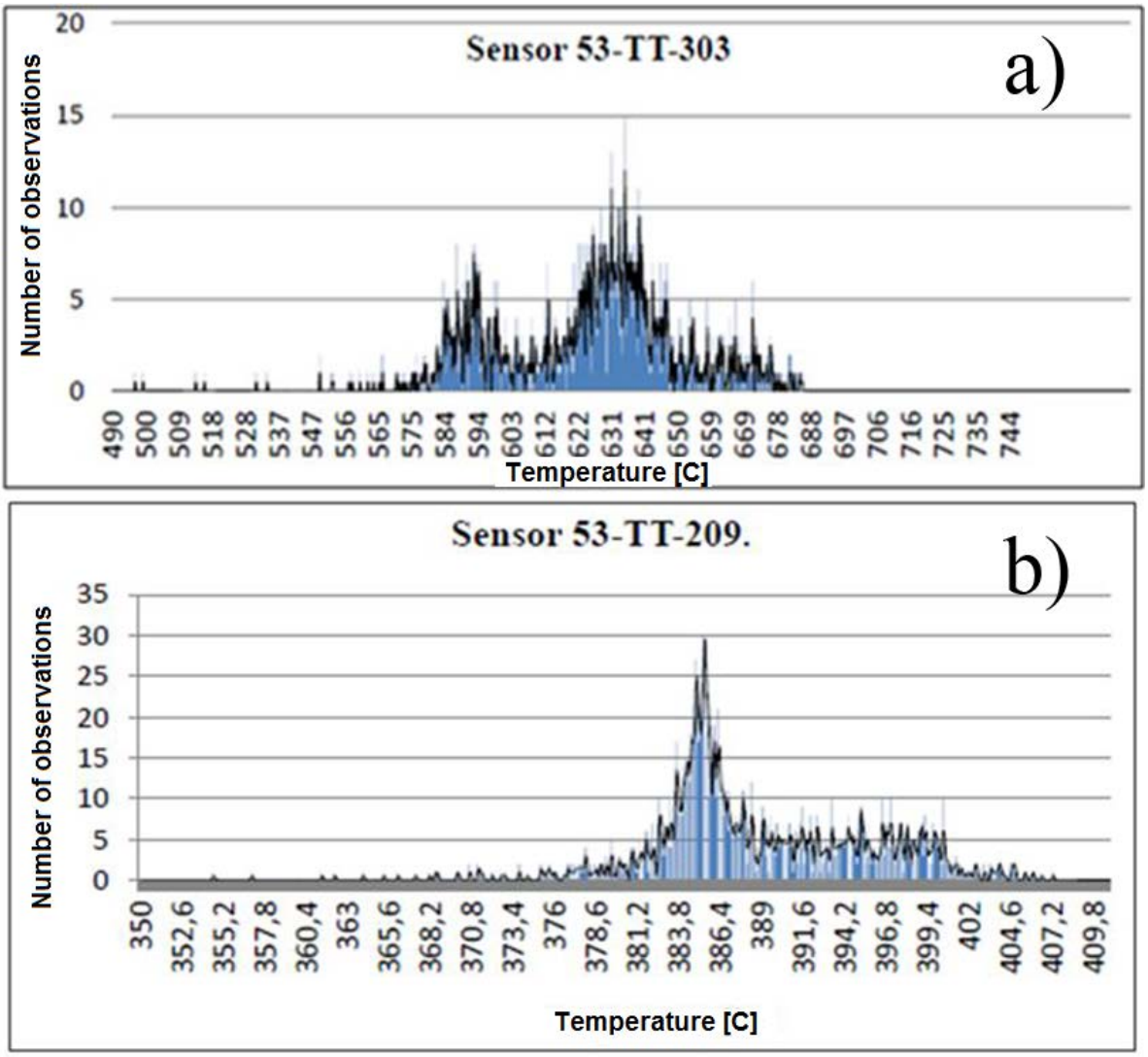

Figure 8. a) Registration of sensor 53-TT-303. b) Registration of sensor 53-TT-299

DETERMINATION OF IDEAL GRINDING PRODUCT SIZE FOR ZINC FLOTATION IN VAZANTE UNIT – VOTORANTIM METAIS

Jorge Lucas Carvalho Bechir[1], Valerio Metsavaht[2], Eder Lúcio de Castro Martins[2], Adelson Dias de Souza[2], Lucas Monteiro Correa e Lopes[2], José Renato Baptista de Lima [3], Carlos Antonio Mendes de Oliveira[2], José Max da Cruz Melo[2]

[1]VOTORANTIM METAIS HOLDING
Highway LMG – KM 65
Vazante, Brasil
jorge.bechir@vmetais.com.br

[2]Votorantim Metais Holding
Highway LMG – KM 65
Vazante, Brasil

[3]Escola Politécnica da USP
380, Prof. Luciano Gualberto avenue
São Paulo, Brasil

24th World Mining Congress
MINING IN A WORLD OF INNOVATION
October 18-21, 2016 • Rio de Janeiro /RJ • Brazil

DETERMINATION OF IDEAL GRINDING PRODUCT SIZE FOR ZINC FLOTATION IN VAZANTE UNIT – VOTORANTIM METAIS

ABSTRACT

The Votorantim Metais plant located in Vazante-MG-Brazil processes zinc from a silicate called Willemite - Zn_2SiO_4 - through froth flotation processes. Through this process, it is possible to obtain high recoveries of zinc. However, we found an opportunity to increase the recovery through reduction in the current grinding product size. Most part of coarser particles of Willemite (above 0.15 mm) are almost entirely lost in the process and sent to the tailings dam. This fact happens mostly because of the current grinding product size that do not achieve optimal liberation of the mineral of interest, so that much of the surface of the particles still have gangue attached to it, making it difficult to be adsorbed by the specific collector of Willemite. Seeking to raise the recovery of zinc and consequently raising the production, studies of mineralogical characterization via SEM/EDS (Scanning electron microscope with energy dispersive X-ray spectroscopy) with MLA (Mineral Liberation Analyzer), optimization in the grinding product sizes and bench scale froth flotation tests were conducted, aiming to determine the optimal grinding product size for the froth flotation process of Willemite. Through the results, we concluded that there were zinc recovery gains by reducing the grinding product size without compromising the zinc grade in the concentrate.

KEYWORDS

Willemite, zinc, liberation, froth flotation, grinding.

INTRODUCTION

Currently, Votorantim Metais has two zinc mines in Brazil represented by Vazante and Morro Agudo units. The Vazante unit has an installed capacity of 142,000 t / year of zinc and is very important to keep Votorantim Metais as 5th largest zinc producer in the world.

The zinc concentration in Vazante unit uses a froth flotation process. In this kind of process, the process engineer must consider several input variables, so that, just choosing the particle size that provides the optimal free surface of the mineral of interest via electron microscope is not sufficient to ensure the best metal recovery. The SEM/EDS (Scanning electron microscope with energy dispersive X-ray spectroscopy) with MLA (mineral liberation analyser) cannot predict, for example, negative consequences of a finer particle size, such as increased reagents consumption (due to the bigger surface area) and increased hydrodynamic drag (which facilitates the passage of finer mineral contaminants to the concentrate).

Considering these particularities, we executed flotation tests in bench scale, considering five different grinding product sizes, aligned to the mineral characterization results obtained by the MLA.

Seeking to optimize the flotation process of Vazante plant, this study aims to increase the zinc recovery by using mineralogical characterization, grinding, and flotation tests. With the mineralogical characterization, it is possible to obtain the ideal grinding product size, which results in the optimal liberation of the mineral of interest with the minimal cost.

TEST EQUIPMENTS AND METHODS

We performed all the tests, except mineralogical characterization in the process laboratory of Votorantim Metais Vazante Unit.

For the study, we needed crushing, grinding, flotation, filtration, chemical analysis and scanning electron microscopy. The following are the equipment used: jaw crusher, ball mill, flotation cell, vacuum filter, chemical analyzer (fluorescence X-ray), analytical balance, heater, SEM/EDS (scanning electron microscope/Energy Dispersive Spectroscopy) with MLA (Mineral Liberation Analyzer), flotation reagents and pH meter.

For this work, we used zinc ore from four different stockpiles that fed the processing plant, sampled with temporal and spatial variability criteria. In Vazante unit, the plant's stockpiles are formed through an automatic stacker, which generates Chevron type piles. We collected the four samples on the conveyor belt that feeds the plant mill. The simplified schematic of the process described before is shown in Figure 1 below:

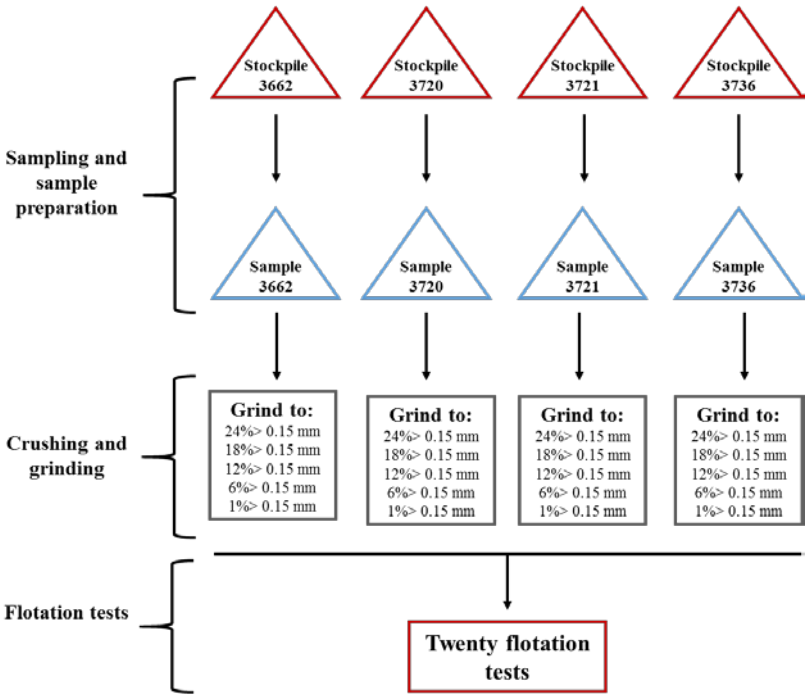

Figure 1 - Simplified schematic of the study

Crushing

The particle size of the stockpile is close to 95% passing 9.5 mm. The laboratory ball mill used in this activity is not able to grind the material of such a high top size as quoted. To grind the ore, we reduced the particle size from 95% passing 9.5 mm to 95% passing 1.18 mm using a jaw crusher with an opening of 1.5 mm and a disc mill.

Mineralogical characterization and grinding

To define the ranges of grinding product sizes that comprised this study, we used historical data of the industrial plant and mineralogical characterization via SEM / EDS with MLA. Currently, the Vazante plant presents grinding product sizes of 18% above 0.15 mm. In order to verify if this grinding product size reaches the ideal liberation of the zinc ore, we conducted a mineral characterization focused in the liberation analysis of the Willemite zinc ore in three different grinding product sizes. To achieve that, we used the mineralogical characterization data from the geometallurgy process database of Vazante mine. The grinding size ranges selected for the liberation study were 16% to 18% above 0.15 mm, 10% - 12% above 0.15 mm and 6% - 8% above 0.15 mm.

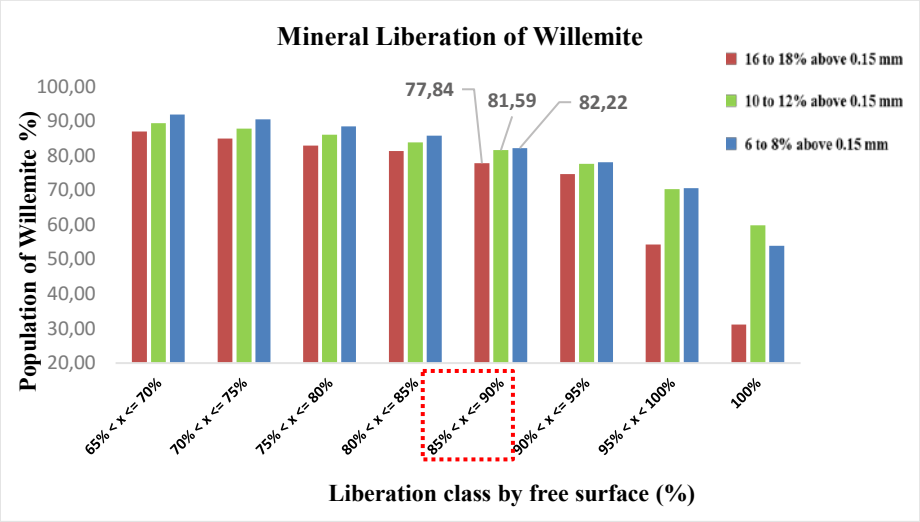

Graph 1 – Willemite liberation by free surface considering three different grinding product sizes

For the flotation process of Willemite, we considered that the ideal liberation occurs in the class that presents more than 85% of liberated perimeter (fraction highlighted in red in the base of Graph 1). Considering Graph 1, we noted that there is an increase in the population of liberated Willemite due to reduction of the grinding product size. For the coarser particle size, we obtained a liberated population of 77.84%; while in the mid grinding product size, the liberated population was 81.59% and the finer grinding product size generated a liberated Willemite population of 82.22%.

Throughout the results shown in Graph 1, we obtained a higher Willemite liberation in the finer grinding product sizes between 6 and 12% above 0.15 mm when compared with from 16 to 18% above 0.15 mm, producing an inversely proportional relationship between grinding product size and Willemite liberation. Thus, we defined five different grinding product sizes to be tested in the flotation process. The grinding product sizes chosen were:

- grinding product size of 24% above 0.15 mm;
- grinding product size of 18% above 0.15 mm - Current practiced in the process plant named as reference;
- grinding product size of 12% above 0.15 mm;
- grinding product size of 6% above 0.15 mm;
- grinding product size of 1% above 0.15 mm.

The ball mill used for grinding the samples has the following parameters and conditions.

- Mill 22cm x 18cm (Length x Diameter) and rubber liners;
- 67% solids and 32% filling degree;
- 72 RPM and 73% critical speed;
- Ball Load of 10500g.

In order to obtain the different grinding product sizes for the study, we generated five grinding curves (one for each stockpile sample) since the hardness of the zinc ore may vary according to the region of the mine.

Using the curves, we could set the grinding times to achieve the targeted product sizes. After submitting the samples to the ball mill grinding with the pre-defined times, we classified the materials by sieving to confirm the results. Table 1 shows the grinding product sizes obtained, along with the grinding time and energy consumed.

Table 1 – grinding product sizes obtained, grinding time and energy consumption calculated by Rowland equation

Percentage above 0.15 mm	P80 (μm)	Average grinding time (min)	Energy consumption (kWh/t)
24,0	176	20	8,26
18,0	145	22	9,09
12,0	124	27	11,15
6,0	102	30	12,39
1,0	69	44	18,17

.

Flotation tests

For the flotation tests, we generated twenty samples with 1300 g each, representing the four different samples (3662, 3720, 3721 and 3736) from the stockpiles. That is, each stockpile sample was grinded into five different grinding product sizes, generating five flotation tests for each sample, totalizing twenty flotation tests that composed the study.

We submitted all samples to an identical flotation process, which includes the same process route, flotation time, reagent consumption, percent of solids, cell level, airflow rate, conditioning time and method of analysis. Table 2 shows the reagents, along with their functions and dosages used in flotation tests.

Table 2 – Parameters and reagents dosage of the flotation tests.

Reagent	Reagent function	Dosage (g/t)	Conditioning time (min)	pH
Sodium Sulfite	Zinc activator and pH regulator	1250	2	10,5
AGLP	Dispersant	320		
Amine	Collector	70	2	
MIBC	Frother	28		

The route used for the flotation tests is located in Figure 2. We performed the tests in a single Rougher stage, at pH 10.5 and a 2-minutes flotation.

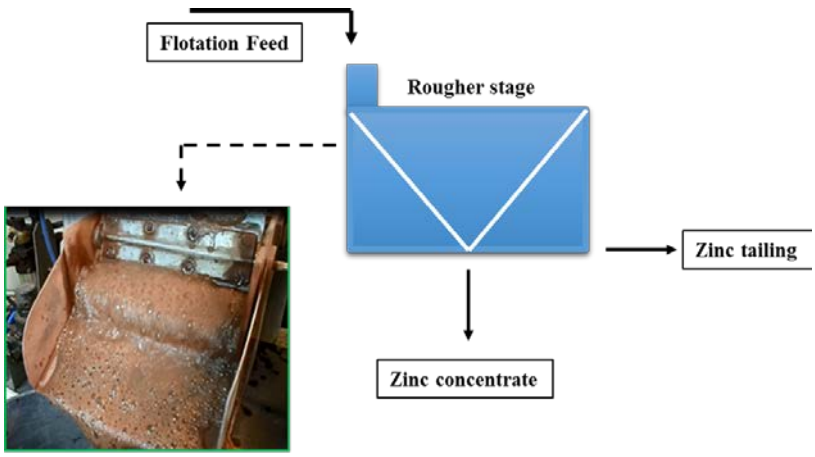

Figure 2 – Schematics of the flotation route used

We analyzed the products obtained from the flotation testing by X-ray fluorescence (XRF).

RESULTS AND DISCUSSION

The flotation results obtained for the four stockpiles samples are showed in the Table 3 below.

Table 3 – Results of the flotation tests

Grinding product sizes	Zinc feed grade (%)	Zinc concentrate grade (%)	Zinc recovery (%)
24% above 0.15 mm	12,13	43,24	63,98
	12,04	35,76	69,94
	11,68	36,19	62,88
	11,44	38,86	64,01
18% above 0.15 mm	12,16	39,76	73,96
	12,17	38,14	64,87
	11,64	38,42	72,26
	11,48	36,87	66,87
12% above 0.15 mm	12,43	39,65	75,68
	12,03	37,24	77,45
	11,44	37,06	80,93
	11,71	38,52	80,00
6% above 0.15 mm	12,33	39,46	79,49
	11,59	37,74	77,23
	11,95	37,49	81,39
	12,03	38,40	83,19
1% above 0.15 mm	12,34	36,23	82,52
	12,24	35,46	84,28
	11,82	32,34	84,55
	12,01	33,95	85,83

We organized the recovery and zinc grade data from the Table 3 in the Graph 2 for a better interpretation of the tests results.

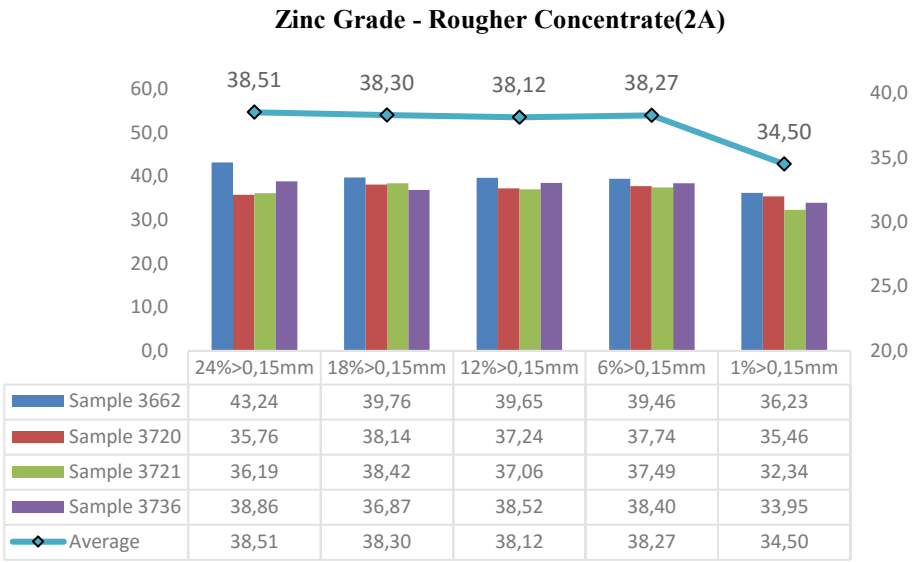

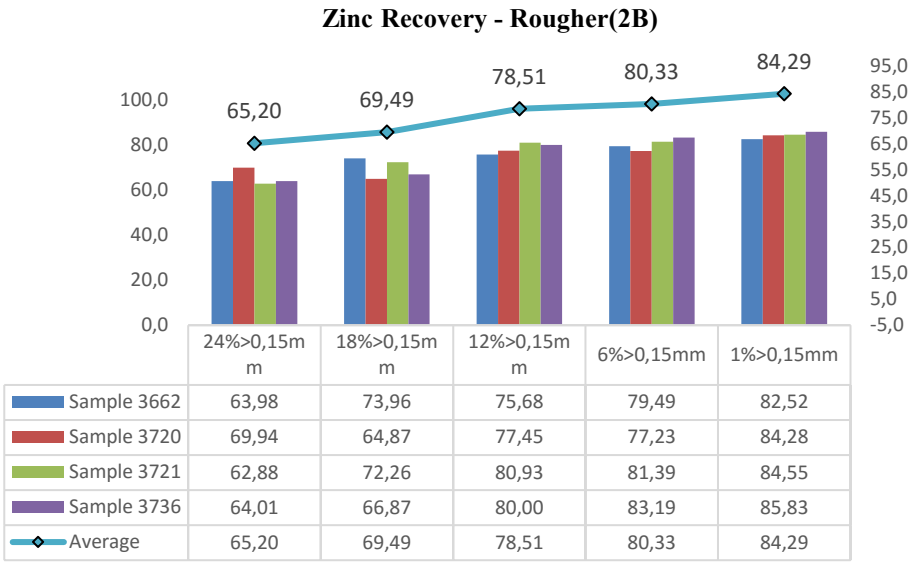

Graph 2A – Zinc concentrate grades. 2B – Zinc recoveries

Interpreting Graph 2A – we noted that the grinding product sizes ranging between 24% > 0.15 mm and 6% > 0.15 mm did not result in significant reduction of zinc grade, generating concentrates of 38.51% and 38.12%, respectively. We cannot say the same for the product size of 1% above 0.15 mm sample. In this grain size, the average grade of zinc in the concentrate was 34.50%.

Interpreting Graph 2B - there is a strong correlation between grinding product sizes and zinc recovery, making it clear that, the finer the particle size, the higher the zinc recovery. Increments on zinc recovery were very significant, going from averages of 65.20% to 84.29% for the four studied stockpile samples.

As previously mentioned, the current grinding product size of Vazante plant is around 18% above 0.15mm. We used this information as reference to help with the interpretation of the results obtained in this study. Transferring the data from Graph 2 to Table 4, we have:

Table 4 – Average results for all flotation tests

Grinding product size	Zinc concentrate grade (%)	Zinc recovery (%)	Mass recovery (%)
18% above 0.15 mm (Reference)	38,30	69,49	21,51
24% above 0.15 mm	38,51	65,20	20,16
12% above 0.15 mm	38,12	78,51	24,51
6% above 0.15 mm	38,27	80,33	25,15
1% above 0.15 mm	34,50	84,29	27,07

The grinding product size of 24 % above 0.15 mm generated a zinc grade of 38,51 % that is similar to the reference grade value (38,30 %), but there was a recovery loss of approximately 4 percentage points over the current reference that is 69.49%. The mineralogical characterization results obtained demonstrated that the grinding product size above 18% > 0.15 mm, the amount of liberated Willemite is low when compared with other finer particle sizes, corroborating with the recovery loss obtained.

The 6 and 12% grinding product size showed similar zinc grades comparing to the 18% > 0.15 mm reference with a significant increase in zinc recovery. Among these two grinding product sizes, the one that presented the best result was 6% above 0.15 mm, with a higher zinc grade (38.27% against 38.12%) and better recovery (84.29% against 80.33%). This information showed that the higher selectivity obtained was caused by the increased liberation of Willemite in this particle size.

The grinding product size of 1% above 0.15 mm displayed the highest zinc recovery, however we believe that the excessive fine particles generated by unnecessary grinding, raised the hydrodynamic drag of carbonate minerals (dolomite) in the flotation, compromising the selectivity of the process and reducing the zinc grade in the concentrate to unacceptable values of 34.71%. Currently, to treat the zinc concentrate in the metallurgy fase, the zinc grade must have closer values to the reference grinding product size of 18% above 0.15 mm, which is 38% of zinc.

CONCLUSION

Results showed that the grinding product sizes of 6 and 12% above 0.15 mm with P80 of 0.102 mm and 0.124 mm, respectively, presented the best flotation results, containing zinc grade within the defined reference (38,30 % zinc), with an increase in the metal recovery. When we reduced the grinding product size to 1% above 0.15 mm, the zinc recovery kept rising, but gangue contamination occurred, reducing the selectivity of the process and consequently dropping the zinc grade in the concentrate.

Through the tests, we demonstrated that the current grinding process of the plant is not sufficient to achieve optimal liberation of Willemite mineral. This fact reduces the best use of the zinc ore in the flotation process, showing that a finer grinding product size is needed in Vazante plant. Considering the results of the bench tests performed, the grinding product size adjustment from 18% above 0.15 mm to 6% above 0.15 mm increased the zinc recovery by approximately 11%, representing a substantial gain that would allow an optimization of the current grinding process of the plant. We must consider that the actual recovery gain to be achieved by grinding product size reduction can only be reached through a robust test campaign in a pilot scale plant, where the entire circuit of the current plant can be simulated with all the particularities and inefficiencies that an industrial plant has. We showed that even finer grinds (1% above 0.15 mm) allow better liberation, but this does not generates gains in the current process. This happens due to the presence of ultrafine carbonate minerals in the flotation process, fact that increases the hydrodynamic drag and reduces the zinc grade in the concentrate.

REFERENCES

Votorantim Metais Holding. Data Report (2014) – *Testes de flotação de zinco e geometalurgia. Internal Report*

Votorantim Metais Holding (2014). *Caracterização Tecnológica em Amostras de Minério de Silicatado de zinco. Relatório Interno.*

Votorantim Metais. *Dados de planilhas de moagem – Trabalhos de flotação de Zinco em escala de bancada 2014. Relatório Interno.*

EVALUATION OF COMMINUTION EFFECTIVENESS FOR SELECTED "CRUSHER-MILL" CIRCUITS IN COPPER ORE PROCESSING

B. Ryszka, D. Saramak*, A. Krawczykowska, D. Foszcz, T. Gawenda and D. Krawczykowski

AGH University of Science and Technology
Department of Mineral Processing and Environmental Engineering
Mickiewicza 30 Av., 30-059 Cracow, Poland
*(*Corresponding author: dsaramak@agh.edu.pl)*

24th World Mining Congress
MINING IN A WORLD OF INNOVATION
October 18-21, 2016 • Rio de Janeiro /RJ • Brazil

EVALUATION OF COMMINUTION EFFECTIVENESS FOR SELECTED "CRUSHER-MILL" CIRCUITS IN COPPER ORE PROCESSING

ABSTRACT

Article concerns problem of raw materials comminution in various crushing devices operating in the circuit with a ball mill. Three types of crushers in laboratory scale were taken into account: jaw crusher, hammer crusher and high-pressure grinding rolls device (HPGR). Effectiveness of crushing process measured through comminution degree, together with flotation recovery, were determined for each comminution circuit. It appeared that the most favorable comminution degree was achieved for the hammer crusher. However, in terms of energy consumption and throughput, HPGR appeared the most suitable device. Results of flotation tests were the least favorable for the jaw crusher.

KEYWORDS

Crushing, grinding, copper ore, ore preparation, comminution circuits

INTRODUCTION – METHODOLOGY APPROACH

Crushing and grinding operations are the basis of sulfide copper ore enrichment processes. These are very first operations in run-of-mine treatment, and their main purpose is to prepare the ore for core beneficiation processes, like flotation or other upgrading operations. The raw material (ore) is crushed in order to liberate useful minerals from the gangue, which primary determines the efficiency of the flotation operations (Smit, 2005, Saramak et. al 2015). The need of fine grinding of the material results in the highest energy consumption of comminution operations, which accounts from 50 to 60% of total processing costs. The efficiency of an entire ore processing circuit depends on many factors, including the feed characteristics, like lithological type, particle size composition, moisture content, type of the crusher, comminution degree, and other operating parameters.

HPGR-based crushing technology is currently one of the most efficient methods of hard ore comminution in terms of the energy consumption (Morrell, 2008). The other benefits include high process efficiency due to the greater comminution effect, easy adaptation for different crushed materials (variable pressure and roller speed values), beneficial PSD of product comparing to conventional crushers, relatively small footprints, stable throughput, low noise emission, low dust emission (Fuerstenau et. al 1991, Morley 2003, Pahl 1993, Rule et. al 2008, Saramak et. al 2010). In general, tumble mills followed by the HPGR unit consume less energy due to the high crushing efficiency of the roller press. Therefore the energy consumption of this circuit is lower because the particle breakage process was partially transferred from the grinding (ball mill) to crushing (HPGR) stage (Smit, 2005, Baum et. al, 1997).

However, it should be emphasized that the design of technological circuit and equipment selection, is based on the analysis of the technological and economic indicators. The values of these indicators will give the operator significant information whether an application of potential solution can be justified or not. The above issues are the subject of the presented paper.

RESEARCH PROGRAMME

Comminution circuit

The test programme included research in laboratory scale over operation effectiveness of three types of technological circuits of two-stage crushing of copper ore. At the first stage of crushing the hammer crusher, jaw crusher and high-pressure grinding roll press, have been operating. Bond's ball mill has been applied at the second stage of each circuit. Figure 1 shows a scheme of investigations.

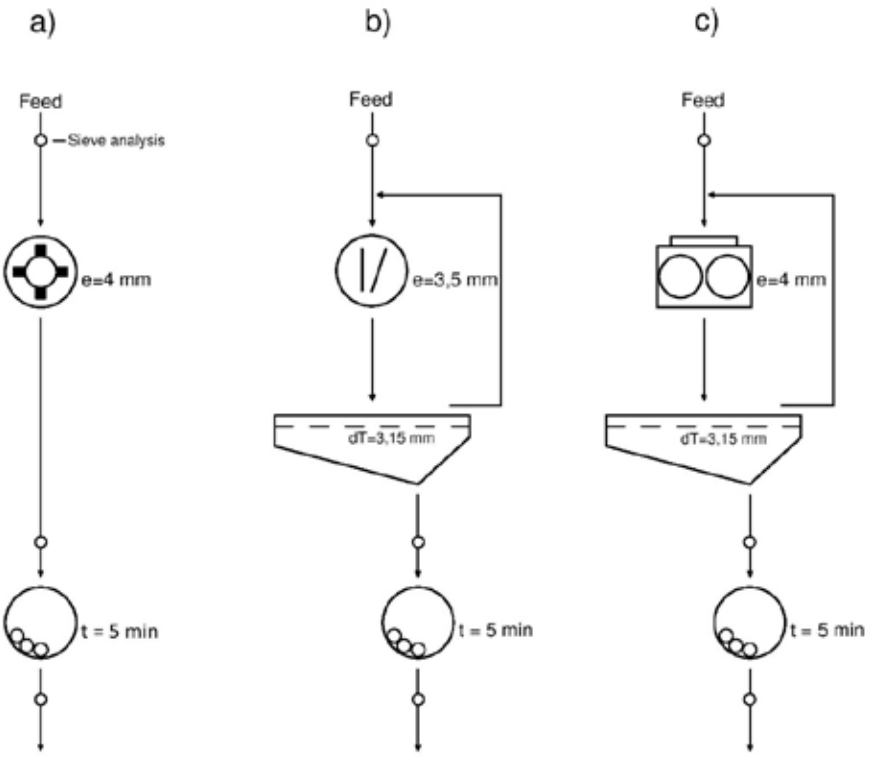

Figure 1 – Comminution circuits under testing: a) hammer crusher, b) jaw crusher, c) high-pressure grinding rolls (HPGR)

Copper ore with particle size from 0 to 12.5 mm was used as feed material and the main aim of the first-stage crushing was to obtain the PSD of product within the range 0 – 3.15 mm, what is an optimal particle size of the Bond's ball mill feed in the second stage of comminution circuit. The grinding device has worked in a closed circuit with the vibrating screen of a mesh size 3.15 mm. Hammer crusher has been operating with a grid of the mesh size 4 mm.

The second comminution stage was the grinding process in Bond's ball mill. The purpose of this stage was to achieve a product with the particle size qualifying it for operations of flotation, that is below 0.1 mm. Each grinding test ran for 5 minutes.

Flotation tests

Flotation tests were carried out in order to verify technological effectiveness obtained for each comminution circuit. The experimental diagram is shown in Figure 3 and flotation tests were performed using the fractional flotation method. Flotation experiments were carried out in constant process conditions for following assumptions:

- the suspended particle matter density for flotation amounted to 1250 g/dm^3
- ethyl xanthate sodium as a depressant was used in an amount of 120 g/mg,
- the Corflot frother reagent was fed in an amount of 30 g / mg
- agitation time after the addition of reagents was 5 minutes,
- flotation concentrates which were collected at the following intervals: 3, 6, 12 and 30 minutes (K1, K2, K3, K4 respectively).

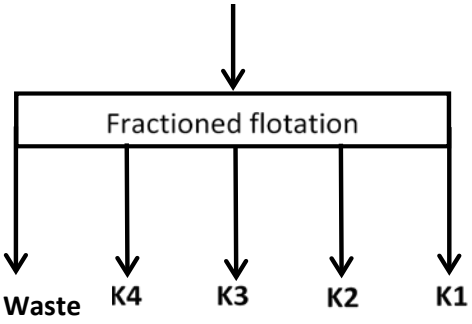

Figure 2 – Scheme of flotation investigations

RESULTS OF INVESTIGATIONS

Figure 3 shows the results of sieve analyses obtained for each crushing device: hammer crusher, jaw and HPGR. Analyzing the figure it is easy to see that the hammer crusher reached more favorable comminution ratio value, compared with jaw crusher and HPGR press. The last two devices reached similar particle size distribution of products. The yield of particle size fraction 0-1 mm for hammer crusher was 78%, while the jaw crusher and HPGR press has resulted 55% and 56%, respectively. Table 1 presents values of comminution degree for each crushing device.

Table 1 – Values of average comminution degree achieved for each tested device

Type of device	S_{50}
Hammer crusher	10.45
Jaw crusher	4.60
HPGR	4.66

These results are consistent with the relationships described in various articles, as hammer crushers are generally characterized by very high comminution degrees, reaching up to 30.

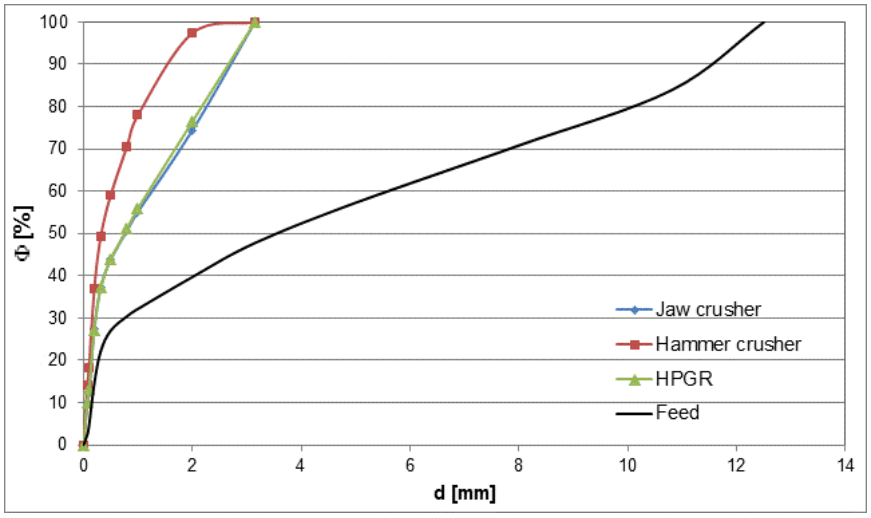

Figure 3 – Particle size distribution curves for feed and products from first stage of crushing

Table 2 – Throughput and Energy consumption of devices under testing

Type of device	Throughput Q [Mg/h]	Energy consumption E_{sp} [kWh/Mg]
Hammer crusher	0.4	4.9

Jaw crusher	0.7	2.8
HPGR	3.3	0.8

Throughput (Q) and energy consumption (E_{sp}) for all devices were determined during the crushing tests. For both indices HPGR appeared the most favorable device. Its unit energy consumption was more than six times lower than the E_{sp} for the hammer crusher and 3.5 times lower for the jaw crusher.
In the next stage of the study the achieved values of comminution degree per energy consumption (E_{sp}/S_{50}) and per throughput (Q/S_{50}), were compared. The calculated values of indicators (Gawenda 2016) are presented in Table 3.

Table 3 – Energy consumption and throughput per average comminution degree

	E_{sp}/S_{50}	Q/S_{50}
Hammer crusher	0.37	0.04
Jaw crusher	0.61	0.16
HPGR	0.17	0.71

The ratio of energy consumption to the achieved comminution degree is a very practical indicator, because it combines both the technological and economic aspects. The analysis from this scope showed that HPGR appeared to be the most preferable device, achieving very low value (0.17), which is several times lower than for the other crushers. Despite the higher energy consumption, hammer crusher appeared more favorable than jaw crusher, due to the higher value of achieved comminution degree. Jaw crusher proved to be the least effective of all tested devices.

The second index expresses the relationship of throughput to the comminution degree, that is the maximum capacity of the device per a single degree of crushing. The highest value of this index has reached the HPGR, while the lowest – the hammer crusher with a value of more than 17 times lower. This has a direct relationship and the nature of the work for the hammer crusher: high comminution degree is achieving due to a long resistance time of the feed material in the working chamber of the crushers, what results in lower throughput.
Analysis of particle size distribution curves for the grinding products indicates that the finest particle size distribution in the ball mill was achieved for the hammer crusher product. This follows directly from the particle size distribution of products from the first stage of crushing, where the device (hammer crusher) reached the highest value of average comminution degree, thus greatly facilitating the operation of a ball mill. Comminution degree for products of jaw crusher and HPGR press contained an average 25% of coarse particles in the particle size class 2-3,15 mm, compared to the 3%, obtained for the hammer crusher. This has also its reflection in yields of fine particle size classes (Table 4).

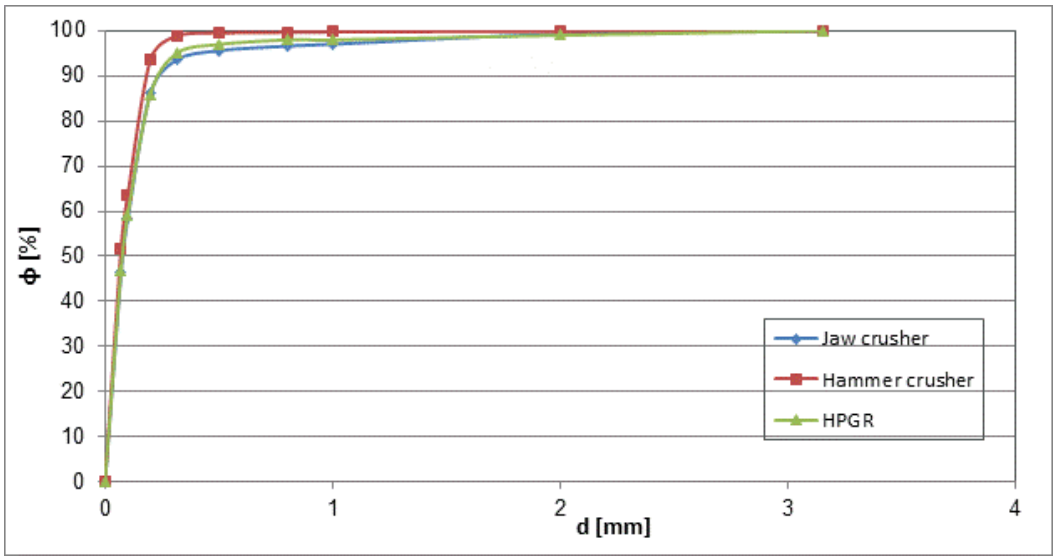

Figure 4 – Particle size distribution curves for products of second comminution stage

Table 4 – Yields of fine particle size classes in second stage of crushing

Type of crusher	Yield of particle size class		Net generation of particle size class 0 – 0.071 mm [%]
	0 – 0.071 mm [%]	0.071 mm – 0.1 mm [%]	
Hammer crusher	52	12	38
Jaw crusher	46	12	36
HPGR	47	11	37

Analyzing the yields of very fine particles (0-0.071 mm) achieved in HPGR and jaw crusher it can be seen that these have decreased by 5-6%, compared to the results achieved for the hammer crusher. The yields of particle size class 0.071 – 0.1 mm are at a comparable level of 11-12% for all three crushers, which proves the stability of the grinding process. In turn, analyzing the net production of particle size class 0 – 0.071 mm in the ball mill, one can see that all three tested devices achieved the values within the range of 36 – 38%.

In the next stage of investigations, flotation tests were carried out in order to verify the work effectiveness of individual comminution circuit. The purpose of flotation tests was a verification of possibility of obtaining possible lowest copper grade in tails. Therefore only one stage of flotation was carried out, without further cleaning of concentrate. Results are presented in Table 5.

Table 5 – Results of flotation tests

Type of circuit	Flotation indices			
	α	β	ϑ	ε
Hammer crusher	1.96	6.31	0.166	94.01
HPGR	1.84	5.85	0.184	92.91
Jaw crusher	1.88	5.07	0.222	92.23

Results of flotations show that the lowest copper grade in tails was achieved for hammer crusher. HPGR enabled us to achieve higher copper grade in tails for about 0.02%, while jaw crusher appeared to be the least effective from this scope. Concentrate grades are low, but it is obvious when only one stage of flotation is carried out. As it was mentioned earlier, the main purpose of flotation tests here was to test the possibility of maximum recovery of the useful mineral. An increase in the concentrate grade would be achieved in further flotation operations (so-called “cleaning flotation”), with possible re-grinding of the concentrate. Summing up the results of flotation one can say that an assessment of operation of crushing and grinding circuit should take into account an entire technological circuit, together with upgrading operations.

CONCLUSIONS AND SUMMARY

The article has presents issues related to the efficiency of grinding of selected crusher-mill circuits. There were analyzed comminution degrees as well as throughput and energy consumption indices for each device. The results of investigations show that the most favorable comminution degrees were achieved for the circuit with hammer crusher, but in terms of throughput and energy consumption the HPGR-based circuit turned out to be the most advantageous.

The results also show that, depending on the configuration of comminution circuit, one can expect various technological and energetic effects of circuit operation. The analysis was supplemented with an assessment of the flotation effectiveness for all crushing products. The obtained results indicate that an overall assessment of the crushing and grinding circuit efficiency is complex and depends on the adopted criterion. In terms of energy the most preferably appeared the HPGR-based circuit, but the most intense comminution degree and the most favorable flotation results were obtained for a circuit with the hammer crusher.

The obtained results proved that the application of suitable crushing device in given copper ore comminution circuit may improve the effectiveness of downstream grinding process what leads to improvement of the entire circuit work efficiency through decreasing the process energy consumption and enhancing the product size reduction.

ACKNOWLEDGMENT

Article has been realized within the frames of research project no. PBS3/B3/28/2015

REFERENCES

Baum, W., Patzelt, N., Knecht, J. (1997). Metallurgical benefits of high pressure roll grinding for gold and copper recovery', *SME*, Denver, Feb. 1997. Conference print pp 111-116.

Fuerstenau, D.W., Shukla, A., Kapur, P.C. (1991). Energy consumption and product size distribution in choke-fed high-compression roll mills. *International Journal of Mineral Processing*, vol. 32, pp. 59-79, 1991

Morley, C. (2003). HPGR in hard rock applications. *Mining Magazine*, September 2003

Morrell, S. (2008). A method for predicting the specific energy requirement of comminution circuits and assessing their energy utilization efficiency. *Minerals Engineering*, vol. 21, issue 3

Pahl, M. H. (1993). Praxiswissen Verfahrenstechnik – Zerkleinerungstechnik. *Fachbuchverlag Leipzig/Verlag*, TÜV Rheinland, Köln 1993

Rule, C.M., Minnarr, D.M., Sauremann, (2008). HPGR – revolution in Platinum? *3rd International Conference „Platinum in Transformation",* The Southern African Institute of Mining and Metallurgy, 2008

Saramak, D., Tumidajski, T., Brożek, M., Gawenda, T., Naziemiec, Z. (2010). Issues of design the comminution circuits In mineral processing. *Mineral Resources Management*, vol.26 issue 4

Smit, I. (2005). Bench scale ore characterization using the High Pressure Grinding Roll. *Workshop 2005*, Perth, August 22, 2005

Saramak D., Młynarczykowska A., Krawczykowska A. (2014). Influence of a high-pressure comminution technology on concentrate yields in copper ore flotation processes. *Archives of Metallurgy and Materials*, vol. 59, issue 3, pp. 951-955

FINE FLOTATION TAILINGS DEWATERING: RESTORING DEWATERING EFFICIENCIES AND SUPPLEMENTING WATER CONSUMPTION IN A GRAVITY GOLD RECOVERY CIRCUIT

*Cameron J.H. Stockman

CEC Mining Systems Corp.
#400 – 602 West Hastings Street
Vancouver, Canada V6B 1P2
*(*Corresponding author: cstockman@cecminingsystems.com)*

24th World Mining Congress
MINING IN A WORLD OF INNOVATION
October 18-21, 2016 • Rio de Janeiro /RJ • Brazil

FINE FLOTATION TAILINGS DEWATERING: RESTORING DEWATERING EFFICIENCIES AND SUPPLEMENTING WATER CONSUMPTION IN A GRAVITY GOLD RECOVERY CIRCUIT

ABSTRACT

Due to a necessary change in grind size to improve mineral recoveries in the gravity/flotation circuit of a 500 tonne per day processing plant in Sonora, Mexico, the Company's process flowsheet was adjusted to include a regrind circuit through installation of a vertical grinding mill. While recoveries did improve, newly introduced fine solids from the regrind circuit caused stress to the existing tailings dewatering circuit as they passed through the existing coarse Dewatering Screen. This process caused a "Recirculating Load" of fines to the Thickener. Equipment efficiencies and availabilities suffered as a result. Proper dewatering circuit operations were restored through the installation of a CX5-80 (80 m^2) Ceramic Disc-Vacuum Filter, employed to recover fine solids from the circuit and discharge them for final disposal. This capital investment has also supplemented fresh process water consumption by equipment in the gravity circuit by 25%. In this case, tailings dewatering has produced a total net annualized fresh water savings of 15% for the Process Plant.

KEYWORDS

Tailings Dewatering, Water Recovery, Water Management, Regrinding, Fines, Operability, Availability, Circuit Optimization, Mineral Processing

INTRODUCTION

Processing variable, heterogeneous ore with fixed capital equipment and circuit arrangement will inevitably come into conflict over time. As company's assets are mined, ore that is unearthed later in a deposit's life may look entirely different than was expected during feasibility or development. In this case, we present the contingent response undertaken by CEC Mining Systems Corp. ("CECMS") and Client to mitigate the impact of regrinding and the presence of a finer particle size distribution ("PSD") of solids than was included in the design in a high-grade gold processing plant's tailings dewatering circuit. Reapplication of this response in other gold processing plants could solve an accelerating, industry wide problem as declining grades and finer liberalization sizes complicate typical water management practices and equipment in tailings dewatering circuits. Conventional solutions, including traditional filtration equipment were deemed unfeasible (technically) and/or not optimal (economically). Through the application of CECMS' CX-Series ceramic disc-vacuum filtration technology with a 1.5-micron pore-size membrane, the circuit was restored to proper operation through collection and discharge of fine solids. Filtrate quality was also drastically improved by lowering total suspended and dissolved solids below 50 ppm. By improving filtrate quality, a water return line was constructed directly between the CX-Series filter and gravity circuit process-water feed/inlet; allowing for the filtration system to supplement 25% of total required process water in the circuit without secondary clarification. Recovery and removal of the fines from the dewatering circuit disrupted the recirculating load and has allowed for restoration of proper thickener operation, settling and overflow water clarity. In total, the installation of the filter has reduced the Process Plant's fresh water consumption by 15%.

THE PROJECT: OPERATIONS & PROCESS PLANT

After acquisition of the Property in February, 2003, the Company conducted a definitive feasibility study used to support a construction decision, which was made in the third (3rd) quarter of 2004. The mine and heap leach operations reached commercial production in April, 2005 and have been in operation since. Numerous expansion projects have been undertaken to grow crushing capacity up to approximately 18,000 tonnes per day ("tpd"). In addition to the Heap Leach Facility, between 2009 and 2012, the Company developed an underground high-grade zone of gold mineralization. To support processing of this high-grade material, the Company designed and built a 500 tpd mill with gravity and flotation concentrate recovery at a cost of USD$ 20 million. Production of the mill which processes ore from the high-grade underground deposit, began in Q3/Q4 2014, with significant improvements made in the lead up to achieving the name plate capacity (500 tpd) in Q1 2015.

Recoveries and Response

While mill throughput targets were eventually attained after the receipt and installation of certain upgraded components in mid-November 2014, improving recoveries to the budgeted level remained a tougher challenge. Recovery rates were negatively impacted by a larger than expected grind size than was designed for. By not attaining the appropriate mineral liberalization size, recoveries of gold mineralization suffered. To meet budgeted recoveries, the Company concluded that they required the installation of a regrind circuit to undertake finer grinding than was achievable by the existing equipment in the crushing circuit (cone crusher and vertical shaft impactor).

Testing and engineering were undertaken for the sizing and performance expectations for a Vertical Grinding Mill in Q4 2014 – Q1 2015. Installation was completed by Q2 2015. As a result of the installation of this equipment, the target mineral liberalization size of p80 < 250 microns, p50 < 105 microns, was achieved, allowing for gold recoveries to improve by 15% to their budgeted level at 75%.

Upon conclusion of this update to the processing circuit, Figure 1 represents the process flowsheet diagram.

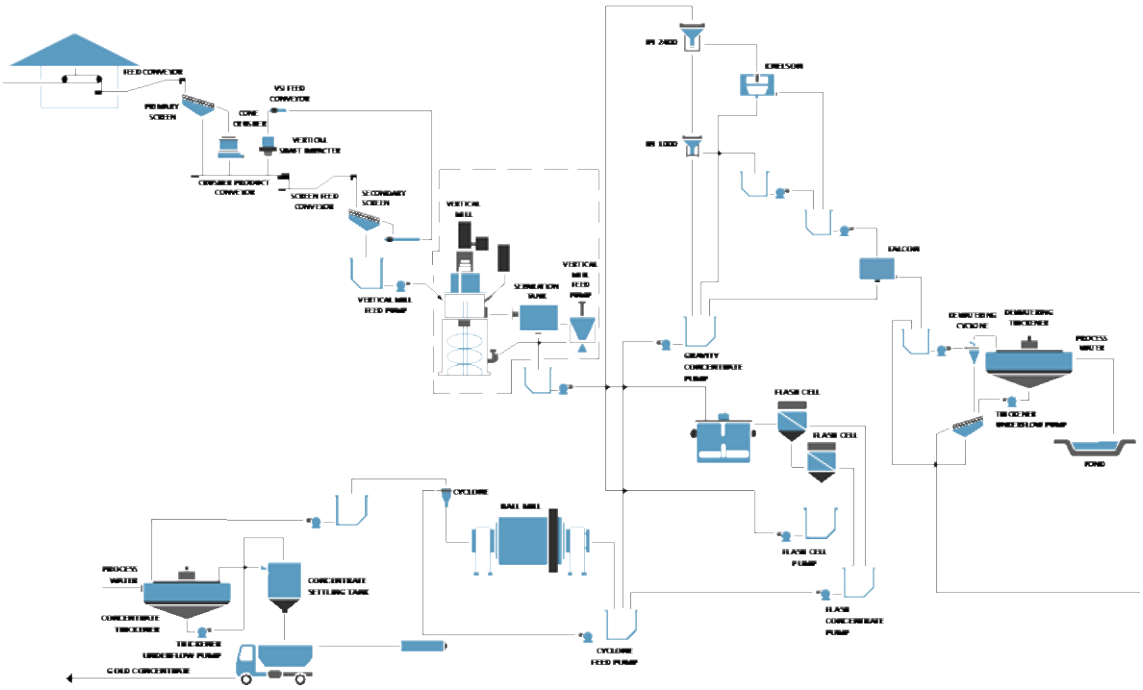

Figure 1 – Process Plant Flowsheet Diagram, Vertical Grinding Mill Installation

Unintended Consequences

The installation of the Vertical Grinding Mill resulted in both intended and unintended consequences. The intended result was the successful liberalization of gold mineralization through finer grinding, hence improved recoveries. The unintended consequence of achieving the appropriate PSD was complications arising in the tailings dewatering circuit due to the presence of a large quantity of fines (25-35% < 10 microns). The existing tailings dewatering equipment was not designed to accommodate that magnitude of fines solids. Neither the tailings thickener, nor the coarse vibratory screen were able to function at their designed performance.

Recirculating Load

The dewatering screen was installed with a sieve size of 300 microns, meaning that any particle smaller than 300 microns could pass through the screen and would re-enter the circuit through the sump pump and be fed back into the Cyclone for physical classification. Over time, more fines were able to accumulate in the circuit, because the Thickener Underflow ("TUF") also reported to the Dewatering Screen. In this paper, we refer to this process as a "Recirculating Load," generated from the equipment arrangement as shown in Figure 2. As seen in Figure 2, the original circuit, which we will title "V1.0", formed an (almost) closed loop with limited ability for the equipment to discharge fines. Attempts to reclaim fines by placing them on top of the coarse bed of coarse material during screen dewatering, what we will define as "Particle Stratification", was done with limited success, as it only served to increase the total residual moisture content of the material by decreasing its permeability.

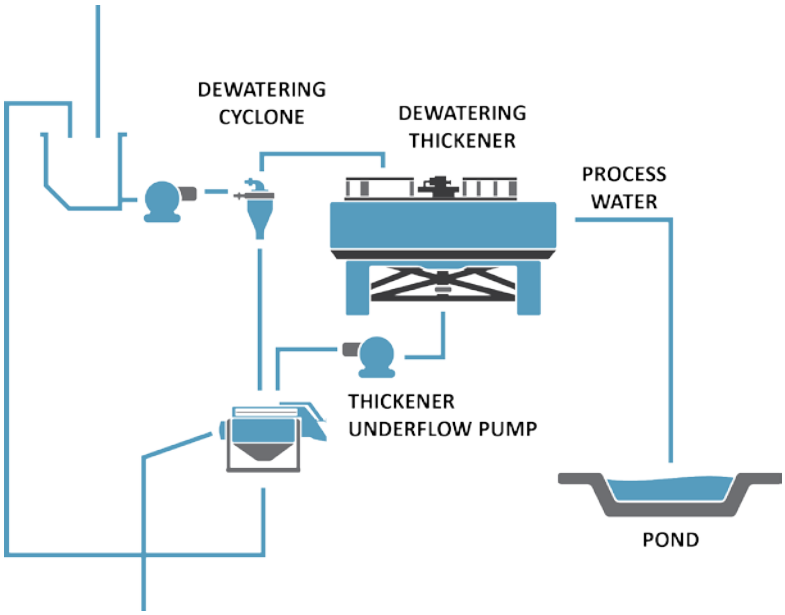

Figure 2 – V1.0 Dewatering Equipment Arrangement, Screen Co-Disposal ("Recirculating Load")

Quantifying the Impact

As fine solids accumulated in the dewatering circuit, they formed a disproportionate fraction of the total solids, distorting the PSD and skewing the tailings to become finer over time. Fines were unlikely to exit the circuit. Therefore, the existing dewatering equipment arrangement began to show escalating signs of stress and decreasing performance.

The following (qualitative) observations were made of the equipment in response to the stress produced by higher than expected load of fines:

- Increasing residual moisture content (% w/w) of 'coarse' tailings being dewatered by the Dewatering Screen;
- Poor settling characteristics in the Thickener;
- Poor (i.e. 'dirty') filtrate quality/clarity achieved in Thickener Overflow ("TOF");
- Increased consumption of flocculant(s) in the Thickener to compensate for poor settling characteristics;
- Accumulation of fine solids in Thickener bed causing higher torque on rake arms;
- Declining Thickener availability due to mandatory manual cleaning at regular intervals;
- Ballooning operating, maintenance, labour costs related to dewatering circuit;

As a result of the challenges stipulated above, the average operating cost for the tailings dewatering circuit increased after the installation of the vertical grinding mill.

DESIGNING A SOLUTION

Thickened Underflow Slurried Tailings Storage

To remedy the issues prevalent in the dewatering circuit, the Company needed to recover the fines from the circuit and to discharge them separately as a new waste stream. The first action taken was to redirect the TUF away from the Dewatering Screen and pump the material directly to a slurried Tailings Storage Facility ("TSF"), as showing in Figure 3, constructed near the Processing Plant.

Challenges

Due to constrictions of the site layout and limits on land use, the small-scale slurried TSF was constructed with substantially less than life-of-mine ("LOM") storage capacity. To increase capacity to LOM-storage, incremental dam embankment raises were to be required at additional capital cost. Moreover, the fines solids settled in the pond at a slower than expected pace. Poor consolidation of the fines resulted in insufficient (in both quantity and quality) reclamation of water from surface pumps placed in the TSF.

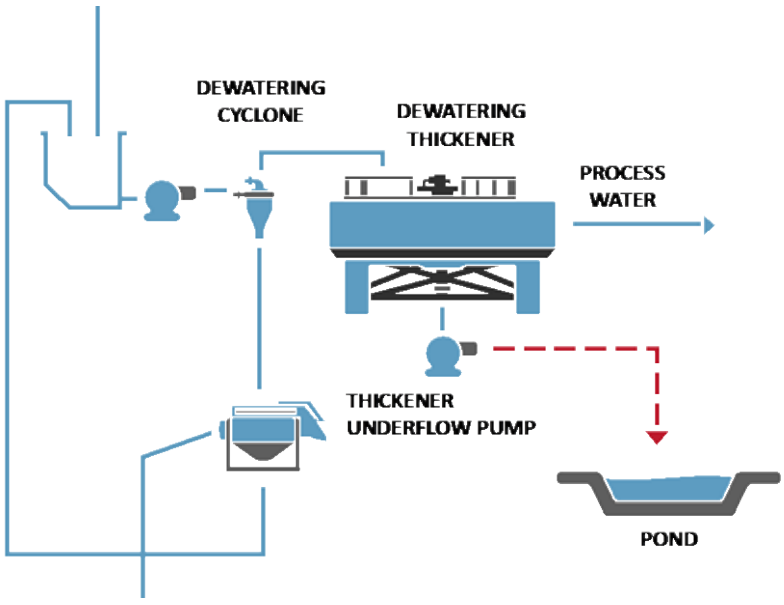

Figure 3 – V2.0 Dewatering Equipment Arrangement, Slurried Tailings Facility Disposal

The Case for Further Dewatering

Due to the Projects location in the east-central portion of the Sonoran Desert, ensuring the Process Plant has sufficient quality and quantity of water is critical to it achieving operational excellence. Therefore, fine tailings dewatering beyond the existing achievable TUF % w/w solids became an opportunity to conduct a cost-benefit analysis on an incremental capital investment. This trade-off scenario, initiated for investigating further dewatering (i.e. filtration), includes the following dimensions:

- Potential impact to fresh water balance by reclaiming more, higher quality water than what was achievable from the slurries TSF;
- Limitation of further, necessary slurried TSF embankment/capacity expansions;
- Recovery and discharge of fines for conveyor transport and heap leaching;
- Mitigation of further, incremental land-use by utilizing the Heap Leach Facility as the fine tailings solid waste dump;

Upon review of the potential qualitative and quantitative benefits associated with the dimensions summarized above, the Company began its own internal feasibility study to evaluate the budgetary capital and operating costs of their alternatives for tailings filtration technologies.

Filtration Testwork and Scoping

To quantify the potential technical and economic benefits that could accrue from further dewatering of the tailings thickener underflow, the Company engaged multiple Vendors (including CECMS) to undertake filtration testwork with the following objectives:

- Receive physical samples (in solid form), prepare slurry using water and add representative amount of flocculant to represent thickening, analyze the samples for their physical properties;
- Evaluate the potential of these slurry samples for optimum filtration method (vacuum, pressure, equipment arrangement);
- Determine maximum achievable rate of filtration while maintaining a residual filter-cake moisture content of no more than 15% w/w;
- Recommend appropriate technology, provide optimum equipment configuration, anticipated budgetary costs (capital/operating) and dewatering performance parameters;

The solid tailings samples provided to the Vendors were characterized predominantly as quartz/silica minerals (using XRD analysis), with a PSD (using Malvern analysis) as summarized in Figure 4.

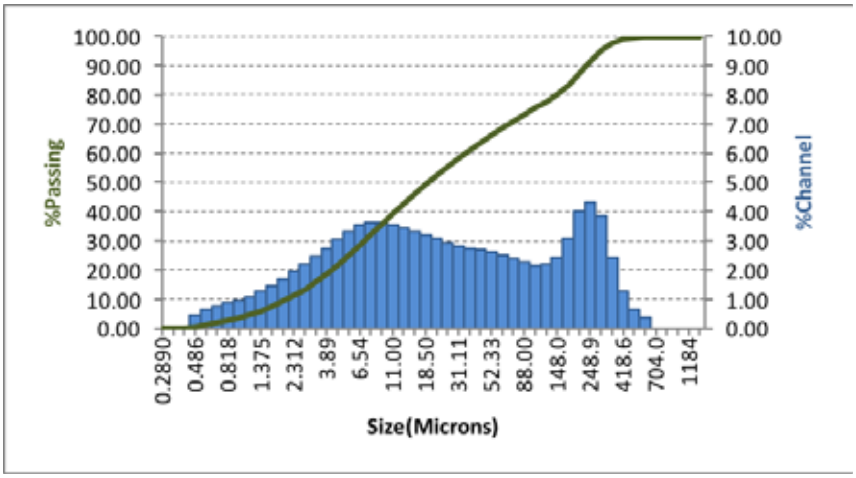

Figure 4 – Solid Tailings Samples (Tested), Particle Size Distribution Characteristics

Upon completion of testwork by the Vendors, the following conclusions were made:

- Horizontal vacuum belt filtration was deemed unsuitable due to poor retention of fines (Turbidity > 1000 NTU), declining rates of filtration above 10 mm filter-cakes, and minimum achievable moisture in the filter-cake was measured at 24% w/w;
- Membrane filter press technology was deemed suitable due to adequate retention of fines (Turbidity ~ 100 NTU) and residual filter-cake moisture content close to the target of 15% w/w;
- Ceramic filter press technology was deemed suitable due to maximum retention of fines (50 ppm of TSS) using 1.5-micron pore size membrane technology, achievable residual filter-cake moisture contents equal between 15 – 20% w/w, and filtration rates of 0.47 t/h/m^2

Equipment Selection

Testwork summaries were collected by the Company, and compiled to form a selection matrix that included the relevant comparison axis', which included physical equipment characteristics, adherence (i.e. compatibility) to the fine tailings as produced by the Process Plant, processing characteristics specific to each equipment, and economic characteristics established by each Vendor in their budgetary scoping proposals.

Based on this multi-variable analysis table and other factors such as equipment energy consumption, time for fabrication and project delivery and rates of spare parts usage, the Company selected CECMS as the Vendor for provision of its CX-Series ceramic disc-vacuum filtration system to dewater the Process Plant's gravity/flotation gold tailings.

CECMS has replicated a representative example of the type of multi-variable analysis undertaken by the Company in Figure 5.

Filtration Equipment Selection Matrix	***Vacuum Dewatering***		***Pressure Dewatering***
	Ceramic Filter	**Belt Filter**	**Horizontal (P&F) Filter Press**
Physical Characteristics			
Footprint	Filtration surface area oriented on vertical, segmented filter discs; ensures high production (tph) / filter footprint (m^2)	Filtration surface area oriented on horizontal cloth surface area. Very large equipment footprint / filtration surface area (m^2)	Filtration surface area oriented on vertical plate membrane inserts. Large infrastructure for auxiliary components and equipment weight
Mechanical Components	Filter frame and slurry basin, drum and filter segments, filtrate receivers, ancillary washing tanks	Filter frame, rollers, guides, drives, vacuum systems and filtrate receivers	Filter frame, recessed filter plates, hydraulic assembly, cloth membrane inserts, auxiliaries and supports
Complexity - Fabrication	Unibody construction, single drive drum, simplistic.	Cloth tracking (rollers, guides) requires high tolerances; medium complexity for fabrication	Numerous moving parts with wear components, pressurized hydraulic system, very complex fabrication and assembly
Filtration Media	Microporous ceramic membrane filters	Unibody cloth media	Cloth membrane inserts
Required Ancillary Equipment	Concentrated, diluted acid tanks; ultrasonic generators, transducers	Cloth washing system	Compressed air blow discharge, cloth washing system, hydraulic system.
Processing Characteristics			
Residual Filter-Cake Moisture Content:	Concentrate, 8% w/w.; Tailings, 12 - 20% w/w	Tailings, 15 - 25% w/w	Concentrate 6 - 8% w/w; Tailings 10 - 25% w/w

Material Applications	Bulk, Base Metal Concentrates; Leach, Gravity, Flotation Tailings	Coarse tailings dewatering	Most versatile system; applies to most materials
Batch vs. Continuous	Continuous	Continuous	Batched
Site Suitability	Vacuum efficiency losses occur at >3,000 mASL.	Vacuum efficiency losses occur at >3,000 mASL.	No considerations.
Particle Size Distribution	Super-fine particles can cause blinding; coarse particles can adhere slowly	Generally more suitable for coarse particle dewatering	Wide application of particle sizes
Economic Characteristics			
Operating Cost	Lowest operating cost of filtration alternatives	Medium average operating cost	High average operating cost
Energy Consumption	Very low energy intensity; up to 85% less consumption than alternatives	Medium average energy consumption	High energy consumption
Filter Media Replacements	8,000 – 12,000 hours	2,500 - 4,000 hours	2,500 – 4,000 hours
Maintenance Regularity / Costs	Irregular; low	Regular; average	Often; intensive
Consumables	Power, air, water, acid (nitric).	Power, air, water.	Power, compressed air, water, hydraulic fluid.
Labour Requirements	Highly automated, low labour inputs	Medium	High

Figure 5 – (Representative) Equipment Selection Matrix

Scope of Filtration Design

Through Vendor-specific bench-scale testing, CECMS established a "Scope of Filtration Design" to act as control for incoming process variables and slurry characteristics. These set of controls, as summarized in Table 1 act as qualifying criteria to produce a set of performance expectations for the CX-Series filter.

Table 1 – Process and Slurry Characteristics

Process Data	Unit	Avg.	~	Design
Material Characteristics:				
Feed Material Description		Gravity/flotation tailings – primarily silica and quartz minerals (minimal clay-like particles)		
Solution Temperature	°C	20 – 26		
Solution pH		8		
Feed:				
Solids Mass Flow - Nominal	t/h	33		37.7
Solids Vol. Flow - Nominal	m^3/h	12.22		13.96
Slurry Mass Flow - Nominal	t/h	55		62.83
Slurry Vol. Flow - Nominal	m^3/h	34.22		39.10
Water Vol. Flow - Nominal		22		25.13
Slurry Percent Solids	% w/w	60		60
Solids Specific Gravity	-		2.7	
Liquids Specific Gravity	-		1.00	
Slurry Specific Gravity	-	1.61		1.61
Particle Size:				
F100	µm	500		500
F80	µm	250		250
F50	µm	100		100

Water Quality:		
Solids Content (TDS)	ppm	N/A
Solids Content (TSS)	ppm	N/A
Operating Conditions:		
Site Elevation	mASL	1,342

CX-Series dewatering performance specifications as established in the Scope of Filtration Design have been summarized in Table 2.

Table 2 – CX-Series Filtration Design

Process Data	Unit	Value
Suggested Equipment		CX5-80
Required Filtration Area	m^2	80
Filter-Cake Product:		
Slurry Mass Flow – Nominal	tph	37.7
Productivity (Minimum)	$t/h/m^2$	0.471
Residual Moisture Content	% w/w	<20
Equipment Availability (Daily Avg.)	%	80
Equipment Utilization	%	100
Filter Cycle Time	sec.	60
Filter-Cake Thickness	mm	9-10

Risk Mitigation

Testwork Scale-Up

To ensure that the testwork effectively scaled to commercial production and conformed with initial design specifications, typical vacuum efficiency loss (0.85) and scale (0.80) factors were applied to the design. In doing this, typical filtration risks were mitigated through start-up and ramp-up allowing for the filtration plant to reach nameplate capacity within a few days of commissioning.

Equipment Availability

CX-Series filters have regularly scheduled washing cycles that employ nitric and ultrasonic cleaning methods. On a daily basis, and with typical tailings characteristics, these washing cycles are required to occur for 1 hour every 7 hours of processing (3/24 hours). This is equal to an 87.5% filter equipment availability. During processing the filter is continuously operating, and does not operate on a batched process such as hydraulic plate-and-frame pressure filters. In the filtration design, a utilization of 80% was selected to provide more flexibility and average filtration capacity in case of mechanical or other necessary downtime.

Ore Variability

Appropriate characterization of representative samples is absolutely critical to ensure the accuracy of testwork and to provide sufficient insulation against a likely heterogeneous ore body. In underground mining, control of ore/waste, grade is more challenging due to the more complex nature and sharper definitions of cut-off grades. Therefore, processing controls and equipment performance specifications may tend to vary. While it is difficult to control for every possible circumstance, adding sufficient contingencies in Testwork Scale-Up factors and required Equipment Availability will provide a defence against external changes in ore.

FILTRATION OUTCOMES

Fine Tailings Dewatering – Ceramic Disc-Vacuum Filtration

Since commissioning in December, 2015, the CX5-80 ceramic disc-vacuum filtration system has been successfully recovering fine solid material directly from the TUF at the appropriate residual moisture content for conveyor transport to, and disposal in, the Heap-Leach Facility where it undergoes further leaching. Filtrate is being returned directly via pipeline from the filter's dual filtrate receivers to an intermediary process water tank, where it is then pumped to the fresh water inlet of the gravity circuit, specifically the Knelson concentrator.

Figure 6 – Ceramic Disc Vacuum Tailings Filtration Plant, Completed (December 2015)

The current process flowsheet diagram for the dewatering circuit equipment arrangement can be referenced in Figure 7.

Water Recovery

When in operation, the filter is able to recover 13 m^3/hr of filtrate from the TUF that would have otherwise been discharged into the TSF. This filtrate is pumped directly back to the process water line and the gravity circuit where it offsets > 25% of total net water consumption in the circuit. There is no secondary clarification or treatment required for this water.

This direct fresh water offset accounts for a total annualized net savings of water consumption of >15% for the entire Process Plant. Due to the aridity of the Sonoran Desert, this accounts for a significant increase in life expectancy of the local aquifer used by both industry and the local municipality.

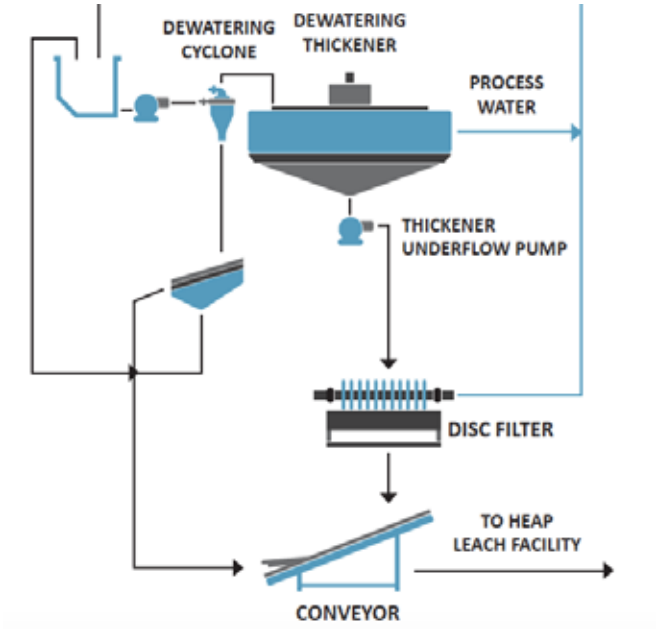

Figure 7 – V3.0 Dewatering Equipment Arrangement, TUF Ceramic Disc-Vacuum Filtration

Filter-Cake Production

Tailings are being dewatered to form a filter-cake between 9 – 10 mm and adequate residual moisture content (<20 %w/w) for appropriate discharge and Conveyor transport (without slumping). The tailings filter-cake from the Process Plant is blended with ROM-ore from the low-grade open pit. These two material streams are agglomerated (with cement) together to maximize leaching rates (i.e. drainage), and conveyed for placement within the Heap-Leach Facility. Visual characteristics of the filter-cake can be seen in Figure 8.

Figure 8 – CX-Series, Filter Cake Production and Discharge (March 2016)

Tailings Storage Footprint

The tailings generated from the Process Plant is now effectively separated into its solid and liquid components. Recovered water from the tailings feed is sent back to the Process Plant, specifically to the gravity circuit. Recovered solids from the tailings feed is sent to the Heap Leach Facility where it undergoes placement and further leaching. While the original TSF has not been de-commissioned in order to act as an emergency disposal catchment for slurried tailings in case of catastrophic filtration equipment failure, there should be no further embankment or capacity increases during the LOM of the Project. By dewatering the Process Plant's tailings and storing the solid waste in the Heap Leach Facility, the Company has neutralized the physical footprint of its tailings production.

CONCLUSIONS

Through implementation of an innovative and cost-effective dewatering technology solution, the Company has been able to optimize the process flowsheet to maximize water recovery, neutralize the Process Plant's tailings footprint and ensure proper operation of the entire dewatering circuit through filtration and removal of fine solids. The capital investment in the installation of the CX-Series filter, and dewatering the Process Plant's entire stream of tailings, has allowed for an average monthly savings of 9,360 m^3 of fresh process water consumption. On an annual basis, the savings accrued to the Process Plant equates to the volume of 45 Olympic size swimming pools.

FLOTATION OF COPPER ORE FROM SOSSEGO MINE UTILIZING PALM OIL AS COLLECTOR AUXILIARY

Raulim O. Galvão[1] Dhiêgo R. Oliveira[1], Moacir R. Neres[1], , Douglas M. Sousa[1] & Denilson da S. Costa[1] Paulo F. A. Braga[2]

[1] Faculdade de Engenharia de Minas e Meio Ambiente,
Universidade Federal do Sul e Sudeste do Pará,
Marabá- Pa, Brazil.
engraulim@gmail.com
[2]Mineral Processes Coordination, Centro de Tecnologia Mineral,
Rio de Janeiro, Brazil,

24th World Mining Congress
MINING IN A WORLD OF INNOVATION
October 18-21, 2016 • Rio de Janeiro /RJ • Brazil

FLOTATION OF COPPER ORE FROM SOSSEGO MINE UTILIZING PALM OIL AS COLLECTOR AUXILIARY.

ABSTRACT

One of currently used methods to improve the fine recovery during ore flotation is the use of diesel oil as hydrophobicity enhancer. However, this compound can be environmentally harmful. Several vegetal oils found in the Amazon area present the potential to be used in the mineral industry, yet are seldom focus of studies. Such supplies are renewable and present a low environmental impact. In that scenery, the present work aims to evaluate the palm oil as a collector auxiliary during the flotation of Copper ore from Sossego mine (Canaã dos Carajás, Pará). With that aim, physical, chemical and mineralogical characterizations of the copper ore were made, as well the refining and physical-chemical characterization of Palm oil. The batch flotation tests used 8 g/t of Xanthates as collector and 30 g/t of MIBC as frothing agent. The collector auxiliary (palm oil) concentrations used were: 60, 80, 100 and 120 g/t. In all concentrations the added nonpolar oil was emulsified. The results were compared as the ones found with diesel oil, which is currently used during the Copper ore processing from Sossego. For the tests using palm oil, the copper content in the concentrated was up to 17.9%, while with diesel oil, the maximal copper content was 15.5%. The average metallurgical recovery found during the tests was 95.74% with palm oil and 97.02% with diesel oil. These results show that palm oil presents a high performance as collector auxiliary during the copper ore flotation, being a relevant option to replace diesel oil total or partially.

INTRODUCTION

Recovery of fine mineral particles (<38 μm) is the main problem that affects sulphide Copper concentration plants. Processing plants are, generally, projected for medium size and high flotation kinetic particles recovery. Furthermore, ore commodity rising demand and high content deposits exhaustion brings the

need to process fine scattered and low content ores. Thus, a finer milling is necessary to release the mineral of interest (Rubio, 2004).

Many techniques have been researched to minimize fine particles flotation issue, including extensor flotation, that consists on utilizing nonpolar oils (emulsified or not) along standard collectors covering hydrophobic mineral surfaces rising the nonpolar character and improving particle-bubble attachment. However, the major importance of extensor flotation lies on fine and ultrafine particles recovery by homoaggregation process, in which occurs the particle size increase through interactions among thousands of colloidal dimension oil drops (1- 5μm) produced during emulsification process (Matiolo, 2005).

Presently this flotation technique is already applied in industrial scale, generally, utilizing diesel oil as collector auxiliary (Capponi et al., 2005; Nankran et al., 2007). Meanwhile, besides not come from a renewable energy source, diesel oil has in its composition: sulphur, aromatic hydrocarbons (BTEX) and polyaromatic hydrocarbons (PAH's), high pollutant elements that are harmful to human being health (Mariano, 2006).

Mineral activity, due to its essence, is the less acceptable activity within the new conceptual framework for sustainable development. Thus, it is necessary a reassessment of inputs and processes used by the mining industry. Accordingly, there is a considerable amount of vegetable oils whose properties indicate the possibility of use as reagents in ore flotation (Costa, 2012).

The present paper objective is show the main results of fine Copper ore recovery by extensor flotation technique utilizing palm oil (*Elaeis guineensis Jaquim*), justified due to its low environmental impact, renewable character, besides the source abundance on Amazon area.

METHODOLOGY

Ore

During this work it was used copper sulphide ore from Sossego mine (VALE), from Canaã dos Carajás, Pará. To prepare the ore its granulometry was reduced to reach a P_{80} of 150 μm, similar to the feed for the rougher stage in the processing plant. Figures 1 and 2 show the granulometric distribution of the samples and the content of copper according to the particle size, respectively.

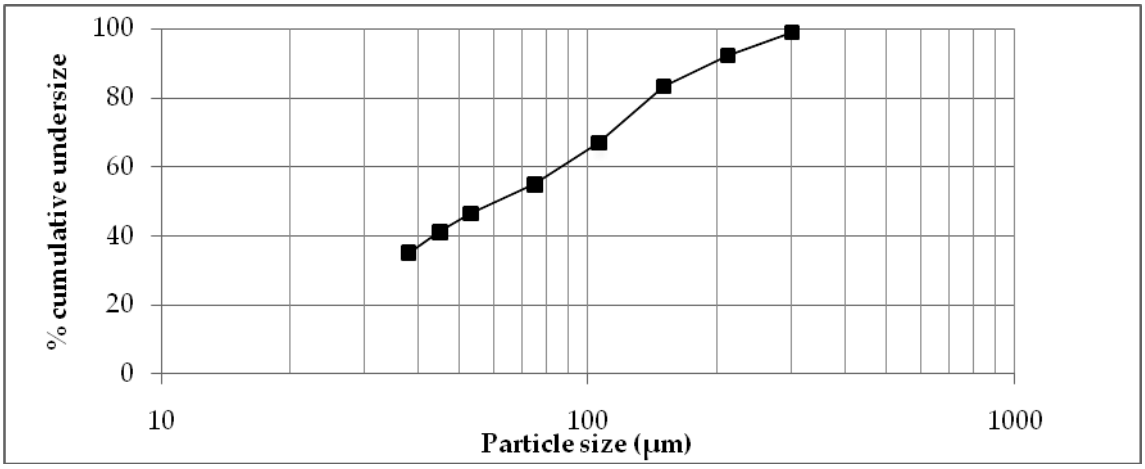

Figure 1: Granulometric distribution of the ore.

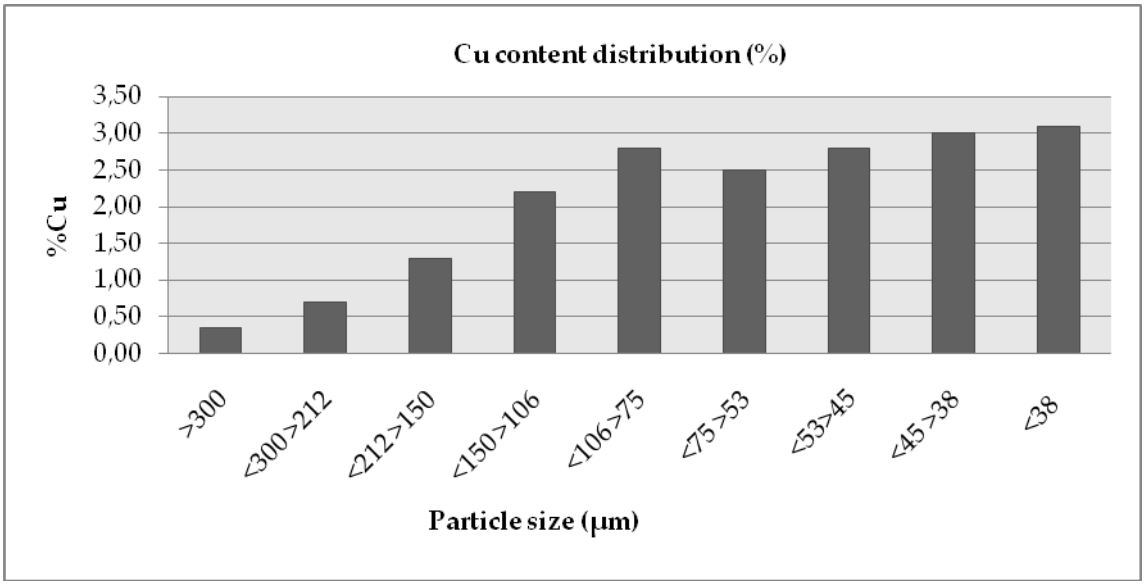

Figure 2: Granulochemical distribution of Cu.

The main minerals found on the sample determined by the X-ray diffraction are shown on the diffractogram from figure 3.

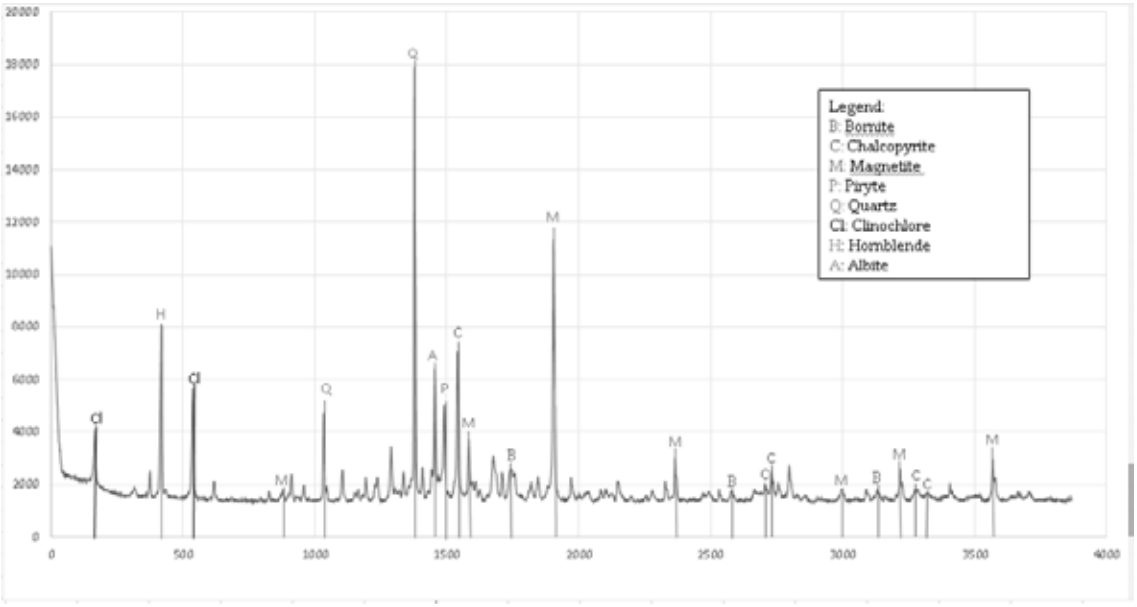

Figure 3**:** X-ray diffractogram of the sample.

Palm oil

The palm oil used during this work was obtained commercially and its acidity and saponification were determined according to AMERICAN OIL CHEMISTS' SOCIETY (AOCS). All analyses were made in the laboratories from the company Indústrias Químicas Ltda. (HIDROVEG), from Rio de Janeiro.

Due to its high acidity presented by the palm oil it was needed to decrease it. The present free fatty acids could lead to fatty acid salts (anionic collectors) once in an alkaline environment. It would bring a dual behaviour to the oil, acting as collector auxiliary and as collector.

Table 1 shows the palm oil before and after the acidity reduction.

Table 1**:** Acidity and saponification of the palm oil.

Palm oil	**Before**	**After**	**Methods**
Acid value (mg KOH/g)	9,33	2,60	A.O.C.S TE IA-54
Saponification value (mg KOH/g)	195,37	193,97	A.O.C.S TG IA-64

Flotation Tests

Tests were performed in a flotation machine (Denver D-12), laboratory scale, and a cell with 1.5L capacity. Pulp, 38% solid in weight, pH 10.5, regulated with lime, was conditioned to 800 rpm for 3 minutes using the following reagents: Potassium amyl xanthate (PAX) (8 $g.t^{-1}$) and Aero 7294 A (5 $g.t^{-1}$) as collectors, emulsified nonpolar oils (different dosages) as collector auxiliary and 30 $g.t^{-1}$ of methyl isobutyl carbinol (MIBC) as frothers (added in this order). After conditioning, cell rotation was increased to 1200 rpm, air was injected and then the ore was floated over 7 minutes. Table 2 presents flotation tests performed and utilized reagents dosages.

Collector auxiliaries (PO and DO) were emulsified in oil/water solution at 6000$mg \cdot L^{-1}$ by mechanical shaking for 10 minutes to ensure uniformity to emulsion.

Table 2**:** Standard flotation (STD) and extension flotation tests using emulsified palm oil (PO) and diesel oil (DO) on different dosages.

NUMBER	TEST	REAGENT (g/t)				
		PAX	Aero 7294A	MIBC	Palm Oil	Diesel Oil
1	**STD**	8	5	30	-	-
2	**POP**	-	-	30	**80**	-
3	**PO-60**	8	-	30	**60**	-
4	**PO-80**	8	-	30	**80**	-
5	**PO-100**	8	-	30	**100**	-
6	**PO-120**	8	-	30	**120**	-
7	**DOP**	-	-	30	-	**80**
8	**DO-60**	8	-	30	-	**60**
9	**DO-80**	8	-	30	-	**80**
10	**DO-100**	8	-	30	-	**100**
11	**DO-120**	8	-	30	-	**120**

By the end of tests the obtained products (concentrate and tailing) were filtered and dried in stove at a maximum temperature of 100°C for approximately 12 hours. After drying, they were sent to the laboratory of chemical analysis to Copper content determination.

RESULTS AND DISCUSSION

At Figure 4 its noticed a Cu content increase to PO dosages over 60 $g.t^{-1}$, and at the 120 $g.t^{-1}$ dosage was reached the best results, with 17.9% Cu at floated. For the tests in which were added DO, gains are also noted in Cu content (14.8% in 120 $g.t^{-1}$) compared to STD tests (13.4%). However, all tests utilizing DO as collector auxiliary presented lower Cu contents when compared to PO tests.

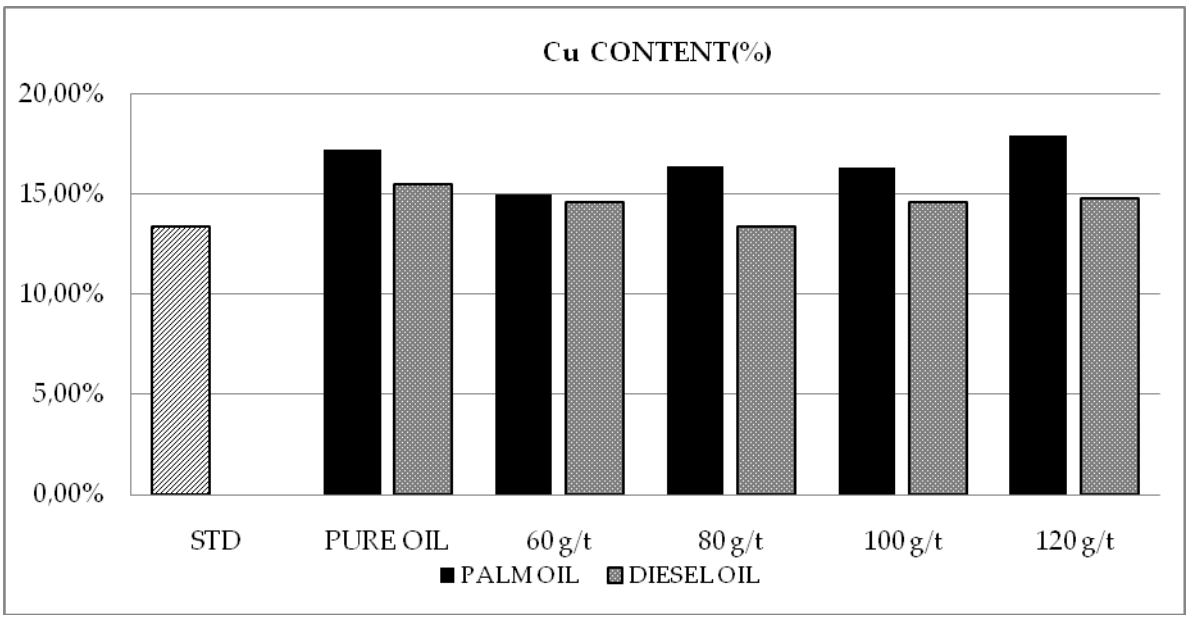

Figure 4: Cu content in the floated

Figure 5 shows Copper metallurgical recovery to tests with PO and DO addition. Generally, tests using emulsified PO and DO presented a increase on Cu recovery, but almost inexpressive relating to STD.

At tests in a dosage of 60 $g.t^{-1}$ to PO and DO o ensaio com dosagem de para OD e OP were obtained more satisfactory metallurgical recovery values, 97,9% e 96,88%, respectively, aganist to 96,59 % from STD.

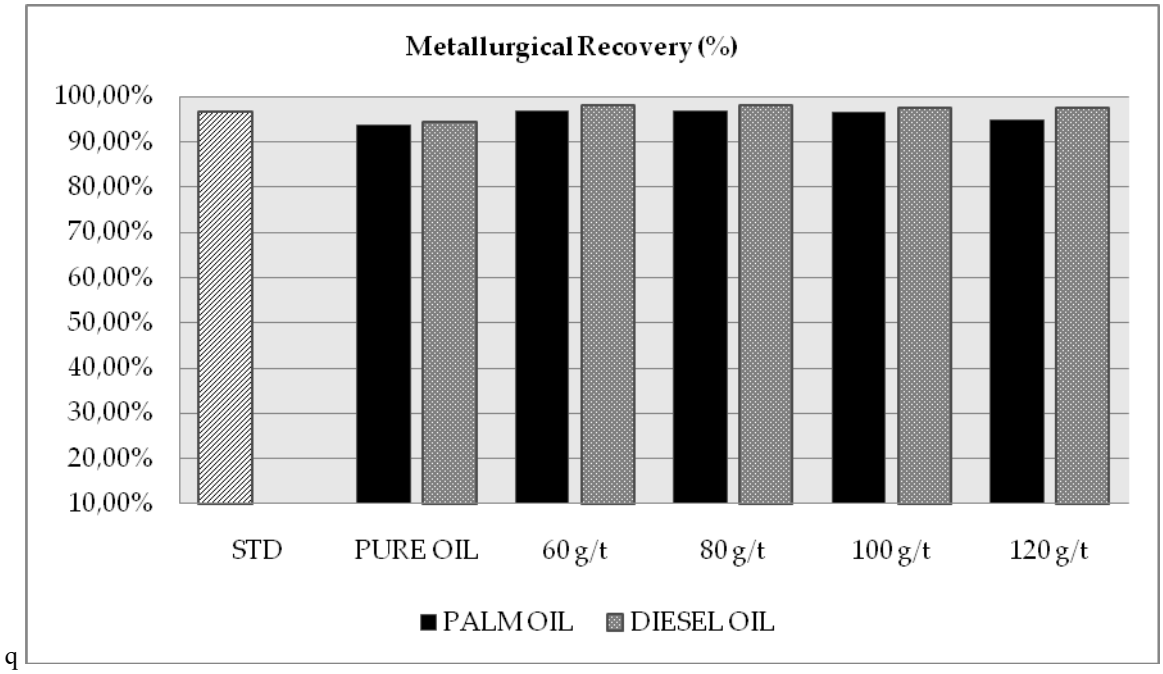

q

Figure 5: Cu metallurgical recovery on the extention and standart flotation tests

Figure 6 shows that emulsified palm oil addition at rougher stage provided, statistically, the same metallurgical gains compared to STD tests, but presented gains until 4.5% at metal of interest content.

Metallurgical recovery and Copper content in the concentrate results were near to the values obtained at Sossego's plant in the rougher stage of flotation, that are average 13 to 17% concentration content and 94 to 96% to metallurgical recovery (Nankran et al., 2007).

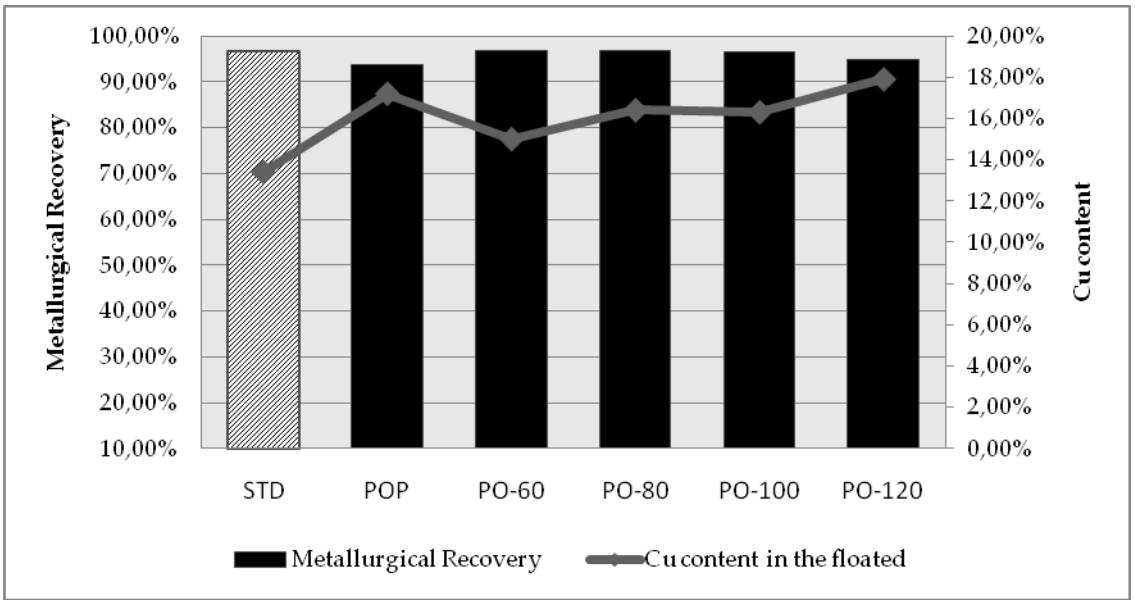

Figure 6**:** Metallurgical recovery and Copper content in the floated at tests utilizing PO.

CONCLUSION

Results found during this work show that the flotation of copper sulphate with the addition of palm oil presents the same metallurgical recovery, but with a higher Cu content in the floated if compared with the studies that utilized diesel emulsified diesel oil to the standard tests.

Considering the similarity of the results between the two nonpolar oils, it can be seen that the OP (as well other Amazonian oils) shows a potential as collector auxiliary. However, deeper studies are needed to a possible total or partial substitution of the DO.

The use of PO, as a substitute for the DO during copper sulphate flotation leads to a higher hydrophobicity of the mineral particles and aggregation of the fine particles, as well a better attachment bubble/particle.

ACKNOWLEDGEMENTS

The authors acknowledge the support from the *Centro de Tecnologia Mineral* to the development of this work.

NOMENCLATURE

STD	Standard flotation test
PO	Palm oil
DO	Diesel oil

REFERENCES

Capponi F, Matiolo E, Rugio J, 2005. Flotação extensora de finos de minério de cobre e molibdênio. *In: Anais do XXI Encontro Nacional de Tratamento de Minérios e Metalurgia Extrativa*. Natal, Brasil vol. 1, pp 235-242.

Costa, D. C, 2012. *Uso de óleos vegetais amazônicos na flotação de minérios fosfáticos*. Tese de Doutorado – Escola de Engenharia, Programa de Pós-Graduação em Engenharia Metalúrgica, Materiais e Minas – PPGEM/UFMG, Belo Horizonte, Brasil, pp 1-176.

Mariano, A. P, 2006. *Avaliação do potencial de biorremediação de solos e de águas subterrâneas contaminados com óleo diesel*. Tese de Doutorado - Programa de Pós-Graduação em Geociências e Meio Ambiente – PPGGMA/UNESP, Rio Claro, Brasil, pp 1-147.

Matiolo, E, 2005. *Recuperação otimizada de finos de minérios de cobre e molibdênio por flotação não convencional*. Dissertação de mestrado – Escola de Engenharia, Programa de Pós-Graduação em Engenharia de Minas, Metalúrgica e Materiais -PPGEM/UFRGS, Porto Alegre, Brasil, pp 1-99.

Nankran, M.; Bergerman, M.; Miranda, A.; Oliveira, J.; Souza, M.; Batista Filho, J.; Cardoso, W, 2007. Controle operacional da usina do sossego. *In: Anais do XXII Encontro Nacional de Tratamento de Minérios e Metalurgia Extrativa*. Ouro Preto, Brasil, 2007. vol. 1, pp 502-512.

Rubio, J., Capponi, F., Matiolo, E., Rosa, J, 2004. Avanços na flotação de finos de minérios sulfetados de cobre e molibdênio. *In: Anais XX Encontro Nacional de Tratamento de Minérios e Metalurgia Extrativa*, Florianópolis, Brasil, Vol. 2, pp 69-77.

FREQUENT AND FAST PROCESS MONITORING DURING MINERAL BENEFICIATION USING MODERN X-RAY TECHNOLOGIES

*U. König[1] and N. Norberg[1]

[1]*PANalytical B.V.*
Lelyweg 1
Almelo, Netherlands, 7600AA
*(*Corresponding author: uwe.konig@panalytical.com)*

24th World Mining Congress
MINING IN A WORLD OF INNOVATION
October 18-21, 2016 • Rio de Janeiro /RJ • Brazil

FREQUENT AND FAST PROCESS MONITORING DURING MINERAL BENEFICIATION USING MODERN X-RAY TECHNOLOGIES

ABSTRACT

Decreasing ore qualities and increasing prices for raw materials require a better control of processed ore and a more efficient use of energy. Traditionally quality control in mining industries has relied on time consuming wet chemistry or the analysis of the elemental composition. The mineralogy that defines the physical properties is often monitored infrequently, if at all. The use of high speed detectors has turned X-ray diffraction (XRD) into an important tool for fast and accurate process control. XRD data and their interpretation do make the difference in the identification of minerals, in describing their distribution in ore bodies and in their beneficiation during processing. The combination of XRD with modern statistical techniques such Partial Least Square Regression (PLSR) enables to directly monitor process relevant parameter during mining and ore processing. The practical use is illustrated on case studies from bauxite mining and iron ore processing.

KEYWORDS

Mineral processing X-ray diffraction, PLSR, bauxite, iron ore, sinter

INTRODUCTION

During the last decades XRD became a analytical standard tool in mining industries due to increasing analysis speed and the use of modern techniques such as the Rietveld method for quantification of the total phase content of a sample. Traditional calibration based methods rely on one peak only and do not analyze the total phase composition. The Rietveld quantification uses structural information to predict information from the full pattern using physical models and fitting techniques. This requires crystallographic knowledge and realistic physical models that fit with the specific materials.

Recently the combination of XRD and partial least squares regression (PLSR) was trialed to directly monitor process parameter such as available element content, element speciation, physical parameters or even reagent consumptions (work in progress). PLSR can run in parallel to the determination of the mineralogical composition using method like Rietveld quantification. PLSR requires neither crystal structures nor complex modeling techniques. Two examples from mining industries and downstream processing are object of this paper to demonstrate the high potential of this method for use in mining industries.

MATERIAL AND METHODS

Sample preparation of powder samples is an important factor to obtain correct results. In order to maximize the accuracy the sample taking should be standardized and optimized to the special needs of the application. To guarantee a reproducible and constant sample preparation for XRD measurements, the samples were prepared using automatic sample preparation equipment. All samples were milled for 30 seconds, resulting in a particle size <73 µm and pressed for 30 seconds with 10 Nm load into steel ring sample holders.

A PANalytical *CubiX³ Minerals* industrial diffractometer with Co anode, incident iron filter and high-speed *X'Celerator* detector was used for the studies, featuring measurement times of less than 8 minutes per scan. Data evaluation was done using the software package HighScore version 4.5, incorporating the partial least squares regression (PLSR) analysis of XRD data.

PLSR (also called soft modeling) is a popular statistical method to predict "hidden" properties directly from the raw data. After the development of a PLSR model it can be used to predict the property from an unknown sample. The PLSR model requires an independent determination of the "reference values". Using PLSR, as developed by WOLD (1966), it is possible to predict any defined property *Y (e.g. process parameter)* directly from the variability in a data matrix *X (XRD measurement)*. The matrix X typically contains non-systematic variations (sample preparation, impurities, different grain sizes) and systematic 'measurable' variations (different quantities). The aim is to correlate the systematic variation with a known property, Y. PLSR for XRD data is a full pattern approach that totally dismisses profile shapes but still uses the complete information present in the XRD data sets. The software HighScore uses the SIMPLS algorithm (DE JONG 1993, LOHNINGER 1999). The PLSR module is easy to use, evaluation and optimization of the regression model is semi-automatic and requires little knowledge of the method.

Cross-validation is used to estimate the errors of a certain PLSR calibration model when a set of independent samples is not available for validation. While performing cross validation one sample is left out of the calibration and this one sample is then used as a validation sample. The process is repeated until all samples have been predicted. However, an independent test set is still the best approach to validate any PLSR model. The rout mean square error of prediction (RMSEP) gives an absolute estimate of the expected error of the predicted parameter.

RESULTS AND DISCUSSION

Analysis of available alumina and reactive silica in bauxite ores

Bauxite ores consists of several mineral phases. The main alumina containing minerals that occur in bauxites are gibbsite, boehmite and diaspore. Other gangue or impurity minerals typically found in bauxites include clays, typically kaolinite, quartz, iron oxide and iron hydroxy-oxide (hematite and Goethite), titanium dioxide in the form of anatase or rutile. The mineralogy is very important as it dictates the refining conditions that must be used and has a large bearing on the economics of processing a particular bauxite. Not all existing elemental aluminium in a bauxite ore can economically be extracted due to the different ways aluminium is bound in the minerals. For that reason bauxite producers monitoring the "available alumina" in bauxite ores. Silicates that react during the refining process make the processing inefficient and need to be monitored as "reactive silica" as well.

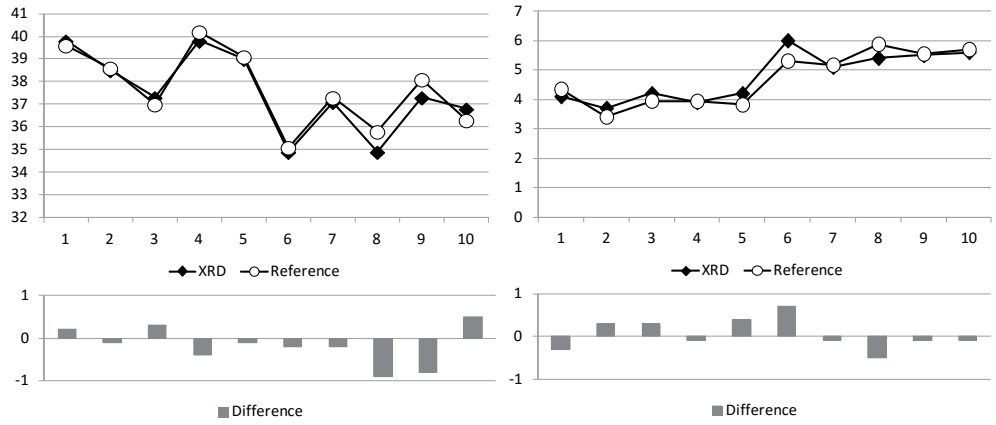

Figure 1 - Comparison of reference values (wet chemical digestion) and the results from XRD/PLSR for available alumina (left) and reactive silica (right) of 10 bauxite ores from one ore deposit

Forty samples from one bauxite deposit were used for the analysis of available alumina and reactive silica using partial least squares regression (PLSR) on X-ray diffraction raw data. For the calibration of the PLSR model the reference values from wet chemical digestion of the samples were used. The forty samples were divided into 30 samples for the development of the PLSR model and 10 samples that were used to validate the PLSR model, figure 1 and table 1. Cross validation was

performed a) theoretical as included in the software package by excluding systematically measurements used for the PLSR model and preferably b) using a set of 10 samples that are measured against the PLSR model.

Table 1 - Comparison of reference values (wet chemical digestion) and the results from XRD/PLSR for available alumina (left) and reactive silica (right) of 10 bauxite samples

	Available alumina			Reactive silica		
Sample	XRD (PLSR)	Reference	Difference	XRD (PLSR)	Reference	Difference
1	39.8	39.6	0.2	4.1	4.4	-0.3
2	38.5	38.6	-0.1	3.7	3.4	0.3
3	37.3	37.0	0.3	4.2	4.0	0.3
4	39.8	40.2	-0.4	3.9	3.9	-0.1
5	39.0	39.1	-0.1	4.2	3.8	0.4
6	34.9	35.1	-0.2	6.0	5.3	0.7
7	37.1	37.3	-0.2	5.1	5.2	-0.1
8	34.9	35.8	-0.9	5.4	5.9	-0.5
9	37.3	38.1	-0.8	5.5	5.6	-0.1
10	36.8	36.3	0.5	5.6	5.7	-0.1

Figure 1 and table 1 show the comparison of the reference values and the obtained results using PLSR for the available alumina and reactive silica content in the 10 bauxite samples. The PLSR models were developed over a range from 32.8% to 40% available alumina and 2.3% to 7.3% reactive silica as available in the samples. Cross validation using the theoretical module as implemented in the software package HighScore with an test set of 3 samples and 5 repetitions gave an expected RMSEP of 1.4% available alumina and 0.6% reactive silica. The differences between the reference values and the measured concentrations of the 10 test samples confirm these expected RMSEP, see figure 1 and table 1 below.

Analysis of iron ore sinter

Iron ore sinter materials are an important feedstock material for the steel industry. Since fines cannot be used in conventional blast furnaces because they impair the upward gas flow, they are agglomerated in sinter plants, GOSH & CHATTERJEE (2008). Most steel plants use coal and iron ores from diverse sites as the major raw material for the sintering process. Raw materials, raw mixtures as well as the sinter material should be controlled carefully to obtain the optimal composition that would lead to a good quality of iron in a blast furnace and an effective use of energy.

The composition of iron ore sinter according to PATRICK & LOVEL (2001) and VAN DEN BERG (2008) includes as main phases hematite (Fe_2O_3), magnetite (Fe_3O_4), ferrites (mostly Silico Ferrite of Calcium and Aluminium, SFCA), a glass phase and dicalcium silicates (C_2S, larnite). Main sources of FeO (total Fe^{2+}) in iron ore sinter is magnetite. Minor amounts are also present within the SFCA phases. Although FeO in sinter is one of the major constituents in making iron and steel, there have been little attempts for the prediction of FeO content in sinter ores using X-ray diffraction (XRD), which has several advantages over conventional analysis methods such as speed, accuracy and the fact the no chemicals are involved for the analysis. Besides the FeO content XRD can quantify the mineralogical phase content and the presence of amorphous phase. Together with statistical methods such as PLSR it is possible to determine also physical parameters such as the sinter strength index (SSI) and the reduction degradation index (RDI).

Forty-eight iron sinter samples were used for the analysis, where 21 samples were used to develop the PLSR model and the rest was used as test samples to validate the model. The results from the PLSR analysis were compared to reference values analyzed with traditional wet chemical methods.

For the determination of the FeO content two XRD method were used, PLSR and full pattern Rietveld quantification, figure 2. Input for all PLSR analysis were the measured XRD scans (range 10 to 88 °2θ) and the reference values for FeO.

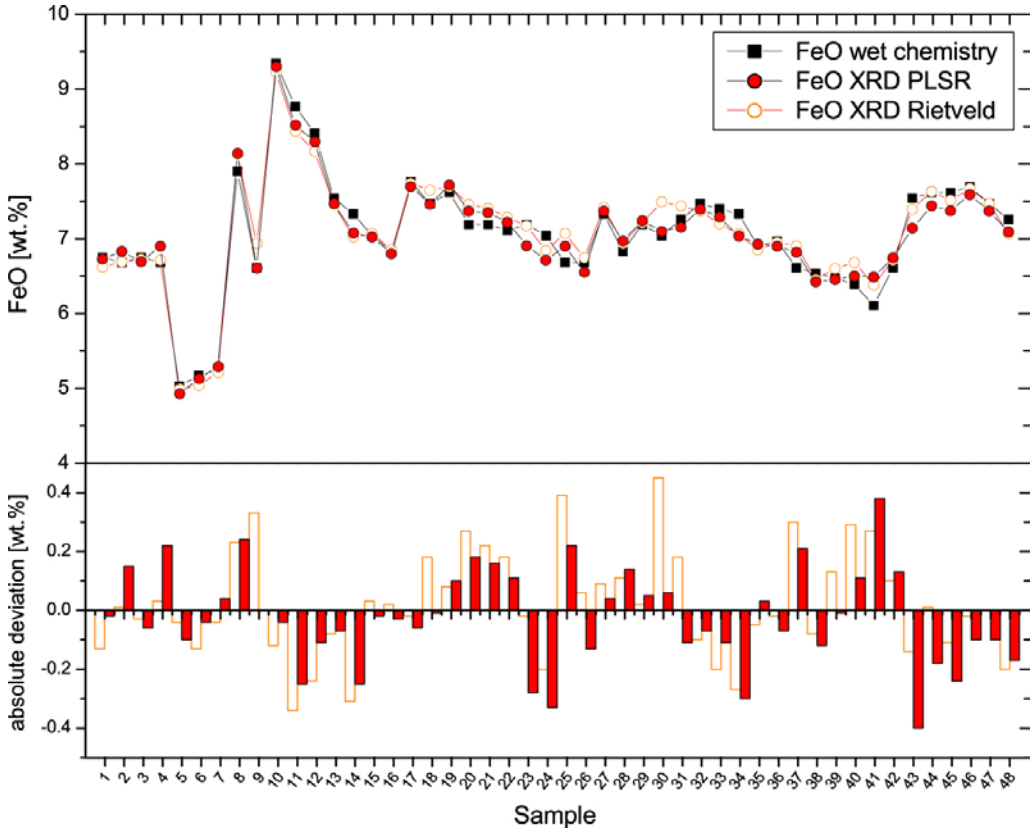

Figure 2 - Comparison of reference values (wet chemistry) and the results from XRD-Rietveld and XRD-PLSR for the FeO content of 48 samples

For testing the model all 48 samples (including the 21 references) were prepared, measured and analyzed. The results are plotted in figure 2 together with the FeO values from the Rietveld quantification and the reference values from wet chemistry. The results from the Rietveld method as well as determined with PLSR match with the given reference values from wet chemistry. Both methods can be used to determine the FeO content in iron sinter. The RMSEP from the results of the test samples matches the expected RMSEP obtained with the cross validation tool in HighScore. In both cases the expected error is with < 0.3 % FeO calculated, see also figure 2 under the graph.

Besides chemistry also physical parameter such as RDI and SSI characterize the quality of iron sinter. PLSR was trialed to correlate XRD raw data with the sinter strength and the RDI value of the same 48 samples. Figure 3 gives a summary about all calculated process parameter obtained from PLSR of the same XRD raw data. Variations in basicity and FeO are can be found back in the variation of the RDI and SSI. All parameter were analyzed simultaneously from the same measurement.

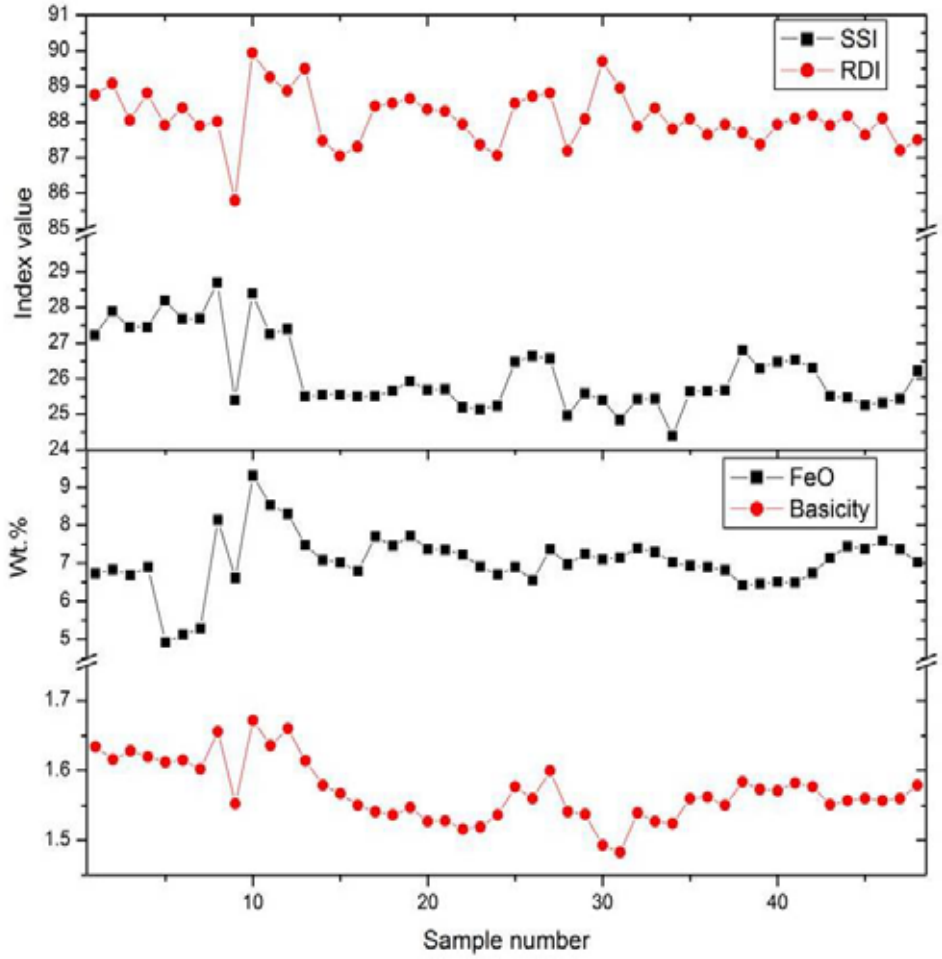

Figure 3- Summary of process parameter obtained XRD measurements (8 minutes) of 48 samples using PLSR (partial least squares regression),
RDI = reduction degradation index, SSI = sinter strength index, basicity = CaO/SiO_2

CONCLUSION

The results prove that XRD in combination with statistical methods such as PLSR is a robust and fast alternative to time and cost consuming wet chemical methods used for characterizing raw ores or processed material. The examples demonstrate the great potential of XRD for controlling and monitoring mining operations and ore processing. High frequent analysis and no use of any chemicals are the main differences between traditional wet chemical methods and fast characterization with XRD. Today's optics, detectors, and software can provide rapid (< 10 minutes) and accurate analyses, suitable for process control environment. The complete analysis is ready for automation and can be easily included in full automation lines. Fluctuations in material streams can be detected and fast counteractions can be directly applied. Obviously this proactive compensation of raw material fluctuations is much faster than waiting to see effects in the processed material.

REFERENCES

DE JONG, S. (1993): SIMPLSR: an alternative approach to partial least squares regression. Chemometrics and Intelligent Laboratory Systems. 18: 251-263.

GHOSH, A. AND CHATTERJEE, A. (2008): Ironmaking and steel making: Theory and practice. 492 p.

LOHNINGER, H. (1999): Teach/Me Data Analysis. Springer-Verlag, Berlin-New York-Tokyo.

PATRICK & LOVEL (2001): Leaching dicalcium silicates from iron ore sinter to remove phosphorus and other contaminants. ISIJ, vol. 41, no. 2, P. 128-135.

VAN DEN BERG, T. (2008): An assessment of the production of fine material in iron ore sinter. University of Pretoria, Department of Materials Science and Metallurgical Engeneering, MSc Dissertation.

WOLD, H. (1966): Estimation of principle components and related models by iterative least squares. In P.R. Krishnaiaah (Ed.) Multivariate Analysis. 391-420. New York. Academic Press.

HEMATITE FLOATABILITY USING HALLIMOND TUBE AND EMDEE-MICROFLOT

D.S. Costa[1], A.E.C. Peres and P.S. Oliveira[2], D.S. da Costa[3]

[1]Universidade Federal do Sul e Sudeste do Pará
Folha 17, Quadra 4, Lote Especial. CEP 68505-080
Marabá/PA-Brazil
Corresponding author: denilson@ufpa.br

[2]Universidade Federal de Minas Gerais
Av. Antônio Carlos, 662. CEP 31270-901
Belo Horizonte/MG-Brazil

.

[3]Universidade Federal do Pará
Rua Augusto Corrêa, 01. CEP 66075-110
Belém/PA-Brazil

24th World Mining Congress
MINING IN A WORLD OF INNOVATION
October 18-21, 2016 • Rio de Janeiro /RJ • Brazil

HEMATITE FLOATABILITY USING HALLIMOND TUBE AND EMDEE-MICROFLOT

ABSTRACT

The main purpose of this paper was to compare recovery values obtained via two techniques widely used as floatability criteria: microflotation in Hallimond tube and EMDEE microFLOT. Hematite was the mineral used and the collector reagent was obtained from alkaline hydrolysis (saponification) of the buriti oil (*Mauritia flexuosa)*, an Amazonian plant specie. The variables used were mineral particle size, collector concentration and pH of flotation. The entrainment was also compared between the two techniques. The results show a qualitative similarity on the behavior of the curve of recovery in function of collector concentration and pH for the coarse fraction. However, the technique which used Hallimond tube recovered more material than the EMDEE microFLOT technique. This result is due to the fact that the systems hydrodynamics are different, because while the Hallimond tube uses gas insertion through the tube base, EMDEE uses vigorous shaking. As a consequence, the bubbles formed by the EMDEE tube have a lower stability in comparison to those formed by the Hallimond tube. Thus, it concludes that, for hematite, the choice of the microflotation technique as floatability criteria will depend on the material particle size. For finer fractions, the EMDEE microFLOT tube showed to be more efficient since the Hallimond tube produces excessive entrainment, even with height extender. For coarser fractions, both techniques are efficient and can be used indistinctly.

KEYWORDS

Flotation, Hallimond, EMDEE.

INTRODUCTION

In the flotation process, it is necessary to use techniques, known as floatability criteria, to evaluate the interactions between reagents and minerals. These techniques provide indications of floatability or hydrophobicity of a certain mineral, what might help to elucidate physic-chemical phenomena that occur in a flotation cell.

Microflotation in Hallimond tube and contact angle measurements are techniques widely used as floatability criteria. Due to the easy manipulation and good reproducibility of results, the microflotation in

Hallimond tube is more used than the angle contact measurements. In this technique, the microflotation is performed with samples of the pure mineral and the air is injected through an orifice below the sintered glass bottom and travels throughout the tube, dragging the hydrophobic particles (property induced for the addition of collectors).

The EMDEE MicroFLOT cell consists of a 100-ml volume glass tube with a removable cover, which is shaken in a controlled manner (number and frequency) by a pneumatic actuator. After shaking the tube, the floated material is separated for drying and weighing. The operational conditions are easily controlled and the results show an excellent repeatability and reproducibility, being almost completely independent of the analyst. Studies performed with EMDEE are common in the current literature about microflotation.

Some minerals present very fine particle size (kaolinite, for example) or significant amount of hematite which, for its ferromagnetic property, adheres on the surface of magnetic stirrer of the Hallimond tube. Thus, it is of utmost importance that the available alternatives can replace equally the most spread technique that is microflotation in Hallimond tube.

Therefore, the main purpose of this paper is to evaluate the differences and similarities on the hematite recovery using two microflotation techniques: Hallimond tube and EMDEE microFLOT.

METHODOLOGY

Mineral Sample

The mineral used in the microflotation tests was hematite, from Mineração Casa da Pedra – Minas Gerais, in the following particle size ranges: -212 µm +150 µm, -150 µm +106 µm, -106 µm +75 µm and -75 µm +45 µm, obtained by wet sieving. The qualitative mineralogical analysis was carried out by X-ray diffraction and the crystalline phases recognition was performed by comparison of the values of interplanar spacing and peak intensities from the sample diffractogram to the ICDD (International Center for Diffraction Data) database. In the diffractogram achieved, it was not observed an amorphous dome, demonstrating the absence of amorphous phases. Hematite was the mineral phase identified in the sample. The sample chemistry composition, ascertained via wet method, contained 69.70% of total iron, 0.049% of aluminum, 0.051% of silica and phosphorus below 0.01%. The loss on ignition was 0.060%. Thus, according to the results shown, the mineral used in this study has acceptable purity for the performance of the proposed floatability tests.

Collector Reagent

The oil used as collector, after alkaline hydrolysis reaction (saponification), was extracted from buriti pulp *(Mauritia flexuosa)* by mechanical pressing. Buriti oil main fatty acids, determined by gas chromatography (GC), were oleic acid (about 70%), palmitic acid (about 17%) and linoleic acid (about 7%). The degree of conversion of saponification reaction was considered as 100%, demonstrated by the results of infrared spectroscopy performed before and after reaction. According to Wang *et al.* (2009), the characteristic band of carbonyl group of triacylglycerols (oils and fats), which appears in the region of 1740 cm^{-1} before reaction, totally disappears after saponification and a band in the region of 1540 cm^{-1} arises, typical of the carbonyl group of fatty acids salts, indicating the completion of the reaction. The amazonian collector Critical Micelle Concentration (CMC), determined by surface tension measurements using du Noüy ring method in KRÜSS K10ST tensiometer, was 48 mg/L.

Microflotation Tests in Hallimond Tube

Microflotation tests were conducted in duplicated and in modified Hallimond tube with height extensor in order to avoid excessive entrainment. Through the preliminary tests were defined the following tests conditions: gas (N_2) flow rate of 40 cm^3/min; conditioning and flotation times of 4 and 1 minute,

respectively; hematite mineral mass of 1 g, in the particle size ranges shown in the item 2.1. The agitation applied was that in which all material (hematite) were suspended. The recovery (%) was determined by the mineral mass floated and the total sample mass ratio.

Microflotation Tests in EMDEE MicroFLOT Tube

Microflotation tests in EMDEE microFLOT tube were conducted in duplicated. After preliminary tests, the pressure was fixed at 300 kPa and the cicle number was fixed at 30, for all tests. The mineral mass used was 1 g and the conditioning time was the same used in the microflotation tests in Hallimond tube (4 minutes). The recovery (in %) was determined by the mineral mass floated and the total sample mass ratio.

RESULTS AND DISCUSSION

The figure 1, 2, 3 and 4 show the recovery curves in function of the collector concentration. The pH used was around 9,0. It is can be seen that as the particle size range rises there are more similarities between the curves obtained by the two microflotation techniques. It is worth noting that, in these cases, the recovery values were obtained without considering the entrainment.

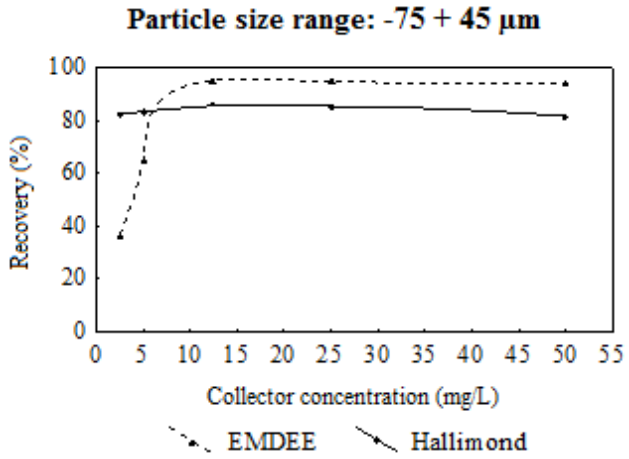

Figure 1 – Recovery of hematite in function of collector concentration for particle size ranges -75+45 µm

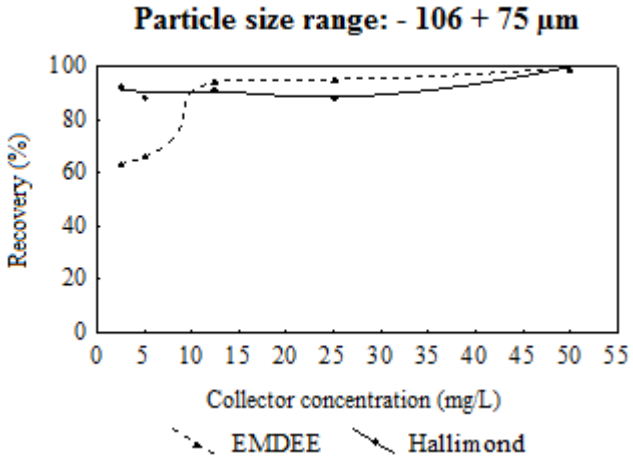

Figure 2 – Recovery of hematite in function of collector concentration for particle size ranges -106+75 µm

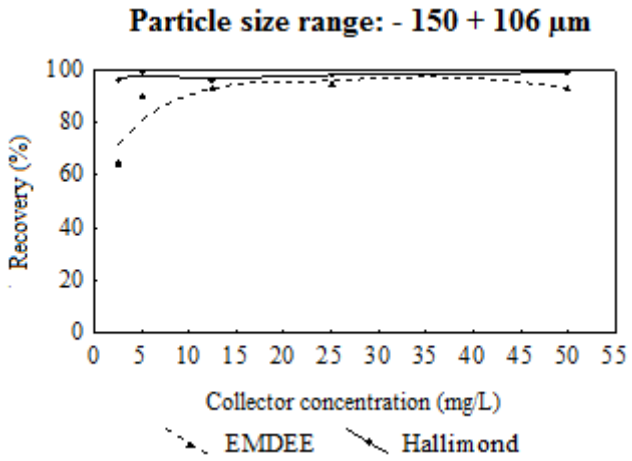

Figure 3 – Recovery of hematite in function of collector concentration for particle size ranges -150+106 µm

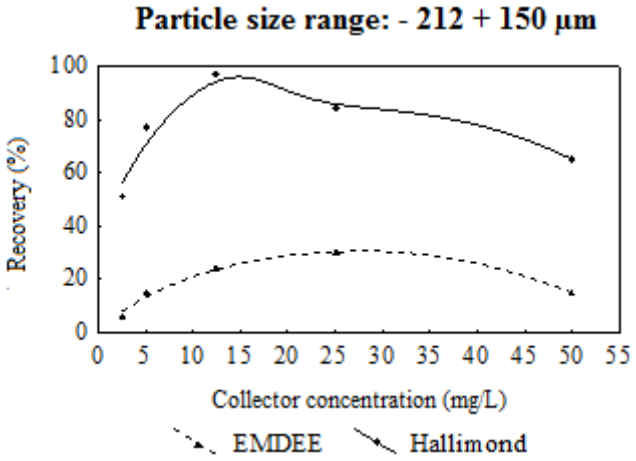

Figure 4 – Recovery of hematite in function of collector concentration for particle size ranges -212+150 µm

It can also been seen, in figures, that in the particle size range of -212 µm + 150 µm, the curves were qualitative identical. However, there was a significant decrease in the recovery using the EMDEE tube technique.

For finer particle size ranges (-75 µm +45 µm, -106 µm +75 µm and -150 µm +106 µm), high recovery was obtained with Hallimond tube, even with low collector concentrations. This is due to the high entrainment of finer particles, according to the entrainment tests results shown in figure 5.

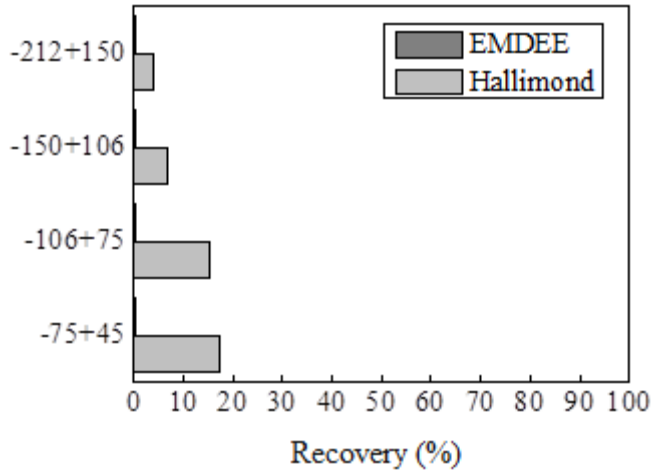

Figure 5 – Entrainment using Hallimond tube and EMDEE tube

In figure 5 is presented that there was no entrainment in the EMDEE cell. In microflotation using Hallimond tube there was an increase of the entrainment as a result of the reduction of the particles size. For the finer particle size range studied (-75 µm + 45 µm) there was the highest entrainment (about 17%) and for the coarser particle size range studied (-212 µm + 150 µm) there was the lowest entrainment (about 4%).

In figure 6 shows the hematite recovery, for particle size range between 212 and 150 µm, in function of pH, using Hallimond tube and EMDEE microFLOT tube. The collector concentration used was 5 mg/L.

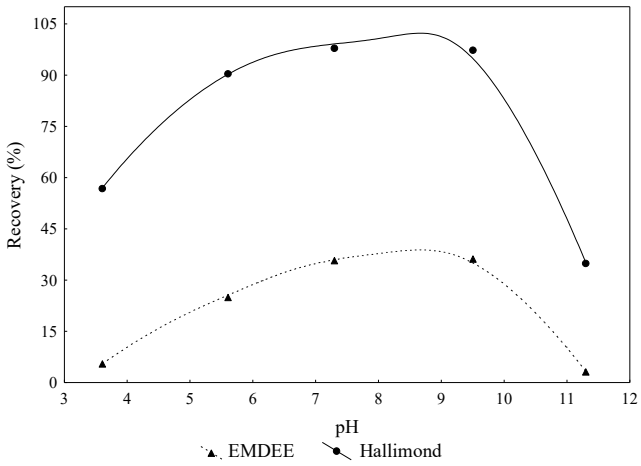

Figure 6 – Recovery of hematite in function of pH for particle size ranges -212+150 µm

From figure 6, it can be seen that there was qualitative similarity on the behaviors of the recovery curves in function of pH for the microflotation tests using both Hallimond tube and EMDEE tube. Though, higher recovery values were obtained in Hallimond tube. This result is due to the fact that the systems hydrodynamics are totally different, because while Hallimond tube uses gas insertion through the tube base, EMDEE uses vigorous shaking. As a consequence, the bubbles formed by the EMDEE tube have a lower stability in comparison to those formed by the Hallimond tube. The pH range in which there was the highest recovery was between 7 and 9,5 (approximately).

CONCLUSIONS

For hematite, the microflotation technique choice to measure the floatability criteria will depend on the material particles size: the EMDEE microFLOT cell shown more efficiency to measure the floatability criteria for the finer fractions. For the coarser fraction, Hallimond tube and EMDEE microFLOT displayed similar performances.

Based on these results, it is suggested the use of EMDEE microFLOT for the microflotation of materials with magnetic properties, since it needs no magnetic stirrer.

REFERENCES

BRANDÃO, P. R. G., CAIRES, L. G., QUEIROZ, D. S. B. Vegetable Lipid Oil-Based Collectors in the Flotation of Apatite Ores. *Minerals Engineering*, v. 7, p. 917-925, 1994.

GUIMARÃES, G. C., ARAUJO, A. C., PERES, A. E. C. Reagents in igneous phosphate ores flotation. *Minerals Engineering*, v. 18, p. 199-204, 2005.

LIMESTONE BRIQUETTES MECHANICAL STRENGTH EVALUATION THROUGH SHATTER TESTS

*M. R. Barros[1], A. C. Silva[2], E. M. S. Silva[3], D. F. Lopes[4], D. N. Sousa[5]

[1, 2, 3, 4] *Federal University of Goiás, Department of Mine Engineering*
Av. Dr. Lamartine Pinto de Avelar, 1120, Catalão, Brazil
*(*Corresponding author: mrezendeb@outlook.com)*

[5] *Goiano Federal Institute, Department of Mining*
Av. Vinte de Agosto, 410, Catalão, Brazil.

24th World Mining Congress
MINING IN A WORLD OF INNOVATION
October 18-21, 2016 • Rio de Janeiro /RJ • Brazil

LIMESTONE BRIQUETTES MECHANICAL STRENGTH EVALUATION THROUGH SHATTER TESTS

ABSTRACT

Brazilian soils are acidic due to the presence of components - H^{+} and Al^{+3} - originated by intense leaching of soil nutrients and the removal of cationic nutrients for culture without proper replacement. Therefore, the need for application of agricultural lime to correct this acidity. The Brazilian Central West was the region that had the highest production of agricultural lime, with 38.2%. Its import and export are non-existent, affirming the self-sustainability of Brazil in its production. But for the processing of this raw material grinding step is required, which generates fine material (through in # 400), which does not have economic viability in the agricultural and metallurgical sectors. This is because this particle size decreases gas percolation in blast furnaces and has slow sedimentation. When employed in agriculture, it can be transported by wind hindering its application and setting environmental liabilities. Therefore we used a process of mineral sintering, briquetting, to take advantage of this waste and reduce environmental problem, as this is the agglomeration of fine particles under pressure, aided or not by agglomerating, allowing obtaining compacts in the shape, size and mechanical parameters. The objective was to agglomerate fine limestone by briquetting, varying amounts of water (used as a caking agent) 0; 5; 7.5; 10; 12.5% and applying briquettes drop test for physical assessment using standardized heights of 30, 60, 90, 120 and 150 cm immediately after its manufacture and 7 days after drying. Its particle size analysis showed that about 10% limestone fine feature colloid particles (<1μm), aiming to further this work, since it is known that any work environment contaminated with dust (aerosols) is a serious problem to the health of workers.

KEYWORDS

Agglomeration, briquetting, limestone, agriculture

INTRODUCTION

Mining is one of the basic sectors of Brazil's economy, contributes decisively to the well-being and improving the quality of life for present and future generations. It is essential for the development of an equitable society, provided it is operated with social responsibility, being always present the principles of sustainable development. However, are considerable environmental impacts caused by the same (FARIAS, 2002). She intensely alters both mined as surrounding areas, which are made deposits of waste and tailings (SILVA, 2007).

Limestones, most commonly used materials in liming, generally vary in the mineralogical, chemical and textural composition jointly determine the overall capacity of soil acidity neutralization. Among the features relating to the quality of limestone, only two have been considered: the neutralizing content and grain size. In evaluating these products, with respect to the aspect particle size, the same has been done in terms of responsiveness on the ground (for short periods of time), disregarding the residual effect (BELLINGIERI et al., 1992).

The current Brazilian legislation, in how to perform the analysis to classify correctives acidity, and based on various levels of calcium, magnesium and RPTN (relative power of total neutralization), and the NP (neutralizing power), they are classified for use.

The Brazilian production of agricultural lime in 2013 showed an unimpressive growth (less than 0.2%) compared to 2012, with the regions and states that produced more agricultural lime in

Figure 1. The import and export of agricultural limestone are missing, confirming the self-sustainability of Brazil in the production of this input (MARTINS JÚNIOR, 2015).

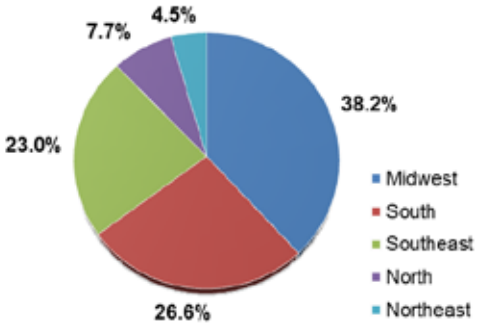

Figure 1 – Production of agricultural lime per region of Brazil in 2013

The treatment of ores is performed through industrial processes for adaptation of minerals, since almost never these are present in nature and in order to be used either for being out of specifications for size or to be associated with other materials, given thus the need these actions (LUZ & LINS, 2010). During the lime processing is required a milling step of the same step which generates this fine material (size less than 400 #), which has no economic viability in production agriculture, coking and calcining. This is because such a particle size may either be carried by the wind, and therefore set up an environmental liability when used in agriculture and reduce the percolation of gas in blast furnaces for having slow sedimentation (GARCIA et al., 2015).

The importance of studying the particle size is linked to the negative effects that these particles, when they take certain size ranges, cause in humans, particularly in relation to the respiratory system. Small particles (<1μm) behave as gas in the atmosphere and are subject to Brownian motion (random motion). The American Lung Association indicates that the particles suspended in air with a diameter smaller than 10 micrometres, the so-called respirable particles are the most harmful to human health (GONÇALVES JÚNIOR, 2014).

Agglomeration processes are designed to recover fine particles from mineral processing and the choice of the process depends on a careful and thorough examination (CARVALHO & BRINCK, 2010). Pelletizing is the agglomeration method used to transform fine fractions of iron ore a suitable product (pellet) to supply blast furnace and direct reduction reactors, which will be transformed into pig iron or sponge iron (MORAES & KAWATRA, 2011). Sintering, which has as its main product iron ore is used in the metallurgical industry to turn ore fines by agglomeration hot together with other raw materials into a product called sinter (TELLES et al, 2013) and finally briquetting, which is a very efficient way to concentrate the available energy in biomass (LUCENA et al, 2008).

The briquetting process is an agglomeration process which consists of applying pressure through a mechanical press in a mass feedstock transforming it into a compact cylindrical solid with high density (FELIPPETO, 2008) The first patent relates to the briquetting was granted to William Easby in 1848 with the development of a process which allowed the formation of solid agglomerates of varying size and shape from fine fractions of any kind of coal, through pressure exerted on the material (CARVALHO & BRINCK, 2010).

The briquette production, besides being a waste reuse form, still has economic advantage to the generation of income for the industry, the marketing of this product (OLIVEIRA, 2003). Other advantages offered are: reducing the volume of waste parked in the yard and reduced transport cost as the briquettes can be stored to reduce the gaps in transit. In Brazil, interest in briquetting process has always been focused on the use of thin steel coming from vegetable coal, taking most of the research for the development of briquettes for use in this second activity (QUIRINO & BRITO, 1991).

Therefore, according to the explained problems throughout the text alternative suggested to alleviate this problem by offering a workable and efficient solution both limestone and for the environment industry is through an agglomeration process, briquetting, having as objective a, which

has as a byproduct a specific type known as filler (through material # 400) in agglomeration processes reducing the environmental liabilities and generating profits for mineral industry.

METHODOLOGY

The experiments were performed in Modeling and Research Laboratory in Mineral Processing at the Federal University of Goiás - Regional Catalão using limestone filler (typically passing material # 400), from the Lagamar region - Minas Gerais. The limestone used was donated by the company Cala Limestone Lagamar LTDA.

In order to characterize the particle size to be used limestone filler samples were prepared to subject them to tests for determining density, grain size and chemical analysis. The mass was determined by pycnometer. The granulometric analysis of limestone was performed with a laser particle analyzer Mastersizer 3000 from Malvern in triplicate. This device uses the technique of laser diffraction for analyzing particle size (ALMEIDA, 2008).

The chemical analysis was performed to determine the Power Neutralization (PN) along with Reactivity of lime (RE), which defines the relative power of total neutralization (RPTN), which is an index commonly used in the selection of scale in Brazil. Knowledge of these values is necessary from the moment that the wrong choice of it can harm the farmers, because often it does not have expertise to apply lime according to your need.

According to the technical report of studies of the Agronomic Institute of Campinas, no matter the calcium: magnesium in the soil when the levels of these nutrients are suitable for crops. Thus, based on soil analysis will be easy to define what kind of corrective use.

This analysis was performed in order to classify the limestone regarding its power neutralization according to its particle size, both analyzes were performed by the Institute of Agricultural Sciences, Federal University of Uberlândia.

We evaluated the potential limestone agglomeration by briquetting, with water as a binder agent using a 15 g mass of limestone each prepared composition. After homogenization of the mixture of lime and water the resulting mass was placed in a mold (Figure 2) and applied uniaxial compression at 3 tons same, so as to promote agglomeration of the material, by a hydraulic press for 2 minutes.

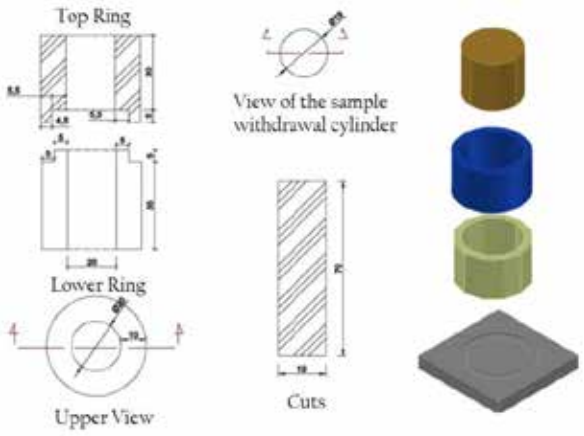

Figure 2 – Views of the cylinder used for briquettes production

The addition of water the lime was carried out using a graduated pipette to guarantee the correct volume as the desired amount of water. In a 250 ml beaker was added 15 g of the limestone and the amount of water split into three times to ensure homogenization of the mixture was the best. Tests

were conducted with 0; 5; 7.5; 10 and 12.5% by weight of water. After all manufacturing briquettes were weighed and measured (diameter and height using a digital calliper) so as to determine the variations in density of manufactured briquettes.

The shatter test determines the briquette strength to withstand repeated drops, simulating impacts that occur naturally during handling and transportation. Before heat treatment (curing), the impact strength of the briquettes can be determined by drop tests from a height of 0.3 m. This test is used as screen, a steel plate with a thickness of 10 mm. If the briquette is subjected to a thermal treatment to increase its mechanical strength, the height of the free fall test will move to 1.5 m (CARVALHO & BRINCK, 2010). The impact resistance is determined by the number of consecutive drops to the briquette can withstand without fragmenting when released standardized heights (30, 60, 90, 120 and 150 cm). To briquettes uncured 3 are considered as a reasonable number of falls, while for briquettes undergo a heat treatment, the number of drops passes to 10. The briquettes were subjected to successive drops until it lost 5% of its initial mass.

In order to analyse the water loss with aging and its influence on the mechanical strength were made briquettes with 7.5% moisture content (percentage that achieved the best results) and their weight monitored for seven days at the end of this period the briquettes They were subjected to impact resistance tests and the relative humidity was monitored using a thermo-hygrometer Minipa MT-241.

One way of assessing the quality of briquettes is in relation to the action of water on them. This information is of great importance for cases where the briquettes can be stored in an open environment, one way to measure the gain of water absorbed by the briquette by immersion thereof in water (CARVALHO & BRINCK, 2010). The test consists in evaluating the mass gain obtained by the briquette after soaking in a container with water. It is common to determine the weight variation over time. According to the authors this information is very important for cases in which the briquettes are stored in external environments (CARVALHO & BRINCK, 2010). The tests should be conducted for 24 hours (CUNHA, 2006). This test was necessary seeking the knowledge of how the briquettes would behave when they came in contact with water when applied directly to the soil with a pH corrective function of it (agricultural use). For this test we were manufactured briquettes five with the highest percentage of tested water (7.5%) and placed in five beakers 25 mL for the analysis of the reaction of the same when they came in contact with water. The test-ended when the briquette lost its cohesiveness and the immersion time thereof was noted.

Information about morphology and characterization of limestone filler microstructure were obtained from the Laboratory of Multi-User High Resolution Microscopy (Labmic) at the Federal University of Goiás by Scanning Electron Microscope (SEM), JEOL JSM - 6610, equipped with EDS, Thermo scientific NSS Spectral Imaging.

RESULTS AND DISCUSSION

The average density of limestone found in picnometry tests was 2.76 +/- 0.05 g/cm^3. The results are in agreement with the values found in the literature (2.72 and 2.87g /cm^3) (SAMPAIO & ALMEIDA, 2005). Figure 3 shows the average particle size analysis using data obtained by testing in triplicate performed in equipment Mastersizer 3000. It is noted that approximately 99.5% of the lime has a particle size less than 74 micrometre (blue line).

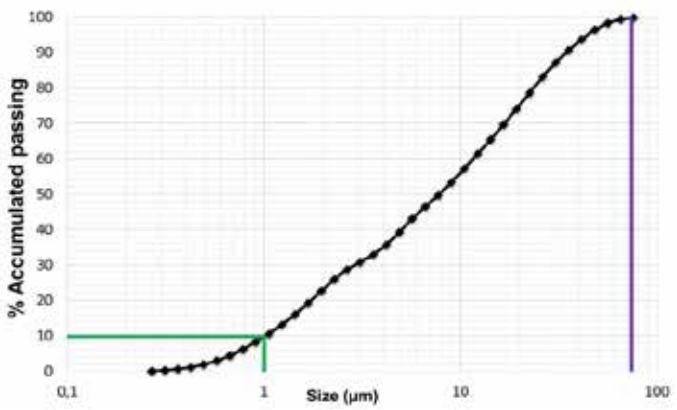

Figure 3 – Particle size analysis average limestone filler

The limestone filler has a low density because it has particles below 1µm. At the time of its application on the ground this becomes a feature as important as worrying as those who apply may be inhaling particulate matter and consequently causing harm to their health, if proper precautions are not taken. In particle size analysis performed 10% of the particles of limestone filler had dimensions which constitute colloidal material (<= 1 µm.). From the application point of view of this particulate matter in agriculture should be remembered that increasing the degree of fineness also increases the difficulties of application, both for applicators fixtures for losses in wind consequence, and also the largest contact concealer with the operator, as mentioned above (ARCADE, 2005).

The type of lime to be used depends on the calcium and magnesium in the soil determined by chemical analysis, and Table 1 shows the results of chemical analysis of lime sample. The obtained value NP 100% and 99.6% RE obtained in this way their RPTN was equal to 99.6%. Lime was rated according to its MgO content and its power neutralization as Dolomitic, since the MgO value was greater than 5% and classified as Group D, as RPTN was greater than 90% (range: D).

Table 1 – Chemical analysis of limestone sample

Oxide	CaO	$CaCO_3$	MgO	$MgCO_3$
%	33.6	59.8	11.1	23.3

Figure 4 shows side and top views of limestone briquettes with additions of 0; 5; 7.5; 10 and 12.5% water by weight before and after the drop test at 30 cm. It is observed that there were fractures only at its ends, and getting large fragments in briquette without moisture, there is also the colour difference due to the absence of binder. The briquettes produced had an average diameter 1.93 cm and height of 2.36 cm. In briquette composition with 12.5% water mechanical conformation thereof had to be difficult, because the water pours out of the mold when applied compression, but the removal of the briquette mold was still possible.

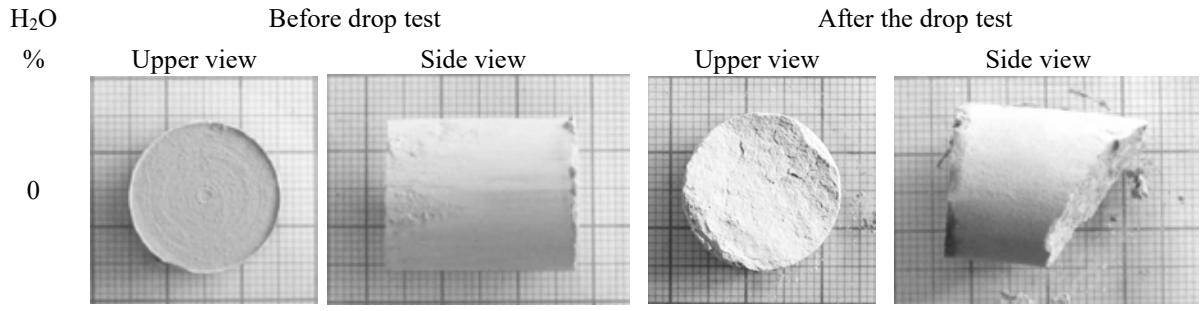

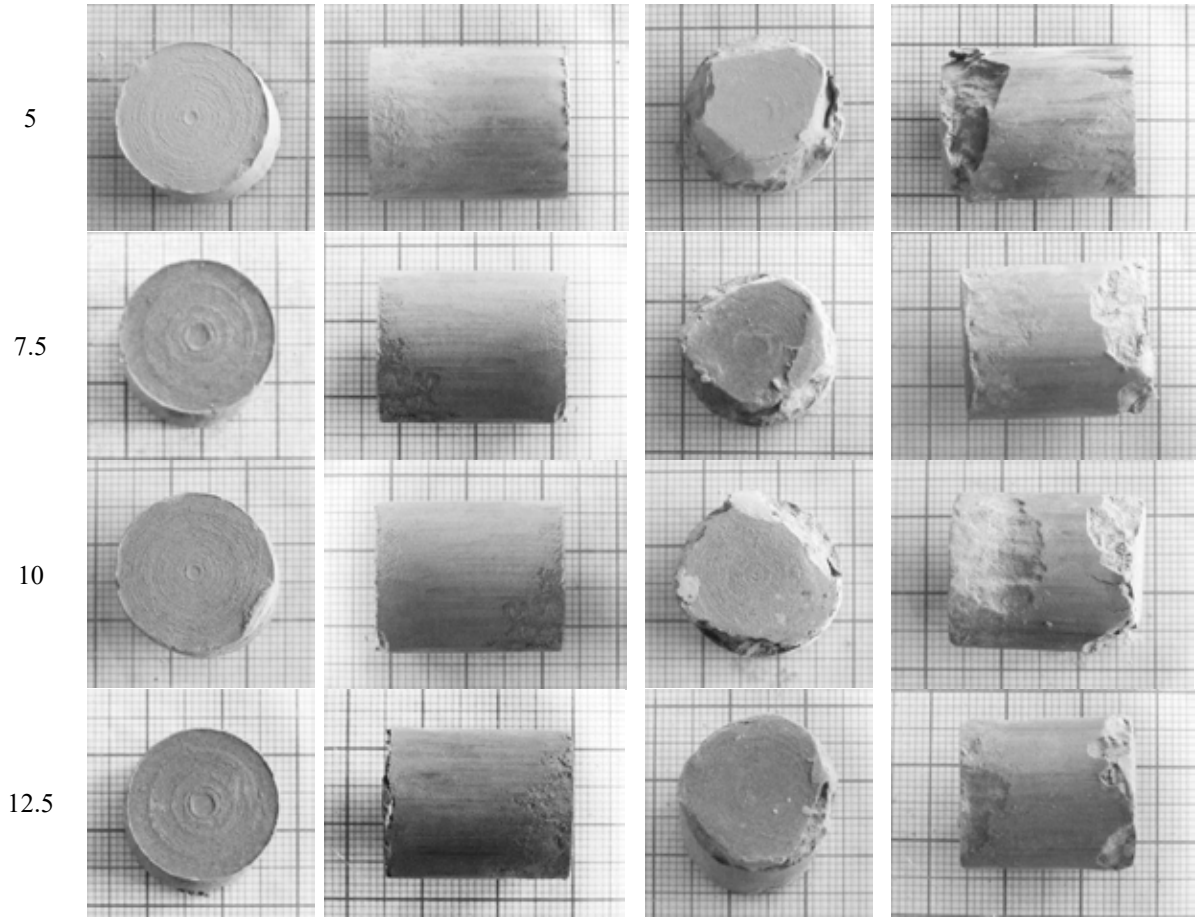

Figure 4 – Top and side views of the briquettes before and after the outputs of the drop test on 30 cm

According to the analysis of Figure 5, one can see that there is a reduction in the number of falls when it raises the heights in the tests. Without the addition of binders in Figure 5 (a) obtained the briquette greater fragility, supporting falls below 5 to 30 cm and reducing its mechanical strength in the other. However, with the addition of water as a binder, Figure 5 (b) and in the other, the briquettes had higher mechanical strength in the first two heights, thus demonstrating their potential in this briquetting material. The higher performance of the briquettes, which had percentage of binder can be explained by the link between particle and binder (water), which increases the impact strength making it more resistant material. The humidity provides the necessary cohesive strength for the adhesion of the particles to be agglomerated. This force also depends on the capacity of adsorption of water by the particles, thus increasing the mechanical resistance (OLIVEIRA, 2003). To analyse the briquettes undergo strength testing after seven days of aging was made a graph (Figure 5f) and compared to the test performed immediately after its manufacture.

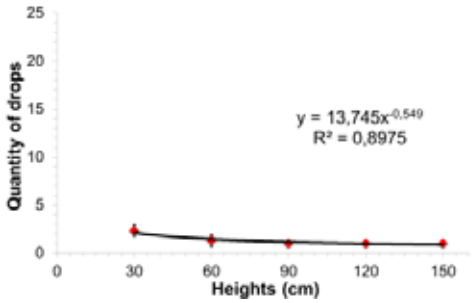

(a)

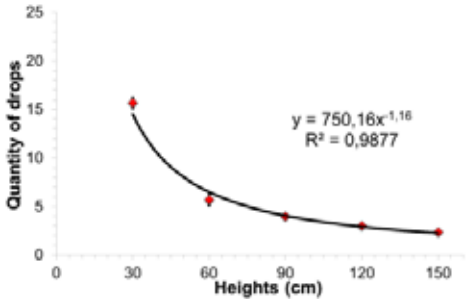

(b)

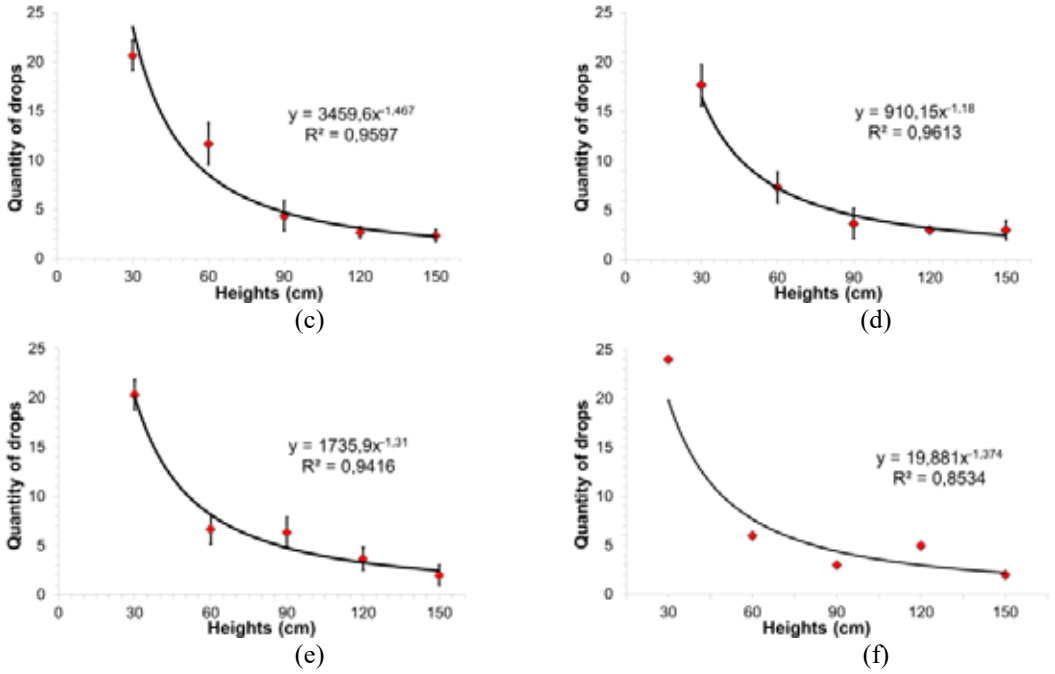

Figure 5 – Quantity of drops in relation to heights of fall: (a) 0; (b) 5; (c) 7.5; (d) 10; (e) 12.5% humidity and (f) drop test with the briquette 7.5% after 7 days of drying

It can be seen that there was no difference between the results of tests performed immediately after the manufacture of briquettes and results of the drop test conducted after 7 days of drying. The briquettes that moisture (7.5%) showed the same pattern of resistance even when subjected to mechanical strength test after seven days. Thus, even losing moisture initially used as a binding agent the product continues to maintain its strength. Table 2 shows average data loss of mass in grams and percent, this loss can be justified due to moisture variation of the air recorded on days weighing.

Table 2 – Weight loss (%) of the briquettes after 7 days drying

Days	Initial Average Mass (g)	Average loss (g)	Average loss (%)	Air humidity (%)
0	15.347	-	-	-
3	14.363	0.984	6.41	81
4	14.341	0.022	0.14	73
6	14.330	0.011	0.08	75
7	14.309	0.021	0.14	45.5

The mass density caused the reduction in porosity occurred over the briquetting where the expulsion of the air by applying pressure. Thus the water adhered to limestone grains through the capillary reducing the amount of empty pores and increasing the mechanical strength of the briquette. With the action of water into the pores by capillarity the briquette becomes denser, demonstrating the increased resistance as can be seen in Figure 5, below.

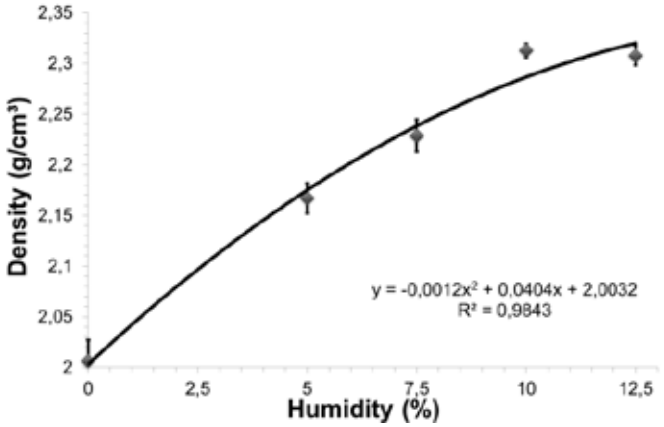

Figure 6 – Variation of the density of briquettes relative humidity

Looking at Figure 7 and the data obtained in the water resistance test action it can be concluded that the briquettes did not receive resistance when submerged. They showed rapid deterioration, totally undoing at an approximate average of 4 to 5 minutes until properties remain within the container. One of the possible purposes of this briquette would be your destination to correct soil acidity. This decay time is relatively accepted. In a case in which occurs a rain or irrigation in longer than 5 minutes briquette this would no longer be visible, thus occurring their dismantling and being incorporated into the soil by means of percolation.

(a) (b) (c) (d)

Figure 7 – Briquettes of immersion time in water: (a) 4 seconds; (b) 1 minute; (c) 2 minutes and (d) 4 minutes

Figure 8 shows the SEM results for limestone filler samples. It's possible to see that the morphology of the particles are not similar, justifying the result obtained by granulometric analysis, which showed that 10% of the material is below 1μm, and the particles were not clear because the shortest distance without losing the quality of the images was of 10μm. Larger particles have size of 25 micrometers and smaller than about 6 micrometers. The particles have anhedral shape, angular/subangular and low degree of sphericity. Some grains are smooth with straight edges well marked, others had their edges smoothed chemically (dissolution). It may be noted evidence of cleavage in some grains rhombohedral.

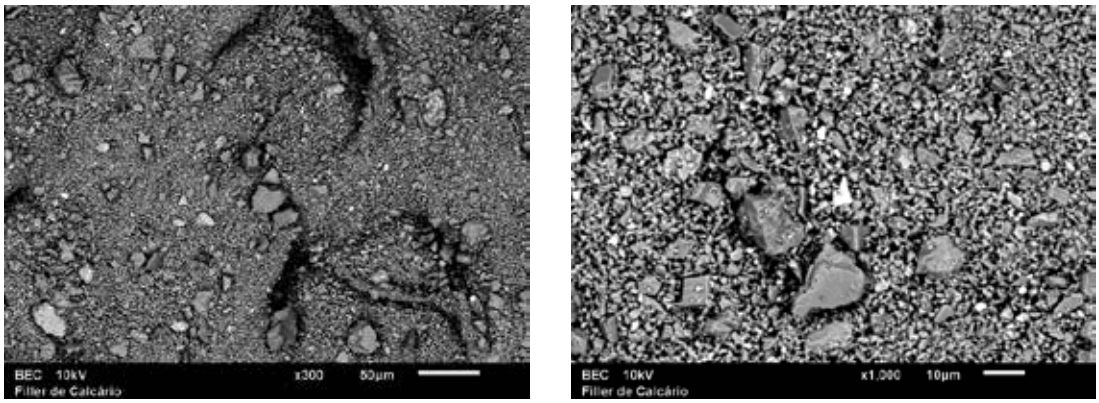

(a) (b)

Figure 8 – SEM results for the distances (a) 50 and (b) 10 micrometres limestone sample

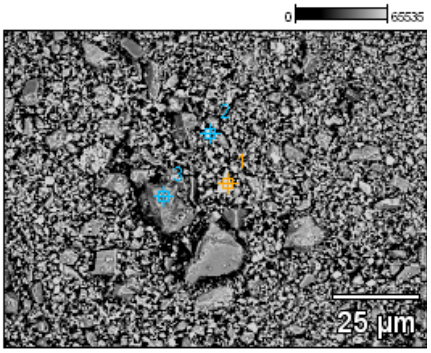

Sample: Limestone Filler
Accelerating Voltage: 10.0 kV
Magnification: 1000
(a)

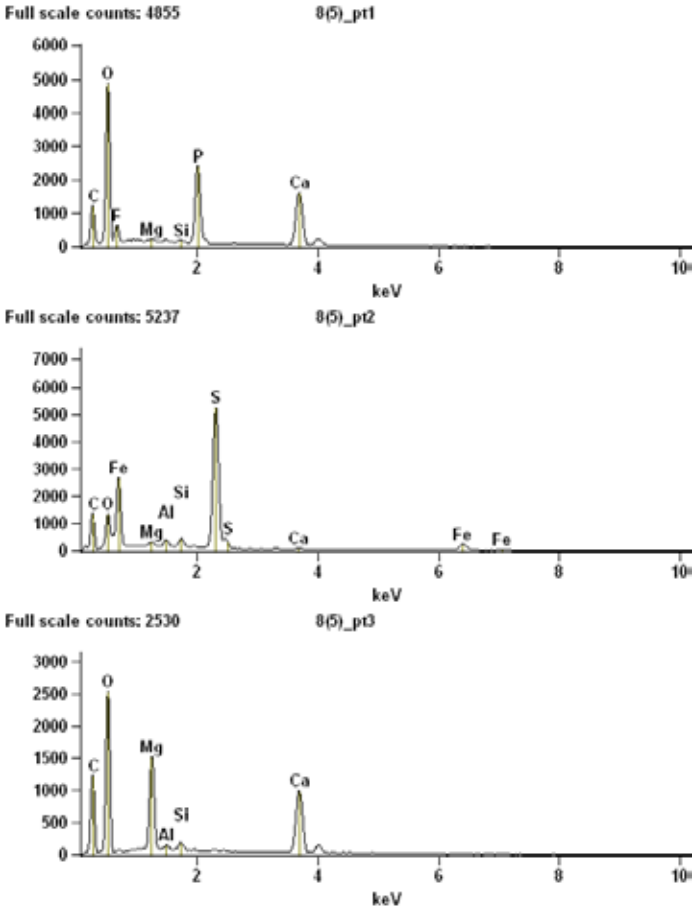

(b)

Figure 9 – EDS results of limestone sample: (a) SEM image and (b) EDS results for three different points

CONCLUSIONS

On the analysis of the results it can be proved that the briquetting is an option both quantitative and qualitative when it comes to the need for reuse because it minimizes the amount of material exposed and assigns value to the end of the process, causing the waste before not used can be finally realized. The limestone fines generated through the mineral limestone treatment showed

characteristics suitable for the generation of briquettes. Thus generating a reduction of exposed material in tailings dams decreasing the environmental impact.

With the discovery of the amount of particulate matter (< 1μm) causes us more of a concern beyond the cause of environmental impact, it would also impact the health of workers. Another reason for briquetting again be a necessary process for the industry, avoiding further damage. The purpose of the end product sought by the agglomeration process is to allow the application of fine limestone in agriculture in the form of briquettes. If before the farmer would have losses from weathering actions using the product conventionally, after the briquetting process would be better use of the product. Another purpose would be the production of quicklime through procedures in muffle.

ACKNOWLEDGEMENTS

The authors thank financial support from the Brazilian agencies CNPq, CAPES, FAPEG and FUNAPE. In addition, we like to thank Anglo American for the samples donation and chemical analyses, Federal University of Goiás and Goiano Federal Institute.

REFERENCES

Alcarde, J. C. *Corretivos da acidez dos solos: características e interpretações técnicas por J.C* (2005). Alcarde. São Paulo, ANDA,

Almeida, C. A. K. *Comportamento do hidrociclone filtrante frente às modificações no diâmetro de underflow e no tubo de vortex finder* (2008). Dissertação de Mestrado, Universidade Federal de Uberlândia – UFU, Uberlândia, MG.

Bellingieri, P. A.; Souza, E. C. A.; Alcarde, J. C.; Shikasho, H. W (1992). *Importância da reatividade do calcário sobre a produção e algumas característica da cultura da soja*. Scientia Agricola. São Paulo - Escola Superior de Agricultura Luiz de Queiroz, v. 49, n. spe, p. 61-71, 1992. Disponível em: <http://hdl.handle.net/11449/4000>.

Carvalho, E. A. & Brinck, V. *Aglomeração – Parte I: Briquetagem* (2010). In: Luz, A. B., Sampaio, J. A., França, S. C. A. Tratamento de Minérios, Edição 5ª. Rio de Janeiro, CETEM/MCT, 683-702 p.

CUNHA, A. F. *Caracterização, Beneficiamento e Reciclagem de Carepas Geradas em Processos Siderúrgicos* (2006). Ouro Preto: REDEMAT/ UFOP.

Farias, C. E. G. *Mineração e o meio ambiente no Brasil* (2002). Relatório Preparado para o CGEE.

Filippeto, D. *Briquetagem de resíduos vegetais: viabilidade técnico econômica e potencial de Mercado* (2008). Dissertação (Mestrado em Planejamento em Sistemas Energéticos) – Faculdade de Engenharia Mecânica, Universidade Estadual de Campinas, Campinas.

Garcia, E. A. S., Silva, A. C., Silva, E. M. S., Barros, M. R. *Pelotização de finos de calcário utilizando água e cal virgem como agentes aglomerantes* (2015). In: Encontro Nacional de Tratamento de Minérios e Metalurgia Extrativa, Outubro 18-22; Poços de Caldas, Brasil. Minas Gerais: XXVI, p. 59-67.

Gonçalves Júnior, S. J. *Avaliação da participação de material particulado e seus impactos à saúde humana em escolas próximas a vias de tráfego veicular e refinaria de petróleo* (2014) [Dissertação de mestrado]. Universidade Federal do Paraná.

Lucena, D. A., Medeiros, R. D., Fonseca, U. T., Assis, P. S. (2008). *Aglomeração de moinha de carvão vegetal e sua possível aplicação em alto-forno e geração de energia*. Tecnol. Metal. Mater. Miner.;4: 1-6.

Luz, A. B., Lins, F. A. F. *Introdução ao Tratamento de Minérios* (2010). In: Luz, A. B., Sampaio, J. A., França, S. C. A. Tratamento de Minérios, Edição 5ª. Rio de Janeiro, CETEM/MCT, 3-18 p.

Martins Júnior, F. L. *Calcário Agrícola* (2015). In: Lima, T. M., Neves, C. A. R. Sumário MINERAL 2014, DEPARTAMENTO NACIONAL DE PRODUÇÃO MINERAL. 2. Ed. Brasília: DNPM, 2015. p. 44-45. [acesso em 10 jan. 2016]. Disponível em: www.dnpm.gov.br.

Moraes, S. L., Kawatra, S. K. *Avaliação do uso de combinações de aglomerantes na pelotização de concentrado de magnetita pela tecnologia de aglomeração em tambor (balling drum)*(2011). Tecnol. Metal. Mater. Miner.; 8: 168-173.

Oliveira, E. R. *Elaboração e caracterização de mini-pelotas utilizando resíduos siderúrgicos e pellet feed para posterior utilização na sinterização de minério de ferro* (2003). 130 f. Dissertação de Mestrado - Universidade Federal de Ouro Preto. Ouro Preto.

Quirino, W. F., Brito, J. O. *Características e índice de Combustão de Briquetes de Carvão Vegetal* (1991). Instituto Brasileiro do Meio Ambiente e dos Recursos Naturais Renovaveis. LPF – SÉRIE TÉCNICA, Nº 13. Brasília.

Sampaio, J. A., Almeida, S. L. M. *Rochas e Minerais Industriais* (2005). In: LUZ, A. B., LINS, F. A. F. 2° edição. Capítulo 15 - Calcário e Dolomito Rio de Janeiro: CETEM/MCT.

Silva, J. P. S. *Impactos ambientais causados por Mineração* (2007). Revista Espaço da Sophia. Nº 08.

Telles, V. B., Espinosa, D. C. R., Tenório, J. A. S. *Produção de sínter de minério de ferro utilizando poeira de aciaria elétrica como matéria prima* (2013). Tecnol. Metal. Mater. Miner.10: 72-77.

MULTISTAGE FLOTATION OF MINE TAILING FOR COPPER AND NICKEL RECOVERY AND UPGRADING

R.S. Magwaneng[1], *K. Haga[1] and A. Shibayama[2]

[1]Graduate School of Engineering and Resource Science
Akita University
1-1 Tegata gakuencmachi Akita 010-8502
Japan
*(*Corresponding author: khaga@gipc.akita-u.ac.jp)*

[2]Faculty of International Resource Sciences
Akita University
1-1 Tegata gakuenmachi Akita 010-8502
Japan

24th World Mining Congress
MINING IN A WORLD OF INNOVATION
October 18-21, 2016 • Rio de Janeiro /RJ • Brazil

MULTISTAGE FLOTATION OF MINE TAILING FOR COPPER AND NICKEL RECOVERY AND UPGRADING

ABSTRACT

Copper (Cu) and Nickel (Ni) processing has been the heart of mining activity in Selebi Phikwe, Botswana. Over 30 years of mining, mine tailing of sulphide ores have been disposed in their tailing dam. The tailing in the dam contain large amount of gangue minerals associated with uncovered metals that have been lost at initial processing. This study serves to investigate the recovery and upgrading of Cu and Ni from mine tailing by multistage flotation. To uncover the potential for economic benefit, an assessment by flotation process, chemical and mineralogical composition analysis were studied. The valuable minerals predominantly hosting Cu and Ni are chalcopyrite and pentlandite respectively, and occur in disseminated matrix with gangue minerals. A two multistage flotation processing was used to recover and concentrate Cu and Ni. XRD, ICP-OES and SEM-EDS analysis were used to characterize the tailing and concentrate at each level. Oxide films were found surrounding the concentrate as well as an interlocking of gangue minerals with valuable minerals indicating incomplete liberation. Size particles distribution of D_{50}: 50 and 70 µm were investigated in flotation process. Addition of 50 g/t of PAX collector and 200 g/t of MIBC frother were used throughout the experiment. Positive results were shown on the particle size distribution of D_{50}: 50 µm. Cu grade improved to 6.52 wt. % from its initial 0.19 wt. % with a recovery of 71 %. Ni also showed an improvement to 2.5 wt. % grade and recovery over 40%.

KEYWORDS

Mine tailings, Multiflotation, Concentrate, Copper, Nickel

INTRODUCTION

Mine tailing have overtime proved to be a major significance in many countries (Lutandala & Maloba, 2013). An interest towards these mineralogical and metallurgical wastes are due to the depletion of minerals from most industrialized countries along with development of processing technologies enabling beneficiation of ores from even the poorest deposits (Senior & Thomas,

2005;Valderrama et al.,2011; Wills & Napier-Munn,2006). Furthermore the current economic price stability of the metal has experienced a downfall, but a consideration in the reprocessing could positively affect their availability (Lutandala & Maloba, 2013). The low cut off grades provide an advantage in the lifeline of the mine and a considerable measure to reuse or even seek byproducts from these waste (Edraki et al., 2014). Recovery of valuable minerals from the mine tailing is not only subjected to their economic benefit but the passive disposal of these materials pose a major threat to the environment. Many countries have already adopted stringent environmental regulations in the mining sector to ensure a green sustainability (Agorhom et al., 2015; Lutandala & Maloba, 2013; Senior & Thomas, 2005). A number of processing alternatives are proposed in the recovery of mineral from mine tailing such as smelting, leaching and concentrating. Different authors, identify the inefficient processing of the primary feed as the main course of mineral loss to the tailing referencing to the reagents used and grinding optimization (Farrokgpay et al., 2011; Karimi et al., 2008; Mudd et al., 2013; Norgate & Jahanshahi 2010).

Flotation is one of the metallurgical process that have been used over a centuries and is highly suggested in many literatures (Karimi et al., 2008; Senior & Thomas, 2005; Valderrama et al., 2011; Wills & Napier-Munn, 2006). Different parameters such as particle size, collector used and dosage, time and frother dosage in flotation are considered in the development of multistage flowsheet to fully optimize recovery. In this research, we study the multistage flotation process to upgrade and recover copper and nickel from mine tailing. The main advantages for the flowsheet design is to ensure efficient selective separation of the gangue minerals from the concentrate, leading to a high upgrading of concentrates and improved recovery. Ultimately the flowsheet design will assist in holistic overviewing of material balance and grind optimization. The present study aims at utilizing flotation processing method to recover copper (Cu) and nickel (Ni) in mine tailing obtained from BCL mine, Botswana. An application of two stage flotation process is used and consequently suggest a flowsheet for the maximum upgrade and recovery of Cu and Ni.

EXPERIMENTAL

Flowsheet Design

The circuit flow sheet design (Figure 1) is composed of two stages. Both stages used a mineral separation (MS) flotation equipment with different cell volumes (250 and 500 mL). Milling was carried in a ceramic ball mill, to avoid metal contamination and ultimately to reduce particle size. The residence time were 10 minutes in both stages of flotation. In the first stage of floatation, particle size and collector dosage are considered. After the first optimization for copper and nickel recovery the concentrate proceeds to second stage flotation. Mineral liberation is further carried out while the

other optimized conditions are kept constant (collector addition, time and frother dosage) as from the first stage flotation.

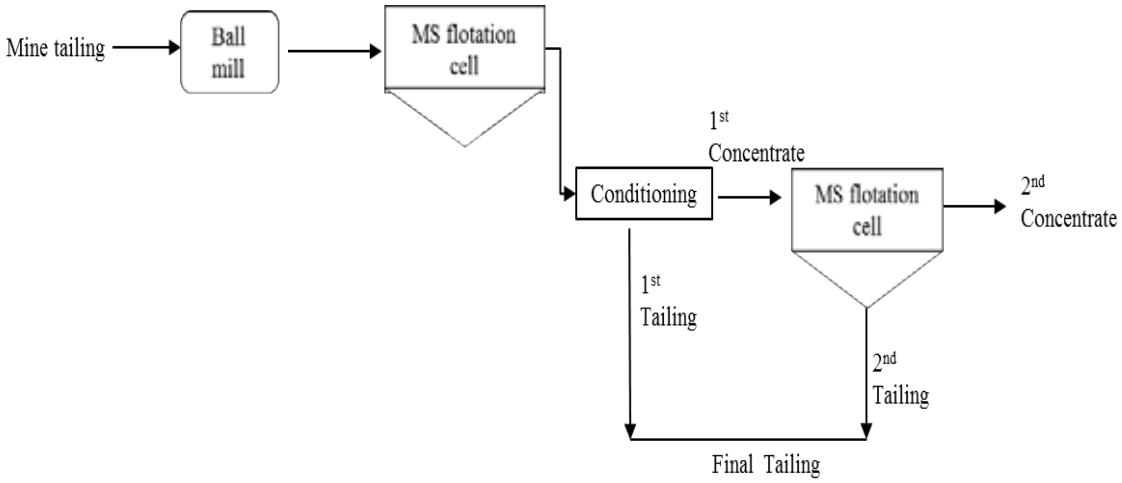

Figure 1-Flow circuit design for Cu and Ni recovery from mine tailing

Mine Tailings/ Ores

The Cu and Ni mineral samples were collected from BCL mine tailing dam. Table 1 shows the chemical mineralogical composition of the sample.

Table 1 - Chemical composition of mine tailing

Elements	Al	Mg	Cu	Ni	Fe
Mass %	1.91	1.32	0.19	0.23	10.38

Analysis performed by X-ray diffraction spectrometry showed a high intensity of associated gangue mineral of quarts and clay minerals (muscovite and kaolinite) in the mine tailing (Figure 2). The detection of chalcopyrite and pentlandite was low as they were highly disseminated and in other instance interlocked with gangue minerals of pyrite and pyrrhotite.

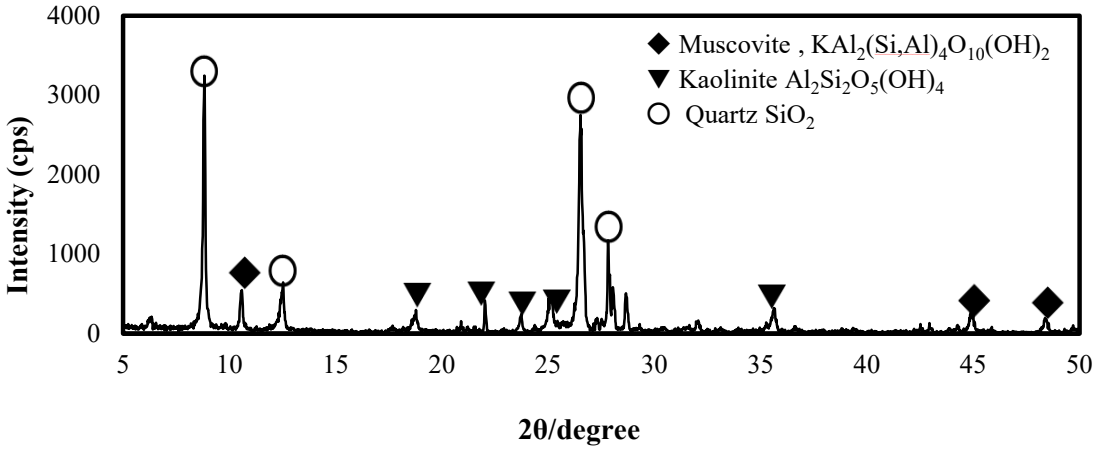

Figure 2- XRD pattern for the mine tailing

Reagents Used

The flotation feed pump was conditioned with the collectors Potassium amyl xanthate (PAX, $C_5H_{11}OCSSK$) and Aerofloat (AF208, sodium diethyl dithiophosphate) at different dosage of 0-200 g/t; frother 200 g/t of methyl isobutyl carbinol (MIBC, $C_6H_{14}O$); sulfurizing agent sodium hydrosulfide (NaHS), and calcium hydroxide ($Ca(OH)_2$) for pH adjustments. Throughout the flotation of the tailing, the pulp was kept at constant addition of 10 % pulp density. The summarized parameters are given in Table 2.

Table 2- Summary of flotation parameters

Mineral	Chemical Formula
Particle size (PS), µm	-53 + 250µm
Type of Collector	PAX, AF208
Collector Dosage	0-200g/t

RESULTS AND DISCUSSION

The recovery and upgrading of copper and nickel in the flotation of mine tailing is highly stressed on the two stage results obtained. Some discussions are made on the chemical and mineralogical analysis of the tailing too.

First Stage Flotation

Effect of Particle Size

The influence of particle size studied in the mine tailing is given in Table 3. Data from Table 3 shows that in sieve fraction of +53 to +250 µm, grade of Cu and Ni was above 1.24 wt% and 0.73 wt% respectively. The observations made on the recovery showed over 79.37 % and 34.08 % for Cu and Ni respectively through all sieved fractions. A high recovery on the smallest fraction was a result of gangue minerals floating therefore giving a poor grade result. The particle size ranges of +53 to +250 µm were mixed and grinded to D_{50} :180 µm for further flotation processing.

Table 3- Effect of particle size on the recovery of Cu and Ni

Sieve fractions	Concentrate			
	Grade wt. %		Recovery %	
(µm)	Cu	Ni	Cu	Ni
+250	1.43	0.73	79.37	34.08
+180~ -250	1.43	0.80	85.47	35.02
+100~ -180	1.44	0.89	90.13	41.46
+53~ -100	1.24	0.93	87.60	50.47
-53	0.82	0.67	87.86	57.13

Effect of Collector Dosage

Bulk flotation of Cu and Ni was achieved by comparing two collectors, PAX and AF208. MIBC frother was used in all experiments. According to the results in Figure 3 (A and B) bulk flotation for Cu and Ni responded well to addition of PAX. The AF208 showed better results for Cu recovery only. The grades of the minerals showed no significant difference to the addition of the two collectors. Therefore PAX addition best suited the collector to recover Cu and Ni.

Recovered concentrates showed increased amount of Fe associated gangue minerals, pyrite (FeS_2) and pyrrhotite ($Fe_{1-x}S$) with increased addition of collector (PAX). Generally flotation of Fe gangue minerals is low, independent of their percentage in a sample, but a high dosage of collector that is not scaled to the amount of Cu and Ni in the sample would spur their flotation (Agorhom et al., 2015). Therefore a dosage of 50 g/t for PAX was decided on.

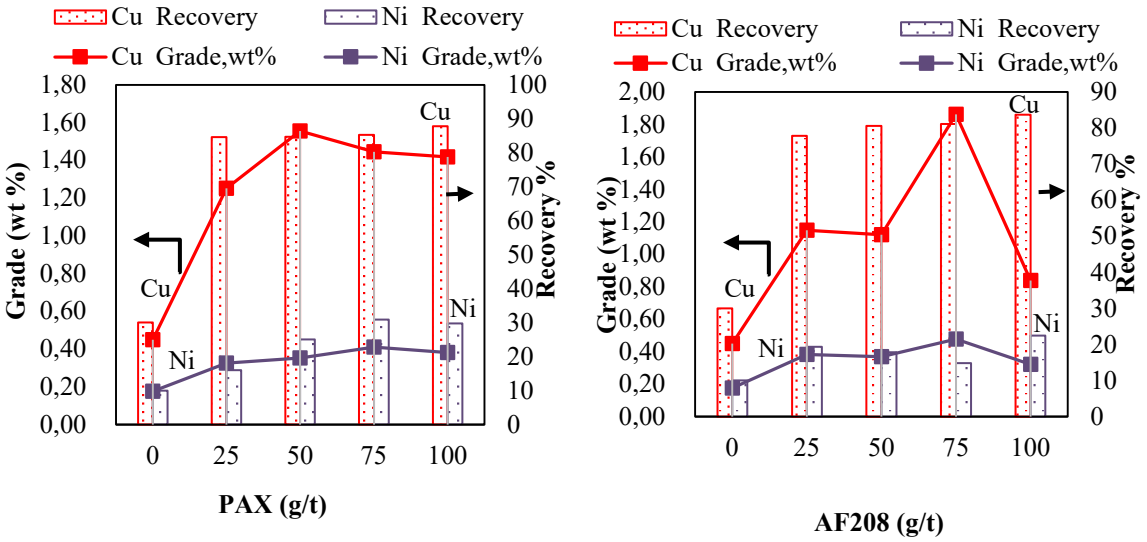

A B

Figure 3(A and B) - Effect of collectors dosage (PAX and AF208) on Cu and Ni recovery

Second Stage Flotation

Effect of Particle Size Distribution

The size distribution of the particles in the concentrates from the first stage of flotation were milled to D_{50}:50 and 70 µm. The finer concentrate showed the highest distribution of Cu and Ni. Using the optimized conditions from first stage flotation, grades of 6.72 wt% and 2.38 wt% for Cu and Ni were achieved respectively. Recoveries of Cu and Ni were recorded at 71.22 % and 44.23 % in the particle size distribution of D_{50}:50 µm. An observation on the concentrate by XRD analysis is shown in Figure 4. The intensity of Cu and Ni bearing minerals is more pronounced in the average sample of D_{50}:50 µm.

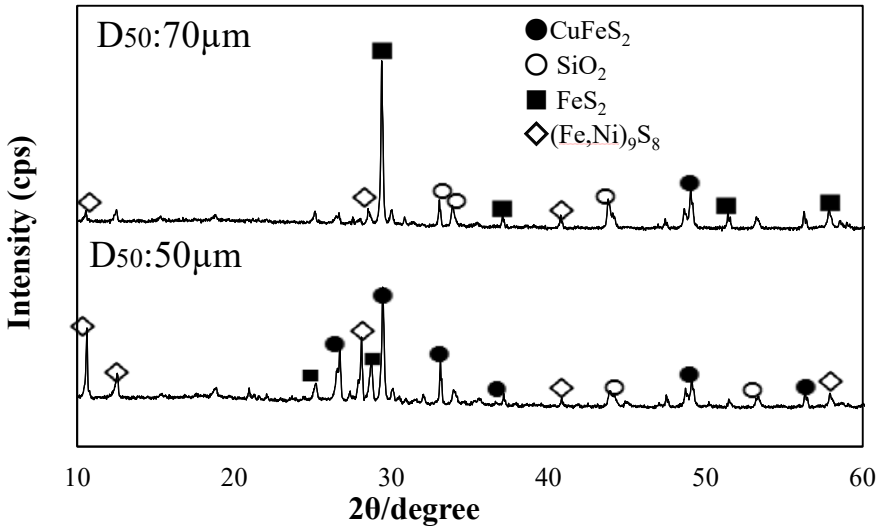

Figure 4- XRD pattern for concentrate of 2nd stage flotation

A summarized recovery and upgrading of Cu and Ni concentrate by multistage flotation is shown in Figure 5.The results show that recovery of Cu and Ni is possible by following a two stage flotation.

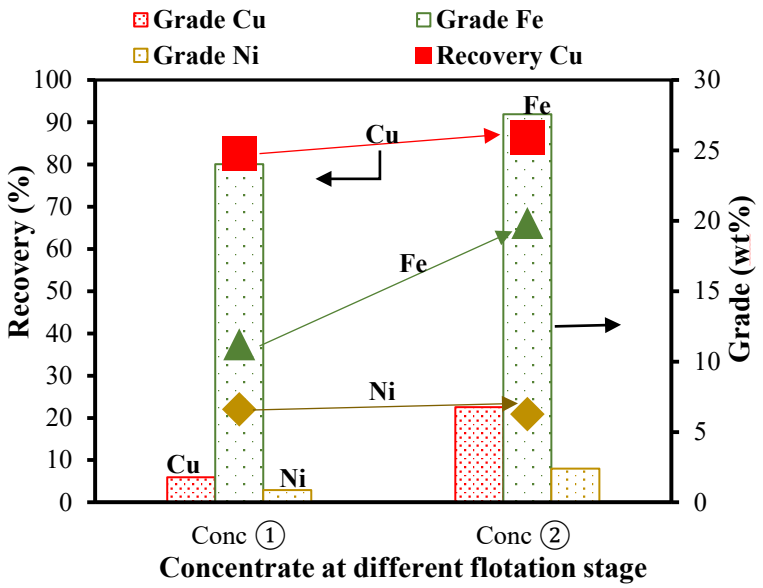

Figure 5- Recovery and grade of Cu and Ni at different levels of flotation

Study of the Final Tailing

The chemical composition of the starting materials to the final tailing is shown in Table 4. Multistage flotation of the mine tailing validated the final recovery of Cu and Ni to 71 % and 44.23 % respectively. Based on these result it has been considered that the final tailing go through another flotation stage to scavenge for Ni by magnetic separation. The Ni in the tailing show that they have magnetic properties because of the pyrrhotite associated with the Ni bearing minerals (pentlandite).

Table 4- Summary of composition of tailing and recovery

Elements	Initial tailings (wt %)	Reprocessed tailings (wt %)	Recovery (%)
Cu	0.19	0.04	71.22
Ni	0.23	0.21	44.23
Fe	10.38	10.67	20.75

CONCLUSION

The study investigated the recovery of copper and nickel from Selebi Phikwe (BCL) mine tailing. The objective was to design a multistage flowsheet to recover Cu and Ni. Characterization and association of the valuable minerals determined the beneficiation method because of their floatability properties. Cu and Ni recoveries were found to rely on particle distribution and collector dosage. Under the optimized condition of particle size D_{50}:180 μm, 50 g/t of PAX for 10 minutes flotation the results were as given below:

- Cu and Ni recoveries of 71 % and 38.83 %, respectively
- The final grade of the minerals at second stage flotation were 6.72 wt% Cu and 2.39 wt% Ni
- Mineralogical analysis on the initial tailing indicated a 62 % of Fe- gangue minerals (pyrite and pyrrhotite) and 21.23 % silicate minerals.
- Nickel recoveries were relatively low suggesting a need for flowsheet design to be adjusted to promote its recovery. In most Cu-Ni flotation circuits, the conditions are fully optimized for copper, while nickel recovery may require magnetic separators.
- Similarly, a comprehensive mineralogical and liberation characteristic of the mine tailing is critically important as they govern the flotation of different minerals.
- The laboratory multistage flotation testing offer an alternative way of copper and nickel recoveries, allowing for economic consideration of mine tailing processing.

ACKNOWLEDGEMENTS

This work was supported by Akita University and the New Frontier Leaders Training Program for Rare Metals and Resource through Japan Society for promotion of Science (JSPS) for all materials and resources required. We are gratefully thankful for their support.

REFERENCE

1. Agorhom, E.A., Lem, J.P., Skinner, W., & Zanin, M. (2015). Challenges and opportunities in the recovery/rejection of trace element in copper flotation-a review. *Mineral Engineering, 78,* 45-57. doi: 10.1016/j.mineng.2015.04.008
2. Edraki, M., Baumgartl, T., Manlaping, E., Bradshaw, D., Franks, D.M., & Moran, C.J. (2014). Designing mine tailings for better environmental, social and economic outcomes: a review of alternative approaches. *Journal of Cleaner Production, 84*, 411-420. doi:10.1016/j.jclepro.2014.04.079
3. Farrokhpay, S., Ametov, I., & Grano, S. (2011). Improving the recovery of low grade coarse composite particles in porphyry copper ores. *Advanced Powder Technology, 22,464*-470. doi:10.1016/j.apt.2011.04.003
4. Karimi, H., Ghaedi, M., Shokrollahi, A., Rajabi, H.R., Soylak, M., & Karami, B. (2008). Development of a selective and sensitive flotation method for determination of trace amounts of cobalt, nickel, copper and iron in environmental samples. *Journal of Hazardous Materials, 151,* 26-32. doi:10.1016/j.jhazmat.2007.05.051
5. Lutandala, M.S, & Maloba, B. (2013). Recovery of cobalt and copper through reprocessing of tailing from flotation of oxidized ores. *Journal of Environmental Chemical Engineering, 1,* 1085-1090. doi:10.1016/j.jec.2013.08.025
6. Norgate, T., & Jahanshahi, S., (2010). Low grade ores- smelt, leach or concentrate? *Minerals Engineering, 23*, 65-73. doi:10.1016/j.mining.2009.10.002
7. Senior, G.D, & Thomas, S.A. (2005). Development and implementation of a new flowsheet for the flotation of a low grade nickel ore. *International Journal Mineral Processing, 78*, 49-61. doi:10.1016/j.minpro.2005.08.001
8. Valderrama L., Santander, M., Paiva, M., & Rubio, J. Modified-three-product Column (3PC) flotation of copper -gold particles in a rougher feed and tailings. *Minerals Engineering, 24*, 1397-1401. doi: 10.1016/j.mineng.2011.05.007
9. Wills B.A. (2006). Froth flotation. In T. Napier-Munn, (Eds.), *Mineral Processing Technology: An Introduction to the Practical Aspects of Ore Treatment and Mineral Recovery*, (7th ed., pp. 267-352) Australia: Elsevier Science & Technology Books.

NEW APPROACH FOR BLASTING DESIGN IN HIGHLY WEATHERED ROCKS

*Vieira[1], J.C. Koppe[2], J.C. Ramos[1], F. Pedrosa[1]

[1]VALE - Departamento de Planejamento de Ferrosos Gerência Geral de Inovação e Desenvolvimento de Mineração. Av. Ligacão, 3580 - Mina de Águas Claras - Prédio 4 - Nova Lima-MG – CEP 34000-000, Brazil.
*(*Coresponding author: andre.luiz.vieira@vale.com)*

[2]Federal University of Rio Grande do Sul, Av. Bento Gonçalves 9500, setor 4, prédio 75, sala 102, Porto Alegre – CEP 91509-900, Brazil

24th World Mining Congress
MINING IN A WORLD OF INNOVATION
October 18-21, 2016 • Rio de Janeiro /RJ • Brazil

NEW APPROACH FOR BLASTING DESIGN IN HIGLY WEATHERED ROCKS

ABSTRACT

Iron ore mines in Brazil usually show significant rock weathering and is very common the occurrence of large blocks of hard rock mixed with softer material. In these mine, we have a problem for blasting design and sometimes the blasting produces large boulders of rock that require a secondary blasting, as well as excavation difficulties. To minimize this situation, geophysical techniques were used to identify the hardest material amid the weathered material. We study the problem using seismic, GPR, electrical resistivity and IP methods in a weathered Brazilian iron ore deposit. The methods of GPR combined with IP, resistivity and seismic showed to be effective in modeling the contrast among hard, friable materials and soil. The geophysical data were used to improve the geological model and create more favorable conditions for the subsequent blast design. The blast design based on geophysical/geological models resulted in significant improvement in the fragmentation of the iron ore. This was achieved by the adoption of a specific drilling pattern for a given geological situation. Several test were carried out and with the new specialized blasting design the formation of boulders was eliminated and the ore fragmentation improved. This methodology increased significantly the productive of mining operation.

KEYWORDS

Blasting design, geophysical survey, iron ore mine, fragmentation.

INTRODUCTION

Brazil is one of the largest producers of iron ore. The Brazilian iron mines are basically banded iron formations intensively weathered. The intensive weathering acting on banded iron formation produced deep soil profiles and extensive rock alteration. In many cases hard material was preserved from the rock alteration process resulting in a mixture of boulders, soil and soft rocky material.

One common problem for blasting in iron ore mines with significant weathering is the occurrence of large blocks of hard rock mixed with softer material. This situation causes a problem for blasting design and excavation difficulties. Blasting in these areas usually produce oversize materials and irregular fragmentation, mixture of fines and coarse material. Large boulders or blocks of rock require a secondary blasting and induce low excavation productivity. This is a typical situation in many Brazilian iron ore deposits.

The main objective of this work is to develop a methodology based on geophysical survey to obtain a geological model that can assist on specific blast design in case of occurrence of hard and friable materials in a mineral deposit. Vieira and Koppe (2015) presented the firs results of this new methodology. In this paper we present new data that confirm the efficiency of this methodology.

The presence of large blocks of rock amid soil and weathered rocks represents a challenge for blasting design. To minimize this problem, we use geophysical techniques to identify where the boulders and hard material are located in such environment. Although geophysics is not a common practice in mining operation, for this study we used seismic, GPR (ground penetrating radar), electrical resistivity and IP methods. The geological model generated by this methodology was compared with drill logs and results showed to be very promising. After that we developed a specific blast design in order to add more blastholes in the areas with the presence of boulders and hard rocks surrounded by friable material.

The case study was performed at the Aboboras Mine, VALE's iron ore deposit located 40 km from Belo Horizonte, Minas Gerais central state of Brazil. The mine produces 21 million tonnes annually of iron ore.

GEOLOGICAL ASPECTS

The Aboboras mine is located in the Quadrilátero Ferrífero (QF) at the southern end of San Francisco Craton (Almeida, 1977). The lithologies of the QF are characterized by a metamorphic complex represented by supracrustal sequences of vulcano sedimentary rocks, clastic and chemical sedimentary rocks, ultramafic, mafic and felsic bodies especially intruded into the Archean lithologies (Chemale Jr. et al., 1994; Alkmim & Marshak, 1998).

The iron ore (*Itabirite*) occurs in the Minas Supergroup representing a Paleoproterozoic sequence of chemical and clastic metamorphic rocks, under conditions of green schist facies. The rock sequence is intensely weathered showing a deep soil profile and intercalations of hard and soft itabirites. This situation favors the formation of large hard rock boulders that mix with the soft material (Rosière & Chemale,1987; Eichler, 1967) (Figure 1).

Figure 1 – Oversize material (boulders and blocks) of hard *itabirite* preserved after regular blasting. The boulders are amid soil and highly altered rocks.

GEOPHYSICAL SURVEY

To study the problem involving the occurrence of boulders amid soil and weathered rocks we selected several geophysical methods including seismic, electrical and electromagnetic methods for the very first field test. The main objectives were to differentiate the friable from the compact itabirites (iron ore) and identify the location of the boulders in the soil with the focus of helping the blasting design.

Geophysical methods are applied when there are physical contrasts among the rocks that will be surveyed. Geophysical methods can be grouped in those that measure natural fields (magnetic and gravity, alpha and gamma radiation, electrical) and those that the response of the terrain to some stimulus is observed (electrical and electromagnetic methods, seismic and down hole methods). Considering the properties of the rock types and soil four methods were selected to be used in this research: seismic, electro resistivity, induced polarization and ground penetrating radar (GPR). Vieira and Koppe (2015) described the geophysical methods applied in this research.

Methodology

The area selected for testing was close to a workbench (Figure 2), thus allowing for direct observation of the geology on the face of the bench. There, alternate hard or compact and friable itabirite, and soil. After selecting the area the geophysical survey was carried out considering 14 sections covering an area of 15,000 m^2(150 x 100 m). The following methods were applied: seismic, electro resistivity, induced polarization (IP)and ground penetrating radar (GPR). The data obtained were compared and integrated to generate the geological/geophysical model. After the geophysical survey a drilling campaign was performed to validate the model. Figure 3 shows a general layout describing the methodology of this study.

Figure 2 – Working bench at Aboboras iron mine. Hard itabirite (prominent on the surface) is mixed with friable itabirite.

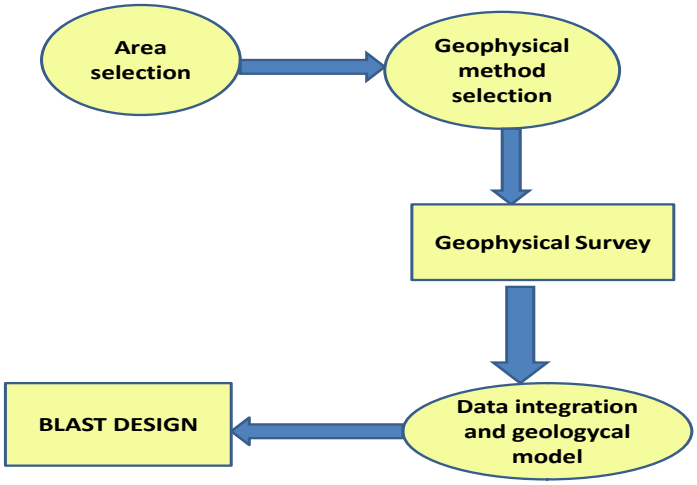

Figure 3- – Methodology for developing a geological model based on geophysical methods to help blast design.

Results

Electro resistivity

The analysis of geophysical sections considered the differences in the profiles on the basis of magnitude in high apparent resistivity zones (ZAR) whose values are above 50,000 ohm.m, and areas of low apparent resistivity (ZBR) whose values are below 2,600 ohm.m. The electric profiles allowed observing at depths ranging 3 to 30 meters. The data were fairly consistent in the differentiation of high and low resistivity anomalies.

A typical section obtained in this method is shown in Figure 4. It is observed in this section (L-18) the predominance of intermediate and low resistivity values areas with occasional ZAR.

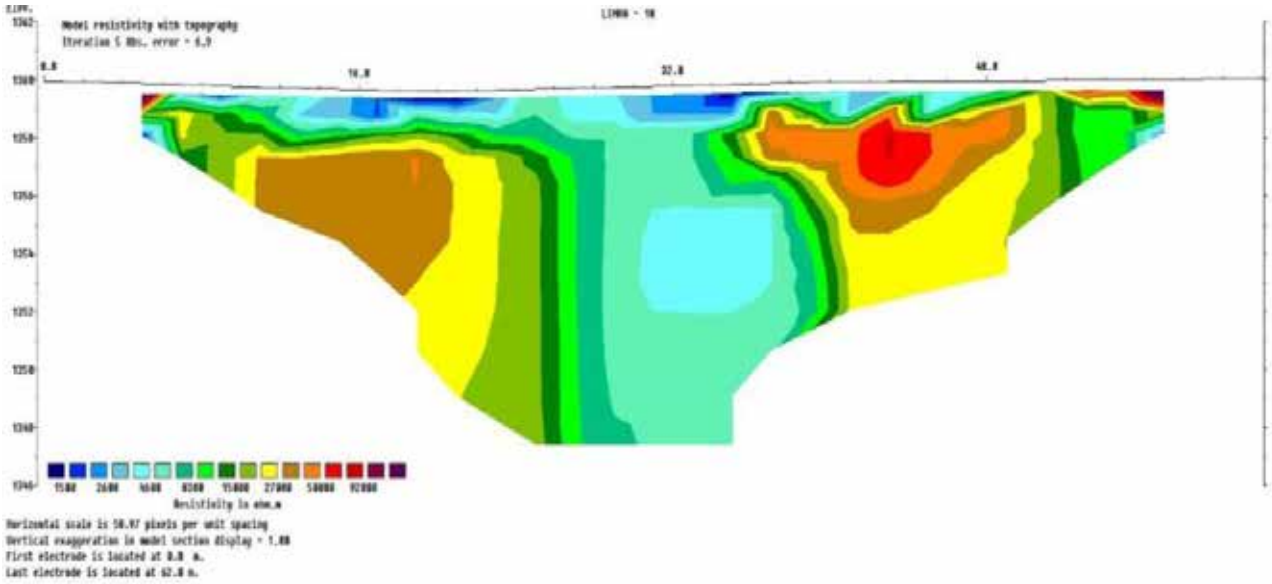

Figure 4 - Electro resistivity section L-18. There are predominance of intermediate (green and yellow) to low (blue) resistivity values areas with occasional ZAR (red colors).

Induced polarization

The IP analyzes considered differences in the profiles on the basis of magnitude in high chargeability apparent zones (ZAC) whose values are above 60 msec and low chargeability apparent zones (ZBC) whose values are below 10 msec. The geophysical sections showed a heterogeneous behavior in relation to distribution of chargeability values, as can be seen in Figure 5.

Ground penetrating radar

The interpretation of GPR profiles sought track reflectors endings to define compartments formed by different materials. Sections reached a depth of approximately 10 meters. Reflectors generally presented plans, semi-continuous in the surface near horizons and inclined and semi-continuous profile next to the base.

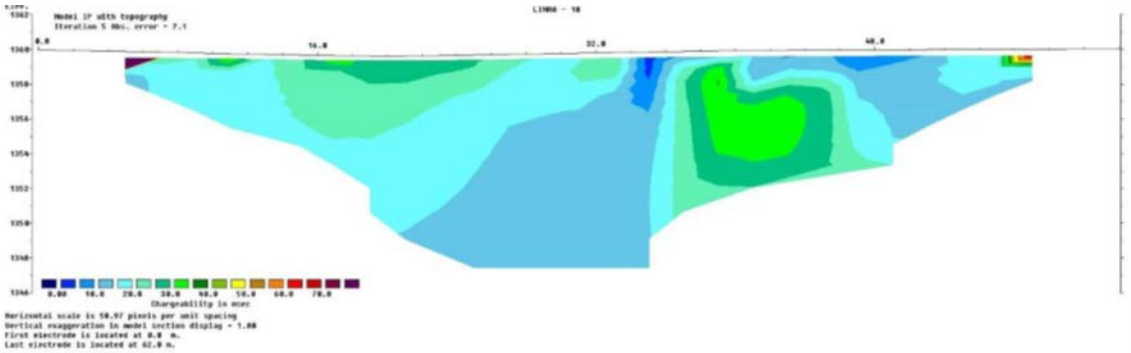

Figure 5 - IP section L-18 section. ZBC (blue colors) dominant in the upper central zone.

Seismic

The interpretations of the material type take into account the average seismic velocity obtained in the profiles. This average rate may vary depending on the size of sections since the velocity takes into account the geometry of the layer. In the studied site were acquired twenty (20) geophysical lines by shallow seismic refraction method. Two different horizons based on average seismic velocity were defined. The first presents seismic velocity between 3,023 to 3,417 m/s. The second records speeds between 3,234 and 3,724 m/s. It is not possible visualize the base of this layer as the refraction occurs in the upper interface and was not displayed other material below this with higher density.

Geophysical data integration

The integration of the profiles obtained from geoelectric, electromagnetic and seismic methods allows us to determine the position of the geological features, with the volume of each geological package and its geographic coordinate.

The analysis of what information is taken from each of the methodologies and inserted into the integrated model depends on the geophysical/geological analysis, describing the deficiencies noted and correlated them.

The geophysical data were integrated to obtain the 3D geological model (Figure 6). The interpretative geophysical model showed the areas with dominant hard *itabirite* and boulders of *itabirite*. The generated model was validated using 10 drill exploratory holes. Only one drill hole resulted unsatisfactory in relation to geophysical interpretation model.

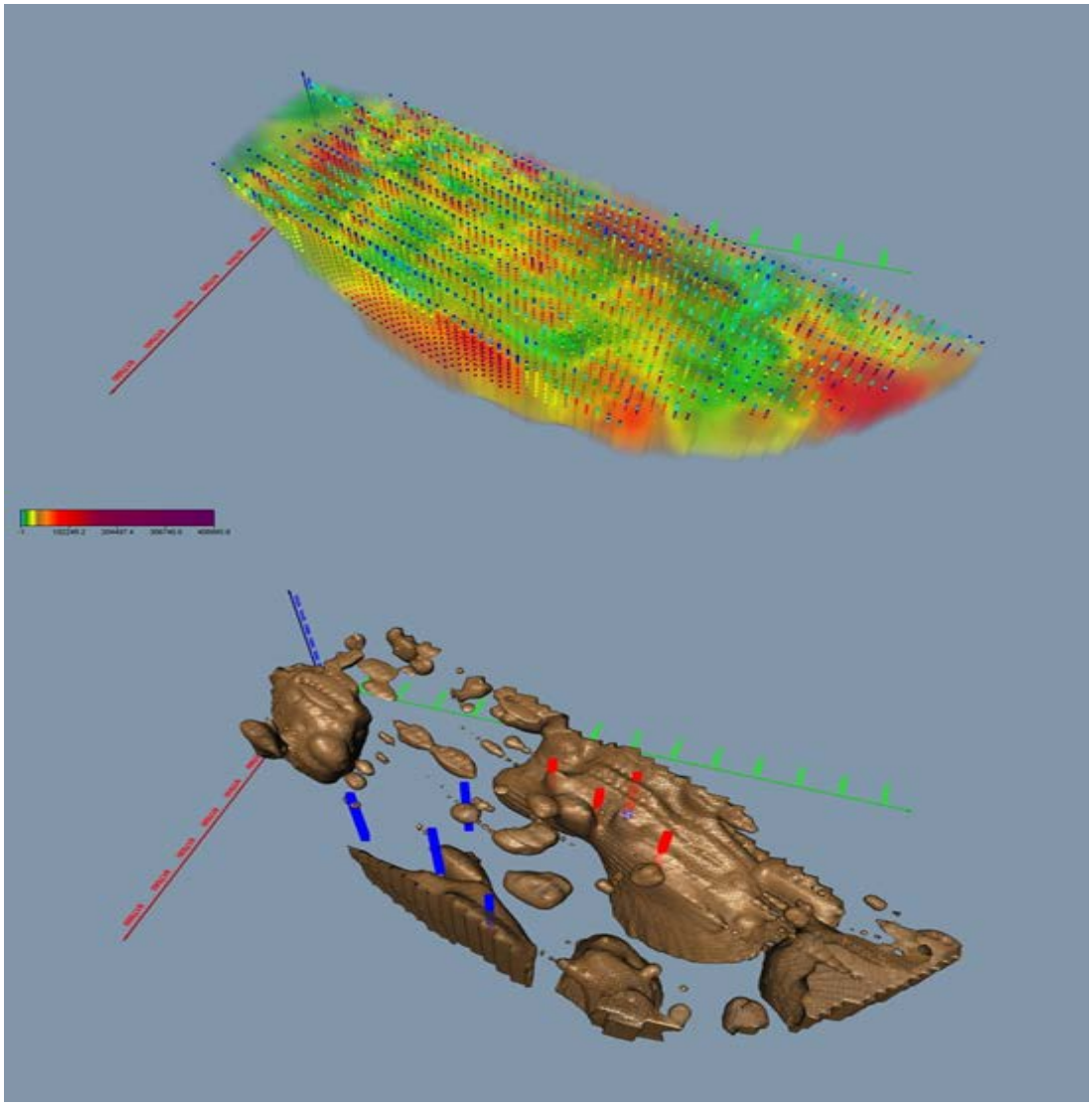

Figure 6 - – Interpretative 3D geological model integrating seismic, GPR, IP and electro resistivity surveys. Above the model including the sections selected for the geophysical survey. Below the model representing the hard *itabirite* and boulders of *itabirite* and the exploratory drill holes.

BLASTING DESIGN BASED ON GEOLOGICAL MODEL: RESULT ANALYSIS

The normal blast pattern (burden x spacing) at the Aboboras mine is 3 x 7 m or 4 x 8 m, bench of 10 m high and powder factor of 150 to 200 g/t. A large number of oversize material results from this blast design. To improve this situation, a new blast design was proposed. This new blast design is based on the geological model developed following the steps described before. Essentially the change was done in the sense of increasing the number of blast holes in areas where boulders or hard *itabirite* were located and decreasing the number of blast holes in areas of friable *itabirite*. Five blasting tests were performed in the areas where the geophysical survey was carried out. Two test were done only changing the blasting design, two tests took the geophysical/geological model into consideration and um test was done with the traditional blasting design. The fragmentation analysis of the blasting tests is shown in the Figure 7. D90 for the two first test reduced 46% compared to the regular blasting design, and D90 for the blasting tests based on geophysical/geological model reduced 75%. In general, a better fragmentation was observed. No boulders were identified in the muckpile. The productivity of the loader Marathon L-1350 (Figure 8) increased 12% considering the blasting test based on the geophysical/geological model.

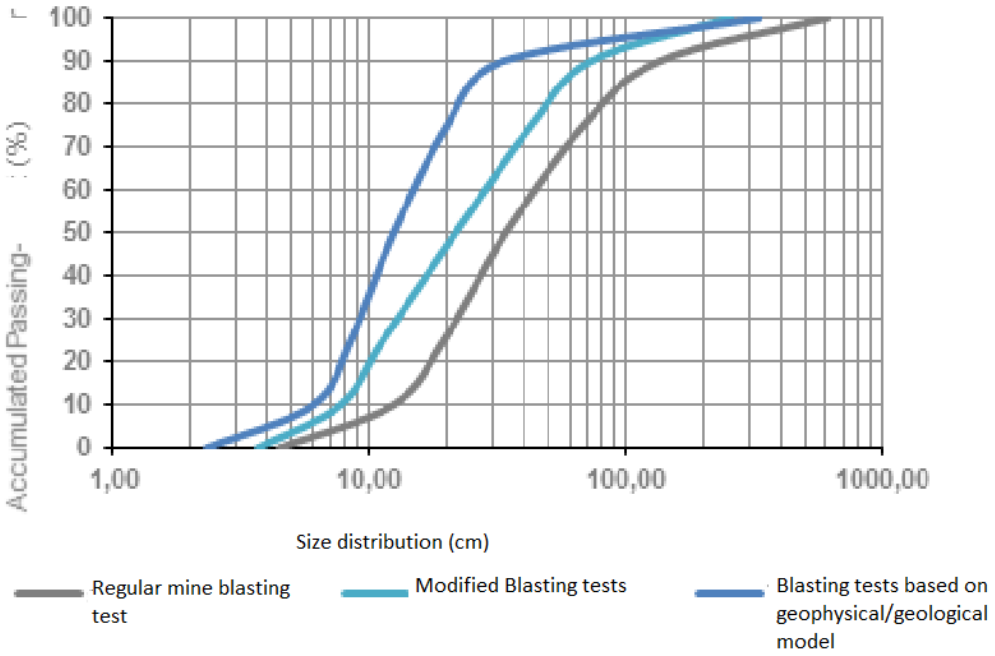

Figure 7 – Fragmentation analysis of the 5 tests carried out at Aboboras mine.

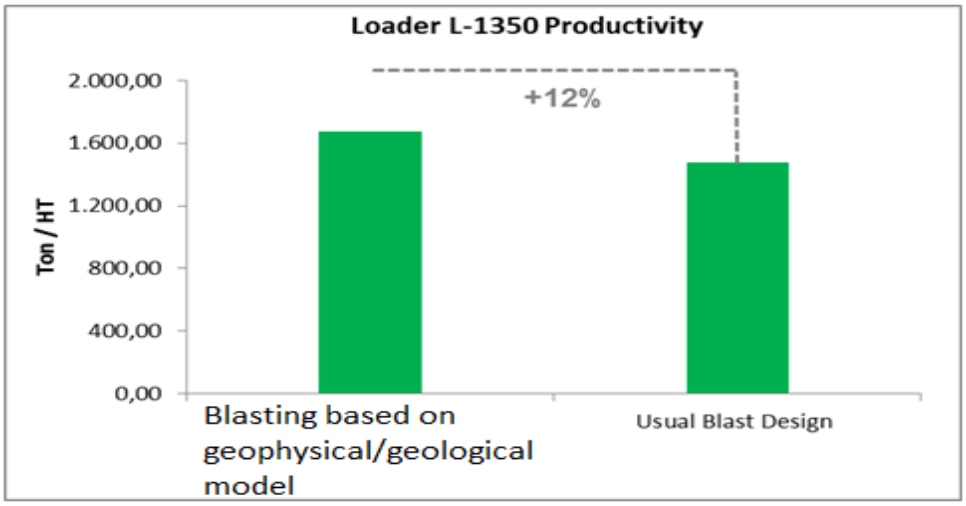

Figure 8 – Loader productivity increased 12% with the blasting test based on geophysical/geological model.

Figure 9 shows the muckpile from conventional blasting at Aboboras mine and the muckpile from blasting based on geophysical/geological model following the methodology described previously. We can see clearly the differences in fragmentation.

Figure 9 – Muckpiles from conventional blasting (left) and blasting based on geophysical/geological model (wright).

CONCLUSIONS

The methods of GPR combined with IP, resistivity and seismic showed to be effective in modeling the contrast among hard, friable materials and soil generating a trustful geophysical/geological model.

The blast design based on geophysical/geological model resulted in significant improvement in the fragmentation of the iron ore at the Aboboras mine. This was achieved by the adoption of a specific drilling pattern for a given geological situation. With the new specialized blasting design, the formation of boulders was eliminated, D90 was reduced in 75%, the productivity of the loader increased 12%, ore blocks transportation to waste dumps were eliminated as well secondary blasting and also the tonnage for ore processing was increased.

ACNOWLEDGEMENTS

The authors would like to thank VALE S.A, for permission to publish the results of this study and DITV-VALE for supporting the research.

REFERENCES

Alkmim, FF, Marshak, S,1998. Transamazonian Orogeny in the Southern São Francisco Craton Region, Minas Gerais, Brazil: evidence for Paleoproterozoic collision and collapse in the Quadrilátero Ferrífero. Precamb. Res., 90:29-58. (Elsevier B. V.).

Almeida, FFM, 1977. O Craton do São Francisco. Revista Brasileira de Geociências, 7(4): 349-364. (SBG, São Paulo).

Chemale Jr., F, Rosiére, CA, Endo, I, 1994. The tectonic evolution of the Quadrilátero Ferrífero, Minas Gerais, Brazil. Precamb. Res. 65: 25-64. (Elsevier B. V.)

Milson, J, 1995. Geophysical Methods, in Introduction to Mineral Exploration, Ed. Evans, A.M., pp. 113-137. (Blackwell Science Ltd, Malden, USA).

Telford, WM, Geldart, L, Sheriff, RA, 1990. Applied Geophysics. 2nd edition. (Cambridge Univ. Press).

Vieira, AL, Rijo, L, Evans, HB, Verma, OP, 1997. Induction Log Modeling. Revista Brasileira de Geofísica. (3): 80-82 (SBGf, São Paulo).

Vieira, A. L., Koppe, J.C, 2014. Geophysical Techniques Applied to Blastng Desing
11th International Symposium on Rock Fragmentation by Blasting. Paper Number: 131.00

NEW ORE CHARACTERISTIZATION METHOD IN HEAVY LIQUID SEPARATION WITH LIQUID INORGANIC AND APPLICATION IN JASPILITE IRON ORE SAMPLES

Ricardo Álvares de Campos Cordeiro[1] and Ronaldo de Moreira Horta[2]

[1] *Rua Carangola, nº 57, apto 1101*
Belo Horizonte (MG), Brazil, CEP: 30.330-240
*(*Corresponding author: ricardoccordeiro@hotmail.com)*

[2] *Rua Holanda Lima, nº 43, apto 400*
Belo Horizonte (MG), Brazil, CEP: 30.441-031

24th World Mining Congress
MINING IN A WORLD OF INNOVATION
October 18-21, 2016 • Rio de Janeiro /RJ • Brazil

NEW ORE CHARACTERISTIZATION METHOD IN HEAVY LIQUID SEPARATION WITH LIQUID INORGANIC AND APPLICATION IN JASPILITE IRON ORE SAMPLES

ABSTRACT

In Brazil, the heavy liquid separation technology, the standard method in ore characterization, is rarely used. The limited supply of ferrosilicon and tungsten carbide in the Brazilian market combined with the difficulties of imports cause delays that make unfeasible the rare scheduled tests. The organic liquids are toxic and their use is regulated by rigid labor laws, which require special equipment for exhaustion. The casual application of this technology in Brazil becomes impractical to maintain trained teams. However, non-routine application of heavy liquid separation for ore characterization inappropriately can exclude the confirmation of feasibility for the production of Lump and Sinter Feed. Not infrequently pre-concentrated in these size ranges are destined, prematurely, for grinding and concentration aiming to generate Pellet Feed product. The industrial dense medium separation process is applied to the density of 3.8 g/cm3, with the potential to go up to 4.5 g/cm^3 in the future. In laboratory, can reach approximately 4.8 g/cm^3 and shall be performed even in drill holes and small bulk samples. Then, a new method heavy liquid separation using inorganic substance (LST) was developed by these authors. Toxic emissions were eliminated and the laboratory was done using only glassware, weighing scales and small equipment with easy training of the workforce. Bench testing were made in samples of iron ore drill holes of the Municipality of Corumbá, State of Mato Grosso do Sul, Brazil, which has microcrystalline hematite from jaspilite rock. Good results at densities between 4.0 g/cm^3 and 4.5 g/cm^3 for Lump and Sinter Feed products with Fe content between 63.00% and 64.00% and mass recoveries between 50% and 60% of ROM. A bench pneumatic stratifier for small samples of drill holes was designed and constructed, and the tests to establish correlations between the new heavy liquid separation method and industrial jigging were initiated.

KEYWORDS

heavy liquid; jigging; jaspilite; lst; corumbá.

INTRODUCTION

The iron-ore deposits and mines in the region of Corumbá, State of Mato Grosso do Sul, Brazil, are well known worldwide for its mineralization originate on jaspilite rock. The studies presented here are related to the deposit named Santa Cruz, owned by Vetorial Mineração. Vetorial, together with two partner companies, is developing a large project aimed at producing 30 Mt/year of iron ore products for export. Currently, Vetorial is mining ore (ROM) in the surface layer limited to 10 m in depth with content around 60% Fe. The current plant, which process is restricted to the crushing and screening operations, has capacity to produce about 1 Mt/year of Lump (- 1 ½ " + ¼") with Fe content between 65% and 66%. The surface ore reserve is only 40 Mt, which are not enough to make feasible a large-scale project.

The ore in the subsurface, beyond this superficial layer, also has origin from jaspilite rock and average content of around 53% Fe with potential resources of up to 10 billion tons. The mineralization has an approximate thickness between 270 m to 300 m from the surface, in an area of about 1,200 hectares. The subsurface ore have a lower degree of alteration in relation to the surface layer and therefore requires the development of new methods of characterization and concentration process routes. Then, a preliminary phase of characterization, called pre-characterization, was programmed, developed and applied to the main lithologies of the deposit of Santa Cruz. The pre-characterization comprised mineralogical analyses, determination of WI for grinding, flotation tests, desliming, magnetic separation, heavy liquid separation, and pneumatic jigging with bench tests. The results of the pre-characterizing tests indicated the need for development of a new heavy liquid separation method using inorganic liquid and project preparation of a

new bench jig for testing small sample mass of drill core. It demonstrated the potential production of Lump and Sinter Feed with 64% Fe content. The bench tests were conducted in laboratories in Brazil and South Africa.

PRE-CHARACTERIZATION PHASE

The objective of the pre-characterization phase was the development of new operational parameters and process for each concentration stage considering the main lithologies of the iron-ore deposit of Santa Cruz. The development of new heavy liquid separation method with the use of inorganic liquid (LST) was shown to be essential according to the results of the pre-characterizing stage. The heavy liquid separation with LST increases greatly the productivity of bench tests and allows rapid evaluation of huge mineral resource of the deposit using only samples of rotary drill cores that is limited to HD diameter. This type of drill core that is available for the process bench tests is limited to an average of approximately 9.5 kg per 5.0 m in length. In bench tests were preferably used samples of rotary drill cores, but also surface samples were used when there was need for large masses. The surveys and related sampling services were made by universal standard methods and ensured the quality of the samples and representativeness of all lithologies. In the case of surface samples also standardized criteria for sampling and preparation were used. However, as surface samples are not representative of the lithologies of subsurface, these samples were only used to define operating parameters of equipment and methods of concentration. The test results with surface samples mainly allowed the correlations between jigging and heavy liquid separation and the preliminary simulations of industrial performances of jig, as well as the development of the heavy liquid method using inorganic liquid and the project preparation of bench pneumatic jig for small mass samples.

Pre-characterization - Mineralogical and Degree of Liberation

In Fundação Gorceix, in Ouro Preto (MG), Brazil, mineralogical analyses and degree of liberation studies were performed in thirty-two samples of drill core, selected according to their coordinates, depths and lithologies. The analyses of natural fraction -1.00 mm to +0.15 mm were conducted in petrographic microscope according to standard methodology of Fundação Gorceix (Ferreira, 2014). Eight samples of the lithology FFB and ten of FND respectively show, microcrystalline hematite (~68.5%, and ~62.0%), microcrystalline quartz (~27.5%, and ~36.5%), carbonates (~3.0% to ~1.0%), and other minerals (~0.25%, and 0.4%). In the average of thirty-two samples, microcrystalline hematite was in ~64%, microcrystalline quartz in ~33.0%, carbonates and other in ~2.5% and ~0.2%, respectively. A summary of the degree of liberation is in the following Table 2.1_1.

Table 2.1_1 – Degree of Liberation – 32 Samples – Summary (Ferreira, 2014)

	(8 samples)	(10 samples)	(3 samples)	(11 samples)	(32 samples)
	Average FND	Average FFB	Average FFC	Average Others	Average
Number of mixed particles	407	454	380	410	420
Number of liberated particles	1	3	0	4	3
Degree of liberation (%)	0.2	0.7	0.0	0.9	0.6
Mixed particles with ≥ 90% of hematite (%)	37.7	39.5	42.3	40.3	38.8
Total of mixed particle (%)	99.8	99.3	100.0	99.1	99.4
Average hematite in mixed particles (%)	54.1	59.5	61.7	56.7	57.4
Fe content (%)	43.38	48.39	45.47	42.83	44.95

The main conclusions of the Fundação Gorceix team were:

- The ore is banded and can be observed bands with more than 95% up to almost 0% by volume of hematite.
- The size of mono-crystals (of both the quartz and hematite) is less than 15 µ, i.e., particles above 10 µ are polycrystalline and there is a high percentage of mixed particles, as shown in Figure 2.1_1 below (Ferreira, 2014).

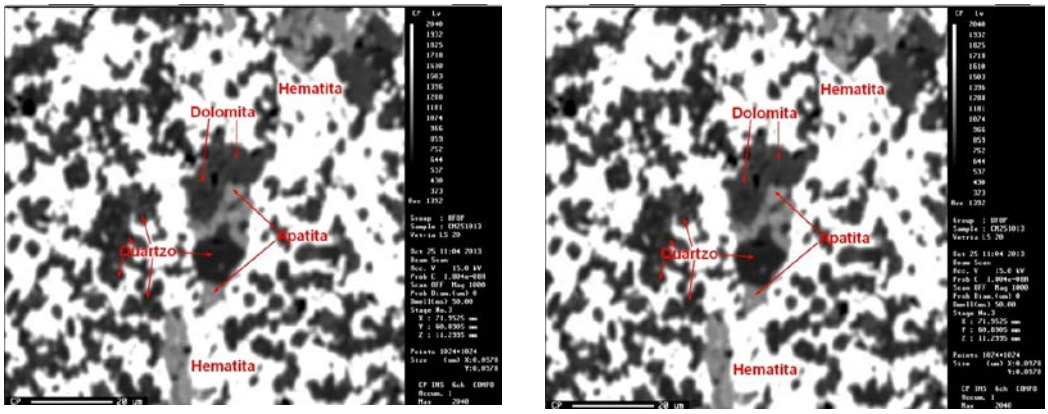

The photo on the left side: sample LS-21 – Image of the backscattered electrons. The photo on the right side: sample jaspilite friable. Photomicrography in reflected light without analyzer. Polycrystalline particle section of quartz mixed with hematite. The size of the quartz monocrystalline varies between 7 µ and 2 µ.

Figure 2.1.1_1 - Sizes - hematite and quartz crystals

- Then, the degree of liberation has no practical significance. The iron content in the mixed particles is the most relevant factor.
- For example, bands with more than 85% by volume of hematite (91.6 % by weight) have more than 64% Fe and less than 8.4% silica.
- The possibility of obtaining salable concentrate for each product type (Lump, Sinter Feed or Pellet Feed) can depend on, among other factors: average thickness of the bands, shape and porosity of the particles and, mainly, the Fe content of each band.

Pre-characterization - Determination of Work Index for Grinding

Fundação Gorceix determined the Work Index of grinding in two surface samples, according to its standard methodology (Gomes, 2012). The most compact texture sample had WI = 19.80 kWh/st and the most fractured WI = 17.98 kWh/st.

Pre-characterization – Particle Size Distribution and Chemical Analyses

In the Table 2.3_1 can be seen a summary of the results of the particle size and chemical analyses of drill core samples from the two main lithologies in subsurface, Banded Iron Formation (FFB) and Nodular Iron Formation (FND) and the most superficial lithology (ECZ). The ECZ lithology is a layer immediately below the superficial ore (elluvium and colluvium) which ore is mined today on a small scale and generates Lump above 65% Fe (Metal Data, 2014). The tests were done on SGS-Geosol, in Vespasiano (MG).

Table 2.3_1 – Particle Size Distribution and Chemical Analyses (Metal Data, 2014)

Lithology	Particle size	% ROM	SiO_2	Al_2O_3	Fe	P	Mn	LOI	FeO
ECZ-17 samp.	Global	100.0	22.44	3.11	50.23	0.089	0.033	1.42	1.60

	(-31.5 +19.0) mm	19.7	17.24	1.08	56.54	0.079	0.019	0.48	1.10
	(-19.0 +6.35) mm	41.4	18.92	1.42	54.86	0.083	0.025	0.70	1.30
	(-6.35 +1.0) mm	17.9	23.08	2.08	51.46	0.099	0.042	1.09	1.09
	(-1.0 +0.15) mm	7.9	30.03	3.69	44.52	0.107	0.052	1.85	1.14
	(-0.15) mm	13.1	29.95	10.10	37.05	0.199	0.069	4.59	0.43
FFB - 148 samples	Global	100.0	23.89	0.73	49.24	0.133	0.213	2.01	1.21
	(-31.5 +19.0) mm	40.0	23.09	0.54	50.34	0.127	0.177	1.77	1.31
	(-19.0 + 6.35) mm	45.9	23.59	0.65	49.72	0.131	0.191	1.88	1.28
	(-6.35 +1.0) mm	10.4	27.15	0.73	46.86	0.136	0.236	2.15	1.28
	(-1.0 + 0.15) mm	2.2	31.01	1.13	43.44	0.147	0.337	2.49	1.41
	(-0.15) mm	2.0	32.07	3.95	37.68	0.287	0.604	4.48	1.03
FND - 137 samples	Global	100.0	23.27	0.63	50.31	0.143	0.159	1.61	1.17
	(-31.5 +19.0) mm	36.8	22.76	0.50	51.11	0.135	0.152	1.46	1.15
	(-19.0 +6.35) mm	48.4	22.82	0.54	50.95	0.141	0.146	1.50	1.20
	(-6.35 +1.0) mm	11.3	26.49	0.65	47.93	0.149	0.173	1.67	1.17
	(-1.0 +0.15) mm	2.2	31.30	1.10	43.96	0.170	0.290	2.03	1.23
	(-0.15) mm	1.8	33.85	3.30	37.20	0.346	0.684	3.98	0.84

Pre-characterization - Flotation

These bench flotation tests were performed and coordinated directly by the authors of this paper in the PCM laboratory, located in Antonio Pereira district, Ouro Preto (MG). All tests were made with composite samples obtained from aliquot of thirty-two samples used for mineralogical analyses. Table 2.4_1 below shows the results of flotation tests on natural fine fractions (-0.15 mm and -1.00 mm +0.15 mm) of the composite samples of the main lithologies of subsurface (Metal Data, 2014). Samples 0004 and 0015 were ground below 74 μ and the remaining below 0.15 mm. The desliming was made by cyclones.

Table 2.4_1 – Flotation - Natural Fines (-0.15 mm and -1.00 mm +0.15 mm) (Metal Data, 2014)

Sample/Lithology	Flux	%							
		Mass	SiO_2	Al_2O_3	Fe	P	Mn	PPC	FeO
Composite-0003 (FFB)	Flotation Feed	57.9	33.26	1.46	42.82	0.077	0.477	1.31	0.48
	Concentrate	45.8	25.50	1.32	48.20	0.076	0.500	1.37	0.41
Composite-0004 (FFB)	Flotation Feed	53.4	33.47	0.82	40.74	0.159	0.592	2.92	2.06
	Concentrate	31.5	15.20	0.53	52.90	0.172	0.670	3.54	2.75
Composite-0006 (FFB)	Flotation Feed	49.4	41.97	3.31	35.59	0.050	0.373	1.31	0.56
	Concentrate	36.4	35.60	2.01	41.60	0.052	0.410	1.11	0.29
Composite-0014 (FND)	Flotation Feed	56.6	43.19	1.18	36.47	0.17	0.527	1.83	0.38
	Concentrate	29.2	40.40	1.10	38.80	0.17	0.820	1.91	0.19
Composite-0015 (FND)	Flotation Feed	53.1	37.77	0.33	41.58	0.07	0.345	0.28	2.68
	Concentrate	12.8	5.51	0.42	64.50	0.06	0.490	-0.48	6.64
Composite-0017 (FND)	Flotation Feed	49.8	35.65	3.87	40.14	0.14	0.177	1.15	0.61
	Concentrate	34.9	29.00	3.02	46.00	0.12	0.180	0.99	0.41

Table 2.4_2 below shows the results of flotation tests on fine fractions (-1.00 mm +0.15 mm), pre-concentrated or desliming (magnetic separation x cyclone) and grounded below 400 mesh (Metal Data, 2014). Magnetic separation has potential for use as a pre-concentration step prior to the flotation, however, the selectivity is also low and the non-magnetic fraction has a high Fe content.

Table 2.4_2 – Flotation - Natural Fines (-0.15 mm and -1.00 mm +0.15 mm) (Metal Data, 2014)

Sample/Test	Flux	%								
		Mass	Rec. Fe	SiO_2	Al_2O_3	Fe	P	Mn	LOI	FeO
Test 01: underflow (501 g/t starch 3x46 g/t amine)	Initial feed	100.0	100.0	16.12	0.92	56.90	0.066	0.015	0.66	0.24
	Overflow	51.2	49.3	19.20	1.28	54.90	0.081	0.020	0.85	0.24
	Flotation feed	48.9	50.9	12.87	0.52	59.28	0.049	0.010	0.54	0.27
	Concentrate	19.1	21.9	3.97	0.49	65.00	0.052	0.010	0.49	0.35
Test 02: Underflow (876 g/t starch 3x81 g/t amine)	Initial feed	100.0	100.0	16.12	0.92	56.90	0.066	0.015	0.66	0.24
	Overflow	51.2	49.3	19.20	1.28	54.90	0.081	0.020	0.85	0.24
	Flotation feed	48.9	50.6	12.87	0.53	58.91	0.049	0.013	0.57	0.25
	Concentrate	13.4	15.5	3.21	0.50	65.50	0.053	0.020	0.47	0.37
Test 03: magnetic (501 g/t starch 3x98 g/t amine)	Initial feed	100.0	100.0	15.97	0.92	57.16	0.065	0.017	0.76	0.25
	No magnetic	30.7	27.1	25.6	1.16	50.30	0.071	0.010	0.88	0.18
	Flotation feed	69.3	72.5	11.75	0.80	59.81	0.061	0.019	0.71	0.32
	Concentrate	20.5	23.4	4.94	0.70	65.20	0.059	0.040	0.65	0.41
Test 04: magnetic (876 g/t starch 3x15 g/t amine)	Initial Feed	100.0	100.0	15.97	0.92	57.16	0.065	0.017	0.76	0.25
	No magnetic	30.7	27.1	25.60	1.16	50.30	0.071	0.010	0.88	0.18
	Flotation feed	69.3	72.0	11.59	0.80	59.43	0.061	0.013	0.74	0.30
	Concentrate	18.3	20.7	3.92	0.65	64.90	0.056	0.020	0.61	0.27

These test results indicate that the flotation must be fed with pre-concentrate with Fe content above 60% and ground under, at least, 400 mesh, but whose concentrate does not exceed 65% of Fe and low mass recovery. In order to continue the development, the authors of this paper programmed bench flotation tests in Mintek laboratory (Johannesburg, South Africa). Mintek performed thirteen flotation bench tests with pre-concentrate (~ 59% Fe) obtained from surface sample and ground ~ 76% -75 µ, whose best result is shown in Table 2.4_3 below.

Table 2.4_3 – Flotation of Superficial Sample – Best Result – Mintek (Shumba, 2014)

Products	**Mass (%)**	**Grade (%)**			
		Fe	**SiO_2**	**Al_2O_3**	**P_2O_5**
RT1	9.8	43.41	32.35	1.48	0.170
RT2	11.0	47.30	27.20	1.41	0.174
RT3	8.7	52.54	19.30	1.46	0.187
RT4	6.0	56.77	14.20	1.41	0.189
RT (calc)	35.5	49.11	24.49	1.44	0.179
RC	64.5	63.41	6.25	1.46	0.182
Head (calc.)	100.0	58.33	12.72	1.45	0.181
Head (meas.)	100.0	59.60	13.35	1.20	0.175

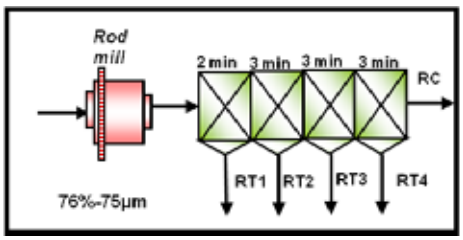

Pre-Characterization - Heavy Liquid Separation

In the first evaluation, the authors of this paper selected ninety-five samples of Coarse Sinter Feed (-6.35 mm +1.0 mm) of drill cores including all lithologies described by geology team and programmed heavy liquid separation (HLS) bench tests at only one density (3.1 g/cm^3). These bench tests were performed in the laboratory of Ferrous, in Brumadinho (MG), Brazil (Metal Data, 2014). Sinter Feed with salable quality was not obtained, but the results showed excellent selectivity and higher densities than 3.1 g/cm^3 should be tested. In sequence, fifty samples of drill cores were scrubbed and screening, generating the Lump (-31.5 mm +6.35 mm), Coarse Sinter Feed (-6.35 mm +1.0 mm) and Fine Sinter Feed (-1.0 mm +0.15 mm). These bench tests were programmed by the authors of this paper and performed in Mintek laboratory, in Johannesburg, South Africa, according to standard methodology of Mintek (Shumba & Tiele, 2014). The densities up to 4.0 g/cm^3 were obtained with TBE (~ 2.96 g/cm^3) and ferrosilicon (~ 7.0 g/cm^3) and above 4.0 g/cm^3 with TBE and tungsten carbide (~ 19.0 g/cm^3). The main objective was successfully reached since products were obtained with 64% Fe content in each range: Lump, in density between 4.5 g/cm^3 and 4.8 g/cm^3; Coarse Sinter Feed between 4.0 g/cm^3 and 4.2 g/cm^3; Fine Sinter Feed between 3.8 g/cm^3 and 4.0 g/cm^3. The selectivity was excellent for Lump and Coarse Sinter Feed. For Fine Sinter Feed, there was generation product with content above 64%, but the selectivity was not as good as for Lump and Coarse Sinter Feed (Shumba & Tiele, 2014). The tests were done in a single stage due to the limited sample masses and use of aliquots of sinks and floats for chemical analyses. The following Table 2.5_2 summarizes the results.

Table 2.5_2 – Results of Heavy Liquid Separation (HLS) - Lump, CSF and FSF (Shumba & Tiele, 2014)

Lump (-31.5 +6.35) mm			Coarse SF (-6.35 +1.0) mm			Fine SF (-1.0 +0.15) mm		
% Fe	Density	% ROM	% Fe	Density	% ROM	% Fe	Density	% ROM
60.5	4.20	45.0	58.0	3.30	8.8	60.0	3.30	1.3
63.7	4.50	13.5	60.0	3.55	8.0	60.0	3.55	1.2
65.0	4.80	2.9	62.0	3.80	71	62.0	3.80	1.2
-	-	-	66.0	4.70	1.9	-	-	-

The Table 2.5_3 below shows a mass balance estimated by the authors based on the results of tests on Mintek and mathematical simulations of: crushing, scavenger stage of heavy liquid separation and flotation for pellet feed production output (Metal Data, 2014).

Table 2.5_3 –Mass Balance HLS – Lump, CSF and FSF – Simulation (Metal Data, 2014)

Product	ROM 52% Fe				ROM 54% Fe			
	FFB 63% + FND 37%		ECZ		FFB 63% + FND 37%		ECZ	
	% ROM	% Fe	% ROM	% Fe	% ROM	% Fe	% ROM	% Fe
Total Lump	5.9 – 20.0	64.00	21.0	64.52	6.5 - 25.0	64.00	25.9	64.52
Coarse SF	17.8 – 15.0	64.00	15.3	64.45	19.4 - 16.0	64.00	16.6	64.45
Fine SF	18.4 – 13.5	64.00	13.7	64.00	20.2 - 14.0	64.00	14.0	64.00
Total SF	36.2 – 29.0	64.00	29.0	64.24	39.5 - 30.0	64.00	30.6	64.24
Pellet Feed	10.0	64.00	10.0	64.00	10.0	64.00	10.0	64.00
Total	52.1 - 59.0	-	59.0	-	56.0 - 65.0	-	66.6	-

2.1 Pre-characterization – Pneumatic Jigging x Heavy Liquid Separation

As already reported in this article, the dense medium separation (DMS) in densities above 3.8 g/cm^3 can't be made industrially yet. Then heavy liquid separation (HLS) and pneumatic jigging bench tests were conducted on six samples of ore superficial. Each sample had 400.0 kg and aliquots of Coarse

Lump, Medium Lump and Coarse Sinter Feed were tested in densities between 3.8 g/cm^3 and 4.8 g/cm^3. The main objective of these tests was to establish correlations between the results of heavy liquid separation and the pneumatic jigging. The most productive operating parameters for the laboratory jig (amplitude, frequency, pressure, residence time, number and thickness of layers, etc.) were tested and defined. The tests and simulations were made in the laboratory Mintek (Shumba, 2014). The results of the heavy liquid separation (HLS) and the respective simulation for industrial pneumatics jigging in one of the six samples are summarized in the following table 2.6_1.

Table 2.6_1 – Results – Heavy Liquid Separation (HLS) Bench Tests x Simulation of Industrial Pneumatic Jigging (Shumba, 2014)

Size Distribution	Coarse Lump			Medium Lump			Coarse Sinter Feed		
	Mass (%)	Fe (%)	SiO_2 (%)	Mass (%)	Fe (%)	SiO_2 (%)	Mass (%)	Fe (%)	SiO_2 (%)
Density	Heavy Liquid Separation (HLS) Results - Bench Test – Mintek								
3.8	84.4	52.47	19.00	88.8	55.88	16.70	65.1	62.85	9.57
4.0	69.0	55.82	17.90	77.8	54.76	17.60	56.1	52.51	9.78
4.2	65.4	59.01	11.60	62.3	60.02	10.60	44.6	61.12	6.69
4.4	49.3	60.94	8.86	39.2	63.29	6.86	31.0	64.07	4.92
4.6	21,5	64.59	5.51	16.0	64.43	5.26	17.7	66.57	3.78
4.8	4.0	66.39	3.72	3.4	66.21	3.50	7.9	67.32	3.35
Density/Layer	Industrial Jigging - Simulation Mintek								
3.8	84.4	59.82	10.68	88.8	60.30	10.57	64.2	61.99	9.59
4.0	69.6	61.39	8.91	78.6	60.88	9.77	56.5	62.13	9.45
4.2	65.6	61.76	8.34	63.6	62.29	7.96	45.4	63.80	7.32
4.4	50.1	62.61	7.32	41.2	63.69	6.32	32.3	65.25	5.52
4.6	23.1	64.64	5.42	18.4	64.58	5.18	19.6	66.34	4.34
ROM	46.5	57.30	16.20	30.9	54.80	18.70	10.4	52.50	22.10

Aliquots of Coarse Lump, Medium Lump and Coarse Sinter Feed of four of these samples of 400.0 kg were also concentrated in the pneumatic jigs of Fundação Gorceix. The main objective was the adjustment of operating parameters of bench jigs of Fundação Gorceix to the equipment of Mintek laboratory, which were successfully obtained. Based on the results of the jigging tests in Fundação Gorceix and Mintek, a new bench pneumatic jig was designed by the authors, for testing HD drill cores samples. This new jig can operate with small masses for Coarse Lump (15.0 kg - 20.0 kg), Medium Lump (7.5 kg - 10.0 kg) and Coarse Sinter Feed (0.5 kg - 1.0 kg).

DEVELOPMEMT OF THE HEAVY LIQUID SEPARATION METHOD WITH LST

The procedures were developed in the laboratory Geomatek, Brumadinho (MG), Brazil, replacing the tetrabromoethane (TBE) for LST (lithium heteropolytungstate), with a density close to 2.89 g/cm^3. The method proved to be efficient for mineral separation in four different ranges of particles size (Coarse Lump, Medium Lump, Coarse Sinter Feed and Fine Sinter Feed) employing densities ranging from 3.10 g/cm^3 to 4.80 g/cm^3. The method using TBE has good process efficiency, as demonstrated by the good results of the tests made in Mintek. But operationally has low productivity due to high toxicity of TBE. The operating procedures of the method with LST were then defined as described below:

- Application of LST + ferrosilicon mixture densities of 3.10 g/cm^3 to 3.80 g/cm^3.
- Application of LST + tungsten carbide mixture densities of 4.0 g/cm^3 to 4.80 g/cm^3.
- Filtering of ferrosilicon or tungsten carbide solutions, reserving LST solution and the ferrosilicon or carbide cake for later use.

- LST recovery for drying in an oven or thermal plate and ferrosilicon and tungsten carbide for filtration.

The simplicity of the method and non-toxicity of LSD, as shown in Figure 4_1, photos of the left side, allows a much higher productivity when compared to tests with organic liquids, resulting in operating efficiency and lower costs. The method is feasible for use in the characterization of high number of small samples, as required in the development of the deposit Santa Cruz.

CHARACTERIZATION - FIRST PHASE

Based on the operating parameters and process obtained in the pre-characterization step, the programming of the definitive characterization, called first stage, was made. For the first phase, concentration tests were scheduled for heavy liquid separation (with LST) and pneumatic jigging bench in about five hundred samples of drill core in each product range. Based on the results of these first five hundred samples testes, a pilot test in continuous scale would be programmed in pneumatic jig and also new bench tests in heavy liquid and jigging until the full characterization of the big deposit. The Figure 4_1 shows as photos of the heavy liquid separation with LST and pneumatic jigs available in Brazil.

Figure 4_1 – Photos of the left side: Geomatek Laboratory - Tests with LSD; photos of center: jigs of Fundação Gorceix; photos of the right side: jig for bench tests of HD drill cores samples

Results – Heavy Liquid Separation with LST

Forty-one samples of drill core were tested in heavy liquid separation (with LST) whose sampling achieved to 30.0 m depth in the deposit (Cordeiro, 2014a). The summary of results is presented in the following Table 4.1_1.

Table 4.1_1 – Heavy Liquid Separation with LST – Geomatek (Cordeiro, 2014a)

Density (g/cm^3)	Particle Size	Product	(% Feed)	(% ROM)	SiO_2	Al_2O_3	Fe	P	LOI
	(-31.5) mm	ROM	100.0	100.0	22.67	1.42	51.60	0.135	1.03
3.8	(-31.5 +19.0) mm	Float (meas.)	9.0	2.4	28.17	0.42	48.46	0.100	0.50
		Sink (calc.)	**91.0**	**23.8**	**12.43**	**0.38**	**60.35**	**0.092**	**0.33**
	(-19.0 +6.35) mm	Float (meas.)	9.4	3.0	26.80	0.54	49.14	0.094	0.69
		Sink (calc.)	**90.6**	**29.2**	**11.09**	**0.41**	**61.24**	**0.089**	**0.43**

4.2	(-6.35 +1.0) mm	Float (meas.)	16.3	1.4	20.14	0.85	53.75	0.116	0.78
		Sink (calc.)	**83.7**	**7.3**	**8.15**	**0.50**	**63.11**	**0.091**	**0.43**
	(-31.5 +19.0) mm	Float (meas.)	37.2	8.9	19.02	0.42	55.75	0.089	0.37
		Sink (calc.)	**62.8**	**15.0**	**8.53**	**0.35**	**63.07**	**0.095**	**0.30**
	(-19.0 +6.35) mm	Float (meas.)	42.4	12.4	16.20	0.47	57.67	0.091	0.59
		Sink (calc.)	**57.6**	**16.7**	**7.32**	**0.37**	**63.87**	**0.087**	**0.31**
	(-6.35 +1.0) mm	Float (meas.)	28.5	2.1	14.08	0.72	58.23	0.097	0.60
		Sink (calc.)	**71.5**	**5.2**	**5.84**	**0.42**	**64.98**	**0.091**	**0.38**
4.5	(-31.5 +19.0) mm	Float (meas.)	49.3	7.4	11.19	0.36	60.92	0.092	0.34
		Sink (calc.)	**50.7**	**7.6**	**6.01**	**0.34**	**65.11**	**0.097**	**0.27**
	(-19.0 +6.35) mm	Float (meas.)	38.5	6.5	10.37	0.39	61.40	0.085	0.36
		Sink (calc.)	**61.5**	**10.3**	**5.40**	**0.35**	**65.43**	**0.088**	**0.28**
	(-6.35 +1.0) mm	Float (meas.)	47.6	2.5	8.34	0.48	63.05	0.089	0.42
		Sink (calc.)	**52.4**	**2.7**	**3.67**	**0.37**	**66.65**	**0.093**	**0.34**
4.8	(-31.5 +19.0) mm	Float (meas.)	84.6	6.4	6.57	0.34	64.78	0.098	0.29
		Sink (calc.)	**15.4**	**1.2**	**3.20**	**0.33**	**66.78**	**0.101**	**0.21**
	(-19.0 +6.35) mm	Float (meas.)	77.9	8.0	6.10	0.37	65.02	0.087	0.31
		Sink (calc.)	**22.1**	**2.3**	**2.93**	**0.31**	**66.87**	**0.092**	**0.18**
	(-6.35 +1.0) mm	Float (meas.)	80.1	2.2	4.26	0.36	66.38	0.098	0.33
		Sink (calc.)	**19.9**	**0.5**	**2.32**	**0.30**	**67.22**	**0.088**	**0.35**

It is observed that the heavy liquid separation was made only at one stage. The floated fractions of each range were not crushed, screened and subjected to the next stage (scavenger) of heavy liquid separation.

Results - Pneumatic Jig Bench Tests

Thirty-nine samples of drill core were tested in bench pneumatic jigging whose sampling also achieved up to 30.0 m deep. The samples were selected in the same regions of the forty-one samples tested in dense liquid. The summary of results is presented in the following Table 4.2_1.

Table 4.2_1 – Pneumatic Jigging Tests – Fundação Gorceix (Cordeiro, 2014b)

Flux	%				
	Mass	SiO_2	Al_2O_3	Fe	P
ROM	100.00	19.94	1.75	53.60	0.12
(-31.5 +19.0) mm	31.05	18.37	0.57	55.85	0.11
(-19.0 +6.35) mm	40.66	17.65	0.84	56.40	0.10
(-6.35 +1.0mm)	13.90	19.89	1.30	54.07	0.10
Coarse Lump	11.91	10.62	-	61.48	-
Medium Lump	10.53	7.50	-	63.88	-
Coarse SF	2.55	7.54	-	63.76	-
LUMP Total	22.44	6.49		62.61	

It is observed that the jigging tests were made only at one stage. The layers with low Fe content were not crushed, screened and subjected to the next stage (scavenger) of jigging or heavy liquid

separation. The tests programmed with the five hundred samples were interrupted due to the iron ore price decline, and especially the current economic situation in Brazil.

CONCLUSIONS

The deposit of Santa Cruz is a BIF (Banded Iron Formation), Neoproterozoic age, characterized by alternating levels rich in hematite, with predominantly silica levels. The iron formation has great alternation of texture and composition, in the various strata. One of the outstanding characteristics is ore texture, very fine-grained hematite and microcrystalline; and silica with micro and cryptocrystalline granulation. The degree of liberation studies (Fundação Gorceix) indicate that the ore is formed by a silica-hematite association that generates products with varying iron content. Lithotipes with higher percentage of hematite to 85.00% generate products with levels above 64.00% Fe. Lithotipes with percentage of hematite over 85.00% generate products with contents up 64.00% Fe.

The flotation process, applied to particles approximately -65 mesh (-0.210 mm), is based on chemistry of the surface for adsorption of reagents by hematite and gangue. The partial liberation of the gangue from the hematite greatly reduces the efficiency and selectivity of this process. The reagents (amine and starch) can be without distinction adsorbed by the surfaces of the mixed particles, which probably causes the low selectivity of the flotation. However, concentration by difference in density exhibited good selectivity for Lump and Sinter Feed, since the current techniques of heavy liquid and pneumatic jigging allow greater separation efficiency.

The results of tests and mathematical modeling presented in this paper indicated the potential for Lump and Sinter Feed production. The results of Pellet Feed concentration are not promising for high quality product, requiring further studies to confirm the potential for the generation of this type of product. The tests with fines in the range of Pellet Feed also indicated the need for grinding development and evaluation of new reagents and their dosages for flotation. The target for Pellet Feed production with 64% Fe content to be mixed with Sinter Feed (- 6.35 mm + 0.15 mm) should also be evaluated because the Fines market may be promising.

The development of the new method of heavy liquid separation with the use of LST was essential because its operational simplicity allows a large increase in productivity in the characterization with bench tests. The design and fabrication of pneumatic jig for small masses samples allow samples of drill core can be tested in bench tests. The establishment of correlations between the results of bench tests (heavy liquid and pneumatic jig) will allow the simulation of industrial results. Then, most of the continuous pilot scale tests could be done with the use of surface samples, with reduced drilling large diameter for this purpose.

REFERENCES

Cordeiro, R.A.C. (2014a). Resultados de testes de meio denso em bancada com LST em 41 amostras. Relatório interno. [Results of heavy liquid separation bench tests with LST in 41 samples. Internal report]. Unpublished manuscript. Vetria Mineração, Belo Horizonte, MG, Brazil.

Cordeiro, R.A.C. (2014b). Resultados de testes de bancada em jig pneumático em 38 amostras. Relatório interno. [Results of bench tests on pneumatic jig in 38 samples. Internal report].Unpublished manuscript. Vetria Mineração, Belo Horizonte, MG, Brazil.

Gomes, F. J. (2012). Relatório de progresso 1. Estudo de caracterização e concentrabilidade de amostras provenientes da Vetria. Relatório Interno. [Progress report. Characterization and concentrability study of samples of Vetria. Internal report]. Unpublished manuscript. Fundação Gorceix, Ouro Preto, MG, Brazil.

Ferreira, C. M. (2014). Considerações sobre o minério de ferro do projeto Santa Cruz – Corumbá – MS. Relatório interno. [Considerations about the iron ore of the Santa Cruz project - Corumbá - MS. internal report]. Unpublished manuscript. Fundação Gorceix, Ouro Preto, MG, Brazil.

Metal Data, 2014. Relatório consolidado de desenvolvimento de processo. Relatório interno. [Consolidated reporting of the process development. Internal report]. Unpublished manuscript. Rio de Janeiro, RJ, Brazil.

Shumba, T., & Tiele, H. (2014). Characterisation of a brazilian iron ore deposit, using heavy liquids separation (HLS). Internal Report. Unpublished manuscript. Mintek, Johannesburg, South Africa.

Shumba, T. (2014). Characterisation of Vetria bulk iron ore samples using heavy liquids separation (HLS) and mineral density separation (MDS). Internal report. Unpublished manuscript. Mintek, Johannesburg, South Africa.

PERFORMANCE EVALUATION OF A DEWATERING CYCLONE BASED ON UNDERFLOW DISCHARGE PATTERN

*Rakesh Kumar Dubey[1], Arun Kumar Majumder[1], K.U.M. Rao[1]

[1]Department of Mining Engineering
Indian Institute of Technology, Kharagpur, India
*(*Corresponding author: dubeyable@gmail.com)*

24th World Mining Congress
MINING IN A WORLD OF INNOVATION
October 18-21, 2016 • Rio de Janeiro /RJ • Brazil

PERFORMANCE EVALUATION OF A DEWATERING CYCLONE BASED ON UNDERFLOW DISCHARGE PATTERN

ABSTRACT

Hydrocyclone separator for classification and dewatering applications has been found to have widespread use in various industrial areas. The performance of a hydrocyclone as a separation device is never perfect and concerted research efforts are still continuing in different directions towards achieving optimum solutions. This complexity is attributable to the turbulent nature of the flow field and also variations in the feed properties as well as design configuration during the operation of a hydrocyclone in industries. As a consequence, due to all the ambiguities associated with the correct understanding of separation characteristics inside a hydrocyclone, practicing professionals, and researchers as well, are, therefore, making constant efforts to monitor the hydrocyclone to meet the specific requirements. It is worth emphasizing that slight variation in operating and design parameters, the performance of a hydrocyclone is significantly affected and will lead to huge economic loss. Therefore, in the present study, applicability of the underflow discharge pattern as an indicator of hydrocyclone performance has been explored. Underflow discharge angle was measured using edge detection technique by an image processing algorithm. In this concern, systematic experimental data was generated to observe the variation of the underflow discharge angle with the relevant operating and design parameters for the dewatering process in a 50.8 mm diameter hydrocyclone. Moreover, the potential of the present concept has also been explored to envisage the significance of rope discharge to rationalize the dewatering process.

KEYWORDS

Hydrocyclones, spray angle, image analysis, rope discharge, dewatering.

INTRODUCTION

The hydrocyclone is a separation device widely used in the chemical and mineral processing industries. Its popularity is promoted by its simple design and operation, compact structure, low maintenance costs, and versatility. Applications of the hydrocyclone include liquid clarification, slurry thickening, solids washing and solids classification. With any of these operations, the overall profitability as well as efficiency of the process relies on the effective performance of the process equipment.

The most important aspect of any process unit is to control and monitor the performance. It helps in increasing the efficiency and reduces the variations in the end product of the unit operation in study. Proper monitoring could also lead to significant financial benefits. The same applies to hydrocyclone too. With the varying feed conditions, which the hydrocyclones are subjected to, even a slight variation in feed properties, the performance of hydrocyclone could significantly be affected and will lead to huge economic loss.

Various operating state has been under investigation which can be an indicative of the present performance of hydrocyclone performance such as shape of air core, internal solids concentration, and shape of underflow discharge. The on/off line continuous/ batch monitoring of these above mentioned state has been attempted using electrical impedance (Williams et al., 1997; Gutierrez et al., 2000), electrical resistance (Williams et al., 1999; West et al., 2000), ultrasound tomography (Schlaberg et al., 2000), mechanical detection (Hulbert, 1993), X-ray tomography (Galvin and Smitham, 1994), Acoustic emission (Hou et al., 1998; 2002) or several sensing techniques. But a robust user-friendly and industrially applicable technique is still to see the day of light due to the relatively costly equipment involved and robustness to develop confidence needed.

It has been long advocated that spray angle can be used as a performance monitoring tool for hydrocyclone. Limited works have also been carried out in the past which indicate the importance of using underflow discharge pattern as one of the most important process control technique as an alternative to various empirical and theoretical modeling techniques, which suffers from inherent disadvantages of their own (Neesse et al., 2004a; Neesse et al., 2004b, Petersen et al., 1996). Industrial application of using spray angle as an indicator is also advantageous as the spray profile is easily visible and spigot is the only design variable which can be easily replaced.

Using the discharge pattern as an indicator cum tool for monitoring the performance of a hydrocyclone, it was imperative to convert the discharge pattern from the underflow of a hydrocyclone in a quantifiable term. Various attempts were made in the past to achieve the same using a number of mathematical, theoretical and video graphic techniques (Van Deventer et al., 2003; Neesse et al., 2004b; Williams et al., 1997; Viljoen, 1993; Petersen et al., 1996; Van Vuuren et al., 2011; Mazumdar et al., 2014).

The classification/dewatering efficiency of a hydrocyclone depends on the different design and operating parameters. These design and operating parameters reflect on changing in underflow discharge pattern. Hence, monitoring the underflow discharge pattern of hydrocyclone can be a useful technique to assess its performance (Viljoen, 1993; Petersen et al., 1996; Neesse et al., 2004a; Van Vuuren et al., 2011; Mazumdar et al., 2014).

MATERIALS AND METHOD

A closed circuit two-inch hydrocyclone test rig consisting of pump and sump assembly was used for generating the requisite experimental data set as shown in Figure 2. The camera for capturing the spray profile was placed at 2m distance from the rig to avoid damage to the lens from water splitting from the sump. At a chosen combination of spigot and vortex finder diameters slurry (mixture of silica sand and water) was introduced through the inlet at inlet pressure ranging from 68948 N/m^2 to 344740 N/m^2. The system was allowed to run for a while to reach the steady state operating condition. Once the steady state condition was reached, the spray discharge through underflow was captured using a digital camera (Sony - DSC HX-300, 50 x zoom, 20.4 MP). The underflow (UF) and overflow (OF) discharge rates were also measured by collecting timed samples for further analysis. This procedure was followed while collecting data at various operating conditions as mentioned in Table1 and 2.

Table 1 - Design and operating variables

Variable	Variable Range

Table 2 - Fixed design parameters

Spigot diameter (mm)	3.2, 4.5, 6.4
Vortex finder diameter (mm)	8, 11, 14
Feed inlet pressure (N/m^2)	68948 - 344738
Feed 1 (d_{50} and d_{90} in micron)	15 and 35.5
Feed 2 (d_{50} and d_{90} in micron)	22 and 55
Feed concentration (% by wt.)	1- 20

Fixed Design parameter	**Value**
Hydrocyclone diameter (mm)	50.8
Cone angle (degree)	7
Inlet area (mm^2)	9×6

Figure 2 show the feed particle size distribution of the solids material used for the experimental purpose and Figure 3 illustrate the laboratory scale experimental set-up.

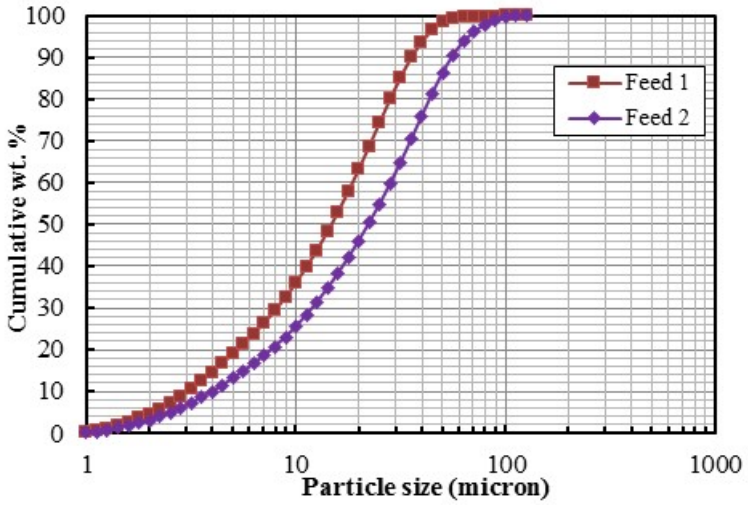

Figure 1 - Feed size distribution

For each experimental condition, ten simultaneous images of underflow discharge pattern were captured. The shutter speed of the camera was fixed at one frame per second. A contrast background was used to proper distinguished between the region of interest (discharge pattern) and its surroundings. Using the developed algorithm on MATLAB^{TM} platform (Mazumder et al., 2014) discharge angles were calculated. Finally, mean of these ten angles was considered as the UF discharge angle for given operating and design condition.

Figure 2 - Experimental test rig

RESULTS AND DISCUSSION

Effect of Outlet Diameter on Underflow Discharge Angle

In the present study, Vortex finder diameter (VFD) and spigot diameter (SPD) as the design parameters have been changed which have significant effect on hydrocyclone performance and UF discharge pattern as well. The diameter of the vortex finder is a very important variable. At the given operating pressure and concentration, an increase in the diameter of the vortex finder will result in a coarser cut point as more feed material reports to the overflow. With higher VFD, underflow flow rate decreases as well as spray angle becomes lower (Figure 3) due to the relative less water recovery through underflow and.

The size of the spigot opening, regulates the underflow density, and must be large enough to discharge the course solids that are being separated by the cyclone. It is found that an increase in either the SPD or cone angle, or a decrease in the area of inlet tangential port increases the air core diameter and UF discharge spray angle. An increase in either SPD or swirl chamber cone angle reduces the resistance offered by the ejection area to the swirling motion of slurry inside it. While a decrease in inlet port area, for a given flow rate, increases the strength of swirling motion by increasing the tangential velocity of injection to the hydrocyclone. It can be observed from Figure 4, increase in SPD leads to increase in underflow discharge angle because this increased spigot diameter allows more fines and excess water to report to the underflow. At fixed operating and design condition, lower SPD leads to the formation of rope discharge.

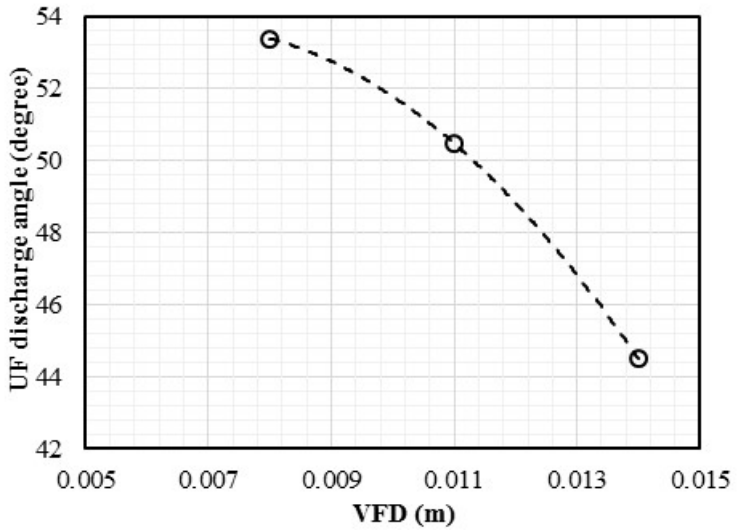

Figure 3 - Effect of VFD on UF discharge angle at 3% feed solid conc. and FIP of 206844 N/m^2 using SPD=4.5mm

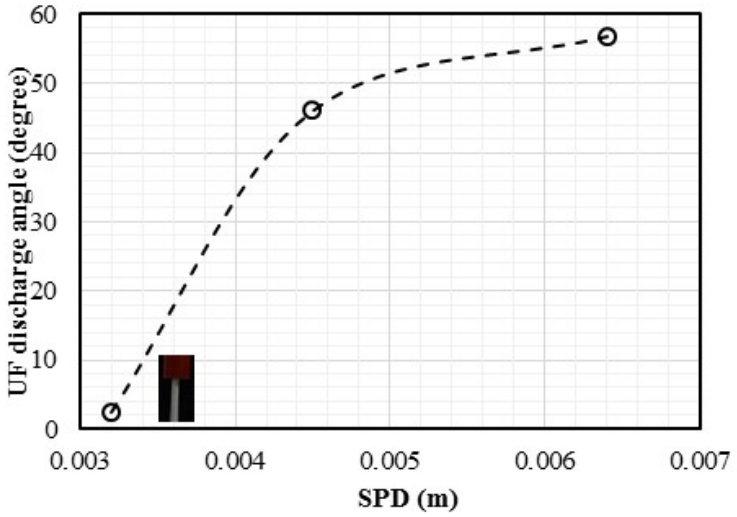

Figure 4 - Effect of SPD on UF discharge angle at 5% feed solid conc. and FIP of 206844 N/m^2 using VFD=11mm

Effect of Feed Inlet Pressure (FIP) on UF Discharge Angle

The discharge spray angle is a visual parameter which immediately identifies normal or aberrant operation and can be directly interpreted to characterise internal flow properties such as pressure drop. An increase in flow rate is accompanied by an increase in the tangential velocity of injection to the hydrocyclone. Inlet feed flow rate is directly reflected by feed inlet pressure. Swirl intensity inside the cyclone increases with increase in feed inlet pressure (increase in inlet Reynolds number) that results,

increase in tangential velocity component at the spigot opening which is responsible for underflow discharge pattern. So, underflow discharge angle increases with increase in inlet pressure till a certain pressure. After this pressure limit, there are nominal effects of change in pressure on spray angle and it moves towards constant while it may be possible that the underflow rate increases due to change in spray thickness at same spray angle. Domouchel et al. (1993) theoretically showed that after a certain point of inlet pressure, an increase in initial fluid spin results in a small or negligible increase in the tangential velocity at the spigot outlet. A visual investigation of the dependency of the feed inlet pressure on spray angle is shown in Figure 5.

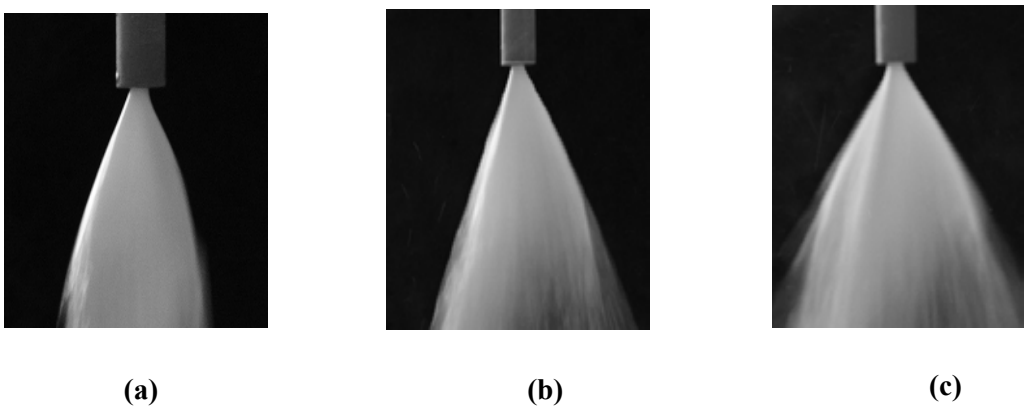

Figure 5 - Effect of increasing feed inlet pressure on underflow discharge shape (a) Low pressure, (b) moderate pressure and (c) high pressure

Figure 5 shows the effect of feed inlet pressure on the discharge angle of the hydrocyclone at three different inlet pressure (68948, 206844 and 344740 N/m^2 respectively) at a fixed geometry and feed solid concentration.

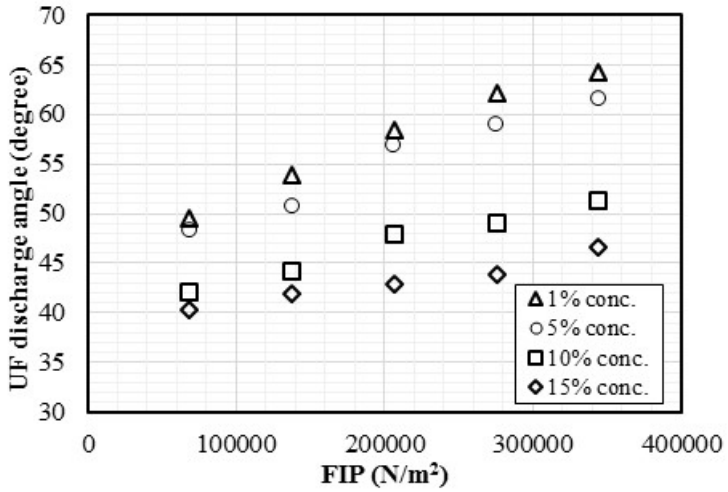

Figure 6 - Effect of feed inlet pressure on UF discharge angle at different feed solid conc. using VFD=11mm and SPD=6.4mm

Effect of Feed Solid Concentration on UF Discharge Angle

Feed solid concentration plays another important role in deciding the shape of the underflow discharge. A visual investigation of the dependency of the feed inlet solid concentration on spray angle is shown in Figure 7. It can easily be demonstrated from Figure 7 that underflow discharge regime gradually shifts from spray to rope discharge with the subsequent increase in feed solid concentration. At lower feed solid concentration, slurry practically behaves like water. An increase in solids concentration increases the cut size and underflow discharge spray angle becomes lower. This is mainly due to the effective increase in viscosity. At higher concentration, relatively a large amount of solids particles is sedimented in conical section (near spigot) and this hindered settling condition leads to the formation of rope discharge.

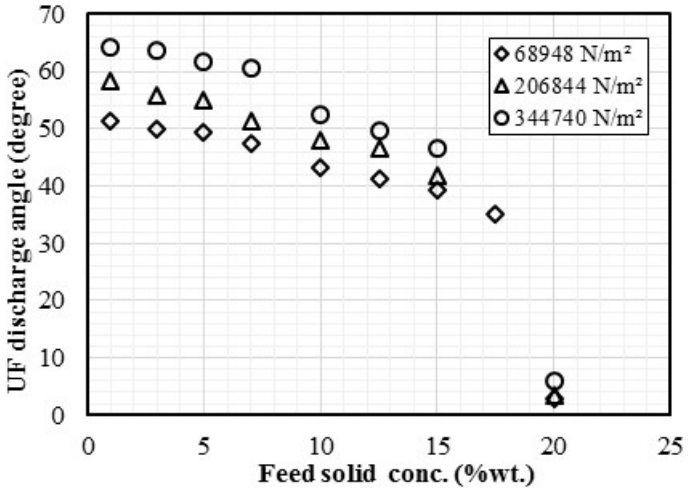

Figure 7 - Effect of feed solids concentration on UF discharge angle at different FIP using VFD=11mm and SPD=6.4mm

Effect of feed size distribution on underflow discharge angle

Feed particle size distribution is also one of the controlling parameters of underflow discharge pattern. Larger feed size distribution (Feed 2) leads to lower discharge angle than relative smaller feed size distribution. At same concentration level, we got lower discharge angle with feed 2. As the concentration increases, the rope condition is found earlier for feed 2 (higher d_{50}). Feed size distribution have strong influence on viscosity and this increased viscosity decreases the discharge angle. In the present study, we are not going to detail of feed size and viscosity relation. For fixed cyclone geometry, we can operate with higher feed solids concentration for relative finer particles (in feed) without commencing the rope condition (undesirable condition).

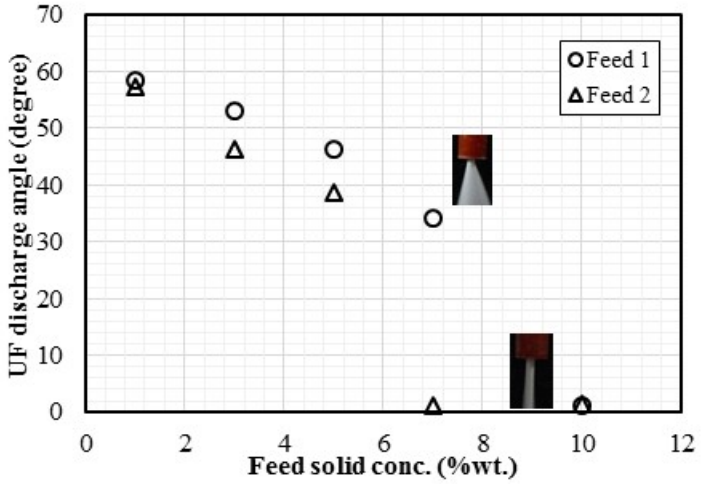

Figure 8 - Effect of feed solids concentration on UF discharge angle with two different feed using VFD=11mm and SPD=4.5mm

Hydrocyclone Performance Indices w.r.t. UF Discharge Angle

It is noticed that the hydrocyclone performance is interrelated with underflow discharge angle. From Figure 9 and 10, it can be observed that performance indices, e.g., cut size (d_{50}), solid split and water split alter with changing in spray angle. Here, solid split and water split are defined as the ratio of underflow solids to feed solids and ratio of underflow water to feed water respectively.

At the same level of feed solids concentration, solid split increases with increase in underflow discharge angle (FIP increases) while water split decreases due to increase in swirl intensity. At higher feed inlet pressure, more solids transport towards the wall side of the cyclone (high centrifugal force than drag force) and report to underflow whereas more water report to overflow. Higher feed solids concentration leads to higher cut size (d_{50}) and lower underflow discharge angle as well. For the given experimental condition, cut size affect the underflow discharge angle (Figure 10).

So, based on the detail experimental observations, it can be interpreted that the spray angle is an indicator of hydrocyclone performance.

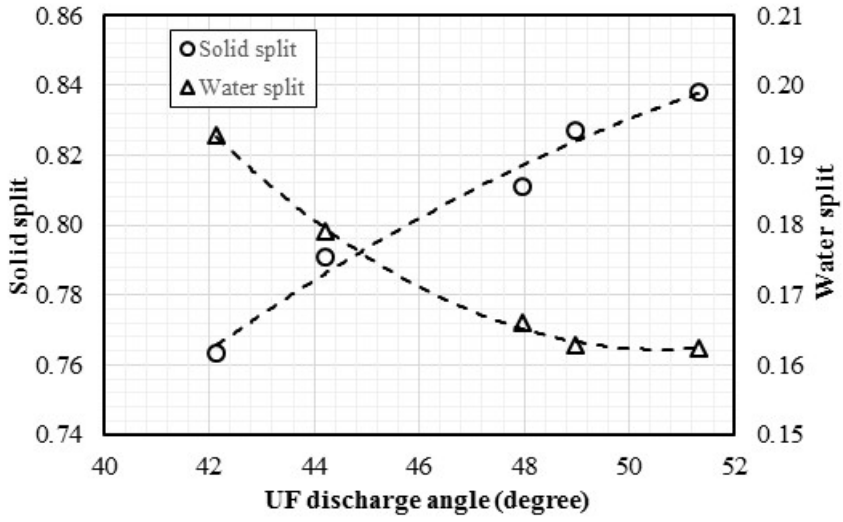

Figure 9 - Variation of solid split and water split w.r.t. UF discharge angle at 10% feed solids conc. (by wt.) using VFD= 11mm and SPD= 6.4mm

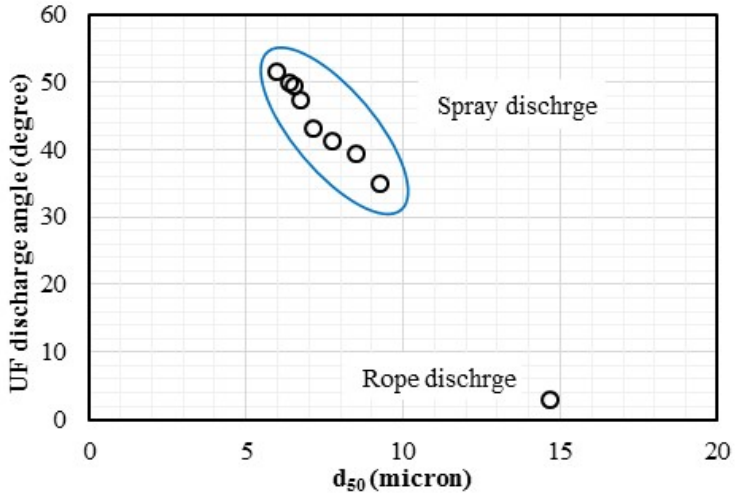

Figure 10 - Variation of UF discharge angle w.r.t. d_{50} at FIP of 68948N/m^2 using VFD= 11mm and SPD= 6.4mm

A small diameter of hydrocyclone having cone angle of 7^0 was used in the present study. Generally, it uses for the dewatering purpose. In terms of dewatering, solids recovery should be maximum with minimum water through underflow. Further, solid split and water split have been studied w.r.t. feed inlet pressures at different concentration levels.

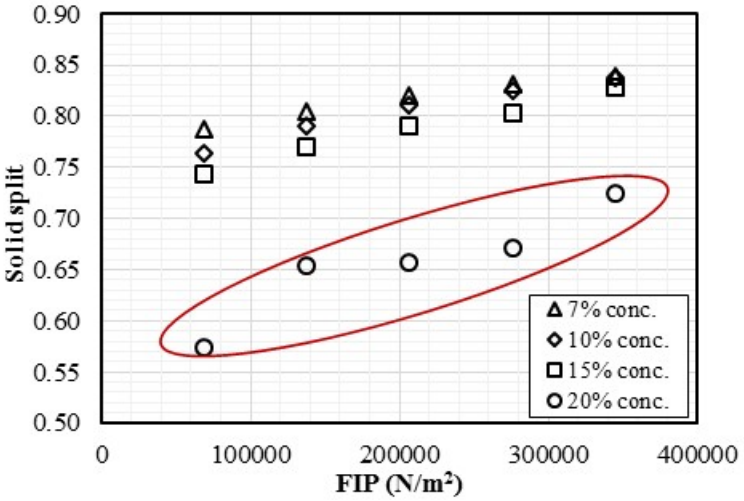

Figure 11 - Effect of feed inlet pressure on the solid split at various feed solids concentration levels using VFD= 11mm and SPD= 6.4mm

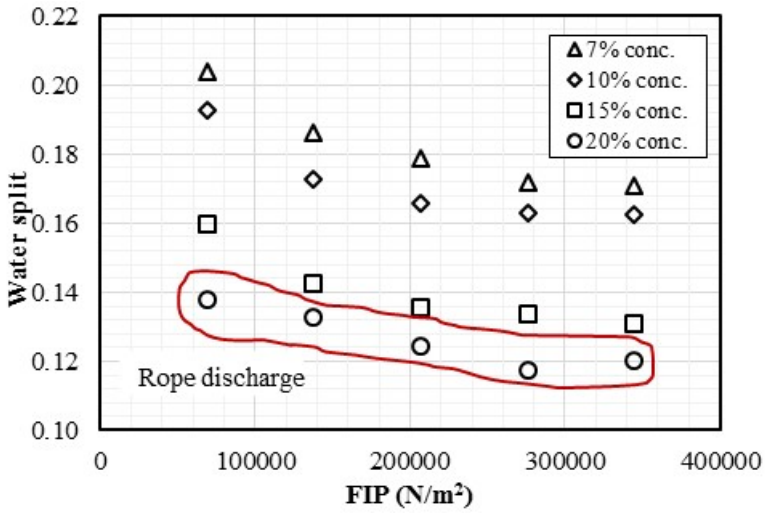

Figure 12 - Effect of feed inlet pressure on water split at various feed solids concentration levels using VFD= 11mm and SPD= 6.4mm

Solid split increases with increase in inlet pressure while water split decreases (Figure 11 and 12) but both decreases with increase in feed solids concentration. Higher concentration (here, 20%) leads to lower water recovery through underflow which is favorable for dewatering purpose but solids recovery through underflow is found lower which is not favorable. So it can be concluded that rope discharge condition, which was formed at higher concentration (here 20%), may not be best for dewatering.

CONCLUSIONS

In this study, the underflow discharge pattern is captured using the photographic and angles are measured using edge detection technique on MATLAB platform. This angle measurement technique is also worked efficiently with slurry as feed. Hydrocyclone design and operating parameters, e.g., VFD, SPD, FIP, feed solids concentration and feed size distribution, have significant effect on its performance and UF discharge angle as well. Each parameter alters the discharge angle which indicates that underflow discharge angle can be good indicator of hydrocyclone performance and the performance of hydrocyclone can be monitored by monitoring the discharge pattern. Performance indices of hydrocyclone w.r.t. underflow discharge angle justify it.

Higher feed solids concentration leads to rope discharge condition. Water recovery in UF is found minimum at rope discharge condition which indicates a good dewatering condition, but relative lessens solids are reported in underflow which indicates rope discharge condition may not be best for dewatering purpose and need to optimize the process further.

However, the present study only intended to show the effect of some design and operating parameters on discharge angle and the variation of discharge angle with some performance indices. Need to further detail

investigation to assess the potential of the approach to provide estimates over a practical range of values for industrial application.

REFERENCES

Dumouchel, C., Bloor, M.I.G., Dombrowski, N., Ingham, D.B., Ledoux, M., 1993. Viscous flow in a swirl atomiser. *Chemical Engineering Science 48 (1)*, 81 – 87.

Galvin, K.P. and Smitham, J.B. (1994). Use of X-rays to determine the distribution of particles in an operating cyclone. *Minerals Engineering, 7(10)*, 1269-1280.

Gutierrez, J.A., Dyakowski, T., Beck, M.S. and Williams, R.A. (2000). Using electrical impedance tomography for controlling hydrocyclone underflow discharge. *Powder Technology, 108 (2-3)*, 180-184.

Hou, R., Hunt, A. and Williams, R.A. (1998). Acoustic monitoring of hydrocyclone performance. *Minerals Engineering, 11(11)*, 1047-1059.

Hou, R., Hunt, A. And Williams, R.A. (2002). Acoustic monitoring of hydrocyclones. *Powder Technology, 124(3)*, 176-187.

Hulbert, D.G. (1993). Measurement Method and Apparatus for Hydrocyclones. *Pat EP0522215A2*, Randburg.

Mazumdar, A., Dubey, R.K., Banerjee, C., Sengupta, K. and Majumder, A. K. (2014). A Study on the characteristics of spray angle formation in a 2 inch hydrocyclone using water only *International Journal of Mineral Processing 126,* 141–145.

Neesse, T., Schneider, M., Golyk, V. and Tiefel, H. (2004a). Measuring the operating state of the hydrocyclone. *Minerals Engineering, 17(5)*, 697-703.

Neesse, T., Schneider, M., Dueck, J., Golyk, V., Buntenbach, S., Tiefel, H. (2004b). Hydrocyclone operation at the transition point rope/spray discharge. *Minerals Engineering, 17,* 733–737.

Petersen, K.R.P., Aldrich, C., Van Deventer, J.S.J., McInnes, C. and Stange, W.W. (1996). Hydrocyclone underflow monitoring using image processing methods. *Minerals Engineering, 9(3)*, 301-315.

Schlaberg, H.I., Podd, F.J.W. and Hoyle, B.S. (2000). Ultrasound process tomography system for hydrocyclones. *Ultrasonics, 38(1-8)*, 813-816.

Van Deventer, J.S.J., Feng, D., Petersen, K.R.P. and Aldrich, C. (2003). Modelling of hydrocyclone performance based on spray profile analysis. *International Journal of Mineral Processing 70, 183–203.*

Van Vuuren, M.J. Janse, Aldrich, C. and Auret, L. (2011). Detecting changes in the operational states of

hydrocyclones. *Minerals Engineering 24*, 1532–1544.

Viljoen, T. (1993). Recent developments in instrumentation. SAIMM School: Process Simulation, Control and Optimisation. The South African Institute of Mining and Metallurgy, Randburg, 18 – 20 August.

West, R., Jia, X. and Williams, R.A. (2000). Parametric modelling in industrial process tomography. *Chemical Engineering Journal, 77(1-2)*, 31-36.

Williams, R.A., Dickin, F.J., Gutierrez, J.A., Dyakowski, T. and Beck, M.S. (1997). Using electrical impedance tomography for controlling hydrocyclone underflow discharge. *Control Engineering Practice, 5(2)*, 253-256.

Williams, R.A., Jia, X., West, R.M., Wang, M., Cullivan, J.C., Bond, J., Faulks, I., Dyakowski, T., Wang, S.J., Climpson, N., Kostuch, J.A. and Payton, D. (1999). Industrial monitoring of hydrocyclone operation using electrical resistance tomography. *Minerals Engineering, 12(10)*, 1245-1252.

PRACTICAL IMPROVEMENTS TO A RING BLASTING TECHNIQUE IN A TRANSVERSE SUBLEVEL STOPING SCENARIO

*L. A. Bündrich[1] and J. C. Koppe[1]

UFRGS[1].
Av. Bento Gonçalves, 9500, setor 4, prédio 75, sala 102
CEP 91509-900 Porto Alegre, RS, Brazil.
*(*Corresponding author: lbundrich@orosur.ca)*

24th World Mining Congress
MINING IN A WORLD OF INNOVATION
October 18-21, 2016 • Rio de Janeiro /RJ • Brazil

PRACTICAL IMPROVEMENTS TO A RING BLASTING TECHNIQUE IN A TRANSVERSE SUBLEVEL STOPING SCENARIO

ABSTRACT

One of the most complex processes concerning underground mining is the blasting of rocks using rings of drilling holes in radial pattern. This technique makes possible to cover a large area, radiating the drill holes from small accesses, maximizing the range of the drilling and minimizing the necessity of creating accesses, which is a costly part of the production in underground operations. In other words, ring drillings generate an increase of the specific drilling, and present itself as a challenging task that requires extensive planning and carefully execution in order to guarantee the effectiveness of the technique. For this reason, it is essential to establish procedures that improve the efficiency of this type of operation in underground mine activities, so it becomes possible to reduce costs and increase the security of related activities. In this context, this paper aims to present methods to improve the processes involved with rock blasting applied to the underground method of Transverse Stopes, in Arenal Deeps mine, where the tests were conducted. The presented methodology could be separated in four parts: first, the implementation of mass blasting concept, in order to accelerate the production cycle and enhance the security of the charging crew; second, the test of different arranges of delays to determine the one that generates the minimum vibration effect; third, the change on the drilling pattern to avoid the roof overbrake in the stopes; and the last and fourth, the test of a new blasting pattern based on the theory of Timothy Hagan. To evaluate the results of those proposals, operational data, seismograph monitoring and Cavity Monitoring Systems (CMS) scanners were used, as well as modeling software, which permits the visualization and manipulation of digital three dimensional models. The implementation of the mass blasting method reduces the number of interventions on stopes from an average of 16 to 5, increasing the productive rate in 20%. The tests of delays performed on the stope TS_N157_E0, reveals that a slower sequence with a ratio between inter-hole delays and inter-row delays of approximately 4 was the less harmful in terms of total vibration. The changes in drilling pattern have successfully reduced the roof overbrake in stopes, saving the cable-bolts, as shown by CMS scanners. The new drilling patterns, based on Hagan's theory, have worse results in real recuperation of stope in comparison with the historical recuperation of the Transverse Stopes. The results show that significantly better outcomes could be achieved in production rate and safety by reducing vibration levels and reducing the roof overbreak in stopes if following the proposed method.

KEY WORDS

Ring Drilling, Mass blasting, Delays, Overbreak, Drilling pattern.

INTRODUCTION

One of the most complex processes concerning underground mining is the blasting of rocks using rings of drilling holes in radial pattern. This technique makes possible to cover a large area, radiating the drill holes from small accesses, maximizing the range of the drilling and minimizing the necessity of creating accesses, which is a costly part of the production in underground operations. In other words, ring drillings generate an increase of the specific drilling, and present itself as a challenging task that requires extensive planning and carefully execution in order to guarantee the effectiveness of the technique. For this reason, it is essential to establish procedures that improve the efficiency of this type of operation in underground mine activities, so it becomes possible to reduce costs and increase the security of related activities.

Ring drilling blasting in underground mines needs a complex planning as well as carefully execution to ensure that the technique would be effective, so it is essential to create operational procedures that could improve its results. In this context, this paper aims to present methods to improve the processes involved with rock blasting applied to the underground method of Transverse Stopes, in Arenal Deeps gold mine, Uruguay with the goal of raising the production rate, safety and stability related problems on the operation of blasting in stopes. This paper focus on four topics: implementation of mass blasting, tests with different delay patterns, overbreak control strategy to reduce the roof damage of stopes, and a test with a new drilling pattern that uses Timothy Hagan's theory (Hagan, 1988).

MINE SITE ASPECTS

Arenal Deeps mine is located in Minas de Corrales, a town at the district of Rivera, in the north portion of Uruguay, approximately 460 km from the country's capital, Montevideo, and 70 km from the Brazil´s border (Figure 1).

Figure 1: Uruguay map showing the location of the Arenal Deeps mine, (Image from prefeasibility study, AMEC, Loryser S.A., 2010)

Geology

The local geology is composed of Proterozoic basement rocks of the Nico Perrez Terrane that are exposed through an erosional window into overlying Paleozoic sediments forming a 110 km long by 20-40 km wide belt called the Isla Cristalina (De Quadros & Koppe,1996). The Arenal deposit is hosted within basement gneissic rocks metamorphosed to amphibolites faces. The gold mineralization was deposited along a moderately south-dipping, east-striking shear zone the highest gold grades are inferred to be controlled by late-stage fracturing, normally the mineralization forms discrete zones (lodes) characterized by silica–sericite–carbonate–pyrite alteration and broader areas of silica–pyrite stockwork veining (Barber, Taylor, Huether, Frost, Coulson & Hertel, 2010).

Mining method

Arenal Deeps mine operated as an open pit from 2004 until 2009, when the development of an underground mine took place and two methods were used to mine the deposit - Inclined Room and Pillar end Transverse Sublevel Stoping, being the last one the focus of this paper.

METHODOLOGY

Mass Blasting

As the Sublevel Stoping is a mass mining method it is essential to practice mass blasting in order to accelerate the rate of production (Haycock & Aelick,1992). Expectations are the implementation of the mass blasting principle to elevate the mining operation to a higher level of quality, but it is important to notice that it requires careful engineering, especially on drilling and blasting, as well as production planning. Also, the design must executed precisely by the production

crew.

In this context, it is important to understand that in order to blast any volume of rock in a confined surrounding, it is recommended to have at least 30% of free space for the expansion of the original volume of the solid and achieve good fragmentation (Sen 1995). Even if this is presented as a limitation to the rock volume that could be blasted from time to time, stopes can be totally blasted in a single event if the necessary volume is respected, which is called one-Shot stopes (Liu, 2013).

The advantages and disadvantages of the mass blasting is presented by Guilfoyle & Bradford (1982 Apud Villaescussa , 2014) :

- The blasting crew is safer when the re-entry number of times into a blasted area is reduced.
- Improved rock fragmentation results from the shearing action of interacting detonation charges and in-flight rock collisions.
- Because fewer individual firings are required, the problem of post blast falloff is reduced.
- Fewer individual blasts are likely to minimize damage to services and other scheduled activities around the stopes.
- The large broken ore tonnages from mass blasts allow uninterrupted production at high extraction rates from the stope drawpoints.

The disadvantages of the mass blasting could possibly include the following:

- If a cut-off occurs, it may be difficult or even impossible to gain re-entry to the areas.
- Mass blast often causes large change of geometry likely to redistribute significant stress around the stope boundaries, which could cause peeling of the walls.
- Any malfunction on the initiation system or the explosive early in the firing sequence can "freeze" the entire mass firing.

1.1. Delays in ring blasting

When ring blasting has a free face with the total area of the row, it could be considered a bench blasting, and this kind of blast is normally is carried out as short period delays, but is important to design the firing pattern carefully, to ensure free breakage faces to each blast hole. The delay time between blast holes and between rows has to be long enough to create space for the blasted rock from succeeding rows (Ollofsson, 1989). The recommended delay for ring blasting is 3-15ms/m of burden and <5ms/m of spacing, when the delay time becomes too short or close to zero or when it becomes much larger than 25ms the fragmentation tend to be coarsely (Onederra & Chitombo, 2007). In ring firing, breakage can be achieved by blasting holes toward a free face in the ring burden direction, and also by providing each hole with at least one extra free face in the direction of the adjacent blast holes in the same ring. Inter-hole delays are normally kept to a minimum to optimize blast hole interaction and improve rock fragmentation. To achieve this, short period delays (MS signal tube initiation systems series) are usually used (Villaescusa, 2014).

Scattering on nominal time of the Nonel detonators could varies from 1- 4% o even more depending of the fabricant, and when the scattering are significant it could make the sequence of firing out of ordering or random (Roy & Singh,1999). For that reason ring-to-ring timing must be designed to avoid out-of-sequence firing, where holes in the second or third ring fire prior to holes in the face row closest to the void. A minimum delay time of 20ms/m of burden is recommended for ring-to-ring timing (Villaescusa, 2014).

To reduce vibration level of the blasting, is recommended to increase the time between the blast holes that contains a significant amount of explosives, the delay time should be more relaxed normally >50ms for drill holes containing more than 100kg (Liu,Tran,Fleury & Lessard, 2000).

Overbreak

There are many causes of over break: geology trends, explosive overcharge, inappropriate delay or the low ratio between the length of the drill holes and the burden. The last one causes the radical break and crack further behind the last row, generally more successful when the length-burden ratio is < 2,

due to the effect of stiffness (Konya,1995).

Drilling pattern based on Hagan's technique

The cost-effectiveness of blasts involving radiating blast holes is currently restricted in the following ways.

- Significant percentages of potential explosion energy are not being liberated; the collar sections of some charges are being dislocated and/or desensitized by the detonations of adjacent earlier-firing charges.
- If the minimum charge spacing is too small, detonation of an early firing charge can initiate an adjacent charge sympathetically.
- The overall distribution of energy is poor.

If the current drilling patterns normally used were replaced by staggered fans/rings having toe spacing/burden ratio of about 4 to 1, they would achieve appreciably better fragmentation. This wide-spaced pattern would enable a higher percentage of the potential energy to be released, would reduce the incidence of sympathetic detonation and would provide a superior overall distribution of energy. (Hagan,1988). Figure 2 explains the effect of changing the spacing-burden ratio, when the drill hole irradiates from a central point.

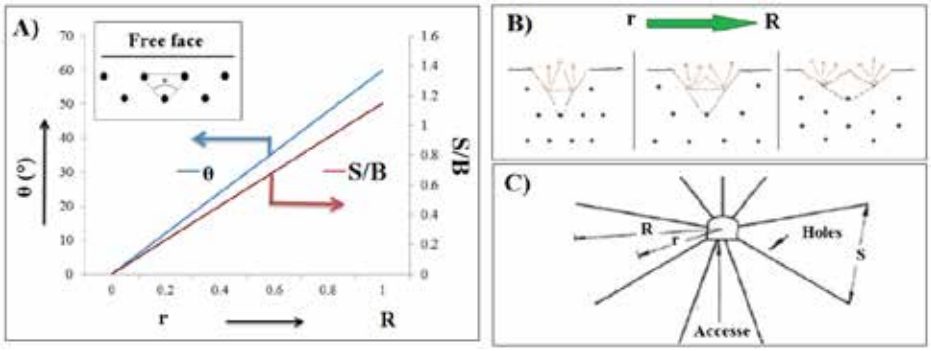

Figure 2: A) Plot of ratio changing between spacing (S) and burden (B); B) Illustration of the spacing increase in a hypothetical firing face; C) Example of ring drilling and nomenclature.

CASE STUDY

Mass blasting

For the implementation of the mass blast method, few aspects were established such as: the number of blasting in the stopes should be kept as minimum as possible; all drilling should be completed before the start of any blasting to avoid interferences between activities; the volume of blasting should not exceed 3.3 times the volume of empty space, necessary for breakage of material; and the free face must have an area larger than the rings or equal to it, which are supposed to be blasted in it. Following the assumption that a blasting needs at least 30% of its volume for its expansion, a generic sequence of blasting applicable to all stopes was created, starting from the opening of a raise that connect two development levels, then a second stage expanding the opening enough in order to generate the void necessary for the complete Slot opening. After that, the radial lines could be blasted respecting the rule of volume for expansion.

For the execution of firing pattern, the following assumptions were considered:

- Each hole was fired with a pyrotechnic nonel detonator that had a specific timing; this is called bottom delay. It was designated to the central hole the shortest timing and from there, increasing delays were designated to the subsequent holes, according to the direction of the sides.
- The holes were charged with the respective detonator series, attached to a 450g booster made of PETN plus ten cartridges (600g) of explosive emulsion as bottom charge, then completed with the main charge of ANFO.

- Each row was initiated with a 10 grams/m detonation cord, designated the timing "ZERO" of the row, and then the order of firing was controlled through bottom delays previously ordered.
- As the rows had exactly the same pattern of bottom delays, it was necessary to use inter-row delays to guarantee the planned sequence of blasting.
- The loading of explosives time should not allow ANFO charges to remain more than 12 hours on the blasting holes, in order to avoid excessive humidity.

The mass blasting concept was applied to fourteen stopes and the results of production were recorded so they could be compared.

Tests with different delay settings

To determine the best delay pattern for vibration control, three blast sequences with distinct delay patterns were performed on the stope TS_N157_E0 on May 2015. The TS_N157_E0 was a secondary stope, remaining between two pillars of cemented rock fill. For that reason, vibration control was a concern in order to avoid overbreak of the fill and consequent dilution.

Each blast had four rows which were very similar, resulting in approximately the same ore tonnage and the same explosive charges. A seismograph Model VMS-2000 was installed in a parallel access, as show in Figure 3, fixed with plaster in a rocky basement, so it was possible to compare the vibration intensity of the three blasts. The monitoring point was chosen to ensure a central position in reference to the three blasts and a regular distance around 22m. The results of vibration monitoring (Table 1) were compared to determine the differences among patterns.

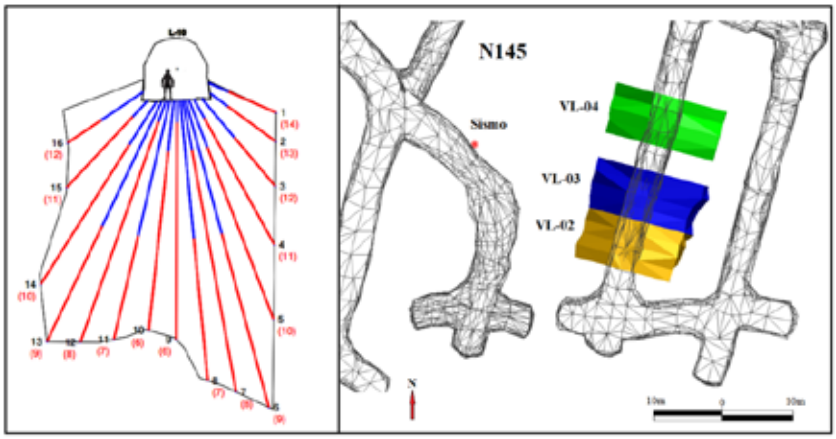

Figure 3: Example of ring drilling of the TS_N157_E0, L-10 (left) and location map of the level -145 (right), showing the three blasts and the seismograph location.

Table 1: Parameters of the three blasts, VL-02, 03 and 04

Blast	Total Explosive Charge (kg)	Mass (t)	Charge concentration (kg/m³)	Delay Hole-Hole (ms)	Delay Row-Row (ms)	Distance to sismograph (m)	Maximum instantaneous charge (MIC) (kg)
VL-02	2140	5800	1.03	25ms	67ms	22	147
VL-03	2144	6200	0.96	50-75ms	75ms	20	194
VL-04	2516	6500	1.08	50-75ms	200ms	23	123

Overbreak

So, the roof of the stopes overbreaks and the subsequent disablement of the cable-bolts could be controlled, then it was suggested a modification on the drilling pattern. The drilling was limited to the height of the access tunnel center, so all holes would have descending orientation, discarding this way the short holes close to the roof with a low length-burden ratio responsible for the rupture of the

roof (Figure 4).

It was expected that the new pattern could preserve the cable-bolts, avoiding the overbreak and preserving the tunnel shape. Afterwards, when the empty stope was filled, this level would have become the haulage level of the superior stope, so it would be important to have had a normal tunnel shape for the operation of mucking that would be performed. Starting on July 2014, the concept was applied to fourteen stopes.

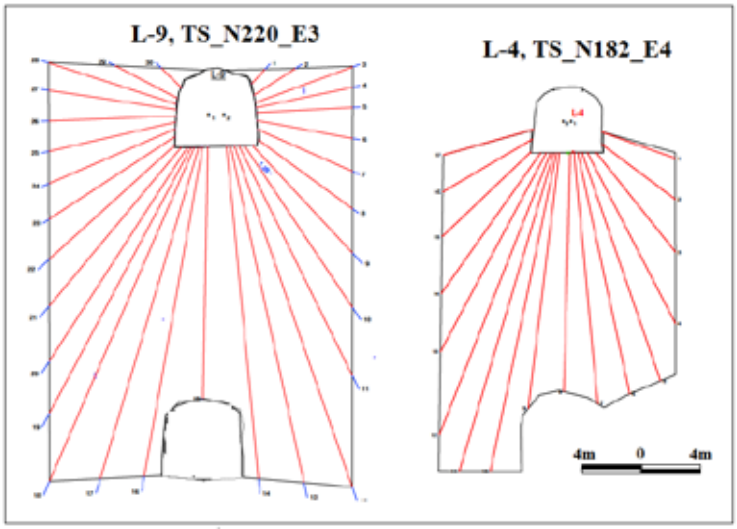

Figure 4: Example of the old ring drilling (left) and new drilling pattern excluding upper holes (right)

Drilling Patterns

Following the idea of increasing the spacing-burden ratio proposed by Hagan (1988), a test with a new pattern of drilling was performed in the stope N181-169_A1. A regular pattern of drilling used during the operation was replaced for a new one that exaggerated the spacing, as well as reduced the burden to maintain the charge-volume ratio of the respective diameter. Table 2 shows the parameters of the drilling patterns.

Table 2: Old drilling pattern parameters and its comparison to the new proposal based on Hagan's Theory

OLD PATTERN					NEW PATTERN				
Diam (mm)	B (m)	S (m)	(S/B)	Pattern	Diam (mm)	B (m)	S (m)	(S/B)	Pattern
64	1.6	1.9	1.19	Square	64	1.4	2.2	1.57	Staggered
76	1.9	2.1	1.11	Square	76	1.4	3.5	2.50	Staggered

The stope 181_169_A1 was a second class type, so it had the regular form of transverse stopes, having both ascendant and descendant drilling, as well as two different drilling diameters of 64mm and 76mm respectively. The two diameters shared the same burden, having varied the spacing. The spacing-burden ratios tested were lesser than the one proposed by Hagan, but the idea was to test the concept partially before a complete change of method.

RESULTS AND DISCUSSION

Reducing the number of interventions on stopes and increasing of production rate

Starting on May 2013, the mass blasting method successfully reduced the total number of interventions in the stope when compared to the old blasting method (Figure 5). The average of blasting tonnage increased from 2,533 to 5,810 tons per blast. During the first three months of

implementation, the production registered an increase of 20.5% when compared to the twelve months before it, which numerically is from 34,942 to 41,086 t.

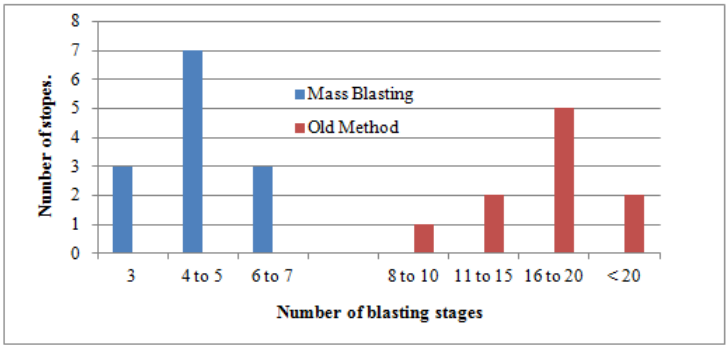

Figure 5: Plot of the total number of blasting stages on stopes after the mass blasting implementation

Seismograph monitoring

The plots of three blasts show that the VL-04 test was the less harmful in terms of vibration intensity, with a maximum peak of 63mm/s, which is not a coincidence since it was the slowest pattern of delay with 1,250 ms of total duration (Figure 6). It reduces the probability of coupling charges due to the scattering on the Nonel nominal delay; the ratio of inter-hole and inter-row delays varies between 2.7- 4 with predominance of the largest value, providing much more relief for the blasting. The same amount of explosive in a longer window of time generates minor peaks, but certainly it has a negative impact on the fragmentation once the cooperation effect between charges was almost none. On the other hand, the VL-03 registered peaks of almost 120 mm/s, because it had a mismatch between the delays of holes and rows, since their ratios were between 0.5-1.5, even with a total duration of 900 milliseconds. The VL-03 presented the largest peaks of vibration, thus vibration intensity seemed not only to depend on blasting total amount of time, but also on the settings of delays. As the ring drilling is always a clustered blast, it is essential to provide correct relief, increasing the delay between rows in relation to the inter-hole delay. The VL-02 demonstrated intermediate values of vibration with a maximum peak of 86 mm/s, and a total duration of only 550 milliseconds. The VL-02 was the fastest configuration of tested delays, but it did not present the largest values of vibration because of a constant ratio between inter-hole and inter-rows delays of approximately 2.68. It reveals that a correct match between holes and rows delays could reduce the vibration peaks, even in a short duration blast.

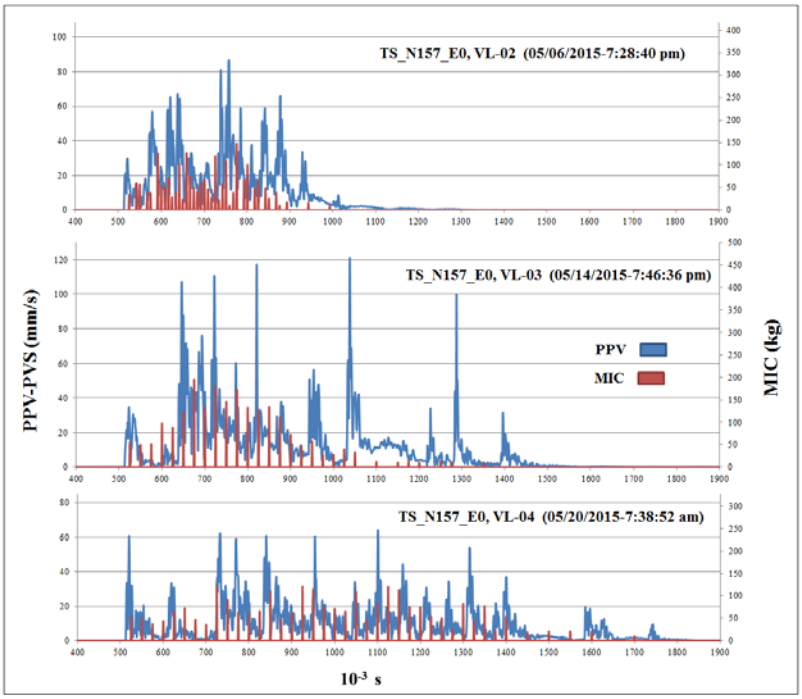

Figure 6: Seismograph register from the three blasting performed, showing the peak particle velocity as well as the maximum instantaneous charge (MIC) of each blast.

Roof overbreak and cable-bolts disablement

Optical scanning made by Cavity Monitoring System shows that the new drilling pattern preserved the gallery shape as well as it was maintained the integrity of the cable-bolts, as shown on figures 7 and 8.

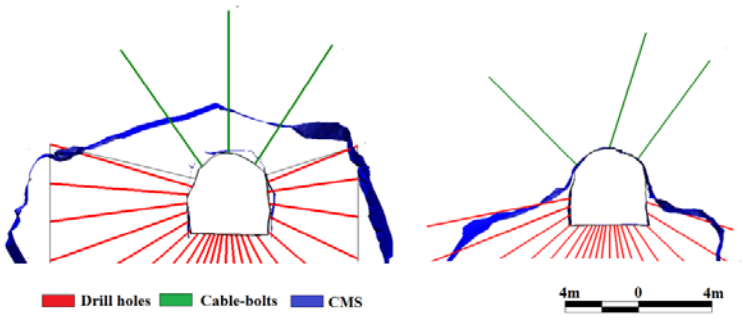

Figure 7: Comparison between CMS scanners superposed to drilling holes and cable-bolts of TS_N182_E3 example of the old pattern (left) and TS_N157_E4 (right) showing the preservation of the cable-bolts.

Figure 8: Photograph of TS_N195_E4 (left) and TS_N157_E4 (right), showing the destruction of cable-bolts and the preservation of the silhouette of the gallery respectively (both photographs are courtesy of the Engineering Department of Orosur Mining Inc.)

New drilling pattern

The new drilling pattern presented a reduction of 19% in the total necessity of drilling holes. The specific drilling value is 0.156m/t, while the expected specific drilling value under the regular pattern would be 0.194m/t. However, the results of stope total recuperation were below historical average for transverse stopes, being 76% against 85%. Such results could be explained by the irregular shape of the stope N181-169_A1, which starts in a thinner section, growing in width along the advance of blasting, meaning that the first slot did not had the total width of the final stope. For that reason, the drilling holes needed constantly enlargement of the opening, transforming the spacing in the real burden, it results in a poor recuperation of the corners since spacing was too exaggerated (Figure 9).

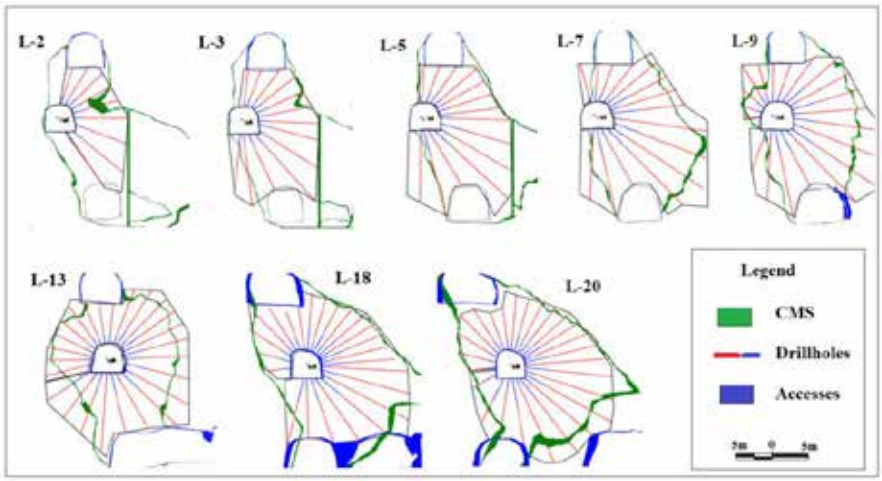

Figure 9: Stope ring drillings 181-169_A1 superposed to the CMS scanning results, showing the poor recuperation of the corners.

CONCLUSIONS AND RECOMMENDATIONS

The results of the mass blast technique as well as the change of drilling pattern near to cable-bolts showed real improvements in blasting operation, increasing production rate and resulting in a safer environment for workers. Future works could aim to reduce the limitations of void necessity for blasting, reducing even more the number of stages. The use of electronic delays could be considered as a support to extremes scenarios such the one studied here.

The tests performed with different delay settings produced valuable information concerning the behavior of blasting vibration on this kind of scenario, as well as the relation between intensity of

vibration and the total duration of the blast. Such approach clarifies the spacing-burden ratio performed and helps on designing future firing patterns, avoiding high vibration peaks. Further studies could test electronical delays in similar conditions to obtain better results by eliminating the Nonel scattering issue. The test with the new drilling pattern did not show better results than the current ones. The technique should be tested in regular stopes with an opening width equal to the final width to obtain more consistent results.

REFERENCES

Barber,J.,Taylor,B.,Huether,K.,Frost,D.Coulson,A.,Hertel,M.(2010). *Arenal Deeps Feasibility Study on Underground Operations* (Tech. Rep. to Orosur Mining Inc.) Rivera, Uruguay: AMEC E&C Services, Inc.

De Quadros ,T. F. P., & .Koppe J.C (1996). Alteração hidrotermal e mineralização do deposíto de aurifero da mina san gregorio-uruguai [Hidrotermal alteration and mineralization of a auriferous deposit of San Gregorio-Uruguay]. In: *GEOCHIMICA BRASILIENSIS, volume 10* (pp 365-377).

Hagan, T.N, (1988). Optimizing the yield and distribution of effective explosion energy in fans and rings of blast holes. In: *Explosive in Mining Workshop* (pp.59-62). Melbourne Australia: Australian Institute of minerals and mining.

Haycocks, C. & Aelick, R.C. (1992). Sublevel stoping. In: Howard L. Hartman. (2ed.,Vol. 1) *Mining engineers' handbook* (pp.1717-1728). Little ton, Colorado: Society for Mining, Metallurgy, and Exploration, Inc.

Liu, Q. (2013). Design and General Practice of mass blast in underground open stopping mining method. In: G. Joshi (Eds.) *Blasting in Mines-New Trends*, (pp. 11-20). London, UK: Taylor & Francis Group.

Liu, Q.;Tran,H.;Fleury,D.;Lessard, J.F. (2000), Evaluation of blasting damage to pastefill at Louvicort mine. In : *International society of explosives Engineers*, vol. 1, 333.

Konya,C.J.(1995). *Blast desing*, Monteville, OH, USA: Interncontinental develpoment corporation (p 153).

Oloffson, S.O. (1988). *Applied explosives technology for construction and mining*, (2ed.), Ärla, Swede: Applex.

Onederra, I. & Chitombo, G., (2007). Design methodology for underground ring blasting. In: *Mining technology*, vol.116, No 4, 180-189. doi:10.1179/174328607X282244

Roy, P.R. & Singh,T.N.(1999). Effect of delay scattering on blasting performance. In: *Procedings*, 25th Annual conference on explosive & Blasting technique (pp.1-18), Nashville,TN, USA.

Sen, G.C. (1995). *Blasting Technology for Mining and Civil Engineers*,Sidney, Australia: University Of South Wales.

Villaescusa, E. (2014). Drilling and Blasting.In a CRC Press (Eds.). In: *Geotechnical Design for Sublevel Open Stoping.* (pp 245-313).Boca Raton, FL, USA: Taylor & Francis.

.

PRE-CONCENTRATION OF SILICATE ZINC ORE USING DENSITY AND MAGNETIC CONCENTRATIONS

*D. José Neto[1] and M.G. Bergerman[1], A.D. Souza[2] and E.L.C. Martins[2] and V.Metsavaht[2] and J.L.C. Bechir[2] and L.M.C. Lopes[2] and M.M. Lopes[2] and C.J. Freitas Neto[2] and J.M.C. Melo[2] and C.A.M. Oliveira[2] and L.M. Resende[2]

[1]Mining Engineering Department of São PauloUniversity
2373 Prof. Mello Moraes Avenue
São Paulo - SP, Brazil 05508-030
*(*Corresponding author: dimasnetosri@gmail.com)*

[2]Votorantim Metais S/A
Km 65 LMG 706 Highway
Vazante – MG. Brazil 38780-000

24th World Mining Congress
MINING IN A WORLD OF INNOVATION
October 18-21, 2016 • Rio de Janeiro /RJ • Brazil

PRE-CONCENTRATION OF SILICATE ZINC ORE USING DENSITY AND MAGNETIC CONCENTRATIONS

ABSTRACT

The pre-concentration consists on the previous discard of a fraction of the mineral processing plant feed with few or none quantity of the mineral of interest, reducing the mass to be processed in the downstream operations, as well the capital and operational costs. In this context, this study aims to verify the susceptibility of the silicate zinc ore from Votorantim Metais, Vazante/MG (Brazil), for pre-concentration by density and magnetic methods. For this purpose, tests have been developed in a magnetic roll separator operating under high field (10,000 gauss) and also on sink/float in dense liquids varying between 2.75 to 2.95 g/cm³ and in coarse particle size: + 6,35, - 6,35 + 3,35 e -3,35 + 1,18 mm. The former results show the possibility to discard more than 50% of the plant mass and zinc metallurgical recoveries above 90%. It also shows that the discard of contaminants, as MgO, can achieve 80%. The results for the magnetic separation have not been meaningful in comparison with the density separation.

KEYWORDS

Pre-concentration, Zinc, Density Separation, Magnetic Separation

INTRODUCTION

According Harkki (2014) the main challenges of modern concentration plants are related to:

i. Processing ores with increasingly lower grade, that exhibit complex mineralogical associations and degree of liberation into the finer particles, which require more elaborate comminution operations and various stages of concentration, increasing installation costs and operation of the plant (Bergerman, José Neto, Tomaselli, Maciel, Del Roveri, & Navarro, 2014).

ii. Management and disposal of processing tailings. Low grade ores generate large amounts of tailings, which are usually stored in containment dams, which are subject to the risk of rupture and have high capital and operating costs (Girodo, 2007).

iii. Shortage and water management. Water scarcity, the necessity to accomplish the legal requirements and the cost of payment for the use of water, will influence directly in mineral production. So wherever possible, the water used in the process, must be recycled and reduced, aiding to reduce "new water" consumption and funding costs (Andrade, Sampaio, Luz, Andrade, Santos, & Grandchamp, 2006).

iv. Energy efficiency. According to Lessard, Bakker and Mchugh (2014), the size reduction operations are the stages of higher energy consumption. For low grade ores and high dilution, most of the required energy is consumed in the grinding of material without economic value, which makes the comminution inefficient and with high operating cost.

An alternative currently used to prevent or minimize the problems already mentioned is to use pre-concentration of the ore before the costly stages, more specifically in grinding. Thus, there is a previous discard of a fraction of the liberated or partially liberated gangue with little or any quantity of metal of interest, reducing the mass to be fed in the mill and in the subsequent operations. This brings a range of benefits to the mine and plant, as reported in Table 1.

Table 1 - Benefits of pre-concentration. Not all of these benefits are occurring simultaneously and depend on the specific application (Source: Adapted from Bergerman *et al*., 2014; Cresswell, 2001; Grigg & Delemontex, 2015)

Benefits	Cause
Reducing energy consumption per ton of metal produced	With the removal of gangue, it reduces the mass fed into the mill, not spending energy grinding material that is not of interest, thus reducing the required power. Further, usually higher WI material is discard, which decreases the specific consumption of the grinding circuit.
Increasing tailing dam life	A smaller volume of gangue is processed; therefore the amount of tailing generated to be disposed in the dam is lower.
Reusing waste	As the waste of the pre-concentration is coarse and easily dewatered, it can be used for paving roads, as loan material (dump), filling galleries (backfill) and depending on their characteristics, it can be sold as by-product generating profits.
Reducing water consumption	There is less mass to be treated.
Increasing mine life	Rejecting part of the gangue, the mine cut-off grade decreases, which allows the exploitation of marginal ores and as a consequence there is the expansion of the reserves.
Positive impact on flotation	Pre-concentration eliminates fluctuations in the grade of the flotation feed throughput. The consumption of reagent is susceptible of being optimized, and the circuit can be simplified with possible cleaner and/or scavenger cells reduction.
Positive impact on the thickening	Reduction of the thickening unit capacity demand and consumption of flocculant, particularly in the tailings, which has been reduced.
Increase the production	The feed throughput of the plant is lower, but offer better grade. Thus, it is possible to produce the same amount of metal at lower feed rates, getting margin for the increase in production without requiring expansion of the capacity of the plant installed.

Based to the this premise, it is possible add some of the various existing mineral processing techniques, before the conventional concentrator, as a standard of good practices to improve the quality of feed at the beginning of the treatment plant. The main techniques used are gravimetric methods (dense medium cyclones, drum separator, conic separator, traditional jigs and pressure jigs), ore sorting, magnetic separation (drum separator) and coarse screening. It even may be done after preferential blasting in mining (Grigg & Delemontex, 2015).

The pre-concentration has been applied in precious metal, uranium and suphides mines worldwide. In Brazil, this practice is incipient but there are several current studies and industrially, just the Maracas Vanadium S/A uses a magnetic pre-concentration, with drum separators in order to separate the magnetite-pyroxenite from the silicate gangue. The process achieves a mass recovery of 68% to 81% vanadium and a reduction of 50% of silicate gangue (Costa, 2014).

Others examples of industrial applications for pre-concentration are shown in Table 2.

Table 2 - Industrial applications of pre-concentration and process performance

Pre-concentration method	Ore type	Mine Localization	Feed size (mm)	Mass rejected (%)	Metal recovery (%)	Reference
DMS cyclone	Ni sulphide	Phoenix/Bostwana	25 ~ 1	60	85	Morgan, 2009
Coarse screening after preferential blasting	Au e Cu sulphide	Telfer/Australia	- 20	60	> 80 (both Au e Cu)	CRC ore, 2016
Pressure jig	Polymetallic (Ag, Zn, Pb)	Pirquitas/Argentina	12 ~ 2	50	80 ~ 90	Grigg and Delemontex, 2015
Ore sorting	Wolframite pipes in quartz	Wolfram Camp/ Australia	100 ~ 15	90 ~ 95	80 ~ 85	Lessard, Bakker and Mchugh, 2014
Magnetic separator	Ni associated with pyrrhotite	Whistle/Canada	5 ~ 2,5	38	80	Vatcha, Cochrane and Rousell, 2000

Motivated by the benefits of discard of the still coarse gangue, Votorantim Metais S/A, Vazante/MG unity, has been developing a series of studies to evaluate the applicability of pre-concentration to its operations. This work is part of such studies and aimed to verify the susceptibility of silicate zinc ore the pre-concentration using density and magnetic techniques.

METHODOLOGY

Three representative samples of Zn ore from Votorantim operations were studied:

- Usicon W: with high Zn content (18.24%);
- Usicon C: low Zn content (5.76%);
- *Extremo Norte*: with high content of Zn (20.77%) and low Fe content (2.42%).

The samples were colected at the primary crusher feed of Votorantim Metais in Vazante, and were sent to the Mineral Processing Laboratory in São Paulo University, where they were comminuted on roll crusher until all the material was passing in an aperture size of 12.7 mm. Then the samples were homogenized and sub-samples of approximately 1 kg wore taken for granulometric analysis by dry sieving using aperture size of 9.5 mm, 6.35 mm, 4.75 mm, 3.35 mm, 2.36 mm, 1.68 mm, 1.18 mm and 0.85 mm. Products obtained in the sieving were quartering and sent for chemical analysis. The remaining samples were separeted into aliquots of approximately 10 kg, reserved for the next steps.

For the test sink and float in heave liquids, 1 kg of material was prepared in each of the following fractions size: + 6.35 mm, - 6.35 + 3.35 mm and - 3.35 + 1.18 mm, for the three samples tested. The fine fraction, below 1.18 mm, was discarded for being too thin to density separations methods with technologies planned for industrial use.

Each fraction described above was separated in three different densities. The densities adopted (Table 3) were chosen based on the specific weight of main minerals present in the samples, willemite ($\rho = 3.9 \sim 4.2$ g/cm³), dolomite ($\rho = 2.85$ g/cm³) and hematite ($\rho = 4.9 \sim 5.3$ g cm³).

Table 3 - Densities for the laboratory tests and correspondent dense medium used

Density (g/cm³)	Dense medium
2,75	Tribromoethane ($CHBr_3$) diluted with alcohol
2,85	Tribromoethane slightly diluted with alcohol
2,94	Tetrabromoethane pure ($CHBr_2CHBr_2$)

The procedures of the tests as well as the safety procedures taken during the tests are detailed in texts of Sampaio and Tavares (2005); Chaves and Chaves Filho (2013).

The medium density, when diluted, was systematically checked before each test, with the aid of volumetric flask and scale.

Figures 1 and 2 illustrates the procedures of the tests. It is important to note that as the floated in 2.85g/cm³ produced low mass for the fractions of the sample *Extremo Norte*, it was decided to take this density as the smallest and adopted 2.9 g/cm³ as intermediate (Figure 2).

For the magnetic separation, 10 kg of each sample were processed by the magnetic separator drum (model: RE – 5/04-1 of Inbrás). A field of 10,000 gauss and a drum rotation of 80.8 rpm was used. The particle size of the test feed was - 12.7 mm for the three samples.

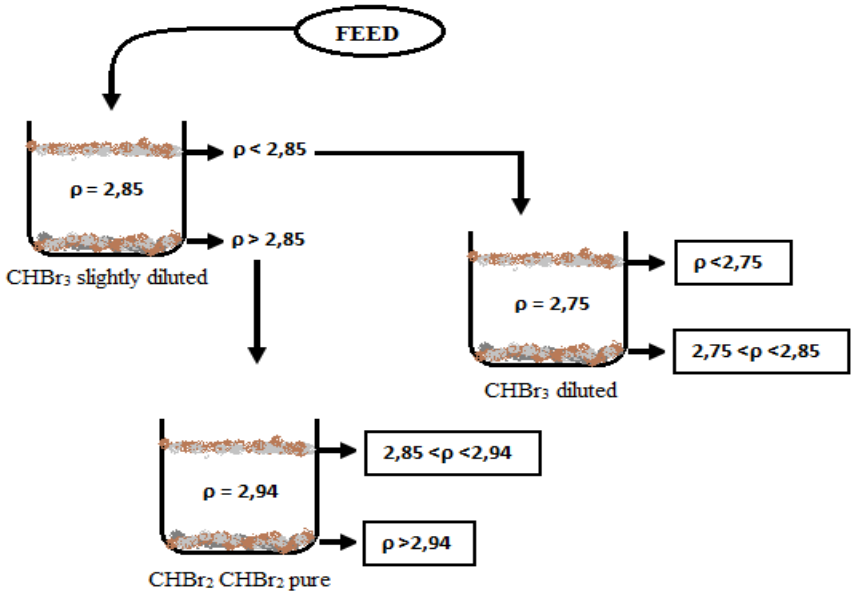

Figure 1 – Procedure for the sink/float test for Usicon W and Usicon C samples

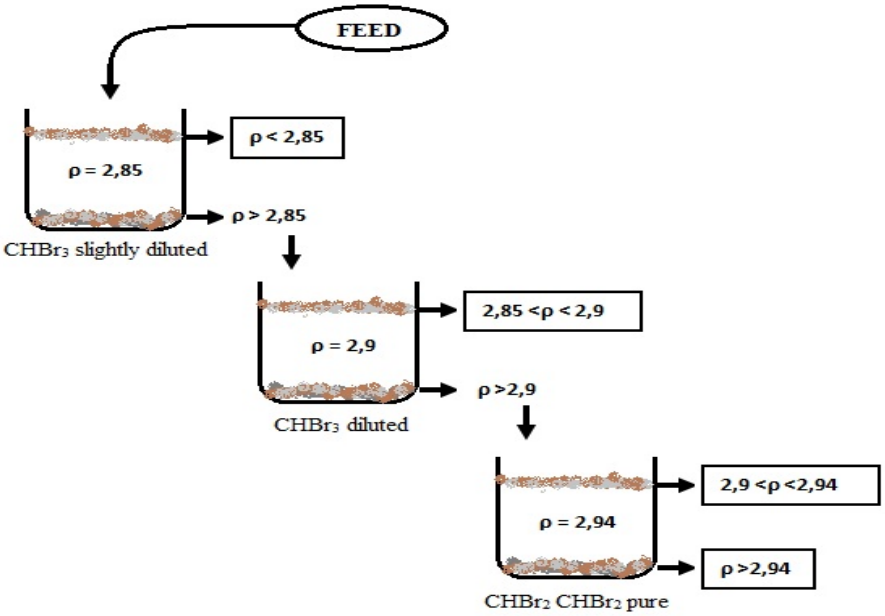

Figure 2 - Procedure for the sink/float test for the *Extremo Norte* sample

RESULTS AND DISCUSSION

The data by chemical analysis shows that the Zn and MgO, the main contaminant, are distributed quite homogeneously in all size fractions, and have proportional distributions to the mass of each fraction. This size behavior was observed for the three samples.

The results of the tests sink/float point to the density 2.94 g/cm³ as more promising for the three samples, as provided sink products with excellent recovery of Zn associated with the lowest MgO recoveries.

Figures 3, 4 and 5 shows the results for the samples Usicon W (- 6.35 + 3.35 mm) Usicon C (+ 6.35mm) and *Extremo Norte* (+ 6.35 mm) respectively. Although other size fractions test also presented excellent separation performance, the fractions that stood out in terms of compromise between better recovery of Zn and lower MgO recovery selected.

The curves mass sinking and floating should be read in the main axis and Zn and MgO curves should be read in axis recovery.

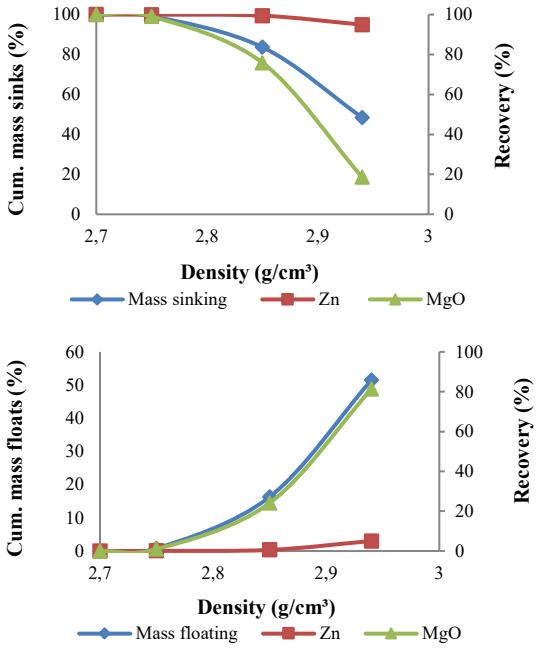

Figure 3 – Separability curves in the sink/float test, sample Usicon W (- 6.35 + 3.35 mm)

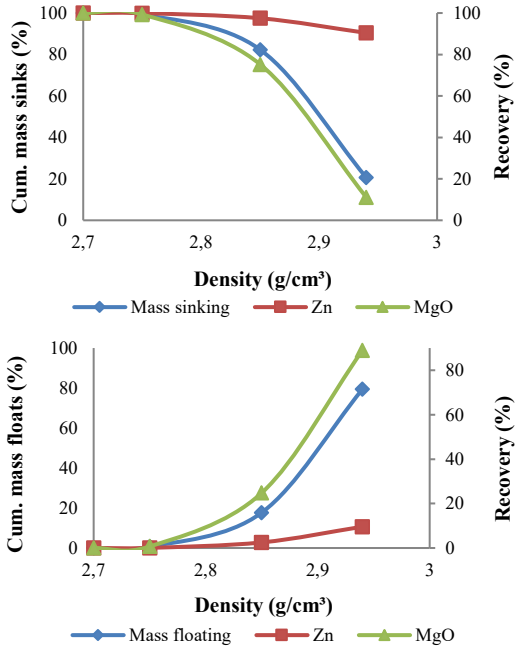

Figure 4 – Separability curves in the sink/float test, sample Usicon C (+ 6.35 mm)

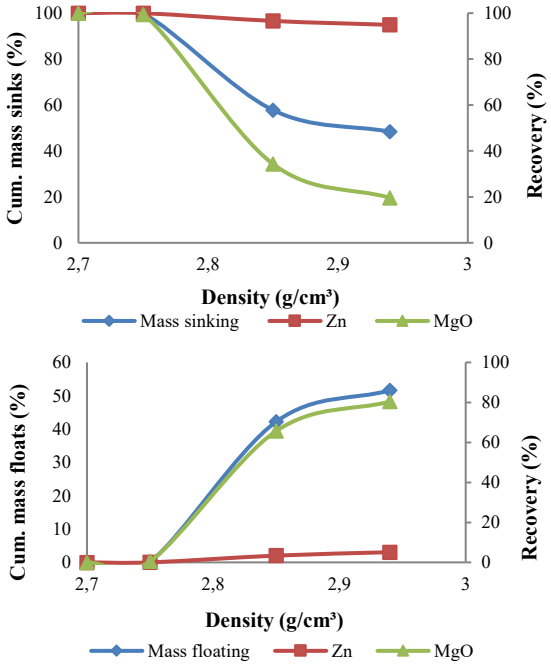

Figure 5 – Separability curves in the sink/float test, sample *Extremo Norte* (+ 6.35 mm)

For Usicon W samples (-6.35 +3.35 mm) and *Extremo Norte* (+6.35 mm), the results indicated the possibility of disposal of approximately 50% of the mass in the floated 2.94 g/cm³, containing nearly 80% of MgO, with only 5% of Zn. Related to the Usicon C sample (+6.35 mm) is possible discard almost 80% of the mass of the float same density, with more than 80% of the MgO. In sink products in the three samples were observed Zn recovery around 90%. This suggests that adoption of a dense mean separation stage becomes technically satisfactory in order to reduce the amount of dolomite feeding rate of the plant. However, tests on a pilot scale and economic viability analysis must be performed to verify the feasibility of a possible industrial installation.

The results of magnetic separation can be seen in Table 4. Note that there were no enrichment of Zn, neither MgO reject as significant as obtained in the dense medium separation.

Table 4 - Results of magnetic separation

Usicon W										
Produto	Massa (g)	Massa (%)	Teores (%)				Distribuição (%)			
			Zn	Fe	Pb	MgO	Zn	Fe	Pb	MgO
Magnético	2.360,00	21,26	16,49	17,59	0,33	4,29	17,43	60,90	8,58	15,74
Não magnético	8.740,00	78,74	21,09	3,05	0,95	6,20	82,57	39,10	91,42	84,26
Alim. Calculada	11.100,00	100,00	20,11	6,14	0,82	5,79	100,00	100,00	100,00	100,00

Table 4 - Results of magnetic separation (continued)

Usicon C										
Produto	Massa (g)	Massa (%)	Teores (%)				Distribuição (%)			
			Zn	Fe	Pb	MgO	Zn	Fe	Pb	MgO
Magnético	1.960,00	17,35	15,93	11,58	0,19	4,99	63,76	62,95	19,00	14,45
Não magnético	9.340,00	82,65	1,90	1,43	0,17	6,20	36,24	37,05	81,00	85,55
Alim. Calculada	11.300,00	100,00	4,33	3,19	0,17	5,99	100,00	100,00	100,00	100,00
Extremo Norte										
Produto	Massa (g)	Massa (%)	Teores (%)				Distribuição (%)			
			Zn	Fe	Pb	MgO	Zn	Fe	Pb	MgO
Magnético	580,00	5,24	17,26	15,95	0,23	4,05	4,55	33,92	4,50	2,94
Não magnético	10.480,00	94,76	20,04	1,72	0,27	7,40	95,45	66,08	95,50	97,06
Alim. Calculada	11.060,00	100,00	19,89	2,47	0,27	7,22	100,00	100,00	100,00	100,00

CONCLUSIONS

- In all the samples studied, we obtained a significant disposal of dolomitic gangue in the float (about 50% in the samples Usicon W and *Extremo Norte* and almost 80% in Usicon C) with Zn recoveries on the order of 90% in sink.
- The best density cut obtained was 2.94 g/cm³.
- The magnetic separation was not efficient in terms of Zn/MgO coarse separation.
- The application of a separation step in dense mean is technically satisfactory. However, tests on a pilot scale and economic viability analysis must be performed to verify the feasibility of the industrial plant.

ACKNOWLEDGMENTS

The authors thank Votorantim Metais for permission to publish this paper and the Mining Engineering Department of Mining Engineering of São Paulo University by ceded the infrastructure for the tests.

REFERENCES

Andrade, M. C., Sampaio, J. A., Luz, A. B., Andrade, V. L. L., Santos, M. L. P., & Grandchamp, C. A. P. (2006). A mineração e o uso da água na lavra e no beneficiamento de minério. In A. F. Domingues, P. H. G. Boson, & S. A. Alípaz (Eds.), *A gestão dos recursos hídricos e a mineração* (pp. 91 – 122). Brasilia, Brazil: ANA.

Bergerman, M. G., José Neto, D., Tomaselli, B. Y., Maciel, B. F., Del Roveri, C., & Navarro, F. C. (2014). Redução do consumo de energia de circuitos de moagem com a utilização de pré-concentração de minerais sulfetados. *Holos*. vol. 3, 176 – 183. doi: http://dx.doi.org/10.15628/holos.2014.1798

Chaves, A. P., & Chaves Filho, R. C. (2013). Teoria e prática do tratamento de minérios: separação densitária. São Paulo, Brazil: Oficina de textos.

Costa, I. A. (2014). *Pré-concentração magnética do magnetita-piroxenito da Vanádio de Maracás S/A* (Monograph). Federal University of Bahia, Salvador, BA, Brazil.

CRC ORE (2016). Optimising resource extraction: coarse liberation circuits. Retrieved on Abril 05, 2016, from http://www.crcore.org.au/main/index.php/case-studies-03/225-coarse-liberation-circuits

Creswell, G. M. (2001). Pre-concentration of base metal ores by dense medium separation. Proceedings of the SAIMM cooper, cobalt, nickel and zinc recovery conference (pp. 1- 10). Joanesburgo: SAIMM

Girodo, A. C. (2007). Manuseio dos materiais. In G. E. S. Valadão, & A. C. Araujo (Eds.), *Introdução ao tratamento de minérios.* (pp. 163 – 178). Belo Horizonte, Brazil: Editora UFMG.

Grigg, N. J., & Delemontex, G. J. (2015). The pre-concentration of precious and base metal deposits using the inline pressure jig (IPJ); higher feed grades and more metal. Retrieved on October 25, 2015, from http://www.ceecthefuture.org/wp-content/uploads/2015/06/IMPC-2014-Pre-concentration-Paper-Revision-CEEC-150825.pdf

Härkki, K. (2014). Overcoming sustainanability challenges of future concentrator plants. In J. Yanatos, A. Doll, C. Gomez, & R. Kuyvenhoven (Eds.), XXVII International Mineral Processing Congress (pp. 2 – 22). Santiago: Gecamin.

Lessard, J., Bakker, J., & Mchugh, L. (2014). Development of ore sorting and its impact on mineral processing economics. *Minerals Engineering*. v. 65. p 88–97. http://dx.doi.org/10.1016/j.mineng.2014.05.0
19

Morgan, P. (2009). The impact of a crushing plant upgrade and DMS pre-concentration on the processing capability of the Tati Nickel Concentrator. In: *Base Metals Conference*, 2009, Kasane. Joanesburgo: SAIMM. pp. 231-244.

Sampaio, C. H., Tavares, L. M. M. (2005). Beneficiamento gravimétrico: uma introdução aos processos de concentração mineral e reciclagem de materiais por densidade. Porto Alegre, Brazil: Editora da UFRGS.

Vatcha, M. T., Cochrane, L. B., & Rousell, D. H. (2000). Pre-concentration by magnetic sorting of Ni - Cu ore at Whistle mine, Sudbury, Canada. *The Institution of Mining and Metallurgy*. Retrieved on October 20, 2015, from http://www.maneyonline.com/doi/abs/10.1179/mpm.2000.109.3.156

QUALITY IMPROVEMENT OF AN IRON ORE JASPER BY SELECTIVE MILLING

*E.L. Souza[1]. O.B. Reis[2]. L.C. Borges[2]. D.F. Pereira[3]

[1]DTECH / CAP / UFSJ
Rod.: MG 443. KM 7
Ouro Branco. MG. Brazil
*(*Corresponding author: souza.erivelto@ufsj.edu.br)*

[2]IFMG – OP
Rua Pandiá Calógeras. 898 – Bauxita
Ouro Preto. MG. Brazil

[3]QTEC
Av. Intendente Câmara. 166
Ouro Branco. MG. Brazil

24th World Mining Congress
MINING IN A WORLD OF INNOVATION
October 18-21, 2016 • Rio de Janeiro /RJ • Brazil

QUALITY IMPROVEMENT OF AN IRON ORE JASPER BY SELECTIVE MILLING

ABSTRACT

One of the most important factors during the process of comminution of minerals is their power consumption rate, which is determined by calculating the WI (work index), which in short is to analyze the amount of kWh consumed per ton of material, to reach a certain particle size and achieve the desired. Along with the quality of the ore is defined and use the classification of the ore. Ores of jaspelíticos type, high hardness, and with lower iron content 60% with silica content above 10.5%, tends to be considered economically unsuitable for merger cases in the Brazilian market. The work presented here consists of a technique that acts by transforming this type of ore at an acceptable quality product and with a lower power consumption than the previously calculated by WI analysis. The procedure presented here recovers a quantity of more than 75% by weight, taking an ore 56% Fe, for an average content of 65% SiO_2 and lowering the 10% to 4.5%. Although reducing by 50% the amount of phosphorus present. The procedure presented here using known methods, but with a variation with respect to the operation, which gives you innovative character, acting together with a selective screening.

KEYWORDS

Selective Milling, Jasper Ore, Quality Improvement

INTRODUCTION

Iron ore coming from Corumbá, Brazilian middle west region, are presented in various ways, lump, medium grained and jaspelitos. The latter, even with a significant iron content, present in coarse particle size and silica layer interleaved and some cases even higher iron content with "pockets" (or Jaspers) silica. The presence of intercalated material and the size of the material leads to the need for treatment for mechanical processing of this ore.

The material studied initially presented a WI curve leading to an average of 18 kWh/t of processed material. At levels ranging from 64% to 48% of Fe, with the silica ranging from 7.5% to 12.5%, and phosphorus often in the range around 0.16%. The grinding has become a problem because the fines generated were high and with great loss of metal content. This led to the study that resulted in the work presented here.

MATERIALS

The material used was the jasper ore with low iron content. The prevailing geology in the region of the city of Corumbá, Mato Grosso do Sul, Brazil, can be seen in the figure 1.

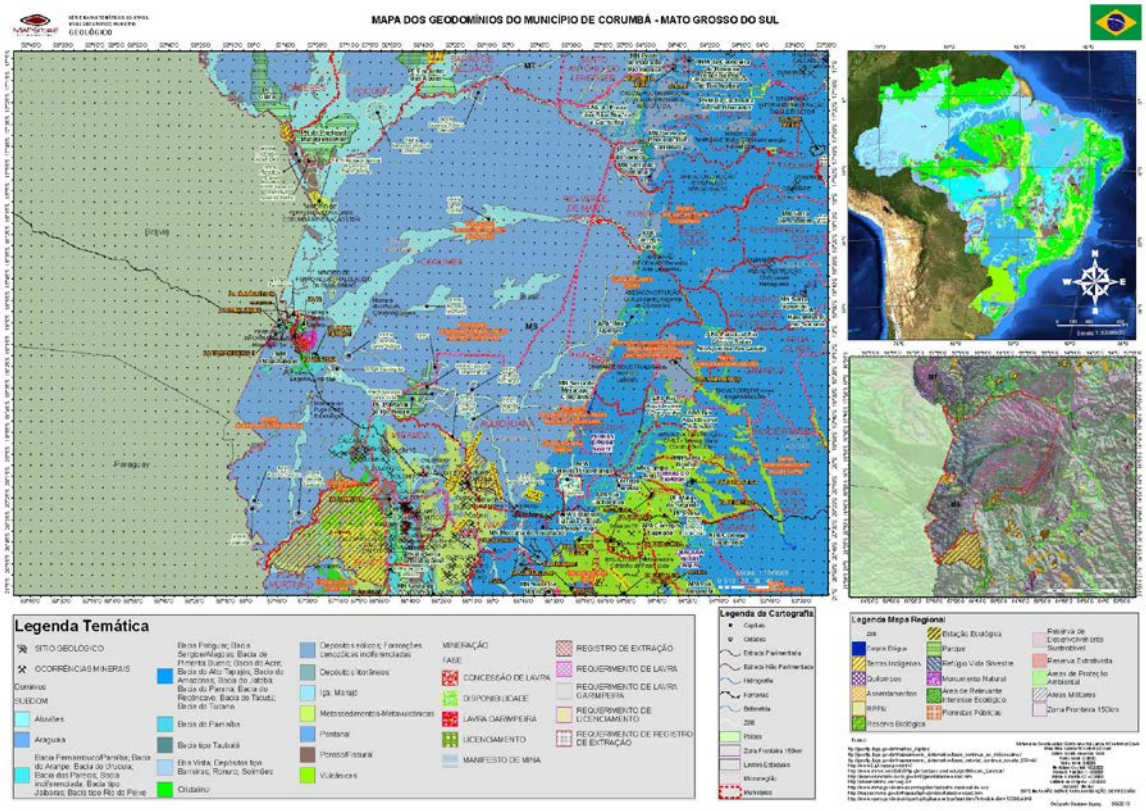

Figure 1 – Map of geological domains of the city of Corumbá, MS, Brazil. [7]

Figure 2 – Samples in the jasper used in the tests. [1]

Figure 3 – Detail of interleaved layers of silica and iron ore in jasper, contaminated by P. [1]

The analyzed ore found in this region has a low iron content compared with the equivalent most used iron ores. Even when its content reaches range considered applicable to economic viability, the hardness and high Work Index makes it initially impractical to use for processing the concentration of the metallic content. The figures 2 and 3 shows this ores and table 1 illustrates the average analysis of the studied ore.

Table 1 – Table showing the initial composition of the tested material. [1]

W.I.	Fe	SiO_2	Al_2O_3	P	Mn	Limonite	Density	Humidity	L.F.
17.75	48.40%	11.27%	2.59%	0.184%	0.010%	2.16%	2.15	3.8%	3.3%

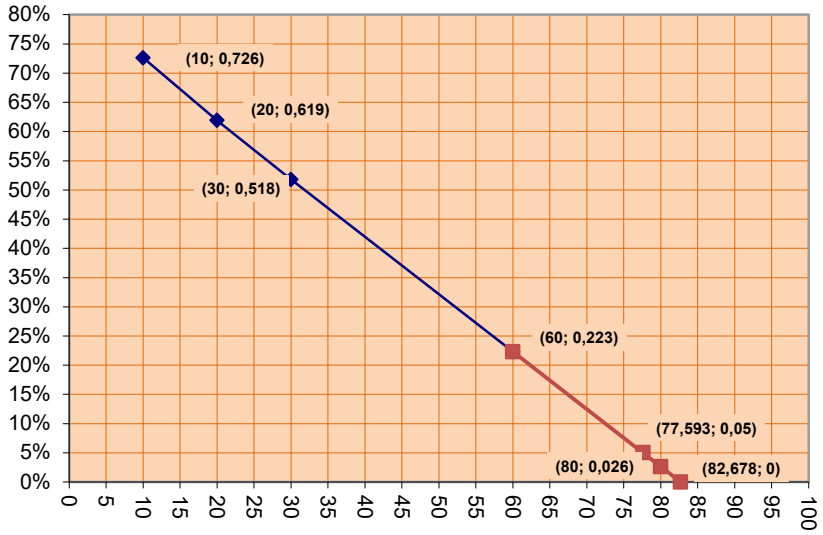

Figure 4 – Time Analysis for definition of Work Index: X-axis: time in minutes; Y-axis: % pass by. [1]

Figures 4 and 5 illustrate, respectively, the Work Index analysis of the work done for this type of ore and the granulometric analysis by milling time for this ore. The test determines the Work Index or grindability (Work Index) for ball mills. The BWI is used with the third comminution theory of Bond to calculate what is the net power requirements for grinding. However, several correction factors may have to be applied.

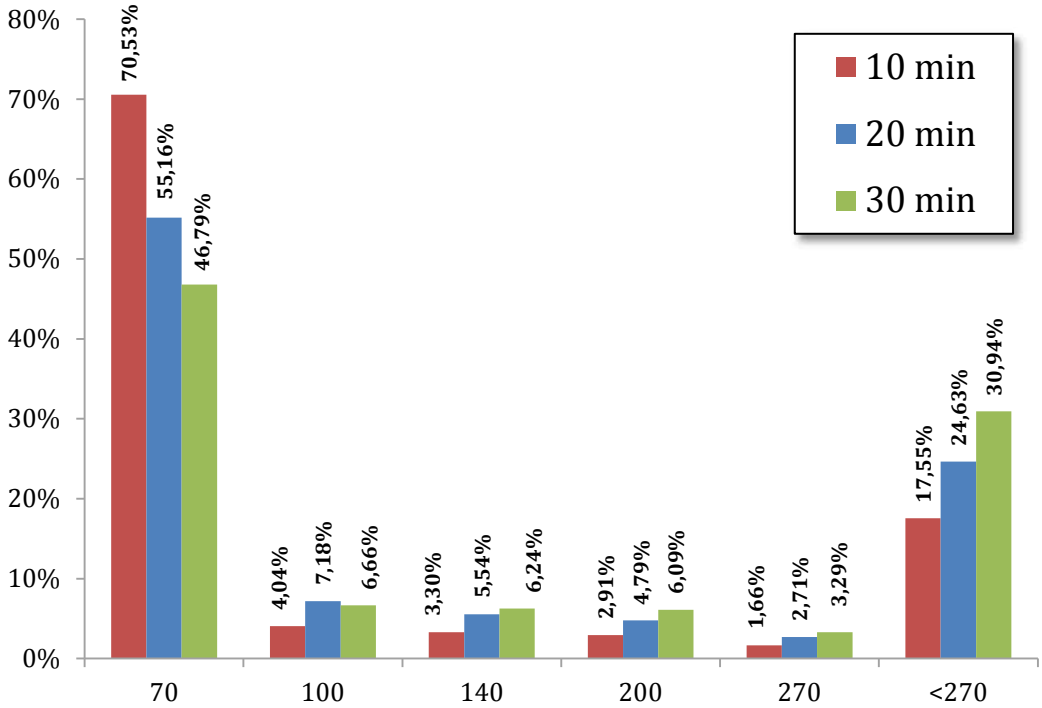

Figure 5 – Comparative graph of the effect of milling time on the comminution of the samples. [1]

ANALYSIS PROCEDURE

The analysis of the milling time shows that the material was concentrated, however, also be realized that the iron content in the thin particles was increased with increasing milling time.

Table 2 – showing the relationship between the grinding time, content and weight distribution of the sample. [1]

Moagem	Malha	R. Massa	%Fe	%SiO_2	%Al_2O_3	%P
10'	70#	70.5%	68.350%	2.973%	0.340%	0.080%
10'	100#	4.0%	65.817%	4.220%	0.688%	0.086%
10'	140#	3.3%	64.220%	5.006%	0.907%	0.090%
10'	200#	2.9%	64.138%	6.720%	1.261%	0.090%
10'	270#	1.7%	64.080%	7.936%	1.512%	0.090%
10'	<270#	17.554%	**54.462%**	**6.664%**	**7.352%**	**0.382%**
30'	70#	46.787%	67.570%	2.588%	0.265%	0.060%
30'	100#	6.658%	66.184%	3.821%	0.150%	0.072%
30'	140#	6.240%	65.310%	4.599%	0.077%	0.080%
30'	200#	6.088%	65.907%	4.975%	0.623%	0.086%
30'	270#	3.285%	66.330%	5.241%	1.010%	0.090%
30'	<270#	30.943%	**62.028%**	**5.503%**	**4.654%**	**0.284%**

METHODOLOGY

Analysis of the Jasper Ores Milling

The analysis of the behavior of the material during the milling led to the calculation of average rate of W.I. around 17.8 kWh/t, led the concentration of this product not economical.

However, the analysis of the background grinding, created a highlight atypical behavior of the sample. It was expected ease in secondary crushing, however, the sample recovered, above 70#, it became more difficult to grind than the initial sample. How is showed in figure 6.

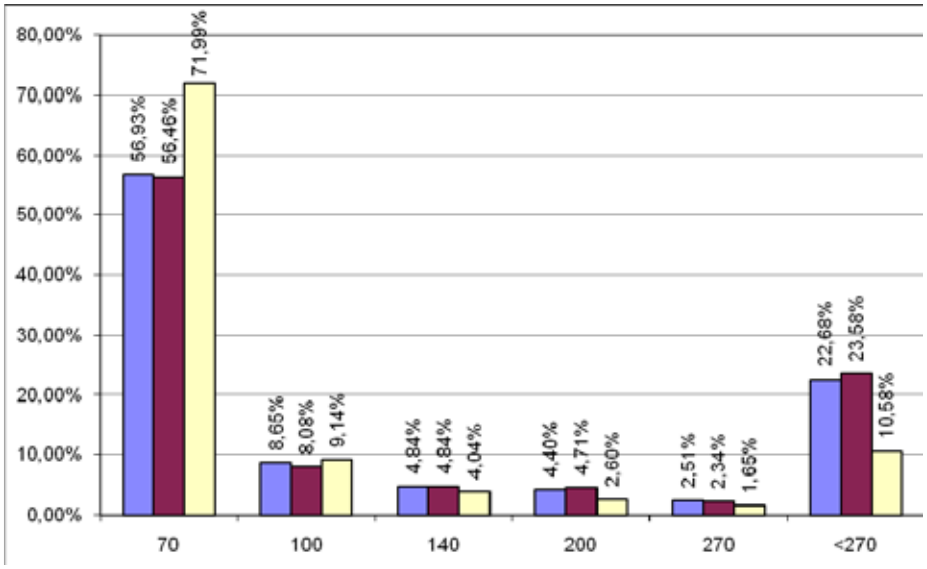

Figure 6 – Graph showing the comparison of the particle size distribution of the primary milling (red and blue) and the second milling (yellow). [1]

After milling it was found that the material was difficult to be ground. So one could deduce that two types of materials were being processed. The softer first and harder second.

The chemical particle size analysis (see table below) shows levels of up to 68% Fe in the retained, indicating that silica present in the ore was crushed first.

Table 3 – Chemical composition of particles size analysis according grinding time. [1]

Milling Time	Participation in the total mass						Participation in specific range			
	Mesh	% Mass	%Fe	%SiO_2	%Al_2O_3	%P	%Fe	%SiO_2	%Al_2O_3	%P
10'	70#	70.5%	68.35%	2.97%	0.34%	0.080%	73.6%	53.7%	14.5%	42.1%
10'	100#	74.6%	68.21%	3.04%	0.36%	0.080%	77.8%	57.9%	16.2%	44.7%
10'	140#	77.9%	68.04%	3.12%	0.38%	0.141%	80.9%	61.9%	18.3%	46.9%
10'	200#	80.8%	67.90%	3.25%	0.41%	0.161%	83.7%	66.9%	20.5%	48.9%
10'	270#	82.4%	67.83%	3.35%	0.46%	0.180%	85.4%	70.3%	21.8%	50.1%
10'	<270#	100%	65.48%	3.93%	1.65%	0.134%	100%	100%	100%	100%
30'	70#	46.8%	67.57%	2.59%	0.27%	0.060%	48.8%	30.8%	7.5%	20.9%
30'	100#	53.4%	67.40%	2.74%	0.25%	0.062%	55.9%	37.8%	8.1%	24.5%
30'	140#	59.7%	67.18%	2.96%	0.23%	0.083%	61.3%	44.6%	8.4%	28.3%
30'	200#	65.8%	67.06%	3.15%	0.27%	0.166%	67.6%	52.3%	10.7%	32.3%
30'	270#	69.1%	67.03%	3.25%	0.34%	0.187%	70.8%	56.7%	12.7%	34.4%
30'	<270#	100%	65.48%	3.93%	1.65%	0.134%	100%	100%	100%	100%

Table 3 shows the evolution of improvement of composition of the ground ore at different times. Comparing the grinding time of 10 and 30 minutes can be seen that the longer time of the milling leads to a

greater participation of the metallic iron content in the finer ranges. With 10 minutes it can be seen that the metallic iron content stands out more in the larger particle size ranges.

Equipment and Process

This process works with a processing line, criated to return the grinding material above 100# for milling; discarding material undersize 270#; and directing the material in the range between 270# and 100# as product, which corresponding to an average of 70% of the mass of the milling feed.

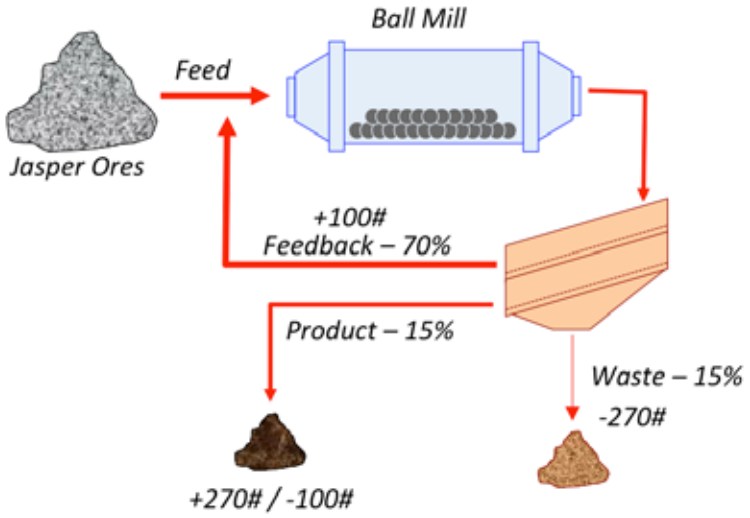

Figure 7 – Graph showing the comparison of the particle size distribution of the primary milling (red and blue) and the second milling (yellow). [1]

Figure 8 – Adjustable plant used for testing in Gorceix Foundation. [1]

RESULTS AND DISCUSSION

A longer milling reduced the iron content in the retained it increased and the thin, allowing to deduce that the silica was acting as an abrasive, leading to iron ore fines, but this abrasion also carried in the first instance phosphorus for fine, reducing it in retained.

To then get a retained with a high iron content, good recovery and decrease in phosphorus, 20 minutes mills were made, separating the part below 270#, passing by 15% every grinding, where the mass retained 100# was 70% allowed in the context of four straight milling, 20' in the range +270#/ –100# to recover more than 68% by weight, with an enrichment of the metallic content of 48 to 67% 5%. Fall of 10% silica content to about 2.28%. Phosphorus reduction of 0.18% to 0.076%. This is all about 11.85 kWh/t. Making this ores viable for commercial use.

Table 4 – This table shows the final composition after selective milling. [1]

W.I.	Fe	SiO_2	Al_2O_3	P	Mn	Limonite	Density	Humidity	L.F.
11.85	68.5%	2.28%	0.59%	0.076%	0.016%	1.04%	3.65	1.8%	2.1%

REFERENCES

1. 21 CBECiMat (2014). *Melhora da Qualidade de um Minério Jaspelítico por Moagem Seletiva*. Cuiabá, MT, Brazil: E.L. Souza; G.S.L. Gomes; L.J.M. Oliveira; D.F. Pereira.
2. CT2004-179-00, CETEM (2004). *Tratamento de Minérios*. Rio de Janeiro, RJ, Brazil: A.B. Luz; F.A.F. Lins.
3. CT2004-182-00, CETEM (2004). *Cominuição*. Rio de Janeiro, RJ, Brazil: H.V.O. Figueira; S.L.M. Almeida; A.B. Luz.
4. U.S. Environmental Protection Agency (1994), Office of Solid Waste, Special Waste Branch. *Extraction and Beneficiation of Ores and Minerals*. 401 M Street, SW, Washington, DC 20460.
5. REM: R. Esc. Minas, 65(2), 247-255, (abr. jun. | 2012). *Simulação de Moagem Mista por Rede Neural Artificial*. Ouro Preto, MG, Brazil: G.M. Rosa; J.A.M. Luz.
6. CETEM/MCT (2001). *Mineração e Desenvolvimento Sustentável: Desafios para o Brasil*. Rio de Janeiro, RJ, Brasil: A.P. Chaves; B. Johnson; F. Fernandes; G.J.C. Sirotheau; M.H.R. Lima; M.L. Barreto; R.C.V. Bôas; S. Nahass.
7. http://mapstore.eco.br/image/data/mapas/geologia/geodominios/municipios/, accessed in 2016, 2nd, May.
8. http://carlosbecker.com.br/site/peneira-giratoria/, accessed in 2016, 2nd, May.

THANKS

My sincere thanks to FAPEMIG, DTECH/CAP/UFSJ, Gorceix Foundation, TecNouveau Engineering, and to my colleagues, partners in this work.

RELEASE DETERMINATION OF GRADE AND STUDY PHYSICAL IRON ORE WASTE AIMING AT ENRICHMENT ON THE STEPS OF MINERAL PROCESSING

*D.D.A. Ferreira[1], J.I.F Santos[1], V..R.N Cordeiro[1] and A.L. Porto[1]

*[1]Federal Institute of Education, Science and Technology of Paraíba - Campina Grande Street Tranquilino Coelho Lemos, Dinamérica- Campina Grande - PB (Brasil) ifpb.edu.br (*Corresponding author: defsson@hotmail.com)*

24th World Mining Congress
MINING IN A WORLD OF INNOVATION
October 18-21, 2016 • Rio de Janeiro /RJ • Brazil

RELEASE DETERMINATION OF GRADE AND STUDY PHYSICAL IRON ORE WASTE AIMING AT ENRICHMENT ON THE STEPS OF MINERAL PROCESSING

ABSTRACT

The iron ore is among the most important substances for maintaining the current technological standards and, about this case, presents itself as a mineral resource highly demanded in the world. Nowadays, Brazil is the second largest producer of this raw material in the world, holding about 17% (IBRAM, 2012) of world production. Despite being one of the highest incidence of metals in the earth's crust, iron ore has shown progressive exhaustion of some mineral reserves of high content due to its large-scale use. In this context, it is necessary to introduce specific procedures that lead to optimal utilization of mineral reserves of medium to low iron content that usually occur associated with high concentrations of gangue minerals, especially quartz and mica. The beneficiation process or treatment of iron ore consists of seek operations that modify particle size, relative concentration and / or the form of minerals, without modifying the physicochemical properties thereof. Aimed at finding routes to the use of iron ore tailings, concentrate samples were studied and tailings from a mine in the state of Ceará, Brazil. Firstly the material was homogenised and quarteado then were made granulometric classification test. After this stage, separated from a fraction of each particle size range (300µm, 180µm, 125 microns and -125µm) and by applying the method Galdin determine the degree of release of the iron particles contained in the waste. Thus, it was determined that the optimum particle size for having the physical release of the iron particles. In addition, physical properties were estimated samples - such as porosity, grain density and grain volume by gas pycnometry. The use of pigmentary properties for obtaining mineral offers the possibility of performing rapid and accurate testing. Analyzing the results obtained, it is concluded that the particle size range below 125µm (-215µm) iron has the best percentage of released particles (70.91%) compared to other particle sizes. Thus, aiming at a higher concentration of this waste, the comminution equipment should be employed so as to provide a product with the said size. With respect to physical properties of the samples, the gas pycnometer determined a density of about 4.4 gm/cc for sample concentrate and 3 gm /cc for the waste, while the porosity and pore volume showed that the sample of tailings is higher than the porosity of the concentrate.

KEYWORDS

Iron ore, exploitation, release.

INTRODUCTION

The iron ore is a mineral that when heated in the presence of a reductant, will produce metallic iron (Fe), and consists mostly of iron oxides, with the primary forms being magnetite (Fe_3O_4) and hematite (Fe_2O_3). Iron ore is the main source of iron and steel industries in the world, so it is essential for the production of steel, which in turn is essential to maintain a strong industrial base.

Treatment or mineral processing operations is seeking to modify the particle size, relative concentration and / or the form of minerals, without modifying the chemical and physical these identities. In this way, the aim is, through mergers, remove the gangue minerals (not usable set of minerals from an ore) of ore minerals (precious minerals, exploitable economically). Furthermore, the fragmentation operations are of great importance for the efficiency of mineral concentration as a release of particles of interest is required in relation to the gangue minerals. Thus, the unit operations of comminution and classification by screening should provide a product within physical demands, which provide a physical release and as a consequent, effective concentration. The products generated from mineral concentration processes are concentrated with a high iron content and containing waste, generally a high content of gangue minerals (quartz and mica), and a percentage of the iron particles.

Getting the iron contained in the residue is an important field for research and academic research leading to determination of parameters and procedures for implementation of scaled plants for metal recovery. This research involves studies rated for estimation of physical properties of the concentrate and tailings, as well as determination of optimum particle size range for obtaining iron (present in the waste). The samples studied were obtained in materials deposition cells from an iron mine located in Quiterianópolis, state of Ceará.

From an economic point of view, the recoveries of the percentage of iron in the tailings contribute to increasing the company's profits, however, for this is necessary a comparative analysis of the costs (with equipment, personnel, energy) and the return to the company's cash . In the environmental area, the contribution is in the processing capability of large volumes of solid waste deposited in some cases, improperly in the environment, which in turn can become a potential pollutant. To start the planning of mineral processing operations necessary for the recovery becomes important to know the following factors:

- In what range of particle size of the iron particles are more liberated in relation to the gangue minerals;
  physical properties (density, porosity, grain, pore volume).

OBJECTIVE

General objective

Determine, through the pigmentary a gas Physical Properties Concentrate samples and iron ore reject , as well as apply the Galdin method to estimate the degree of liberation in different grain sizes paragraph iron particles contained in the tailings.

Specific objectives

- Analyze the particle size distribution of the concentrate and tailings samples;
- Determine , through the analysis of microscopic magnifying glass , which the majority minerals that make up the samples studied ;
- Estimate, based on the results obtained, which is the optimal particle size for better recovery of iron contained in the waste, but also determine what size the iron is more assimilated to the gangue minerals.

DEVELOPMENT WORK

Our work was developed in conjunction with the Comminution and Mineral Concentration Laboratory of the Federal Institute of Paraíba, Campina Grande, and the petrophysics laboratory of the Federal University of Campina Grande.

EXPERIMENTS

Sampling and preparation

To conduct the survey about 20 kg of each material were collected . The first part of the work was the homogenization in conical piles of the total sample and quartering into smaller fractions (Figure 1) using Jones splitter . After preparation, the samples were broken parts in 0,74mm sieve to remove aliquots of 0.2 kg (a concentrate and reject the other) to be sent to the gas pycnometer tests. In addition, fractions were removed from 1 kg to the particle size distribution analysis.

Figure 1- Procedure for homogenization and quartering samples.

Particle size distribution analysis

To study the particle size behavior of the samples, assays were carried out in dry, with 1 kg of concentrate and tailings using sieve shaker (300 sieves, 180, 125, 106, 74μm and blind bottom) operating at 10 minutes 5Hz cycle equipment vibration intensity.

Degree release

Small fractions were separated (the reject) in four different particle sizes - 300, 180, 125, and through 125μm for applying the method proposed by Galdin. with the display in microscopic magnifying glass, the separation was made with a needle, the mineral phases. In addition, for each size range was taken to count individual particles of each constituent mineral particles and mixed.

Knowing the amount of iron particles, the amount of mixed particles (iron mineral assimilated to another), it becomes possible to apply equation (1) below to determine the percentage of particles physically released in each of the four particle sizes.

$$degree\ of\ release = \frac{free\ amount}{free\ amount + free\ amount}.100 \quad (1)$$

Picnometry gas

The tests carried out to determine physical properties were carried out using a gas permoporosímetro, Corelab brand, model UltraPoroPerm 500, available in petrophysics laboratory of the Federal University of Campina Grande.

Couto *et al.* (2012), it states that the application of pinometric procedure is practical and effective contributing less time and lower costs in tests to determine the physical properties of rocks and minerals.

The measurement of density, porosity and other properties of the samples was carried out by weighing the same on a digital balance accurate, then the sample was introduced in a glass matrix array coupled to a glass equipment. After the glass matrix to be filled with sample, weighing was made and then the tests were performed on a gas permoporosímetro. Using matrix glass was measured volume of the sample grain. The difference between the grain volume and the total volume of the sample, is its void volume. To calculate the porosity sufficient to determine the ratio of the void volume and total volume.

Once the sample is dry it can be assumed that its mass corresponds to the mass of a solid phase, the grain density being given by the ratio between the sample mass and volume of grain measured. With the porosity and grain density can estimate the total density of the rock despising the

density of the air, which fills the pores of the rock.

Software installed on your computer (connected to permoporossímetro) in a few moments generates a spreadsheet with the data on the physical properties of the samples. This procedure was applied to both sample of the concentrate and the tailings. Figure 2 expresses briefly the method applied.

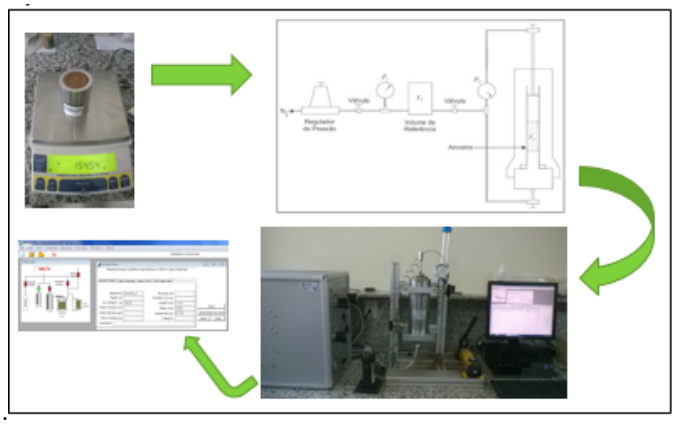

Figure 2- Basic flowchart of the procedure for determining physical properties

RESULTS AND DISCUSSIONS

Sieve analysis

Tables 1 and 2 represent, respectively, the results obtained after the particle size to classification tests for samples of concentrate and reject iron ore. By viewing the tables can determine which bands are the largest weights of the samples, thereby estimating the majority sizes which in each case.

Table 1. Representation of the distribution of particle sizes in the concentrated.

Sieve (#)	Opening (µm)	Withheld (gm)	Percentage		
			Withheld	Accumulated	Passing
50	300	528	52,8	52,8	47,2
80	180	273	27,3	80,1	19,9
120	125	113	11,3	91,4	8,6
140	106	29	2,9	94,3	5,7
200	74	28	2,8	97,1	2,9
>200	>74	29	2,9	100	0
Total	-	1000		-	-

Table 2. Representation of the distribution of particle sizes in the waste

Sieve (#)	Opening (µm)	Withheld (gm)	Percentage		
			Withheld	Accumulated	Passing
50	300	597	59,7	59,7	40,3
80	180	219	21,9	81,6	18,4
120	125	92	9,2	90,8	9,2

140	106	27	2,7	93,5	6,5
200	75	35	3,5	97	3
-200	74	30	3	100	0
Total	-	1000	-	-	-

The results obtained by analyzing the tables show that the two samples have basically the same grain size behavior. The larger aperture sieve retained most of the mass of the sample, 52.8% and 59.7% in the concentrate in the waste. Therefore, we can define the samples were mainly composed of coarser grains since the amount of material passed into the lower sieve opening (125 74µm) was relatively low.

Figure 3 depicts the passing granulométrica- distribution curves due to the opening (uM) - and it shows a distinct behavior in the first sieve (300µm) However, from the second screen, the distribution is strongly similar between the two samples.

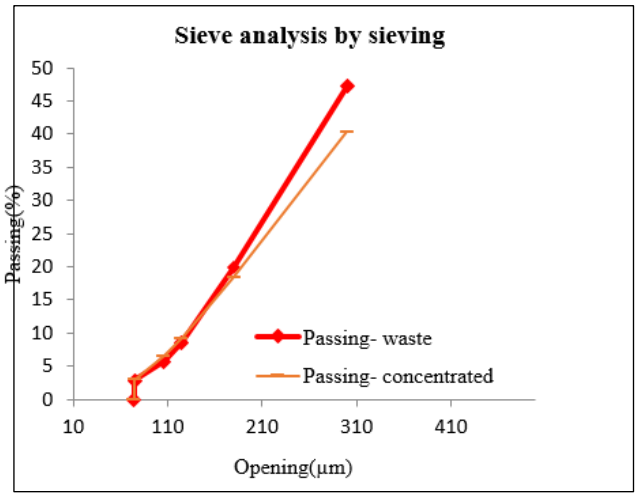

Figure 3- Graph of particle size distribution curves.

Degree release

Figure 4 shows the mineral particles counted and secreted in accordance with the mineral species. By viewing loupe, identify minerals of major proportions that make up the samples. particles were identified: quartz, mica and iron, mixed (iron and other mineral). However, the method is not sufficient to identify the mineral phases in minor proportions. Thus, the authors of this study also seek to submit samples for mineralogical characterization by X-ray diffraction, to estimate the proportion of components. The results calculated by applying the Galdin method are shown in Table 3.

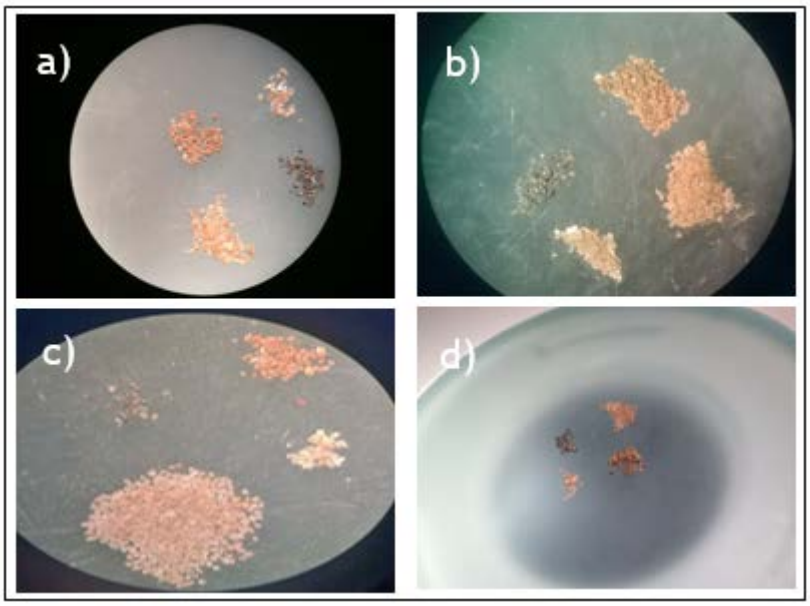

Figure 4 Separation and individual particle counts of each mineral phase: a) withheld to 300µm; b) Withheld of 180µm, c) Withheld to 125µm; d) Passing 125µm.

Table 3: Data and results of the determination of the degree of release *(degree).*

Granulometry	Free Particles (iron)	Iron Composite Particles	Equation	Dedree
withheld to 300µm	62	105	(62/ 167) x 100	**37,13%**
withheld to 180µm	98	156	(98/254) x 100	**39,36%**
withheld to 125µm	44	98	(44/142) x 100	**30,99%**
Passing 125µm	233	91	(233/324) x 100	**70,91%**

Looking at the table above, we can see that among the particle sizes studied the track with a particle size below 125µm has 70.91% of the contained iron, released physically, that is, within the requirement for efficient mineral concentration. However, the above groups and 125µm, the particles of iron found were treated as other mineral phases, stopping a low degree of release.

In this context, the fractions that have low release should be fragmented to the particle size below 125µm, targeting a further concentration with better metal recovery.

Picnometry

Through the gas pycnometer tests the following results were obtained:

Table 4. Physical property data obtained by gas picnometry

Sample	Dry weight (gm)	Volume of Grain (cc)	Density (gm/cc)	Volume Pore(cc)	Porosity (%)
Concentraded	248,97	56,51	4,41	34,6	37,98
Waste	154,55	49,43	3,13	41,68	45,75

As was expected, due to the high iron content, the density of the estimated concentrate sample (4,41gm / cc) was higher than the density calculated for the sample of waste (3.13 gm / cc). Knowing that the quartz has d = 2.65 gm / cc (DANA 1974), and this is mainly mineral that comprises the waste sample, the density is estimated to reject as expected. However, also in this case, knowledge of contents of mineral material for forming a conclusion grounded and accurately is required.

With regard to data volume of pores and porosity, it appears that the waste has pore volume and porosity higher than the concentrate. The aim is also to study this work, the influence of the concentrations of mineral components in the results of pore volume and porosity.

Work Continuity

For enrichment and improving results, it needs to be evaluated, through analysis by X-ray diffraction and fluorescence X-rays, the concentrations of the minerals which compose the sample. In order to define which method enables the highest degree of content of enrichment waste from iron ore, it is suggested that tests are carried out with different methods and mineral concentration equipment, such as gravitational (concentrator table jig, spirals , etc.), magnetic and flotation. Thus, it is possible to define which methods may be used in a processing plant for the recovery of iron contained in the waste.

CONCLUSIONS

The use of iron ore reserves with low content and the waste generated in the stages of mineral processing is essential for rational and sustainable development of the mineral sector in Brazil. Therefore, aimed at finding routes to appropriate treatment of the material, it is necessary to know, in other parameters, the degree of release and physical properties.

It was identified that much of the material, both concentrate and tailings, have Coarse. Knowing the best result degree of release was 70.91% thin- range in size below 125µm steps are necessary comminution (crushing and grinding) and classification to generate as much material below 125µm and thus physically free iron particles, so that an ideal material to be forwarded to promote efficiently, the subsequent concentration.

About the results of psychometric tests, we concluded that the physical characteristics can be obtained quickly and conveniently by this method. A density of about 4.4 gm/cc for sample concentrate and 3 gm/cc for the waste, and porosity values and pore volume show that the sample of tailings is higher than the porosity of the concentrate was calculated.

REFERENCES

COUTO, H. J. B.; BRAGA, P. F. A & FRANÇA, S. C. A. **Use of gas pycnometry for estimating the iron content in mineral samples.** Minerals Engineering, 39, pp. 45-47, 2012

Dana, J. D. **Manual de Mineralogia**. Livros Técnicos e Cientificos Editora S.A, 1974.

LUZ, A. B. & LINS, F. A. F. **Rochas & Minerais Industriais: usos e especificões.** 2. Ed. Rio de Janeiro: CETEM/MCT, 2008.

LUZ, A. B.; SAMPAIO, J. A. & FRANÇA, S. C. A. **Tratamento de Minérios.** 5. ed. Rio de Janeiro: CETEM/MCT, 2010.

REPRESENTATIVE SAMPLING – THE WAY TO THE PRECISE METAL ACCOUNTING

M. Ranchev[1], L. Tsotsorkov[2], D. Nikolov[2], A. Angelov[2], T. Pukov[2], I. Grigorova[1] and *I. Nishkov[1]

[1] *University of Mining and Geology "St. Ivan Rilski"*
Department of Mineral Processing and Recycling
Prof. Boian Kamenov Street
1700 Sofia, Bulgaria
*(*Corresponding author: inishkov@gmail.com)*

[2] *ASSAREL-MEDET AD*
4500 Panagyurishte, Bulgaria

24th World Mining Congress
MINING IN A WORLD OF INNOVATION
October 18-21, 2016 • Rio de Janeiro /RJ • Brazil

REPRESENTATIVE SAMPLING – THE WAY TO THE PRECISE METAL ACCOUNTING

ABSTRACT

The key starting point for accurate metallurgical accounting is the collection of representative samples of the process streams. An official examination (Technological Audit) and assessment of the equipment, procedures and practices applied in the concentrator of Assarel copper mine have been conducted. Besides the detailed survey of the sampling procedures, laboratory equipment, documents, personnel carrying out the sampling activities and those concerned with the performing of the metallurgical accounting, an experimental procedure of the main input and output streams has been performed. However, a special attention has been paid to the mechanical sampling of the slurry feed and tailings product, required for the primary metal accounting. Furthermore, the impact of the sample cutter design, in particular the cutter aperture and speed, the turbulence around the cutter and the segregation have been evaluated. Over a period of one work shift, pilot tests with different size of the cutter gap, sampling the feed and the final tailings streams have been conducted. The experimental results clearly showed the necessity of an increasing of the cutter opening size for both, the feed and final tailings streams, which definitely will result in more precise and representative samples for primary metal accounting.

KEYWORDS

Sampling, metal accounting, cutter aperture

INTRODUCTION

The key starting point for accurate metallurgical accounting is the collection of representative samples for determining the grades of process streams. However, while many examples of good sampling practices can be found in the mineral and coal industries, the collection of samples and the need for them to be representative is often not given the necessary attention (Morrison, 2008). There is little point in using the latest metallurgical accounting package to improve metal balancing if the data used are unreliable in the first place. The basic rule for correct sampling is that all parts of the ore, concentrate, slurry or other material being sampled must have an equal probability of being collected and becoming part of the final sample for analysis. Unfortunately, this rule is not respected in many processing plant environments, resulting in both bias and poor precision of the analyses. Of these, bias is the more serious, because no amount of replicate sampling and analysis will reduce bias once it is present (Holmes, 2004) and it is often quite difficult and expensive to rectify the problem subsequently due to space limitations in the processing plants (Morrison, 2008).

Correct sampling means that all constituent elements of the lot have an equal opportunity of being in the sample, and the integrity of the sample is preserved both during and after sampling (Gy, 1998). Correct sampling is a generalization to bulk materials (solids, liquids, gases) of statistical random sampling. Sampling procedures may be vague, and sampling practices may not follow correct procedures. Sampling equipment may not perform well in practice even though it is designed correctly. Operators (those taking the samples) may not be properly trained in correct sampling. Without correctness, sampling bias is introduced and sampling variation is increased, sometimes substantially, beyond the unavoidable statistical sampling variation. Since samples are only as good as the sampling systems that generate them, incorrect sampling will remain undetected without an examination and evaluation of the sampling systems (Smith, 2004).

In the assessment of the metallurgical balance and for control around a metallurgical plant it is necessary to have unbiased measurements of the metal contents of the main input and output streams and to know the confidence that can be placed on the results. The determination of content involves measurement of the dry mass of the process streams, the taking of accurate, or unbiased samples, and accurate analysis in the laboratory of the samples that are taken (Barlett, 2002). Since most of the decisions made on a metallurgical plant, such as process flowsheet developments, methods of improving recoveries and grades and reducing losses etc., are based on the results obtained from sampling, it is imperative that the reliability of the samples and the methods used in obtaining them are carefully controlled and quantified (Simukanga, 2005). Sampling theory according to Gy (Gy, 1982; Pitard, 1989) deals very well with all that needs to be known about sampling from a particulate material that is not segregated in some way (Gy, 1982; Pitard & Gy, 1989). The theory of sampling covers all aspects of particulate sampling, ranging from the origin of seven types of sampling errors, via principles of sampling correctness, to a long line of physical sampling procedures and practices essential for everybody doing practical sampling, or working with sampling procedure optimization.

By definition, the measurement error of particulate value is the differences between the actual and the measured value. It is generally accepted, that the individual measurements are the elements of the probability distribution of the errors. This means that it is expected most of the repeated measurements to pile up around the mean value, with fewer measurements retreating from the central value.

Any sampling process will itself generate sampling errors. The only way to be able to eliminate, or to reduce these errors to an acceptable level, is to be able to understand how these sampling errors originate and are propagated. The theory of sampling combines the technical part of sampling (i.e., to cut and correctly extract the sample) and the statistical part (to characterize the heterogeneity of the sampling target, to estimate the uncertainty generated by sampling operations and to generalize the results) (Petersen, 2005). Samples for metallurgical accounting are taken from a range of locations in processing plants, but the best method is to take a sample from a moving stream either at a transfer point between two conveyor belts or at the end of a slurry pipe. In these two locations two locations the stream can be intersected at predetermined times or tonnage and increments can be collected by taking a full cross-section of the stream with a sample cutter, thereby satisfying the fundamental requirements for correct sampling. The presence of bias is a major problem for metallurgical accounting, because it causes serious difficulties in reconciling production figures and does not average out over time (Holmes, 2004).

A clearer understanding of the sources of sampling errors and how to eliminate sampling bias and minimize variance can be obtained by splitting the total sampling error TE_i for a given sampling stage ''i'' into a number of independent components as follows (Gy, 1982; Pitard & Gy, 1989):

$$TE_i = FE_i + GE_i + QE2_i + QE3_i + WE_i + DE_i + EE_i + PE_i \quad (1)$$

where: FE_i = fundamental error; GE_i = grouping and segregation error; $QE2_i$ = long-range quality fluctuation error; $QE3_i$ = periodic quality fluctuation error; WE_i = weighting error; DE_i = increment delimitation error; EE_i = increment extraction error; PE_i = preparation error.

The equation shown above (Report, 2014), applies principally to sampling from moving streams, so not all the above components of error apply to every sampling situation. For example, the long-range and period quality fluctuation and weighting errors do not apply to blast hole sampling, but the fundamental error, increment delimitation, increment extraction and preparation errors definitely apply. The last three components require special attention, particularly when sampling for metallurgical accounting purposes, because they can introduce sampling bias. However, they can be eliminated. The others are largely random errors that can never be completely eliminated, but they can be reduced to acceptable levels by careful design of the sampling system (Holmes, 2004).

The correct design of sample cutter is critical to obtaining representative samples from process streams. Sample cutters must satisfy the following design rules to eliminate increment delimitation and extraction errors (Petersen, 2005):

- The sample cutter must be non-restrictive and self-clearing discharge completely each increment without any rebounding, overflowing or hang-up in the cutter;
- The geometry of the cutter opening must be such that the cutting time at each point in the stream is equal;
- For linear-path cutters, the cutter edges (called lips) must be parallel, while for cutters travelling in an arc or circle (e.g. Vezin samplers) the cutter lips must be radial;
- No materials other than the sample must be introduced into the cutter, e.g. dust or slurry must be prevented from accumulating in the cutter when in the parked position;
- The cutter should intersect the stream in a plane normal to the mean trajectory of the stream;
- The cutter must travel through the stream at a uniform speed. Electric drives are best in this respect;
- The cutter aperture must be not less than three times the nominal top size, with a minimum size of 10 mm for slurries;
- The cutter must have sufficient capacity to accommodate the increment mass at the maximum flow rate of the stream;
- For slurries, loss of sample material due to dribbles must be avoided;
- The maximum cutter speed should not exceed 0.6 m/s. This rule is taken from Gy (1988) who conducted experiments to quantify the extent to which particles of known particle size bounce from the cutting edges of a horizontal cutter, either into or out of, the cutter with a measured gap and travelling at set speeds. These measurements do not necessarily apply to slurries.

The cutter speed is important for cross-stream cutters. In the absence of well-documented evidence to the contrary, it should not exceed 0.6 m/s at the minimum cutter aperture w_0 (i.e., 3d or 10 mm, whichever is the greater) to avoid extraction bias (Pitard & Gy, 1989; Gy & Marin, 1978). However, if the cutter aperture (w) is increased above this minimum, the maximum cutter speed (v_c) can be increased as follows, subject to an absolute maximum of 1.2 m/s:

$$v_c = 0.3.\left(1 + \frac{w}{w_0}\right) \tag{2}$$

Cutters can be found in mineral processing plants with speeds in excess of these limits to reduce the sample mass that needs to be collected. However, the ‘‘effective’’ cutter aperture decreases as the cutter speed increases, which can preferentially exclude the coarser particles and thereby introduce bias (Holmes, 2004).

The increment mass m_I (kg) taken by a cross-stream cutter is determined by the cutter aperture A (m), the cutter speed (v_c) and the stream flow rate G (t/h) as follows:

$$m_I = \frac{GA}{3.6\, v_c} \tag{3}$$

Consequently, for a given flow rate, the minimum increment mass that can be correctly taken to avoid bias is determined by the minimum cutter aperture and the maximum cutter speed. It is not possible to take unbiased increments of smaller mass unless the flow rate of the stream is reduced or the ore is crushed prior to sampling so that the cutter aperture can be reduced accordingly (Morrison, 2008).

This paper is based on the results, conclusions and recommendations, which are being obtained after the technological audit (Report, 2014) and assessment process of the equipment, sampling and measurement practices, conducted in Assarel concentrator. By examining the written sampling procedures, sampling equipment and by observing the ongoing sampling practices in the plant, a useful and practical

reference could be given, to ensure that the extracted samples are representative, which is vital for the accurate metallurgical accounting process.

METHODS AND MATERIALS

Sampling procedure (time-basis) for examination and assessment the performance of the cross-stream cutters, sampling the flotation feed and final tailings streams (primary metallurgical streams) have been developed. In Table 1 below, are presented the general sampling procedure conditions, such as: the existing and the experimental cutter opening sizes (cutter aperture), the sampling duration time and frequency of sampling, as well as the total number of the extracted individual samples. During the experimental sampling procedure, a four times intersection of the both streams at each sampling interval (10 min.) has been maintained. Each individual sample was analyzed for: solids content (wt.,%); Cu grade (%) and particle size distribution (+200 μm; -200 +100 μm; -100 +0.00 μm).

In addition, in the course of the experiment, a manual sampling – taking manual cuts from the upper part of the slurry stream in order to evaluate whether or not any segregation exist in both process streams have been conducted. The results of the material particle size (μm) and density (wt.%) were than compared with the samples, extracted automatically from the cross-stream cutter.

Table 1 – Sampling procedure conditions

No.	Cross-stream cutter	Cutter aperture (mm)	Sampling duration (h)	Sampling frequency (min.)	Total number of samples
1	Flotation feed	2.00 mm (current size)	3 hours	10 minutes	18
2	stream	4.00 mm (experimental size)			18
3	Final tailings	3.00 mm (current size)	3 hours	10 minutes	18
4	stream	4.00 mm (experimental size)			18

A comparison of the probability density functions (PDF) of the obtained results for Cu grade (%) in the extracted individual samples from the flotation feed (2.00 mm and 4.00 mm) and final tailings streams (3.00 and 4.00 mm), with the corresponding size of the cutter gap have been presented.

RESULTS AND DISCUSSION

In Figures 1 and 2 below are presented the percentage content of fractions -100 μm and +200 μm in the extracted increments (18 individual samples) during the sampling of the flotation feed and final tailings streams, with sample cutter apertures - 2.00 mm (current size) / 4.00 mm (experimental size) and 3.00 mm (current size) / 4.00 mm (experimental size), respectively for both streams.

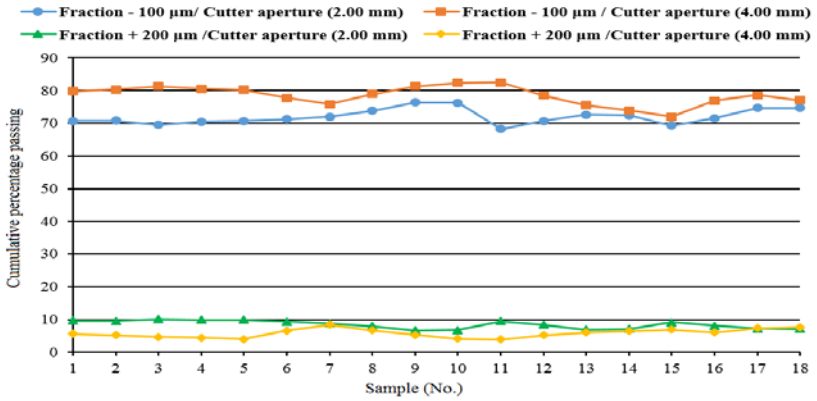

Figure 1 - Cumulative distribution of the fractions -100 μm and +200 μm in the extracted increments from flotation feed stream, with sample cutter opening size - 2.00 and 4.00 mm

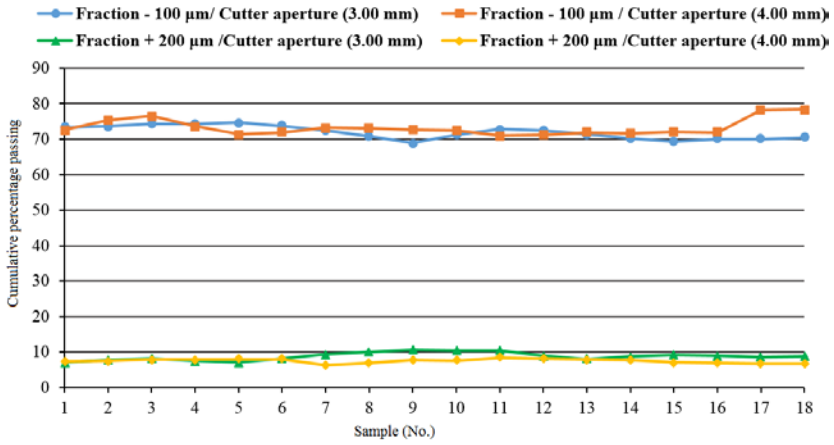

Figure 2 - Cumulative distribution of the fractions -100 µm and +200 µm in the extracted increments from flotation tailings stream, with sample cutter opening size - 3.00 and 4.00 mm

The results shown in Fig. 1, indicated that higher fine fraction content (-100 µm) in the samples extracted from the experimental (4.00 mm aperture) cross-stream cutter have been achieved, compared to the results obtained with the existing (2.00 mm) sampling cutter. Meanwhile, the contrast in the fine fractions (-100 µm) distribution in the samples obtained from both (current 3.00 mm and experimental 4.00 mm) cross-stream cutters (Fig. 2) of the final flotation tailings, was not so obvious. Furthermore, the course fractions (+200 µm) distribution in the extracted samples from both process streams, indicated almost negligible differences. The main material losses are introduced in the fine fractions, which therefore affect the copper distribution (metal content) in the samples, required for the primary metallurgical accounting.

In Figures 3 and 4 below are presented the percentage Cu grade in the extracted increments during the sampling of the flotation feed and final tailings streams. In the Figure 3 are shown the results after the performed sampling procedure of the flotation feed stream with opening size of the cutter gap - 2.00 mm and 4.00 mm, the present and the experimental size, respectively. In Figure 4 are presented the obtained results after the completed sampling experiment of the final tailings stream with opening size ot the cutter gap - 3.00 mm and 4.00 mm, the present and the experimental size, respectively.

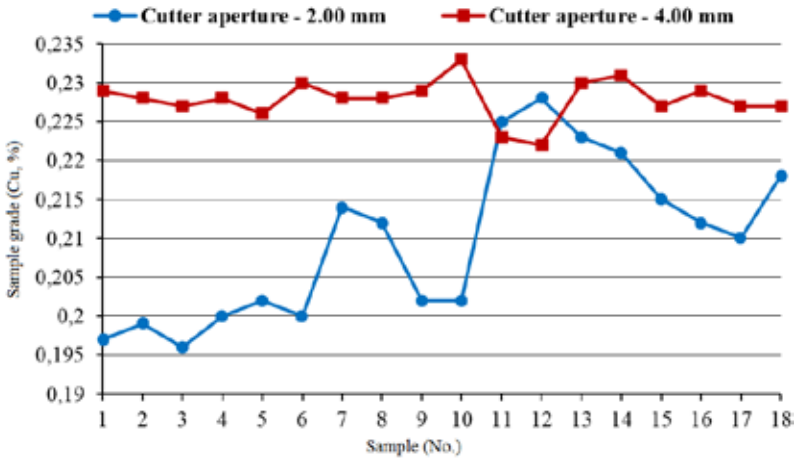

Figure 3 - Extracted increments Cu grade (%) from the flotation feed stream with sample cutter aperture - 2.00 mm and 4.00 mm

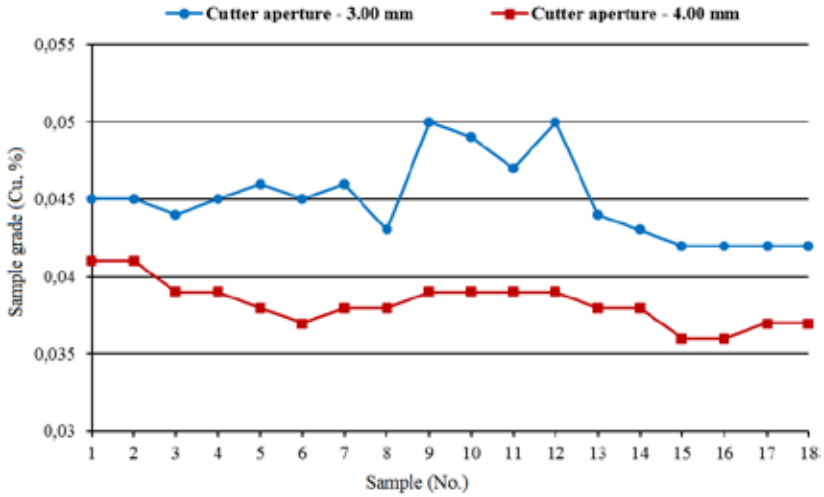

Figure 4 - Extracted increments Cu grade (%) from the flotation tailings stream with sample cutter aperture - 3.00 mm and 4.00 mm

In Table 2 are presented the summarized statistical results obtained after the experimental sampling procedure of the flotation feed (2.00 / 4.00 mm – cutter aperture) and the final tailings streams (3.00 / 4.00 mm – cutter aperture).

Table 2 – Summarized experimental sampling results

Stream	Flotation feed				Final tailings			
Cutter aperture	2.00 (mm) reference size		4.00 (mm) experimental size		3.00 (mm) reference size		4.00 (mm) experimental size	
Assay and Solids content	Cu (%)	(wt. %)	Cu (%)	(wt. %)	Cu (%)	(wt. %)	Cu (%)	(wt. %)
Average value	0.210	25.242	0.227	23.410	0.045	24.990	0.038	24.970
Min. value	0.196	23.320	0.222	21.930	0.042	23.350	0.036	22.570
Max. value	0.228	26.860	0.233	25.270	0.050	25.970	0.041	27.350
SD	0.010	0.950	0.00240	0.842	0.00251	0.687	0.00130	1.121
Variance	0.00010	0.897	0.00006	0.710	0.00060	0.472	0.00002	1.257
SEM	0.00230	0.212	0.00055	0.188	0.00056	0.154	0.00031	0.251

The obtained experimental results, showing the copper grade (Cu, %) in the extracted individual samples and the subsequent statistical analysis presented in Table 2, confirmed the expectations that an increase in the cross-stream cutters gap size, would result in more accurate measurements (closed to the "true" value or at least to the mean of a repeated set of measurements) with smaller standard deviation (SD) proportion and low variance of the distributed values.

Figures 5 and 6 show the distribution density of the copper assay for both process streams (flotation feed and final flotation tailings).

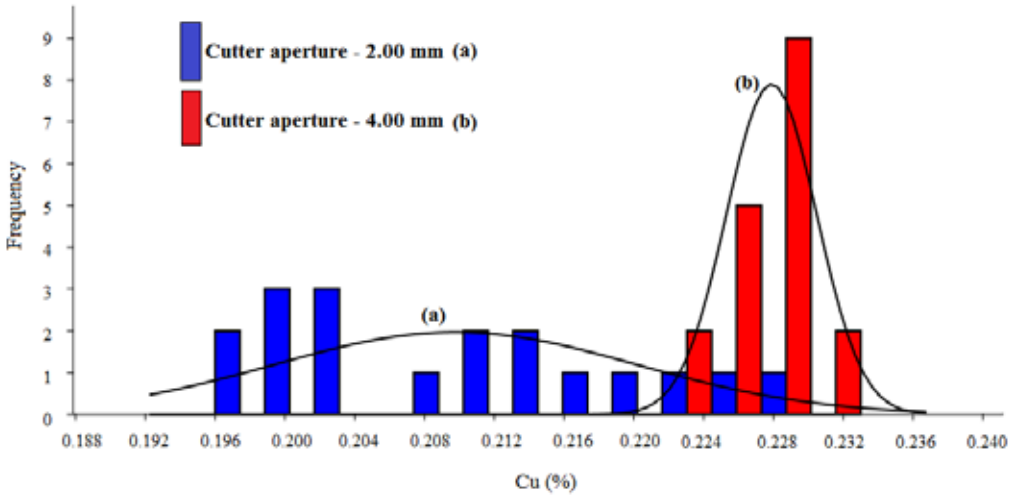

Figure 5 - Copper assay distribution density in the samples of the flotation feed stream

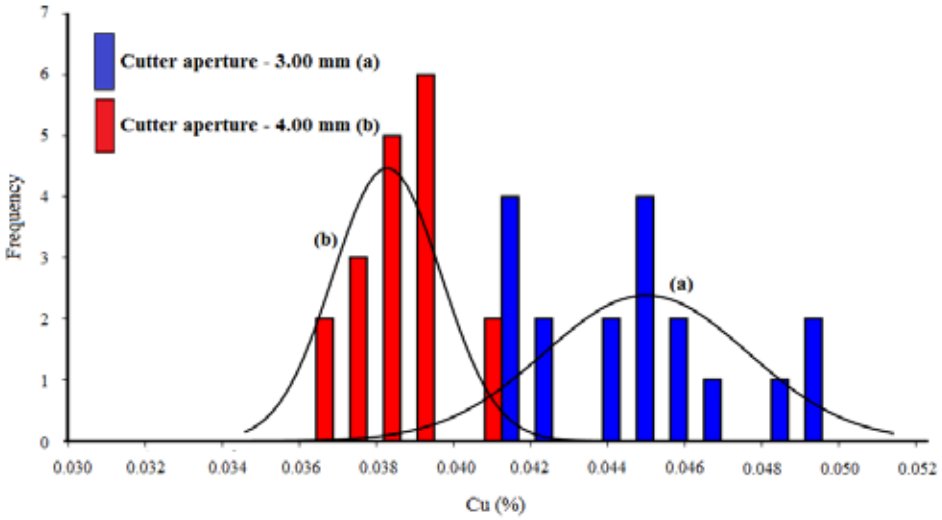

Figure 6 - Copper assay distribution density in the samples of the final tailings stream

The higher data scattering of the percentage copper distribution in the individual samples (2.00 mm cutter aperture), obtained during the sampling procedure of the flotation feed stream and both poorly formed peaks (Fig. 5a), could be interpreted as indication of error distribution law deviation. The average Cu grade (%) in the flotation feed stream was found in the area of 0.21 %. However, the lower data scattering around the mean value and the clearly indicated single peak, is an indication of limited scattering of the measured values in the extracted increments during the sampling process of the flotation feed stream – 4.00 mm cutter aperture.

The results presented in Figure 6 showed a symmetrical copper content (%) data distribution (Fig. 6a) around the average value of 0.045 % (cutter aperture 3.00 mm) with shapely peak and higher dispersion compared to curve (b), showing an average copper grade of 0.038 %, lower dispersion and higher peak.

A comparison of the particle size distribution in the manual and automatically extracted samples during the experimental procedure of the flotation feed (2.00 and 4.00 mm cutter aperture) and final tailings streams (3.00 and 4.00 mm, cutter aperture) is shown in Figures 7 and 8.

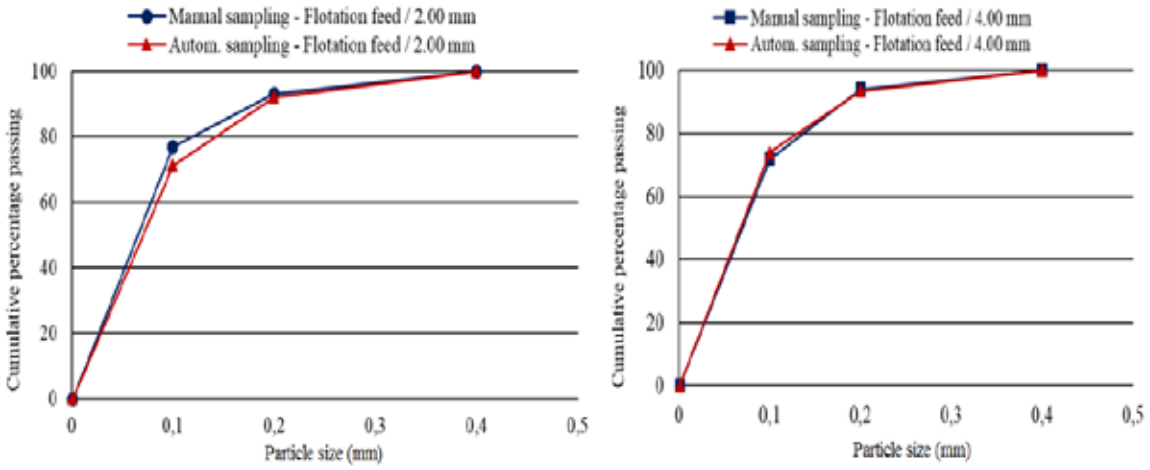

Figure 7 - Flotation feed stream - manual and automatically extracted samples during the sampling procedures – cutter aperture 2.00 and 4.00 mm

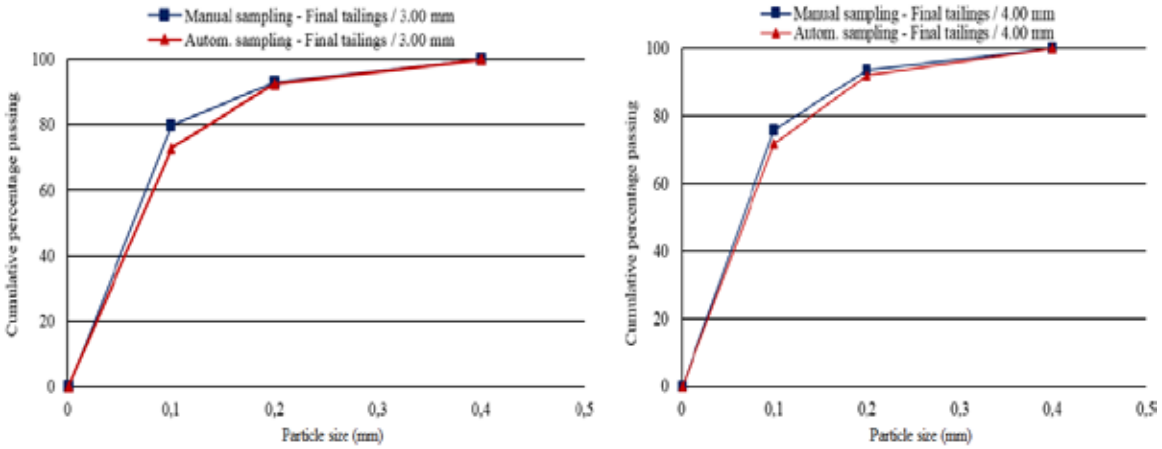

Figure 8 - Final tailings stream - manual and automatically extracted samples during the sampling procedures – cutter aperture 3.00 and 4.00 mm

Manually extracted samples from the upper part of the flotation feed and final tailings streams have been collected and analyzed, in order to determine the degree of segregation in both primary accounting streams. From the cumulative particle size distribution curves presented in Figures 7 and 8, could be concluded that a very low degree of segregation have been observed. In short, the reasons could be summarized as: when sampling from the moving streams, the flow is not laminar enough; local segregation of the different particle sizes could occur, due to the formation of stream vortices.

CONCLUSION

The fundamental rule for taking representative samples is that all parts of the material being sampled must have an equal probability of being collected and becoming part of the final sample for analysis. If this rule is not respected, the samples taken are likely to be seriously biased and the precision impaired, thereby compromising the value of the resultant analyses for metallurgical accounting (Morrison et al., 2008).

Based on the technological audit and assessment process of the equipment, procedures and practices applied in Assarel-Medet JSC, the biggest and leading copper concentrator in Bulgaria, the results from the experimental procedure, covering the mechanical sampling of the flotation feed and final tailings streams with different apertures (mm) of the linear cross-stream cutters and also from the presented in the beginning of the article sampler design rules, the following conclusions and recommendations have been made:

- Any contamination of the process slurry splitters and the cross-stream cutters should be avoided. An accidental "sludge" detachment (sticky material), which inevitably happen and its presence in the primary accounting samples, certainly will vitiate the measurement results;
- The appropriate dimensions of the primary sampling equipment (static multiple cutter device; crosscut samplers, etc.) sampling the main input and output process streams should be correctly established in accordance with continuously increasing plant capacity;
- Necessarily increase the width of the opening gap size of the linear cross-stream cutters for both process streams.

In order to minimize the possible bias during the sampling procedures and to ensure that each increment carries the correct weighting and assay information, the following examination should be carried out:

- A detailed examination, in order to determine the optimal cutter aperture, corresponding to constantly variations in quality (Cu content, %) and flow rate of the process streams;
- A detailed examination, in order to identify the appropriate sampling interval, confirmed by precisely determined autocorrelation functions of the process streams parameters.

Improving the mechanical sampling practices and procedures, will ensure that representative sample is delivered in the laboratory, where the quality control and the metallurgical accounting of the processing plant have been carried out.

ACKNOWLEDGEMENTS

Financial support for these studies and permission to publish this paper from ASSAREL-MEDET JSC is gratefully acknowledged.

REFERENCES

Barlett, H. E. (2002). Design of primary samplers for slurries in concentrators and statistical methods for measuring components of variance in sampling. *Journal of the South African Institute of Mining and Metallurgy, 102 (8)*, 485 – 490.

Gy, P., Marin, L. (1978). *International Journal of Mineral Processing, 5,* 297 - 315.

Gy, P. (1982). *Sampling of particulate materials, theory and practice*. 2nd ed., Elsevier.

Gy., P. (1998). *Sampling for Analytical Purposes*, Wiley, West Sussex, England.

Holmes, R. J. (1992). Sampling of mineral processing streams. *Sampling Processes in the Minerals Industry Mount Isa, 7*.

Holmes, R. J. (2004). Correct sampling and measurement – The foundation of metallurgical accounting, *Chemometrics and Intelligent Laboratory Systems, 74*, 71-83.

Morrison, R., Wortley, M., Holmes, R., Randolph, N., & Dunglison, M. (2008). *An introduction to Metal Balancing and Reconciliation*. (Ed.) Morrison, R. D. Julius Kruttschnitt Mineral Research Centre Monograph Series #4, pp. 141 - 170.

Petersen, L., Minkkinen, P., & Esbensen, K. (2005). Representative sampling for reliable data analysis: Theory of Sampling. *Chemometrics and Intelligent Laboratory Systems, 77*, 261– 277.

Pitard, F., F., Gy., P. (1989). *Sampling theory and sampling practice*, CRC Press Inc.

Technological audit and assessment of the sampling and metallurgical accounting systems in Assarel-Medet concentrator (Project № D-III - 155/2014), *University of Mining and Geology "St. Ivan Rilski"*, Sofia (In Bulgarian), 157 p.

Simukanga, C. P., et al., (2005). Designing and testing the representative samplers for sampling a milling circuit at Nkana copper/cobalt concentrator. *African Journal of Science and Technology, Science and Engineering Series, 6*, pp. 102 – 112.

Smith, L. P. (2004). Audit and assessment of sampling systems. *Chemometrics and Intelligent Laboratory Systems, 74*, 225 – 230.

REVOLUTION IN SENSOR TECHNOLOGIES: USES OF DE-XRT AND CCD CAMERA IN ORE PROCESSING

*A. Young[1], M. Veras[1,2], C. Petter[1], C. Sampaio[1]

[1]Universidade Federal do Rio Grande do Sul
Av. Bento Gonçalves, 9500
Porto Alegre/RS, Brazil, 91501-970
*(*Corresponding Author: Aaronsyoung@gmail.com)*

[2]*Instituto Federal do Amapá*
Rodovia BR 210 Km 3, s/n -Brasil Novo
Macapá/AP, Brasil, 68909-398

24th World Mining Congress
MINING IN A WORLD OF INNOVATION
October 18-21, 2016 • Rio de Janeiro /RJ • Brazil

REVOLUÇÃO DA TECNOLOGIA DE SENSORES DE RAIOS-X E CÂMERAS CCD NOS ESTÁGIOS DE BENEFICIAMENTO DE MINÉRIO

ABSTRACT

Automation is a common goal of the mining industry in the 21st century. From improving the safety and productivity of haul trucks through the use of cameras and GPS, to the divination of slope failures, sensors of various kinds have been used as steps towards automation in recent years (Wotruba *et al.* 2014). Just as with other mining areas, one of the most impacting developments in mining within the last ten years has been the application of sensor technology into automated sorting systems to create pre-concentrations of mine ore (Jönsson 2014). Unfortunately, the greatest challenge with the implementation of sensor technology within mining is the general inability of miners and mill operators to keep pace with the breaking technology (Lessard et. al. 2015). To face this challenge, this article discusses breakthrough sensor technologies, specifically, Dual Energy X-Ray Transmission (DE – XRT) and charge-coupled device (CCD) cameras.

KEYWORDS

Sorter, sensor, x-ray, ccd, preconcentration, mineral.

INTRODUCTION

To meet the demands of the future mining industry, an improvement in gravimetric processes with a focus on improving pre-concentration to ensure better ore content is needed (Sampaio and Tavares, 2005). By implementing Sensor Based Sorting (SBS) during the onset of beneficiation, particles of poor grade can be removed from the system before participating in more energy intensive processes downstream. The reduction in the mass of tailings to be processed equates to savings in energy and water usage and equipment maintenance, ultimately increasing the efficiency of the entire beneficiation process (Wotruba *et al.* 2014).

SBS is the use of spectromatic sensors to identify intrinsic characteristics of particles and separate them by either mechanical or pneumatic means into different product streams (Wotruba *et al.* 2014). SBS can be used with great effectiveness to improve gravimetric beneficiation through the selective separation or pre-concentration of run of mine ores (ROM), however SBS is not a replacement for the gravimetric beneficiation process. The ability to sort material effectively is therefore dependent on the ability to measure it correctly and rapidly.

Lindner (2010) suggests that correct and rapid measurement of ROM is only possible if there exists an electromagnetic interaction present in all of the wave spectra interacting with the solid ore. The frequencies of the wave spectra which may interact with the solid ore vary between 1000 and 10^{20}Hz. ROM material varies greatly and is as diverse as there are solid ores. Both the frequencies irradiated at the material and the intrinsic characteristics of the material govern the response of the material. After receiving a spectrum of electromagnetic waves by irradiation, the material responds in a way which is unique to intrinsic characteristics resulting in a reduced wavelength from the material. The response from the material manifests through one or

many of the differing types of radiation such as fluorescence, reflection, remission, absorption, and/or transmission.

Depending on the ore to be processed, some wave spectra are more effective at distinguishing material characteristics than others. Figure 1 outlines sorting equipment which uses frequencies ranging from x-ray to visible light and can be applied to most of the minerals and metals presently known.

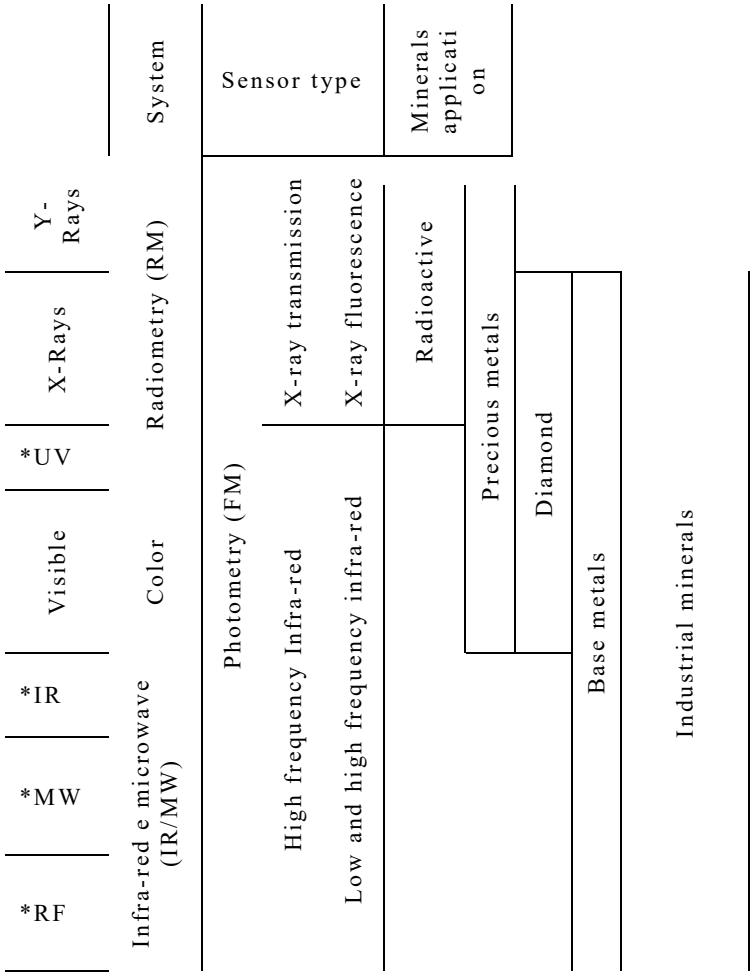

Figure 1. The sensor application range by the electromagnetic spectrum. (Adapted from Gaastra, 2014 and Lessard *et al.* 2014).
Legends: *WL = wave-length, *UV = ultraviolet rays, *IR = infra-red rays, *MW = micro-wave, *RF = radio frequency.

The most common sensors used in SBS are charge-coupled device (CCD) cameras, which allow the qualitative classification and sorting of material based on on a representation of its appearance in the visible light spectrum. CCDs allow through a Red, Green, and Blue (RGB) coloring system, the separation of minerals with different colors, tones. They are capable of distinguishing brightness and colors at a pace and accuracy in step

with the demands of industry.

More recently, the development and use of Dual Energy X-Ray Transmission (DE - XRT) to enable the separation of ROM by atomic density of the constituent minerals within a given rock has become a reality. This reality is also indebted to increased computational capacity (Lessard et. al. 2015).

CCD Cameras

The name charge-coupled device (CCD) refers to the architecture of the semiconductor which is capable of collection, transfer, and conversion of charge (Holst and Lomheim, 2011). More specifically, in the context of SBS, CCD signifies a visual sensor, which recognizes material radiation within the visible range of the electromagnetic spectrum and convert the information into usable form (Cremers *et al.* 2006). CCDs are light-integrating detectors, which collect plasma over several microseconds before compiling and exporting the corresponding electrical charge (Miziolek et al. 2006).

A main advantage of CCD is that the data measured can be displayed on a monitor for human interpretation or processed electronically by algorithm. ROM processed by CCD may sort automatically or may be inspected manually. Reviewing images on monitors is an effective method for operators and quality control to gain an understanding of the material in question (Wotruba *et al.* 2014).

De-xrt

Dual Energy X-Ray Transmission (DE – XRT) sensors are named for after capability of combining measurements from both high and low (dual) energy levels simultaneously (Reidel e Dehler, 2010). They are ideal for the mineral industry because they are capable of determining the mineral characteristics of samples which do not appear on the surface. Analyses with DE-XRT are not only non-intrusive and non-destructive, but they are also resilient to the effects of sample contamination through dirt or corrosion. These analyses can create a full composition read-out of the material, which can be represented on a monitor just like information displayed with CCD (Wotruba et al. 2014).

The sorting process

The x-ray sorting process, depicted in Figure 2, begins with samples passing an x-ray emitter towards a sensor, usually by means of conveyor. The sensor reads the level of x-radiation and converts it into usable data. This process involves the synchronization of the sensor with the speed of the conveyor and the processing of the data taken. From the data, colors are assigned to each region within the image according to a set color scheme. Pixels meant to represent areas of high atomic mass equivalent within the sample are given certain colors, while pixels corresponding to areas of low atomic mass equivalent are assigned contrasting colors (Kleine, 2010).

Each pixel within the images created represents the compilation of quantifiable data for a given area of the sample into a single value. After assigning quantitative values to each area of the material in question, the equipment then analyses the material as a whole particle and determines to which category (ore, or waste) the sample pertains, at which point the material is separated by simple mechanical means, either by chute or compressed air depending on particle size (Wotruba et al. 2014).

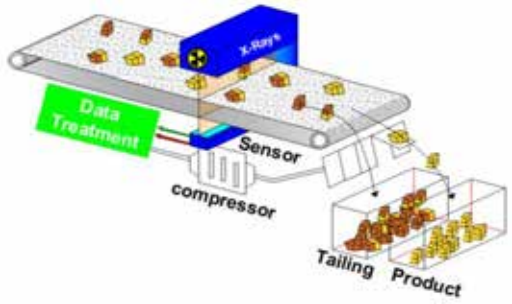

Figure 2. Layout of x-rays sensor separation.

In the case of DE-XRT sorters, the emitter used is an x-ray tube. DE-XRT implements a detection system which is depicted in Figure 3 and comprises of two layers of scintillators and photodiodes separated by a filter, with the first layer detecting longer wavelengths of low energy, and the second layer detecting smaller wavelengths of high energy (Kiehlmann 2011).

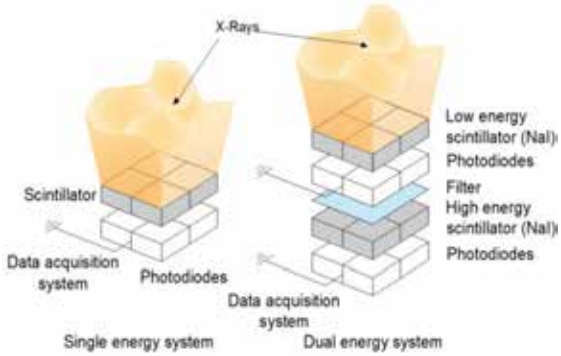

Figure 3. Configuration layout of a simple energy and dual energy sensor (Adapted from Wotruba et al 2014).

Challenges of X-Ray Sorting

Due to the fact that the intensity represented in each pixel of an x-ray spectrometer is an agglomeration for the attenuation of the x-rays as a function of the thickness of the particle examined, x-ray sensors generate results which assume homogeneity of material. The displays rendered do not account for a difference between the position of a measurement relative to the object between the x-ray emitter and the sensor. Therefore, all non-uniform objects present different results from different measurements, depending on the relative orientation of the material as illustrated in Figure 4. Also, the analysis of certain materials can cause interference and generate inaccurate data inducing unwanted separation. (Kleine, 2010).

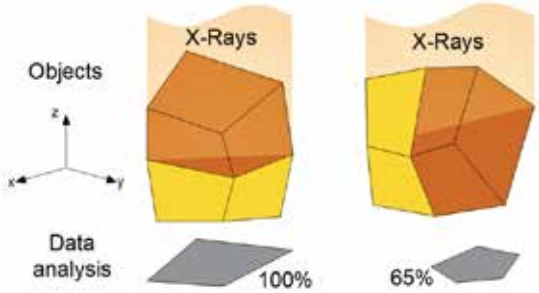

Figure 4. Position of material during the scan and the resulting compiled data (Adapted from Wotruba et al 2014).

MINING APPLICATIONS

Bergman (2009) estimated that there were up to 300 classifying machines that used sensors in the mineral industry, with a belief that the number is much higher. This technology has been applied to industrial minerals, precious metals and others such as coal, uranium, diamonds, gold, etc., and often presents a positive economic return on investment.

Lessard et. al. (2015) discussed how the technology has been so slow to become adopted in spite of its great potential, partially due to the fact that initial forms of SBS were unable to meet processing demands. Undoubtedly, there is room for more research and more detailed discussion among academic literature with regard to the economic, environmental and safety benefits of including automatic SBS into mineral processing systems.

The authors of this article currently operate a COMEX Lab-Sorter shown in Figure 5, at the Federal University of Rio Grande do Sul in Porto Alegre, Brazil. The Lab-Sorter has been used to sort coal from near density rock, rare earths, industrial minerals, recycled construction materials, and gravel.

Figure 5. COMEX Lab-Sorter MSX-400-VL-XR-3D at the Federal University of Rio Grande do Sul in Porto Alegre, Brazil.

Examples of sample image collection from DE-XRT are shown as Figures 6-(a,b) through 8. When masses present atomic density differences between product and waste, it becomes possible to sort them with the use of DE-XRT. These density differences which were hidden in the visible spectrum (the photos on the right),

become apparent in the x-ray spectrum (photos on the left).

[a] [b]

Figure 6. Samples of coal (Yellow) and Waste Rock (Green) in [a], and samples of Tungsten ore particles in [b] (Photos courtesy of COMEX).

When masses exhibit nearly identical atomic density differences but color or other characteristics are different, CCD may be used effectively for sorting.

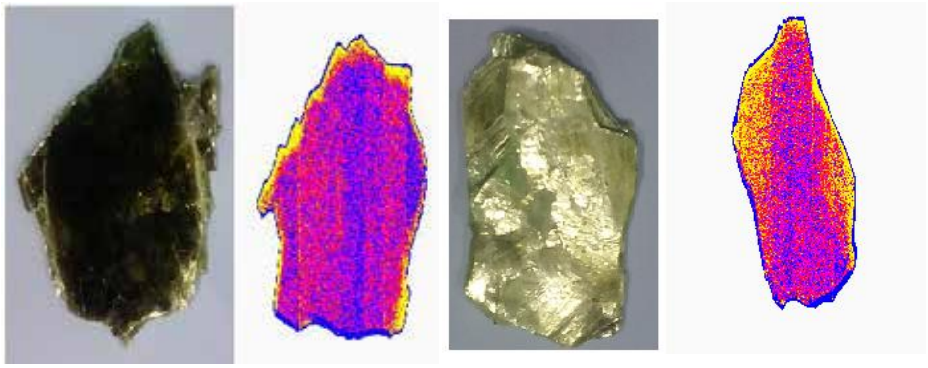

Figure 8: Samples of Muscovite and Hematite Micas (Photo taken from Authors using Lab-Sorter)

CONCLUSION

SBS can be employed in the primary or secondary separation of commercially valuable minerals and in dry processes. DE-XRT and CCD are among the most used sensor technology and can be applied to most mining operations. Sensor technology has been studied by various fields and its industrial applications and are still expanding. Previous studies have shown that this separation technology has been tested successfully between, among others, kimberlites, iron ores, gold, limestone, talc, coal, oil shale, magnesium ore, cobalt ore and slag, nickel ore and slag (Wotruba et al., 2014) and, more recently, rare-earth minerals in its pegmatitic form. The SBS technology has for many years now, been considered a breakthrough in mining the mining industry.

References

Bergman, C (2009), *Desenvolviments in ore sorting technologies*, s.l.: Mintek.

Cremers D and Radziemski L (2006), *Handbook of Laser-Induced Breakdown Spectroscopy*, John Wiley & Sons Ltd, Chichester, England.

Jong T and Harbeck H (2005), *Automatic sorting of minerals: current status and future outlook*, In: Process of the 37th canadian Mineral Processors Conference, Canadian, p 629-648.

Holst G and Lomheim T (2011), *CMOS/CCD Sensors and Camera Systems*, JCD Publishing, Winter Park, 2 Ed.

Kiehlmann, S (2011), *Atomund molekülphysik Röntgenstrahlung*, Lernportal Georg-August-Universität Göttingen.

Killmann, D (2009), *Betrachtung des Eisfluesses der Lagaverteilung von Abfallstücken im Zuförderstrom einer sensorgestützten Sortiermachine auf dei Erzielbare Wertschopfung pro Ziet diese sortierprozesses*, PhD thesis, RWTH, Aachen, In: Nienhaus, K Pretz, T and Wotruba H (2014), *Sensor Technologies: impulses for the raw Materials Industry*, RWTH, Aachen.

Kleine, C (2010) *Deshaling of ROM coal using XRT-sorting*, Tech, Rep. AMR, RWTH, Aachen University.

Lessard, J, Sweester, W, Bartram, Figueroa, J, de and McHugh, L (2015) *Bridging the gap: Understanding the economic impact of ore sorting on a mineral processing circuit* Minerals Engineering, 65; 88-97.

Lessard, J Bakker, J de and McHugh, L (2014) *Development of ore sorting and its impact on mineral processing economics* Minerals Engineering, 65; 88-97.

Lindner, H (2010) *Physik für ingenieuere*, Carl Hansenr Verlag, München, 18a ed.

Miziolek A, Palleschi V, and Schlechter I (2006) *Laser-Induced Breakdown Spectroscopy (LIBS) Fundamentals and Applications*, University Press, Cambridge.

Nave, R (2012) *The electromagnetic spectrum,* HyperPhisics, Department of Physics and Astronomy, Geogia States Universitiy, GA

Nienhaus, K Pretz, T Wotruba, H (2014) *Sensor Technologies: impulses for the raw Materials Industry*, Aachen: RWTH, Chapter 4, Berwanger, M Gaastra, M "Technical and physical principles of sensor technologies applied in the raw materials industry", p 47-199.

Oliveira, I B de (2006) *Desenvolvimento de cristal semicondutor de brometo de tálio para aplicações como detector de radiação e fotodetector*, Tese, USP.

Riedel, F and Dehler, M (2010) *Recovery of unliberated diamonds by x-ray transmission sorting*, In: Conferences Diamonds - Source to Use; March 1-3; Gaborone, Botswana. (SAIMM; 4th Colloquium on Diamonds), p 193-199.

Sampaio, C H and Tavares, L M M (2005) *Beneficiamento gravimétrico: Uma introdução aos processos de concentração mineral e reciclagem de materiais por densidade* 1ª ed, Porto Alegre, UFRGS.

Schubert, H (1988) *Aufbereitung mineralischer Rohstoffe*, 1ª ed, Vol 4, Dt. Verl, für Grundstoffindustrie, Cap 13, Leipzig.

Straydom, H (2010) *The aplication of dual energy x-ray transmission sorting to the separation of coal from Torbanite*, PhD Thesis, Faculty of Engineering and the Built Enviroment, Univerty of Witwatersrand, Johanesburg.

Wotruba, H Knapp, H Neubert, K and Schropp C (2014) *Anwendung der sensorgestützten Sortierung für die Aufbereitung mineralischer Rohstoffe*, Chemie Inginieur Techik, 86 (6), 773-783.

SAMPLING TESTS OF METAL ACCOUNTING STREAMS IN ASSAREL CONCENTRATOR

M. Ranchev[1], L. Tsotsorkov[2], D. Nikolov[2], A. Angelov[2], T. Pukov[2], I. Grigorova[1] and *I. Nishkov[1]

[1] *University of Mining and Geology "St. Ivan Rilski"*
Department of Mineral Processing and Recycling
Prof. Boian Kamenov Street
1700 Sofia, Bulgaria
*(*Corresponding author: inishkov@gmail.com)*

[2]*ASSAREL-MEDET AD*
4500 Panagyurishte, Bulgaria

24th World Mining Congress
MINING IN A WORLD OF INNOVATION
October 18-21, 2016 • Rio de Janeiro /RJ • Brazil

SAMPLING TESTS OF METAL ACCOUNTING STREAMS IN ASSAREL CONCENTRATOR

ABSTRACT

Based on the results of the technological audit carried out in Assarel concentrator, a continuous industrial experiment has been conducted. Time-basis sampling procedure, in order to examine the influence of the cross-stream cutter aperture on the sampling representativeness of the final flotation tailings stream has been carried out. Moreover, a comprehensive monitoring program of the various conditions (mass flow rate, turbulence, clogging, segregation, etc.) occurring throughout the industrial experiment has been accomplished. In order to perform a more precise analysis of the obtained data and to determine the accuracy of the sampling procedure, a statistical technique such as standard deviation functions and relative differences between the sampling errors has been evaluated. In addition, a principle steps in establishing a sampling regime have been presented. Stand on the collected results and their statistical treatment the optimum technological parameters, such as sample cutter aperture and sampling interval have been evaluated.

KEYWORDS

Sampling interval, cross-stream cutter

INTRODUCTION

Sampling procedures cover the practice of selecting representative quantities of test material in the field, to evaluate bulk materials. Examples of the test materials are bulk granular solids, slurries, sludges, grains, and solid fuels. It is necessary to be able to sample bulk materials during shipment and during processing operations. Taggart (1945) defined sampling as: “The operation of removing a part convenient in size for testing, from a whole which is of much greater bulk, in such a way that the proportion and distribution of the quality to be tested (e.g. specific gravity, metal content, recoverability) are the same in both the whole and the part removed.”After the primary sampling stage, the increments taken by mechanical sampling system are usually processed on-line to reduce the sample mass that is taken back to the laboratory for final sample preparation and analysis. Primary increments are either processed individually or combined into sub-lot or gross sample in a number of stages of crushing, division and drying if necessary (Morrison et al., 2008).

Correct sampling means that all parts of the ore, concentrate or slurry being sampled must have an equal probability of being collected and becoming part of the final sample for analysis (Gy, 1982; Pitard & Gy, 1993), otherwise bias is easily introduced and the sample is not representative. The presence of bias is one of the main problems for metallurgical accounting, because it causes serious difficulties in reconciling production figures and does not average out over time (Holmes, 2004).

The normal practice when sampling a process stream is to divide the stream into “strata” of equal mass or time and then take increments with a sample cutter from a fixed point in mass or time within each stratum. This is called mass-basis and time-basis systematic sampling respectively. Alternatively, increments can be taken at random within each stratum on a mass or time basis, which is called, stratified random sampling. This alternative approach is recommended to eliminate possible bias when periodic variations in quality are suspected to be presented in the stream being sampled (Morrison et al., 2008).

At all sampling steps, the sampling correctness should be controlled by respecting the rules about sampling hardware and procedures provided by TOS (“Theory of sampling”), as this will eliminate the incorrect sampling errors, and simultaneously ensure unbiased samples. A benefit of this is that the general sampling variances will also be reduced. The choice of exactly which mechanical sampler or procedure to use is always dependent on the material to be sampled and rests heavily on experience, etc. Slurries, liquids and dusty gases need different equipment from particulate solids, but the principles are the same (Petersen, 2005).

Assarel-Medet is the largest Bulgarian open pit mining and copper ore processing company, and maintains a long history of implementing new technology and processing methods. The Assarel-Medet Mine is located in the Sashtinska Sredna Mountain in Bulgaria, 11 km northwest from the town of Panagyurishte, and 90 km east of the capital city of Sofia. Assarel concentrator processes over 14 million Mt. of copper porphyry ore per year.

In 2014, an official examination and assessment of the equipment, procedures and sampling practices applied in the concentrator of Assarel copper mine have been conducted. Based on the results and conclusions obtained during the technological audit the following recommendations have been proposed:

- Any contamination of the process slurry splitters and the cross-stream cutters should be avoided. An accidental "sludge" detachment (sticky material), which inevitably happen and its presence in the primary accounting samples, certainly will vitiate the measurement results;
- The appropriate dimensions of the primary sampling equipment (static multiple cutter device; crosscut samplers, etc.) sampling the main input and output process streams should be correctly established in accordance with continuously increasing plant capacity;
- Necessarily increase the width of the opening gap size of the linear cross-stream cutters for both process streams.
- In order to minimize the possible bias during the sampling procedures and to ensure that each increment carries the correct weighting and assay information, the following examination should be carried out:
- A detailed examination, in order to determine the optimal cutter aperture, corresponding to constantly variations in quality (Cu content, %) and flow rate of the process streams;
- A detailed examination, in order to identify the appropriate sampling interval, confirmed by precisely determined autocorrelation functions of the process streams parameters.

Improving the mechanical sampling practices and procedures, will ensure that representative sample is delivered in the laboratory, where the quality control and the metallurgical accounting of the processing plant have been carried out (Ranchev et. al., 2016).

In regards to the suggestions presented above, an additional experimental procedure covering the mechanical sampling of the final tailings and flotation feed streams with different cutter aperture have been implemented.

Due to the ongoing experimental procedure of the flotation feed stream, the aim of this article is to present the results and discussions from the first part of the industrial tests, and particularly the results from the sampling test of the flotation tailings stream, with 3.00 mm opening gap size (reference cutter aperture) of the first cross stream cutter and experimental – 5.00 mm; 7.00 mm and 9.00 mm of the second cross stream cutter.

METHODS AND MATERIALS

Sampling procedure

The experimental procedure include sampling the moving stream (flotation tailings stream) with two linear cross cut samplers, one of which is with 3.00 mm (reference size) opening size and the other is with the corresponding experimental size – 5.00 mm (I week – 30 min. sampling interval), 7.00 mm (II week – 30 min. sampling interval), 7.00 mm (III week -35 min. sampling interval) and 9.00 mm (IV week – 35 min. sampling interval).

The sampling interval and cutter speed have been complied with the requirements of the laboratory, where the collected shift samples are delivered for further preparation and analyses. The conditions of the sampling procedure are presented in Table 1.

Table 1 - Sampling procedure conditions

Sampling period	Cutter aperture		Sampling interval
	Reference cutter	Experimental cutter	

I week	3.00 mm	5.00 mm	30 min.
II week		7.00 mm	30 min.
III week		7.00 mm	35 min.
IV week		9.00 mm	35 min.

Figure 1 shows the design and aperture (A – 3.00 mm; B – 7.00 mm) differencesfor both cross stream cutters, during the sampling procedure of the final tailings stream.

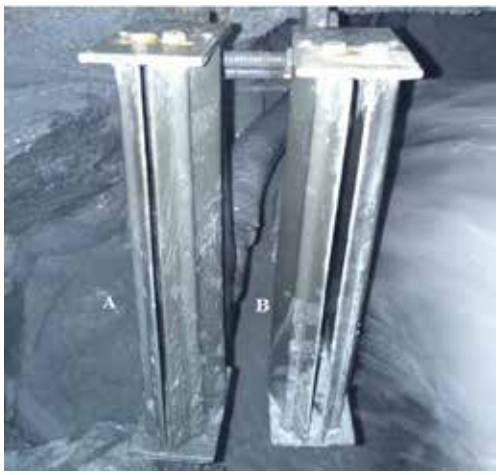

Figure 1 – Falling stream cutters (A – reference cutter; B – experimental cutter) sampling the final tailings stream

Chemical analysis methods

Atomic absorption spectrophotometry (AAS) and X-ray fluorescence spectroscopy (XRF) analysis have been used to determine the copper content in the extracted samples. The average results (Cu, %) from both analysis and the corresponding standard deviation (St. Dev.) measurements are presented in Table 2.

Particle size distribution

Screening tests were performed using Fritsch's Vibratory Sieve Shaker "Analysette 3 Pro". In fact, the size fractions -100 μm and +200 μm, were selected because these are the critical fractions monitored by the on-line slurry particle size analyzer right after the grinding circuits. In Table 3 are presented the average percentage content of fractions -100 μm and +200 μm and the corresponding standard deviation measurements in the extracted samples during the sampling procedures.

Statistical data analysis

As a measure of the sampling error the standard deviation functions (St. Dev.) have been estimated and presented in the "Results and discussion" section below. In order to identify more clearly the sampling error as percentage difference between the St. Dev. values of the reference (3.00 mm) and the experimental (5.00; 7.00 and 9.00 mm) cutter aperture, the estimated relative differences have been presented. The relative differences are obtained by dividing the estimated St. Dev. value of the set of data for the reference cutter by the St. Dev. value of the set of data for the experimental cross stream cutter:

$$\Delta_{SD} = \frac{\text{St. Dev 3.00 mm}}{\text{St. Dev (5.00; 7.00; 9.00 mm)}} \cdot 100, \% \quad (1)$$

Results and discussion

The following tables represent the summarized results from the estimated statistical data, obtained during the sampling procedures. Tables 2 and 3 show the results from the chemical and particle size distribution analysis, respectively.

Table 2 - Summarized sampling results from the performed chemical analysis

Sampling period	I week (21 shifts) 30 (min.) sampling interval				II week (21 shifts) 30 (min.) sampling interval				III week (21 shifts) 35(min.) sampling interval				IV week (21 shifts) 35(min.) sampling interval			
Assay	XRF		AAS		XRF		AAS		XRF		AAS		XRF		AAS	
Aperture, mm	3.00	5.00	3.00	5.00	3.00	7.00	3.00	7.00	3.00	7.00	3.00	7.00	3.00	9.00	3.00	9.00
Average Cu, (%)	0.049	0.053	0.049	0.051	0.050	0.053	0.050	0.051	0.052	0.052	0.052	0.050	0.055	0.057	0.054	0.054
St. Dev	10.90	7.76	5.42	5.66	8.97	5.45	8.39	6.16	11.48	7.50	10.38	8.59	12.88	10.85	12.68	10.89
Δ_{SD} Relative differences	28.79		-4.45		39.20		26.59		34.66		17.22		15.77		14.16	
	1		2		3		4		5		6		7		8	

Figures 2 and 3 show the relative differences of the standard deviation values (Δ_{SD}), between the average results from the chemical and sieve size analysis data, respectively obtained during the sampling procedures of the cross-stream cutters.

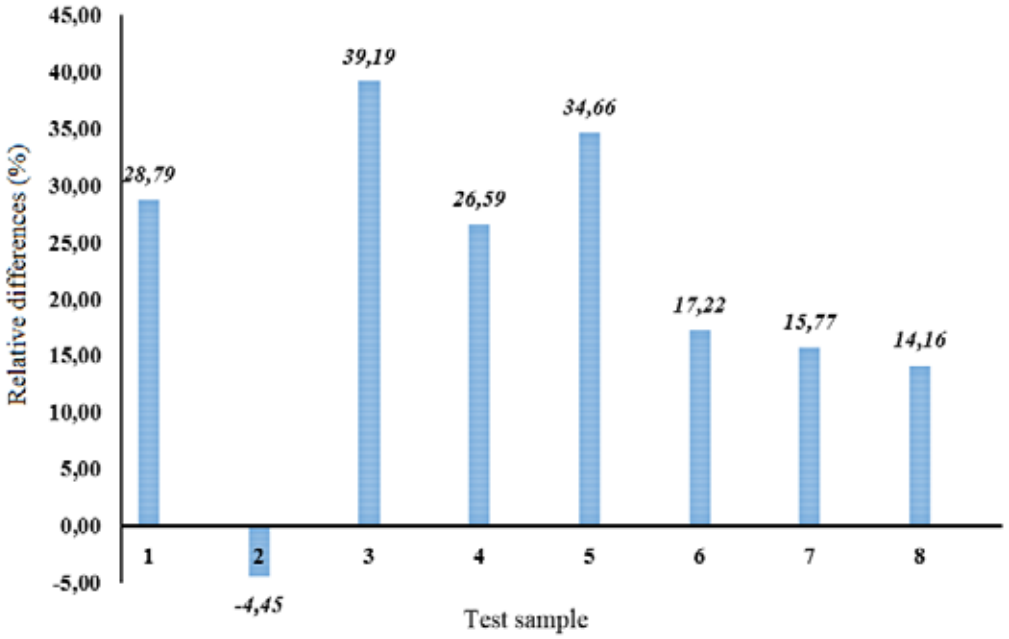

Figure 2 –Relative differences of the St. Dev. values of the average chemical analysis results

Table 3 - Summarized sampling results from the performed particle size distribution analysis

Sampling period	I week (21 shifts) 30 (min) sampling interval				II week (21 shifts) 30 (min) sampling interval				III week (21 shifts) 35(min) sampling interval				IV week (21 shifts) 35(min) sampling interval			
Sieve size	- 100 (μm)		+200 (μm)		- 100 (μm)		+200 (μm)		- 100 (μm)		+200 (μm)		- 100 (μm)		+200 (μm)	
Aperture, mm	3.00	5.00	3.00	5.00	3.00	7.00	3.00	7.00	3.00	7.00	3.00	7.00	3.00	9.00	3.00	9.00
Average, (%)	78.49	74.88	5.56	6.96	74.89	74.83	6.50	6.60	72.25	73.46	8.01	7.44	71.78	72.72	8.51	7.98
St. Dev.	3.16	2.38	20.52	11.73	3.62	1.91	17.84	10.58	3.78	3.39	18.56	19.15	3.51	2.35	12.78	11.46
Δ_{SD} Relative differences	24.41		42.80		47.45		40.67		10.24		-3.14		32.79		10.38	
	1		2		3		4		5		6		7		8	

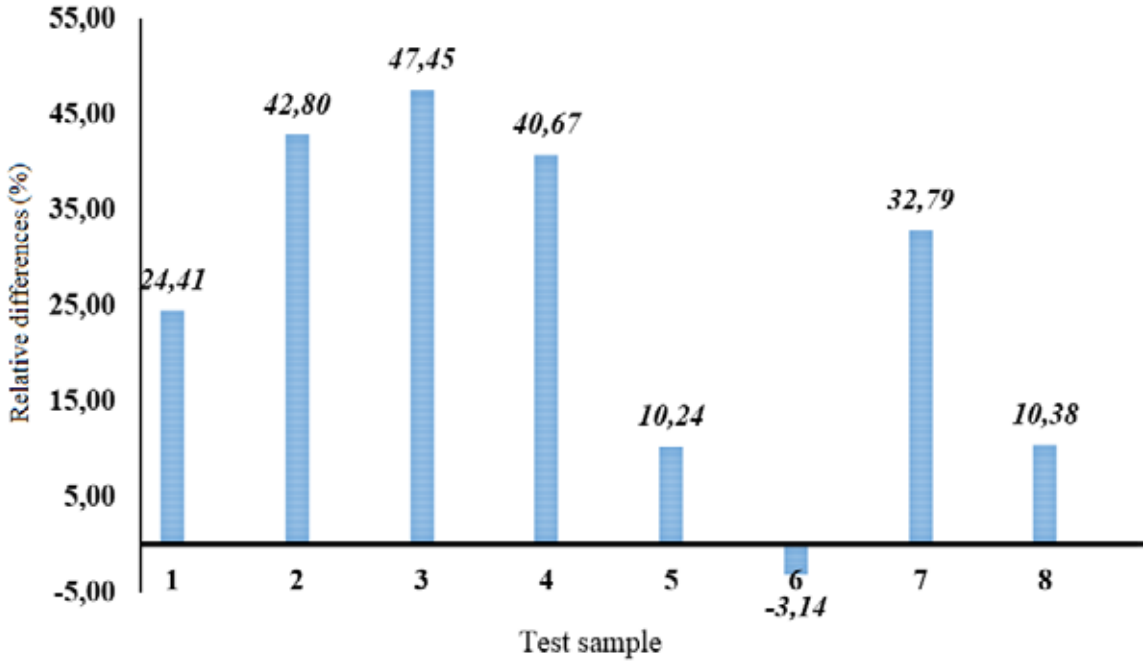

Figure 3 - Relative differences (Δ_{SD}) between the average particle size distribution results

Observing the results from the XRF and AAS chemical analyses for the first two experiments with cutter aperture 3.00/5.00 mm and 3.00/7.00 mm with 30 minutes sampling interval and the second series of experiments with 3.00/7.00 and 3.00/9.00 mm and 36 min. sampling interval respectively, the following statements could be made:

For the assessment of the sampling error – the standard deviation function, a significant difference for the XRF data analysis in the first series (3.00 and 5.00 mm) of experiments has been observed – 10.90 and 7.80 %, respectively. For the opening gaps of 3.00 and 7.00 mm in the second series of experiments (II week), the differences in the sampling errors indicate a decrease of about 39 %. In addition, the decrease in sampling error according to the AAS analysis is around 27 %.

In the next series of experiments with 35 minutes sampling interval (III week) the sampling error for the 7.00 mm cutter aperture has a value of approximately 35 % lower for the XRF analysis and about 18 % decrease for the AAS test results, compared to the reference aperture – 3.00 mm.

The last experiment (IV week) with cutters aperture 3.00 and 9.00 mm, respectively and 35 minutes sampling interval, the tendency of reducing the error from the wider opening size is clearly defined (about 16 and 14 % for both chemical analysis).Considering all aspects of the experimental results, regarding the chemical analysis, there is only a difference in the first AAS analysis for the 3.00 and 5.00 mm cutter aperture. In the sequence of the industrial series, the tendency of the experimental error reduction occurs in the following order: 3.00 – 5.00 – 7.00 mm, both for AAS and XRF average results.

It could be assumed that the expansion of cutter aperture, the increasing of the sampling interval and as well as the time distance of the individual series, definitely affects the statistical correlation, which increases the suspicious about the correctness of the assessments. However, for the estimated average values of the fractions -100 and +200 μm and the standard deviation functions, as an assessment of the sampling error, the following comments could be made:

- For the fine fraction -100 μm the reduction of the sampling error by increasing the aperture size could be observed in the following order – 3.00; 5.00 ; 7.00 mm at 30 min. sampling interval. While at 35 min. sampling interval the estimated standard deviations of the reference (3.00 mm) and the experimental (7.00 and 9.00 mm) cross-stream cutters, show a slight increase at 7.00 mm (St. dev. 3.39 %) aperture, which on the other hand decreases for the 9.00 mm (2.35 %) opening size;

- For the coarse fraction +200 μm, which has relatively low mass recovery and the sampling error assessments are undoubtedly much higher, the estimated error decreases almost twice at the 30 min. sampling interval and in the following sequence 3.00, 5.00 and 7.00 mm. On the other hand, at 35 minutes sampling interval the same abnormality as well as in the fraction -100 μm could be observed.

Decreasing the sampling error at cutter apertures 3.00 – 5.00 mm with 24 % and for the 3.00 – 7.00 mm with 47 % being the tendency in the relative differences in the standard deviation functions for fraction -100 μm at 30 min. sampling interval. Once again, the tendency during the 35 min. sampling interval indicated above, shows that the sampling error decreases with 10 % at 3.00 / 7.00 mm experimental sizes and increases up to 33 % for the 3.00/9.00 mm cutter apertures. For the fraction +200 μm the assessment error differences for the obtained results, decreases almost twice for the first week of the experimental procedure (3.00/5.00 mm). The tendency continues during the II week of the experiments, as the estimated error decreases with approximately 40 % (7.00 mm). At 35 minutes sampling interval the assessments of the sampling error for the 3.00/7.00 and 3.00/9.00 mm cutter apertures have an insignificant variation.

CONCLUSION

Based on the detailed analysis presented above, the following summarized conclusions could be made:

- For more than 30 minutes sampling interval the tendency of changing the value of the error assessment, for both copper content assays (XRF and AAS) and particle size distribution analysis, decreases significantly;
- The behavior of the particles (-100μm; +200μm) during the separation of the final sample in the cutter it is affected not only from the cutter aperture, but also from the flow rate and the nature of the stream motion.
- An absence of laminar flow conditions of the final tailings stream during the sampling procedures has been observed.

The obtained experimental results and the subsequent statistical treatment of the collected data showed regularity in expanding the cutter aperture from 3.00 to 7.00 mm and do not exceeded30 min. sampling interval, which is in a good agreement with the best practices and recommendations around the world. The second part of the industrial experiments covering the sampling procedures of the flotation feed stream is currently ongoing with reference (2.00 mm) and experimental (4.00; 6.00 and 8.00 mm) cross-stream cutter apertures and various sampling intervals from the range of 20 to 30 minutes.

ACKNOWLEDGEMENTS

Financial support for these studies and permission to publish this paper from ASSAREL-MEDET JSCis gratefully acknowledged.

REFERENCES

Gy, P. (1982). *Sampling of particulate materials, theory and practice*. 2nd Edition, Elsevier

Holmes, R. J. (2004). Correct sampling and measurement – The foundation of metallurgical accounting, *Chemometrics and Intelligent Laboratory Systems, 74,* 71-83.

Morrison, R., Wortley, M., Holmes, R., Randolph, N., & Dunglison, M. (2008). *An introduction to Metal Balancing and Reconciliation.* (ed.) Morrison, R. D. Julius Kruttschnitt Mineral Research Centre Monograph Series #4, pp. 141 - 170.

Petersen, L., Minkkinen, P., & Esbensen, K. (2005). Representative sampling for reliable data analysis: Theory of Sampling. *Chemometrics and Intelligent Laboratory Systems, 77,* 261– 277.

Pitard, F., Gy, P.(1993).*Sampling Theory and Sampling Practice*. 2nd edition, CRC Press, Florida.

Ranchev, M., Tsotsorkov, L., Nikolov, D., Angelov, A., Pukov, T., Grigorova, I., & Nishkov, I.(2016). Representative sampling – the way to the precise metal accounting,*Twenty-fourthWorld Mining Congress*, Rio de Janeiro (Brazil), October 18-21, in press.

Taggart, M.(1945)*Handbook of Mineral Dressing*. Section 19, Wiley.

SILO DESIGN CODES: RECOMMENDATIONS FOR A BRAZILIAN STANDARD

* John Carson[1] and Rogério Ruiz[2]

[1] *Jenike & Johanson, Inc.*
400 Business Park Drive, Tyngsboro, Massachusetts 01879 USA
(Corresponding author: jwcarson@jenike.com)*

[2] *Jenike & Johanson Ltda.*
Rua Monteiro de Barros, 513, Vinhedo/SP, 13.280-000, Brazil

24th World Mining Congress
MINING IN A WORLD OF INNOVATION
October 18-21, 2016 • Rio de Janeiro /RJ • Brazil

SILO DESIGN CODES: RECOMMENDATIONS FOR A BRAZILIAN STANDARD

ABSTRACT

In a recent publication, one of the authors discussed the limits and contradictions of the four most common codes in use in the world today: BS EN 1991-4:2006; ACI 313-97; ANSI/ASAE EP433 JUN2000 (R2015); and AS 3774-1996. There is no Brazilian standard that covers this subject in detail and, in the best case, local engineering firms and manufacturers adopt either one of the above or ISO 11697:1995. The limitations of these standards, the inconsistency between them, and the lack of a Brazilian regulatory code, leave room for subjective interpretation, resulting in poor and perhaps even unsafe designs. The authors present a comparison between the above codes and the conditions that are not covered by them. The result is a valuable source of information for code users, and more importantly, guidelines for Brazilian code writers so that they can develop their own standard without the same flaws and inconsistencies of the existing ones.

KEYWORDS

Silo design codes; solids-induced loads; structural design

INTRODUCTION

Silos for storing and handling bulk materials are common in virtually every industry including the mining industry, where silos for iron ore, bauxite, concentrates, pellets, etc. are common. (NOTE: Various terms are used to describe a container for bulk solids, such as bin, silo, tank, bunker, vessel, elevator, etc. Since none of these terms has a commonly accepted definition, they are used interchangeably in this paper.) In order to design such equipment, the engineer must consider both its functional requirements as well as its structural integrity under expected operating conditions.

The solids-induced loads that act on the walls and internals of bins and silos are not easily determined or understood. As a result, these structures fail with a frequency that is much greater than almost any other industrial structure. Sometimes the failure only involves distortion or deformation that, while unsightly, does not pose a safety or operational hazard. In other cases, failure involves complete collapse of the structure with accompanying loss of use and even loss of life. (Carson, 2000)

Given the importance of determining silo loads, the obvious question is, “Why isn’t this better understood?” Part of the problem lies in the lack of training in this subject. Many engineers when faced with the need to analyze a container storing a bulk solid wrongly assume that a flowing bulk material behaves like a flowing liquid. Nothing could be further from the truth! Solid particles can transfer shear stresses between each other and between themselves and silo walls even if there is no relative motion between them. In addition, the magnitude of these shear stresses is, for most bulk solids, independent of shear strain rate or velocity. Solids can form stable pile surfaces and sometimes stable flow interruptions known as *arches* and *ratholes*. Fluids do not exhibit such behavior. Therefore, using a fluids-based approach to calculate silo loads is doomed to produce unrealistic values. For example, a silo containing a fluid will have the highest wall pressure at the bottom, whereas the same vessel storing a bulk solid will almost always have the highest wall pressure somewhere near its mid-height.

HISTORY OF SILO CODES

Various attempts have been made over the last 50 years to codify solids-induced pressures acting on silo walls. The first code to provide helpful rules for calculating silo loads, German Standard DIN 1055 Part 6 “Design loads for buildings: Loads in silo bins”, was developed based on extensive testing performed by Pieper and Wenzel (1964). This standard, which was first published in 1964, has

been significantly revised and reissued twice -- 1987 and 2005. Other groups in other countries have codified solids-induced silo wall pressures, and this process continues today.

Various terms are used to describe these documents: Standard, Code, Guidelines, Recommended Practice, Engineering Practice, etc. Documents titled "Code" or "Standard" require compliance, whereas those titled "Recommended Practice", "Guidelines" or "Engineering Practice" might be considered recommendations only, not requiring mandatory compliance. While that may be true in a strict legal sense, this does not absolve an engineer from responsibility for what should be his/her primary focus: safety, regardless of pressure that may come from clients or others. Safety, and then economy, must determine the design.

For practical purposes, "Guidelines", "Recommended Practices" and "Engineering Practices" should be considered minimum mandatory standards. In other words, an engineer has the right to exercise independent engineering judgment when creating a design, and he/she may even go back to first principles. However, if a problem occurs and the engineer is required to justify the design, there will be a strong presumption against the engineer that will be very difficult to overcome in most cases if the engineer has not at least considered all applicable "Guidelines", "Recommended Practices" and "Engineering Practices". (Samuels, 2001)

SILO DESIGN CODES COVERED IN THIS PAPER

The focus of this paper is limited to the five most commonly used silo design codes in the world today. Other, specialized codes exist, but, to the authors' knowledge, they are not in general use.

BS EN 1991-4:2006 "Eurocode 1 – Actions on structures – Part 4: Silos and Tanks"

Adopted by the European Committee for Standardization (CEN) in October 2005, this is the most modern and complete silo design code in use today. It is commonly called "the Eurocode", although that is like referring to "the ASTM Standard" as if there is only one. The formal designation for the English version of this code, which was published in May 2006, is British Standard BS EN 1991-4:2006 "Eurocode 1 - Actions on structures - Part 4: Silos and Tanks". A German standard was produced from a late draft of this standard and published as DIN 1055-6:2005-03 "Actions on structures – Part 6: Design loads for buildings and loads in silo bins" in March 2005. DIN EN 1991-4: 2010-12, which is essentially a German translation of the British Standard, has superseded the previous version.

BS EN 1991-4:2006 exploits extensive European research on silos starting in the mid-1970s. It was extensively reviewed by civil, mechanical and chemical engineering specialists before it was adopted, and it is widely recognized as most advanced standard of its kind in the world.

This code divides silos into three classes – from simple, small structures (Action Assessment Class 1) to large and/or complex structures (Action Assessment Class 3). These distinctions permit appropriate procedures to be used for given conditions, and they eliminate debates on complexity vs. dangerous over-simplifications.

Silos are further classified by aspect ratio h_c/d_c, where h_c is the height of the cylindrical section from the cylinder/hopper intersection to the centroid of the top pile, and d_c is the cylinder diameter:

- Slender ($h_c/d_c \geq 2$)
- Intermediate slenderness ($1 < h_c/d_c < 2$)
- Squat ($0.4 < h_c/d_c \leq 1$)
- Retaining ($h_c/d_c \leq 0.4$)

Each geometry has special loading features with different conditions being critical for design, and each class blends smoothly with the next.

Design conditions depend on silo geometry, the stored bulk solid, and conditions of filling and discharge. This is the first silo design code to identify so many different conditions and regulate how each should be treated. It allows careful identification of requirements according to safety implications.

This code recommends that the three key material properties (μ, coefficient of wall friction between the stored bulk solid and the wall surface, γ, bulk density, and k, lateral pressure ratio) be determined by tests, which are detailed in Annex C. Recognizing that variations occur when the same bulk solid is tested repeatedly, the code recommends a procedure by which upper and lower characteristic values can be obtained.

Eccentric loads cause more silo failures than any other condition, and this is the first standard to provide rational treatment of this phenomenon, adopting the simple model proposed by Rotter (1986, 2001). The complexity of treatment depends on the Action Assessment Class, with "patch loads" used to deal with smaller eccentricities.

This is the first code to recognize and fully treat the fact that characteristic actions for different parts of a silo are controlled by different ends of the statistical distribution of values of properties of the stored bulk solid. When calculating maximum lateral pressures in a silo's cylindrical section, a combination of minimum coefficient of wall friction, μ, with maximum lateral pressure ratio, k, is specified. This calculation is what usually dictates silo wall thickness when hoop tension governs, e.g., a thick-walled silo. On the other hand, if vertical buckling dictates wall thickness (such as for a thin-walled metal silo), a combination of maximum coefficient of wall friction with maximum lateral pressure ratio is used, since this results in maximum frictional drag. As a result, a significant reduction in empirical over-pressure factors is possible.

ACI 313-97 "Standard practice for design and construction of concrete silos and stacking for storing granular materials"

The current version of this publication by the American Concrete Institute (ACI) was adopted in January 1997. Unlike BS EN 1991-4:2006 which has broad applicability, this document is focused solely on methods to calculate pressures exerted on the walls of concrete silos, although one could argue that the calculation methods – but not the values used in the equations – should be independent of a silo's material of construction.

Consistent with BS EN 1991-4:2006, this publication correctly recognizes that the three key bulk solid properties almost always vary for a given bulk solid, and that this variation should be taken into account depending on the calculations that one is performing. In all cases bulk density is to be taken at its maximum value, since solids-induced pressures and shear stresses vary linearly with bulk density. The coefficient of wall friction is determined by test or reference to tabulated values.

In an attempt to cover the many unknowns when calculating silo wall pressures, the writers of this publication specify the use of a large factor-of-safety, specifically: *"4.4.2.2 Concentric flow -- The horizontal wall design pressure above the hopper for concentric flow patterns shall be obtained by multiplying the initial filling pressure ... by a minimum over-pressure factor of 1.5".*

Eccentric loads are treated poorly, providing practically no guidance to the design engineer: *"4.4.2.3 Asymmetric flow -- Pressures due to asymmetric flow from concentric or eccentric discharge openings shall be considered".* The Commentary provides little additional guidance on this topic: *"R4.4.2.3 Asymmetric flow can result from the presence of one or more eccentric outlets or even from non-uniform distribution of material over a concentric outlet. Methods for evaluating the effects of asymmetric flow have been published. None of these methods has been endorsed by the Committee".* Thirteen publications are referenced.

Unlike BS EN 1991-4:2006, which includes patch loads to cover non-uniform silo wall pressures that are known to develop even in silos with concentric fill and discharge (Ooi, Pharm & Rotter, 1990), ACI 313-97 makes no mention of patch loads.

As with almost all silo design codes, this publication includes a table of example physical properties of common bulk solids. However, Table 4-A in this Standard Practice's Commentary is

more simplistic and therefore more dangerous than most. For example, the value given for coefficient of wall friction for bituminous coal against steel is a single value, 0.3. There is no indication of the type of steel (e.g., carbon steel or stainless steel) or its surface finish (hot rolled, cold rolled, polished, corroded, etc.), nor any suggestion that the coal's moisture, ash or other variables have any effect on wall friction. The footnote to this table states: "*The properties listed here are illustrative of values which might be determined from physical testing. Ranges of values show variability of some materials. Design parameters should preferably be determined by tests and the values shown used with caution"*. While meant to provide a warning to the reader, this footnote is easily overlooked.

ISO 11697:1995 - Bases for design of structures -- Loads due to bulk materials

ISO 11697 was prepared by the Technical Committee ISO/TC 98, *Bases for design of structures*, Subcommittee SC 3, *Loads, forces and other actions* and last reviewed in 2015.. The scope of this code is limited to a narrow range of applications, with dynamic effects excluded and eccentricities of filling and discharge limited to less than one-quarter the silo cylinder's diameter. Action Assessment Classes are not defined. Instead, this standard states that it can be used for the design of any silo smaller than 50 m in diameter and 100 m high provided the cylinder height-to-diameter ratio is no greater than 10.

The methodology for calculating hopper loads is claimed to be applicable for any hopper provided that its walls are inclined at 20° or more from horizontal. There is no differentiation between conical and planar hopper geometries. A "kick pressure" is added for mass flow hoppers.

Tables of material properties are presented (Tables 1 and 2 in this code) for ten materials. These tables are more dangerous than most, since, for example, "coal" is listed with no further distinction (e.g., "bituminous") Table 1 in the code presents mean values of wall friction coefficient said to be applicable for any smooth surface (e.g., carbon steel, stainless steel, aluminum or even plastic). For rough surfaces (e.g., concrete), 0.1 is added to the tabulated values. Other properties (i.e., bulk density and lateral pressure ratio) are also tabulated. Factors of 0.9 and 1.15 are applied to wall friction coefficients and lateral pressure ratios to account for inherent variability of bulk material properties.

For designs that require "a more accurate description of the material parameters or if materials other than those listed in Table [2] are to be stored, appropriate values of material parameters may be obtained by testing" using the methodologies described in Section 5 and Annex A .

ANSI/ASAE EP433 JUN2000 (R2015) "Loads exerted by free-flowing grain on bins"

The latest version of this Engineering Practice was adopted by the American Society of Agricultural Engineers (ASAE) in December 1988 and approved by the American National Standards Institute (ANSI) in September 1991. It was reaffirmed yearly thereafter and revised editorially by ASAE in March 2000. The current version was reaffirmed by ANSI in December 2015.

As its title indicates, this publication was developed solely for vessels storing free-flowing, agricultural whole grains. Furthermore, its application is limited to a silo flow (i.e., discharge) pattern classically called *funnel flow*, although in this document that term is restricted to a flow pattern in which the flow channel does not intersect the cylinder wall. (See discussion below concerning flow patterns.) This publication states, "Funnel flow will normally occur in bins which have H/D ratios less than 2.0", where H is the total height of material from lowest point of discharge, i.e., including hopper section, to one-third height of pile surcharge at the top surface, and D is bin diameter. It should be noted that, if the flow channel were to open up more than about 14° (from vertical), the condition of *funnel flow* would no longer occur, since the flow channel would intersect the cylinder wall. This document calls this condition *plug flow* and specifies that an over-pressure factor, F, equal to 1.4 be used when calculating silo wall pressures.

For coefficient of wall friction a simplistic table of values similar to that in ACI 313-97 and ISO 11697:1995 is included, but the numbers are different as shown in Table 1:

Table 1 - Tabulated coefficients of wall friction for grain on two different wall surfaces

Wall Surface	ANSI/ASAE EP433 2011, Table 1	ACI 1997 Table 4-A	ISO 11697:1995, Table 1
Steel	0.3	0.26 – 0.42	0.3 – 0.5
Concrete	0.4	0.29 – 0.47	0.4 – 0.6

This publication is limited to silos that are centrally filled and discharged, so eccentric loads are not included. Patch loads are also not included, even though it is well recognized that non-uniform wall pressures develop during symmetric fill and discharge.

AS 3774-1996 "Loads on bulk solids containers"

The first Australian publication on solids-induced pressures on silo walls was titled "Guidelines for the assessment of loads on bulk solids containers". It was published in 1986 by a working party on bins and silos of the Australian Institution of Engineers' National Committee of Structural Engineering. This was followed by Australian Standard AS 3774, which was first published in 1990 and then revised in 1996. This standard can be considered one of the precursors of BS EN 1991-4:2006, since Michael Rotter was the lead author of both documents.

Unlike BS EN 1991-4:2006 this standard does not include Action Assessment Classes, but it does include upper and lower characteristic values of key material parameters. It includes four classifications of loads (dead loads, normal service loads, environmental loads and accidental loads) and a table describing load combinations that must be considered. Some often-overlooked conditions such as permissible geometric deviations in silo geometry and effects of wall flexibility are described.

Even though it includes methods to calculate wind and seismic loads, this is perhaps best handled using the most up-to-date general design code such as the Universal Building Code (UBC).

LOAD CONDITIONS

Table 2 summarizes various load conditions covered by these five codes.

Table 2 - Load conditions covered by various codes

Load condition	EN 1991-4 2006	ACI 313-97	ISO 11697 1995	ANSI/ASAE EP433-1988	AS 3774 1996
Hopper geometry					
-Symmetric single cone	Yes	Yes	Yes	Yes	Yes
- Square pyramid	Yes	No	No	No	Yes
- Wedge with vertical end walls	Yes	No	No	No	Yes
Fill and discharge conditions					
- Patch loads	Yes	No	Yes	No	No
- Eccentric fill and discharge	Yes	Poorly	Poorly	No	Yes
- Mass flow	Yes	No	Yes	No	Yes
- Funnel flow					
- Pipe/Internal flow	Yes	Yes	Yes	Yes	Yes
- Mixed flow	Yes	No	Yes	Yes	No
- Expanded flow	No	No	Yes	No	No
- Impact loads on filling	No	No	No	No	Yes
- Silo quaking	No	No	No	No	No
Internals	No	No	No	No	Yes
Thermal ratcheting	Yes	No	No	Yes	Yes
Grain swelling	No	No	No	Yes	Yes
Effects of gas pressures					
- Completely fluidized contents	Yes	Yes	Yes	No	Yes
- Partially fluidized contents	No	No	No	No	No
External equipment	No	No	No	No	Yes

Hopper geometries

Only a few, common hopper geometries are covered by all five codes. In industrial practice many other hopper geometries are commonly used, including transition, chisel, non-symmetric pyramid, wedge with non-vertical end walls, asymmetric cone, multiple hoppers joined together one above the other (e.g., a cone below another cone, etc.), see Figure 1. None of these geometries is covered by any of these codes. BS EN 1991-4:2006 notes that there are problems in some of these cases, but it simply requires a rational analysis be used in addressing them.

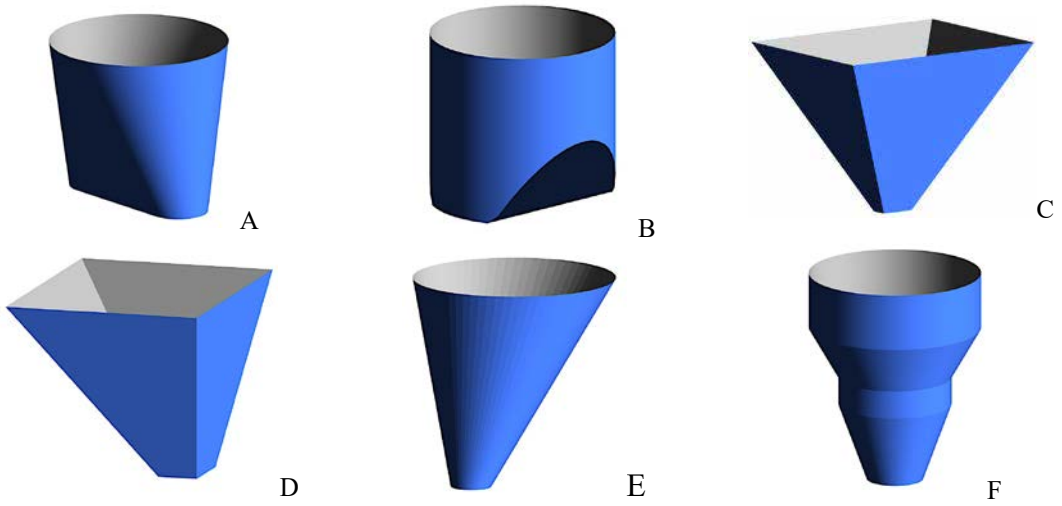

Figure 1 - (A) transition hopper; (B) chisel hopper; (C) wedge hopper with converging end walls; (D) non-symmetric pyramid; (E) asymmetric cone; (F) multi hopper

Patch loads

Even the simple case of symmetric fill and discharge involves accidental asymmetries that can result in non-uniform pressures around the circumference of a silo (Nielsen, 1996; Zhong, Ooi & Rotter, 2001). BS EN 1991-4:2006 and ISO 11697:1995 handle this issue by requiring use of patch loads.

Flow patterns

Codes BS EN 1991-4:2006, AS 3774-1996, and ISO 11697:1995 cover the flow pattern called *mass flow,* which occurs when a silo's hopper walls are sufficiently low in friction and steep so that all the material is in motion whenever any is withdrawn.

Funnel flow occurs with less steep and/or less frictional hopper walls. As a result, some of the material remains stagnant while the rest (directly over the outlet) is flowing. These five codes use somewhat different terms to describe this flow pattern. BS EN 1991-4:2006 and AS 3774-1996 use the term *mixed flow* to describe the condition of the flow channel intersecting the silo wall, whereas ANSI/ASAE EP433 calls this *plug flow*. BS EN 1991-4:2006 and AS 3774-1996 use the term *pipe flow* to describe the condition when the flow channel does not intersect the silo wall, whereas ISO 11697:1995 calls this *internal flow* and ANSI/ASAE EP433 calls it *funnel flow*.

Only ISO 11697:1995 mentions *expanded flow*, which is a combination of mass flow and funnel flow. However, that code does not provide any guidance on calculation of loads at the transition between the funnel flow and mass flow regions.

Internals

Structures are often placed within a silo in an attempt to alter the flow pattern, facilitate introduction of a gas into the bulk solid for processing, heating, cooling, etc., reduce pressures on silo walls, or to reduce loads on the outlet region. These structures include so-called Chinese hats, cone-in-cone inserts, and cross beams as shown in Figure 2. Loads on such internal structures can be extremely high, and many have failed or caused the silos in which they are located to fail. Only AS 3774-1996 addresses loads on such internals, but the calculations are rather simplistic and do not include the effects of internals on the silo wall. BS EN 1991-4:2006 identifies these problems and requires a rational analysis to be used in addressing them.

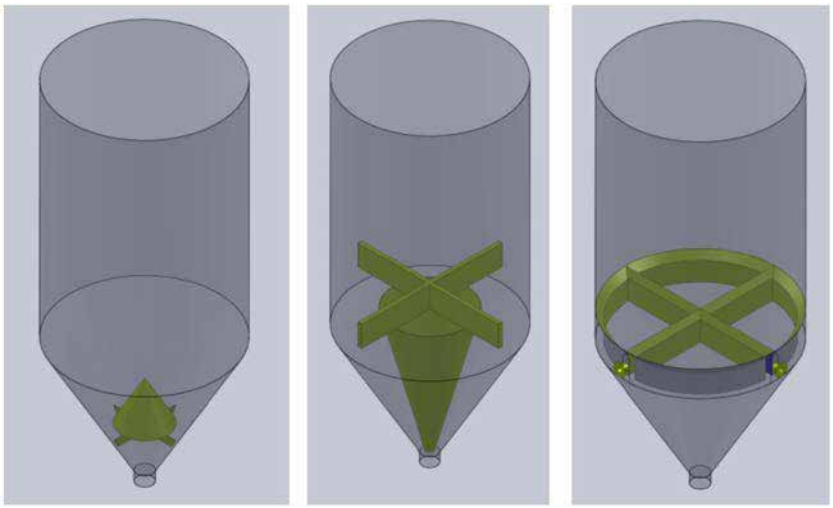

Figure 2 – From left to right: Chinese hat insert; Binsert ; and J-Purge cross beams

Anti-dynamic tubes are sometimes used to convert a silo's flow pattern to last-in-first-out, thereby eliminating pressure increases on silo walls that develop during discharge. Only ANSI/ASAE EP433 covers the loads acting on such tubes.

Material properties

All five codes start with the premise that the stored bulk solid is free flowing. Unfortunately many bulk solids handled and stored in industrial plants are not in this category. BS EN 1991-4:2006, AS 3774-1996, and ISO 11697:1995 note that they can be used when "the stored solid can be guaranteed to flow freely within the silo container as designed", but neither ACI 313-97 nor ANSI/ASAE EP433 provides any guidance on how to design storage vessels for non-free-flowing bulk solids. .

All five codes recommend that the stored material's relevant properties be determined by tests, if possible. Nevertheless, they all provide a table of typical values. These must be used with caution, particularly the tables in ACI 313-97, ANSI/ASAE EP433 and ISO 11697:1995, as noted above. All codes except ISO 11697:1995 warn against over-reliance on tabulated values, but the warnings can be easily overlooked. ISO 11697:1995 recommends testing only when the design requires more accurate properties or when the material is not listed in its table.

Thermal ratcheting

Thermal ratcheting is a condition in which successive temperature cycles cause increasing pressures on metal silo walls. Metals have a higher coefficient of thermal expansion than bulk solids, and metal silo walls react more quickly to ambient temperature changes than the stored bulk solid. Thus metal walls expand with increasing temperature, and the stored material settles (assuming no discharge). When the ambient temperature drops, the walls attempt to contract, but the bulk solid can only be pushed upward to its previous level if the direction of wall friction between the walls and bulk solid is reversed. This is impossible, so stresses within the wall increase significantly (Carson, 2000), and the phenomenon continues ("ratcheting") with each succeeding temperature cycle.

ANSI/ASAE EP433 provides an estimate of this effect on silo walls in 4.4.1 but notes in the Commentary that this estimate is based on laboratory studies using model circular silos fabricated from steel. It states that qualitative results collected from full size silos are available in the literature, but that "quantitative results needed for design purposes are not available from large silos".

AS 3774-1996 and BS EN 1991-4:2006 cover this phenomenon much more completely than ANSI/ASAE EP433, while ACI 313-97 and ISO 11697:1995 do not address it at all.

Grain swelling

This is a known cause of a number of silo failures. ANSI/ASAE EP433 notes in 4.4.2.1 that "moisture increases during storage of 4% or more can cause lateral pressures to increase several times static load conditions." It notes in the Commentary: *"5.4.2 Stored grains are hygroscopic; that is, they absorb moisture from liquid sources and from the atmosphere. When grains absorb moisture, they expand. When grains are confined within a structure, the expansion is restrained. The consequence is an increase in bin wall pressure".*

It notes that data in the literature on this subject is limited in number and scope, but that some studies have reported that lateral pressures increased by a factor of six as grain moisture increased by 4%, and by a factor of ten for a 10% increase in grain moisture content (Rotter, 1983).

AS 3774-1996 also covers this phenomenon, but none of the other three codes covers it.

Effects of gas pressures

Sometimes gas is added to storage vessels to cause or suppress chemical reactions, cool or heat the bulk solid, etc. If sufficient gas is added, a completely fluidized condition develops, and the wall pressures change to essentially hydrostatic. ACI 313-97, BS EN 1991-4:2006, AS 3774-1996, and ISO 11697:1995 provide guidance on this condition.

If less gas is added, the effect is not as dramatic as a fluidized column, but the wall loading can certainly be affected in a major way. Sometimes the entire vessel is operated at above-atmospheric pressure, while at other times it is close to atmospheric but differential gas pressures are present. None of the five codes addresses such conditions.

External equipment

External equipment such as electric or pneumatic vibrators, vibrating bin dischargers (bin activators), localized aeration devices, and air cannons impart significant forces to a silo structure that must be taken into account. They can also affect the stored bulk solid in such a way that its properties change, resulting in different silo loads. AS 3774-1996 provides some limited guidance on this phenomenon, but it does not cover loads acting on external equipment itself by the stored bulk solid. The other four silo design codes do not cover this at all.

Feeders and gates are also critical to a safe and properly functioning silo. AS 3774-1996 provides guidance regarding loads imposed on them, but the other four codes do not.

CONCLUSIONS

Knowledge of the loads applied to the walls and internals (if any) of a silo is extremely important. Such loads must not be ignored if a stable, safe silo is to be designed.

Much progress has been made in the last 50 years in providing silo load guidance to design and structural engineers. BS EN 1991-4:2006 is a significant advance over all previous codes, but even it does not cover many common load cases.

For load cases not covered by the codes, the design/structural engineer is left with two choices:

- Be extremely conservative in estimating applied loads. This approach can be quite expensive and yet still may not be conservative enough to prevent problems.
- Rely on design engineers who have significant experience in calculating silo loads.

Hopefully the information presented herein will be useful to Brazilian code writers so that they will be able to develop their own standard without the same flaws and inconsistencies of the existing ones. A well-written Brazilian standard will not only provide guidance for silo designers, but also allow regulatory agencies to inspect and impose a methodology that ensures a reliable and safe

design, and ultimately, contribute to the country's economy by promoting the development of more reliable and more efficient equipment.

REFERENCES

ACI 313-97. *Standard practice for design and construction of concrete silos and stacking tubes for storing granular materials.* American Concrete Institute, Farmington Hills, MI.

ANSI/ASAE EP433 JUN2000 (R2015). *Loads exerted by free-flowing grain on bins*. American Society of Agricultural and Biological Engineers, St. Joseph MI

AS 3774-1996. *Loads on bulk solids containers.* Standards Australia, Homebush, NSW.

BS EN 1991-4:2006. *Eurocode 1 – Actions on structures – Part 4: Silos and Tanks*. British Standards Institution, London.

Carson, J. W. (2000). Silo failures: Case histories and lessons learned, *Proceedings of the 3rd Israeli Conference for Conveying and Handling of Particulate Solids*, Dead Sea, Israel, ,4.1-4.11.

ISO 11697:1995. *Bases for design of structures - Loads due to bulk materials.* International Organization for Standardization, Switzerland.

Nielsen, J. (1996). Pressures from flowing granular solids in silos. *Phil. Trans. Royal Society of London: Mathematical, Physical and Engineering Sciences, Series A, 356(1747),* 2667-2684.

Ooi, J. Y., Pharm, L., & Rotter, J. M. (1990). Systematic and random features of measured pressures on full-scale silo walls, *Engineering Structures, 12(2),* 74-87.

Pieper, K. & Wenzel, F. (1964). *Druckverhältnisse Silozellen*, Wilhelm Ernst und Sohn, Berlin,.

Rotter, J. M. (1983). The effect of increasing grain moisture content on the stresses in silo walls. *Investigation Report S444,* School of Civil and Mining Eng., Univer

Rotter, J. M. (1986). The analysis of steel bins subject to eccentric discharge. *Proc., Second International Conference on Bulk Materials Storage Handling and Transportation Engineers*, Australia, 264-271.

Rotter, J. M. (2001). *Guide for the Economic Design of Circular Metal Silos*. Spon, London.

Samuels, B. (2001). Personal communication.

Zhong, Z., Ooi, J. Y., & Rotter, J. M., (2001). The sensitivity of silo flow and wall stresses to filling method. *Engineering Structures, 23(7)*, 756-767.

SITE SPECIFIC TECHNOLOGY FOR PREVENTION AND CONTROL OF FIRE IN MINES DURING EXTRACTION OF COAL USING BLASTING GALLERY METHOD

*R. V. K. Singh[1] and N. K. Mohalik[1] , P. K. Singh[2]

[1]Senior Principal Scientist and Senior Scientist
Mine Fire Division
CSIR-Central Institute of Mining & Fuel Research,
Dhanbad, 826015, Jharkhand, India
*(*Corresponding author: drrvksingh@yahoo.com)*

[2] Director
CSIR-Central Institute of Mining & Fuel Research,
Dhanbad, 826015, Jharkhand, India

24th World Mining Congress
MINING IN A WORLD OF INNOVATION
October 18-21, 2016 • Rio de Janeiro /RJ • Brazil

ABSTRACT

The problem of spontaneous heating in Blasting Gallery (BG) panels during extraction is a major threat to safety and productivity in Singareni Collieries Company Limited (SCCL) coal mines of India. Most of the BG panels have been sealed due to occurrences of spontaneous heating during extraction of the panel. After sealing of the panel, it is much difficult to re-open the panel. The basic principle of BG method is to extract thick coal seams through drilling and blasting of roof and sides of galleries, which are driven at the bottom of the seam at regular intervals. Authors are presenting the successful case studies of Godavarikhani (GDK) No. 11 mine of SCCL, where all precautionary measures were implemented and panels were successfully extracted. The purpose of this paper is to describe the different site specific technology for prevention and control of spontaneous heating/fire in coal mines using blasting gallery method for extraction of coal safely.

KEYWORDS

Coal Mine, Spontaneous heating, Fire, Blasting Gallery method, Inertisation, Carbondioxide

INTRODUCTION

In India, there are number of thick seams with good quality of coal. Mechanisation of mine in India is not much successful and the percentage of coal production is less. Sand stowing for working the thick seams cannot be considered as an option because the cost is prohibitive. Extraction of thick seams by conventional hand section is neither productive nor effective from the conservation point of view. The percentage of extraction by hand section mining in the thick seams is as low as 25 to 30%. A lot of good grade coal has been irretrievably lost. Besides, millions of tones of good grade coal in thick seams are locked in pillars. In order to meet the ever increasing demand of coal in Southern India, SCCL has taken up various steps like re-organization of existing mines, introduction of mechanization for higher rate of production and liquidation of long standing good quality coal pillars. In the past, thick seams were extracted with sand stowing. But, presently due to unavailability of sand in sufficient quantity and also high transportation cost for stowing in underground mines, this method is not being commonly practiced. Therefore, SCCL is of the opinion that Blasting Gallery method is the suitable method for the extraction of thick seams at least up to a thickness of 8m. BG method is likely to produce about 1000 tons/ day on an average with peaks being as high as 2000 tons/day, when sufficient and proper evacuation capacity is being provided.

The basic principle of BG method is to extract thick coal seams through drilling and blasting of roof and sides of galleries, which are driven at the bottom of the seam at regular intervals. Width of the gallery left between the two adjacent galleries is between 8 and 13 m. (Ring holes up to 10m long are drilled in the roof and sides of the galleries at regular distances varying between 1 to 2m by means of a crawler mounted JUMBO drill). Blasting is done using explosive cartridges separated by inert spacers and detonating fuse, so that the explosive spreads all along the length of the hole. The load haul dumpers (LHDs) fitted with remote control systems carry out loading of coal, which enables the operator to stand under the supported roof and operate the LHDs. The LHDs carry the coal from the face and thereby discharge into the armored chain conveyors, which fed to the belt conveyor network and transport to the surface (CSIR-CIMFR Project Report, 2002). Blasting gallery method envisages blasting the entire thickness of the seam by successive blasts and retreating along the level gallery, which is driven along the floor of the seam. A large panel of about 1000m X 120 to 150m is divided into sub panels of 150m X 120 to 150m by driving main rise. A barrier of about 20m is left in between the panels. It is necessary to adopt this sub paneling to restrict the size of panel so that the extraction is completed within the incubation period. The sub panel is further sub-divided into two parts by driving a central main dip and after extraction of coal will be sealed off. From this central dip rooms are driven at slightly rising gradient (1 in 60) to reach the boundary of the panel. Such rooms are driven at 13 – 15m apart and are of 4.2m wide. Thus a solid barrier pillar of about 9 to 11m x 60 to 65m is formed in between the rooms. The width of the main rise and the central main rise is about 4.7m to facilitate the housing of chain conveyor and also the movement of LHDs and Jumbos. All the development is done along the floor of the seam to the height of 3m. It is very essential to stick to the correct dimensions of rooms and rises to avoid roof control problems at the later stage. This development has been carried out by conventional drilling and blasting and lifting the coal by LHDs. Authors are presenting the

successful case study of GDK No. 11 mine of SCCL, where all precautionary measures were implemented and panels were successfully extracted.

CASE STUDY

Godavarikhani (GDK) No. 11 Incline mine under Ramagundam Area-I is located in the north central part of Ramagundam area, lies between north latitude 18° 41'30" and 18° 41'10" and east longitude 79°32'58" and 79°32'54". The full dip of the seam is 1 in 8 to 10 in the direction of N 60 E. The nearest railway station is Ramagundam on Kazipet - Ballarsha section of South Central Railway and is 24 km away from the mine. The mine is opened on 15-02-1979, production started from 25-09-1985. Total mine take area is 901.907 Ha. In this area 6 No's of seams are existing known as 1A, 1, 2, 3A, 4 &4 seams, out of these only 1,2,3&4 seams are workable. Over this surface there are three nos. of tanks and a seasonal nallah called Jallaram vagu, PWD Road to Manthani, three villagers named Singareddy pally, Dubbapally and Harijan wada exists (CSIR-CIMFR Project Report, 2014).

Workable seams

Description	**1 Seam**	**2 Seam**	**3 Seam**	**4 Seam**
Thickness	6.0m	6.0m	10.0m	3.0m
Parting	18m-22m		65m-70m	9.5m-12m
Grade of coal	G10	G11	**G9**	G8
Degree of gassiness	1 Degree			
Extractable reserves	16.70 MT	14.20MT	55.37 MT	13.50MT
RMR	51 (class II fair)	41 (class III fair)	50.40 (class IIIB fair)	42 (class IIIA fair)
Target of the year 2012-13 (8,70,000 T)	4,50,000T	-	3,00,000 T	1,20,000T

Seam wise reserves: (as on 31-03-2013)

SEAM	RESERVES	AVERAGE THICKNESS (M)
1 Seam	22.599	5 to 6 m
2 Seam	24.84	3.25m
3 Seam	60.502	8.5m to 11m
4 Seam	24.82	3.0m
Total	132.761	
Life of the mine	100years/10 Lakhs	

Production with method of mining

1 Seam	Depillaring with continuous miners	4,70,000 T
2 Seam	Temporary closed	
3 Seam	Depillaring with Blasting gallery Method	3,00,000 T
4 Seam	Sand stowing with Load Haul Dumpers	1,20,000 T

Details of outlets:

(a) Inclines

Description	Length	Gradient	Connected to
Main Incline	400	1 in 5	1 Seam
Man Way	400	1 in 5	1 Seam
III entry	300	1 in 4	1 Seam

(b) Air shaft:

SI.No.	Number/ name of the shaft	Diameter (in mtr.)	Depth (in mtr.)	Seams connected with the shaft	Purpose

1	Air shaft	6.00	80.00	Only 1 seam	Intake airway
2	Air shaft	6.00	190.00	Up to 3S Top	Return airway

SCIENTIFIC INVESTIGATION

Scientific investigation of the BG-J(1) Panel has been carried out from very beginning with respect to thermocompositional monitoring and application of preventive and control measures to avoid occurrences of spontaneous heating. The thickness of the seam is 3.0 to 10.0m and developed in one section 3.0m along the floor (Fig.-1). The dimension of BG-5 panel is 111mx127.5m (14150 Sq. m area). Extraction of the coal has been started from 30th October 2013. Total number of pillars in this panel was 9 and the surface cover of this panel varies from 242m to 256m. The actual reserve of the panel is 222000 tonne coal but the extractable reserve is 190000 tonne coal. The adjoining panel BG-1H3 was extracted successfully and no history of fire. Coal of seam 3 is more prone to spontaneous heating due to high moisture and high V.M. The method of ventilation in this panel is descentional and flow of air quantity in this panel is 2500m^3/minute. During the period of extraction regular thermo-compositional monitoring has been carried out in all the available goaf edge, return point and application of CO_2 was also carried out in the running BG-J(1) panel and adjoining panel as preventive measures and situation of the panel. CO_2 flushing has been started in this panel from 18th December, 2013 at the rate of 9.6t/day in both the running as well as adjoining panel. Pipelines arrangement was also carried out in all the levels for injection of inert gases and collection of air samples. Main fall have not been noticed and some of the local fall have been observed. Panel was inspected during the scientific investigation and measured temperature, oxygen and carbonmonoxide at the available goaf edge to know the status of the panel and accordingly suitable advice has been provided to the mine management for application of preventive measures (Table-1). CO_2 was injected in running as well as adjoining panel. The pipe lines laid down in the floor of coal, gets damaged due to movement of machinery/mining equipments. The frequency and quantity of CO_2 infusion in the goaf will decide as per the situation of the panels. A total quantity of 1063.61cum, t carbondioxide has been injected for inertisation as well as cooling of the running and adjoining goaf. The summarised detail of the panel BG-J(1) has been mentioned in Table-2. Goaf edge returns air sample and details of CO_2 flushing and are shown in Table 3 and 4.

Table 1- Measurement of D.B., W.B. O_2 and CO on spot during scientific investigation

Locations	Date	Hygrometer Reading, ^{0}C		O_2% reading on spot	COppm reading on spot
		W.B.	D.B.		
26level south of 15 dip	06.12.2013	26.0	27.0		00
26.5 level south of 15 dip		26.0	27.0		00
27 level south of 15 dip		26.5	27.5		00
27.5 level south of 15 dip		27.5	28.5		00
28 level south of 15 dip		28.0	29.0		00
28level of 15 dip		26.5	28.5		00
28.5 level south of 14 dip		27.5	29.0		00
29 level south of 14 dip		27.5	28.5		00
26level 15 dip junction	01.02.2014	24.0	25.0	20.9	00
26.5 level south of 14 dip		24.5	26.5	20.9	00
27 level south of 14 dip		25.0	26.0	20.9	00
27.5 level south of 14 dip		25.0	26.0	20.9	00
28 level south of 13 dip		24.5	26.0	20.9	00
28.5 level of 13 dip		26.0	27.0	20.9	00
29th level south of 13 dip		27.00	28.00	20.9	00
16th rise of 30 level I.S.				1.90	00
15th rise of 30 level I.S.				3.80	00

14th rise of 30 level I.S.				6.30	00
15 dip of 25th level	07.03.2014	26.0	27.0	20.9	00
26level south of 14 dip junction		26.0	27.0	20.9	00
26.5 level south of 13 dip		25.0	26.0	20.9	00
27 level south of 13 dip		26.0	27.0	20.9	00
27.5 level south of 13 dip		26.5	27.0	20.9	00
28 level south of 13 dip		28.0	29.0	20.9	00
28level of 13 dip		26.0	27.5	20.9	00
29th level south of 12 dip				8.1	00
16th rise of 30 level I.S.				1.8	00
15th rise of 30 level I.S.				5.1	00
14th rise of 30 level I.S.				5.8	00
13th rise of 30th level I.S.				7.7	00
Adjoining sealed off panel 1H3 17 dip of 25th level				1.8	00

Table 2 - BG-J(1) panel details of seam 3

Name of the Panel	BG-J(1)
Size of the Panel, m^2	14,150
Depth range, m	242 – 256
Extractable reserves, T	1,90,000
Panel starting date	30.10.2013
Panel sealing date	26.04.2014
Progressives working days	180
Progressives production as on 26.04.14, t	1,63,462 T
Goaf line velocity, mtr/day average	0.95
Air quantity in the panel, m^3/min	2500
Ventilation system in the panel	Descentional
Min & Max temperatures in the workings, ^0C	27.0 – 28.5
CO_2 flushing starting in working panel on:	18.12.2013
CO_2 flushing rate, t/day	10.5# (# 3.5 tones of CO2 flushing in to BG 1H-3)
Status of Nitrogen (N_2) Plant	Plant is working, Nitrogen purity is checked and it is 95.9%.(O_2-4.1%)
Oxygen (O_2) % in remote goaf of working panel	J1-Panel: At 29L: < 7 At 28L: < 7 At 16R/30L: < 3.6 At 15R/30L: < 6.5 At 14R/30L: < 7
Name of adjacent Panel/Panels & Oxygen (O_2) %	BG-1 H/3 : < 4
	BG-1 I : < 1
	BG-1G : < 5
Main fall occurred	Nil
Last Level Closing Status (no of days from starting of the panel)	• 29L/13D closed on 23.02.14(after 117 days)

RESULTS & DISCUSSIONS

In Godavarikhani No. 11 Incline mine Ramagundam SCCL, some of the previous panels have no history of fire and successfully extracted. Extraction of coal from seam 3, panel BG-J(1) has been started on 30th October, 2013. In this panel, regular thermocompositional monitoring of the panel is being carried out along with injection of carbondioxide as per the site specific condition and situation of the panel. The pipelines are layout along the barrier of the panel from rise side to dip for taking samples of goaf air from each level and injection for inert gases. In this mine ventilation is descentional. Some time, the temperature increases more than the ambient temperature surrounding the panel due to heavy machineries operation, roof fall in the goaf. Thus proper inertisation of the goaf, CO_2 has been flushed since 18th December, 2013 regularly as per panel condition. Last level gallery (bottom most portion) of the 29 level 13 dip was sealed on 24th February, 2014. In the adjoining BG-1H3 panel, the percentage of the oxygen was 1.8% and no CO and CH_4 were found on 7th March, 2014. Due to proper flushing of CO_2, the oxygen percentage is below 8.0% in 30th level of 13 rise and 1.9% in 30th level bottom most level of 16th rise. Quantity of carbondioxide (CO_2) flushing mentioned in table 4 clearly predict that, it has been injected in the running goaf as per the situation and need of the panel as preventive and control measures. Thus after taking suitable preventive measures as per requirement, BG-J(1) panel has been successfully extracted. The frequency and location for infusion of carbon dioxide depends upon the site specific condition and temperature found in the goaf edge. This panel was sealed on 26th April, 2014 after successful extraction and 1,63,462 tonnes (85%) of coal was extracted without any occurrences of spontaneous heating. Duration of the Panel BG-J(1) was up to five months twenty eight days.

CONCLUSION

After carrying out scientific investigation, authors conclude that to avoid further loss of valuable natural resources like coal, due to fire, the coal industry should give consistent efforts to stop further occurrences of spontaneous combustion in BG panel of coal mines. Based on the scientific study of BG-J(1) panel at GDK 11 Incline mine, Ramagundam, the following suggestions may be strictly followed for the safe extraction of BG panel without any occurrences of spontaneous heating.

1. Regular thermocompositional monitoring of the goaf edge, return of the panel should be carried out for early detection of spontaneous heating. Measurement of temperature of BG working panel goaf may be carried out using Heat spy Infra-red thermometer (Laser guided or Telescopic) at regular intervals.
2. Minimum quantity of coal should be left in the goaf and adjoining panel should be regularly monitored and try to maintain the percentage of oxygen below two percent.
3. Measurement of the air quantity of the panel should be carried out at certain interval to maintain the adequate required quantity of air on the basis of available number of rooms/working faces.
4. Ventilation arrangement should be made such that the maximum possible heat is extracted from exposed strata without allowing much oxygen in the goaf so that inert atmosphere, created in the goaf is not being disturbed.
5. Application of CO_2 should be carried out in the running panel as per the situation of site specific condition for proper inertisation of goaf. It may be injected in the panel when the trend of temperature increase may observe, but it will depend upon the site specific situation. Injection of nitrogen may be carried out in adjoining sealed off panel for inertisation. If nitrogen will not be available then area should be flushed with CO_2.
6. Faster rate of extraction may be adopted for safe extraction of panel and goaf line velocity should be maintained between 0.90 to 1.0m/day depending upon the panel condition. The pipe line laid down in the floor of the panel may damaged due to movement of machinery, thus it is not necessarily required.
7. Bottom most portion of the panel should be sealed as early as possible and inertise properly.
8. After final extraction of the BG panel, it should be isolated by explosion proof stopping for safety of the next panel.

ACKNOWLEDGEMENT

Authors are grateful to Dr. P. K. Singh, Director, CSIR-Central Institute of Mining & Fuel Research, Dhanbad for giving permission to present the paper. Authors are also grateful to the SCCL mine officials of GDK No. 11 Incline mine, Ramagundam and R&D officials of Kothagudem for providing all facilities and full co-operation during scientific investigation of the project. Authors are also thankful to the other colleagues of Mine Fire

Division, CSIR-CIMFR for their full support in scientific investigation of the project. Views expressed in this paper are of authors not necessarily of CSIR-CIMFR.

REFERENCES

CSIR-CIMFR S&T Unpublished Project report, " Study for early detection of the occurrences of spontaneous heating in the blasting gallery method and to evaluate suitable measures for prevention & control of spontaneous heating in thick coal seams", Project No. GAP/25/MF/MOC/2000 (CSIR-CMFRI & SCCL), November 2002.

CSIR-CIMFR Unpublished project report, "Scientific study and advice for safe extraction of BG-J(1) panel of No. 3 seam to avoid occurrences of spontaneous heating at GDK 11 Incline Mine, Ramagundam Area - I, SCCL", Project No. CNP/3921/2014-15, May 2014, P. 4-30.

Table 3 - Goaf edge return air sample (in %) of BG-J(I) Panel

Date	P.No	Location	Gas Analysis result					
			$C0_2$	O_2	CH_4	CO	H_2	N_2
01.12.2013	J-1	26LS/15D	0.284	19.997	0	0	0	78.8
15.12.2013	J-1	26LS/15D	0.224	20.785	0	0	0	78.08
22.12.2013	J-1	26LS/15D	0.035	20.633	0	0	0	78.425
29.12.2013	J-1	26LS/15D	0.102	20.93	0	0	0.0001	78.065
05.01.2014	J-1	26LS/15D	0.301	20.206	0	0	0	78.58
12.01.2014	J-1	26LS/15D	0.864	19.651	0	0	0	78.57
19.01.2014	J-1	26LS/15D	0.239	20.886	0	0	0	77.97
26.01.2014	J-1	26LS/15D	0.47	17.568	0	0	0	81.024
09.02.2014	J-1	26LS/15D	0.353	19.23	0	0	0	79.4987
15.02.2014	J-1	26LS/15D	1.0878	19.25	0	0	0	78.7481
16.02.2014	J-1	26LS/15D	0.1764	19.7577	0	0	0	79.1517
17.02.2014	J-1	26LS/15D	0.0479	20.8812	0	0	0	78.1676
18.02.2014	J-1	26LS/15D	0.8781	17.9738	0	0	0	80.2214
19.02.2014	J-1	26LS/15D	0.3703	18.6636	0	0	0	80.0415
20.02.2014	J-1	26LS/14D	0.0209	20.3559	0	0	0	78.7132
20.02.2014	J-1	26LN/16D	14.7088	17.856	0	0	0.0001	66.6647
21.02.2014	J-1	26LS/14D	0.1041	20.7735	0	0	0.0001	78.2182
21.02.2014	J-1	26LN/16D	6.7491	18.4109	0	0	0.0001	73.9849
22.02.2014	J-1	26LS/14D	0.4932	18.4636	0	0	0	80.1175
23.02.2014	J-1	26LS/14D	0.3947	20.7583	0	0	0.0001	77.9464
24.02.2014	J-1	26LS/14D	0.284	20.8249	0	0	0.0001	78.0257
24.02.2014	J-1	26LN/16D	8.7889	17.1507	0	0	0.0002	73.2142
25.02.2014	J-1	26LS/14D	0.0793	18.5012	0	0	0	80.5012
25.02.2014	J-1	26LN/16D	6.8688	18.1508	0	0	0	74.1239
26.02.2014	J-1	26LS/14D	0.3081	20.2278	0	0	0.0001	78.5563
26.02.2014	J-1	26LN/16D	4.0152	19.8293	0	0	0.0001	75.2855
27.02.2014	J-1	26LS/14D	0.9437	20.2296	0	0	0	77.9264
27.02.2014	J-1	26LN/16D	4.1717	19.7409	0	0.0008	0.0005	75.2172
28.02.2014	J-1	26LS/14D	1.5309	19.1201	0	0	0	78.4428
28.02.2014	J-1	26LN/16D	5.0547	17.1412	0	0	0	76.9154
01.03.2014	J-1	26LS/14D	0.1415	19.6159	0	0	0	79.3262
01.03.2014	J-1	26LN/16D	5.9982	18.7395	0	0	0	74.4027
02.03.204	J-1	26LS/14D	1.361	19.5905	0	0	0	78.1506
02.03.2014	J-1	26LN/16D	7.308	18.0908	0	0	0	73.7491
03.03.2014	J-1	26LS/14D	0.9291	19.7	0	0	0	78.4646
03.03.2014	J-1	26LN/16D	7.7833	18.5078	0	0	0	72.867
04.03.2014	J-1	26LS/14D	0.3186	20.5783	0	0	0	78.1997
04.03.2014	J-1	26LN/16D	7.0682	20.2662	0	0	0	71.8357
05.03.2014	J-1	26LN/16D	6.1197	19.8816	0	0	0	73.1536
05.03.2014	J-1	26LS/14D	1.2494	20.7731	0	0	0	77.0871
06.03.2014	J-1	26LN/16D	9.0984	16.7622	0	0	0	73.2925

06.03.2014	J-1	26LS/14D	0.2193	19.3937	0	0	0	79.4691
07.03.2014	J-1	26LN/16D	5.7226	19.334	0	0	0	74.0875
08.03.2014	J-1	26LN/16D	5.4358	18.8323	0	0	0	74.867
08.03.2014	J-1	26LS/14D	0.2073	20.683	0	0	0	78.2063
09.03.2014	J-1	26LN/16D	5.0212	19.7939	0	0	0.0002	74.326
09.03.2014	J-1	26LS/14D	0.9674	20.4874	0	0	0	77.6481

Table 4 - Details of CO_2 flushing/day

Date	CO_2 Flushing shift wise, T			CO_2 Flushing /day, T	CO_2 Flushing cum,t
	I Shift	II Shift	III Shift		
18.12.2013	0.5	1.5	1.5	3.5	3.50
19.12.2013	1.5	1.5	1.5	4.5	8.00
20.12.2013	1.5	1.5	1.5	4.5	12.50
21.12.2013	1.5	1.5	1.5	4.5	17.00
22.12.2013	1.5	1.5	1.5	4.5	21.50
23.12.2013	1.5	1.5	1.5	4.5	26.00
24.12.2013	1.5	1.5	1.5	4.5	30.50
25.12.2013	1.5	1.5	1.5	4.5	35.00
26.12.2013	1.5	2	2	5.5	40.50
27.12.2013	2	2	2	6	46.50
28.12.2013	2	2	2	6	52.50
29.12.2013	2	2	2	6	58.50
30.12.2013	2	2	2	6	64.50
31.12.2013	2	2	2	6	70.50
01.01.2014	2	2	2	6	76.50
02.01.2014	2	2	2	6	82.50
03.01.2014	2	2	2	6	86.50
04.01.2014	0.56	2	2	4.56	93.06
05.01.2014	2	2	2	6	99.06
06.01.2014	2	2	2	6	105.06
07.01.2014	2	2	2	6	111.06
08.01.2014	2	2	2	6	117.06
09.01.2014	2	2	2	6	123.06
10.01.2014	2	2	2	6	129.06
11.01.2014	1.5	1.5	1.5	4.5	133.56
12.01.2014	1.5	1.5	1.5	4.5	138.06
13.01.2014	1.5	1.5	1.5	4.5	142.56
14.01.2014	1.5	1.5	1.5	4.5	147.06
15.01.2014	1.5	1.5	1.5	4.5	151.56
16.01.2014	1.5	1.5	1.5	4.5	156.06
17.01.2014	1.5	1.5	1.5	4.5	160.56
18.01.2014	1.5	1.5	1.5	4.5	165.06
19.01.2014	1.5	1.5	1.5	4.5	169.56
20.01.2014	1.5	1.5	1.5	4.5	174.06
21.01.2014	1.5	1.5	1.5	4.5	178.56
22.01.2014	1.97	2.5	2.5	6.97	185.53
23.01.2014	2.5	2.5	2.5	7.5	193.03
24.01.2014	2.5	2.5	2.5	7.5	200.53
25.01.2014	2.5	2.5	2.5	7.5	208.03
26.01.2014	2.5	2.5	2.5	7.5	215.53
27.01.2014	2	2.5	2.5	7	222.53
28.01.2014	1.9	2.5	2.5	6.9	229.43
29.01.2014	2.5	2.5	2.5	7.5	236.93
30.01.2014	2	2	2.06	6.06	242.99
31.01.2014	1.5	1.5	1.5	4.5	247.49
01.02.2014	2	2.5	2.5	7	254.49

02.02.2014	2.5	2.5	2.5	7.5	261.99
03.02.2014	2.5	2.5	2.5	7.5	269.49
04.02.2014	2.5	2.5	2.5	7.5	276.99
05.02.2014	2.48	2.5	2.5	7.48	284.47
06.02.2014	2.5	2.5	2.5	7.5	291.97
07.02.2014	2.5	2.5	2.5	7.5	299.47
08.02.2014	2.5	2.5	2.5	7.5	306.97
09.02.2014	1.88	2.5	2.41	6.79	313.76
10.02.2014	2.5	2.5	2.5	7.5	321.26
11.02.2014	2.5	2.5	2.5	7.5	328.76
12.02.2014	2.5	2.5	2.5	7.5	336.26
13.02.2014	2.5	2.5	2.5	7.5	343.76
14.02.2014	2.5	2.5	2.5	7.5	351.26
15.02.2014	2.5	2.5	2.5	7.5	358.76
16.02.2014	2.5	2.5	2.5	7.5	366.26
17.02.2014	2.5	2.5	2.5	7.5	373.76
18.02.2014	2.5	2.5	2.5	7.5	381.26
19.02.2014	2.5	2.5	2.5	7.5	388.76
20.02.2014	2.5	2.5	2.5	7.5	396.26
21.02.2014	2.5	2.5	2.5	7.5	403.76
22.02.2014	2.5	3	3	8.5	412.26
23.02.2014	3	3	3	9	421.26
22402.2014	3	2.03	0	5.03	426.29
25.02.2014	1	3	3	7	433.29
26.02.2014	3	3	3	9	442.29
27.02.2014	3	3	3	9	451.29
28.02.2014	3	3	1	7	458.29
01.03.2014	3	3	3	9	467.29
02.03.2014	3	3	3	9	476.29
03.03.2014	3.2	3.3	3.3	9.8	486.09
04.03.2014	3.3	3.3	3.3	9.9	495.99
05.03.2014	3.3	1.89	3.3	8.49	504.48
06.03.2014	3.3	3.3	3.3	9.9	514.38
07.03.2014	3.3	3.5	3.5	10.3	524.68
08.03.2014	3.5	3.5	3.5	10.5	535.18
09.03.2014	3.5	3.5	3.5	10.5	545.68
10.03.2014	3.00	3.00	3.00	9.00	554.68
11.03.2014	3.50	3.50	3.50	10.50	565.18
12.03.2014	3.50	3.45	3.50	10.45	575.63
13.03.2014	3.50	3.50	3.50	10.50	586.13
14.03.2014	3.50	3.50	3.50	10.50	596.63
15.03.2014	3.50	3.50	3.50	10.50	607.13
16.03.2014	3.50	3.50	3.50	10.50	617.63
17.03.2014	3.50	3.50	3.50	10.50	628.13
18.03.2014	3.50	3.50	3.46	10.46	638.59
19.03.2014	3.50	3.50	3.50	10.50	649.09
20.03.2014	3.50	3.50	3.50	10.50	659.59
21.03.2014	3.50	3.50	3.50	10.50	670.09
22.03.2014	3.50	3.50	3.50	10.50	680.59
23.03.2014	3.50	3.50	3.50	10.50	691.09
24.03.2014	3.50	3.50	3.50	10.50	701.59
25.03.2014	3.50	3.50	3.50	10.50	712.09
26.03.2014	3.50	3.50	3.50	10.50	722.59
27.03.2014	3.00	3.50	3.50	10.00	732.59
28.03.2014	3.50	3.50	3.50	10.50	743.09
29.03.2014	3.50	3.48	3.50	10.48	753.57

30.03.2014	3.00	3.50	3.50	10.00	763.57
31.03.2014	3.50	3.50	3.50	10.50	774.07
01.04.2014	3.50	3.50	3.50	10.50	784.57
02.04.2014	3.50	3.50	3.50	10.50	795.07
03.04.2014	3.50	3.50	3.50	10.50	805.57
04.04.2014	3.50	3.50	3.50	10.50	816.07
05.04.2014	3.50	3.50	3.50	10.50	826.57
06.04.2014	3.43	3.50	3.50	10.43	837.00
07.04.2014	3.50	3.50	3.50	10.50	847.50
08.04.2014	3.50	3.50	3.50	10.50	858.00
09.04.2014	4.51	0.00	2.00	6.51	864.51
10.04.2014	2.50	2.50	2.50	7.50	872.01
11.04.2014	2.50	2.50	2.50	7.50	879.51
12.04.2014	2.50	2.50	2.50	7.50	887.01
13.03.2014	2.50	2.50	2.43	7.43	894.44
14.04.2014	2.50	2.50	2.50	7.50	901.94
15.04.2014	2.50	2.50	2.50	7.50	909.44
16.04.2014	2.50	2.47	2.50	7.47	916.91
17.04.2014	2.50	2.50	2.50	7.50	924.41
18.04.2014	2.50	2.50	2.50	7.50	931.91
19.04.2014	2.50	2.50	2.50	7.50	939.41
20.04.2014	2.50	2.50	2.50	7.50	946.91
21.04.2014	2.50	2.50	2.50	7.50	954.41
22.04.2014	2.50	2.50	2.50	7.50	961.91
23.04.2014	2.50	2.50	2.50	7.50	969.41
24.04.2014	2.50	2.50	2.50	7.50	976.91
25.04.2014	2.50	2.50	2.50	7.50	984.41
26.04.2014	2.50	2.50	2.50	7.50	991.91
27.04.2014	2.50	2.50	2.50	7.50	999.41
28.04.2014	3.50	3.50	3.50	10.50	1009.91
29.04.2014	3.50	3.50	3.50	10.50	1020.41
30.04.2014	3.50	3.50	3.50	10.50	1030.91
01.05.2014	2.00	2.00	2.00	6.00	1036.91
02.05.2014	1.50	1.50	1.50	4.50	1041.41
03.05.2014	1.50	1.50	1.20	4.20	1045.61
04.05.2014	1.50	1.50	1.50	4.50	1050.11
05.05.2014	1.50	1.50	1.50	4.50	1054.61
06.05.2014	1.5	1.5	1.5	4.50	1059.11
07.05.2014	1.5	1.5	1.5	4.50	1059.11
08.05.2014	1.5	1.5	1.5	4.50	1063.61
09.05.2014	1.5	1.5	1.5	4.50	1063.61

STUDY OF A NICKEL TAILING FLOCCULENT OF SUSPENSION DURING THICKENING

Raulim O. Galvão

Sílvia Cristina A. França

David Marzzoni Nogueira

Faculdade de Engenharia de Minas e Meio Ambiente,

Universidade Federal do Sul e Sudeste do Pará,

Marabá- Pa, Brazil.

engraulim@gmail.com

24th World Mining Congress

MINING IN A WORLD OF INNOVATION

October 18-21, 2016 • Rio de Janeiro /RJ • Brazil

STUDY OF A NICKEL TAILING FLOCCULENT OF SUSPENSION DURING THICKENING

engraulim@gmail.com

ABSTRACT

The flocculation processes involving the action of the polymer chains dispersed in pulp with small size particles resulting in the formation open aggregate of larger diameter and greater rate sedimentation. In general, flocculation of finely particles dispersed in suspensions is affected by properties such as pH, quality of water, and parameters that affect the hydrodynamics and the nature and dosage of flocculating agents. This article consists in evaluating the behavior of a flocculent suspension nickel reagents with different flocculants, pH, dosage of flocculant, percent solids and shear rate and effects on the settling velocity of the flocs. The tests consisted sedimentation test bench in beakers to analyse the settling time with or without the use of flocculants and testing agitators jartest to analyze the effect of stirring speed on the sedimentation rate. In the study of the behavior of this suspension was found that slurry and flocculent suspensions with higher percentages of solids have minor settling velocities and this effect happen due to population. It was observed that higher speeds of agitation in the range above 250 rpm in 30 seconds time the sedimentation flocs is decreased due to the breakdown of the structure and when the studied keep the same shear rate and flocculent time by half did not have a homogeneous and clear suspension.

KEYWORDS

Flocculation, Flocculating agents, Shear rate, Settling velocity

INTRODUCTION

The fine particles ores are considered waste from the beneficiation process and concentration of minerals that are usually discarded in the condition of a fluid pulp and have their disposal a large area confined by dikes or dams. To reduce this amount of water in dams a large number of solid-liquid separation operations in order to promote the thickening of the pulp. The various solid-liquid separation operations, the thickening is the activity with lower unit costs among the activities dewatering (FRANÇA AND MASSARINI, 2010). This shows the importance of developing and optimizing techniques and process parameters to improve the use and efficiency.

Another tests to be investigated in the characterization and design of solid-liquid separation equipment is the percentage of fine particles. This finely mineral demand for its sedimentation, flocculation agents that modify the stability and allows the particles get together creating a larger diameter structure called floc. In general flocculation characterized by the action of a polymer necessarily water soluble, called flocculant, which promotes the aggregation of fine particles in flake form. The organic flocculants are polymers responsible for creating bridges between particles that are suspended in the slurry, allowing increase in its effective diameter and, consequently, in the solid-liquid separation rates (ATTIA, 1992).

This article studied the flocculation of a nickel ore slurry (-20 microns) comparing conditions and types of flocculants, pH, reagent dosage, percentage of solid and agitation. The relevance of this work is the optimization of settling time of the particulates and recovery of water that can be reused in the process.

MATERIALS AND METHODS

To study the behavior of a flocculent suspension of fine nickel particles ranging the conditions of agitation by rotating the Jar Test had to set some initial parameters as appropriate choice of flocculant, flocculant dosing, percent solids and pH.

Planning of tests

Planning for the development of this article is based on a review and the appropriate laboratory procedures were grouped in phases, as described below and illustrated in the flow chart shown in Figure 01.

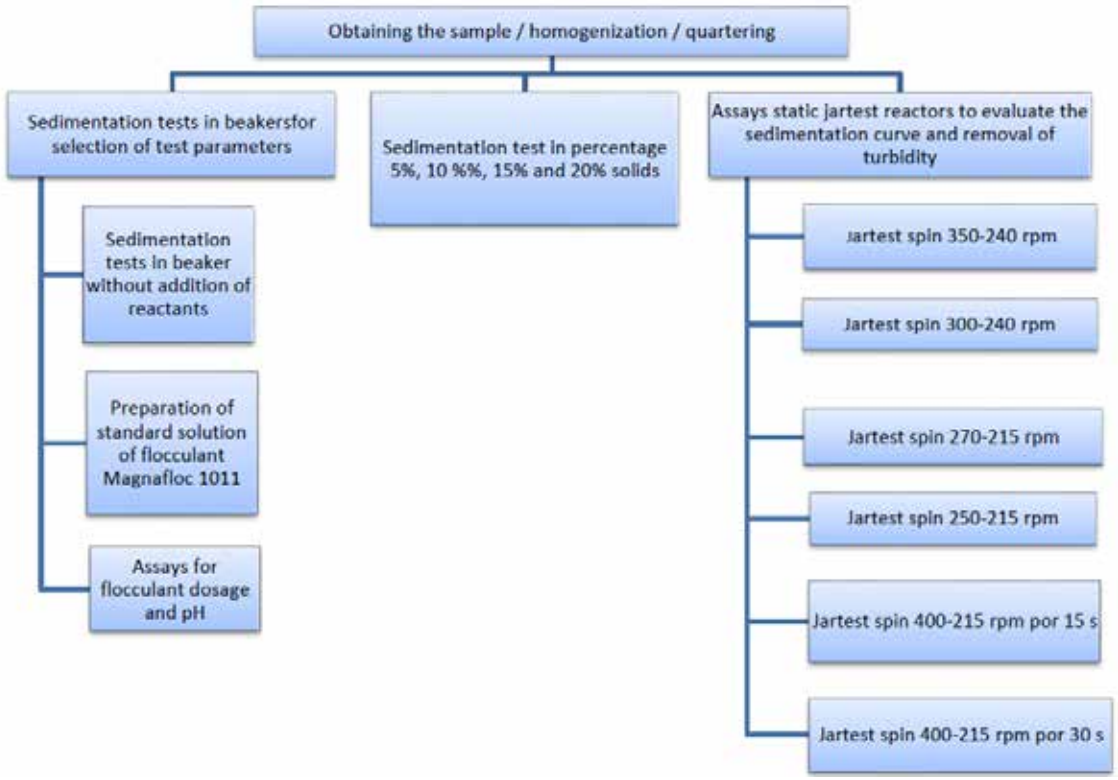

Figure 01: Planning of laboratory tests.

Sample characterization

The samples mineral used in sedimentation tests was the hydrocyclone overflow in the desliming (1,5 ') of a nickel ore slurry, which was desired cut 20 micrometers. The desliming operation was performed in the Mineral Technology Center pilot plant (CETEM). The particle density was determined by pycnometry and the value is 2.786 g / cm^3.

The micro grain size analysis of the material was in the Malvern equipment Instruments®. The graphic analysis shows larger percentages of fines particles present in the ranges between 2 and 20 micrometers. Figure 01 shows the particle size distribution curves generated showing significant amounts of particles below 5µm.

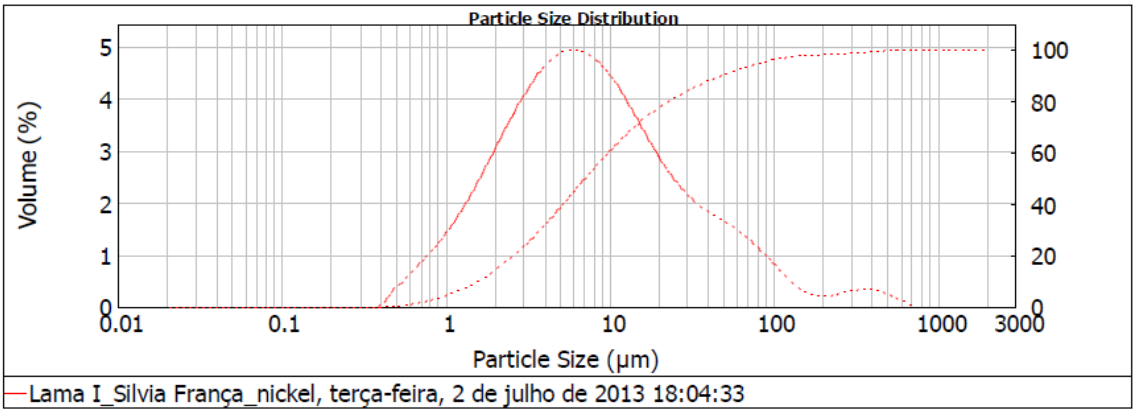

Figure 02: Particle size analysis Malvern.

.

RESULTS AND DISCUSSION

Effect of pH and concentration of flocculating agent

The results of the sedimentation velocity for dosage of flocculant and pH and settling time are shown in figure 03. It is observed that the settling times for the tests ranged between 4 and 20 seconds, depending on the dosage that has been established to reach compression stage. In lower dosages in the range of 40 to 60 g/t larger settling times and consequently less sedimentation was obtained. The choice of the optimal dosage of flocculant to be scheduled for tests will be when observed the lowest settling. This way 200 g/t Magnafloc 1011 is the dosage that gives lower settling times being less than 8 seconds. For tests with pH correction 10 was better performance of the polymer observed by the decrease by 57% the settling time for the same dosage of 200 g / t.

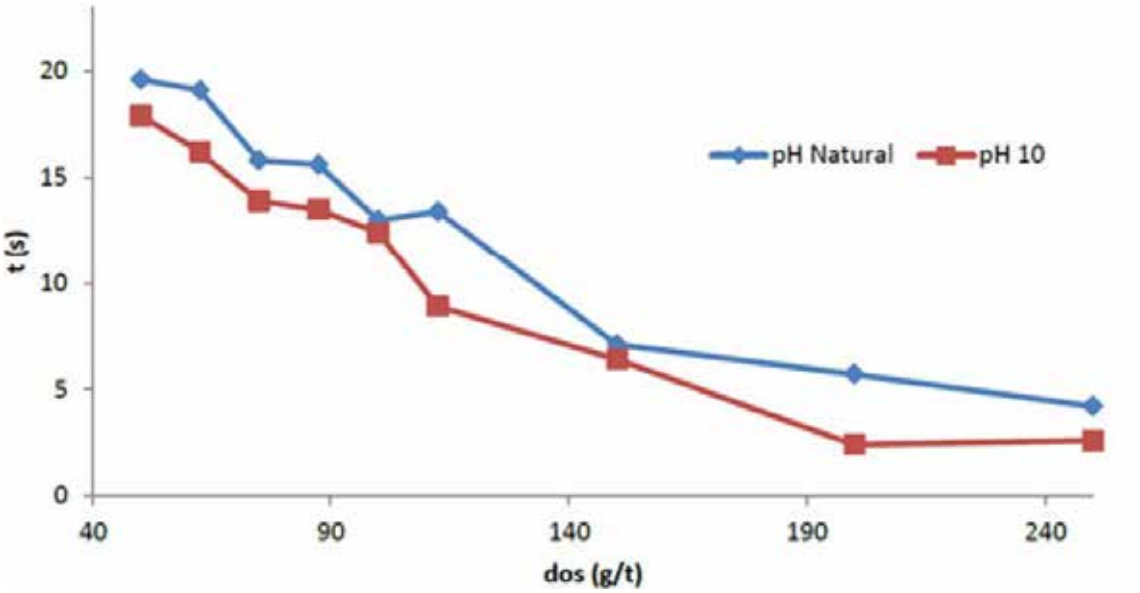

Figure 03: Settling time pH 10 and natural pH.

Comparison tests with and without flocculants

In terms of the percentage of solids it found that the displacement of the lines thats separates the solis of a pulp with 5% solids in both tests (without addition or with addition of flocculating agents) occurs more rapidly. This is because the sedimentation free where an inorganic particle or flake in a fluid undergo only the liquid's resistance to its movement and when isolated describes a free downward trend and set down, using it only one time t (FRANÇA AND CASQUEIRA , 2007).

When there are many particles or flakes in the pulp, lot of particles have the same trajectory. Thus sedimented simultaneously with different velocities. Thus, the higher the percentage of solids in a pulp, the lower the sedimentation rate of the solid particles, due to the deceleration caused by possible interactions between these particles while they go through the settling path to the bottom of cylinder.

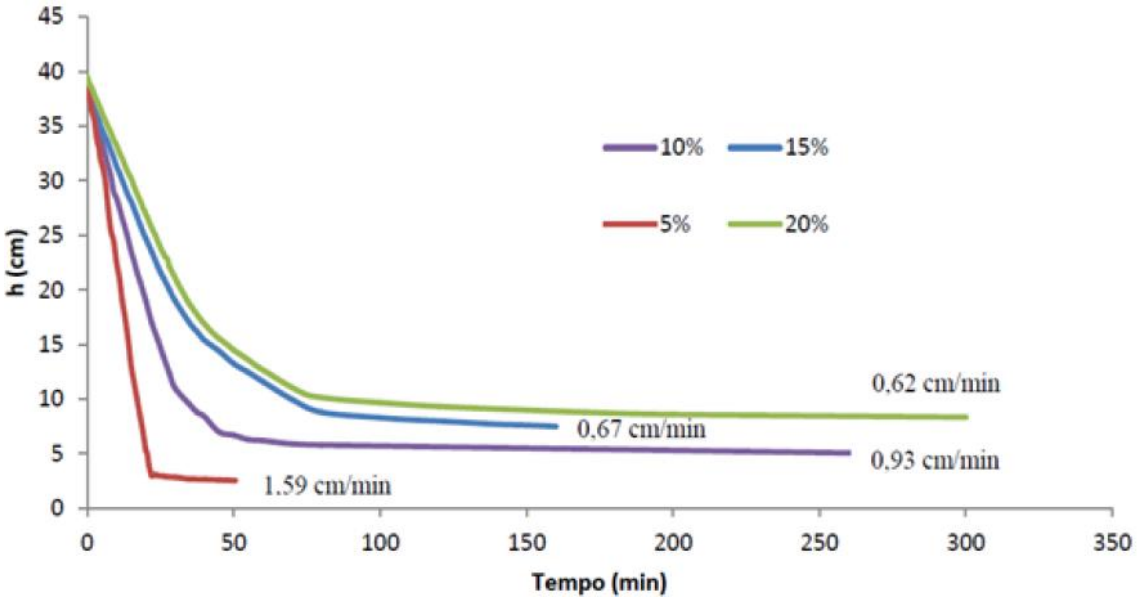

Figure 04: Test bench without settling flocculant use.

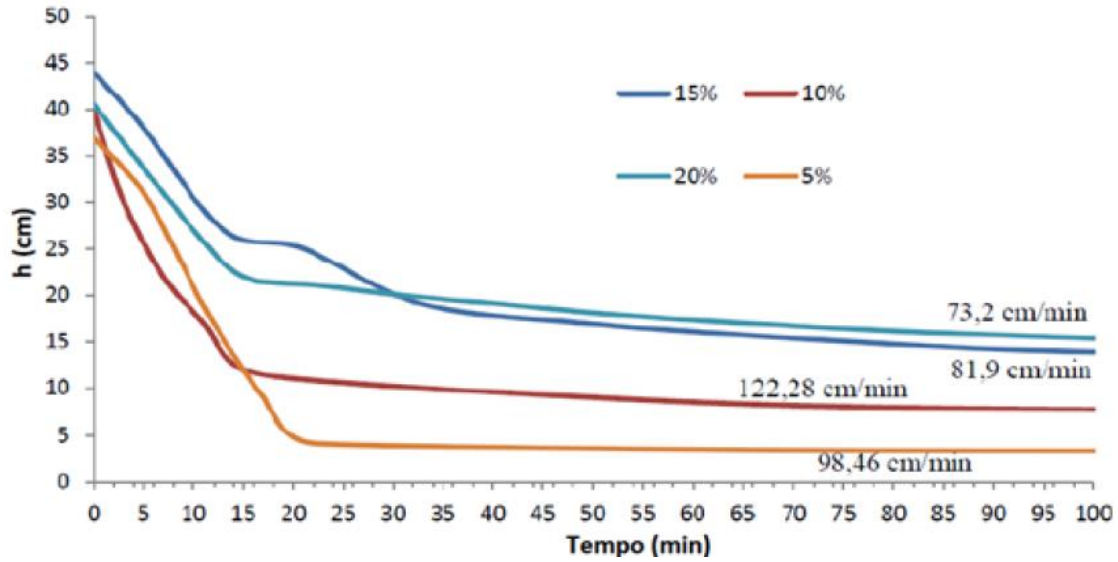

Figure 05: Test bench sedimentation with flocculant use.

Effect of rotation

The results of the tests whose sedimentation rate parameters were analyzed fast and slow stirring the mixture with a flocculant dosage 200 g/t natural pH of the pulp are shown in Figure 06, 07 and 08. The residual turbidity was used as parameter evaluation of flocculation and sedimentation efficiency of the particles, have their values is presented in figure 09.

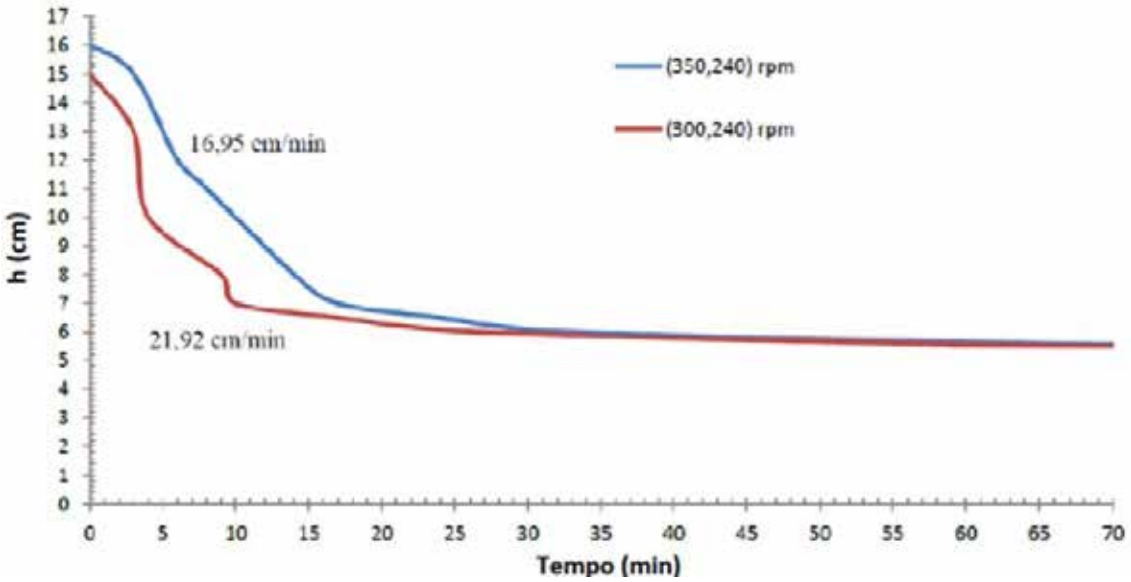

Figure 06: sedimentation curve in rotation 350 and 300 rpm.

In the test with increase of 300 agitation speed to 350 rpm there were a reduction in the sedimentation rate of around 23% which leads to view as cited by Voltan (2007) the effect of excessive agitation has a negative effect causing rupture the flocs formed, which reduce the sedimentation rate. The breaking of the flakes leads to production of smaller flakes, indicating a more turbid supernatant as cited by Tridibid (2006). Residual turbidity values for the testing shown in figure 09 confirm that at higher shear rates turbidity values were higher.

In the test with increasing agitation speed 250 to 270 rpm promoted a reduction in the sedimentation rate of around 56%, but the residual turbidity values remained close around 5.5 NTU.

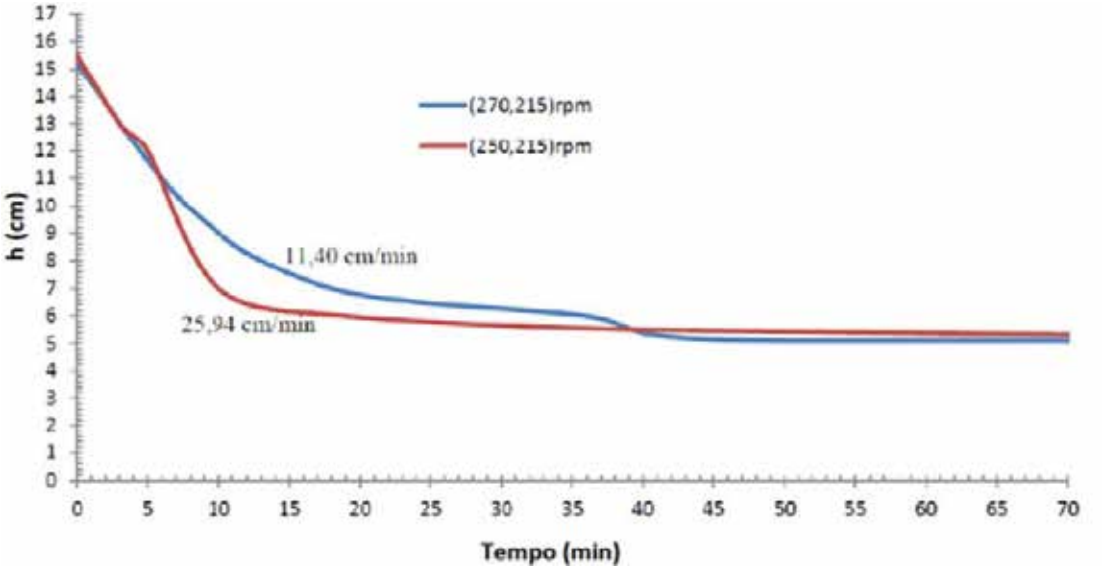

Figure 07: sedimentation curve in the rotations of 250 and 270 rpm.

In the test with increasing stirring speed is 300 350 rpm to promoted a reduction in the sedimentation rate of around 23%

For the third test and final test (Figure 08) proposed to evaluate the stirring time in rapid mixing setting t1 15 seconds and t2 30 seconds in order to understand the time needed for the formation, growth and rupture of the flakes. The stirring time as quoted by Baltar (2010) has the function of promoting the

various dispersed particles come into contact with the polymer chain and form considerably larger flakes. However, when printing the same shear rate for a long time results in disruption of the formed structure.

In the third test a decrease was observed on the settling velocity printed when the shear rate in the least time. This leads us to understand that this time was not enough to promote the aggregation of suspended particles and which in this part of the pulp not flocullate.

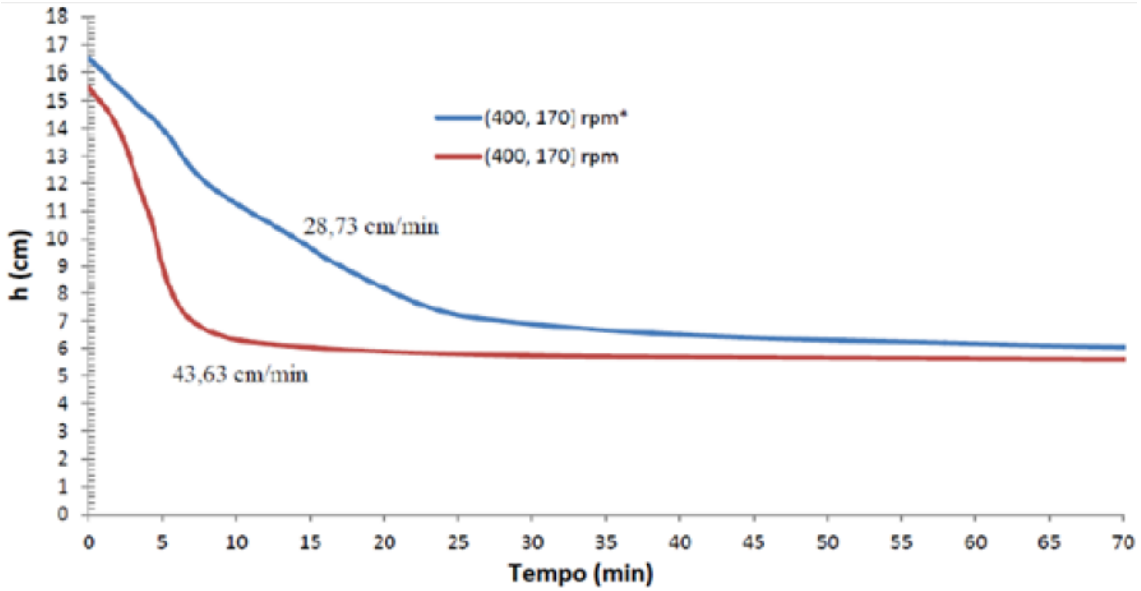

Figure 08: sedimentation curve in rotation 400 rpm for times of 15 and 30 seconds.

Figure 09 shows the graph of the variation of turbidity as a function of agitation speed for the tests. Note that the turbidity is greater when the stirring speed is increasing, it follows that by applying higher shear rate promotes breaking of the flakes and some of these smaller structures remain in suspension for a longer period of time.

For the purposes of speeds faster and slower shaking 400 and 170 rpm, respectively, it was found that the application time of this rate for 15 seconds, the turbidity value was higher than when applied to the same stirring conditions over a period of time 30 seconds. This fact reveals that the value of high turbidity can be related to insufficient time for the formation of flakes, leaving some individual particles still in suspension which leads to high values of remaining turbidity.

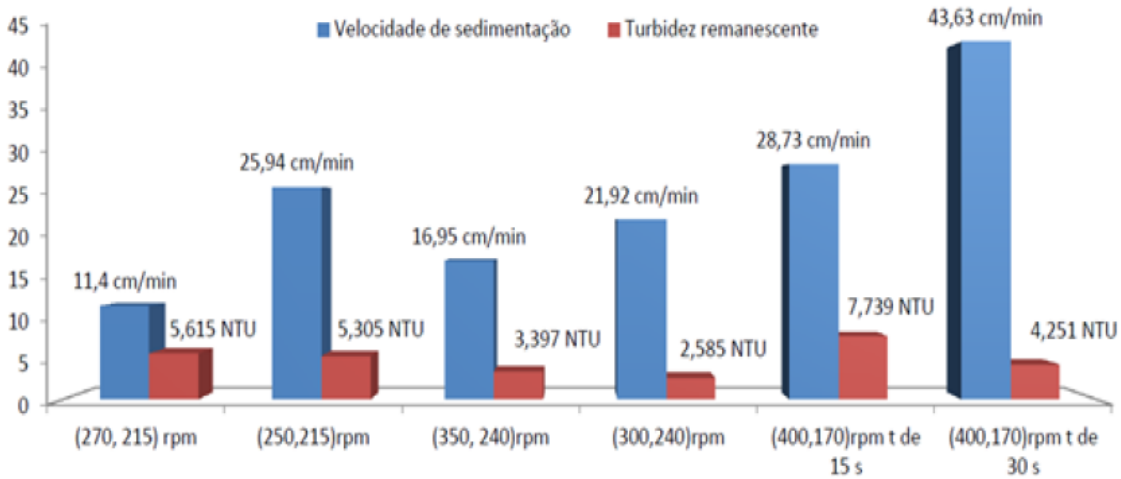

Figure 09: Comparative graph of sedimentation velocity and residual turbidity value

CONCLUSION

.

For the study variables, the results showed that the reagent best suited to the nickel tailings particles is Magnafloc 1011 and raising the pH to the value of 10 has a better performance of the polymer even if the decrease in settling time 57% justify not work all other tests with pH correction. In all tests, it was found that the higher the percent solids, the lower the sedimentation velocity both when working on slurries sedimenting system of individual particles or sedimentation of flocculated aggregates.

The results also indicate that the stirring speed is a sensitive parameter to be studied. In all trials Jar Test increasing agitation speed (300 to 350; 250 to 270) resulted in the breakdown of flocculated structures, particularly the time required for sedimentation and a higher percentage of particles in suspension, which was confirmed by the values higher residual turbidity. It was also concluded that the print equal shear rates, both rapid stirring, as in slow agitation did not provide satisfactory values in sedimentation velocity, because the short time of 15 seconds was not sufficient to allow adsorption and complete aggregation of the reagents polymer particles in promoting flocculation.

REFERENCES

ATTIA, Y.A., 1992. Flocculation. In.: Colloid Chemistry in Mineral Processing. Laskowski, J.S.; Ralston, J. (eds.). Elsevier Science Publishers, Chapter 9, p. 277-308.

BALTAR, A. M.. Processos de agregação In: Tratamento de Minérios. 5a ed. Rio de Janeiro: CETEM/MCT, 2010, Cap. 13, p. 559-594.

FRANÇA, S. C. A.; CASQUEIRA, R. R. Ensaios de sedimentação em :Tratamentos de minérios- Práticas laboratoriais. Rio de Janeiro: CETEM/MCT, 2007, Cap. 23, p. 393-422.

FRANCA, S. C. A.; MASSARANI, G. Separação Sólido Liquido. In: Tratamento de Minérios. 5a ed. Rio de Janeiro: CETEM/MCT, 2010, Cap. 15, p. 637-680.

TRIDIBID, T. Flocculation: a new way to treat waste water. Journal of Physical Sciences, Vol. 10, 2006, 93 – 127

VOLTAN, PAULO E. N., Avaliação da ruptura e do recrescimento de flocos na eficiência de sedimentação em agua com turbidez elevada. Tese de mestrado. USP: 2007, São Carlos, SP.

STUDY OF TIME INFLUENCE IN STATIC LAY LEACHING USING H_2SO_4 OF COPPER ORE FROM SOSSEGO MINE

Torben Ulisses da Silva Carvalho[1]
Renan Correa Aranha[2]
Adielson Rafael Oliveira Marinho[3]
João Henrique Assunção Oliveira[4]
Amanda Maria Machado de Oliveira[5]
Leonardo Vilarinho Antunes Junior[6]
Ana Rosa Rabelo de Lima[7]
Lucas de Freitas Brasil Marins[8]
Raulim Oliveira Galvão[9]

1 Graduando em Engenharia de Materiais, Estudante, Faculdade de Engenharia de Materiais, Universidade Federal do Sul e Sudeste do Pará, Marabá, Pará, Brasil.
2 Graduando em Engenharia de Materiais, Estudante, Faculdade de Engenharia de Materiais, Universidade Federal do Sul e Sudeste do Pará, Marabá, Pará, Brasil.
3 Graduando em Engenharia de Materiais, Estudante, Faculdade de Engenharia de Materiais, Universidade Federal do Sul e Sudeste do Pará, Marabá, Pará, Brasil.
4 Graduando em Engenharia de Materiais, Estudante, Faculdade de Engenharia de Materiais, Universidade Federal do Sul e Sudeste do Pará, Marabá, Pará, Brasil.
5 Graduanda em Engenharia de Materiais, Estudante, Faculdade de Engenharia de Materiais, Universidade Federal do Sul e Sudeste do Pará, Marabá, Pará, Brasil.
6 Graduando em Engenharia de Materiais, Estudante, Faculdade de Engenharia de Materiais, Universidade Federal do Sul e Sudeste do Pará, Marabá, Pará, Brasil.
7 Graduanda em Engenharia de Materiais, Estudante, Faculdade de Engenharia de Materiais, Universidade Federal do Sul e Sudeste do Pará, Marabá, Pará, Brasil.
8 Graduando em Engenharia de Materiais, Estudante, Faculdade de Engenharia de Materiais, Universidade Federal do Sul e Sudeste do Pará, Marabá, Pará, Brasil.
9 Graduado em Engenharia de Minas e Meio Ambiente, Bacharel, Faculdade de Engenharia de Materiais, Universidade Federal do Sul e Sudeste do Pará, Marabá, Pará, Brasil.

24th World Mining Congress
MINING IN A WORLD OF INNOVATION
October 18-21, 2016 • Rio de Janeiro /RJ • Brazil

STUDY OF TIME INFLUENCE IN STATIC LAY LEACHING USING H_2SO_4 OF COPPER ORE FROM SOSSEGO MINE

ABSTRACT

Leaching is a hydrometallurgical process that consists in the separation of the metal and the gangue by dissolution in aqueous solution of the ore containing the metals of interest. The present study utilized the oxidized copper ore from Sossego Mine, leached in laboratory scale with different periods, using sulfuric acid. With the data found through these test, graphics were made showing the metallurgical recovery and the metal content in the waste and in the liquor. The results were found using the titration technique. There were changes in the content levels, which increased proportionally with the leaching period. This behavior demonstrates the need for a larger number of steps in a certain period for proper metallurgical recovery.

KEYWORDS

Leaching; Copper ore; Sossego Mine; Hydrometallurgy

INTRODUCTION

World reserves of copper ore recorded in 2012 a total of 680 million tons in metal content, amount 1.4% lower than in 2011. The Brazilian mineable reserves of copper in 2012 totaled 11.42 million tonnes of contained copper, an increase of 3.2% compared to the previous year, with highlights to the states of Pará, with 81% of this total, Goiás, Bahia and Alagoas [1].

Leaching is a hydrometallurgical process consisting in processing of ores in which the metal of interest is separated from the gangue by dissolving in an aqueous medium of the copper from the ore. This type of metallurgical processing is already being widely used for the subsequent production of high purity

cathode copper (about 99.99%) [1; two]. Its high visibility for the treatment of copper oxidized ores, can be seen as the leaching cells is the most important industrial technique for treating such ores.

Its commercial importance is likely to grow even more with the fact that the most appropriate form of processing for recycling and for the treatment of low-grade ores. [3] The importance gain results in the need for constant study to the appropriate technological development, optimizing the hydrometallurgical extraction of oxidized copper.

MATERIALS AND METHODS

The sample used copper ore originated from Sossego Mine, located in Canaan, Pará state Southeast. The sample was crushed, sieved, homogenized and quarteada. The size fraction used in the acid leach described in this paper was close to 5 mm.

Leaching

For this study were made Leaching tests with four static bed oxidized copper ore having particle size rates around 5 mm. As leaching agent was used sulfuric acid (H2SO4) at a concentration of 8%. Aliquots containing 100 grams of ore were leached and homogenized in a beaker by adding 250 ml of solution, resulting in a relation solid / liquid 1: 2.5. The leaching took place during certain periods of 0.25, 0.5, 1, 2, 3.5, 12, 19, and 24 hours.

The leaching of oxidized coppers is usually done with sulfuric acid solutions, a combination of economy and efficiency issues. Among the copper oxidized ores are species that are characterized by ore leaching time [4]. After certain times, samples were filtered to promote the separation of liquor containing metal of interest and reject the solid.

Liquor analysis

A sample of each previously separated and reserved liquor was diluted, with a new concentration of 10% over the previous. In an Erlenmeyer flask were added to the samples, plus 2g of potassium iodide (KI) and 4 drops of concentrated sulfuric acid. The mixture was placed at rest, without the presence of light, during the period required for the reaction was complete.

Then the titration was started with the release of iodine using sodium thiosulphate solution (0.1N Na2S2O3). Thereafter the samples were subjected to addition of 2 ml of starch. quantities of sodium thiosulfate for each sample were then recorded.

We used the results of the analysis of the liquor, whose values can be found in Table 02, to calculate the mass of copper present in the liquor by Equation 1. Where mCu is the weight in grams of copper present in the sample liquor ; N normality of the sodium thiosulphate solution used; V is the volume, in liters, thiosulfate used for the titration; MMCu the Copper molar mass; and Fdiluição the dilution factor used in the case, equal to 4.

$$m_{Cu} = N \; x \; V \; x \; MM_{Cu} \; x \; F_{diluição} \quad (1)$$

Figure 1 shows some of the volumetric flasks with the liquor to the leaching tests carried out for each sample.

Figure 1. Liquors from leaching tests.

Reject Analysis

For the analysis of the solid residue obtained after leaching, it was dried using an oven at 100 ° C. A solid sample whose mass can be found in Table 03, was taken and pulverized using a mortar and pestle. In an Erlenmeyer flask, the copper contained in the sample was dissolved using 15 ml of perchloric acid (HClO4 72%). In a chapel, the flask was heated by a plate for five minutes counted after the start of boiling. Then it was cooled for five minutes and then were added 50 ml of distilled water. After this the sample was again heated by the plate for five minutes counted after boiling.

After cooling, were added five drops of ammonia solution (NH3 1: 1), 2 g of ammonium hydrofluoride ((NH4) HF2), and 6 ml of the solution potassium iodide solution. Then he began to titration with sodium thiosulfate while adding 20 ml of thiocyanate 10% potassium solution. Thus were obtained the values found in Table 03 for the volume of titrant used.

the values of the content of the waste produced during leaching were obtained according to equation 2.

Where this is Curej% copper content in the waste sample; N normality of the sodium thiosulphate solution used; V is the volume, in liters, thiosulfate used for the titration; MMCu the molar mass of copper; MSAMPLE and the mass of the tailings sample used for titration, in this case, equal to 0.6.

$$\%Cu_{rej} = N \times V \times MM_{Cu} / m_{amostra} \qquad (2)$$

As the oxidized copper ore this region has copper content of 0.74% [5], it was possible to obtain metallurgical recovery. Equation 3 determines the metallurgical recovery in which RM is a metallurgical recovery in percentage; mCu1 the mass, in grams, of copper present in the sample liquor; and feeding content of 0.74%.

$$\mathbf{RM} = \frac{\mathbf{m_{Cu1}}}{\mathbf{teor\ da\ alimentação}} \mathbf{x\ 100} \qquad (3)$$

RESULTS AND DISCUSSION

The results of the analysis of the resulting liquor leaching process, for certain times and metallurgical recovery values calculated through Equation 3 are shown in Table 1.

Table 1. Results of stemmed liquor from the leaching process at different time periods

AMOSTRA	PERÍODO DE LIXIVIAÇÃO (h)	TIOSSULFATO DE SÓDIO UTILIZADO (mL).	MASSA DE COBRE NO LICOR (g/L)	RECUPERAÇÃO METALÚRGICA (%)
I	0,25	5,6	0,142	19,235
II	0,50	9,2	0,233	31,601
III	1,00	7,5	0,190	25,761
IV	2,00	5,7	0,144	19,579
V	3,50	11,0	0,279	37,784
VI	12,00	12,5	0,317	42,936
VII	19,00	11,9	0,302	40,875
VIII	24,00	20,0	0,508	68,698

A discrepancy was noted in the eighth sample value in time of 24 h. Because this, the point can be disregarded, making the sample VI was obtained that longer separation of the mineral of interest in the process, reaching 0.317 g / L of copper. As the process was done in static beds, the extracted copper content was minimal. The pressure leaching liquid on the ore may also have been important because it limits the formation of copper sulphate in the liquor, besides decreasing the copper solubility limit, occurring thereby saturating the solution. In view of this, some mistakes can be generated in the solids content of copper results in the liquor.

The use of agitation leaching increases in recovered copper content. In the literature there are works that use the agitated tank leaching where they obtained results with recovery above 60% for this type of ore. [5]

From the data presented, it was possible to plot a graph (Figure 2) for the recovery of copper by leaching time.

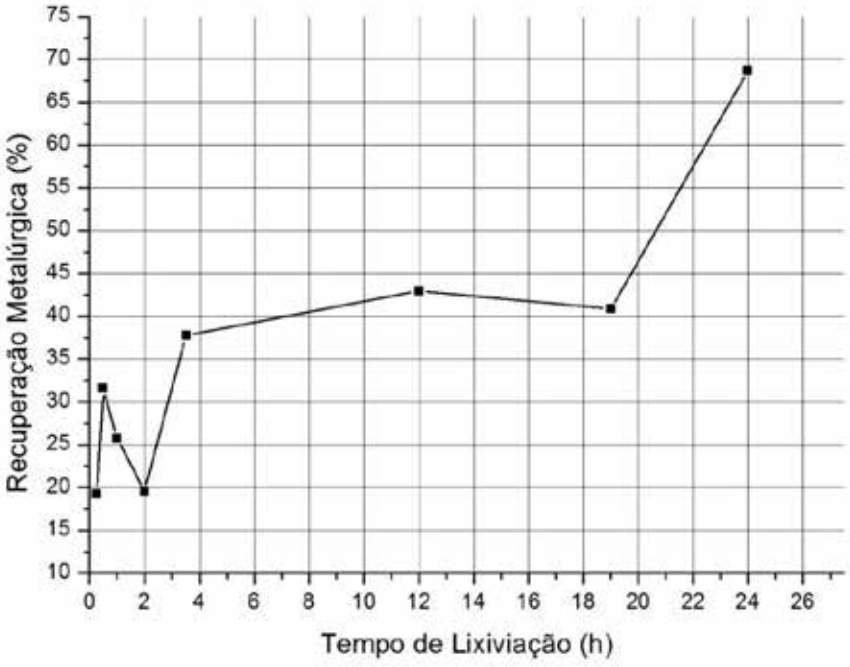

Figure 2. Metallurgical recovery by leaching time

The results obtained from Equation 02, the masses obtained were present in each of the tailings coming from the leaching process of this work. These data are presented in Table 2.

Table 2. Results of the analyzes of the mass of waste originated from the leaching process

AMOSTRA	TEMPO (h)	VOLUME DE SOLUÇÃO TITULANTE (mL)	MASSA DE COBRE (g/L)	TEOR DE COBRE (%)	COBRE NÃO RECUPERADO (%)
I	0,25	54,0	0,343	0,572	77,29
II	0,50	50,4	0,320	0,534	72,13
III	1,00	40,1	0,255	0,425	57,39
IV	2,00	36,5	0,232	0,387	52,33
V	3,50	50,0	0,317	0,529	71,56
VI	12,00	48,0	0,305	0,508	68,69
VII	19,00	51,1	0,324	0,541	73,13
VIII	24,00	52,0	0,330	0,550	74,42

It can be observed the high copper content not recovered above 50% for all times analyzed, which on an industrial scale would be totally impractical for the process. The sample point VIII remains the most divergent among the calculated exclusion being passive again. There was a high rate of copper which is not recovered directly connected to the liquid / solid ratio of the process.

This relationship causes an interference to occur at the solubility limit, precipitating copper crystals in liquor, after filtering, are located in the waste. Unlike liquor analysis results, we see the decrease in copper content in the waste with time to sample IV, within what was expected. Figure 3 shows the copper points analyzed not recovered in time.

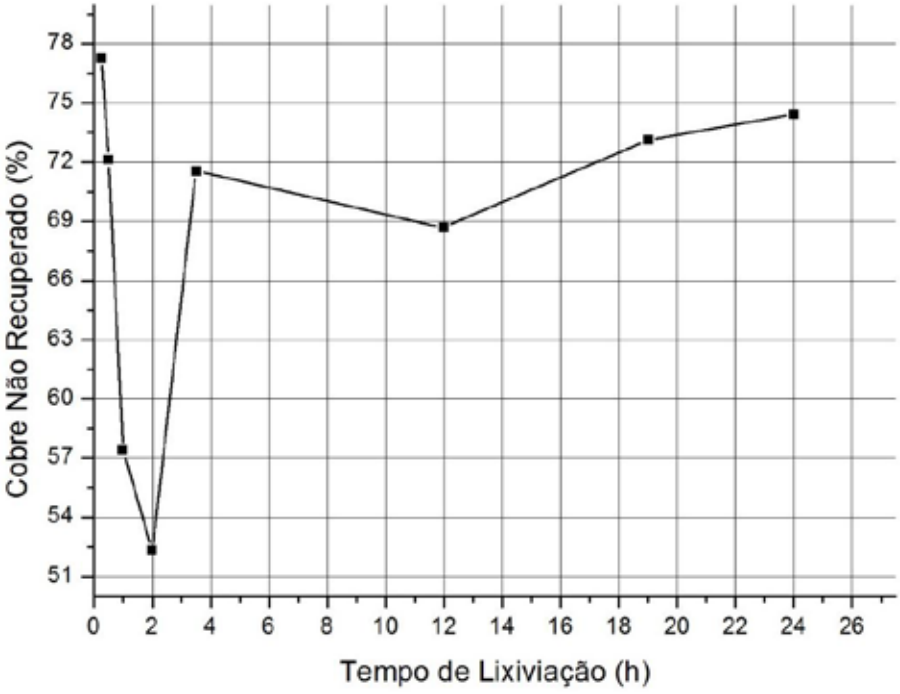

Figure 3. Copper not recovered by leaching time

For a clearer analysis, made a liquor treatment of data was plotted a metallurgical recovery versus time curve, shown in Figure 4.

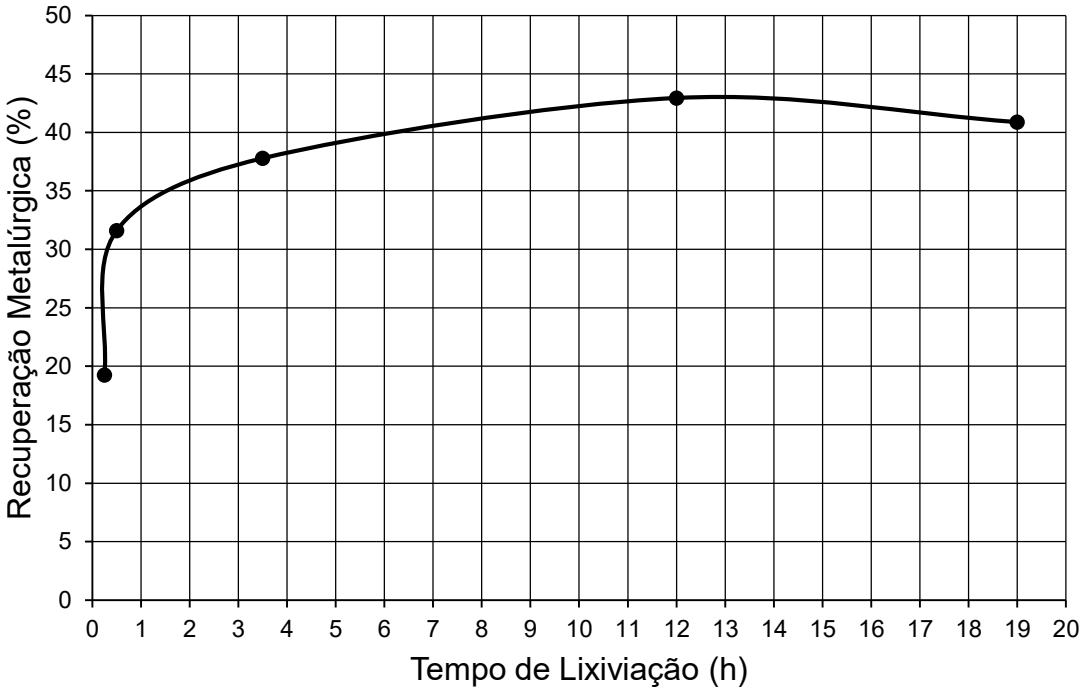

Figure 4. Curve recovery versus leaching time

In the curve you can see that the optimum leaching time was 12 hours, with 42.93% metallurgical recovery. It may be noted that after this time there is a decrease in recovery, instead of its consistency, which can be explained by the copper concentration in the liquor exceeding the solubility limit in the solution, causing the formation of crystals and their subsequent precipitation preventing there is passage through the filter paper.

CONCLUSION

The results obtained for the copper leaching tests Sossego mine can not be regarded as conclusive yet, since Ideally, the experiment was repeated a few times to get a representative sample universe, since the values are divergent with results found by other authors. The analysis of the periods of leaching and copper levels in the liquor and waste adopted in this work made it possible to determine the best extraction time was 12 hours with metallurgical recovery of 42.94%.

However, further study can be done to make you check the influence of the factor particle size versus leaching time and the solid relationship / liquid, parameters that can be error accumulators and makeup actual results, even for an analytical analysis, it usually fails.

Finally, it is important to highlight the prevalence of acid leaching of copper for its metallurgical recovery, making the process of paramount importance to the knowledge in the field of hydrometallurgy, accustomed to this work provided obtaining a great practical and theoretical knowledge on the subject .

REFERENCES

1 Ribeiro JAS. Cobre. DNPM. Salvador; 2013.

2 Masson IOC, Soares PSM. Recuperação do Cobre do Minério Oxidado de Caraíba por Extração por Solventes em Escala Semi-piloto. CETEM. Brasília; 1981.

3 Ferreira AE, Agarwal S, Machado RM, Gameiro LF. Extraction of Copper from Acidic Leach Solution with Acorga M5640 Using a Pulsed Sieve Plate Column. Hydrometallurgy. 2010; 30.

4 Carriconde LL. Estudo prévio da Viabilidade de Extração de Cobre a partir de Minérios Oxidados por Lixiviação Ácida. Porto Alegre: Universidade Federal do Rio Grande do Sul; 2011.

5 Braga ACL, Júnior RNC, Paiva RS, Vale SB. Estudo do Comportamento da Recuperação Metalúrgica do Cobre Oxidado da Mina do Sossego de Canaã dos Carajás Submetido à Lixiviação com H_2SO_4. In: XXIV ENTMME. Bahia, 2011.

TAILINGS DAMS – MONITORING AND REHABILITATION

Stefan Schwank[1] , Axel Oppermann and Dr. Uta Alisch[2], Alessander Kormann[3]

[1] BAUER Mining Solutions at BAUER Maschinen GmbH
BAUER Str.1
Schrobenhausen, D-86529 Germany
(Corresponding author: stefan.schwank@bauer.de)

[2] Fugro Consult GmbH
Wolfener Straße 36 U
D 12681Berlin, Germany

[3] Fugro In Situ Geotecnia, Rua do Geólogo
76 - Zona Especial de Negócios / ZEN
CEP: 28.890-000 - Rio das Ostras / RJ, Brazil

24th World Mining Congress
MINING IN A WORLD OF INNOVATION
October 18-21, 2016 • Rio de Janeiro /RJ • Brazil

TAILINGS DAMS – MONITORING AND REHABILITATION

ABSTRACT

Current dam failures and breaches drive the attention to a more reliable understanding of risks related to tailing dams. The mining industries face a lot of challenges for identifying and mitigate such potential risks. Smart innovative technologies are required for tailing dam characterization as well as for rehabilitation measures for tailings dams at risk.

KEYWORDS

Risks, Dam Failure, Investigation, Monitoring, Dam Rehabilitaion, Seepage, Dam Stability, Seismic liquefaction

INTRODUCTION

Tailing dam failures create significant environmental impacts and economical losses. The worldwide number of tailing dams is increasing and has been estimated as about 3,500 (Martin 2000) with increasing failure rates. The important economic consequences of failures include business interruption or down time of mining and processing operations, environmental damage and cleanup, the socio-economic and political issues associated with transboundary migration of effluent in rivers (Kossoff et al. 2014; Lucas 2001). The cost for catastrophic tailing dam failures can easily exceed $500 million.

TAILING DAM STRUCTURES

Two different types of construction methods for the impoundment of tailings in mining are common:

- Water-retention type tailings dams
- Sequentially raised tailings dams

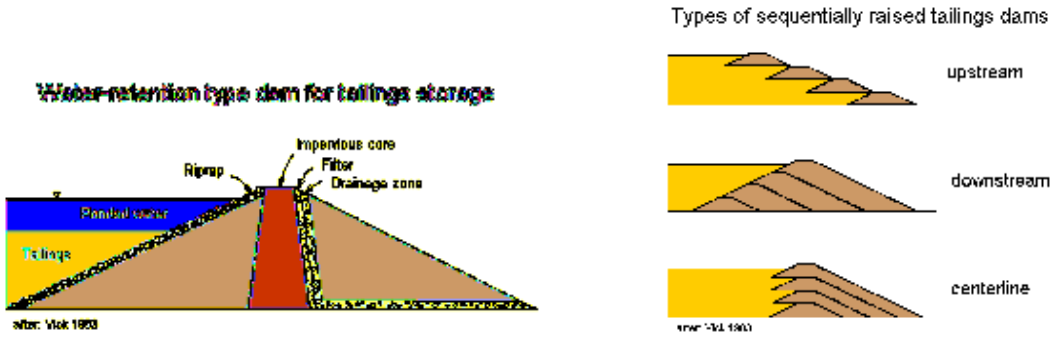

Figure 1 – Tailing Dam Structures by WISE

Retention dams design is very similar to water retention dikes and suitable for any types of tailings and deposition method. They are constructed initially with the construction of the mine to contain the maximum volume of tailings at the end of mine life and impose therefor relative high costs already during the construction phase. The dam is built with material specifically made for dam construction with an impervious core and designed filter and drainage zone.

Raised embankments, be it up-stream, down-stream or centerline dams, are raised step-by step during the life of the mine and have therefore much lower initial construction costs. Raised embankments use usually waste rock or tailings, which are easily available from mining. No special core materials as well filter and drainage zones are installed.

Tailing dams are in most cases constructed by material which is available from the ore processing plants. This is rather a fine grained sand and silt than a qualified construction material as it is used for other dam constructions like hydro dams. The safety integrity of such dams is dependent on design, maintenance and monitoring.

TAILING DAM RISKS

As tailings impoundments are almost never removed, the dams need to be designed for perpetuity. However due to improper construction, settlements in the dam or foundation, flood events and seismic events or increased environmental requirements, rehabilitation of existing dams is requisite to avoid catastrophic consequences in future.

External risks to dams imposed by

- over topping and thus surface erosion
- Increased environmental and mine water regulations
- Increase of pond volume by raising the dam and thus increased hydrogeological conditions for dam and foundation

Internal risks to dam imposed by:

- Uncontrolled seepage through the dike
- Uncontrolled seepage through the foundation of the dike
- Risk of dike stability by seismic events which may cause liquefaction
- Risk of foundation stability by seismic events which may cause liquefaction
- Uncontrolled and untreated seepage water
- Overtopping by flood water with rapid increase of pore pressure and risk of static liquefaction

TAILING DAM RISK ANALYSIS

It is very likely that most of the failures of tailing dams could have been avoided by improved design and sophisticated tailings management. The initial step for any improvements is a tailing dam risk analysis. Execution of analysis for safety assessment should be completed such as stability of the foundation and the operating conditions, liquefaction potential assessment in dams, check the sizing of spillway structures and the adequacy of extreme events adopted in terms of full design and maximum possible earthquake, flood and stability of the foundation when subjected to extreme events, and additional analyses that are identified as necessary after field visits and evaluation of the collected information.

Verification of stability of the foundation and the spillway must consider the static and seismic applications in both operating conditions and in extreme conditions. The number of sections depends on the complexity of the analysed dam geometry (topography and dam).

By waste characteristics (unconsolidated and saturated similar particle size material) verification of the liquefaction potential is always recommended. Among the factors that must be evaluated are the type of soil (through particle size distribution), the specific gravity (density control trials) value of in situ stresses, intensity and duration of dynamic stresses (induced by the mine operation and resulting earthquakes) and position of the water table. Checks should be made considering the potential for liquefaction considering static and dynamic liquefaction. These assessments may be achieving through the use of internationally recognized methodologies as proposed by Seed and Idriss (1971), Robertson and Wride (1997), Andrus and Stokoe (2000), Olson (2001) and Olson and Stark (2003), among others.

A proper design and risk analysis for tailing dams requires accurate and reliable basic data. Fugro, as a world leader in data acquisition has developed a toolbox of smart solutions and specialist technologies for tailing dam investigation and monitoring.

Cone Penetration Testing (CPT)

A tailing dam investigation should besides drilling, sampling and lab testing always includes Cone Penetration Testing (CPT). CPT is the state of the art technology for assessing soil types and their distribution in a tailing dam or a tailing pond. The technology is based on measuring the tip resistance of the probe and the sleeve friction. The ratio between sleeve friction and tip resistance provides fundamental information about soil strength and other properties.

The standard CPT cone has an end area of 10 m^2 or 15 m^2 and is being pushed by static force at a constant speed of 2 cm/sec. Figure 1 shows a standard CPT Piezocone as it was developed by Fugro and TNO 1965. The CPT is a fast and accurate technology, the average daily testing performance is about 200 m.

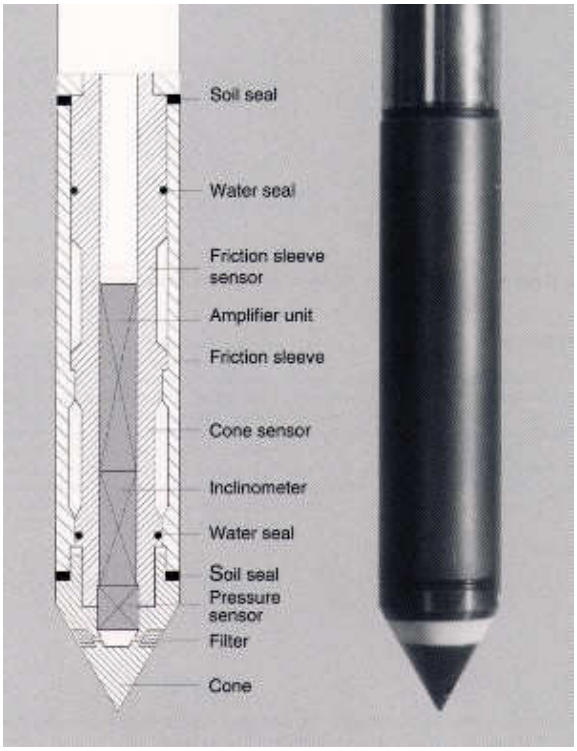

Figure 2 - Standard CPT cone

The CPT can be used to provide design parameters based on a number of indirect methods and correlation's. The data gained from the CPT data allow for:

- Determining soil profiles and estimated soil types
- Determining estimated shear strength of clays
- Estimate settlement and bearing pressures (granular soils)
- Pile capacity and pile tip levels (granular soils)
- Compaction control
- Finding cavities \ swallow holes
- Hydraulic characteristics
- Stiffness measurements (Cone Pressuremeter)
- Dynamic properties (Seismic Cone)

The standard CPT cone can further be combined with other special cones for gaining more specific parameter. In the following, four examples for special cones with valuable use for tailing dam characterization are given:

Seismic CPT Cone (SCPT)

The SCPT is a CPT Cone with an integrated Geophone array build in a sub behind the cone. It allows for testing of dynamic properties without drilling boreholes and with minimal disturbance of soil. Since the cone is pushed directly into the formation the position of the cone is accurately known and the direct contact to the surrounding formation provides an excellent acoustic coupling. The seismic data are collected at 1.0 m intervals. Besides the seismic data the CPT cone provides full geotechnical data. It is a rapid method for acquiring seismic data, the average performance is about 60 – 80 m / day. Figure 2 shows a schematic set-up of a SCPT testing procedure. Figure 3 gives an example for a shear wave velocity profile.

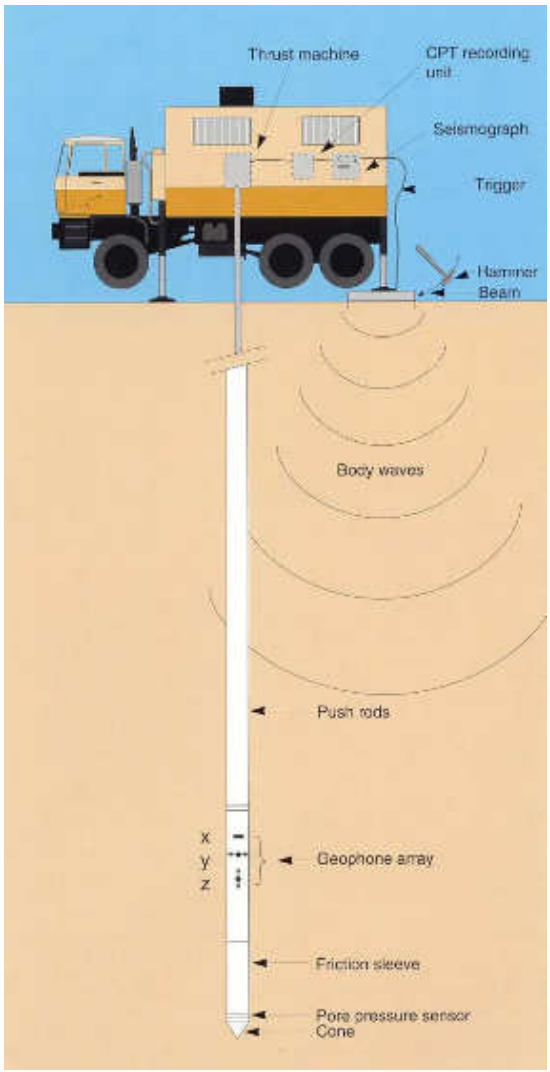

Figure 3 - Schematic set-up of SCPT testing

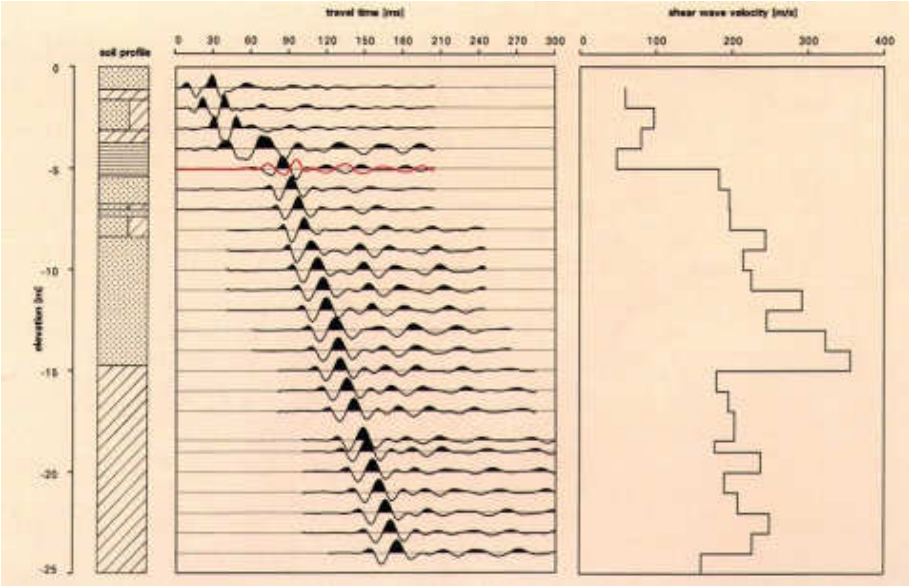

Figure 4 – Travel time and shear wave velocity profile obtained at a CPT location till 25 m depth.

The Cone Pressuremeter (CPM)

The cone pressuremeter is designed for in-situ stiffness measurements. It provides reliable In situ data of the in-situ strength and load deformation behaviour of the soil. In addition it provides undrained shear strength, shear modules, effective horizontal stress and relative density. The CPM uses standard CPT rigs. The test is carried out by controlled expansion of a rubber membrane using nitrogen. At 2 or 3 intervals during the expansion the inflation is stopped and small unload / reload loops are carried out. The test terminates when the maximum expansion or pressure is reached. As a result of testing a pressure strain curve is obtained using applied pressure versus volume expansion. Since the CPM is also coupled with a CPT cone, the soils to be tested are clearly identified via CPT data.

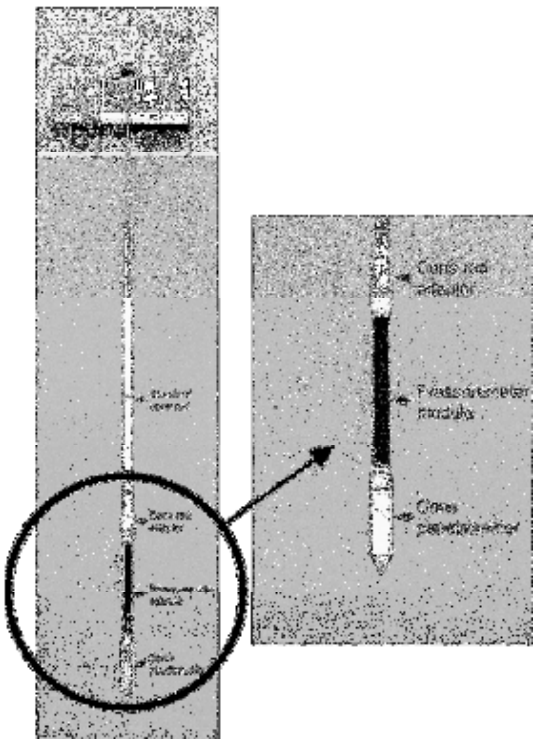

Figure 5 - Schematic set-up of Cone Penetrometer

The Hydraulic Profiling Tool (HPT)

The HPT is designed to evaluate the hydraulic properties of the site subsurface. While the probe is advanced through the subsurface, water is injected at a constant rate Q (up to 5000ml/min) through a screen on the side of the probe. An in-line pressure sensor measures the pressure response p (kPa) of the soil/groundwater system against water injection. Low pressure response means large grain size and the ability to easily transmit water. High pressure response means small grain size and the low ability to transmit water.
The interpretation of recorded profile is preliminary judged in terms of Q/p as relative hydraulic conductivity. The application of variable head tests in wells constructed on the site allows the site specific hydraulic behaviour (as derived from the HPT results) to be validated and, under favourable conditions, be translated into K values (hydraulic conductivity). Through its ability of high resolution k-data acquisition the HPT tool is a valuable tool for identifying piping effects in dams and levees. It has gained a wide acceptance in the levees community for risk assessments related to piping.

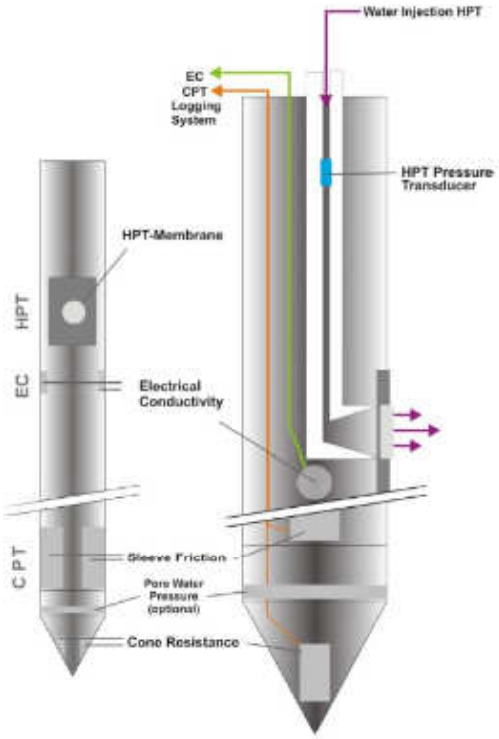

Figure 6 - Schematic sketch of the HPT tool

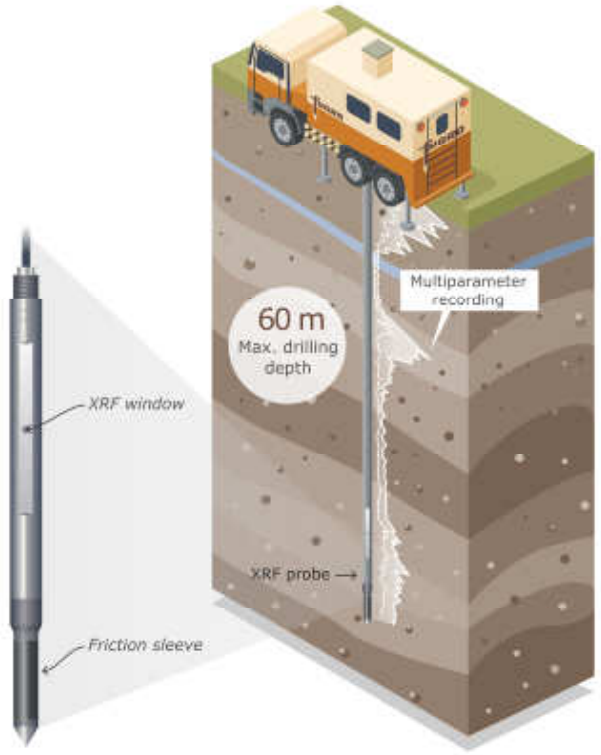

Figure 7 - XRF-CPT tool in operation. While pushed into the tailing material the probe collects geotechnical data (CPT = soil type and soil properties) and elemental date (XRF = element concentrations)

The X-Ray Fluorescence Tool (CPT-XRF)

The CPT-XRF tool has a miniaturized X-ray assembly (x-ray tube and detector) build in a sub behind the CPT cone. This unique tool provides elemental information in a ppm range real time and in high resolution while being pushed into the ground. The probe was specially designed for tailings characterization and delivers valuable data about element contend of a tailing and its remining potential.

Case Study - Copper and Zinc Tailings in Chile

The technology was first applied in Chile in an historic tailing having a complex processing history. The method allowed for a fast and high resolution screening of copper and zinc content in the tailing material down to tailing base at about 25m below surface. The data provided a good understanding of the 3D copper distribution within the tailings sediments and the geotechnical situation as a basis for mine engineering evaluation.

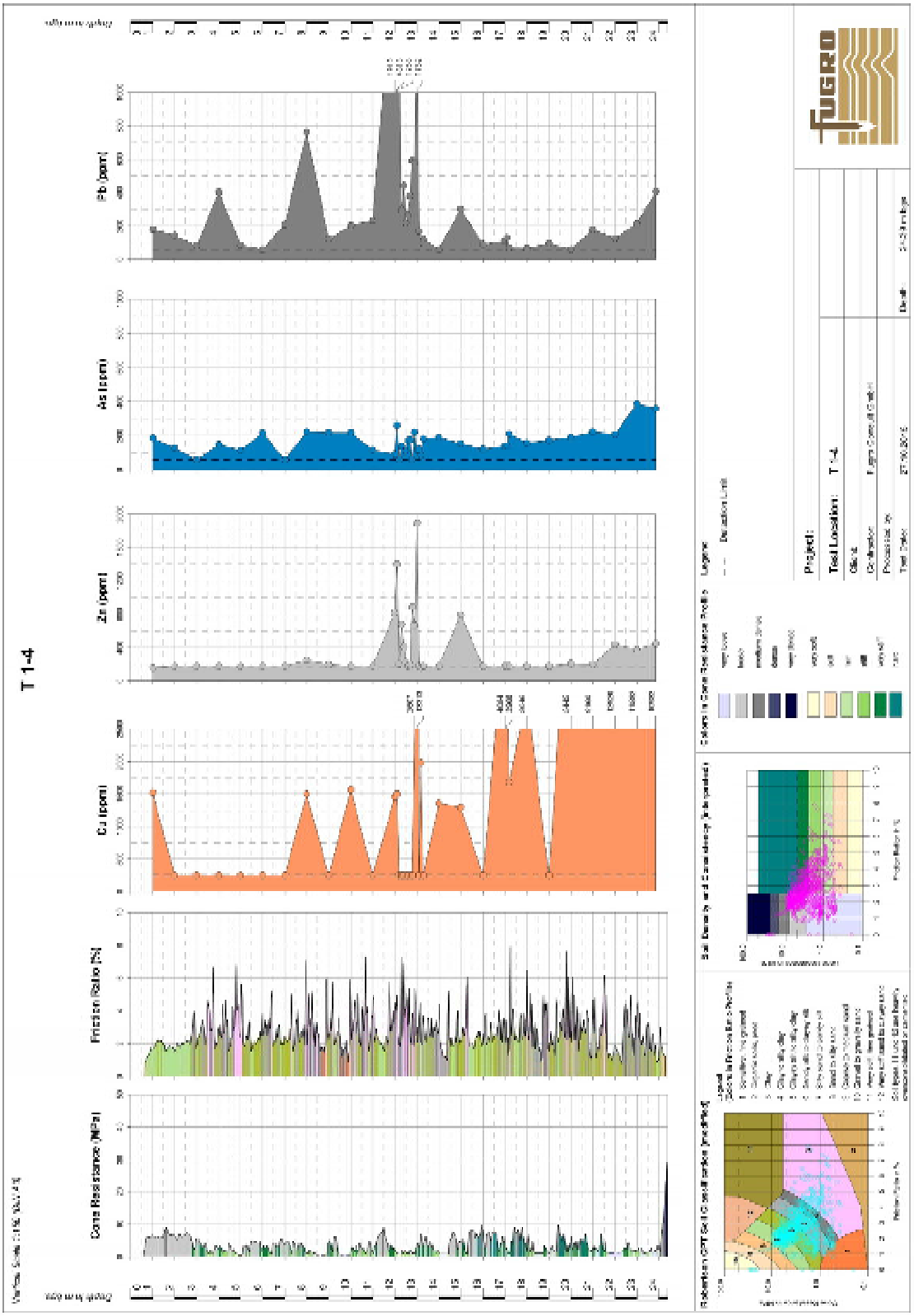

Figure 8 - CPT-XRF log showing soil type, density and metal concentrations (Cu, Zn, As, Pb) in a tailing. At the deeper part of the tailing copper concentrations above 1% could be proved.

Besides the special cone explained above, several other probes are available. The most important ones for tailing dam characterization are:

- In-Situ vane testing: Deployed from a CPT rig, provides in-situ strength like the CPM
- Thermal conductivity probe: Provides continuous temperature profile.

Maintenance and Monitoring

Maintenance and monitoring of tailing dams includes the design of the monitoring scheme (i.e. number of inclinometers, standpipes… and locations), through installation of the monitoring equipment up to a web-based monitoring portal.

Monitoring and maintenance activities during operation should include the following steps:

- Identification of the main risks
- Design of a monitoring plan/system
- Equipment selection and installation
- Equipment control
- Determination of alarm levels and action plans
- Web portal interface
- Continuous assistance during production
- Staff training

For real time monitoring tailored software solutions **integrates and combines** soil investigation data, monitoring, model results and interpretations, so that geotechnical risks can be identified **more rapidly**. The software should include an interactive data platform providing **a single point of truth** for designers, construction teams, geotechnicians and decision makers. This supports teams to manage risks in complex construction projects.

The software portal is ideally accessible via an online working environment and yields real-time insight into geohydrological processes, the effects of construction activities and deformations. The objective presentation of measurement results is a major source of confidence for stakeholders and enables informed decision-making.

REHABILITATION OF DAMS

Different specialized technologies to control and reduce seepage and to improve the stability of tailings dam are available from civil engineering.

For each individual tailings dam, the optimum solution must be determined based on the dike design, materials used in the dike, underground conditions, tailings and mine water composition and static and seismic loading, but also in regard to cost efficiency and environmental sustainability.

Seepage control

Seepage through the dam and the dam foundation which quite often results in piping, impose the highest risk of dam failures. Such risks can be significantly lowered by deliberately drain the seepage water into filter gravel columns or collect the seepage water in large diameter downstream pressure relive wells.

Gravel columns

Both systems are keeping the phreatic line well in the dam body and lower the internal pore water pressure. At the same time they reduce the risk of piping since both systems act as filters with controlled drainage of the mine water, keeping the fines in place inside the dam not being transported as when piping occurs. The seepage water collected can be recirculated with or without treatment back into the mining process or if appropriate, released controlled into ground or surface waters.

Figure 9 – Installation of gravel columns

Gravel columns are installed by bottom feed vibrators with fed material designed to complement the dam or foundation material to create the required filter system for drainage and at the same time due the vibrations introduced, compact the material and increase the internal shear resistance of the dam or foundation. The gravel is fed through a delivery pipe to the tip of the heavy vibrator .

Large Diamater Wells

Large diameter dewatering wells are standard solution, but special care must be taken in case of tailings dams to the proper selection of the material of the filter and of the well screens in respect to the chemical properties of the mine water to achieve a long-lasting wells

Figure 10 – Large Diameter Well Drilling

Reduction / Elimination of Seepage by Cut-off Wall Technologies

To avoid piping and internal erosion and to minimize environmental hazards by mine water seepage, cut-off walls (COW) are the most efficient system to stop the flow of water in both the dam body as well as the foundation of the dam. COWs are especially suited for retention dam improvements. They provide also the best solution for retention dams which have to be raised to accommodate for higher tailings volumes and as a result of the raise have to cope with higher hydraulic gradients. Various COW technologies are available to achieve an optimum effect in regards to seepage reduction or almost elimination and cost. Depending on the dam material, but even more important the geology of the foundation and the hydraulic gradient, soil - bentonite, cement - bentonite or 2 phase concrete walls are proven technologies derived from civil engineering.

The mix design of the cut-off system must be adjusted to each dam separately to achieve best results in water tightness, chemical resistance and flexibility to allow for certain deformation and settlements of the dam.

High standard COWs require the safe penetration through all different soil and rock conditions and the successful seating into even very hard layers is mandatory. Cutter based excavation equipment in combination with a project based slurry mix design provide the optimum seepage barrier for deep COW in highly sensitive environmental areas.

Figure11 - Cut-off wall installation with trench cutter BC 40 at Red Dog mine, Alaska

Cutter Soil Mixing (CSM) walls combine the advantages of the cutter system being able to penetrate trough hard layers with the use of the in-situ dam and foundation material. Actively mixing the soil with a pre-mixed cement-slurry eliminates disposal of excavated soils and at the same time, minimizes trucking to site by only adding cement slurry.

Figure 12 - BAUER BCM 5 CSM Cutter wheel assembly

Alternative solutions for cut-off systems can also be secant pile walls as well as sheet pile walls for easy and fast installation.

Improvement of Internal Dam Stability

Raised embankments in particular, built of uniform fine grained tailings are susceptible to liquefaction if the internal pore pressure cannot dissipate fast enough in case of loading. Especially in case of cyclic loads such as wave action or seismic events, pose a threat to such dikes but also static liquefaction can occur when overloading the dam. The rise of internal pore water pressure reduces the internal friction of the particles and in consequence the dike stability. The same risk applies also to a fine grained foundation especially in seismic events.

In all such cases the soil behaves similar to liquids and when these liquefied zones extends over a large area, the soil mass in motion becomes very large with high energy contained.

The key to improve the dam stability is therefore to increase the internal friction and case of risk of liquefaction reduce the masses in motion and improve the drainage capacity. As shown above gravel columns are a good system for dewatering and seepage control, but at the same time increase the internal friction and improve the dam stability also in case of seismic events (FEMA 2005 and Jansen 2004).

Cutter Soil Mixing web cells are another method to reduce the shaking masses in case of seismic events by partition into small, single, low mass cells. Since the cutter mixing system can be applied also in specific layers only, it is an ideal tool to reduce the risk of liquefaction while concentrating on the sensitive layers. In addition, the CSM cells increase of internal friction of the sensitive layers significantly.

Similar to CSM also high pressure cement grouting is mixing the in-situ soil with a hardening cement slurry, forming any shape of cell structures to reduce the large swinging masses into multiple smaller ones and at the same time increase the internal friction of the soil layer.

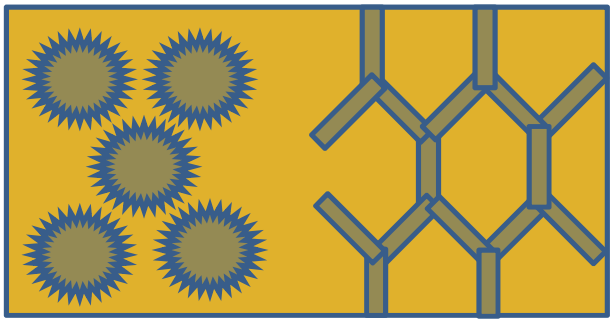

Figure 13 – Single Columns and CSM Web Cell Structures

CONCLUSIONS

Intensive site investigation and monitoring is required to assess the risk of dam failure due to internal problems like piping or external problems like seismic liquefaction. Once the problems of the individual tailing dam are identified, specific solutions can be selected from various methods of civil engineering technology for rehabilitation.

REFERENCES

Andrus, R. and Stokoe II, K. (2000). "Liquefaction Resistance of Soils from Shear-Wave Velocity." J. Geotech. Geoenviron. Eng., 10.1061/(ASCE)1090-0241(2000)126:11(1015), 1015-1025.

FEMA, Federal Guidelines for Dam Safety: Earthquake Analyses and Design of Dams, FEMA 65, printed May 2005

Jansen R.B. Weighing the ways to fix a dam, Water Power and Dam Construction, 25 August 2004

Kossoff, D., Dubbin, W.E., Alfredsson, M., Edwards, S.J., Macklin, M.G., Hudson-Edwards, K.A. 2014. Applied Geochemistry, Vol. 51: pp 229–245.

Lucas, C., 2001. "The Baia Mare and Baia Borsa accidents: cases of severe transboundary water pollution." *Environ. Policy Law*, Vol. 31: pp 106–111.

Martin, T.E., Davies, M.P., 2000. "Trends in the stewardship of tailings dams." In: Proceedings of Tailings and Mine Waste'00, Fort Collins, January, Balkema Publishers, pp 393–407.

Olson, S. M. and Stark, T. D. (2003), yield strength ratio and liquefaction analysis of slopes and embankments, ASCE JGGE, 727-737.

Olson, S. M. (2001), liquefaction analysis of level and sloping ground using field case histories and penetration resistance. Ph.D. thesis, University of Illinois.

Robertson P. K. and Wride, C.E. (1997) Cyclic liquefaction and its evaluation based on the SPT and CPT NCEER Workshop on Evaluation of liquefaction Resistance of Soils, Technical Report NCEER-97-0022, 90pp, National Centre for Earthquake Resistance of Soils.

Vanden Berghe, J.-F., Ballard, J-C., Wintgens, J-F. and List, B. 2011. "Geotechnical Risks Related to Tailings Dam Operations", Proceedings Tailings and Mine Waste 2011, Vancouver, BC, November 6-9.

THE QUESTION: WHICH EXPLOSIVE TO USE? ANFO, EMULSIONS OR BLENDS?

*P. N. Worsey, Ph.D. EurIng

Director of Explosives Education and Professor of Mining Engineering
Department of Mining and Nuclear Engineering
Missouri University of Science and Technology
1400 North Bishop Avenue
Rolla, MO 65409-0450
USA.
*(*Corresponding author: pworsey@mst.edu)*

24th World Mining Congress
MINING IN A WORLD OF INNOVATION
October 18-21, 2016 • Rio de Janeiro /RJ • Brazil

THE QUESTION: WHICH EXPLOSIVE TO USE? ANFO, EMULSIONS OR BLENDS?

ABSTRACT

Traditionally ANFO has been used for dry holes and emulsion for wet conditions. ANFO is less dense, so is loaded in a condensed pattern, whereas emulsions are significantly denser, which allows expanded patterns. Traditionally economic analysis has pitted drilling against explosives costs. However, when using ANFO, conditions are not always completely dry and wet holes have to be loaded with emulsion. In this paper an economic analysis is provided based on the percentage of wet holes encountered. Actual costs from the mid 2000's are used for a crushed limestone operation as an example. At less than 7% wet holes, emulsion on an expanded pattern is more economically attractive. In this scenario using emulsion on an expanded pattern eliminates risk and simplifies the charging process. The adoption of this strategy has made some blasting contractors in the United States very successful. The effect of cost differential between ANFO and emulsion is explored, along with variation in drilling cost, which move the transition percentage. In addition the use of dry and wet blends on an expanded pattern is explored, which can provide additional cost savings.

KEYWORDS

Economic, analysis, bulk, explosive, blasting, ANFO, emulsion, blend, wet, holes

INTRODUCTION

Bulk ANFO (Ammonium Nitrate Fuel Oil (mix)) and emulsions and their predecessors, slurries, have been around for over 50 years. Traditionally ANFO was used in dry holes and stick product in wet holes. However stick explosive is very expensive and has been replaced in most mining operations in the United States by bulk emulsion, which is a much cheaper alternative. Besides rumors, there is no waterproof ANFO that can be loaded in wet holes, just water resistant ANFO, which can be loaded in dewatered holes and only resists the residual moisture on the borehole walls and minor water infiltration back into the hole.

Past decisions for using ANFO vs. emulsion in dry conditions have been made by comparing the economics of ANFO on a condensed pattern vs. emulsion on an expanded pattern using the same weight of explosive to blast the same volume of rock (constant powder factor). As emulsion is typically considerably denser than ANFO less holes are required. Thus increased explosive cost is balanced against reduced drilling cost. However, most operations are not totally dry and have mixed conditions i.e. dry holes with some wet holes. In addition there are dry and wet seasons and a dry pattern may be inundated by heavy rain and the holes fill up with water. This particularly makes explosives shot service (contracted blasting) a risky business if the contractor is being paid by the ton of rock blasted.

If a wet hole is encountered, typically the blaster will be forced to load with bulk emulsion. The emulsion is both more expensive than ANFO per unit weight and also significantly denser such that a second extra cost is incurred because more kg end up being placed in the hole. In this paper a real life example is used of a typical limestone quarry in the United States with explosives and drilling costs supplied by a very successful shot service contractor. (These are actual costs from the 2000's to avoid any competitive issues with the release of these numbers.). The scenario is modeled using a simple spreadsheet and the break-even point for emulsion is calculated. The rational is presented such that any engineer can

make similar calculations for his or her operations. The sensitivity of the break-even point is explored for both price differential between emulsion and ANFO and changing drilling costs.

Rationale for calculations

There are two main spreadsheet design factors that are key to simple calculation:

1. A complex spread sheet and calculations can be confusing. Keeping to a constant powder factor allows us to compare apples to apples.

2. All we need to do is design a single hole. It is not necessary at this stage to design a complete blast. This significantly simplifies the process.

To design a single hole we require: hole diameter, blast depth, subdrill and stemming. This determines the volume of hole for placement of explosive. Explosive density determines the weight of explosive we can get into that volume. Powder factor, once chosen is kept constant.

Example spread sheet

The scenario used: crushed stone quarry with horizontal closely bedded limestone in the Midwestern US, typical hole diameter and face height. 4 in. (100 mm) hole, 40 ft (12 m) bench height.

The units used in the example spreadsheet are US, both measurements and costs, but a spreadsheet can be easily written in metric units and currency appropriate for any country.

The explosives materials, costs, hole diameter and bench height can be seen in the first seven rows of Figure 1. This is the basic information required for the design of a single loaded hole and calculation of its ultimate cost. The powder factor is chosen as 0.5 lb of explosives per short ton of rock (~0.25 kg per tonne), which is a typical value used in US quarrying in this type of rock.

In the next eight rows the hole design is calculated for ANFO, Emulsion, and three different blend ratios (%emulsion/%ANFO). A readily available explosive TITAN is used in this example. Note that the densities for 100%, 70% and 40% are very close. This allows the same expanded pattern to be used later on for both straight emulsion and emulsion ANFO blends. In the design of the hole, the rock is closely bedded and therefore no sub drill is required. The stemming is crushed stone approximately 1/8th of the hole diameter and a length of 2/3 of the burden, estimated at 16 times the hole diameter for ANFO and 20 times for emulsion. The remainder of the hole is filled with explosives.

The total cost of a single hole is then calculated, including the costs of the explosive, initiators, primers and drilling. Finally the cost per ton is calculated by taking the total cost per hole and dividing by the total tons blasted by that hole (weight of explosive in hole/powder factor).

In this example the bottom line cost of blasting per ton is $0.41 for ANFO and $0.42 for emulsion on an expanded pattern. Obviously ANFO is cheaper in dry ground than emulsion. However when a wet hole is encountered the emulsion is loaded into a hole on a smaller ANFO pattern, so the cost of that hole is significantly higher and the cost per ton of that hole on the shrunk pattern is the cost of the hole divided by the total tons for an ANFO hole. This cost per ton is calculated at $0.59 per ton, significantly higher.

Wet or Dry								
Input	AN		Emulsion					
Dry Hole		Wet Hole		Drilling		Units	Initaiton costs	
SG Explosive	0.86	SG explosi	1.25	Hole diam	4	inches	EZdet	$4.50
Cost/lb	$0.310	Cost/lb	$0.480	Bench heig	40	feet	Primer	$3.00
				Subdril 1=y	0		Primers #	1
				Cost/ft	$1.900			
Powder factor		0.5	lb/ton					
Hole calculations								
	ANFO	Emul	70/30	40/60	30/70			
Stemming	5.33	6.67	6.67	6.67	6.67			
Hole depth	40.00	40.00	40.00	40.00	40.00			
ex col ht	34.67	33.33	33.33	33.33	33.33			
density	0.86	1.25	1.29	1.25	1.15			
#/ft	4.69	6.81	7.03	6.81	6.27			
#/hole	162.42	227.00	234.26	227.00	208.84			
Cost								
Explosive	$50.35	$108.96	$100.50	$85.81	$75.39			
Cap	$4.50	$4.50	$4.50	$4.50	$4.50			
Primer	$3.00	$3.00	$3.00	$3.00	$3.00			
Drilling	$76.000	$76.000	$76.000	$76.000	$76.000			
						Emul Shrunk		
Total Cost	$133.85	$192.46	$184.00	$169.31	$158.89	$192.46		
Total tons	324.8461	454	468.528	454	417.68	324.8461		
Cost/ton	$0.41	$0.42	$0.39	$0.37	$0.38	$0.59		

Figure 1 - Screenshot of the calculation part of the excel spread sheet

A blast pattern is a multitude of blast holes usually drilled on a constant fixed pattern. The cost of wet holes vs ANFO can then be plotted and the break-even point established. As it is a straight line relationship with respect to percentage wet holes it can be done using two points, those for completely dry and completely wet, as illustrated in Figure 2. In this figure, the increasing cost of replacing ANFO with emulsion on a shot is graphed along with that for emulsion on an expanded pattern. Note that the emulsion on an expanded pattern is ultimately not affected by whether the hole is wet or dry and is therefore a horizontal straight line. The calculated breakeven point between the two scenarios is 6.58% wet holes. This is not many wet holes. For this scenario choosing the expanded emulsion pattern avoids risk for a shot service contractor, and simplifies his blast crew's job, making them more efficient.

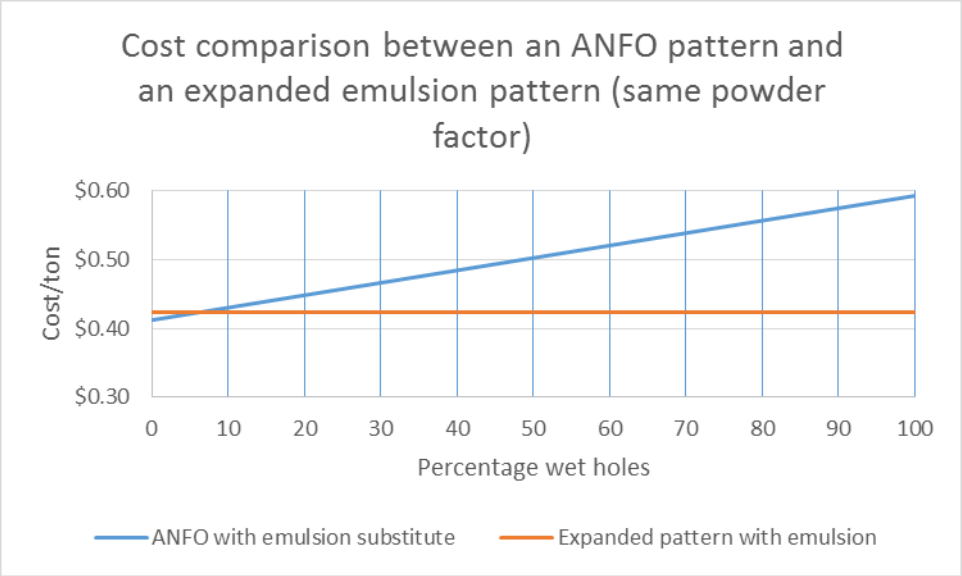

Figure 2 - The cost comparison between an ANFO pattern and an expanded emulsion pattern (same powder factor) vs percentage wet holes

As one changes the costs in the spreadsheet the breakeven point moves accordingly and each mining operation will have a different break-even point for the use of emulsion on an expanded pattern. The effect of these changing parameters on the emulsion/ANFO breakeven point was investigated further using the spreadsheet. First, the effect of changing the cost of the emulsion was looked at. Data for both increments and decrements in the cost of the emulsion was generated and plotted in Figure 3.

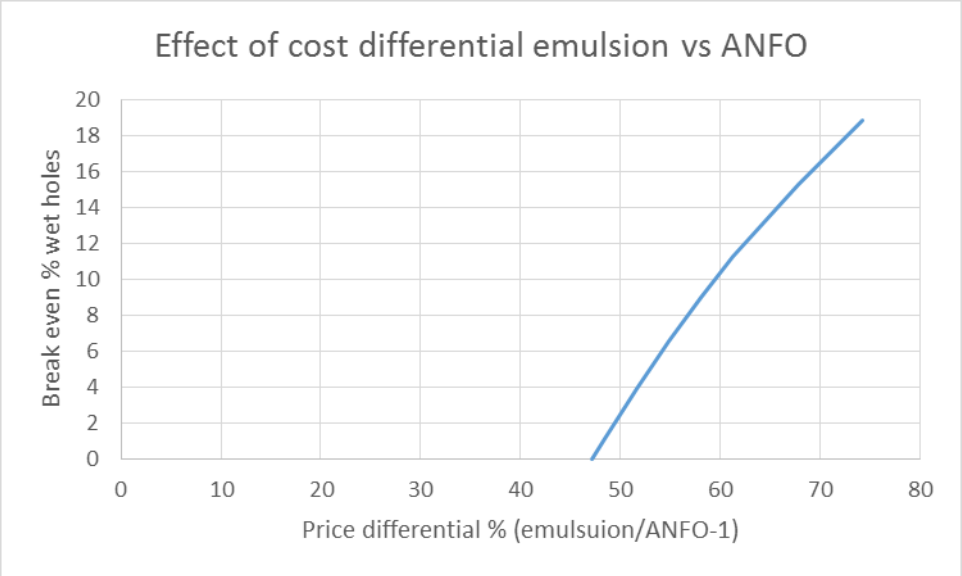

Figure 3 - Effect of cost differential between emulsion and ANFO on the break-even point

The % break-even is plotted against the price differential in percent. For example a price differential of 50% means that the emulsion costs 50% more than ANFO per kg. For reference the price differential for the original scenario is approximately 55%. As expected, as the price differential increases

the break-even point increases making the use of emulsion less attractive. In this scenario when the price differential drops to around 47%, the break-even point drops below zero which means that emulsion on an expanded pattern is now cheaper than ANFO on a constricted pattern regardless of conditions.

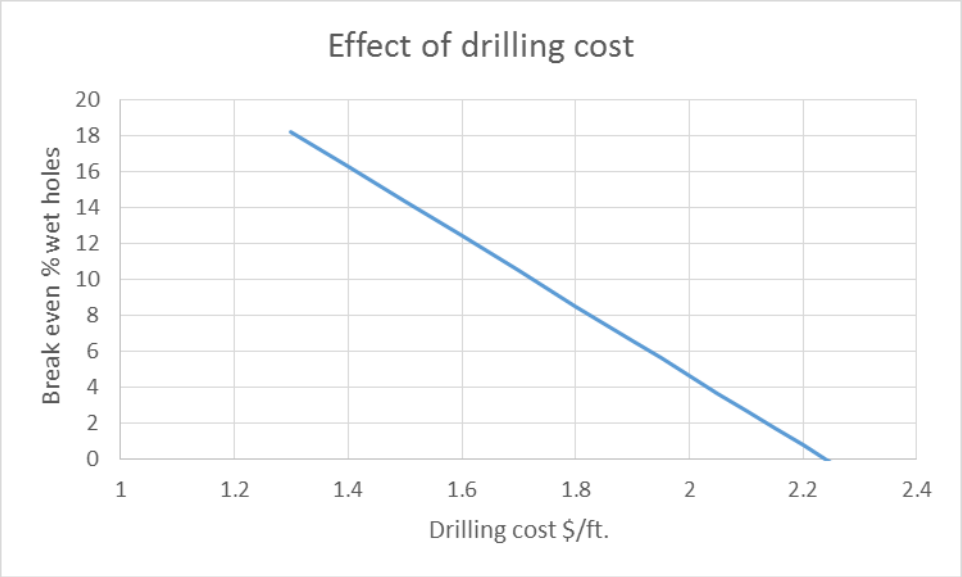

Figure 4 - Effect of drilling cost on the break-even point

The current drilling cost is $1.90/ft. for a break-even of 6.58%. Drilling costs can vary based on three major categories comprising, drilling contractor bids, the hardness and drillabilty of the rock, and varying economic considerations. Let's take for instance differing rock conditions. If easier drilling is encountered, the drilling rate will increase and the drilling cost will go down, and vice versa for harder rock. As can be seen in Figure 4, for fixed explosive costs, as the drilling cost increases, emulsion on an expanded pattern becomes more attractive. In this scenario the break-even point drops to zero (completely dry) at a drilling cost of approximately 2.24 $/ft. However, when drilling costs decrease the break-even point increases and the use of emulsion becomes less attractive.

USE OF BLENDS

Blends hit the mining scene in a big way in the late 1980's. Blends are a mixture of emulsion and ANFO. They are usually reported as emulsion/ANFO mix such as 70/30. Some manufactures, example Dyno in Figure 5 below, report the emulsion percentage as the last 2 numbers of the name. Titan emulsion was used in example as the densities were readily available and consistent from 100% through 40%.

Senario	ANFO	TITAN 1000	Titan 1070	Titan 1040	Titan 1030
SG	0.86	1.25	1.29	1.25	1.15
Emulsion	0%	100%	70%	40%	30%
ANFO	100%	0%	30%	60%	70%
Cost/lb	$0.31	$0.48	$0.43	$0.38	$0.36

Figure 5 - Snapshot from spreadsheet showing the explosives designated and projected blend costs

ANFO is cheap compared to emulsion but ANFO is very light in comparison. Because of this you can usually put up to as much as 50% extra kg of emulsion in a blast hole. The actual density of a single

ANFO prill is comparable to that of emulsion. However, the air gaps between the prill reduce the density significantly. By placing emulsion in the gaps between the prill, the density can be appreciably increased, and conversely adding ANFO prill to emulsion can reduce the explosive cost. The problem is that the prill is highly water soluble, whereas the emulsion is relatively insoluble. If the prill touch each other in the blend they will dissolve in wet holes, but if the prill is completely encapsulated by the emulsion it will be waterproof. Unfortunately a 50/50 mix is not waterproof and a higher percent emulsion is required. In this example I have selected a 70/30 mix for wet holes and a 40/60 mix for dry holes. It is important to note that their densities are comparable so that an approximately constant powder factor is maintained. This means they can be used on the same expanded pattern as emulsion and interchanged depending on the conditions.

In Figure 6 below the purple line represents emulsion on an expanded pattern with less expensive 60/40 blend substituted for dry holes. In this scenario it is cheaper than ANFO even for dry holes. Additional cost savings can be obtained by replacing straight emulsion with 70/30 waterproof blend (yellow line). It is for this reason that blend trucks have become so popular in the United States.

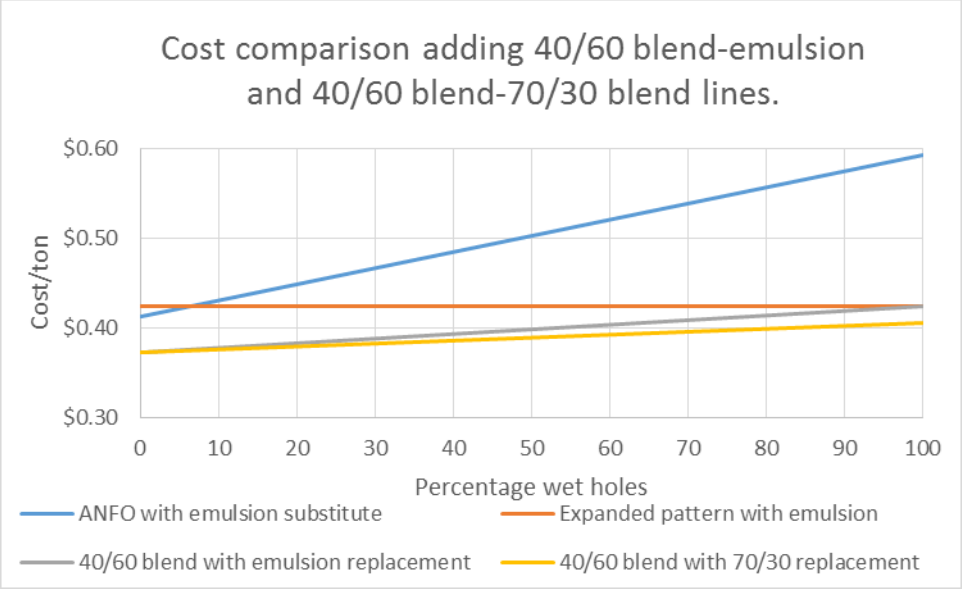

Figure 6 - The cost comparison adding blends to the scenario

Further comments and discussion

Of course blends require a specialist charging truck with both ANFO and emulsion tanks, with the ability to discharge either explosive or a mixture of the two. Because of cost and requirement to have an adequate return on investment the equipment needs high usage. Therefore we see blend trucks used most often in large scale mining operations and by shot service contractors who service multiple smaller quarry operations.

Emulsion has less energy per kg, as it contains a small percentage of inert water. However, this is compensated by its superior detonation velocity, which increases blast fracturing and fragmentation. In most mining blasting, fragmentation is the desired outcome. However, in the United States in the last 30 years blast casting has been popular in large scale strip pit coal mining, where the explosive energy is used to move the overburden. If using for overburden movement the relative bulk energy of the explosive can be easily factored into the spread sheet.

CONCLUSIONS

The economics of using ANFO vs emulsion can be easily modeled using a simple spreadsheet based on single hole charging configurations and by maintaining a constant powder factor. For comparison purposes it is not necessary to design a full blasting pattern.

If the use of ANFO is more economic for dry holes, there will be a break-even point for its replacement by emulsion using an expanded pattern as the percentage of wet holes increases. This break-even point is raised with increasing cost differential between ANFO and emulsion and it is decreased by increasing drilling cost.

The use of blends as a substitute for straight emulsion can be very attractive when using an expanded pattern and is part of the explanation for the surge of the use of blends in the US.

ZINC DEPRESSION IN THE GALENA FLOTATION OF ERMA REKA CONCENTRATOR

M. Ranchev[1], N. Valkanov[2], I. Grigorova[1] and *I. Nishkov[1]

[1]*University of Mining and Geology "St. Ivan Rilski"*
Department of Mineral Processing and Recycling
Prof. Boian Kamenov Street
1700 Sofia, Bulgaria
*(*Corresponding author: inishkov@gmail.com)*

[2]*MINSTROY HOLDING JSC*
57 G.M. Dimitrov Blvd.
1172 Sofia, Bulgaria

24th World Mining Congress
MINING IN A WORLD OF INNOVATION
October 18-21, 2016 • Rio de Janeiro /RJ • Brazil

ZINC DEPRESSION IN THE GALENA FLOTATION OF ERMA REKA CONCENTRATOR

ABSTRACT

Lead-zinc ores are dressed in "Erma Reka" concentrator. These ores are characterized with variable and complex mineral composition and physical properties. Due to this fact, a collective-selective flotation circuit was established. Two-stage selective flotation is used, where the zinc and iron minerals are depressed, allowing the galena to float, followed by the activation of the zinc minerals in the lead tailings to allow a zinc float. Mineralogical studies in polished sections and quantitative electron microprobe analysis of the lead-zinc ores from the three exploited deposits were held. These surveys showed the presence of an iron rich sphalerite (marmatite) containing 10.50 – 12.00 % iron, which was found in two of these tree main deposits. The existence of marmatite in the run-of-mine, would mostly lead to poor technological parameters, production of lead concentrate contaminated with zinc minerals and subsequent decreasing of the zinc concentrates grade. The aim of this study is to minimize the flotation of marmatite during the separation of the lead and zinc minerals into the galena rougher flotation. Laboratory flotation tests were conducted, where the role of pH and the consumption of zinc sulphate and modified sulfides complex MINFIT® were established. The results from the laboratory flotation tests, showed the possibility of marmatite depression under certain conditions. Therefore, pilot tests were held, where in the presence of zinc sulphate (800 g/t) and MINFIT® (200 g/t) at the pH value of 9.5, the recovery of lead concentrate reached 94.00 % at a grade of 73.40 % Pb and only 3.30 % Zn in the final lead concentrate.

KEYWORDS

Zinc depression, galena flotation, marmatite

INTRODUCTION

Flotation is an important and versatile mineral processing step used to achieve selective separation of minerals and gangue. It utilizes the hydrophobic (aerophilic) nature of mineral surfaces and their propensity to attach to rising air bubbles in a water–ore pulp as the basis for separation (Biswas & Davenport, 1994). Metal sulphide minerals, for which this process was originally developed, are generally weakly polar in nature and consequently most have a hydrophilic surface (Wills, 1997). The flotation recovery of a mineral particle is dependent on the efficiency of collision of the particle with an air bubble, the efficiency of attachment of the particle to the bubble and the stability of the bubble particle aggregate during its transport and recovery from the froth. The efficiency of collision decreases with decreasing particle diameter for a given bubble size and various models have been proposed to describe this effect (Dai, Dukhin, Fornasiero & Ralston, 1998; Reay & Ratcliff, 1973).

The minimum contact angle required to ensure the stability of the bubble particle aggregate has been shown to be particle size dependent (Crawford & Ralston, 1988). The factors affecting attachment efficiency have also been identified (Hewitt, Fornasiero & Ralston, 1994) and are linked to both particle size and hydrophobicity effects. The decreased flotation recovery of fine sulphide minerals can be attributed to their decreased mass and higher surface area. This is because a decreased mass and inertia decreases the collision efficiency, whereas an increased surface area increases the reagent addition requirements per unit mass. A decrease in particle size may increase the degree of surface oxidation and the degree of interaction of the finer particles with other fine hydrophilic or slime particles (Gaudin, Fuerstenau & Miaw, 1960). These effects are primarily attributable to an increased surface area but may also be the result of finer particles having a higher surface energy per unit area (Sivamohan, 1990).

Flotation separation and recovery of lead and zinc concentrates from ores containing galena (PbS) and sphalerite (ZnS) is well established and generally achieved quite effectively. The two principal minerals containing lead and zinc are galena and sphalerite. They are frequently found together along with other sulphide minerals, but one or the other may be predominant. Galena may

contain small amounts of impurities including Ag, Bi, Sb, Te etc. When silver is present in sufficient quantities, galena is regarded as a silver ore and called argentiferous galena. Sphalerite is an important Zn-bearing mineral and the primary source of zinc metal (Biswas & Davenport, 1994). Natural sphalerite commonly contains impurities such as Fe, Cd, Mn and Cu substituted for Zn^{2+}, which displays a wide range of colors in nature. The Fe content of sphalerite varies from 0.40 % to 22.00 % (wt) with different temperatures and chemical environments of the crystallization. Sphalerite is called marmatite (Zn, Fe) S when the content of Fe is over 6% (Tong Xiong, Song Shao-xian & He Jian, 2007). Some of the difficulties associated with processing of the ores containing marmatite can be described as follows: the flotation kinetics of marmatite (Zn, Fe)S is much lower than that of sphalerite ZnS; during the flotation of ore containing marmatite, the consumption of activator ($CuSO_4$) is much higher than that normally used for flotation of low Fe sphalerite. Surveys from about 30 operating plants that treat varieties of sphalerite have indicated that the consumption of $CuSO_4$ required to activate sphalerite is proportional to the amount of Fe present in the sphalerite (Bulatovic, 2007). The hydrometallurgical requirements connected with the zinc impurities in the flotation lead concentrates and lead or iron (pyrite, pyrrhotite) contaminants in the final zinc concentrates, must be strictly followed, in order to avoid any penalties which are usually different for each individual smelter.

Zinc sulphide minerals (sphalerite, marmatite) always occur in association with other sulphide minerals. The concentration and separation of these minerals by flotation requires the use of modifying procedures: activation to render the zinc mineral susceptible to reaction with sulfhydryl collectors, deactivation and depression to prevent their inadvertent flotation together with other components of the ores (Finkelstein, 1997). The non-values include iron sulphides such as pyrite and pyrrhotite that, while are often floatable, could be controlled. Being the most abundant sulfide mineral pyrite is undesirably associated, and in most cases fine grained and intimately intergrowth, with minerals of economic value (Dimitrijevic, Antonijevic & Jankovic, 1996). This gangue pyrite is a cause of reduced concentrate grade and increased smelting costs, for most minerals such as galena, sphalerite and chalcopyrite. Pyrite is also a primary contributor towards the substantial environmental problem of acid mine drainage resulting in acidification of natural water systems.

Lead-zinc ores from hydrothermal lead-zinc deposits disposed at the southeastern part of Madan ore field, Central Rhodopes, Bulgaria are dressed in Erma reka concentrator. The Madan deposits comprise the largest region producing Pb-Zn ore in Bulgaria. The ore mineralization has been represented by three morphogenetic types of ore bodies – ore veins, marble-hosted skarn-ore bodies and stockworks. These ores are characterized with variable and complex mineral composition and physical properties. Due to this fact, a collective-selective flotation circuit was established. The main ore minerals are presented by galena, sphalerite, pyrite and chalcopyrite and as subordinate and minor could be found - arsenopyrite, marcasite, pyrrothite, tetrahedrite – tennantite, Fe-oxides etc. The ore minerals associated with quartz, carbonates, clinopyroxenes skarns – johannsenite – hedenbergite. Lead and zinc concentrates and pyrite product are obtained in Erma reka concentrator during the treatment of the lead – zinc ore. Hydrometallurgical company subsequently treats the concentrates and the pyrite product is combined with the final flotation tailings and directed to the tailings pond.

Two-stage selective flotation is performed, where the zinc and iron minerals are depressed with $ZnSO_4$ and sodium cyanide at pH 8.00 – 8.50, allowing the galena to float, followed by the activation of the zinc minerals found in the lead scavenger tailings and subsequent zinc flotation. The lead circuit includes two rougher, scavenger, re-scavenger and four cleaner stages. After the galena flotation, the tailings are treated with copper sulphate, which reactivates the surface of zinc minerals, allowing them to float. Lime is used to depress pyrite, as has no depressing effect on the activated zinc minerals, and high pH (10-12) is used in circuit. The zinc circuit includes Zn-Py rougher, Zn-Py scavenger and two re-scavenger, Zn-Py cleaner, Zn rougher, Zn scavenger and re-scavenger, Zn-cleaner and three Zn re-cleaner stages. Finally, the concentrator produces lead and zinc sulphide concentrates (Nishkov & Grigorova, 2010).

At the last two years (2013, 2014) ineffective results during the selective-collective flotation treatment and relatively poor concentrate grades of the final lead and zinc concentrates have been observed, which leads to technological difficulties along the hydrometallurgical operations and the recovery of the Pb and Zn metals. Studies of the run-of-mine showed the presence of Fe-rich sphalerite. The existence of this high iron variety of sphalerite called marmatite (Zn, Fe)S in the lead rougher flotation feed would result in poor technological parameters, contamination of the lead

concentrate with zinc minerals and subsequent decreasing of the zinc concentrate grade, metal losses in the final tailings and possible penalties by the metallurgical companies.

Research and development program has started to improve the lead – sphalerite separation in the Erma reka flotation plant. The aim of this study is to determine and minimize the causes for the ineffective selective flotation (marmatite recovery in the rougher lead concentrate) and the subsequently production of metal concentrates with deteriorated technological parameters. A special attention was paid to the improvement of the galena – marmatite selectivity process, which was achieved under the conditions detailed below. This paper describes the results of the model physicochemical investigations, laboratory and industrial experimental work in the frame of the research program and the development of new reagent regime in the flotation section of Erma reka concentrator.

METHODS, MATERIALS AND EQUIPMENT

Ore Characterization

The representative lead-zinc ore sample (50 kg) was provided from the currently exploited by underground mining lead-zinc deposits. The chemical composition of the lead-zinc ore sample was Pb-2.56%; Zn - 2.70 %; SiO_2–53.00 %; CaO - 7.25 %. In order to evaluate the mineral composition of the run-of-mine and zinc flotation concentrate, polished sections studied with polarizing microscope MEIJI MT 9430 (provided with digital camera) have been prepared. Quantitative electron microprobe analyses for determination of the composition of the main ore and gangue minerals with scanning electron microscope JSM-6010 Plus/LA, with EDS analytical system have been established. A special attention of the sphalerite composition and the presence of Fe in the mineral have been paid, considering that the increase Fe content affect the physicochemical properties and flotation kinetics of the sphalerite. By using Mössbauer and Raman spectroscopy, it was determined that, when the Fe is more than 6 %, a part of the iron it is presented by Fe^{3+}, while in the sphalerite matrix could be found lamellas of pyrrothite (FeS) (Lepetit, Bente, Doering & Luckhaus, 2003).

Contact Angle Measurements

The wetting properties of the marmatite were characterized by means of the three-phase contact angle. The three-phase contact angle on the flat mineral substrate submerged in the solution was studied using the microscopy technique. By forcing a meniscus from a capillary against the mineral surface, a non-equilibrium liquid film was formed and by its thinning, at a critical thickness value, a three-phase contact was formed spontaneously, the latter expanding at constant pressure till the moment when meniscus took a new equilibrium shape, characterized by the angels of wetting of the flat mineral surface and of the cylindrical glass one. The formation of a thin film and the expansion of the three-phase contact perimeter were monitored by a metallographic microscope. Several marmatite samples were selected and studied. The mineral sample pretreated as described above was immersed in deionized distilled water and potassium ethyl xanthate was added. After 15 minutes conditioning time the contact angle was determined. Following these measurements, the clean marmatite sample was conditioned in zinc sulphate and MINFIT® solution at pH 9.5 for period of 15 minutes after which potassium ethyl xanthate was added to the system. After an additional 15 min. conditioning, contact-angle measurements were obtained.

Laboratory Flotation Tests

The flotation feed samples were ground in a laboratory stainless steel ball mill in order to achieve a P_{80} = 75 μm, determined by traditional sieving. Laboratory, batch flotation experiments were conducted using a 2.5 L Denver self-aerated flotation machine. The pulp was conditioned at 660 rpm for 2 min. The solids content during the flotation experiments was maintained within the scope of 25 - 27 wt. % and the employed pH regulator was lime ($Ca(OH)_2$). Potassium ethyl xanthate (PEX) was used as collector and MIBC was use as a frother for the lead rougher flotation tests. The depressants reagent used in the laboratory flotation tests were zinc sulphate and MINFIT® – representing a complex of modified sulphites.

Industrial Tests

In the period of several months an industrial tests have been conducted in order to determine the optimum reagent regime in the cycle of lead rougher flotation. The aim of the industrial tests was to minimize the recovery of zinc minerals in the lead rougher concentrate during the separation of galena from the Fe-rich sphalerite minerals. The experimental conditions that were tested during the industrial test were as follows: Throughout the grinding operation the pH of the pulp was changed in the range of 7.5– 9.5; the depressants – zinc sulphate and MINFIT® were added alone or together in various proportions.

RESULTS AND DISCUSSION

Ore Characterization

The results from the conducted studies by optical microscope and the implemented quantative electrone microprobe analysis, showed that in the metasomatic ore bodies in some deposits the Fe content in the sphalerite minerals in most cases is more than 6.00 % and could reach 11.00 – 12.00 %. Selected electron microprobe data on marmatite from the Madan ore field are presented in Table 1, and microphotographs of the analyzed mineral particles on Figures 1-4.

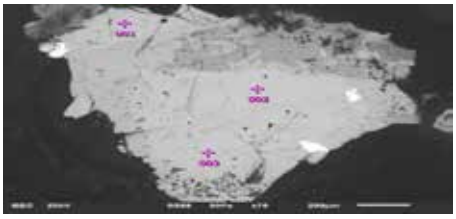

Figure 1 - Marmatite (greyish), with inclusions of gangue mineral (dark grey) and galena (white). BSE image, SEM, X 200

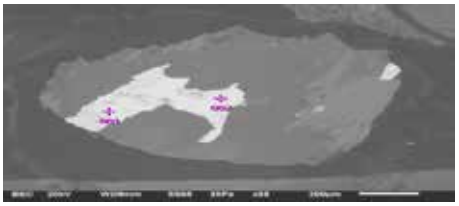

Figure 3 - Marmatite (greyish), irregular inclusions in matrix of skarn pyroxene aggregates (dark grey). BSE image, SEM, X 200

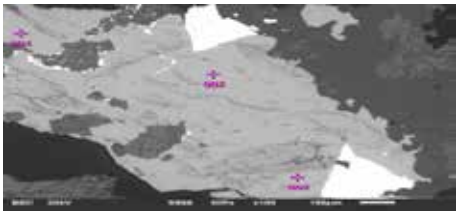

Figure 2 - Marmatite (greyish), with inclusions of galena (white) and clinopyroxenes (dark grey). BSE image, SEM, X 100

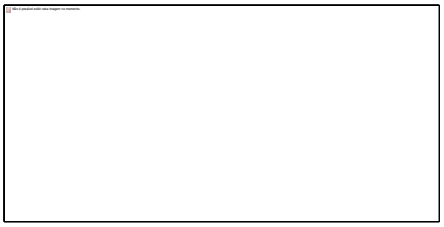

Figure 4 - Marmatite (greyish) - large particle in the centre and smaller one around it. Flotation Zn concentrate. BSE image, SEM, X 100

Table 1 - Selected electron microprobe analyses of marmatite (Zn, Fe)S from Pb-Zn ore and flotation Zn concentrate, Madan ore field

№	Fig. (№)	№ (Zn,Fe)S particle № analyses	Element (wt. %)					
			Zn	Fe	Mn	Cd	Cu	S
1	1	1.1 / lead-zinc ore	52.80	10.59	1.06	-	0.61	34.95
2	1	1.2/ lead-zinc ore	52.60	10.85	1.14	0.48	0.45	34.48
3	1	1.3/ lead-zinc ore	53.14	10.93	1.11	-	-	34.82
4	2	2.1/ lead-zinc ore	52.37	11.17	0.92	0.84	-	34.70
5	2	2.2/ lead-zinc ore	52.43	11.25	0.92	0.59	-	34.81
6	2	2.3/ lead-zinc ore	50.61	12.00	0.88	0.58	1.23	34.69
7	3	3.1/ lead-zinc ore	52.87	10.44	0.92	-	-	35.77
8	3	3.2/ lead-zinc ore	53.67	10.34	0.75	-	-	35.24
9	4	4.1/ zinc concentrate	54.89	9.68	0.72	-	-	34.72
10	4	4.2 / zinc concentrate	55.56	8.91	0.77	-	-	34.76

Contact Angle Measurements

The results obtained by using the microscope technique outlined in the experimental section are as follows: The mean value of the three-phase contact angle on the mineral substrates after the treatment with potassium ethyl xanthate solution is approximately 52°. After the treatment with the selected depressants ($ZnSO_4$ and MINFIT®) at pH of 9.5, the contact angles drastically decrease from 52° to 3°, i.e., the marmatite surface become unfloatable. The obtained very low values of the contact angel measurements after using the modified sulphite reagent MINFIT®, suggested that on the surface of marmatite a hydrophilic coating layer have been formed, which results in a significant reduction of xanthate adsorption on its mineral surface. It was established that the depressing action increase after the addition of lime (pH 9.5) and zinc sulphate. Another possible mechanism have been suggested for the depressing effect of $ZnSO_4$ and MINFIT® on marmatite during the selective flotation is the formation of insoluble heavy metal sulfite salts and subsequent reduction in the heavy metals ion concentration in the pulp, thus preventing unintentional activation.

Laboratory Flotation Tests

Laboratory flotation tests were conducted to investigate the role of pH, zinc sulphate and MINFIT® addition in the flotation of galena and Fe-rich sphalerite ore from the Erma reka concentrator. The laboratory rougher flotation tests with representative lead – zinc ore samples from "Erma reka" concentrator, have been conducted. The open cycle flotation tests results are presented on the graphs in Figures 5 – 14.

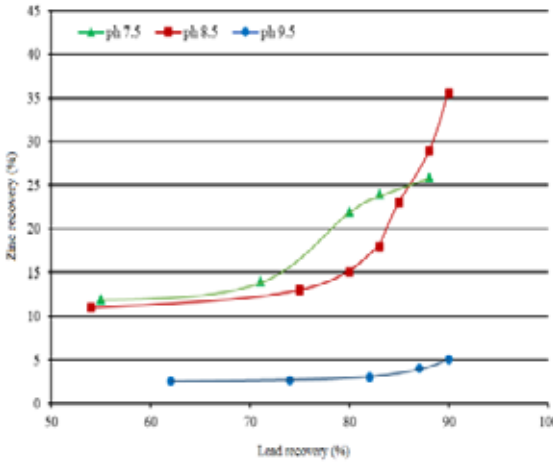

Figure 5 – Lead/zinc selectivity – effect of pH

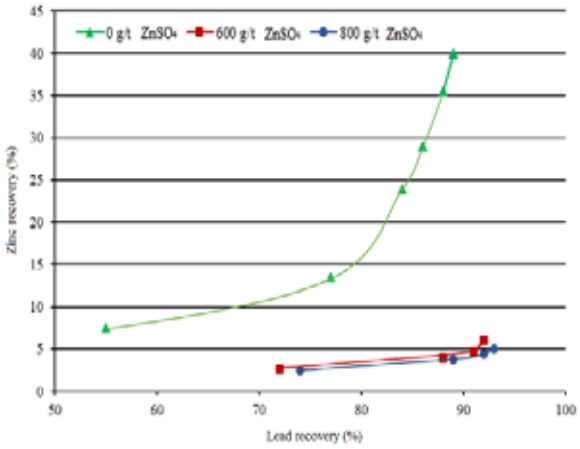

Figure 7 – Lead/zinc selectivity - effect of $ZnSO_4$ (g/t) at constant pH 8.5

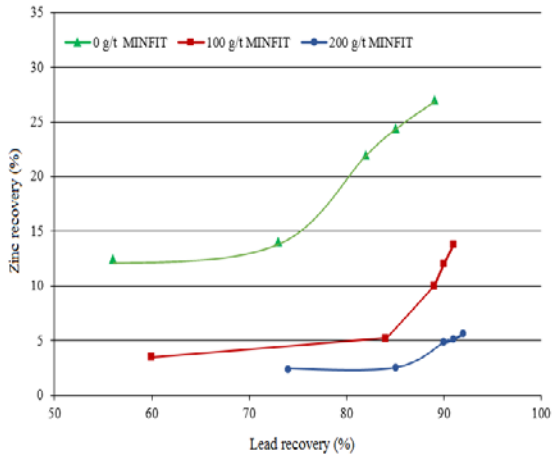

Figure 9 – Lead/zinc selectivity - effect of MINFIT® (g/t) at constant pH 7.5

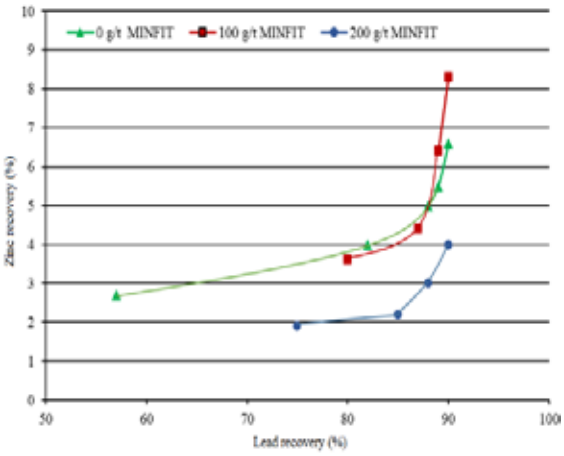

Figure 10 – Lead/zinc selectivity - effect of MINFIT® (g/t) at constant pH 8.5

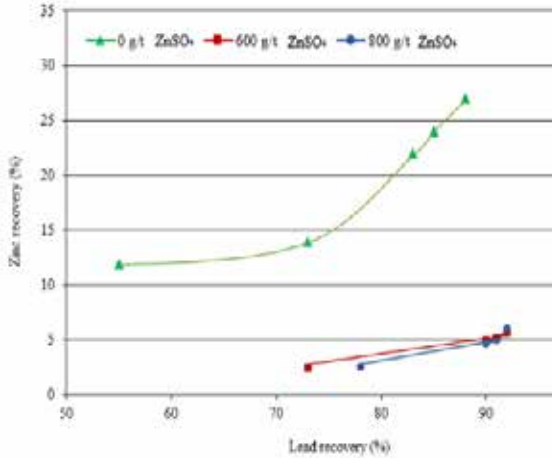

Figure 6 - Lead/zinc selectivity - effect of $ZnSO_4$ (g/t) at constant pH 7.5

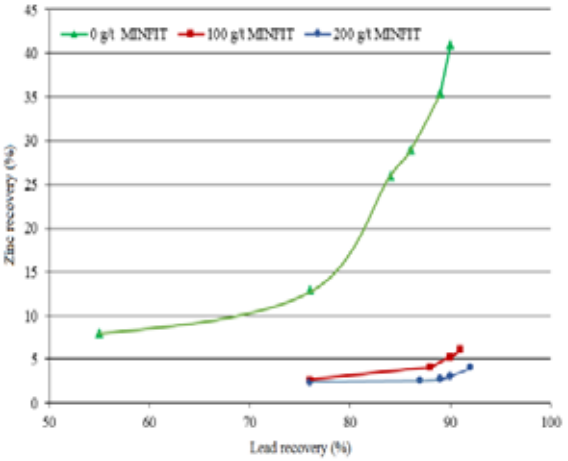

Figure 11 – Lead/zinc selectivity - effect of MINFIT® (g/t) at constant pH 9.5

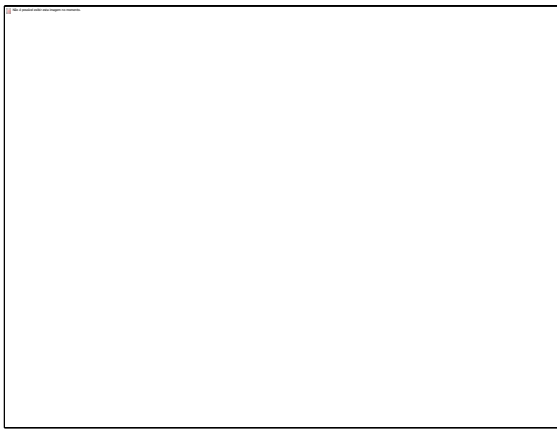

Figure 8 – Lead/zinc selectivity - effect of $ZnSO_4$ (g/t) at constant pH 9.5

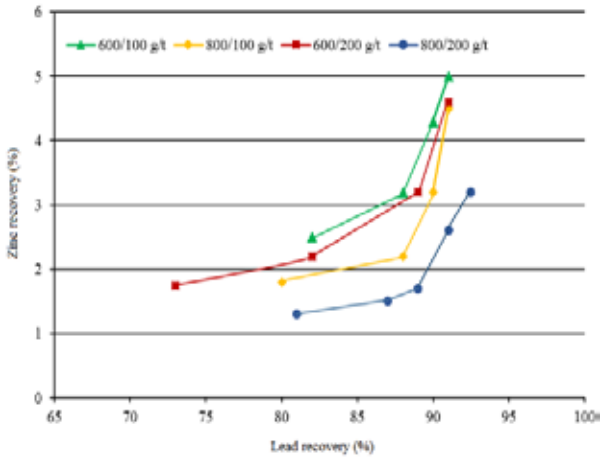

Figure 13 – Lead/zinc selectivity at pH 8.5 - effect of combined depressant addition ($ZnSO_4$ /MINFIT®, g/t)

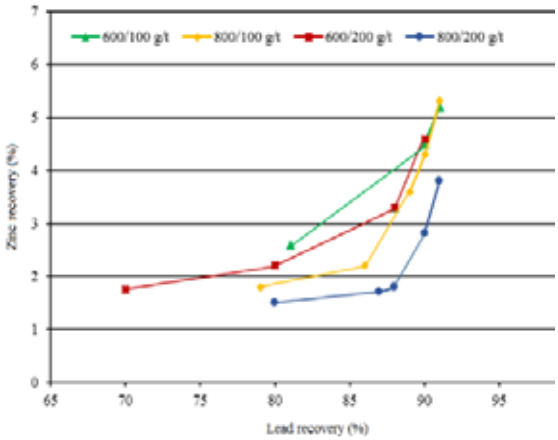

Figure 12 – Lead/zinc selectivity at pH 7.5 - effect of combined depressant addition ($ZnSO_4$ /MINFIT®, g/t)

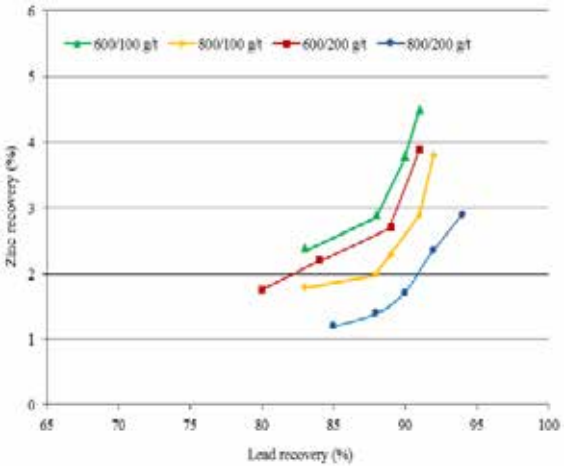

Figure 14 – Lead/zinc selectivity at pH 9.5 - effect of combined depressant addition ($ZnSO_4$ /MINFIT®, g/t)

The presented results on Figure 5 shows that the most successful depression action of marmatite was obtained at pH 9.5, where the zinc minerals recovery in the lead rougher concentrate was around 5.00 %. It's assumed that the addition of lime tended to slightly depress galena flotation, but substantially depress marmatite flotation (Misra, Miller & Song, 1985). Sutherland and Wark (1955) observed that the depressant action of lime was due to the formation of a finely dispersed hydrophilic film of lime on the surface of the sphalerite (Higgins & Quast, 1992).

Figures 6, 7 and 8 shows that with increasing the pH values of the pulp (from 7.5 to 9.5), along with increasing the quantity of $ZnSO_4$ addition (g/t), the depressing effect on the surface of the sphalerite is significantly improved and the lead concentrate grades are notably higher. The obtained results are in good agreement with the work of Malinovsky and Livshitz (cited by Klassen and Mokrousov, 1963) in that more alkaline conditions provided an increase in hydroxyl ions, and, along with the greater presence of zinc ions, more colloidal zinc hydroxide will be formed. This would precipitate on the surface of the marmatite and prevents the adsorption of the xanthate, and Livshitz and Idelson demonstrated that the extent of sphalerite depression was related to the concentration of colloidal zinc hydroxide in the pulp (Sutherland & Wark, 1955). The results presented in Figures 9, 10 and 11, shows that at pH 8.50 and 9.50 of the pulp and relatively low reagent consumption (MINFIT®) leads to very low recovery of zinc minerals in the rougher lead concentrates. The best results are obtained under the following conditions: pH value of the pulp 9.5 and 200 g/t MINFIT®.

The effect of combined depressant addition ($ZnSO_4$ and MINFIT®) is presented in Figures 12 - 14. In Figure 12 it could be seen that the best selectivity at the lower alkalinity (pH 7.5) of the lead and Fe-rich sphalerite minerals was obtained when using 200 g/t MINFIT® and 800 g/t $ZnSO_4$. However, the higher Pb recovery and the lower zinc minerals contamination in the lead rougher concentrate occurred with the addition of 200 g/t MINFIT® and 800 g/t $ZnSO_4$, while the pH of the pulp was 9.5. The depression action of the Fe-rich sphalerite when both reagents are included in the flotation tests is most likely due to the formation of zinc sulphite. When this forms, it is adsorbed onto the surface of the marmatite, resulting in competition for surface sites between those anions and xanthate under alkaline conditions (Klassen & Mokrousov, 1963).

Industrial Tests

Based on the results from the laboratory flotation experiments, industrial tests in the Erma reka concentrator have been conducted. During the industrial tests, the following conditions have been examined: pH range from 7.5 – 9.5; reagent dosage - Zinc Sulphate 600 – 800 g/t and MINFIT® 100 – 200 g/t. The obtained lead and zinc concentrates have been analyzed in the chemical laboratory. The corresponding grades and recoveries in the final lead and zinc concentrates were discussed.

The results obtained from the continued industrial experiment certainly showed the great depression effect of the marmatite during the rougher lead flotation operation. It could be clearly noticed that applying both depressants ($ZnSO_4$ and MINFIT®) with reagent dosage of 800 and 200 g/t, respectively, at maintained pH of the pulp - 9.5, would definitely lead to limited presence of Zn minerals in the final lead concentrate and therefore will increase the grade of final zinc concentrates.

APPLICATION RANGE

Since the beginning of 2015 a new flotation reagent regime in the rougher lead flotation section has been introduced. Based on the results from the industrial pilot plants tests, the following reagents and consumption rates $ZnSO_4$ – 800 g/t and MINFIT® 200 g/t have been implemented at pH 9.5 for the depression of the Fe-rich sphalerite (marmatite) in the Erma reka concentrator. In Figure 15 is presented the average monthly Zn content (%) in the final lead concentrates in 2015 versus the results from 2013 and 2014.The results presented in Figure 16, shows the average monthly lead content in the final zinc concentrates, during the period when the reagent regime was implemented (2015) and compared with the results from previous years. Furthermore, on Figure 17 is presented the average monthly quartz (SiO_2) content in the final zinc concentrate. In all three figures (15, 16 and 17) is clearly evident that in 2015 there are no values crossing the line, showing the hydrometallurgical limits for certain elements.

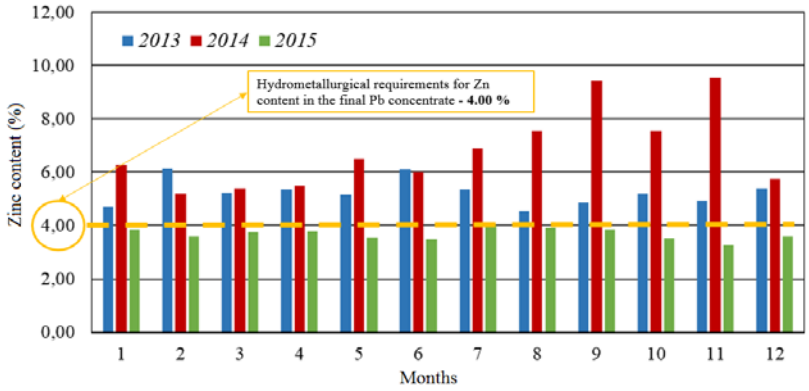

Figure 15-An average monthly zinc content (%) in the final lead concentrates during 2013, 2014 and 2015

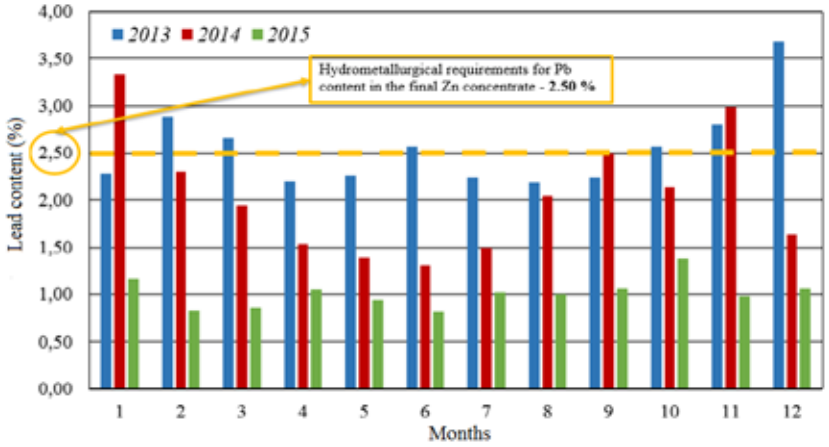

Figure 16 – An average monthly lead content (%) in the final zinc concentrates during 2013, 2014 and 2015

Figure 17 – An average monthly quartz content (%) in the final zinc concentrates during 2013, 2014 and 2015

CONCLUSION

Based on the model physicochemical investigations, the laboratory and industrial flotation tests and the results showing the performance of the Erma reka concentrator, since the new flotation regime have been maintained, it could be concluded that under these conditions the production of high quality lead and zinc concentrates with significantly lower recovery of undesirable contaminants in the

overall concentrates have been achieved. During the whole 2015 the hydrometallurgical requirements for less than 4.00 % zinc in the final lead concentrates and less than 2.50 % and 3.20 %of lead and quartz content in the final zinc concentrates have been followed and maintained.

ACKNOWLEDGEMENT

Financial support for this studies and permission to publish this paper from MINSTROY HOLDING JSC is gratefully acknowledged.

REFERENCES

Biswas, A. K., & Davenport, W. G., (*Eds*). (1994). *Extractive metallurgy of copper*. 3rd ed. Oxford: Pergamon.

Bulatovic, S. (2007). *Handbook of Flotation Reagents Chemistry, Theory and Practice: Flotation of Sulfide Ores*. Elsevier Science & Technology Books, 331 – 332.

Crawford, R., & Ralston, J. (1988). The influence of particle size and contact angle in mineral flotation. *International Journal of Mineral Processing*, *23*, 1-24.

Dai, Z. F., Dukhin, S., Fornasiero, D., & Ralston, J. (1998). The inertial hydrodynamic interaction of particles and rising bubbles with mobile surfaces. *Journal of Colloid and Interface Science, 197*, 275-292.

Dimitrijevic, M., Antonijevic, M. M., & Jankovic, Z. (1996). *Hydrometallurgy, 42*, 377.

Energy and Environmental Profile of the U.S. Mining Industry. Lead and Zinc. (Tech. Rep. (2013), 1-27).

Finkelstein, N. P. (1997). The activation of sulphide minerals for flotation: a review. *International Journal of Mineral Processing, 52*, 81–120.

Gaudin, A. M., Fuerstenau, D. W., & Miaw, H. L. (1960). Slimes coatings in galena flotation, *Canadian Mining and Metallurgy Bulletin*, 960-963.

Hewitt, D., Fornasiero, D., & Ralston, J. (1994). Bubble particle attachment efficiency. *Minerals Engineering, 7*, 657-665.

Higgins, S., & Quast, K. B. (1992). Zinc depression in the flotation of Broken Hill lead–silver concentrates. *Proceedings of the Metallurgy workshop*, AusIMM Annual Conference, Broken Hill, The Australasian Institute of Mining and Metallurgy, Melbourne, Australia.

Klassen, V. I., & Mokrousov, V. A. (1963). *An Introduction to the Theory of Flotation*. Butterworths, 304.

Lepetit, P., Bente, K., Doering, T. & Luckhaus, S. (2003). Crystal chemistry of Fe-containing sphalerites. *Physics and Chemistry of Minerals*, *30*, 185-191.

Misra, M., Miller, J. D., & Song, Q. Y. (1985). The effect of SO_2 in the flotation of sphalerite and chalcopyrite. In: Forssberg, K. S. E. (*Ed.*), *Flotation of Sulphide Minerals.* Elsevier, Amsterdam, 175– 196.

Nishkov, I., & Grigorova, I. (2010). Peculiarities of quartz distribution in zinc flotation products and their influence to mineral processing. *Twenty-fifth International Mineral Processing Congress* (pp. 2197 – 2203). Brisbane, Australia

Reay, D., & Ratcliff, G. A. (1973). Removal of fine particles from water by dispersed air flotation: effects of bubble size and particle size on flotation efficiency. *Canadian Journal of Chemistry Engineer*, *51*, 178-185.

Sivamohan, R. (1990). The problem of recovering very fine particles in mineral processing - A review. *International Journal of Mineral Processing*, *28*, 247-288.

Sutherland, K. L., & Wark, I. W. (1955). *Principles of Flotation*. Australasian Institute of Mining and Metallurgy, Melbourne, Australia.

Tong Xiong, Song Shao-xian, & He Jian. (2007). Activation of high-iron marmatite in froth flotation by ammoniacal copper solution. *Journal of Mineral Engineering, 20 (9)*, 259−263.

Wills, B. A., (*Ed.*), (1997). *Mineral processing technology: an introduction to the practical aspects of ore treatment and mineral recovery*. 6th ed. Boston: Butterworth-Heineman.

Institucional Support:

Editorial Support:

Communication Agency:

Operations Management:

Executive Producer and Marketing:

Commercial Partner – India:

Commercial Partner – Canada/USA:

Promotion:

IBRAM
INSTITUTO BRASILEIRO DE MINERAÇÃO
Brazilian Mining Association
Cámara Minera de Brasil

24th World Mining Congress
MINING IN A WORLD OF INNOVATION

October 18-21, 2016
Rio de Janeiro /RJ • Brazil